



Earth Resources
A Continuing
Bibliography
with Indexes

NASA SP-7041(54)
August 1987

National Aeronautics and
Space Administration

es Earth Resources
s Earth Resources
Earth Resources E
th Resources Far
Resources Earth
Resources Earth R
resources Earth Res

(NASA-SP-7041(54)) EARTH RESOURCES: A
CONTINUING BIBLIOGRAPHY WITH INDEXES (ISSUE
54) (NASA) 164 P Avail: NTIS HC A08

N87-27315

CSCI 05B

Unclas
00/43 0092568

* ACCESSION NUMBER RANGES

Accession numbers cited in this Supplement fall within the following ranges.

STAR (N-10000 Series) N87-15160 — N87-20170

IAA (A-10000 Series) A87-19611 — A87-31362

EARTH RESOURCES

A CONTINUING BIBLIOGRAPHY WITH INDEXES

Issue 54

A selection of annotated references to unclassified reports and journal articles that were introduced into the NASA scientific and technical information system and announced between April 1 and June 30, 1987 in

- *Scientific and Technical Aerospace Reports (STAR)*
- *International Aerospace Abstracts (IAA).*



Scientific and Technical Information Office

National Aeronautics and Space Administration

Washington, DC

1987

This bibliography was prepared by the NASA Scientific and Technical Information Facility operated for the National Aeronautics and Space Administration by RMS Associates.

INTRODUCTION

The technical literature described in this continuing bibliography may be helpful to researchers in numerous disciplines such as agriculture and forestry, geography and cartography, geology and mining, oceanography and fishing, environmental control, and many others. Until recently it was impossible for anyone to examine more than a minute fraction of the Earth's surface continuously. Now vast areas can be observed synoptically, and changes noted in both the Earth's lands and waters, by sensing instrumentation on orbiting spacecraft or on aircraft.

This literature survey lists 562 reports, articles, and other documents announced between April 1 and June 30, 1987 in *Scientific and Technical Aerospace Reports (STAR)*, and *International Aerospace Abstracts (IAA)*.

The coverage includes documents related to the identification and evaluation by means of sensors in spacecraft and aircraft of vegetation, minerals, and other natural resources, and the techniques and potentialities of surveying and keeping up-to-date inventories of such riches. It encompasses studies of such natural phenomena as earthquakes, volcanoes, ocean currents, and magnetic fields; and such cultural phenomena as cities, transportation networks, and irrigation systems. Descriptions of the components and use of remote sensing and geophysical instrumentation, their subsystems, observational procedures, signature and analyses and interpretive techniques for gathering data are also included. All reports generated under NASA's Earth Resources Survey Program for the time period covered in this bibliography are also included. The bibliography does not contain citations to documents dealing mainly with satellites or satellite equipment used in navigation or communication systems, nor with instrumentation not used aboard aerospace vehicles.

The selected items are grouped in nine categories. These are listed in the Table of Contents with notes regarding the scope of each category. These categories were especially chosen for this publication, and differ from those found in *STAR* and *IAA*.

Each entry consists of a standard bibliographic citation accompanied by an abstract. The citations include the original accession numbers from the respective announcement journals.

Under each of the nine categories, the entries are presented in one of two groups that appear in the following order:

IAA entries identified by accession number series A87-10,000 in ascending accession number order;

STAR entries identified by accession number series N87-10,000 in ascending accession number order.

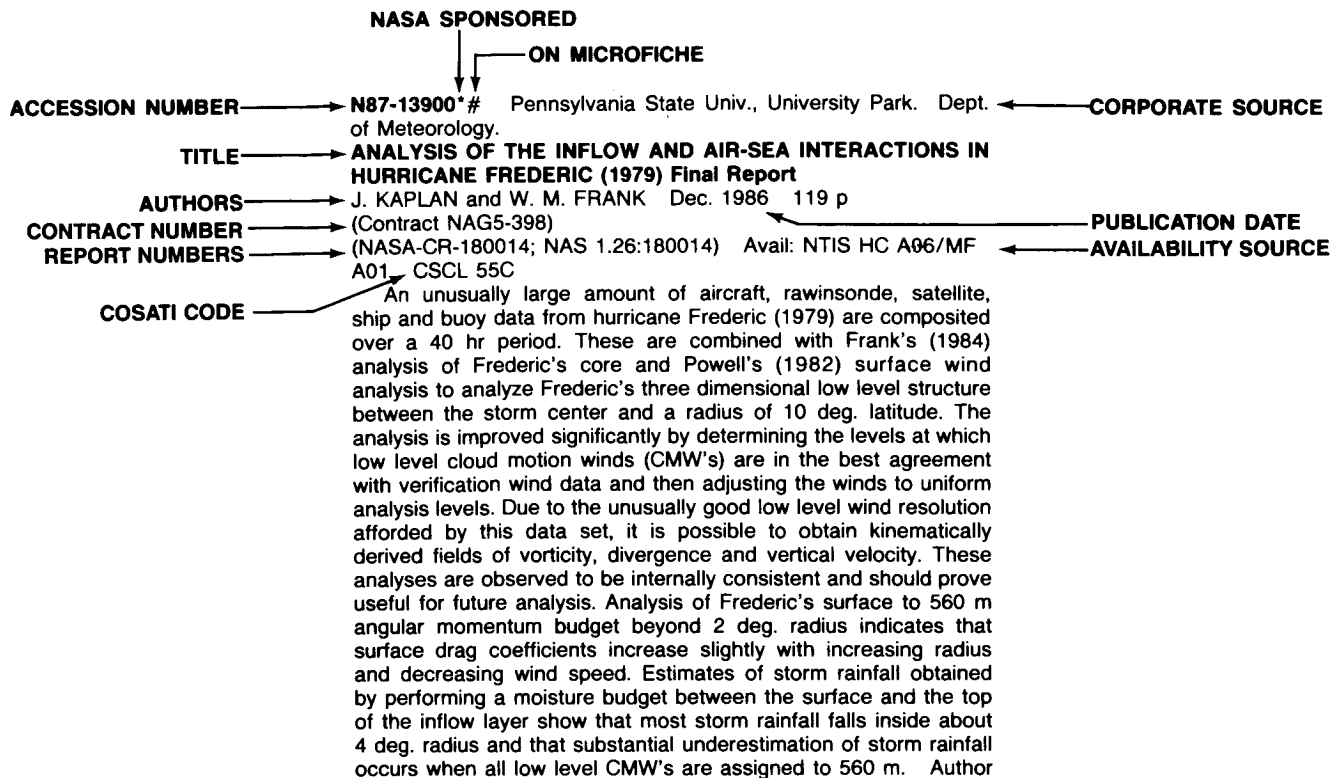
After the abstract section, there are seven indexes:

subject, personal author, corporate source, foreign technology, contract number, report/ accession number, and accession number.

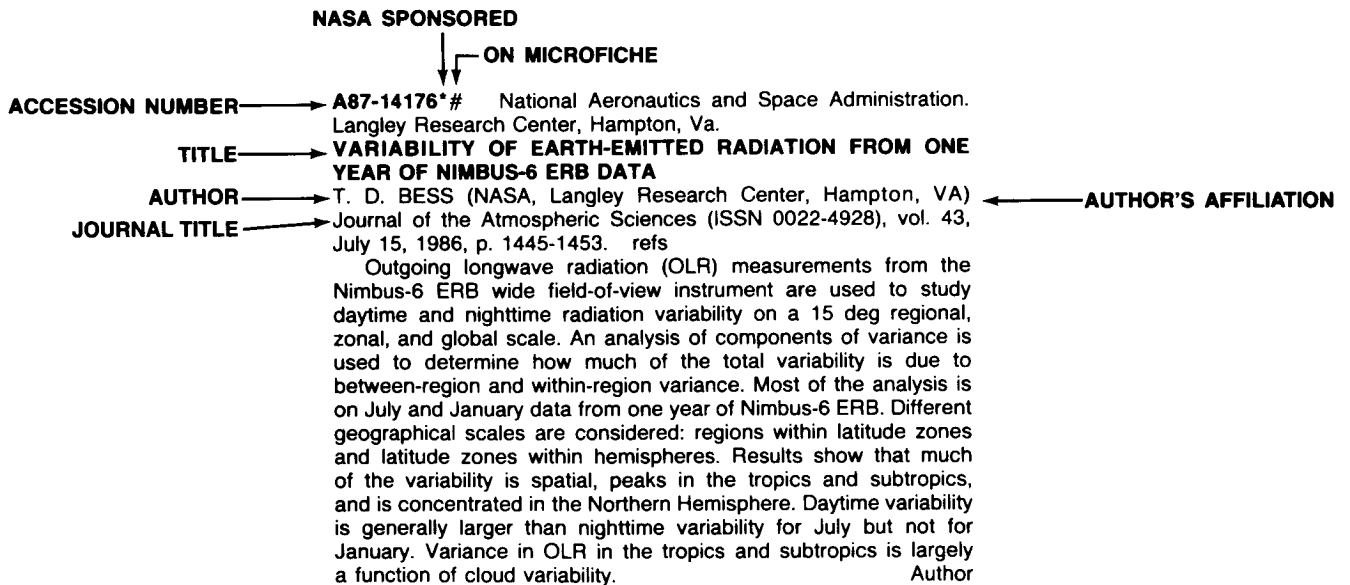
TABLE OF CONTENTS

	Page
Category 01 Agriculture and Forestry Includes crop forecasts, crop signature analysis, soil identification, disease detection, harvest estimates, range resources, timber inventory, forest fire detection, and wildlife migration patterns.	1
Category 02 Environmental Changes and Cultural Resources Includes land use analysis, urban and metropolitan studies, environmental impact, air and water pollution, geographic information systems, and geographic analysis.	24
Category 03 Geodesy and Cartography Includes mapping and topography.	26
Category 04 Geology and Mineral Resources Includes mineral deposits, petroleum deposits, spectral properties of rocks, geological exploration, and lithology.	27
Category 05 Oceanography and Marine Resources Includes sea-surface temperature, ocean bottom surveying imagery, drift rates, sea ice and icebergs, sea state, fish location.	37
Category 06 Hydrology and Water Management Includes snow cover and water runoff in rivers and glaciers, saline intrusion, drainage analysis, geomorphology of river basins, land uses, and estuarine studies.	56
Category 07 Data Processing and Distribution Systems Includes film processing, computer technology, satellite and aircraft hardware, and imagery.	62
Category 08 Instrumentation and Sensors Includes data acquisition and camera systems and remote sensors.	73
Category 09 General Includes economic analysis.	86
Subject Index	A-1
Personal Author Index	B-1
Corporate Source Index	C-1
Foreign Technology Index	D-1
Contract Number Index	E-1
Report Number Index	F-1
Accession Number Index	G-1

TYPICAL REPORT CITATION AND ABSTRACT



TYPICAL JOURNAL ARTICLE CITATION AND ABSTRACT



EARTH RESOURCES

A Continuing Bibliography (Issue 54)

AUGUST 1987

01

AGRICULTURE AND FORESTRY

Includes crop forecasts, crop signature analysis, soil identification, disease detection, harvest estimates, range resources, timber inventory, forest fire detection, and wildlife migration patterns.

A87-20671
AN INITIAL EVALUATION OF TWO DIGITAL AIRBORNE IMAGERS FOR SURVEYING SPRUCE BUDWORM DEFOLIATION

F. J. AHERN (Department of the Environment, Canada Centre for Remote Sensing, Ottawa), W. J. BENNETT (INTERA Technologies, Ltd., Ottawa, Canada), and E. G. KETTEL (Canadian Forestry Service, Maritime Forest Research Centre, Fredericton, Canada) *Photogrammetric Engineering and Remote Sensing* (ISSN 0099-1112), vol. 52, Oct. 1986, p. 1647-1654. refs

The comparative effectiveness of mechanical and pushbroom airborne multispectral scanners in detecting differences in budworm spruce defoliation is investigated on the basis of data obtained in flights over a test site in New Brunswick, Canada, during July 1983. The data are presented in tables, graphs, and sample images and characterized. The superior performance of the pushbroom scanner is attributed to its higher spectral resolution. T.K.

A87-20758
REMOTE SENSING OF THE STATE OF CROPS AND SOILS

K. IA. KONDRATEV (AN SSSR, Institut Ozerovedeniia, Leningrad, USSR), V. V. KOZODEROV (AN SSSR, Otdel Vychislitel'noi Matematiki, Moscow, USSR), and P. P. FEDCHENKO (Vsesoiuznyi Nauchno-Issledovatel'skii Institut Sel'skokhoziastvennoi Meteorologii, Obninsk, USSR) *International Journal of Remote Sensing* (ISSN 0143-1161), vol. 7, Oct. 1986, p. 1213-1235. refs

Various techniques as well as some general problems of agricultural remote sensing are discussed, with emphasis on the development of techniques to assess soil productivity (humus content) and the state of crops (weediness, etc.). The techniques considered were tested for the conditions of the southern part of the USSR European territory (the Ukraine and Moldavia). Sample applications of the technique are shown. Author

A87-20759
MACHINE PROCESSING OF LANDSAT DATA FOR SOIL SURVEY - THE BENUE VALLEY SAVANNA CASE STUDY

A. FAGBAMI (Ibadan, University, Nigeria) *International Journal of Remote Sensing* (ISSN 0143-1161), vol. 7, Oct. 1986, p. 1237-1250. refs

A ground-truth (GT) map, produced by fieldwork and the interpretation of large-scale B&W aerial photographs, was compared with digital/graphical output from Landsat data of the savanna around Makurdi in central Nigeria. The GT maps were digitized, grid-converted and then aggregated, while the Landsat data were resampled for the purpose of rectification on the ERDAS 400 microcomputer at Michigan State University. A visual comparison of the maps was done by overlaying the digital maps on the GT map, while the histogram listing provided an approximate quantitative comparison. Two algorithms of supervised classification

(maximum likelihood and minimum distance) produced similar results, but the third unsupervised algorithm, (cluster analysis), produced a far simpler map that is ideal as a reconnaissance soil/resource survey map. Author

A87-20761* New York State Univ., Binghamton.
ESTIMATION OF CANOPY PARAMETERS FOR INHOMOGENEOUS VEGETATION CANOPIES FROM REFLECTANCE DATA. II - ESTIMATION OF LEAF AREA INDEX AND PERCENTAGE OF GROUND COVER FOR ROW CANOPIES

N. S. GOEL and T. GRIER (New York, State University, Binghamton) *International Journal of Remote Sensing* (ISSN 0143-1161), vol. 7, Oct. 1986, p. 1263-1286. NASA-supported research. refs

The canopy reflectance (CR) model for row-planted vegetation proposed earlier has been tested for soybean canopies in three different stages of growth and for corn canopies at early and full growth stages. The model fits the field-measured bidirectional CR data quite well. It is shown that, by inverting this model, one could estimate the leaf area index as well as the percentage of ground cover quite accurately from measured canopy reflectances. Author

A87-20762
THEMATIC MAPPER ANALYSIS OF CONIFEROUS FOREST STRUCTURE AND COMPOSITION

J. FRANKLIN (California, University, Santa Barbara) *International Journal of Remote Sensing* (ISSN 0143-1161), vol. 7, Oct. 1986, p. 1287-1301. Research supported by the University of California. refs

Simple regressions of single-band TMS reflectance data against stand basal area and leaf biomass show that the spectral feature most strongly related to vegetation amount is visible reflectance (TM bands 1.2 and 3), which decreases as conifer basal area increases. Principal-components analysis of TMS spectral data for sample stands, and stepwise multiple regression of transformed axes, showed the first principal component, interpreted as scene brightness, to be the composite spectral feature most correlated to vegetation amount. TMS data showed some ability to discriminate spectrally between coniferous forest stands dominated by different species. Author

A87-20763* Jet Propulsion Lab., California Inst. of Tech., Pasadena.

ASSESSING FOREST DECLINE IN CONIFEROUS FORESTS OF VERMONT USING NS-001 THEMATIC MAPPER SIMULATOR DATA

J. E. VOGELMANN and B. N. ROCK (California Institute of Technology, Jet Propulsion Laboratory, Pasadena) *International Journal of Remote Sensing* (ISSN 0143-1161), vol. 7, Oct. 1986, p. 1303-1321. NASA-supported research. refs

This study evaluates the potential of measuring/mapping forest decline in spruce-fir forests using airborne NS-001 TMS data. Using field instruments, it was found that ratios of 1.65/1.23 and 1.65/0.83-micron reflectance discriminated between spruce samples of low and high-damage sites. Using TMS data, band ratios were found to be strongly correlated with ground-based measurements of forest damage. Ratio color-density slice images using these band ratios, and images using 0.56 and 1.65-micron bands with either of these band ratios in a false-color composite,

provide accurate means of detecting, quantifying and mapping levels of forest decline. Author

A87-21239 REMOTE SENSING OPTIONS FOR SOIL SURVEY IN DEVELOPING COUNTRIES

AYODELE FAGBAMI (Ibadan, University, Nigeria) (Working Group on Remote Sensing for Soil Survey, Symposium, Wageningen and Enschede, Netherlands, Mar. 3-8, 1985) ITC Journal (ISSN 0303-2434), no. 1, 1986, p. 3-8. Research supported by Ette Aro and Partners. refs

The ability of developing countries to take full advantage of remote sensing applications has been limited by poor technology and financial constraints. In this article, four sources of remote sensing data are assessed (aerial photographs, Landsat diazo prints and CCTs, and Skylab photographs), emphasizing the best combinations of simplicity of technology, utility and flexibility of the data, and affordable costs, without compromising accuracy of results, speed of inventorying or development implementation programmes. Author

A87-21240 NMR INSTRUMENT FOR SOIL MOISTURE GROUND-TRUTH DATA COLLECTION

RON F. PAETZOLD (USDA, Hydrology Laboratory, Beltsville, MD) (Working Group on Remote Sensing for Soil Survey, Symposium, Wageningen and Enschede, Netherlands, Mar. 3-8, 1985) ITC Journal (ISSN 0303-2434), no. 1, 1986, p. 9-13. refs

Research was conducted to develop an instrument capable of measuring volumetric soil-water content using nuclear magnetic resonance (NMR) techniques. NMR is very attractive since it is both non-destructive and non-invasive. An NMR instrument was designed to continuously measure volumetric water content in the soil surface while moving at ground speeds of up to 17 km/h. The instrument will be used to gather ground data for calibration and verification of data collected by remote sensing instruments. This use requires a method that is relatively accurate, rapid and independent of soil type, organic matter content, texture and clay mineralogy. Calibration measurements were made on large soil samples with varying water content. The average correlation coefficient of the NMR results with the soil moisture content for six combinations of measurement depth and sensor configuration was 0.97. Author

A87-21241 SOIL SCIENCE INTERPRETATION OF PHOTOGRAPHS TAKEN BY SPACELAB 1 [INTERPRETATION PEDOLOGIQUE DES PHOTOGRAPHIES PRISES PAR SPACELAB 1]

MICHEL C. GIRARD (Institut National de la Recherche Agronomique, Paris, France) (Working Group on Remote Sensing for Soil Survey, Symposium, Wageningen and Enschede, Netherlands, Mar. 3-8, 1985) ITC Journal (ISSN 0303-2434), no. 1, 1986, p. 14-18. In French.

High-resolution color infrared photographs obtained by the Spacelab 1 metric camera were enlarged to a scale of 1:300,000 and used to determine the principal morphologic landscape forms. Towns, in addition to soil elements such as humid uncovered soils and hydromorphic soils, could be distinguished. A distinction is made between directly detectable elements and those which are deduced from intermediary elements such as vegetation cover. A three-level study permits the production of preinterpretation maps of the distribution of soils at different scales and at various levels of precision. R.R.

A87-21242 SPECTRAL BRIGHTNESS AND SURFACE SOIL CHARACTERISTICS IN AN ARID MEDITERRANEAN REGION (SOUTHERN TUNISIA) [LUMINANCE SPECTRALE ET CARACTERES DE LA SURFACE DES SOLS EN REGION ARIDE MEDITERRANEENNE /SUD TUNISIEN/]

RICHARD ESCADAFAL (Office de la Recherche Scientifique et Technique Outre-Mer, Gabes, Tunisia) and MARCEL POUGET (Office de la Recherche Scientifique et Technique Outre-Mer, Bondy, France) (Working Group on Remote Sensing for Soil Survey, Symposium, Wageningen and Enschede, Netherlands, Mar. 3-8, 1985) ITC Journal (ISSN 0303-2434), no. 1, 1986, p. 19-23. In French. refs

A87-21243 THE THEMATIC MAPPER - A NEW TOOL FOR SOIL MAPPING IN ARID AREAS

MICHEL A. MULDER and GERRIT F. EPEMA (Landbouwhogeschool, Wageningen, Netherlands) (Working Group on Remote Sensing for Soil Survey, Symposium, Wageningen and Enschede, Netherlands, Mar. 3-8, 1985) ITC Journal (ISSN 0303-2434), no. 1, 1986, p. 24-29. refs

The application of thematic mapper (TM) data to soil mapping is studied. The basic capabilities and operation of the TM are described. The TM provides improved spatial resolution, spectral resolution, and band allocation. The TM was utilized to evaluate the gypsiferous, calcareous, and clayey surfaces of the Kasserine and Sefimi areas in Tunisia; the generated TM maps are compared with aerial photographs. It is noted that the TM is useful for soil mapping in arid area if combined with aerial photographs. I.F.

A87-21244 PROCESSING THEMATIC MAPPER DATA FOR MAPPING IN TUNISIA

GERRIT F. EPEMA (Landbouwhogeschool, Wageningen, Netherlands) (Working Group on Remote Sensing for Soil Survey, Symposium, Wageningen and Enschede, Netherlands, Mar. 3-8, 1985) ITC Journal (ISSN 0303-2434), no. 1, 1986, p. 30-34. refs

The structure of thematic mapper (TM) data was investigated using various methods to assess the information content for an area in North Africa. One of the most effective methods of displaying TM data was obtained by using ratio images in combination with total intensity images. This allowed preparation of thematic maps which could be subsequently checked during fieldwork. Author

A87-21245 AN APPLICATION OF THEMATIC MAPPER DATA IN TUNISIA - ESTIMATION OF DAILY AMPLITUDE IN NEAR-SURFACE SOIL TEMPERATURE AND DISCRIMINATION OF HYPERSALINE SOILS

MASSIMO MENENTI, ALOISIUS LORKEERS, and MARTIN VISSERS (Landbouwhogeschool, Wageningen, Netherlands) (Working Group on Remote Sensing for Soil Survey, Symposium, Wageningen and Enschede, Netherlands, Mar. 3-8, 1985) ITC Journal (ISSN 0303-2434), no. 1, 1986, p. 35-42. refs

A87-21246 EXPERIMENTAL RESULTS IN SOIL MOISTURE MAPPING USING IR THERMOGRAPHY

SUNE AXELSSON (Linkoping, Universitet, Sweden) and BENGT LUNDEN (Stockholms, Universitet, Stockholm, Sweden) (Working Group on Remote Sensing for Soil Survey, Symposium, Wageningen and Enschede, Netherlands, Mar. 3-8, 1985) ITC Journal (ISSN 0303-2434), no. 1, 1986, p. 43-50. Research supported by the Swedish Board for Space Activities. refs

To evaluate aerial thermography for soil moisture mapping, thermal images of an agricultural area in central Sweden were obtained in the early afternoon and the following night. Eighty soil samples were analyzed with respect to volumetric water content, grain size distribution, porosity and organic material. Aluminium plates were placed at the sampling sites for location in the thermal images. Analysis of the relationship between thermal image data

and soil data showed a significant correlation between soil moisture and temperature in both day and nighttime images. The accuracy increased considerably with the addition of meteorologic data and soil type information in the interpretation procedure. Author

A87-21247**THERMOGRAPHY - PRINCIPLES AND APPLICATION IN THE OOST-GELDERLAND REMOTE SENSING STUDY PROJECT**

GERARD J. A. NIEUWENHUIS (Landbouwhogeschool, Wageningen, Netherlands) (Working Group on Remote Sensing for Soil Survey, Symposium, Wageningen and Enschede, Netherlands, Mar. 3-8, 1985) ITC Journal (ISSN 0303-2434), no. 1, 1986, p. 51-58. refs

A study project conducted in The Netherlands is described in which both thermal images and agro-hydrologic models were assessed. Linear relationships were established between the increase in crop surface temperature derived from thermal images and the reduction in daily evapotranspiration. With these relationships, digital images in the visual and thermal infrared spectral regions could be transformed automatically into an evapotranspiration map. Thermography was found valuable in itself and also as an important check for the agro-hydrologic models. The two techniques correlated reasonably well in estimating the hydrologic regime in a mostly agricultural area. Author

A87-21249**TIMELY THERMAL INFRARED DATA ACQUISITION FOR SOIL SURVEY IN HUMID TEMPERATURE ENVIRONMENTS**

DAVID W. LYNN (Reading, University, England) (Working Group on Remote Sensing for Soil Survey, Symposium, Wageningen and Enschede, Netherlands, Mar. 3-8, 1985) ITC Journal (ISSN 0303-2434), no. 1, 1986, p. 68-76. refs

A87-21250**THEORETICAL APPROACH TO RADAR BACKSCATTERING OF SOILS**

LEO KRUL (Delft, Technische Hogeschool, Netherlands) (Working Group on Remote Sensing for Soil Survey, Symposium, Wageningen and Enschede, Netherlands, Mar. 3-8, 1985) ITC Journal (ISSN 0303-2434), no. 1, 1986, p. 77-81. refs

Models which describe the relationship between the radar signal and the object parameters for radar-based remote sensing are developed. The models need to predict the amplitude and phase of the scattered wave as a function of polarization, incidence angle, and wavelength of the illuminating wave. The material properties are expressed in terms of a dielectric constant and the structural interaction effects are classified into Rayleigh, Mie, and optical regions. Procedures and equations for solving the electromagnetic field problem are presented. A procedure for simulating the backscattering of soil is described. I.F.

A87-21251**RADAR IMAGES FOR SOIL SURVEY IN ENGLAND AND WALES**

ROBERT EVANS (Cambridge University, England) and DOUGLAS M. CARROLL (Working Group on Remote Sensing for Soil Survey, Symposium, Wageningen and Enschede, Netherlands, Mar. 3-8, 1985) ITC Journal (ISSN 0303-2434), no. 1, 1986, p. 88-93. refs

A87-23360**FOREST FIRE MONITORING USING THE NOAA SATELLITE SERIES**

M. D. FLANNIGAN (Canadian Forestry Service, Petawawa National Forestry Institute, Chalk River, Canada) and T. H. VONDER HAAR (Colorado State University, Fort Collins) IN: Conference on Satellite Meteorology/Remote Sensing and Applications, 2nd, Williamsburg, VA, May 13-16, 1986, Preprints. Boston, MA, American Meteorological Society, 1986, p. 168-172. refs

A87-23388* National Aeronautics and Space Administration, Goddard Space Flight Center, Greenbelt, Md.

THE EFFECT OF LOCAL ADVECTION ON THE INFERENCE OF SOIL MOISTURE FROM THERMAL INFRARED RADIANCES

PETER J. WETZEL (NASA, Goddard Space Flight Center, Greenbelt, MD) and ROBERT H. WOODWARD (General Software Corp., Landover, MD) IN: Conference on Satellite Meteorology/Remote Sensing and Applications, 2nd, Williamsburg, VA, May 13-16, 1986, Preprints. Boston, MA, American Meteorological Society, 1986, p. 307-312.

The degree to which the GOES-VISSR infrared data can be used to infer area-averaged soil moisture is explored for a five-day case study period. Chosen variables are transformed and incorporated into a multiple linear regression. The actual observations, rather than a simplified model, are used to determine the relationship between soil moisture and GOES-IR radiance. It is shown that a depletion coefficient of 0.92 produces an index of ground truth which is best correlated with soil moisture as inferred from GOES thermal infrared data. When all individual daily soil estimates during the case study period are averaged at each point and compared to the average observed soil moisture, the data correlate at 0.85. This implies that the algorithm can distinguish at least four categories of soil moisture. C.D.

A87-23389**SOIL MOISTURE ESTIMATES FROM SATELLITE INFRARED TEMPERATURES AND THEIR RELATION TO SURFACE MEASUREMENTS**

TOBY N. CARLSON (Pennsylvania State University, University Park) IN: Conference on Satellite Meteorology/Remote Sensing and Applications, 2nd, Williamsburg, VA, May 13-16, 1986, Preprints. Boston, MA, American Meteorological Society, 1986, p. 313-316. refs

The use of a time-dependent, initial-valued, one-dimensional boundary layer model in conjunction with measured surface temperatures to obtain the surface energy balance, a soil moisture parameter called the moisture availability, and the thermal inertia of the soil is addressed. Recent results are reported which show agreement between moisture values calculated with the model using satellite infrared temperatures as input and ground-based measurements of related parameters. The approach can detect large spatial and temperature changes in soil moisture but cannot yet provide a completely consistent measure of the real soil water content or the soil depth over which it applies. C.D.

A87-23797**AN ITERATIVE LANDSAT-MSS CLASSIFICATION METHODOLOGY FOR SOIL SURVEY**

M. C. PARTON and O. A. CHADWICK (Arizona, University, Tucson) IN: American Congress on Surveying and Mapping and American Society for Photogrammetry and Remote Sensing, Annual Convention, Washington, DC, Mar. 16-21, 1986, Technical Papers. Volume 4. Falls Church, VA, American Congress on Surveying and Mapping and American Society for Photogrammetry and Remote Sensing, 1986, p. 380-387. refs

A procedure for the integration of digital Landsat multispectral scanner and photographic remotely sensed data into pre-mapping activities of a soil survey was developed and tested for 170,000 hectares of southern Arizona rangeland. Image enhancement, classification and stratification of the digital data were used to derive output products employed to accelerate field sampling site selection and mapping. Digitized map data on established ground sites and the thermic/hyperthermic temperature boundary were overlaid with classified MSS data to produce a second-order classification for improved soil map units. Benefits from this methodology included the design of more appropriate map units, enhanced prediction of soil occurrence outside of the intensively studied field sites, creation of a digital data base for the resulting general soils map and time savings during subsequent detailed mapping. Author

A87-23806

AGRICULTURAL REMOTE SENSING IN SOUTH CAROLINA - A STUDY OF CROP IDENTIFICATION CAPABILITIES UTILIZING LANDSAT DATA

BASIL G. SAVITSKY (Research Planning Institute, Inc., Columbia, SC) and JOHN R. JENSEN (South Carolina, University, Columbia) IN: American Congress on Surveying and Mapping and American Society for Photogrammetry and Remote Sensing, Annual Convention, Washington, DC, Mar. 16-21, 1986, Technical Papers. Volume 4 . Falls Church, VA, American Congress on Surveying and Mapping and American Society for Photogrammetry and Remote Sensing, 1986, p. 476-484. refs

Remote sensing of agricultural resources in the southeastern United States is constrained both by relatively small field sizes and by persistent cloud cover during the growing season. This study examined the crop identification capabilities of Landsat MSS data during the summer of 1980 when only one date of imagery of acceptable quality was available. The phenological calendars of four major crops (soybeans, corn, cotton, and tobacco) were prepared, and the theoretical discriminability evident in the spectral reflectance curves of the crops was compared to actual results. The Landsat data were transformed using Kauth-Thomas and principal component analyses, and supervised and unsupervised classifications were performed on all three sets of imagery. There was no major change in overall classification accuracy associated with the transformed data, but the classification accuracies of the unsupervised classifications were significantly higher than the supervised classifications. The unsupervised classification of the principal component data yielded the highest information content and had an overall accuracy of 65.9 percent. Author

A87-23807

USING LANDSAT TO ASSESS TROPICAL FOREST HABITAT FOR MIGRATORY BIRDS IN THE YUCATAN PENINSULA

J. F. LYNCH (Smithsonian Environmental Research Center, Edgewater, MD) and K. M. GREEN IN: American Congress on Surveying and Mapping and American Society for Photogrammetry and Remote Sensing, Annual Convention, Washington, DC, Mar. 16-21, 1986, Technical Papers. Volume 4 . Falls Church, VA, American Congress on Surveying and Mapping and American Society for Photogrammetry and Remote Sensing, 1986, p. 495-499. refs

A87-23810

AMERICAN CONGRESS ON SURVEYING AND MAPPING AND AMERICAN SOCIETY FOR PHOTOGRAMMETRY AND REMOTE SENSING, ANNUAL CONVENTION, WASHINGTON, DC, MAR. 16-21, 1986, TECHNICAL PAPERS. VOLUME 5 - REMOTE SENSING

Falls Church, VA, American Congress on Surveying and Mapping and American Society for Photogrammetry and Remote Sensing, 1986, 310 p. For individual items see A87-23811 to A87-23834.

Papers are presented on Landsat image map production methods at the U.S. Geological Survey, an image analysis workstation for geologic data integration, the use of hand-held color oblique 35 mm slides for littoral zone mapping, the use of remote sensing for evaluating the canopy reflectance of two drought-stressed shrubs, phenological effects on grass canopy/spectral relationships, and remote sensing estimation of sugarcane yield using a spectroradiometer. Topics discussed include a new method for measuring suspended sediment content in different depth water using a spectroradiometer, the use of TM data for temperature mapping in the Great Lakes, image processed sidescan sonar data, and Space Shuttle radargrammetry results. Consideration is given to techniques for deriving land use information from Landsat data using a geographic information system, the identification of forest and agricultural edges using Landsat TM data, and vegetable crop inventoring with Landsat TM data. I.F.

A87-23811

LAND SURFACE CLIMATIC VARIABLES MONITORED BY NOAA-AVHRR SATELLITES

K. P. GALLO, J. D. TARPLEY, and D. F. MCGINNIS, JR. (NOAA, National Environmental, Data, and Information Service, Washington, DC) IN: American Congress on Surveying and Mapping and American Society for Photogrammetry and Remote Sensing, Annual Convention, Washington, DC, Mar. 16-21, 1986, Technical Papers. Volume 5 . Falls Church, VA, American Congress on Surveying and Mapping and American Society for Photogrammetry and Remote Sensing, 1986, p. 1-8.

Data collection and analysis has begun at the National Environmental Satellite Data and Information Service to determine the usefulness of satellite data for monitoring land surface climatological variables. The objective of this study is to determine if relationships can be developed between satellite obtained information and routinely available ground-based quantities such as the crop moisture index (CMI), Palmer drought index (PDI), soil moisture status, and shelter temperature. Collection of satellite data from the Great Plains area of the United States has begun and includes mapped Global Area Coverage data from the Advanced Very High Resolution Radiometer (AVHRR) on the NOAA-9 satellite. Conventional (ground-based) weather observations are accessed daily from the National Meteorological Center's operational data files. Derived climatic indices (CMI, PDI, etc.) produced by the NOAA Climate Analysis Center are acquired on a weekly basis and merged with the AVHRR data for further analysis. The coincident satellite and ground data will be used to evaluate AVHRR data and products with respect to ground observations. Author

A87-23816

AN ASSESSMENT OF EVAPOTRANSPIRATIONAL WATER LOSSES IN A SIERRAN MIXED CONIFER FOREST USING REMOTELY SENSED DATA

RUSSELL G. CONGALTON and LARS L. PIERCE (California, University, Berkeley) IN: American Congress on Surveying and Mapping and American Society for Photogrammetry and Remote Sensing, Annual Convention, Washington, DC, Mar. 16-21, 1986, Technical Papers. Volume 5 . Falls Church, VA, American Congress on Surveying and Mapping and American Society for Photogrammetry and Remote Sensing, 1986, p. 53-62. Research supported by the University of California. refs

A87-23818

PHENOLOGICAL EFFECTS ON GRASS CANOPY/SPECTRAL RELATIONSHIPS

WILLIAM J. RIPPLE (Oregon State University, Corvallis) IN: American Congress on Surveying and Mapping and American Society for Photogrammetry and Remote Sensing, Annual Convention, Washington, DC, Mar. 16-21, 1986, Technical Papers. Volume 5 . Falls Church, VA, American Congress on Surveying and Mapping and American Society for Photogrammetry and Remote Sensing, 1986, p. 69-79. refs

The utility of the Landsat Thematic Mapper bands for estimating grass canopy variables during three different phenological stages was studied. Spectral data were collected from annual ryegrass (*Lolium multiflorum*) plots using in situ remote sensing techniques with a Barnes Modular Multiband Radiometer. Data sets were collected at three plant stages; early stem extension (June), anthesis (July), and senescence (August). The highest correlations between the spectral and canopy variables were found for the June data set while the August data set yielded the poorest relationships. High levels of biomass (July) and plant senescence (August) both adversely affected the reflectance/canopy relationships. Principal component analysis was successful at reducing the seven original spectral bands to only two dimensions while maintaining nearly all of the variability found in the original data. Author

A87-23819

ESTIMATION OF DENSITY IN YOUNG PINE PLANTATIONS USING 35MM AERIAL PHOTOGRAPHY

RICHARD C. HEER and JAMES L. SMITH (Virginia Polytechnic Institute and State University, Blacksburg) IN: American Congress on Surveying and Mapping and American Society for Photogrammetry and Remote Sensing, Annual Convention, Washington, DC, Mar. 16-21, 1986, Technical Papers. Volume 5. Falls Church, VA, American Congress on Surveying and Mapping and American Society for Photogrammetry and Remote Sensing, 1986, p. 80-84.

In this study, stem counts were determined for plots established in young pine plantations using 35 mm vertical aerial photography. Color slides, at a scale of 1:6000, taken during the fall color change period provided the basis for this interpretation. A difference in the photo-obtained stem counts and those obtained in ground appraisals of the plots was observed. The age of the plantation being evaluated seemed to have an effect on the results, with the youngest stand showing the strongest relationship between the ground and photo counts. Author

A87-23822

DIURNAL-SEASONAL LIGHT INTERCEPTION, LEAF AREA INDEX, AND VEGETATION INDEX INTERRELATIONS IN A WHEAT CANOPY - A CASE STUDY

ARTHUR J. RICHARDSON and CRAIG L. WIEGAND (USDA, Agricultural Research Service, Weslaco, TX) IN: American Congress on Surveying and Mapping and American Society for Photogrammetry and Remote Sensing, Annual Convention, Washington, DC, Mar. 16-21, 1986, Technical Papers. Volume 5. Falls Church, VA, American Congress on Surveying and Mapping and American Society for Photogrammetry and Remote Sensing, 1986, p. 103-111. refs

Diurnal measurements of photosynthetically active radiation (PAR), intercepted by wheat canopies (IPAR), were adjusted for solar zenith angle (Z) effect on canopy solar path length and related to leaf area index (LAI) and perpendicular vegetation index (PVI) for semidwarf durum wheat (cv. Yavaros). Solar zenith angle adjustments permitted diurnal-seasonal IPAR data obtained during the canopy development portion of the 1983-1984 growing season to be correlated with $LAI/\cos Z$ and with the PVI calculated from diurnal radiometer radiance. Regressing IPAR data from light bar sensors against $LAI/\cos Z$ and PVI yielded $IPAR = 1 - 0.96\exp(-0.78 LAI/\cos Z)$ and $IPAR = 1 - 3.26\exp(-0.144 PVI)$. Also, $LAI/\cos Z = 0.155\exp(0.116 PVI)$. These studies indicate that LAI and IPAR are associated with spectral data such as the PVI until senescence begins. Correlations ranged from $r^2 = 0.86$ to 0.94 . The PVI appeared sensitive over a greater $LAI/\cos Z$ range than the normalized difference. These relations may be useful for large-scale agrometeorological crop growth models driven by satellite acquired spectral data. Author

A87-23830* George Mason Univ., Fairfax, Va.

LANDSAT THEMATIC MAPPER DIGITAL INFORMATION CONTENT FOR AGRICULTURAL ENVIRONMENTS

BARRY HAACK (George Mason University, Fairfax, VA), NEVIN BRYANT, and STEVEN ADAMS (California Institute of Technology, Jet Propulsion Laboratory, Pasadena) IN: American Congress on Surveying and Mapping and American Society for Photogrammetry and Remote Sensing, Annual Convention, Washington, DC, Mar. 16-21, 1986, Technical Papers. Volume 5. Falls Church, VA, American Congress on Surveying and Mapping and American Society for Photogrammetry and Remote Sensing, 1986, p. 260-268. refs
(Contract NAS7-918)

Landsat Thematic Mapper (TM) data collected for Imperial Valley, California in December, 1982 were digitally examined to assess their utility to distinguish among agricultural and other land-covers. Statistics for thirty-seven training sites representing a variety of crops plus urban, water and desert land-covers were obtained and analyzed using transformed divergence (TD) calculations. TD values were employed to assess intraclass variability and the best bands for classification. Four subscenes

were selected for clustering or unsupervised signature extraction. These areas were agriculture, urban, desert and water land-covers. The number of clusters for these subscenes were examined and the best TM bands for interclass separability were identified. The results of the clustering and training site analyses for interclass separability were compared. The TM data were useful for the digital delimitation of most crops and other cover types in this analysis. Four bands of data are adequate for classification with the best results obtained by the selection of one band from each of the available portions of the electromagnetic spectrum. Different band combinations are best for various land-cover intraclass separability. Author

A87-23832

IDENTIFICATION OF FOREST AND AGRICULTURAL EDGES USING LANDSAT THEMATIC MAPPER DATA - PRELIMINARY RESULTS

D. A. GILLESPIE, D. L. CIVCO, and W. C. KENNARD (Connecticut, University, Storrs) IN: American Congress on Surveying and Mapping and American Society for Photogrammetry and Remote Sensing, Annual Convention, Washington, DC, Mar. 16-21, 1986, Technical Papers. Volume 5. Falls Church, VA, American Congress on Surveying and Mapping and American Society for Photogrammetry and Remote Sensing, 1986, p. 279-289. Research supported by the Storrs Agricultural Experiment Station. refs

Portions of a Landsat 4 Thematic Mapper (TM) scene imaged October 19, 1982 were analyzed to identify vegetation 'edges' (boundaries between cover types). Three study sites in northeastern Connecticut were used to determine the effectiveness of using TM data to identify both forest and agricultural cover types and edges between these covers. Channels 3, 4, 5, and 6 (middle IR) were the most effective bands for accurate cover type classification based on an evaluation of maps produced utilizing various channel combinations. Also, a channel consisting of spectral texture data was utilized in several analyses to evaluate its ability to affect edge classification. Maps identifying only homogeneous cover types had consistently higher overall accuracy values compared to maps identifying edge cover types. Author

A87-23833

VEGETABLE CROP INVENTORY WITH LANDSAT TM DATA

V. L. WILLIAMS, W. R. PHILIPSON, and W. D. PHILPOT (Cornell University, Ithaca, NY) IN: American Congress on Surveying and Mapping and American Society for Photogrammetry and Remote Sensing, Annual Convention, Washington, DC, Mar. 16-21, 1986, Technical Papers. Volume 5. Falls Church, VA, American Congress on Surveying and Mapping and American Society for Photogrammetry and Remote Sensing, 1986, p. 290-296. USDA-supported research.

Landsat thematic mapper (TM) data are being evaluated for inventorying or monitoring the planted areas of vegetables in New York State. TM scenes for western New York were acquired in July and August 1984, and were analyzed digitally with spectral characterizations, enhancements, and supervised classifications being compared to field-measured reflectances and cropping records. Preliminary testing has shown single-date classification accuracies of at least 85 percent for three vegetables grown on organic soils (muckland), and over 70 percent for 3 of 4 vegetables grown on mineral soils (upland). Author

A87-24388

A PHOTOGRAPHIC TECHNIQUE FOR STUDYING REFLECTION INDICATRICES OF VEGETATION COVER [FOTOGRAFICHESKII SPOSOB IZUCHENIIA INDIKATRIS OTRAZHENIIA RASTITEL'NOGO POKROVA]

A. E. KUUSK (AN ESSR, Institut Astrofiziki i Fiziki Atmosfery, Tartu, Estonian SSR) Issledovanie Zemli iz Kosmosa (ISSN 0205-9614), July-Aug. 1986, p. 113-118. In Russian. refs

A photographic method for measuring the reflection indicatrices of a canopy is presented, using a camera with a 180-deg field-of-vision for rapid aerial photography. Three-dimensional plots of indicatrices obtained for a birch forest and a barley field are compared with the plot calculated from the Nilson-Kuusik (1984)

model. The advantages and drawbacks of the photographic method of indicatrix determination are compared with those of direct photometric measurements. I.S.

A87-24776* National Aeronautics and Space Administration. Goddard Space Flight Center, Greenbelt, Md.

MAXIMUM NORMALIZED DIFFERENCE VEGETATION INDEX IMAGES FOR SUB-SAHARAN AFRICA FOR 1983-1985

C. J. TUCKER (NASA, Goddard Space Flight Center, Greenbelt, MD) International Journal of Remote Sensing (ISSN 0143-1161), vol. 7, Nov. 1986, p. 1383, 1384.

A87-24777* National Aeronautics and Space Administration. Goddard Space Flight Center, Greenbelt, Md.

SATELLITE REMOTE SENSING OF PRIMARY PRODUCTION

C. J. TUCKER and P. J. SELLERS (NASA, Goddard Space Flight Center, Greenbelt, MD) International Journal of Remote Sensing (ISSN 0143-1161), vol. 7, Nov. 1986, p. 1395-1416. refs

Leaf structure and function are shown to result in distinctive variations in the absorption and reflection of solar radiation from plant canopies. The leaf properties that determine the radiation-interception characteristics of plant canopies are directly linked to photosynthesis, stomatal resistance and evapotranspiration and can be inferred from measurements of reflected solar energy. The effects of off-nadir viewing and atmospheric constituents, coupled with the need to measure changing surface conditions, emphasize the need for multitemporal measurements of reflected radiation if primary production is to be estimated. Author

A87-24779* Reading Univ. (England).

ANALYSIS OF THE DYNAMICS OF AFRICAN VEGETATION USING THE NORMALIZED DIFFERENCE VEGETATION INDEX

J. R. G. TOWNSHEND (Reading University, England) and C. O. JUSTICE (Maryland, University, College Park) International Journal of Remote Sensing (ISSN 0143-1161), vol. 7, Nov. 1986, p. 1435-1445. refs (Contract NAG5-399)

Images at a resolution of 8 km are currently being generated for the whole of Africa, displaying the normalized difference vegetation index (NDVI). These images have undergone a process of temporal compositing to reduce the effects of cloud cover and atmospheric variation. When the NDVI is plotted against time, different cover types are shown to have characteristic profiles corresponding closely with their phenology. The resultant pattern of NDVI values displayed on the images is analyzed in terms of the cover types present and local variations in rainfall. Comparison between images for 1983 and 1984 overall showed considerable similarities, but significant differences were observed in the northward extent of the greening wave in the Sahel, the greening up of the Kalahari Desert and East African communities. It is concluded that vegetation monitoring using NDVI images needs to be associated with scene stratification according to cover type. Author

A87-24780

REFLECTIONS ON DROUGHT - ETHIOPIA 1983-1984

B. L. HENRICKSEN (International Livestock Centre for Africa, Addis Ababa, Ethiopia) International Journal of Remote Sensing (ISSN 0143-1161), vol. 7, Nov. 1986, p. 1447-1451.

AVHRR images collected in August and September 1983 and 1984 displaying drought conditions in Ethiopia are compared. The normalized difference vegetation indices and difference ratios of IR and red reflectances are analyzed. The vegetation growth and topography detected from the images and the climate of Ethiopia are described. The effects of topography and a reduction in rainfall during August 1984 on vegetation growth are discussed. I.F.

A87-24781* Maryland Univ., College Park.

MONITORING EAST AFRICAN VEGETATION USING AVHRR DATA

C. O. JUSTICE (Maryland, University, College Park), B. N. HOLBEN (NASA, Goddard Space Flight Center, Greenbelt, MD), and M. D. GWYNNE (UN, Environment Program, Global Environmental Monitoring System, Nairobi, Kenya) International Journal of Remote Sensing (ISSN 0143-1161), vol. 7, Nov. 1986, p. 1453-1474. refs (Contract NAG5-399)

NOAA Advanced Very High Resolution Radiometer satellite data are applied to regional vegetation monitoring in East Africa. Normalized Difference Vegetation Index (NDVI) data for a one-year period from May 1983 are used to examine the phenology of a range of vegetation types. The integrated NDVI data for the same period are compared with an ecoclimatic zone map of the region and show marked similarities. Particular emphasis is placed on quantifying the phenology of the Acacia Commiphora bushlands. Considerable variation was found in the phenology of the bushlands as determined by the satellite NDVI, and is explained through the high spatial variability in the distribution of rainfall and the resulting green-up of the vegetation. The relationship between rainfall and NDVI is further examined for selected meteorological stations existing within the bushland. A preliminary estimate is made of the length of growing season using an NDVI thresholding technique. Author

A87-24782* Maryland Univ., College Park.

MONITORING THE GRASSLANDS OF THE SAHEL USING NOAA AVHRR DATA NIGER 1983

C. O. JUSTICE (Maryland, University, College Park) and P. H. Y. HIERNAX (Centre International pour l'Elevage en Afrique, Bamako, Mali) International Journal of Remote Sensing (ISSN 0143-1161), vol. 7, Nov. 1986, p. 1475-1497. refs (Contract NAG5-399)

A87-24783

RAINFALL AND VEGETATION MONITORING IN THE SAVANNA ZONE OF THE DEMOCRATIC REPUBLIC OF SUDAN USING THE NOAA ADVANCED VERY HIGH RESOLUTION RADIOMETER

J. U. HIELKEMA (UN, Ford and Agriculture Organization, Rome, Italy), S. D. PRINCE, and W. L. ASTLE (Queen Mary College, London, England) International Journal of Remote Sensing (ISSN 0143-1161), vol. 7, Nov. 1986, p. 1499-1513. refs

A87-24784

MONITORING VEGETATION IN THE MALI SAHEL DURING SUMMER 1984 [SUIVI DU DEVELOPPEMENT VEGETAL AU COURS DE L'ETE 1984 DANS LE SAHEL MALIEN]

P. H. Y. HIERNAX (Centre International pour l'Elevage en Afrique, Bamako, Mali) and C. O. JUSTICE (Maryland, University, College Park) International Journal of Remote Sensing (ISSN 0143-1161), vol. 7, Nov. 1986, p. 1515-1531. In French. refs

A ground data-collection program was initiated to establish a calibration between the normalized difference vegetation index (NDVI) from the NOAA Advanced Very High Resolution Radiometer (AVHRR) and grassland biomass. Thirty sites were selected representing a range of Sahelian vegetation communities in the Gourma region of Mali and monitored during the 1984 growing season. The herbaceous and woody strata were sampled every fourteen days, and above-ground green biomass and rainfall data were collected. NDVI values were extracted for the ground sites and correlation analysis performed. Low correlation coefficients were calculated for the ground measured green biomass and satellite NDVI (0.67). The correlation between the maximum NDVI and the total biomass produced during the season was 0.73. A value of 0.05 was determined as the NDVI associated with the minimum vegetation cover identifiable by the satellite (100 kg/ha). Explanation is given for the possible causes for such low correlations, including the very low biomass production associated with the 1984 drought conditions, atmospheric haze and dust and poor locational accuracy of the satellite data. Author

A87-24785

SATELLITE REMOTE SENSING OF RANGELANDS IN BOTSWANA. I - LANDSAT MSS AND HERBACEOUS VEGETATION

S. D. PRINCE and W. L. ASTLE (Queen Mary College, London, England) *International Journal of Remote Sensing* (ISSN 0143-1161), vol. 7, Nov. 1986, p. 1533-1553. refs

The ability of Landsat MSS data to measure palatable forage of vegetation is examined. The relationships between MSS data and ground measurements of vegetation in three sites in Botswana during the 1983-1984 growing season are studied; the sites and vegetations observed include the *Colophospermum mopane* woodland in Tamasane, the *Combretum apiculatum-Acacia nigrescens* woodland in Shakwe, and the *Terminalia sericea* woodland in Masama. The canopy cover and biomass of live and dead herbaceous vegetation and the canopy cover of trees and shrubs were measured. The data reveal that there is a positive relationship between live herbaceous biomass and band ratio; however, the correlation between herbaceous vegetation cover and band ratio is more variable than for biomass. Multiple regression analysis and multitemporal integration were applied to the band ratios. It is noted that cover, biomass, and production of herbaceous vegetation can be accurately measured using the MSS. Graphs of canopy cover and biomass for ground measurements and MSS are presented. I.F.

A87-24786* London Univ. (England).

SATELLITE REMOTE SENSING OF RANGELANDS IN BOTSWANA. II - NOAA AVHRR AND HERBACEOUS VEGETATION

S. D. PRINCE (Queen Mary College, London, England) and C. J. TUCKER (NASA, Goddard Space Flight Center, Greenbelt, MD) *International Journal of Remote Sensing* (ISSN 0143-1161), vol. 7, Nov. 1986, p. 1555-1570. refs

The relation between the normalized difference vegetation index (NDVI) and the herbaceous vegetation in Tamasane, Shakwe, and Masama in eastern Botswana is studied using 1983-1984 AVHRR data. The procedures for Landsat MSS interpolation of ground measurements and the data processing of the AVHRR data are described. The temporal sequence AVHRR global-area coverage (GAC) composite NDVI is examined. The AVHRR GAC composite NDVI and biomass and Landsat MSS interpolations of field measurements are analyzed and compared. I.F.

A87-24787* National Aeronautics and Space Administration. Goddard Space Flight Center, Greenbelt, Md.

MONITORING THE GRASSLANDS OF THE SAHEL 1984-1985

C. J. TUCKER (NASA, Goddard Space Flight Center, Greenbelt, MD), C. O. JUSTICE (Maryland, University, College Park), and S. D. PRINCE (Queen Mary College, London, England) *International Journal of Remote Sensing* (ISSN 0143-1161), vol. 7, Nov. 1986, p. 1571-1581.

Normalized difference vegetation index data obtained from polar-orbiting meteorological satellites were used to compare the growing or rainy seasons of 1984 and 1985 for the Sahelian zone of Africa. A substantial difference was found between these two years, with 1985 generally having higher normalized difference vegetation index values indicating higher levels of primary production in 1985 than in 1984. 1 km data were compared for Senegal, Mali, Niger and Sudan, and 7 km data were compared for sub-Saharan Africa. The qualitative comparison of these data suggests the use of similar data to assist in centralized monitoring of rangeland conditions, to identify areas of deficiencies in primary production and provide synoptic information in support of regional drought monitoring. Author

A87-24788

GROWING PERIOD AND DROUGHT EARLY WARNING IN AFRICA USING SATELLITE DATA

B. L. HENRICKSEN and J. W. DURKIN (International Livestock Centre for Africa, Addis Ababa, Ethiopia) *International Journal of Remote Sensing* (ISSN 0143-1161), vol. 7, Nov. 1986, p. 1583-1608. refs

A87-24789* Food and Agriculture Organization of the United Nations, Rome (Italy).

ASSESSMENT OF ECOLOGICAL CONDITIONS ASSOCIATED WITH THE 1980/81 DESERT LOCUST PLAGUE UPSURGE IN WEST AFRICA USING ENVIRONMENTAL SATELLITE DATA

J. U. HIELKEMA, J. ROFFEY (UN, Food and Agriculture Organization, Rome, Italy), and C. J. TUCKER (NASA, Goddard Space Flight Center, Greenbelt, MD) *International Journal of Remote Sensing* (ISSN 0143-1161), vol. 7, Nov. 1986, p. 1609-1622. refs

A87-24933*# National Aeronautics and Space Administration. Ames Research Center, Moffett Field, Calif.

AIRCRAFT AND SATELLITE THERMOGRAPHIC SYSTEMS FOR WILDFIRE MAPPING AND ASSESSMENT

J. A. BRASS, J. C. ARVESEN (NASA, Ames Research Center, Moffett Field, CA), V. G. AMBROSIA (Technicolor Government Services, Inc., Moffett Field, CA), P. J. RIGGAN (USDA, Forest Service, Riverside, CA), and J. S. MYERS (ATAC, Inc., Moffett Field, CA) *AIAA, Aerospace Sciences Meeting, 25th, Reno, NV, Jan. 12-15, 1987*. 8 p. refs
(AIAA PAPER 87-0187)

Two complementary sensors, the DAEDALUS DEI-1260 Multispectral Scanner aboard the NASA U-2 aircraft and the Advanced Very High Resolution Radiometer aboard National Oceanographic and Atmospheric Administration orbiting satellites were tested for their applicability in monitoring and predicting parameters such as fire location, temperature and rate of spread, soil heating and cooling rates, and plume characteristics and dimensions. In addition, the satellite system was tested for its ability to extend the relationships found between fire characteristics and biospheric consequences to regional and global scales. An overall system design is presented, and special requirements are documented for the application of this system for fire research and management. Author

A87-25586

THE SPECTRAL REFLECTANCE OF STANDS OF NORWAY SPRUCE AND SCOTCH PINE, MEASURED FROM A HELICOPTER

JOHAN KLEMAN (Stockholm, Universitet, Sweden) *Remote Sensing of Environment* (ISSN 0034-4257), vol. 20, Dec. 1986, p. 253-265. Research supported by the Swedish Board for Space Activities. refs

Radiometer measurements were made from a helicopter over selected stands of Norway spruce (*Picea abies*) and Scotch pine (*Pinus sylvestris*) near Stockholm, Sweden. Continuous reflectance spectra in the wavelength range of 0.4-1.7 microns were measured over forest stands having different species, ages, crown densities, and understories. The irradiance was measured continuously with a cosine receptor on board the helicopter. The average reflectances of pine stands with an age over 40 years were higher in all bands than the reflectances for comparable spruce stands. In rank order, bands centered at 0.67, 1.6, and 0.48 microns offered the best separation possibilities. The reflectance changes through the summer for the two species were small. The reflectance of the pine stands varied less with deviations in look angle away from the nadir than the reflectance of the spruce stands. Author

A87-25589

MOORLAND PLANT COMMUNITY RECOGNITION USING LANDSAT MSS DATA

A. J. MORTON (Imperial College of Science and Technology, Ascot, England) *Remote Sensing of Environment* (ISSN 0034-4257), vol. 20, Dec. 1986, p. 291-298. Research supported by the Imperial College of Science and Technology. refs

Landsat MSS data are examined to determine what extent moorland plant community types can be recognized in the Plynlimon area of Wales. A detailed comparison is made between spectral radiance data and community composition. Attention is drawn to the importance of a phenological understanding of the dominant plant species and in particular the proportion of living and standing

dead plant parts as an important aid to distinguishing between species and communities. Author

A87-25590

ASSESSMENT OF GRASSLAND PHYTOMASS WITH AIRBORNE VIDEO IMAGERY

J. H. EVERITT, D. E. ESCOBAR, P. R. NIXON (USDA, Agricultural Research Service, Weslaco, TX), M. A. HUSSEY, and B. PINKERTON (Texas A & M University, Weslaco) Remote Sensing of Environment (ISSN 0034-4257), vol. 20, Dec. 1986, p. 299-306. refs

Airborne video imagery was evaluated for assessing phytomass production within grass plots fertilized with five rates of nitrogen. Video imagery was taken with two black-and-white video cameras, one visible light and the other visible/near-infrared light sensitive. Red and infrared narrowband filters were used with the visible and visible/near-infrared light sensitive cameras, respectively. Hand-held red and infrared radiometric reflectance and phytomass measurements were made on the day that imagery was obtained. Red and infrared digital video data were obtained from the plots using an image processor. The plots were studied on two dates: April 15 and May 22, 1985. On April 15, three phytomass levels could be distinguished within the infrared video image. Moreover, a infrared/red ratio video composite produced on an image processor enhanced differences among nitrogen treatments to the extent that generally four levels of phytomass could be identified. Coefficients of determination, obtained by regressing red, infrared, and infrared/red reflectance, and red, infrared, and infrared/red digital video data on phytomass measurements were significant statistically. Imagery acquired on May 22, however, showed few differences among treatments. This may have been caused by plant phenological and canopy architectural differences among the grass species. Nevertheless, video imagery should be a useful tool to assess phytomass production on rangelands when grasses are actively growing. Author

A87-26197* Jet Propulsion Lab., California Inst. of Tech., Pasadena.

REMOTE DETECTION OF FOREST DAMAGE

B. N. ROCK, J. E. VOGELMANN, A. F. VOGELMANN, T. HOSHIZAKI (California Institute of Technology, Jet Propulsion Laboratory, Pasadena), and D. L. WILLIAMS (NASA, Goddard Space Flight Center, Greenbelt, MD) Bioscience (ISSN 0006-3568), vol. 36, July-Aug. 1986, p. 439-445. NASA-supported research. refs

The use of remote sensing to discriminate, measure, and map forest damage is evaluated. TM spectral coverage, a helicopter-mounted radiometer, and ground-based surveys were utilized to examine the responses of the spruces and firs of Camels Hump Mountain, Vermont to stresses, such as pollution and trace metals. The basic spectral properties of vegetation are described. Forest damage at the site was estimated as 11.8-76.0 percent for the spruces and 19-43.8 percent for the balsam firs. Shifts in the spectra of the conifers in particular in the near IR region are analyzed, and variations in the mesophyll cell anatomy and pigment content of the spruces and firs are investigated. The relations between canopy moisture and damage is studied. The TM data are compared to aircraft data and found to be well correlated. I.F.

A87-26535

THE DEVELOPMENT OF PROCEDURES FOR FOREST INTERPRETATION FROM TEXTURE-SELECTIVE IMAGES [RAZRABOTKA METODIKI DESHIFRIROVANIYA LESOV NA STUKTUROZONAL'NYKH SNIMKAKH]

V. I. KRAVTSOVA (Moskovskii Gosudarstvennyi Universitet, Moscow, USSR) Issledovanie Zemli iz Kosmosa (ISSN 0205-9614), Sept.-Oct. 1986, p. 55-66. In Russian.

Texture processing of multispectral aerial photographs obtained over the Central Yakutsk Plain, which is overgrown with exceedingly heterogeneous forests, was used, along with geophysical and geological data, for identification of the forest types. Recognition of texture-selective images made it possible to identify the

signatures of larch and pine forests of different quality classes as spectral frequency curves. A scheme for successive interpretation of a set of such images is presented. I.S.

A87-26536

DETERMINATION OF THE PROPERTIES OF A PLOWED SOIL LAYER FROM MULTISPECTRAL SPACE IMAGERY [OPREDELENIE SVOISTV PAKHOTNOGO GORIZONTA POCHV PO MNOGOZONAL'NYM KOSMICHEKIM SNIMKAM]

L. N. VASILEV and V. M. MAZIKOV (AN SSSR, Institut Geologii, Moscow, USSR) Issledovanie Zemli iz Kosmosa (ISSN 0205-9614), Sept.-Oct. 1986, p. 67-77. In Russian.

A procedure is presented for estimating the quality of a plowed soil layer from multispectral space imagery, using multivariate analysis of the spectral radiance and soil components. The method relates the contents of organic matter and mineral composition of plowed layers with their spectral luminosity and identifies the most informative indicators. The application of this procedure for the interpretation of space images (obtained with the Fragment multispectral scanner aboard the Meteor satellite) of a territory 90 km wide and with an area of 27,000 sq km made it possible to evaluate the plowed horizon in terms of its two most significant components, humus and carbonate, as well as soluble salts, iron, and silica. I.S.

A87-26539

AUTOMATION OF THEMATIC PROCESSING OF SPACE IMAGES IN EVALUATING CROP CONDITION [AVTOMATIZATSIYA TEMATICHESKOI OBRABOTKI KOSMICHEKIKH IZOBRAZHENII PRI OTSENKE SOSTOIANIYA SEL'SKOKHOZIAISTVENNYKH KULTUR]

G. G. ANDREEV, V. P. BOCHAROV, N. V. SAZONOV, and L. N. CHABAN (Vsesoiuznyi Nauchno-Issledovatel'skii Tsentr AIUS-Agroresursy, Moscow, USSR) Issledovanie Zemli iz Kosmosa (ISSN 0205-9614), Sept.-Oct. 1986, p. 95-102. In Russian. refs

A flexible interactive scheme is presented for computer-aided thematic processing of space imagery of large crop areas, which can be applied to different classes of problems related to crop status. The thematic processing software is built around nonparametric stochastic segmentation and controlled classification packages. To illustrate the potential of this scheme, space imagery, obtained with the Fragment MSS over fields of winter wheat in the Stavropol Region, is analyzed with respect to wheat condition, classifying wheat crops into good, medium, and poor. I.S.

A87-26974

PROPOSAL OF A REMOTE SENSING METHOD FOR MEASURING SOIL MOISTURE OF BARE SOILS IN THE FREQUENCY RANGE 100 MHZ-1 GHZ

K. SASSI and A. TABBAGH (CNRS, Centre de Recherches Geophysiques, Pouilly-sur-Loire, France) Annales Geophysicae, Series B - Terrestrial and Planetary Physics (ISSN 0755-0685), vol. 4, Dec. 1986, p. 625-637. refs

A87-28316

MICROWAVE BACKSCATTERING FROM A LAYER OF RANDOMLY ORIENTED DISCS WITH APPLICATION TO SCATTERING FROM VEGETATION

S. S. SEKER (University of the Bosphorus, Bebek, Turkey) IEE Proceedings, Part H - Microwaves, Antennas and Propagation (ISSN 0950-107X), vol. 133, pt. H, no. 6, Dec. 1986, p. 497-502. refs

A87-28387

FRUIT TREE INVENTORY WITH LANDSAT THEMATIC MAPPER DATA

DANIEL K. GORDON, WARREN R. PHILIPSON, and WILLIAM D. PHILPOT (Cornell University, Ithaca, NY) Photogrammetric Engineering and Remote Sensing (ISSN 0099-1112), vol. 52, Dec. 1986, p. 1871-1876. USDA-supported research. refs

The use of Landsat TM data to inventory New York State fruit trees is evaluated. Image processing of TM scenes of Orleans

County obtained on August 28 and September 13, 1982 and June 22, 1984 was performed on a digital analysis system. The TM data were employed to classify orchards by fruit tree type and to isolate orchards as a class. The data reveal that the classification of the orchard by fruit tree type using unenhanced single date TM data is not possible due to the reflectance of young and mature orchards. It is observed that it is possible to distinguish orchards from nonforest vegetation using multivariate classification with bands 3, 4, and 5 for August 1982 and June 1984, and to differentiate orchards from forest using a texture-extraction procedure. I.F.

A87-28388* National Aeronautics and Space Administration, Goddard Space Flight Center, Greenbelt, Md.
UTILITY OF AVHRR CHANNELS 3 AND 4 IN LAND-COVER MAPPING

A. G. KERBER and J. B. SCHUTT (NASA, Goddard Space Flight Center, Greenbelt, MD) Photogrammetric Engineering and Remote Sensing (ISSN 0099-1112), vol. 52, Dec. 1986, p. 1877-1883. refs

Imagery collected on July 11, 1981 from the Advanced Very High Resolution Radiometer aboard the NOAA-7 spacecraft was used in a four-channel (channels 1 to 4) classification study for forest, agriculture/grass, and urban categories. The class signatures composing these categories were compared using the transformed divergence algorithm. Separability in all instances was found to be dominated by emitted radiation more so by channel 3 (3.55 to 3.93 microns) than by channel 4 (10.5 to 11.3 microns). Laboratory spectra obtained for the 3.55 to 3.93-micron region showed that for leaves the transmission was virtually zero, and the reflectances on the leaves and soil investigated were about three percent. Thus, emitted radiation dominated reflected radiation as the mechanism responsible for class separability in this spectral region. The enhancement in the separability contributed by channel 3 over that of channel 4 resulted primarily from the temperature dependence of the Planck function, and to a lesser extent by the increased transmission within channel 3 relative to channel 4.

Author

A87-28414* Texas Univ., Austin.
TREE ATTENUATION AT 869 MHZ DERIVED FROM REMOTELY PILOTTED AIRCRAFT MEASUREMENTS

WOLFHARD J. VOGEL (Texas, University, Austin) and JULIUS GOLDBIRSH (Johns Hopkins University, Laurel, MD) IEEE Transactions on Antennas and Propagation (ISSN 0018-926X), vol. AP-34, Dec. 1986, p. 1460-1464. refs
 (Contract N00024-85-C-5301; JPL-956520)

Attenuation due to single trees is experimentally investigated using UHF transmissions at 869 MHz between a remotely piloted aircraft and a ground receiver system located in a stationary vehicle. Single trees of each tree type in full foliage were found to attenuate from 10-20 dB, with an average median value of about 12 dB. Attenuation coefficients associated with path lengths through the foliage may on average be about 1 dB/m, with maximum values closer to 2 dB/m.

R.R.

A87-29003
IMPACT OF ENVIRONMENTAL VARIABLES ON SPECTRAL SIGNATURES ACQUIRED BY THE LANDSAT THEMATIC MAPPER

MARK A. KARASKA (Indiana State University, Terre Haute), STEPHEN J. WALSH (North Carolina, University, Chapel Hill), and DAVID R. BUTLER (Georgia, University, Athens) International Journal of Remote Sensing (ISSN 0143-1161), vol. 7, Dec. 1986, p. 1653-1667. refs

Eleven environmental variables, elevation, slope angle, slope aspect, surface roughness, soil type, geology, percentage of vegetation, percentage of trees, percentage of shrubs, percentage of herbs, and percentage of bare ground, are evaluated as to their impact on Landsat Thematic Mapper (TM) spectral signatures. Multiple regression models indicate that a combination of percentage of trees and shrubs have the most significant impact on TM spectral response, and, in fact, mask the effects of other tested environmental variables. Regression models are also

developed for major soil types which significantly predict the amount of trees and shrubs present on a site. Author

A87-29004
ESTIMATING PRE-HARVEST PRODUCTION OF MAIZE IN KENYA USING LARGE-SCALE AERIAL PHOTOGRAPHY AND RADIOMETRY

D. G. PEDEN, W. K. OTTICHILO, and H. MWENDWA (Kenya Rangeland Ecological Monitoring Unit, Nairobi) International Journal of Remote Sensing (ISSN 0143-1161), vol. 7, Dec. 1986, p. 1669-1677. refs

A87-29005
ESTIMATING AND MAPPING GRASS COVER AND BIOMASS FROM LOW-LEVEL PHOTOGRAPHIC SAMPLING

K. J. DANCY, R. WEBSTER (Rothamsted Experimental Station, Harpenden, England), and N. O. J. ABEL (East Anglia, University, Norwich, England) International Journal of Remote Sensing (ISSN 0143-1161), vol. 7, Dec. 1986, p. 1679-1704. Research supported by the International Livestock Center for Africa. refs

Using data obtained of 700 sq km in Botswana in four seasonal surveys, it is found that low-level aerial photography can provide accurate estimates of grass cover and biomass at any season, and that kriging can project these estimates with adequate precision over a region of several hundred square kilometers. Sample semivariograms were modeled as anisotropic power functions to lags of 10 km by least square approximation, and grass cover and biomass were mapped from the sample data by interpolating a figure field of cover on a fine mesh by kriging, and then contouring the figure field. A strong regional pattern is noted which remains fairly constant at different seasons and from which four distinct subregions are delineated, with biomass ranging from 185-1700 kg/ha.

R.R.

A87-29006
COMPARISON OF SOME CLASSIFICATION METHODS ON A TEST SITE (KISKORE, HUNGARY) - SEPARABILITY AS A MEASURE OF ACCURACY

FERENC CSILLAG (Foldmeresi Intezet, Budapest, Hungary) International Journal of Remote Sensing (ISSN 0143-1161), vol. 7, Dec. 1986, p. 1705-1714. refs

The purpose of this study was to compare some classification methods on a typical Hungarian lowland agricultural area. For a multicrop test area of approximately 20,000 ha several one-date and multivariate Landsat MSS data sets were classified using supervised methods. The best results were obtained by clustering two-band Kauth-Thomas transforms for each date, using Swain-Fu intercluster distance. In general, clustering Kauth-Thomas bands always showed slightly better accuracy than the ones for the MSS 5 and MSS 7 data sets. The accuracies achieved by polygon-vector classification were lower (3-6 percent) than those of multivariate clustering. An effort was made to explain the results in terms of spectral separability of agricultural cover classes. The ratio of the average separability of an individual class and the total data set is proposed to measure classification accuracy on areas similar to the Kiskore test site.

Author

A87-29008
CALIBRATION OF LANDSAT DATA FOR SPARSELY VEGETATED SEMI-ARID RANGELANDS

R. P. PECH, R. D. GRAETZ (CSIRO, Div. of Wildlife and Rangelands Research, Lyneham, Australia), A. W. DAVIS, and R. R. LAMACRAFT (CSIRO, Div. of Mathematics and Statistics, Glen Osmond, Australia) International Journal of Remote Sensing (ISSN 0143-1161), vol. 7, Dec. 1986, p. 1729-1750. refs

A Landsat-based rangelands monitoring system has been designed for semi-arid chenopod shrublands in southern Australia. Simultaneous ground and Landsat measurements were used to test multivariate calibration methods for estimating vegetation cover. Of three methods compared, the Lwin-Maritz and inverse estimators outperformed the classical approach. Data were analyzed by rangeland type and as a combined set. Calibration

curves, with errors of estimation, are presented for five major rangeland types. Author

A87-29012
CLASSIFICATION OF REFLECTANCE ON COLOUR INFRARED AERIAL PHOTOGRAPHS AND SUB-TROPICAL SALT-MARSH VEGETATION TYPES

P. E. R. DALE, K. HULSMAN, and A. L. CHANDICA (Griffith University, Nathan, Australia) International Journal of Remote Sensing (ISSN 0143-1161), vol. 7, Dec. 1986, p. 1783-1788. Research supported by the Gold Coast City Council and University Research Grants Committee of Australia. refs

A87-29017
PRELIMINARY ANALYSIS OF SPOT HRV MULTISPECTRAL PRODUCTS OF AN ARID ENVIRONMENT

N. A. QUARMBY and J. R. G. TOWNSHEND (NERC, Dept. of Geography, Reading, England) International Journal of Remote Sensing (ISSN 0143-1161), vol. 7, Dec. 1986, p. 1869-1877. refs

(Contract NERC-F60/G6/12; NERC-F60/G6/03)

A preliminary analysis of a SPOT HRV multispectral scene centered on the Chott el Djerid in southern Tunisia is presented. All three HRV bands are very strongly correlated for this scene, and statistically it has an overall one-dimensional structure, although the near-infrared band provides unique information on the variability within vegetated areas. Each of the three bands has discriminatory potential. Inter-detector variability is clearly visible in HRV band 2, and there are also systematic changes in level. The improved spatial resolution of the HRV sensor is notable, compared with the Thematic Mapper. Author

A87-29018
PRELIMINARY MEASUREMENTS OF LEAF SPECTRAL REFLECTANCE IN THE 8-14/MICRON

JOHN W. SALISBURY (USGS, Reston, VA) International Journal of Remote Sensing (ISSN 0143-1161), vol. 7, Dec. 1986, p. 1879-1886. refs

Previous broad band measurements of the spectral reflectance of leaves indicate variations in spectral emissivity that, although small, might be detected with current airborne thermal infrared imaging systems. Preliminary high spectral resolution measurements of the spectral reflectance of leaves of four different species reported here show a different spectral response for each species. These data suggest that species discrimination using remote sensing data in the thermal infrared may be feasible, and raise the possibility that other factors that might affect leaf surface composition and spectral response, such as metal stress, might also be detected. Author

A87-30129
EXTRACTION OF AREAS INFESTED BY PINE BARK BEETLE USING LANDSAT MSS DATA

YUKIO MUKAI, TOSHIRO SUGIMURA (Remote Sensing Technology Center of Japan, Tokyo), HIROSHI WATANABE, and KUNIYASU WAKAMORI (Japan Forest Technical Association, Tokyo) Photogrammetric Engineering and Remote Sensing (ISSN 0099-1112), vol. 53, Jan. 1987, p. 77-81. Research sponsored by the Forestry Agency of Japan. refs

Areas infested by pine bark beetle (pine nematode) in Japan have been expanding in recent years. Two sites in heavily infested areas of Ibaragi and Chiba Prefectures were selected as study areas. Images of the study areas were generated from two temporal Landsat MSS scenes. Pine areas were extracted by multispectral classification using the four bands composed of bands 5 and 6 for each of the scenes. The areas infested by the pine bark beetle were extracted by detecting the areas where the value of band 5 increased and the value of band 6 decreased within the pine areas. The infested areas could be classified into light, moderate, and heavy damage in proportion to the increase of band 5 and the decrease of band 6. Ground surveys were collected by local government forestry officials to estimate damage volume. There was a high correlation ($r = 0.824$) between the timber volume of

the damaged pines estimated from Landsat data and that surveyed on the ground. Author

A87-30130
MICROCOMPUTER-ASSISTED VIDEO IMAGE ANALYSIS OF LODGING IN WINTER WHEAT

D. M. GERTEN and M. V. WIESE (Idaho, University, Moscow) Photogrammetric Engineering and Remote Sensing (ISSN 0099-1112), vol. 53, Jan. 1987, p. 83-88. Research supported by Merck and Co., and University of Idaho. refs

Microcomputer-assisted video image analysis (VIA) was used to measure lodging in winter wheat, a symptom of foot rot disease. The percent area of lodged versus erect winter wheat in seven fields was measured from 35-mm true color and color-infrared aerial photos and from manually prepared photointerpretations made onto frosted Mylar sheet. Lodged wheat areas measured from these standard images ranged from 0.5 to 7.6 ha per field. Measurements made directly from photos consistently underestimated lodging by 0.2 to 2.4 ha per field relative to measurements from the standard images. Manual measurement of foot rot symptoms and grain yield in the seven fields showed 9 percent more severe lesions, and grain yield reductions of 1389 to 3416 kg/ha, in lodged wheat relative to erect wheat. Yield measurements combined with VIA lodging measurements made from the standard images showed the lodging-foot rot complex reduced yields by 138 to 796 kg/ha per field. Author

A87-30894
GROUND RADIOMETRY AND AIRBORNE MULTISPECTRAL SURVEY OF BARE SOILS

E. J. MILTON and J. P. WEBB (Southampton, University, England) International Journal of Remote Sensing (ISSN 0143-1161), vol. 8, Jan. 1987, p. 3-14. refs
 (Contract NERC-GR/3/4994)

Soil survey data collected in southern and eastern England are examined in order to describe the intercalibration between measurements made at ground level and by the Airborne Thematic Mapper (ATM). The effects of solar-sensor geometry and cultivation practices on intercalibration are investigated. The relation between ATM reflectance and ground reflectance are analyzed. It is observed that the reflectances correlate well at the first three bands; however, for the middle IR band the ATM values are higher than the ground level data. The soil surface data reveal that only the samples close to nadir show good correlation with the reflectance data. I.F.

A87-30896
REMOTE SENSING OF STRUCTURALLY COMPLEX SEMI-NATURAL VEGETATION - AN EXAMPLE FROM HEATHLAND

N. W. WARDLEY, E. J. MILTON, and C. T. HILL (Southampton, University, England) International Journal of Remote Sensing (ISSN 0143-1161), vol. 8, Jan. 1987, p. 31-42. refs

A87-30897
SPECTRAL SEPARATION OF MOORLAND VEGETATION IN AIRBORNE THEMATIC MAPPER DATA

R. E. WEAVER (Durham, University, England) International Journal of Remote Sensing (ISSN 0143-1161), vol. 8, Jan. 1987, p. 43-55. refs

Simulated Thematic Mapper (TM) data are examined for an area of the North Yorks Moors, northern England. The aim of analysis is to determine the number and identity of wavebands needed distinguish specific moorland vegetation types from the surrounding community. The interband correlation and dimensionality of the data are found to be different for each of the vegetation types studied. Calculation of the transformed divergence measure shows that the major communities of bracken, heather and sedges are clearly separated with the use of one or two wavebands; four or five bands are needed to distinguish the stages of heather growth. In all cases, the combination of wavebands which maximizes discrimination is specific to the vegetation types

to be separated. The work has practical implications for the use of TM data in the monitoring of the moorland landscape. Author

A87-30898**AIRBORNE MSS DATA TO ESTIMATE GLAI**

P. J. CURRAN and H. D. WILLIAMSON (Sheffield, University, England) *International Journal of Remote Sensing* (ISSN 0143-1161), vol. 8, Jan. 1987, p. 57-74. refs
(Contract NERC-GR/3/5096)

The use of airborne multispectral scanner data collected in June 1984 to estimate the green leaf area index (GLAI) for 60 sq km of grassland in England is examined. The processing of the data involves: (1) radiometric and atmospheric correction, (2) production of a vegetation index image, (3) calculation of a calibration relationship between a vegetation index and GLAI, (4) production of an image of estimated GLAI, and (5) accuracy assessment. The application of six refinements to this methodology is discussed. The effects of these refinements on the ability of the MSS data to accurately estimate the GLAI are investigated. It is observed that the refined methodology increased the GLAI estimation accuracy to + or - 0.09 GLAI for an area, and 60-82 percent at the 95 percent confidence level for a five-class classification. The repeatability of this refined methodology when using a different data set is evaluated. I.F.

N87-15507# Institut fuer Angewandte Geodaesie, Frankfurt am Main (West Germany).

MAPPING OF AGRICULTURAL LANDS IN THE USSR

ANATOLY I. PANFILOVICH *In its Contributions to Geodesy, Photogrammetry, and Cartography, Series 2, No. 44* p 101-104 1986

Avail: NTIS HC A10/MF A01

Development of cadastral data acquisition through the inclusion of remote sensing procedures, and development of cartographic methods of representation and analysis are described. Mathematical methods for the investigation of national land resources and their evaluation in the context of the decision-making process are considered. Creation of a land resources data base with corresponding retrieval system for the entire national territory is discussed. Improvement of the integration of data acquisition, processing, and output as well as of the organization of land exploration at the national level is treated. ESA

N87-15514*# Massachusetts Inst. of Tech., Cambridge. Dept. of Civil Engineering.

ESTIMATION OF VEGETATION COVER AT SUBPIXEL RESOLUTION USING LANDSAT DATA Interim Technical Report, 1 Jun. - 30 Nov. 1986

MICHAEL F. JASINSKI and PETER S. EAGLESON Nov. 1986 64 p

(Contract NAG5-510)

(NASA-CR-177077; NAS 1.26:177077) Avail: NTIS HC A04/MF A01 CSCL 02C

The present report summarizes the various approaches relevant to estimating canopy cover at subpixel resolution. The approaches are based on physical models of radiative transfer in non-homogeneous canopies and on empirical methods. The effects of vegetation shadows and topography are examined. Simple versions of the model are tested, using the Taos, New Mexico Study Area database. Emphasis has been placed on using relatively simple models requiring only one or two bands. Although most methods require some degree of ground truth, a two-band method is investigated whereby the percent cover can be estimated without ground truth by examining the limits of the data space. Future work is proposed which will incorporate additional surface parameters into the canopy cover algorithm, such as topography, leaf area, or shadows. The method involves deriving a probability density function for the percent canopy cover based on the joint probability density function of the observed radiances. M.G.

N87-15517*# South Dakota State Univ., Brookings.

MODELING ENERGY FLOW AND NUTRIENT CYCLING IN NATURAL SEMIARID GRASSLAND ECOSYSTEMS WITH THE AID OF THEMATIC MAPPER DATA Semiannual Progress Report

JAMES K. LEWIS 1987 16 p Original contains color illustrations

(Contract NAS5-28766)

(NASA-CR-179903; NAS 1.26:179903; SAPR-2) Avail: NTIS HC A02/MF A01 CSCL 13B

Energy flow and nutrient cycling were modeled as affected by herbivory on selected intensive sites along gradients of precipitation and soils, validating the model output by monitoring selected parameters with data derived from the Thematic Mapper (TM). Herbivore production was modeled along the gradient of soils and herbivory, and validated with data derived from TM in a spatial data base. B.G.

N87-15518*# California Univ., Santa Barbara. Dept. of Geography.

CANOPY REFLECTANCE MODELING IN A TROPICAL WOODED GRASSLAND Final Report

DAVID SIMONETT and JANET FRANKLIN 1986 64 p

(Contract NAGW-788)

(NASA-CR-180097; NAS 1.26:180097) Avail: NTIS HC A04/MF A01 CSCL 02F

Geometric/optical canopy reflectance modeling and spatial/spectral pattern recognition is used to study the form and structure of savanna in West Africa. An invertible plant canopy reflectance model is tested for its ability to estimate the amount of woody vegetation from remotely sensed data in areas of sparsely wooded grassland. Dry woodlands and wooded grasslands, commonly referred to as savannas, are important ecologically and economically in Africa, and cover approximately forty percent of the continent by some estimates. The Sahel and Sudan savannas make up the important and sensitive transition zone between the tropical forests and the arid Sahara region. The depletion of woody cover, used for fodder and fuel in these regions, has become a very severe problem for the people living there. LANDSAT Thematic Mapper (TM) data is used to stratify woodland and wooded grassland into areas of relatively homogeneous canopy cover, and then an invertible forest canopy reflectance model is applied to estimate directly the height and spacing of the trees in the stands. Because height and spacing are proportional to biomass in some cases, a successful application of the segmentation/modeling techniques will allow direct estimation of tree biomass, as well as cover density, over significant areas of these valuable and sensitive ecosystems. The model being tested in sites in two different bioclimatic zones in Mali, West Africa, will be used for testing the canopy model. Sudanian zone crop/woodland test sites were located in the Region of Segou, Mali. Author

N87-15519# Instituto de Pesquisas Espaciais, Sao Jose dos Campos (Brazil). Dept. de Sensoriamento Remoto.

THE USE OF AERIAL REMOTE SENSING IN A CASE STUDY OF DESERTIFICATION: QUIXABA-PE [O USO DE SENSORIAMENTO REMOTO AEREO PARA UM ESTUDO DE CASO DE DESERTIFICACAO: QUIXABA-PE]

VITOR CELSO DECARVALHO Jul. 1986 19 p In

PORTUGUESE Presented at the 1st National Meeting of the Middle Atmosphere Study, Garanhuns, Brazil, 6-11 Oct. 1986

(INPE-3963-PRE/980) Avail: NTIS HC A02/MF A01

The Brazilian semiarid northeast, pointed out as one of the problem regions of the land, is presented, as a consequence of its fragile environment and high risk of desertification. A case of vegetative development in one of the problem sectors, a region of Quixaba', between the cities of Ouricuri and Parnamirim-PE, is found and analyzed qualitatively by interpretation of multi-seasonal area photographs (during 1955, 1965, and 1983). The results show an increase and notable agrarian shift in the region, but no change in the process of rapid degradation of its land. The situation at present is alarming, with almost 15% of its land now unproductive through human or natural action. Author

N87-15554# Centre de Recherches en Physique de l'Environnement, Issy-les-Moulineaux (France).

MODELISATION OF EVAPOTRANSPIRATION AND SOIL AVAILABLE WATER OVER AN AGRICULTURAL REGION APPLICABLE FOR REMOTE SENSING

O. TACONET *In* ESA Proceedings of an International Satellite Land-Surface Climatology Project (ISLSCP) Conference p 65-71 May 1986

Avail: NTIS HC A99/MF A01

It is shown that in evaluating evapotranspiration over an agricultural region, serious errors can arise by neglecting the influence of vegetation. Using Dardorff's formalism (1978), the single midday temperature is sufficient over dense canopies for obtaining the bulk canopy resistance to evaporation, from which the surface fluxes are derived. The two methodologies (with and without vegetation) are tested by examining the evolution of simulated fluxes (using NOAA-7 images) and the measured surface fluxes during a 10 day period of soil drying. Surface heat flux is effectively captured by the inversion method using measured radiative temperatures and a vegetation parameterization. The inversion methodology with bare soil formalism reveals inferior performance, especially for great sensible heat flux, when applied to a wheat canopy. However, while the agreement between measured and modeled sensible heat fluxes support the vegetation formalism, more field measurements are needed in order to determine if this modeling is valid for different situations and crops. ESA

N87-15572# Osnabrueck Univ. (West Germany). General Ecology Group.

EVALUATION OF CLIMATE RELEVANT LAND SURFACE CHARACTERISTICS FROM REMOTE SENSING

G. ESSER and H. LIETH *In* ESA Proceedings of an International Satellite Land-Surface Climatology Project (ISLSCP) Conference p 205-211 May 1986

Avail: NTIS HC A99/MF A01

Land surface characteristics visual evaluation methods in remote sensing are investigated. Discrimination of vegetation formations and anthropogenically influenced communities is discussed. Land use changes in South America were evaluated, showing a mean annual increase of cleared areas of 9500 sq km. ESA

N87-15583# Freie Univ., Berlin (West Germany). Inst. of Meteorology.

SATELLITE-DERIVED VEGETATION INDEX OVER EUROPE

KLAUS BLUEMEL and W. TONN *In* ESA Proceedings of an International Satellite Land-Surface Climatology Project (ISLSCP) Conference p 281-285 May 1986 Original contains color illustrations

Avail: NTIS HC A99/MF A01

Data from NOAA-AVHRR were used for deriving vegetation indices. Indices depend on atmospheric influences, viewing geometry, surface topography, and vegetation density. Results for the most significant indices are presented. Bi-dimensional histograms of spectral channel are performed in different regions of Central Europe and North Africa for vegetation type analysis. ESA

N87-15584# Durham Univ. (England). Dept. of Geography. **VEGETATION INDEX MODELS FOR THE ASSESSMENT OF VEGETATION IN MARGINAL AREAS**

R. HARRIS *In* ESA Proceedings of an International Satellite Land-Surface Climatology Project (ISLSCP) Conference p 287-291 May 1986 Sponsored by Durham Univ.'s Middle East Center, England

Avail: NTIS HC A99/MF A01

Ground radiometer data and LANDSAT thematic mapper data for four terrain types in the Sidi Ali ben Aoun region of central Tunisia are analyzed. The effects of the band ratio and the normalized difference vegetation index on the near infrared/red feature space are shown. The results show the sensitivity of the vegetation indices to the data distribution. ESA

N87-15585# New Zealand Meteorological Service, Wellington. **CALIBRATION OF NORMALIZED VEGETATION INDEX AGAINST PASTURE GROWTH**

B. F. TAYLOR, P. W. DINI, and J. W. KIDSON *In* ESA Proceedings of an International Satellite Land-Surface Climatology Project (ISLSCP) Conference p 293-297 May 1986 Original contains color illustrations

Avail: NTIS HC A99/MF A01

The normalized vegetation index (NVI) was calculated from direct-readout NOAA-7 data for a pastoral farming area of New Zealand. The correlation between monthly-mean NVI and monthly pasture growth, averaged over 7 measurement sites, is 0.8. Variations in NVI on time scales < 1 month agree qualitatively with estimates of regional daily rainfall and soil moisture. Results suggest that routine monitoring of pasture growth by meteorological satellites may be valuable to the agricultural industry. ESA

N87-15589# Consiglio Nazionale delle Ricerche, Florence (Italy).

CONTRIBUTION OF PASSIVE MICROWAVE REMOTE SENSING IN SOIL MOISTURE AND EVAPOTRANSPIRATION MEASUREMENTS

P. PAMPALONI, S. PALOSCIA, and L. CHIARANTINI (Segnalamento Marittimo ed Aereo S.p.A., Florence, Italy) *In* ESA Proceedings of an International Satellite Land-Surface Climatology Project (ISLSCP) Conference p 327-332 May 1986

Avail: NTIS HC A99/MF A01

Microwave and infrared measurements (at 3 and 0.8 cm wavelengths) on bare and vegetated soils are reported. Results suggest that the 0.8 cm polarization index is related to leaf water potential. The absorption properties of corn and alfalfa, computed by means of the measured brightness temperature and a model based on the radiative transfer theory, are correlated to plant water content. ESA

N87-15593*# Jet Propulsion Lab., California Inst. of Tech., Pasadena.

OBSERVATIONS OF THE SEASONAL VARIABILITY OF SOIL MOISTURE AND VEGETATION COVER OVER AFRICA USING SATELLITE MICROWAVE RADIOMETRY

ENI G. NJOKU and INDU R. PATEL *In* ESA Proceedings of an International Satellite Land-Surface Climatology Project (ISLSCP) Conference p 349-353 May 1986

Avail: NTIS HC A99/MF A01 CSCL 04B

Multispectral passive microwave data from the scanning multichannel microwave radiometer (SMMR) on the Nimbus-7 satellite were processed selectively for a 1 yr period over Africa. The data show a wide dynamic range of brightness temperature (180 to 290 K), corresponding to variations in surface features such as moisture, temperature, vegetation, roughness, and large-scale topography. It appears that soil moisture variability is detectable with the SMMR over large regions of Africa. To what extent roughness and vegetation affect this capability is not clear. The lowest SMMR frequency is C-band (6.6 GHz), thus any soil moisture sensitivity at this frequency would be much improved by a sensor at L-band (1 to 2 GHz) less affected by roughness and vegetation. ESA

N87-15604# Lund Univ. (Sweden). Remote Sensing Lab. **DESERTIFICATION MONITORING: REMOTELY SENSED DATA FOR DROUGHT IMPACT STUDIES IN THE SUDAN**

ULF HELLDEN *In* ESA Proceedings of an International Satellite Land-Surface Climatology Project (ISLSCP) Conference p 417-428 May 1986

Avail: NTIS HC A99/MF A01

The relationship between a vegetation index based on LANDSAT and NOAA AVHRR GAC data and precipitation data in the Sudan was studied. Results indicate that the magnitude of the desertification problem in Kordofan is strongly exaggerated in many reports and described in an incorrect and misleading way. The impact of man on the environment, as to productivity of natural vegetation and crops, seems to be of a minor importance in the semi-arid Sudan compared to the climatic impact. Different

perceptions of the course of desertification create a need for an objective instrument for land degradation monitoring. The results imply a high potential to develop an operational satellite based system for productivity and drought impact monitoring and possibly for crop yield and drought impact prediction. ESA

N87-15605# Calabar Univ. (Nigeria). Dept. of Geography and Regional Planning.

REGIONAL STUDIES WITH SATELLITE DATA IN AFRICA ON THE DESERTIFICATION OF THE SUDAN-SAHEL BELT IN NIGERIA

D. O. ADEFOLALU *In* ESA Proceedings of an International Satellite Land-Surface Climatology Project (ISLSCP) Conference p 429-438 May 1986

Avail: NTIS HC A99/MF A01

Airborne side-looking radar and LANDSAT data were used to map vegetation in the Sudan-Sahelian region (SSR). Results show that because of its balance of payments deficit, the SSR continues to put too much pressure on the land, encouraging desertification. Nigeria was classified as a member of the SSR after appraisal of the events sequel to the 1969 to 73 drought showed evidence of desertification in the West African sub-region. Desertification is now threatening areas north of latitude 10 N in the country. (

ESA

N87-15607# Kenya Meteorological Dept., Nairobi.
USE OF REMOTE SENSING APPLICATION FOR AGRICULTURAL EXPANSION INTO SEMI-ARID AREAS OF KENYA

SILVERY B. B. OTENGI *In* ESA Proceedings of an International Satellite Land-Surface Climatology Project (ISLSCP) Conference p 443-448 May 1986

Avail: NTIS HC A99/MF A01

Principles underlying agricultural planning for semiarid areas are reviewed. During the Kenyan long rains period, that is March, April and May rains, satellite pictures were used to monitor trends of moisture from highland areas where rainfall is abundant to semiarid areas of the country. Results support agricultural expansion into the semiarid areas of the country. ESA

N87-15610# Innsbruck Univ. (Austria). Inst. of Meteorology and Geophysics.

VEGETATION IDENTIFICATION AND VARIABILITY IN THE TAHOUA AREA, NIGERIA

H.-J. BOLLE *In* ESA Proceedings of an International Satellite Land-Surface Climatology Project (ISLSCP) Conference p 461-466 May 1986 Original contains color illustrations

Avail: NTIS HC A99/MF A01

Seven LANDSAT images were analyzed for vegetation cover and strength. The data were homogenized using unchanging test areas for calibration before a normalized vegetation index (NVI) algorithm was applied. Vegetation changes are quantified in terms of the area covered by vegetation of specific NVI and 600/700 mm reflectance. The MSS-5 signal was used in addition to the NVI to discriminate sparse vegetation from soil with increasing reflectance in the near infrared. The vegetation pattern provides information about soil moisture distributions. In dry years or seasons, vegetation concentrates in areas which carry open water during rainy seasons. The high resolution information clearly supplements global vegetation index maps. ESA

N87-15612# Ghent Univ. (Belgium). Lab. for Regional Geography.

ASSESSMENT OF WIND AND FLUVIAL ACTION BY USING LANDSAT-MSS COLOR COMPOSITES IN THE LOWER NILE VALLEY (EGYPT)

A. GAD and L. DAELS *In* ESA Proceedings of an International Satellite Land-Surface Climatology Project (ISLSCP) Conference p 473-476 May 1986

Avail: NTIS HC A99/MF A01

Black and white LANDSAT images were used to study wind and water erosion in the Nile Valley (Egypt). Wind action, especially upon the Western Desert, causes the erosion of the limestone

plateau and is responsible for the accumulation of eolian deposits along the western boundaries of the Nile Valley. Fluvial action, by occasional thunderstorms, causes the erosion of the Eastern Desert plateau and hills and causes the accumulation of debris in the eastern side of the Nile valley. The Diazo-chrome-film sandwich technique was used to get false color composites with an optimal contrast. The interference zone between the eolian deposits of the Western Desert and fluvial deposits of the Nile Valley is well recognized. ESA

N87-15614# Kasetsart Univ., Bangkok (Thailand). Faculty of Forestry.

THE APPLICATION OF LANDSAT IMAGERY FOR LAND COVER ASSESSMENT

S. WACHARAKITTI *In* ESA Proceedings of an International Satellite Land-Surface Climatology Project (ISLSCP) Conference p 483-486 May 1986

Avail: NTIS HC A99/MF A01

Satellite imagery was used to study deforestation in Thailand. The forest land cover of the northeastern region in 1973 was 50,671 sq km (30%), decreased to 31,221 sq km (18.49%) in 1978, and to 25,886 sq km (15.33%) in 1982. The average forest land depletion in the period 1973 to 1978 is 8.4% annually, while the most critical locations are at Phen and Chi watersheds, at 10.85% and 10.21% per annum respectively. In the period 1978/1982, the average forest land depletion is 6.95% annually; the most critical locations are at Chi and Phen, at 8.58% and 8.18% per annum respectively. It is proved that LANDSAT imagery in term of black and white, and false color composite prints of 1: 250,000 scale can provide enough information on forest land cover and other land uses. ESA

N87-15615# Lund Univ. (Sweden). Lab. of Remote Sensing.
SURFACE ALBEDO CHANGE IN ARID REGIONS IN THE SUDAN

L.-O. ZELL *In* ESA Proceedings of an International Satellite Land-Surface Climatology Project (ISLSCP) Conference p 487-491 May 1986

Avail: NTIS HC A99/MF A01

Albedo change for 8 regions in arid to semiarid zones in central Sudan was calculated using LANDSAT 1 and 3 images registered in Oct./Nov. 1972 and Oct. 1979. Areas with low cultivation intensities show a decrease in surface albedo indicating a better green biomass cover at the end of the rainy season in 1979 than in 1972. Increases in albedo occur in areas with high cultivation intensities. ESA

N87-15618# Zurich Univ. (Switzerland). Dept. of Geography.

MONITORING OF LAND-SURFACE CHANGE IN SRI LANKA

H. HAEFNER and S. D. F. C. NANAYAKKARA (Survey Dept., Colombo, Sri Lanka) *In* ESA Proceedings of an International Satellite Land-Surface Climatology Project (ISLSCP) Conference p 501-507 May 1986

Avail: NTIS HC A99/MF A01

A method to continuously monitor land transformation processes and land-cover changes by satellite technology in Sri Lanka was developed. Land-use maps 1:100,000 (benchmark maps) and masking techniques form the basis for qualifying and quantifying the seasonal variations and long-term modifications results show worrying rates of deforestation and tea plantation disappearance. Paddy land remains constant. Data on other land use categories is insufficient. The Center for Remote Sensing at the Survey Department is executing the mapping and monitoring procedure and serves as focal point for introducing techniques and transferring results to the users, e.g., government agencies engaged in planning, resources management, and development. ESA

01 AGRICULTURE AND FORESTRY

N87-15619# University of the West Indies, Kingston (Jamaica).
VEGETATION CHANGE AND DESERTIFICATION IN THE CARIBBEAN

L. ALAN EYRE *In* ESA Proceedings of an International Satellite Land-Surface Climatology Project (ISLSCP) Conference p 509-514
May 1986

Avail: NTIS HC A99/MF A01

Evidence that surface climatology is changing in many parts of the Caribbean region is discussed. The trend is from humid tropical and dry seasonal forest towards increasing aridity, with savanization and actual desertification being apparent. There is a debate as to the degree to which the changes are anthropogenic and due to misuse of the environment. All evidence points to overexploitation of essentially fragile island ecosystems. Field studies and sampling of time-sequential satellite imagery, including LANDSAT, suggest that a combination of remotely sensed and ground verified data is useful in documenting trends in land surface climatology. ESA

N87-15621# Consiglio Nazionale delle Ricerche, Florence (Italy).

AN INTEGRATED SYSTEM TO ASSESS AGRICULTURAL PRODUCTIVITY

C. CONESE, G. MARACCHI, F. MIGLIETTA, V. CAPPELINI, R. CARLA, and V. SACCO *In* ESA Proceedings of an International Satellite Land-Surface Climatology Project (ISLSCP) Conference p 523-530 May 1986 Original contains color illustrations
Avail: NTIS HC A99/MF A01

An approach to an integrated system for the assessment of agricultural productivity is presented. It uses LANDSAT data to extract information on a field scale, connected with farm activity, while meteorological satellites give information on the thermal behavior of the ground, on a global scale. By correlating the satellite data with ground information such as digital cartography, land soil biological parameters, and meteorological data acquisition by a conventional network, an intermediate or simplified crop model was developed to integrate conventional ground data with satellite data, to assess agricultural productivity. ESA

N87-15622# Indian Space Research Organization, Ahmedabad. Space Applications Centre.

AVHRR AND MSS DATA BASED VEGETATION INDICES STUDIES OVER INDIAN SITES

R. K. GUPTA (National Remote Sensing Agency, Hyderabad, India), B. K. RANGANATH (National Remote Sensing Agency, Hyderabad, India), S. T. CHARI (National Remote Sensing Agency, Hyderabad, India), and R. P. S. CHHONKAR *In* ESA Proceedings of an International Satellite Land-Surface Climatology Project (ISLSCP) Conference p 531-535 May 1986 Original contains color illustrations

Avail: NTIS HC A99/MF A01

Images from NOAA AVHRR normalized vegetation index (NVI) over Shivalik forest range (India) and adjoining regions for the months of May and November were analyzed with the help of LANDSAT/MSS data based interpretation maps to bring out the differential biomass signatures of different forest types, and canopy cover, and their variations after the rainfall season. The results of Allapalli forest region AVHRR NVI image analysis are presented. The results of comparative analysis of ratio and normalized vegetation indices, principal components images over a Palmaner taluk subscene are discussed. First level result of improved vegetation discrimination with the use of NVI, and bands 7 and 5 as components of false-color composite are presented. ESA

N87-15623# Thessaloniki Univ. (Greece). Dept. of Biology.
THE USE OF REMOTE SENSING TECHNIQUES IN THE STUDY OF VEGETATION RECOVERY AFTER FIRE IN MEDITERRANEAN COUNTRIES (A PRELIMINARY STUDY)

J. DIAMANTOPOULOS and S. PARASKEVOPOULOS *In* ESA Proceedings of an International Satellite Land-Surface Climatology Project (ISLSCP) Conference p 537-538 May 1986

Avail: NTIS HC A99/MF A01

The possible contribution of the International Satellite Land Surface Climatology Project (ISLSCP) to studying the impact of

fire on the biomass of Greece is discussed. The ISLSCP could help in long term monitoring activities and the constitution of archives for retrospective studies. It could also complete climatological data, especially in mountainous areas, and develop indexes and algorithms to follow the regeneration process. ESA

N87-15629*# National Aeronautics and Space Administration. Goddard Space Flight Center, Greenbelt, Md.

THE FIRST INTERNATIONAL SATELLITE LAND SURFACE CLIMATOLOGY PROJECT (ISLSCP) FIELD EXPERIMENT - FIVE

T. J. SCHMUGGE and P. J. SELLERS *In* ESA Proceedings of an International Satellite Land-Surface Climatology Project (ISLSCP) Conference p 567-571 May 1986
Avail: NTIS HC A99/MF A01 CSCL 08B

The International Satellite Land Surface Climatology Project (ISLSCP) will verify the use of satellite data for the estimation of land-surface properties through field experiments using point measurements on the ground and areal measurements from aircraft overflights. It will study approaches for obtaining areal averages of the radiation, moisture, and heat fluxes made using remotely sensed data, by combining the surface point measurements of the fluxes with the aircraft areal observations using a surface energy balance model. Surface parameters to be estimated from aircraft observations include: surface radiation temperature, albedo, land cover or vegetation index, and surface soil moisture. The latter will be obtained using passive and active microwave approaches. The area-averages of the surface properties will be compared with satellite data. The First ISLSCP Field Experiment is planned for a site having relatively uniform vegetation cover in the central great plains of the U.S.A. ESA

N87-17122*# National Aeronautics and Space Administration. Earth Resources Lab., Bay St. Louis, Miss.

MONITORING VEGETATION RECOVERY PATTERNS ON MOUNT ST. HELENS USING THERMAL INFRARED MULTISPECTRAL DATA

KENNETH J. LANGRAN *In* JPL, California Inst. of Technology The TIMS Data User's Workshop p 53-54 1 Nov. 1986
Previously announced in IAA as A86-46106
Avail: NTIS HC A05/MF A01 CSCL 02C

The Mount St. Helens 1980 eruption offers an opportunity to study vegetation recovery rates and patterns in a perturbed ecosystem. The eruptions of Mount St. Helens created new surfaces by stripping and implacing large volumes of eroded material and depositing tephra in the blast area and on the flanks of the mountain. Areas of major disturbance are those in the blast zone that were subject to debris avalanche, pyroclastic flows, mudflows, and blowdown and scorched timber; and those outside the blast zone that received extensive tephra deposits. It was observed that during maximum daytime solar heating, surface temperatures of vegetated areas are cooler than surrounding nonvegetated areas, and that surface temperature varies with percent vegetation cover. A method of measuring the relationship between effective radiant temperature (ERT) and percent vegetation cover in the thermal infrared (8 to 12 microns) region of the electromagnetic spectrum was investigated. Author

N87-17123*# National Aeronautics and Space Administration. Earth Resources Lab., Bay St. Louis, Miss.

INVESTIGATION OF FOREST CANOPY TEMPERATURES RECORDED BY THE THERMAL INFRARED MULTISPECTRAL SCANNER AT H. J. ANDREWS EXPERIMENTAL FOREST

STEVEN A. SADER *In* JPL, California Inst. of Technology The TIMS Data User's Workshop p 55-57 1 Nov. 1986
Avail: NTIS HC A05/MF A01 CSCL 02F

Thermal Infrared Multispectral Scanner (TIMS) data were collected over the H. J. Andrews Experimental Forest in Western Oregon on July 29, 1983 at approximately 1:30 p.m., Pacific Standard Time. The relation of changes in canopy temperature to green leaf biomass levels in reforested clearcuts and old-growth forest was investigated. A digital data base was generated in order to isolate that portion of the thermal emission that could be

attributed to surface properties other than the vegetation biomass component. The TIMS appears to be capable of detecting subtle differences in ERT as related to canopy closure and green lead biomass, however calibration techniques are needed to correct for emissivity and atmospheric effects. B.G.

N87-17124*# National Aeronautics and Space Administration. Earth Resources Lab., Bay St. Louis, Miss.

APPLICATIONS OF TIMS DATA IN AGRICULTURAL AREAS AND RELATED ATMOSPHERIC CONSIDERATIONS

R. E. PELLETIER and M. C. OCHOA *In* JPL, California Inst. of Technology The TIMS Data User's Workshop p 57-58 1 Nov. 1986 Prepared in cooperation with Auburn Univ., Ala.

Avail: NTIS HC A05/MF A01 CSCL 02C

While much of traditional remote sensing in agricultural research was limited to the visible and reflective infrared, advances in thermal infrared remote sensing technology are adding a dimension to digital image analysis of agricultural areas. The Thermal Infrared Multispectral Scanner (TIMS) an airborne sensor having six bands over the nominal 8.2 to 12.2 μ m range, offers the ability to calculate land surface emissivities unlike most previous singular broadband sensors. Preliminary findings on the utility of the TIMS for several agricultural applications and related atmospheric considerations are discussed. Author

N87-17126*# Nebraska Univ., Lincoln. Inst. of Agriculture and Natural Resources.

TIMS DATA APPLICATIONS IN NEBRASKA

LLOYD QUEEN and GENE MURRAY *In* JPL, California Inst. of Technology The TIMS Data User's Workshop (date) p 60 1 Nov. 1986

Avail: NTIS HC A05/MF A01 CSCL 08B

A total of 172 flight-line miles of Thermal Infrared Multispectral Scanner (TIMS) data were acquired in the state of Nebraska; and an additional mission is planned for August of this year. Data collected by the scanner were generally applied to investigations in four general areas: hydrology, geology, soils, and vegetation analysis. Relatively simple manipulations of these thermal-emittance data led to excellent classifications of vegetation communities established along topographic gradients in the Nebraska Sandhills. Similar procedures were used to study variations in soil parameters along those same routes. Proposed geologic applications include mapping of the surficial geology along a portion of the Platte River and the delineation of a segment of the Cambridge Arch, a structural feature in central Nebraska. Author

N87-17127*# Pennsylvania State Univ., University Park. Dept. of Agronomy.

THE APPLICATION OF REMOTELY SENSED DATA TO PEDOLOGIC AND GEOMORPHIC MAPPING ON ALLUVIAL FAN AND PLAYA SURFACES IN SALINE VALLEY, CALIFORNIA

D. A. MILLER, G. W. PETERSEN, and A. B. KAHLE *In* JPL, California Inst. of Technology The TIMS Data User's Workshop p 61 1 Nov. 1986

Avail: NTIS HC A05/MF A01 CSCL 08G

Arid and semiarid regions yield excellent opportunities for the study of pedologic and geomorphic processes. The dominance of rock and soil exposure over vegetation not only provides the ground observer with observational possibilities but also affords good opportunities for measurement by aircraft and satellite remote sensor devices. Previous studies conducted in the area of pedologic and geomorphic mapping in arid regions with remotely sensed data have utilized information obtained in the visible to near-infrared portion of the spectrum. Thermal Infrared Multispectral Scanner (TIMS) and Thematic Mapping (TM) data collected in 1984 are being used in conjunction with maps compiled during a Bureau of Land Management (BLM) soil survey to aid in a detailed mapping of alluvial fan and playa surfaces within the valley. The results from this study may yield valuable information concerning the application of thermal data and thermal/visible data combinations to the problem of dating pedologic and geomorphic features in arid regions. Author

N87-17132*# Nevada Univ., Reno. Dept. of Geological Sciences.

APPLICATION OF THERMAL INFRARED MULTIBAND SCANNER (TIMS) DATA TO MAPPING OF PLUTONIC AND STRATIFIED ROCK AND ASSEMBLAGES IN ACCRETED TERRAINS OF THE NORTHERN SIERRA, CALIFORNIA

JAMES V. TARANIK, DAVID DAVIS, and MARCUS BORENGASSER *In* JPL, California Inst. of Technology The TIMS Data User's Workshop p 71-73 1 Nov. 1986

Avail: NTIS HC A05/MF A01 CSCL 08B

The Thermal Infrared Multispectral Scanner (TIMS) data were acquired over the Donner Pass area in California on September 12, 1985. The higher peaks in the area approach 9,200 feet in elevation, while the canyon of the north fork of the American River is only 3000 feet in elevation. The vegetation is dominated by conifers, although manzanita and other shrubs are present in areas where soils have developed. The data contain noise patterns which cut across scan lines diagonally. The TIMS data were analyzed using both photointerpretative and digital processing techniques. Preliminary image interpretation and field analysis confirmed that TIMS image data displays the chert units and silicic volcanics as bright red. The imagery appears to display zoning in the batholithic and hypabyssal intrusive rocks, although this was not field checked at this time. Rocks which appear to be more dioritic in composition appear purple on the imagery, while rocks more granitic in composition appear shades of red and pink. Areas that have more than 40% vegetative cover appear green on the imagery. Author

N87-17156*# Purdue Univ., West Lafayette, Ind. Dept. of Forestry and Natural Resources.

ANALYSIS OF MULTIPLE INCIDENCE ANGLE SIR-B DATA FOR DETERMINING FOREST STAND CHARACTERISTICS

R. M. HOFFER, D. F. LOZANO-GARCIA, D. D. GILLESPIE, P. W. MUELLER, and M. J. RUZEK (Jet Propulsion Lab., California Inst. of Tech., Pasadena) *In* JPL The Second Spaceborne Imaging Radar Symposium p 159-164 1 Dec. 1986

Avail: NTIS HC A10/MF A01 CSCL 02F

For the first time in the U.S. space program, digital synthetic aperture radar (SR) data were obtained from different incidence angles during Space Shuttle Mission 41-G. Shuttle Imaging Radar-B (SIR-B) data were obtained at incidence angles of 58 deg., 45 deg., and 28 deg., on October 9, 10, and 11, 1984, respectively, for a predominantly forested study area in northern Florida. Cloud-free LANDSAT Thematic Mapper (T.M.) data were obtained over the same area on October 12. The SIR-B data were processed and then digitally registered to the LANDSAT T.M. data by scientists at the Jet Propulsion Laboratory. This is the only known digitally registered SIR-B and T.M. data set for which the data were obtained nearly simultaneously. The data analysis of this information is discussed. Author

N87-17160*# Michigan Univ., Ann Arbor.

SIR-B MEASUREMENTS AND MODELING OF VEGETATION

FAWWAZ T. ULABY and M. CRAIG DOBSON *In* JPL The Second Spaceborne Imaging Radar Symposium p 191-200 1 Dec. 1986

Avail: NTIS HC A10/MF A01 CSCL 02C

A summary is presented of the results derived from analysis of six SIR-B data takes over an agricultural test site in west central Illinois. The first part describes the procedure used to calibrate the SIR-B imagery, the second part pertains to the observed radar response to soil moisture content, and the last part examines the information derivable from multiangle observations. Author

N87-17165# Freiburg Univ. (West Germany).

COMPARISON OF THEMATIC MAPPER (TM) AND SPOT SIMULATION DATA FOR AGRICULTURAL APPLICATIONS IN SOUTH WEST GERMANY

W. MAUSER, H.-J. STIBIG, and W. KIRCHHOF (Deutsche Forschungs- und Versuchsanstalt fuer Luft- und Raumfahrt, Oberpfaffenhofen, West Germany) *In* ESA Proceedings of the 1986 International Geoscience and Remote Sensing Symposium (IGARSS '86) on Remote Sensing: Today's Solutions for Tomorrow's Information Needs, Volume 1 p 9-13 Aug. 1986
 Avail: NTIS HC A99/MF E03; ESA, Paris, France, 3 volume set \$90 Member States, AU, CN, and NO (+20% others)

Data sets of pixel-sizes of 10, 20, 30, 50, and 80m created from data of a LANDSAT Thematic Mapper (TM) simulation were used for a comparative analysis between TM and SPOT-data of the information content in agricultural and forestry applications. The discrimination of objects depending on pixel-size and spectral bands was investigated. The TM-bands together with the improved resolution brought strong improvements in the separation of vegetated and built-up areas as well as growth stages of vegetation in comparison to MSS. The TM is found to be well suited for application in areas with average field sizes of 1.5 ha. The information content of the SPOT-multiband data-set is found to not essentially differ from that of TM. The results of a classification of the SPOT-multiband data are slightly less accurate than those using the TM-data. ESA

N87-17173# Stanford Univ., Calif.

SPATIAL ANALYSIS OF THE DYNAMICS OF AN ECOSYSTEM BY MULTISTAGE REMOTE SENSING IN KENYA

H. R. GOETTING and R. MAECKEL (Freiburg Univ., West Germany) *In* ESA Proceedings of the 1986 International Geoscience and Remote Sensing Symposium (IGARSS '86) on Remote Sensing: Today's Solutions for Tomorrow's Information Needs, Volume 1 p 53-56 Aug. 1986
 Avail: NTIS HC A99/MF E03; ESA, Paris, France, 3 volume set \$90 Member States, AU, CN, and NO (+20% others)

Satellite data, an aerial survey, and ground reference data were used as a database for the analysis of the carrying capacity and the desertification process in the Uaso Nyiro River Basin of Northern Kenya. The carrying capacity in terms of the population density of the semi-arid Leroghi Plateau is 7 P/sqkm. But there are 14.5 P/sqkm currently living there and the population is growing. Due to the desertification process, the vegetation to support the livestock decreased by 11% in the last 16 yr. In the arid river basin the calculated carrying capacity is 2 P/sqkm. If one assumes that this calculation is still up to date, then the area south of the river is overpopulated by 275%. The overpopulation in the area north of the river reaches 490%. Due to the desertification process and the shrinking grazing land, today's carrying capacity of the river basin is a mere 1 P/sqkm. The dangerous overpopulation points toward a human tragedy in the near future in the arid lands of Northern Kenya. ESA

N87-17238# Florence Univ. (Italy). Dipt. di Ingegneria Elettronica.

MULTISPECTRAL CLASSIFICATION OF MICROWAVE REMOTE SENSING IMAGES

G. BENELLI, V. CAPPELLINI, E. DELRE, and L. NIGRO *In* ESA Proceedings of the 1986 International Geoscience and Remote Sensing Symposium (IGARSS '86) on Remote Sensing: Today's Solutions for Tomorrow's Information Needs, Volume 1 p 463-466 Aug. 1986

Avail: NTIS HC A99/MF E03; ESA, Paris, France, 3 volume set \$90 Member States, AU, CN, and NO (+20% others)

Methods for the automatic classification and discrimination of crops are described. Microwave images in bands X and C collected during the European SAR 580 campaign are used. One and two dimensional classification algorithms using Bayes rule or the block distance are analysed. The probability of correct classification for different crops is presented. ESA

N87-17250# Cranfield Inst. of Tech., Bedford (England). Silsoe Coll.

THE INFLUENCE OF RESAMPLING METHOD AND MULTITEMPORAL LANDSAT IMAGERY ON CROP CLASSIFICATION ACCURACY IN THE UNITED KINGDOM

A. S. BELWARD and J. C. TAYLOR *In* ESA Proceedings of the 1986 International Geoscience and Remote Sensing Symposium (IGARSS '86) on Remote Sensing: Today's Solutions for Tomorrow's Information Needs, Volume 1 p 529-534 Aug. 1986

Avail: NTIS HC A99/MF E03; ESA, Paris, France, 3 volume set \$90 Member States, AU, CN, and NO (+20% others)

Six sequential LANDSAT MSS scenes for a test site were geometrically corrected. Resampling to 50m pixel size was carried out with bilinear interpolation and nearest neighbor. Spectral coincident plots and decision boundaries were used for feature selection, and supervised maximum likelihood classification used for crop classification. Bilinear interpolation gives a mean increase in classification accuracy of 1.95% over nearest neighbor. Multitemporal data give better overall classification accuracies than single date images. A spring/early summer combination gives a mean classification purity of 70%, a 6% increase over the best single date classification from May, and 46% better than the worst from February. ESA

N87-17262# Bern Univ. (Switzerland). Inst. of Applied Physics.
DIELECTRIC AND SURFACE PARAMETERS RELATED TO MICROWAVE SCATTER AND EMISSION PROPERTIES

E. STOTZER, U. WEGMUELLER, R. HUEPPI, and C. MAETZER *In* ESA Proceedings of the 1986 International Geoscience and Remote Sensing Symposium (IGARSS '86) on Remote Sensing: Today's Solutions for Tomorrow's Information Needs, Volume 1 p 599-603 Aug. 1986

Avail: NTIS HC A99/MF E03; ESA, Paris, France, 3 volume set \$90 Member States, AU, CN, and NO (+20% others)

A correlated study of the dielectric properties, surface roughness, and the backscatter and emission behavior of bare soil is presented. For the measurement of the permittivity of the soil field proof dielectric sensors at frequencies between 0.5 and 1 GHz were developed. A surface sensor measures the dielectric constant of a top 1 cm layer and a volume sensor averages over a depth of 15 cm. For the measurement of surface roughness, a laser distance measurement system was designed. It measures a 1 m long surface height profile. Quantities like distribution and standard deviation of heights and slopes, or the autocorrelation function are computed and used in scattering models. Temperature profiles, soil moisture, and texture are determined. Together with the soil parameters, the microwave signatures are measured with an L to X-band radiometer-scatterometer. Emissivities and backscattering coefficients are related to the soil parameters, and compared with model calculations. ESA

N87-17265# Centre d'Etude Spatiale des Rayonnements, Toulouse (France).

EXTRACTION OF THE BACKSCATTER COEFFICIENT OF AGRICULTURAL FIELDS FROM AN AIRBORNE SAR IMAGE

A. LOPES and R. TOUZI *In* ESA Proceedings of the 1986 International Geoscience and Remote Sensing Symposium (IGARSS '86) on Remote Sensing: Today's Solutions for Tomorrow's Information Needs, Volume 1 p 621-628 Aug. 1986

(Contract ESA-6153/WL-MS)

Avail: NTIS HC A99/MF E03; ESA, Paris, France, 3 volume set \$90 Member States, AU, CN, and NO (+20% others)

Relative and absolute calibration was performed on an X-band SAR image of an agricultural area. The image presented distortions due mainly to aircraft motions and to the antenna gain function. Distortions due to aircraft motions, resulting in dark rays perpendicular to the flight direction, are corrected by a spectral filtering method. The thermal noise is estimated and subtracted from the image. The antenna gain is evaluated by using a distributed target of a priori known angular variation. A correction taking into account the antenna gain and the range is applied to the image.

The scattering coefficient is estimated using a Luneberg lens located in the scene. Errors in this estimation are assessed.

ESA

N87-17266# Freiburg Univ. (West Germany). Abt. Luftbildmessung und Fernerkunde.

MICROWAVE REMOTE SENSING: ITS APPLICATIONS AND LIMITATIONS IN OPERATIONAL TASKS OF LAND USE INVENTORY AND FOREST MANAGEMENT

R. KESSLER *In* ESA Proceedings of the 1986 International Geoscience and Remote Sensing Symposium (IGARSS '86) on Remote Sensing: Today's Solutions for Tomorrow's Information Needs, Volume 1 p 629-631 Aug. 1986

Avail: NTIS HC A99/MF E03; ESA, Paris, France, 3 volume set \$90 Member States, AU, CN, and NO (+20% others)

Woodland and agricultural aspects of land use, based on experience with Seasat-SAR, SAR-580 and SIR-B imagery are reviewed. Potential applications and the limitations of microwave remote sensing sensors for operational tasks of land use inventory are described.

ESA

N87-17273# Zurich Univ. (Switzerland). Remote Sensing Labs. **VIEWING ANGLE CORRECTIONS OF AIRBORNE MULTISPECTRAL SCANNER DATA ACQUIRED OVER FORESTED SURFACES**

K. STAENZ, P. MEYER, K. I. ITTEN, D. G. GOODENOUGH (Canada Centre for Remote Sensing, Ottawa (Ontario).), and P. M. TEILLET *In* ESA Proceedings of the 1986 International Geoscience and Remote Sensing Symposium (IGARSS '86) on Remote Sensing: Today's Solutions for Tomorrow's Information Needs, Volume 1 p 671-676 Aug. 1986

Avail: NTIS HC A99/MF E03; ESA, Paris, France, 3 volume set \$90 Member States, AU, CN, and NO (+20% others)

Airborne MSS BENDIX M2S Scanner data obtained over a forested area were analyzed in order to assess the viewing angle effect. All of the bands situated within 0.4 to 1.1 microns are affected by the viewing angle. The magnitude of this effect results in a gray level difference of up to 35% within a viewing angle range from 0 (nadir) to 40 deg. In order to remove this radiometric distortion due to off-nadir viewing, two correction procedures, the additive adjustment technique and different band transformations (NIR-red ratio, NIR-red difference, vegetation and biomass index) were applied to the image data. The additive adjustment technique gives the best result. Due to the viewing angle correction, a significant improvement of the classification accuracy is achieved.

ESA

N87-17284# Canada Centre for Remote Sensing, Ottawa (Ontario).

AN OVERVIEW OF REMOTE SENSING AGRICULTURAL APPLICATIONS IN NORTH AMERICA: PAST, PRESENT AND FUTURE

R. J. BROWN *In* ESA Proceedings of the 1986 International Geoscience and Remote Sensing Symposium (IGARSS '86) on Remote Sensing: Today's Solutions for Tomorrow's Information Needs, Volume 2 p 733-737 Aug. 1986

Avail: NTIS HC A17/MF A01; ESA, Paris, France, 3 volume set \$90 Member States, AU, CN, and NO (+20% others)

The use of remote sensing for crop condition monitoring and crop area determination is reviewed. The Large Area Crop Inventory Experiment and the AGRISTARS project are recalled. The LANDSAT and NOAA satellite instruments used in agricultural remote sensing are described.

ESA

N87-17285# Agricultural Research Service, Beltsville, Md. **APPLICATIONS OF REMOTE SENSING IN THE US DEPARTMENT OF AGRICULTURE**

J. C. PRICE *In* ESA Proceedings of the 1986 International Geoscience and Remote Sensing Symposium (IGARSS '86) on Remote Sensing: Today's Solutions for Tomorrow's Information Needs, Volume 2 p 739-742 Aug. 1986

Avail: NTIS HC A17/MF A01; ESA, Paris, France, 3 volume set \$90 Member States, AU, CN, and NO (+20% others)

The U.S. Department of Agriculture uses remote sensing to monitor and assess crop conditions and to manage renewable resources. The Foreign Agriculture Service uses meteorological satellite data and LANDSAT data to monitor the status of crops in major agricultural regions of the world. The National Agricultural Statistics Service uses LANDSAT data to improve estimates of crop acreage in the central U.S. The Soil Conservation Service will use aircraft data to aid in the inventory of U.S. agricultural lands. Research to improve agency procedures is described.

ESA

N87-17286# Kansas State Univ., Manhattan. E.T. Lab. **ASSESSING GRASS CANOPY CONDITION AND GROWTH FROM COMBINED OPTICAL-MICROWAVE MEASUREMENTS**

G. ASRAR, E. T. KANEMASU, and R. D. MARTIN *In* ESA Proceedings of the 1986 International Geoscience and Remote Sensing Symposium (IGARSS '86) on Remote Sensing: Today's Solutions for Tomorrow's Information Needs, Volume 2 p 743-744 Aug. 1986

Avail: NTIS HC A17/MF A01; ESA, Paris, France, 3 volume set \$90 Member States, AU, CN, and NO (+20% others)

The potential of a combined optical-microwave sensor system for monitoring canopy condition and development in a natural tallgrass prairie was assessed. A set of linear classification functions was derived for distinguishing among tallgrass prairie surface cover types based on their spectral characteristics. An indirect procedure for estimating green leaf area index and phytomass for measurements of red and near infrared canopy reflectance was developed. Microwave (C-band) scatterometer measurements are found to strongly correlate with near-surface soil water content of the grassland.

ESA

N87-17287# Laval Univ. (Quebec). **ANALYSIS OF THE SPATIAL STRUCTURE OF SYNTHETIC APERTURE RADAR (SAR) IMAGERY FOR A BETTER SEPARABILITY OF CEREAL CROPS, WHEAT AND BARLEY**

C. DUBE, H. PROULX, and K. P. B. THOMPSON *In* ESA Proceedings of the 1986 International Geoscience and Remote Sensing Symposium (IGARSS '86) on Remote Sensing: Today's Solutions for Tomorrow's Information Needs, Volume 2 p 745-750 Aug. 1986

Avail: NTIS HC A17/MF A01; ESA, Paris, France, 3 volume set \$90 Member States, AU, CN, and NO (+20% others)

The analysis of the statistical characteristics of radar data for wheat and barley is discussed. The SAR data set is of good quality and comprises two depression angles, two row directions for each field, and three flight dates. A methodology of image processing which concerns the examination of structure and texture in image data is outlined. Results reveal two important characteristics in separating wheat from barley: the degree of homogeneity and the row effect. The texture analysis can be used to separate wheat and barley.

ESA

N87-17288# Centre National d'Etudes des Telecommunications, Issy-les-Moulineaux (France).

TOWARD A SATELLITE SYSTEM TO MONITOR THE SPATIAL AND TEMPORAL BEHAVIOR OF SOIL WATER CONTENT

R. BERNARD, O. TACONET, and D. VIDAL-MADJAR *In* ESA Proceedings of the 1986 International Geoscience and Remote Sensing Symposium (IGARSS '86) on Remote Sensing: Today's Solutions for Tomorrow's Information Needs, Volume 2 p 751-753 Aug. 1986

Avail: NTIS HC A17/MF A01; ESA, Paris, France, 3 volume set \$90 Member States, AU, CN, and NO (+20% others)

It is shown that using proper simple parameterizations of the soil/vegetation/atmosphere system it is possible to derive soil water content and surface atmospheric fluxes at satellite pixels scale. Though the algorithms must be further tested, it is anticipated that a future space system (geostationary satellites and polar platforms) using visible, thermal infrared, and microwave remote sensing may be used on an operational basis as a hydrologic observatory. ESA

N87-17289# California Univ., Berkeley. 260 Space Sciences Lab.

UTILITY OF REMOTE SENSING DATA IN RENEWABLE RESOURCE SAMPLE SURVEY

R. W. THOMAS *In* ESA Proceedings of the 1986 International Geoscience and Remote Sensing Symposium (IGARSS '86) on Remote Sensing: Today's Solutions for Tomorrow's Information Needs, Volume 2 p 755-758 Aug. 1986

Avail: NTIS HC A17/MF A01; ESA, Paris, France, 3 volume set \$90 Member States, AU, CN, and NO (+20% others)

It is shown how remote sensing technology offers possibilities for sample-based estimation of renewable resource means and totals. Studies show that significant improvements in estimate precision, cost, or timeliness are available for estimation of crop and irrigated area, forest wood volume and growth, and useable livestock forage when satellite data and/or aerial photography are included as sample stages. Land satellite data often provide a highly cost-effective, rapid alternative for stratifying a region into strata having a smaller range of variation in the ground parameters(s) of interest. Satellite and aircraft data can provide sample unit-specific measurements, correlated to corresponding ground measurements, reducing required ground sample size and inventory time. ESA

N87-17304# Texas Instruments, Inc., Dallas.

THE EFFECT OF MEASUREMENT ERROR AND CONFUSION FROM VEGETATION ON PASSIVE MICROWAVE ESTIMATES OF SOIL MOISTURE

S. W. THEIS and A. J. BLANCHARD *In* ESA Proceedings of the 1986 International Geoscience and Remote Sensing Symposium (IGARSS '86) on Remote Sensing: Today's Solutions for Tomorrow's Information Needs, Volume 2 p 847-851 Aug. 1986

Avail: NTIS HC A17/MF A01; ESA, Paris, France, 3 volume set \$90 Member States, AU, CN, and NO (+20% others)

The sensitivity of error in soil moisture estimates to passive microwave measurement error as a function of vegetation was studied using a simple model and measurements. Roughness confusion is not considered. The direct problem is defined as investigating the sensor response as the dependent variable to the parameter of interest while the inverse problem uses the parameter of interest as the dependent variable. The inverse method must be used for operational remote sensing applications. It is shown that this difference becomes very important when both confusion and measurement error are considered. A methodology whereby the sensitivity to measurement error attributed to vegetation can be estimated from the perpendicular vegetation index is presented. ESA

N87-17305# Helsinki Univ. of Technology, Espoo (Finland). Radio Lab.

CLASSIFICATION OF FOREST AND SURFACE TYPES BY SATELLITE MICROWAVE RADIOMETRY

M. HALLIKAINEN and P. JOLMA *In* ESA Proceedings of the 1986 International Geoscience and Remote Sensing Symposium (IGARSS '86) on Remote Sensing: Today's Solutions for Tomorrow's Information Needs, Volume 2 p 853-858 Aug. 1986

Avail: NTIS HC A17/MF A01; ESA, Paris, France, 3 volume set \$90 Member States, AU, CN, and NO (+20% others)

Scanning Multichannel Microwave Radiometer 10-GHz and 18-GHz data from Nimbus-7 were employed to investigate the classification of forest and surface types. Data for Falls 1978 and 1979 were compared against a digital map that shows 7 different forest and surface types for Southern Finland. The results indicate that four different categories can be discriminated: pine-dominant forest, other forest types (spruce-dominant and deciduous) and bogs, farmland, and water. ESA

N87-17313# INTERA Environmental Consultants Ltd., Ottawa (Ontario).

SAR IMAGERY FOR FOREST MANAGEMENT

R. T. LOWRY, P. VANECK, and R. V. DAMS *In* ESA Proceedings of the 1986 International Geoscience and Remote Sensing Symposium (IGARSS '86) on Remote Sensing: Today's Solutions for Tomorrow's Information Needs, Volume 2 p 901-906 Aug. 1986

Avail: NTIS HC A17/MF A01; ESA, Paris, France, 3 volume set \$90 Member States, AU, CN, and NO (+20% others)

A high resolution, digital, airborne, HH polarized, X-band SAR was tested for forest management. The SAR was compared with conventional panchromatic aerial photography in terms of information content, aerial coverage and costs; and with existing forest cover-type maps in which vegetation types, tree density, and height classes are provided. The evaluation of clearcut areas and other types of forestry and industry environmental effects (e.g., loss of timber volume through extensive seismic line clearing activities) was also assessed. Results show that if suitable base maps do not exist, they can be derived from SAR imagery; broad forestry inventories can be developed; and changing land use patterns can be mapped and existing inventories updated. The SAR is inferior to photography for classifications, but is not weather dependent. ESA

N87-17316# Zurich Univ. (Switzerland). Dept. of Geography. **SNOW COVER RECESSION IN AN ALPINE ECOLOGICAL SYSTEM**

M. KELLER and K. SEIDEL (Eidgenossische Technische Hochschule, Zurich, Switzerland) *In* ESA Proceedings of the 1986 International Geoscience and Remote Sensing Symposium (IGARSS '86) on Remote Sensing: Today's Solutions for Tomorrow's Information Needs, Volume 2 p 921-924 Aug. 1986

Avail: NTIS HC A17/MF A01; ESA, Paris, France, 3 volume set \$90 Member States, AU, CN, and NO (+20% others)

In the Man and Biosphere project, an ecological survey in a high Alpine valley was carried out. Data from climatology, forestry, game biology, land use history, pedology, and vegetation were assembled into a Geographic Information System. A LANDSAT based snow cover recession map is found to be a fundamental variable influencing a number of layers within the ecological data set. It is shown quantitatively, for example, how snow cover recession and floral associations are related. This assists in vegetation mapping and can be used to simulate vegetation. ESA

N87-17344*# National Aeronautics and Space Administration.
Goddard Space Flight Center, Greenbelt, Md.
EVALUATING ROUGHNESS MODELS OF RADAR BACKSCATTER

E. T. ENGMANN (Agricultural Research Service, Beltsville, Md.) and J. R. WANG *In* ESA Proceedings of the 1986 International Geoscience and Remote Sensing Symposium (IGARSS '86) on Remote Sensing: Today's Solutions for Tomorrow's Information Needs, Volume 2 p 1097-1101 Aug. 1986

Avail: NTIS HC A17/MF A01; ESA, Paris, France, 3 volume set \$90 Member States, AU, CN, and NO (+20% others) CSDL 171

Three radar backscatter roughness models were assessed using soil moisture data collected by the Space Shuttle flight 41G SIR-B SAR in an intensively farmed area. The SIR-B data swath included a large number of bare, dry fields with a large variety of surface roughnesses. The small perturbation model gives the best results, particularly when fields with a definite periodic row structure were omitted. The standard deviation of surface heights appears to be a good measure of relative roughness conditions, but the correlation length is not a good descriptor of the surface, and does not seem to be related in any way to the measured backscatter.

ESA

N87-17347# Bern Univ. (Switzerland). Inst. of Applied Physics.
L TO X-BAND SCATTER AND EMISSION MEASUREMENTS OF VEGETATION

R. HUEPPI and E. SCHANDA *In* ESA Proceedings of the 1986 International Geoscience and Remote Sensing Symposium (IGARSS '86) on Remote Sensing: Today's Solutions for Tomorrow's Information Needs, Volume 2 p 1113-1118 Aug. 1986

Avail: NTIS HC A17/MF A01; ESA, Paris, France, 3 volume set \$90 Member States, AU, CN, and NO (+20% others)

A broad-band H and V polarization radiometer was combined with a noise transmitter to an instrument for measuring active and passive microwave signatures at seven frequencies between L and X band. This radiometer-scatterometer is operated from a cherry picker over agricultural fields. During the growing seasons the development of sugar-beet, wheat, and corn was measured. The geometrical structure of the vegetation cover was described by recording the crop type, the distances between the plants, and the canopy height. The soil underneath was characterized by moisture, temperature profile, and dielectric constant. Another variable was the seasonal change in water content of the plants. Relating these parameters to the microwave signatures reveals the interaction of scatter and emission processes between soil and vegetation. Significant differences of the emission and scattering behavior for the measured crops are found.

ESA

N87-17350# Joint Research Centre of the European Communities, Ispra (Italy).
RURAL LAND USE INVENTORY AND MAPPING IN THE ARDECHE AREA (FRANCE) USING MULTITEMPORAL THEMATIC MAPPING (TM) DATA

J. HILL and J. MEGIER *In* ESA Proceedings of the 1986 International Geoscience and Remote Sensing Symposium (IGARSS '86) on Remote Sensing: Today's Solutions for Tomorrow's Information Needs, Volume 2 p 1135-1141 Aug. 1986

Avail: NTIS HC A17/MF A01; ESA, Paris, France, 3 volume set \$90 Member States, AU, CN, and NO (+20% others)

A set of 4 Thematic Mapper scenes (LANDSAT-5) covering the Ardecche region (Southern France) was examined. Image rectification was performed by least squares solution of polynomial equations using 39 to 45 GCP per TM half frame. Since a digital terrain model was not available, image registration was performed for restricted subimages (600 x 600 pixel) which were mosaiced with reference to one master scene. Problems result from relief dependent dislocations which affect the superposition of images, especially from different orbits and in mountainous areas. Further image analysis included the generation of multitemporal normalized vegetation index, image enhancement by edge preserving

smoothing, verification and refinement of ground truth information, and supervised classification (maximum likelihood). ESA

N87-17351# Istanbul Univ. (Turkey). Faculty of Forestry.
LANDSAT-5 THEMATIC MAPPING (TM) DATA APPLICATIONS TO LAND USE CLASSIFICATION ON AROUND THE BOSPHORUS AREA, TURKEY

K. ERDIN, A. HIZAL, and E. ATAMAN *In* ESA Proceedings of the 1986 International Geoscience and Remote Sensing Symposium (IGARSS '86) on Remote Sensing: Today's Solutions for Tomorrow's Information Needs, Volume 2 p 1143-1148 Aug. 1986

Avail: NTIS HC A17/MF A01; ESA, Paris, France, 3 volume set \$90 Member States, AU, CN, and NO (+20% others)

Data from LANDSAT-5 TM were evaluated to delineate forest land use classifications by means of computer assisted techniques. The land use map was checked in the field. Results show that LANDSAT-5 TM Band 5/4 combination is the most convenient to classify forest land use types.

ESA

N87-17352# Aston Univ., Birmingham (England). Dept. of Civil Engineering.

DISCRIMINATION OF LAND FEATURES USING LANDSAT FALSE COLOUR COMPOSITE IN N IRAN

H. TAKERKIA and W. G. COLLINS *In* ESA Proceedings of the 1986 International Geoscience and Remote Sensing Symposium (IGARSS '86) on Remote Sensing: Today's Solutions for Tomorrow's Information Needs, Volume 2 p 1149-1153 Aug. 1986

Avail: NTIS HC A17/MF A01; ESA, Paris, France, 3 volume set \$90 Member States, AU, CN, and NO (+20% others)

Multispectral LANDSAT data was studied as a source of information for land and water resources (inventories). Two false color composite images, scale 1:250,000, were used as the data source. Forestry, rice cultivation, and drainage networks were mapped and the results compared with data from published 1:250,000 topographic maps. The results show that LANDSAT provides an acceptable degree of accuracy to permit first order mapping of surface drainage, forestry, and rice fields in Iran, where there is an acute shortage of information relating to the land and water resources.

ESA

N87-17395# Los Alamos National Lab., N. Mex. Theoretical Div.

CANOPY HOT-SPOT AS CROP IDENTIFIER

S. A. W. GERSTL, C. SIMMER, and B. J. POWERS May 1986 10 p Presented at the 12th International Conference on Very Large Databases, Kyoto, Japan, 25 Aug. 1986

(Contract W-7405-ENG-36)

(DE86-011258; LA-UR-86-1596; CONF-860888-1) Avail: NTIS HC A02/MF A01

Illuminating any reflective rough or structured surface by a directional light source results in an angular reflectance distribution that shows a narrow peak in the direction of retro-reflection. This is called the Heiligenschein or hot-spot of vegetation canopies and is caused by mutual shading of leaves. The angular intensity distribution of the hot-spot, its brightness and slope, are therefore indicators of the plant's geometry. We propose the use of hot-spot characteristics as crop identifiers in satellite remote sensing because the canopy hot-spot carries information about plant stand architecture that is more distinctive for different plant species than, for instance, their spectral reflectance characteristics. A simple three-dimensional Monte Carlo/ray tracing model and an analytic two-dimensional model are developed to estimate the angular distribution of the hot-spot as a function of the size of the plant leaves. The results show that the brightness-distribution and slope of the hot-spot change distinctively for different leaf sizes indicating a much more peaked maximum for the smaller leaves.

DOE

N87-18143# IBM France S. A., Paris.

THERMAL INERTIA AND SOIL FLUXES BY REMOTE SENSING

D. HO *In* ESA Proceedings on the 1986 International Geoscience and Remote Sensing Symposium (IGARSS '86) on Remote Sensing: Today's Solutions for Tomorrow's Information Needs, Volume 3 p 1215-1220 Aug. 1986 Sponsored by CNES and CNRS

Avail: NTIS HC A21/MF A01; ESA, Paris, France, 3 volume set \$90 Member States, AU, CN, and NO (+20% others)

The diurnal surface temperature cycle is shown to be insensitive to the initial temperature profile and the lower boundary conditions, allowing the soil to be treated with an analytic steady state model as a transmission line problem. It is possible to calculate the soil conducting flux directly from the satellite temperature data, without the knowledge of the energy exchange process at the ground surface, provided that the soil thermal inertia is known. A simple inverse model can then be derived to calculate the soil thermal inertia and soil fluxes using visible and infrared satellite data along with standard meteorological data. The model requires neither the linearization of the flux terms at the ground surface nor the knowledge of the lower boundary condition and the soil initial temperature profile. The model, applied to a lake, yields an error less than 4% in the estimate of thermal inertia and sensible heat flux. The model can be extended to generate thermal inertia and heat flux maps without any in - situ measurements. ESA

N87-18146# Centre National de la Recherche Scientifique, Garchy (France). Centre de Recherches Geophysiques.

THE USE OF THERMAL AIRBORNE REMOTE SENSING FOR SOIL IDENTIFICATION: A CASE STUDY IN LIMOUSIN (FRANCE)

F. GAUTHIER and A. TABBAGH *In* ESA Proceedings of the 1986 International Geoscience and Remote Sensing Symposium (IGARSS '86) on Remote Sensing: Today's Solutions for Tomorrow's Information Needs, Volume 3 p 1231-1234 Aug. 1986

Avail: NTIS HC A21/MF A01; ESA, Paris, France, 3 volume set \$90 Member States, AU, CN, and NO (+20% others)

Thermal airborne remote sensing in a test area where a pedological 1/10 000 scale map already existed is described. Two specific types of soil can be recognized and delimited on the thermographies. Flight took place at 10 am local time after a 4 days cold period. The radiometer was used with the 10 to 12.5 microns thermal channel. Apparent temperatures are higher on shallow soils (on granitic rock) and on hydromorphic soils than on well drained slope soils. In situ measurements of soil thermal properties allow thermal inertias to be calculated for each type of soil, and verify that pebbly soils of high heat capacity have higher thermal inertias. The differences in thermal inertias explain the observed difference in apparent temperature for a flux variation corresponding to that prevailing during the days preceding the flight. ESA

N87-18147# Comision Nacional de Investigaciones Espaciales, Buenos Aires (Argentina). Centro de Sensores Remotos.

SOIL DEGRADATION EVALUATION BY DIGITAL IMAGE PROCESSING

L. GUILLON and S. NAVONE (Buenos Aires Univ., Argentina) *In* ESA Proceedings of the 1986 International Geoscience and Remote Sensing Symposium (IGARSS '86) on Remote Sensing: Today's Solutions for Tomorrow's Information Needs, Volume 3 p 1235-1240 Aug. 1986

Avail: NTIS HC A21/MF A01; ESA, Paris, France, 3 volume set \$90 Member States, AU, CN, and NO (+20% others)

A satellite digital imagery technique was used to study an area where soil erosion processes (hydric and eolic) are common. The study area has a subhumid, temperate climate. Landscape is gently rolling and soils are mainly medium to deep argiudolls, with loamy to silty-loamy texture. To enhance both types of soil degradation identification, digital processes were tried. The LANDSAT MSS second principal component depicted eolic erosion areas; linear enhancement of B7 (MSS) identified hydric erosion areas; B5 (MSS) helped in detecting soil with lime-rock problems. Soil degradation

is accurately assessed through the effects on vegetation and when processes are intensive. ESA

N87-18148# Ghent Univ. (Belgium). Lab. for Regional Geography.

ASSESSMENT OF SOIL DEGRADATION IN AN ARID REGION USING REMOTE SENSING

A. GAD and L. DAELS *In* ESA Proceedings of the 1986 International Geoscience and Remote Sensing Symposium (IGARSS '86) on Remote Sensing: Today's Solutions for Tomorrow's Information Needs, Volume 3 p 1241-1246 Aug. 1986

Avail: NTIS HC A21/MF A01; ESA, Paris, France, 3 volume set \$90 Member States, AU, CN, and NO (+20% others)

The FAO/UNEP and UNESCO methodology for assessing soil degradation in arid lands was tested in Egypt. The false color diazo technique was applied on MSS LANDSAT images for visual interpretation. Different enhancements made it possible to study the soil, the land-use, and the topography factors which are used in the evaluation of the different degradation processes. Results confirm the usefulness of the methodology. They show that the Nile valley is subject to wind and water erosion and salinization. Desert fringes, considered for agricultural expansion, are affected by the same processes. ESA

N87-18149# Istanbul Univ. (Turkey). Faculty of Forestry.

THE USE OF REMOTE SENSING (INCLUDING AERIAL PHOTOGRAPHS) TO DEVISE COST-EFFECTIVE METHODS FOR SOIL CONSERVATION IN THE KOCAELI PENINSULA, TURKEY

A. HIZAL *In* ESA Proceedings of the 1986 International Geoscience and Remote Sensing Symposium (IGARSS '86) on Remote Sensing: Today's Solutions for Tomorrow's Information Needs, Volume 3 p 1247-1250 Aug. 1986

Avail: NTIS HC A21/MF A01; ESA, Paris, France, 3 volume set \$90 Member States, AU, CN, and NO (+20% others)

The use of aerial photographs and LANDSAT images to help devise cost-effective methods to stabilize erosion features in the Kocaeli peninsula (Turkey) is discussed. The basic maps, such as detailed erosion and land use maps, must immediately be produced using remote sensing techniques. Critical areas having serious erosion problems in terms of producing water have to be designated using the maps in order to decide cost-effective treatment methods. If the erosion control works are carried out using the small scale maps produced by conventional ground surveys, control works may be expensive and may not achieve the expected conservation objectives. ESA

N87-18150# Haryana Agricultural Univ., Hisar (India).

APPLICATION OF REMOTE SENSING IN THE STUDY OF THE SOIL HAZARDS OF HARYANA STATE, INDIA

M. SINGH and V. P. GOYAL *In* ESA Proceedings of the 1986 International Geoscience and Remote Sensing Symposium (IGARSS '86) on Remote Sensing: Today's Solutions for Tomorrow's Information Needs, Volume 3 p 1251-1256 Aug. 1986

Avail: NTIS HC A21/MF A01; ESA, Paris, France, 3 volume set \$90 Member States, AU, CN, and NO (+20% others)

Multispectral and multitemporal LANDSAT images of Haryana state (India) and of representative areas were interpreted to delineate the soil hazards and normal soils. The major soil hazards of different intensity levels identified are saline-alkali soils, wind erosion, water erosion, river deposition, and water-logging. The soil associations at great group level are Udipsamments, Ustipsamments, Torripsamments, Ustorthents, Ustifluvents, Ustochrepts, Haplaquepts, Calciorthids, Camborthids, Ochraqualfs and Natrustalfs. A map depicting intensity and distribution of soil hazards in Haryana state was prepared. ESA

N87-18153# Consiglio Nazionale delle Ricerche, Florence (Italy). Ist. di Analisi Ambientale e Telerilevamento Applicati all' Agricoltura.

AN INTEGRATED DATA BANK FOR AGRICULTURAL PRODUCTIVITY BY REMOTE SENSING

C. CONESE, L. BACCI, G. MARACCHI, V. CAPPELLINI, and R. CARLA *In* ESA Proceedings of the 1986 International Geoscience and Remote Sensing Symposium (IGARSS '86) on Remote Sensing: Today's Solutions for Tomorrow's Information Needs, Volume 3 p 1273-1278 Aug. 1986

Avail: NTIS HC A21/MF A01; ESA, Paris, France, 3 volume set \$90 Member States, AU, CN, and NO (+20% others)

A methodology for the assessment and evaluation of natural resources in order to establish the land actual and potential agricultural productivity is proposed. The main sources of information are conventional cartography, LANDSAT TM image processing, NOAA and Meteosat satellite image processing, soil cartography, meteorological data, and models of main crop productivity. The integrated information obtained from these different sources are used to simulate crop productivity and build up a map of land capacity. ESA

N87-18154# Swedish Space Corp., Solna.

MARRYING GEOCODED IMAGE DATA WITH OTHER TYPES OF GEOGRAPHIC INFORMATION IN A PC ENVIRONMENT

S. ZENKER, A. ENGBERG, G. GRAPE, and H. MALMSTROEM *In* ESA Proceedings of the 1986 International Geoscience and Remote Sensing Symposium (IGARSS '86) on Remote Sensing: Today's Solutions for Tomorrow's Information Needs, Volume 3 p 1279-1280 Aug. 1986

Avail: NTIS HC A21/MF A01; ESA, Paris, France, 3 volume set \$90 Member States, AU, CN, and NO (+20% others)

The power of interactive analysis of geographic data on an IBM-AT image processing system was demonstrated in a forestry application. By pointing with a cursor within a LANDSAT TM image on the screen, associated timber stand boundaries and ancillary data are immediately displayed. ESA

N87-18156# Rand Afrikaans Univ., Johannesburg (South Africa).

INTEGRATING VECTOR AND SATELLITE DATA TO EVALUATE THE ADEQUACY OF A GRAIN SILO NETWORK

E. J. VANVUUREN, P. A. J. VANRENSBURG, and S. H. VONSOLMS *In* ESA Proceedings of the 1986 International Geoscience and Remote Sensing Symposium (IGARSS '86) on Remote Sensing: Today's Solutions for Tomorrow's Information Needs, Volume 3 p 1287-1290 Aug. 1986 Sponsored by the CSIR

Avail: NTIS HC A21/MF A01; ESA, Paris, France, 3 volume set \$90 Member States, AU, CN, and NO (+20% others)

A computerized method for preparing vector type geocoded geographical data to be overlaid on to a LANDSAT 4 MSS image is described. The geographical data sets consisted of silo range boundaries digitized from 1:250 000 maps, and soil potential contours generated by computer-aided modeling procedures. These geocoded geographical data were initially line segments represented by their coordinates. After rasterizing the geocoded data sets, they were overlaid on to classification maps generated from the LANDSAT data to calculate potential grain production per silo range. ESA

N87-18171*# National Aeronautics and Space Administration. Ames Research Center, Moffett Field, Calif.

REMOTE SENSING OF WETLAND PLANT STRESS

B. WOOD and L. BECK (California Univ., Berkeley) *In* ESA Proceedings of the 1986 International Geoscience and Remote Sensing Symposium (IGARSS '86) on Remote Sensing: Today's Solutions for Tomorrow's Information Needs, Volume 3 p 1383-1386 Aug. 1986

Avail: NTIS HC A21/MF A01; ESA, Paris, France, 3 volume set \$90 Member States, AU, CN, and NO (+20% others) CSCL 13B

High resolution laboratory, field, and airborne spectrometer data were correlated with plant tissue chemistry in order to characterize wetland plant spectral response due to high trace element concentrations. Wavelengths found to be important for distinguishing trace element stress were extended to broadband, regional remote sensing systems. Results indicate that LANDSAT Thematic Mapper bands 2, 3, and 5 may be the most useful for distinguishing between stressed and nonstressed wetland species. ESA

N87-18173# Technische Univ., Graz (Austria). Inst. for Image Processing and Computer Graphics.

INFLUENCE OF CANOPY SHADOW ON STRESS DETECTION IN CONIFEROUS FORESTS USING LANDSAT DATA

C. BANNINGER *In* ESA Proceedings of the 1986 International Geoscience and Remote Sensing Symposium (IGARSS '86) on Remote Sensing: Today's Solutions for Tomorrow's Information Needs, Volume 3 p 1397-1400 Aug. 1986

Avail: NTIS HC A21/MF A01; ESA, Paris, France, 3 volume set \$90 Member States, AU, CN, and NO (+20% others)

The effects of canopy shadow decreasing the spectral response of stressed canopies in the visible and shortwave near-infrared, contrary to what is expected in these spectral regions, on stress detection of coniferous forests by remote sensing systems are discussed. If a reduction in leaf pigment and water content also takes place, one would expect to see an increase in canopy reflectance in the visible and shortwave infrared LANDSAT bands, due to an increase in leaf transmittance and reflectance and a corresponding decrease in canopy shadow. This does not appear to happen, at least not in a sufficient amount to negate the increase in canopy shadow caused by morphological changes in the canopy. ESA

N87-18174# Technische Univ., Graz (Austria). Inst. for Image Processing and Computer Graphics.

RELATIONSHIP BETWEEN TREE DENSITY, LEAF AREA INDEX, SOIL METAL CONTENT, AND LANDSAT MSS CANOPY RADIANCE VALUES

C. BANNINGER *In* ESA Proceedings of the 1986 International Geoscience and Remote Sensing Symposium (IGARSS '86) on Remote Sensing: Today's Solutions for Tomorrow's Information Needs, Volume 3 p 1401-1404 Aug. 1986 Sponsored by the Austrian Ministry of Science and Research and the Syrian Scientific Research Office

Avail: NTIS HC A21/MF A01; ESA, Paris, France, 3 volume set \$90 Member States, AU, CN, and NO (+20% others)

Measurements from a coniferous tree stand in soils containing high concentrations of copper, lead, and zinc of soil metal concentrations and tree density and stem diameter helped to establish relationships between canopy structure (stand density and leaf area index), soil metal content, and LANDSAT canopy radiance values. Canopy properties that most affect the spectral response of metal-stressed coniferous tree stands in LANDSAT scene data were defined. Results suggest that subtle or incipient levels of heavy metal stress in coniferous trees are most likely manifested by morphological rather than physiological changes in a canopy, and that these changes are capable of being detected by rather coarse spatial, spectral, and radiometric resolution sensor systems operating from space platforms, such as the LANDSAT Multispectral Scanner. ESA

N87-18175*# Jet Propulsion Lab., California Inst. of Tech., Pasadena.

USE OF TMS/TM DATA FOR MAPPING OF FOREST DECLINE DAMAGE IN THE NORTHEASTERN UNITED STATES

B. N. ROCK and J. E. VOGELMANN *In* ESA Proceedings of the 1986 International Geoscience and Remote Sensing Symposium (IGARSS '86) on Remote Sensing: Today's Solutions for Tomorrow's Information Needs, Volume 3 p 1405-1410 Aug. 1986

Avail: NTIS HC A21/MF A01; ESA, Paris, France, 3 volume set \$90 Member States, AU, CN, and NO (+20% others) CSDL 02F

Remote sensing systems were used to monitor forest decline damage suspected of being due to air pollution. Field activities and aircraft overflights were centered on montane spruce/fir forest sites. Using aircraft data acquired with the Thematic Mapper Simulator (TMS) and LANDSAT Thematic Mapper (TM) during the growing season, extensive areas of forest decline damage were accurately mapped. Seven levels of decline damage are discriminated and mapped and the levels of discriminated damage agree well (rsq-0.94) with visual assessment conducted on the ground. New areas of high damage were discovered. A band ratio (TM5/TM4) is most useful in discriminating and quantifying the various levels of forest decline damage. ESA

N87-18183# Los Alamos Scientific Lab., N. Mex. Theoretical Div.

OFF-NADIR OPTICAL REMOTE SENSING FROM SATELLITES FOR VEGETATION IDENTIFICATION

S. A. W. GERSTL *In* ESA Proceedings of the 1986 International Geoscience and Remote Sensing Symposium (IGARSS '86) on Remote Sensing: Today's Solutions for Tomorrow's Information Needs, Volume 3 p 1457-1460 Aug. 1986

Avail: NTIS HC A21/MF A01; ESA, Paris, France, 3 volume set \$90 Member States, AU, CN, and NO (+20% others)

It is shown that angular reflectance distribution from vegetated surface in the visible and near infrared regimes contain angular signatures that may be used as crop identifiers. The canopy hot spot is such an angular signature and is invariant to atmospheric perturbations. It is proposed as a crop identifier from satellite observations. The value of angular signatures for scene identification is clearly established and considered complementary to the spectral signatures. Off-nadir satellite remote sensing of the Earth's land surface, which consists almost exclusively of non-Lambertian surfaces, may provide very valuable information for surface feature identification that is not otherwise attainable. The provision of directional pointing capabilities in future Earth observing satellites is thus highly desirable. ESA

N87-18184# Freiburg Univ. (West Germany). Inst. for Physical Geography.

MULTITEMPORAL ANALYSIS OF THE PHENOLOGICAL STAGE OF VEGETATION USING TM-DATA IN THE SOUTHERN BLACK FOREST (WEST GERMANY)

W. MAUSER *In* ESA Proceedings of the 1986 International Geoscience and Remote Sensing Symposium (IGARSS '86) on Remote Sensing: Today's Solutions for Tomorrow's Information Needs, Volume 3 p 1461-1464 Aug. 1986

Avail: NTIS HC A21/MF A01; ESA, Paris, France, 3 volume set \$90 Member States, AU, CN, and NO (+20% others)

A multitemporal dataset of a mountainous watershed was created including elevation, slope and aspect, LANDSAT Thematic Mapper bands 3 and 4 of 2 scenes taken in April and July, and the solar irradiance for each point at the time and date of each overflight. Through modeling of the irradiance, slope and aspect influences due to different illuminations were eliminated and the ratio -vegetation-index (RVI) of selected grass plots of different elevation and aspect was calculated for the two dates. The RVI shows an exponential decline with elevation in April, whereas in July the RVI of the grass areas is almost constant throughout the watershed. This shows that the RVI, after proper correction of illumination differences, can be used as indicator for the phenological stage of grassland in mountainous terrain. ESA

N87-18185# Environmental Research Inst. of Michigan, Ann Arbor.

VEGETATION AND SOILS INFORMATION CONTAINED IN TRANSFORMED THEMATIC MAPPER DATA

E. P. CRIST, R. LAURIN, and R. C. CICONE *In* ESA Proceedings of the 1986 International Geoscience and Remote Sensing Symposium (IGARSS '86) on Remote Sensing: Today's Solutions for Tomorrow's Information Needs, Volume 3 p 1465-1470 Aug. 1986

Avail: NTIS HC A21/MF A01; ESA, Paris, France, 3 volume set \$90 Member States, AU, CN, and NO (+20% others)

The LANDSAT Thematic Mapper (TM) Tasseled Cap data transformation method for reorienting TM data such that vegetation and soils information can be more easily extracted, displayed, and understood is outlined. The transformation applied as to any temperate climate scene produces invariant features which can be directly compared (i.e., between scenes or sensors), thereby simplifying the development of automatic signal processing algorithms and minimizing the need for recalibration of either algorithms or expectations (i.e., of human interpreters). In the TM Tasseled Cap features space, information on vegetation type, stage of development, and condition, and soil type and moisture status, is readily available. Atmospheric condition can be estimated from the data themselves, with minimal impact from ground class response differences. ESA

N87-18186# Ecole Polytechnique Federale de Lausanne (Switzerland). Inst. of Agricultural Engineering.

DESCRIPTION OF A METHODOLOGY FOR BIOMASS CHANGE MAPPING WITH THE USE OF LANDSAT TM DATA

R. CALOZ, B. ABEDNEGO, P. MEYLAN, and C. COLLET (Fribourg Univ., Switzerland) *In* ESA Proceedings of the 1986 International Geoscience and Remote Sensing Symposium (IGARSS '86) on Remote Sensing: Today's Solutions for Tomorrow's Information Needs, Volume 3 p 1471-1476 Aug. 1986

Avail: NTIS HC A21/MF A01; ESA, Paris, France, 3 volume set \$90 Member States, AU, CN, and NO (+20% others)

A methodology to obtain a vegetation change index (VCI) computed from non calibrated radiometric data in the red and near infrared bands is proposed. Perpendicular vegetation indices for two dates are first normalized and then subtracted to produce a VCI. The whole procedure was developed for an interactive user-friendly use on an I2S image processing system. It is illustrated with the use of two Thematic Mapper bands on a region of western Switzerland. ESA

N87-18187# Haryana Agricultural Univ., Hisar (India).

REMOTE SENSING APPLICATIONS IN THE STUDY OF LAND USE AND SOILS OF AEOLIAN COVER OF THE WESTERN PART OF HARYANA STATE, INDIA

V. P. GOYAL, S. DEV, J. NATH, and M. SINGH *In* ESA Proceedings of the 1986 International Geoscience and Remote Sensing Symposium (IGARSS '86) on Remote Sensing: Today's Solutions for Tomorrow's Information Needs, Volume 3 p 1477-1481 Aug. 1986

Avail: NTIS HC A21/MF A01; ESA, Paris, France, 3 volume set \$90 Member States, AU, CN, and NO (+20% others)

Multispectrum and multitemporal LANDSAT false color composites of 1:250,000, and transparencies on 1:1 million scales of bands 4,5,6, and 7 were interpreted to identify and delineate areas under varying intensities of dunal activity in the western part of Haryana state comprising an area of 12610 sq.km. Some CCTs of representative areas were also interpreted on the Multispectral Interactive Data Analysis System. Field checks were made to correlate the laboratory interpretation and the ground truth. The study area was differentiated into: sandy desert zone: no cultivation on dune tops except some shrubs; aeolian cover with sandy hummocks: low intensity cultivation; plain with aeolian cover: moderately cultivated; plain: moderately to intensively cultivated. ESA

N87-18193# IBM France S. A., Paris. Centre Scientifique.
FIRST STEP IN THE USE OF REMOTE SENSING FOR REGIONAL MAPPING OF SOIL ORGANIZATION DATA: APPLICATION IN BRITTANY (FRANCE) AND FRENCH GUIANA

M. DOSSO and F. SEYLER (Societe Europeenne de Propulsion, Puteaux, France) /n ESA Proceedings of the 1986 International Geoscience and Remote Sensing Symposium (IGARSS '86) on Remote Sensing: Today's Solutions for Tomorrow's Information Needs, Volume 3 p 1521-1524 Aug. 1986

Avail: NTIS HC A21/MF A01; ESA, Paris, France, 3 volume set \$90 Member States, AU, CN, and NO (+20% others)

Two analyses showing correlations between soil organization data and aerial photography features are presented. Image processing is useful to express structural pedological information which is present in the pictures. ESA

N87-18207# Oldenburg Univ. (West Germany).
LASER-INDUCED CHLOROPHYLL-A FLUORESCENCE OF TERRESTRIAL PLANTS

R. ZIMMERMANN and K. P. GUENTHER /n ESA Proceedings of the 1986 International Geoscience and Remote Sensing Symposium (IGARSS '86) on Remote Sensing: Today's Solutions for Tomorrow's Information Needs, Volume 3 p 1609-1613 Aug. 1986

Avail: NTIS HC A21/MF A01; ESA, Paris, France, 3 volume set \$90 Member States, AU, CN, and NO (+20% others)

A modified oceanographic lidar system operating over forest regions detected the chlorophyll A fluorescence at 685 nm and 735 nm. Inspecting the fluorescence signal ratio along the flight lines confirms that the fluorescence ratio reflects the physiological state of the plant. Results correspond to the evaluation of multispectral scanner data and terrestrial investigation. ESA

N87-18220# Freiburg Univ. (West Germany). Abteilung Luftbildmessung und Fernerkundung.

FOREST COVER ANALYSIS USING SIR-B DATA

D. A. ANTHONY /n ESA Proceedings of the 1986 International Geoscience and Remote Sensing Symposium (IGARSS '86) on Remote Sensing: Today's Solutions for Tomorrow's Information Needs, Volume 3 p 1683-1688 Aug. 1986

Avail: NTIS HC A21/MF A01; ESA, Paris, France, 3 volume set \$90 Member States, AU, CN, and NO (+20% others)

Synthetic aperture radar L-band HH polarized data were obtained by SIR-B over a forest, to analyze the digitally obtained SIR-data at 41 deg incidence angle. Density slicing and visual interpretation of single radar images shows no further discriminations than forest/nonforest. The test area was segmented into individual stands based on the ground inventory data. The quantitative evaluation of the backscattering signatures shows that five different forest cover types can be determined although classification is made difficult if the stands have the same structure. ESA

N87-18222*# Reading Univ. (England). Dept. of Geography.
MONITORING SEDIMENT TRANSFER PROCESSES ON THE DESERT MARGIN

ANDREW C. MILLINGTON, R. JONES ARWYN, NEIL QUARMBY, and JOHN R. G. TOWNSHEND 1987 47 p
 (NASA-CR-180181; NAS 1.26:180181) Avail: NTIS HC A03/MF A01 CSCL 08H

LANDSAT Thematic Mapper and Multispectral Scanner data have been used to construct change detection images for three playas in south-central Tunisia. Change detection images have been used to analyze changes in surface reflectance and absorption between wet and dry season (intra-annual change) and between different years (inter-annual change). Change detection imagery has been used to examine geomorphological changes on the playas. Changes in geomorphological phenomena are interpreted from changes in soil and foliar moisture levels, differences in reflectances between different salt and sediments and the spatial expression of geomorphological features. Intra-annual change phenomena that can be detected from

multidate imagery are changes in surface moisture, texture and chemical composition, vegetation cover and the extent of aeolian activity. Inter-annual change phenomena are divisible into those restricted to marginal playa facies (sedimentation from sheetwash and alluvial fans, erosion from surface runoff and cliff retreat) and these are found in central playa facies which are related to the internal redistribution of water, salt and sediment. Author

N87-18912*# Illinois Natural History Survey, Champaign. Section of Botany and Plant Pathology.

INTERPRETING FOREST AND GRASSLAND BIOME PRODUCTIVITY UTILIZING NESTED SCALES OF IMAGE RESOLUTION AND BIOGEOGRAPHICAL ANALYSIS Progress Report

LOUIS R. IVERSON, ELIZABETH A. COOK, ROBIN L. GRAHAM, JERRY S. OLSON, THOMAS FRANK, YING KE, COLIN TREWORYG, and PAUL G. RISSER 4 Feb. 1987 35 p Prepared in cooperation with Oak Ridge National Lab., Tenn.

(Contract NAS5-28781)

(NASA-CR-180213; TMWR-PR-3; NAS 1.26:180213;

TS-BPP-1987-1) Avail: NTIS HC A03/MF A01 CSCL 05B

This report summarizes progress made in our investigation of forest productivity assessment using TM and other biogeographical data during the third six-month period of the grant. Data acquisition and methodology hurdles are largely complete. Four study areas for which the appropriate TM and ancillary data were available are currently being intensively analyzed. Significant relationships have been found on a site by site basis to suggest that forest productivity can be qualitatively assessed using TM band values and site characteristics. Perhaps the most promising results relate TM unsupervised classes to forest productivity, with enhancement from elevation data. During the final phases of the research, multi-temporal and regional comparisons of results will be addressed, as well as the predictability of forest productivity patterns over a large region using TM data and/or TM nested within AVHRR data. Author

N87-18916# Los Alamos National Lab., N. Mex. Theoretical Div.

OFF-NADIR OPTICAL REMOTE SENSING FROM SATELLITES FOR VEGETATION IDENTIFICATION

S. A. W. GERSTL 30 May 1986 5 p Presented at the IGARSS '86 Symposium, Zurich, Switzerland, 8 Sep. 1986

(Contract W-7405-ENG-36)

(DE86-012387; LA-UR-86-1927; CONF-860997-1) Avail: NTIS HC A02/MF A01

Today's satellite remote sensing systems rely heavily on spectral signatures for scene identification from nadir observations. We propose to use angular signatures as complementary scene identifiers when off-nadir sensing is possible. Specifically, the hot spot (Heiligenschein) of plant canopies is recognized as an atmosphere-invariant angular reflectance signature that carries information about the plant stand architecture which may be useful for instant crop identification from off-nadir satellite measurements. DOE

N87-18919# National Aerospace Lab., Amsterdam (Netherlands). Space Div.

THE PROCESSING OF AND INFORMATION EXTRACTION FROM AIRBORNE SLAR DATA

P. BINNENKADE 24 Dec. 1985 23 p Presented at a Canada Center for Remote Sensing Seminar, Ottawa, Canada, 10 Oct. 1985

(NLR-MP-86004-U; B8679799; ETN-87-99511; AD-B107864L)

Avail: NTIS HC A02/MF A01

Side-looking airborne radar crop identification in The Netherlands is discussed. Only a selected number of crops may be unambiguously identified, and crop growth stages must be closely monitored in order to select optimal flight dates and acquisition geometry. In order to proceed to operational conditions it is necessary to include internal and external calibration of the radar to allow for cross-comparison of data. Although external targets (corner reflectors) were placed at a number of locations

throughout the test areas, consequences on processing and classification need further evaluation. It is argued that airborne programs will become largely obsolete due to the multitemporal and synoptic characteristics of spaceborne systems. ESA

N87-19786# Instituto de Pesquisas Espaciais, Sao Jose dos Campos (Brazil).

AGRICULTURAL CROP ESTIMATES USING INFORMATION GATHERED BY REMOTE SENSING SATELLITES, AS WELL AS GROUND DATA, THROUGH SAMPLES OF GEOGRAPHIC LAYERS [ESTIMATIVA DE SAFRAS AGRICOLAS UTILIZANDO DADOS COLETADOS POR SATELITES DE SENSORIAMENTO REMOTO E DADOS TERRESTRES, ATRAVES DE AMOS TRAS DE SUBSTRATOS GEOGRAFICOS]

THELMA KRUG and CORINA DACOSTAFREITASYANASSE Jan. 1986 48 p In PORTUGUESE; ENGLISH summary (INPE-4102-RPE/534) Avail: NTIS HC A03/MF A01

A statistical methodology is presented for estimating areas cultivated with several cultures using information gathered by the LANDSAT satellite, as well as ground data collected by trained enumerators. Paper strata constructed within analysis district are used to improve the precision of the desired estimates. Direct expansion estimators to be used over ground data and regression estimator combining the results of LANDSAT classification with survey data on those areas where these two sources of data are available are proposed. Author

N87-19790# Instituto de Pesquisas Espaciais, Sao Jose dos Campos (Brazil).

CANASATE: SUGAR CANE MAPPING BY SATELLITE, AREA 3 [CANASATE- MAPEAMENTO DA CANA-DA-ACUCAR POR SATELITE - AREA 3]

FRANCISCO JOSE MENDONCA, DANIEL ALFREDO ROSENTHAL, KLEBER DEFARIA, MARCOS COVRE, RENATO DOSSANTOS, and RICARDO L. VIANNARODRIGUES Dec. 1986 20 p In PORTUGUESE; ENGLISH summary (INPE-4068-RPE/526) Avail: NTIS HC A02/MF A01

The CANASATE Project, Sugarcane Mapping by Satellite, has the objective of obtaining the spatial distribution and area estimations of sugarcane plantations, at national level, using remote sensing techniques. To achieve this objective, Brazil was divided into three areas: Area 1, which includes Rio de Janeiro, Sao Paulo and Parana states; Area 2, which includes Alagoas and Pernambuco states; and Area 3, which includes Minas Gerais, Espirito Santo, Goias and Mato Grosso do Sul states. The results are shown for Area 3, which represents approximately 7% of the national sugarcane plantations. Author

N87-19797# Technische Hogeschool, Delft (Netherlands). Dept. of Electrical Engineering.

BARE SOIL MEASUREMENTS WITH THE DELFT UNIVERSITY SCATTEROMETER (DUTSCAT) SYSTEM (L-BAND) Ph.D. Thesis

H. J. C. VANLEEUWEN 30 May 1986 75 p (REPT-64-220-86-T-1LH; ETN-87-99074) Avail: NTIS HC A04/MF A01

A pulse modulated radar obtained information about bare soils in agricultural fields. The radar signal was transmitted and received by the Delft University Scatterometer system in L-band. The corrections of the scatterometer data to obtain an accurate backscatter coefficient were performed by antenna measurements. The antenna radiation pattern and the maximal gain were determined. Ground truth measurements together with scatterometer data (at different incidence angles) were gathered to test the inverse use of a scatter model for bare soil. With the help of video recordings (airborne) angular dependency of the radar backscatter and its possible relation with the measured soil moisture content and roughness was confirmed by the model of Attema, Kats, and Krul (1982). ESA

N87-19826*# Washington State Univ., Pullman. Dept. of Agronomy and Soils.

SPECTRAL CHARACTERISTICS AND THE EXTENT OF PALEOSOLS OF THE PALOUSE FORMATION Semiannual Progress Report

B. E. FRAZIER, ALAN BUSACCA, YAAN CHENG, DAVID WHERRY, JUDY HART, and STEVE GILL 1987 22 p (Contract NAS5-28758)

(NASA-CR-180357; NAS 1.26:180357; SAPR-3) Avail: NTIS HC A02/MF A01 CSCL 08G

Thematic mapping data was analyzed and verified by comparison to previously gathered transect samples and to aerial photographs. A bare-soil field with exposed paleosols characterized by slight enrichment of iron was investigated. Spectral relationships were first investigated statistically by creating a data set with DN values spatially matched as nearly as possible to field sample points. Chemical data for each point included organic carbon, free iron oxide, and amorphous iron content. The chemical data, DN values, and various band ratios were examined with the program package Statistix in order to find the combinations of reflectance data most likely to show a relationship which would dependably separate the exposed paleosols from the other soils. Cluster analysis and Fastclas classification procedures were applied to the most promising of the band ratio combinations. B.G.

02

ENVIRONMENTAL CHANGES AND CULTURAL RESOURCES

Includes land use analysis, urban and metroplitan studies, environmental impact, air and water pollution, geographic information systems, and geographic analysis.

A87-23777 ACCURACY OF POPULATION ESTIMATION FROM MEDIUM-SCALE AERIAL PHOTOGRAPHY

C. P. LO (Georgia, University, Athens) IN: American Congress on Surveying and Mapping and American Society for Photogrammetry and Remote Sensing, Annual Convention, Washington, DC, Mar. 16-21, 1986, Technical Papers. Volume 4. Falls Church, VA, American Congress on Surveying and Mapping and American Society for Photogrammetry and Remote Sensing, 1986, p. 1-10. refs

An Old Delft Scanning Stereoscope with 4.5 times magnification, and 1:12,000 black-and-white panchromatic aerial photographs obtained on January 6, 1983, were used to estimate the population of Athens, Georgia. Land use and land cover checks were performed to identify residential structures and to establish a photointerpretation key which identified three dwelling types. Using population factors of 2, 3, and 4 per dwelling for multiunit, small single-family, and large single-family dwellings, respectively, comparison with population census data revealed a relative error of -1.74 percent, which was improved to +0.73 percent when the larger census tracts were used. R.R.

A87-23828 TECHNIQUES FOR DERIVING LAND USE INFORMATION FROM LANDSAT DATA THROUGH THE USE OF A GEOGRAPHIC INFORMATION SYSTEM

GARY S. SMITH (Vermont, University, Burlington) IN: American Congress on Surveying and Mapping and American Society for Photogrammetry and Remote Sensing, Annual Convention, Washington, DC, Mar. 16-21, 1986, Technical Papers. Volume 5. Falls Church, VA, American Congress on Surveying and Mapping and American Society for Photogrammetry and Remote Sensing, 1986, p. 243-249. refs

The use of geographic information systems to generate land use data from satellite imagery is examined. Geographic information systems can be grid, raster, polygon, or vector based.

The procedures for developing a geographic reference system are described. Techniques for reducing the spectral and spatial resolution limitations of classified satellite maps and improving the ability of the maps to classify heterogeneous areas are discussed. I.F.

A87-23829**DETECTION OF NEW URBAN BUILD-UP IN ARDMORE AND MCALESTER, OKLAHOMA USING LANDSAT MSS DATA**

ARTHUR J. RICHARDSON (USDA, Remote Sensing Research Unit, Weslaco, TX) and EARL BLAKLEY (USDA, South National Technical Center, Fort Worth, TX) IN: American Congress on Surveying and Mapping and American Society for Photogrammetry and Remote Sensing, Annual Convention, Washington, DC, Mar. 16-21, 1986, Technical Papers. Volume 5. Falls Church, VA, American Congress on Surveying and Mapping and American Society for Photogrammetry and Remote Sensing, 1986, p. 250-259. refs

A87-29007**PERFORMANCE OF LANDSAT-5 TM DATA IN LAND-COVER CLASSIFICATION**

MIKIHIRO IOKA and MASATO KODA (IBM Japan, Ltd., Science Institute, Tokyo, Japan) International Journal of Remote Sensing (ISSN 0143-1161), vol. 7, Dec. 1986, p. 1715-1728. Research supported by the National Land Agency of Japan. refs

An experimental analysis has been conducted on the performance of the new Landsat-5 Thematic Mapper (TM) data for detailed land-cover classification using a maximum-likelihood method. Data used is the TM test data of the Tokyo metropolitan area (path-107, row-035) of November 4, 1984. Map-precision geometric correction is performed and TM data are resampled to 30 m pixel spacing. The experiment is designed to determine how well TM categories land-cover types in comparison with the Detailed Numerical Information digitally formatted data (Geographical Survey Institute of Japan, 10 m spatial accuracy), together with ground truth data in a representative test area. Classification accuracy for aggregated 12 categories within the test area is about 47 percent with the application of the explicit filtering technique utilizing 3 x 3 neighborhood operations. This increases to 70 percent using a majority logic filter with a larger 5 x 5 neighborhood function. Associated with the classification accuracy, effects of the mixed pixels are also investigated. The results show that the improved characteristics of TM aided the overall classification accuracy.

Author

A87-30128* National Aeronautics and Space Administration. National Space Technology Labs., Bay Saint Louis, Miss.

USE OF TOPOGRAPHIC AND CLIMATOLOGICAL MODELS IN A GEOGRAPHICAL DATA BASE TO IMPROVE LANDSAT MSS CLASSIFICATION FOR OLYMPIC NATIONAL PARK

WILLIAM G. CIBULA (NASA, National Space Technology Laboratories, Bay St. Louis, MS) and MAURICE O. NYQUIST (National Park Service, Geographic Information Systems Field Unit, Denver, CO) Photogrammetric Engineering and Remote Sensing (ISSN 0099-1112), vol. 53, Jan. 1987, p. 67-75. NASA-supported research. refs

An unsupervised computer classification of vegetation/landcover of Olympic National Park and surrounding environs was initially carried out using four bands of Landsat MSS data. The primary objective of the project was to derive a level of landcover classifications useful for park management applications while maintaining an acceptably high level of classification accuracy. Initially, nine generalized vegetation/landcover classes were derived. Overall classification accuracy was 91.7 percent. In an attempt to refine the level of classification, a geographic information system (GIS) approach was employed. Topographic data and watershed boundaries (inferred precipitation/temperature) data were registered with the Landsat MSS data. The resultant boolean operations yielded 21 vegetation/landcover classes while maintaining the same level of classification accuracy. The final classification provided much better identification and location of the major forest types within the park at the same high level of

accuracy, and these met the project objective. This classification could now become inputs into a GIS system to help provide answers to park management coupled with other ancillary data programs such as fire management. Author

A87-30882**LAND APPLICATIONS FOR REMOTE SENSING FROM SPACE**

ROBERT N. COLWELL IN: Space science and applications: Progress and potential. New York, IEEE Press, 1986, p. 77-122. refs

The benefits and limitations of space-based remote sensing of the earth as a tool for resource mapping are discussed and illustrated with numerous photographic reproductions. The need for such capability, i.e., for a whole-earth view, is driven by an explosively increasing population growth rate, the finite, dwindling amount of accessible terrestrial resources, and the growth per capita demand for those resources. The methods used for applying remote sensing imagery for resource assessment are summarized, along with criteria for selecting the type of imagery to be collected and the constraints on the usefulness of the images. A comparison is made between the capabilities of spaceborne and airborne photography. Techniques which are used to enhance remotely-sensed images are illustrated with an integrated set of NOAA Nimbus 7 Coastal Zone Color Scanner images. M.S.K.

N87-15579# Universite Catholique de Louvain (Belgium). Inst. d'Astronomie et de Geophysique.

ESTIMATION OF SURFACE ALBEDO USING SATELLITE DATA. A SIMPLE FORMULATION FOR ATMOSPHERIC EFFECTS

J. L. MELICE /n ESA Proceedings of an International Satellite Land-Surface Climatology Project (ISLSCP) Conference p 263-265 May 1986

Avail: NTIS HC A99/MF A01

Using a short wave radiative transfer model, a simple formulation (a set of graphical representations) to help eliminate the effects of large aerosol amounts on measurements of surface albedo from LANDSAT multispectral scanner data was derived. Monitoring of surface reflectivity over large areas using the model may be performed after determining the spectral reflectivity of calibration areas from ground truth observations. The total optical depth over the calibration area may then be determined and, after assuming that the aerosol concentration is laterally homogeneous, this optical depth may be used to recover the albedo of large surfaces surrounding the calibration area. Limitations of the method are outlined. ESA

N87-17175# Instituto de Pesquisas Espaciais, Sao Paulo (Brazil).

ENVIRONMENTAL MODIFICATION OF METROPOLITAN AREAS THROUGH SATELLITE IMAGES: STUDY OF URBAN DESIGN IN THE TROPICS

M. A. LOMBARDO /n ESA Proceedings of the 1986 International Geoscience and Remote Sensing Symposium (IGARSS '86) on Remote Sensing: Today's Solutions for Tomorrow's Information Needs, Volume 1 p 63-65 Aug. 1986

Avail: NTIS HC A99/MF E03; ESA, Paris, France, 3 volume set \$90 Member States, AU, CN, and NO (+20% others)

The application of remote sensing to identification of Sao Paulo's urban land use patterns, and the relationships between these uses and urban heat island effects, including air pollution, is described. Results show a pattern of temperature according to urban land use class. Highest temperatures are registered where the concentration of industries and buildings is heaviest. Conversely, municipalities, large green areas, and water reservoirs register the lowest readings. The horizontal thermal gradient in Sao Paulo, in stable atmospheric conditions, shows the greatest gradients in temperature. The thermal gradient intensity in the heat island is over 10 C, far surpassing measurements taken among cities in midlatitudes. ESA

N87-17388# World Meteorological Organization, Geneva (Switzerland).

AN OVERVIEW OF THE IMPLEMENTATION OF THE WORLD CLIMATE RESEARCH PROGRAM

THOMAS KANESHIGE *In* ESA Proceedings of an ESA Workshop on ERS-1 Wind and Wave Calibration p 169-172 Sep. 1986
 Avail: NTIS HC A11/MF A01

The meteorological, oceanic, satellite observation, data management, and global environmental monitoring aspects of the World Climate Research Program (WCRP) are outlined. The WCRP was established to study climate variability and its causes, of natural or human origin. The research strategy is formulated in terms of three specific objectives or streams. Each objective is a stepping stone for the next, which encompasses a wider range of interactions between the atmosphere, ocean, ice, and land surface, and calls for a more refined treatment of energy sources and sinks. ESA

N87-18151# Zurich Univ. (Switzerland). Dept. of Geography.
MONITORING LAND USE CHANGES IN SRI LANKA FOR LAND USE PLANNING USING A GEOGRAPHIC INFORMATION SYSTEM AND SATELLITE IMAGERY

P. SCHMID *In* ESA Proceedings of the 1986 International Geoscience and Remote Sensing Symposium (IGARSS '75) on Remote Sensing: Today's Solutions for Tomorrow's Information Needs, Volume 3 p 1259-1265 Aug. 1986
 Avail: NTIS HC A21/MF A01; ESA, Paris, France, 3 volume set \$90 Member States, AU, CN, and NO (+20% others)

A digital approach for updating land use maps is introduced. A geographic information system with information from existing maps and satellite imagery is used to update digitized land use maps for planning purposes. The superimposing of land use maps and satellite imagery simplifies the classification of the satellite images using the maps as digital masks. ESA

N87-18246# Washington Univ., St. Louis, Mo.
OZONE FORMATION IN POLLUTANT PLUMES: A REACTIVE PLUME MODEL WITH ARBITRARY CROSSWIND RESOLUTION Final Report

N. V. GILLANI Aug. 1986 96 p Sponsored by EPA (PB86-236973; EPA-600/3-86-051) Avail: NTIS HC A05/MF A01 CSCL 04A

A new two-layer reactive plume model is developed, in which arbitrary crosswind resolution of the emission field of each precursor is preserved, and dynamic plume-plume and plume-background interactions are explicitly accommodated. The model has a hybrid formulation, having Lagrangian downwind transport and Eulerian crosswind spread. It is applied in a diagnostic mode to simulate the observed behavior of plumes of the metropolitan St. Louis area and the Labadie power plant. The RAPS emissions inventory gave detailed spatial resolution of the emission field, numerous stationary and mobile upper air wind soundings provided the basis for transport simulation, and aircraft data provided detailed crosswind profiles of pollutant concentrations across the plumes at downwind sections. Model simulations of ozone were generally good, even in crosswind detail, given an appropriate background characterization. Simulated values of the rate of SO₂ oxidation were quantitatively not as satisfying. GRA

GEODESY AND CARTOGRAPHY

Includes mapping and topography.

A87-21931* Jet Propulsion Lab., California Inst. of Tech., Pasadena.

MOBILE VERY LONG BASELINE INTERFEROMETRY AND GLOBAL POSITIONING SYSTEM MEASUREMENT OF VERTICAL CRUSTAL MOTION

PETER M. KROGER, JOHN M. DAVIDSON (California Institute of Technology, Jet Propulsion Laboratory, Pasadena), and ELAINE C. GARDNER (Kalamazoo College, MI) *Journal of Geophysical Research* (ISSN 0148-0227), vol. 91, Aug. 10, 1986, p. 9169-9176. NASA-supported research. Previously announced in STAR as N86-10401. refs

Mobile Very Long Base Interferometry (VLBI) and Global Positioning System (GPS) geodetic measurements have many error sources in common. Calibration of the effects of water vapor on signal transmission through the atmosphere, however, remains the primary limitation to the accuracy of vertical crustal motion measurements made by either technique. The two primary methods of water vapor calibration currently in use for mobile VLBI baseline measurements were evaluated: radiometric measurements of the sky brightness near the 22 GHz emission line of free water molecules and surface meteorological measurements used as input to an atmospheric model. Based upon a limited set of 9 baselines, it is shown that calibrating VLBI data with water vapor radiometer measurements provides a significantly better fit to the theoretical decay model than calibrating the same data with surface meteorological measurements. The effect of estimating a systematic error in the surface meteorological calibration is shown to improve the consistency of the vertical baseline components obtained by the two calibration methods. A detailed error model for the vertical baseline components obtained indicates current mobile VLBI technology should allow accuracies of order 3 cm with WVR calibration and 10 cm when surface meteorological calibration is used. Author

A87-28442

THE SHAPE OF THE EARTH IN THE SPACE AGE [LA FIGURE DE LA TERRE A L'ERE SPATIALE]

JEAN KOVALEVSKY Academie des Sciences (Paris), *Comptes Rendus, Serie Generale, La Vie des Sciences* (ISSN 0762-0967), vol. 3, no. 4, July-Aug. 1986, p. 399-420. In French. refs

Geodesic measurements made of the shape of the earth using instrumentation with space-based components are described. Precise measurements became possible with laser systems for bouncing beams off satellites and reflectors on the moon. Accurate satellite orbit predictions are necessary to account for terrestrial flattening in the northern hemisphere, gravity waves and atmospheric drag. Simultaneous soundings of satellite position from several earth stations provide satisfactory data for the location of the satellite, and can therefore furnish data for determining the subsatellite geoid. Radio-based interferometry has proven reliable for determining the position of the poles and irregularities in the rotation of the earth. Sample geoid maps are provided from satellite soundings of the whole earth and for a small region of the Mediterranean Sea. M.S.K.

A87-28504

THE USE OF DOPPLER OBSERVATIONS TO OBTAIN INITIAL GEODETIC DATA AND TO DERIVE PLUMBLINE DEVIATIONS AND QUASI-GEOID HEIGHTS [ISPOL'ZOVANIE DOPPLEROVSKIKH NABLIUDENII DLIA USTANOVLENIIA ISKHODNYKH GEODEZICHESKIKH DAT I VYVODA UKLONENII OTVESA I VYSOT KVAZIGEOIDA]

F. KH. LAN (Moskovskii Institut Inzhenerov Geodezii, Aerofotos'emki i Kartografii, Moscow, USSR) Geodeziia i Aerofotos'emka (ISSN 0536-101X), no. 4, 1986, p. 33-38. In Russian.

A87-29977* Colorado Univ., Boulder.

THE EARTH'S C21 AND S21 GRAVITY COEFFICIENTS AND THE ROTATION OF THE CORE

JOHN M. WAHR (Colorado University; Cooperative Institute for Research in Environmental Sciences, Boulder) Geophysical Journal (ISSN 0016-8009), vol. 88, Jan. 1987, p. 265-276. refs (Contract NAG5-485; NSF EAR-84-07110)

Observational results for the earth's C21 and S21 gravity coefficients can be used to constrain the mean equatorial rotation of the core with respect to the mantle. Current satellite gravity solutions suggest the equatorial rotation rate is no larger than 1 x 10 to the -7th times the earth's diurnal spin rate, a limit more than one order of magnitude smaller than the polar rotation rate inferred from the westward drift of the earth's magnetic field. The next generation gravity solutions should improve this constraint by more than one order of magnitude. Implications for the fluid pressure at the core-mantle boundary and for the shape of that boundary are discussed. Author

N87-17415*# Ohio State Univ., Columbus. Dept. of Geodetic Science and Surveying.

BASIC RESEARCH FOR THE GEODYNAMICS PROGRAM Semiannual Status Report, Jul. - Dec. 1986

Dec. 1986 20 p

(Contract NSG-5265; OSURF PROJ. 711055)

(NASA-CR-180137; NAS 1.26:180137; SASR-17) Avail: NTIS HC A02/MF A01 CSCL 08G

Further development of utility program software for analyzing final results of Earth rotation parameter determination from different space geodetic systems was completed. Main simulation experiments were performed. Results and conclusions were compiled. The utilization of range-difference observations in geodynamics is also examined. A method based on the Bayesian philosophy and entropy measure of information is given for the elucidation of time-dependent models of crustal motions as part of a proposed algorithm. The strategy of model discrimination and design of measurements is illustrated in an example for the case of crustal deformation models. B.G.

N87-17416*# Ohio State Univ., Columbus. Dept. of Geodetic Science and Surveying.

IMPROVEMENT OF THE EARTH'S GRAVITY FIELD FROM TERRESTRIAL AND SATELLITE DATA Status Report, 1 Nov. 1984 - 31 Dec. 1986

Jan. 1987 9 p

(Contract NGR-36-008-161; OSURF PROJ. 783210)

(NASA-CR-180139; NAS 1.26:180139; SR-42) Avail: NTIS HC A02/MF A01 CSCL 08G

The terrestrial gravity data base was updated. Studies related to the Geopotential Research Mission (GRM) have primarily considered the local recovery of gravity anomalies on the surface of the Earth based on satellite to satellite tracking or gradiometer data. A simulation study was used to estimate the accuracy of 1 degree-mean anomalies which could be recovered from the GRM data. Numerous procedures were developed for the intent of performing computations at the laser stations in the SL6 system to improve geoid undulation calculations. B.G.

N87-18225# Defense Mapping Agency, Washington, D.C. Hydrographic-Topographic Center.

PRELIMINARY EVALUATION OF DOPPLER-DETERMINED POLE POSITIONS COMPUTED USING WORLD GEODETIC SYSTEM 1984 Final Report

JOHN A. BANGERT and JAMES P. CUNNINGHAM Oct. 1986 13 p Presented at the 128th IAU/IAG Symposium on Earth Rotation and Reference Frames for Geodesy and Geodynamics, Coolfront, W. Va., 20-24 Oct. 1984

(AD-A173467) Avail: NTIS HC A02/MF A01 CSCL 08E

Since 1975, the Defense Mapping Agency (DMA) has been determining polar motion as a byproduct of computing the precise orbits of the Navy Navigation Satellite System (NNSS) satellites. The orbit determination process currently incorporates the NSWC 922 terrestrial reference system and the NWL 10E-1 Earth Gravitational Model (EGM) to degree 28 and order 27. The World Geodetic System 1984 (WGS 84), developed by DMA, will replace the NSWC 922/10E-1 system for NNSS orbit determination. The WGS 84 EGM to degree and order 41 will be used. This paper presents the results of two experiments which compared pole positions computed in the two systems. These comparisons indicate that use of WGS 84 improves agreement between pole position values resulting from the Nova-class satellite orbit solutions and the values determined by other modern techniques. GRA

N87-18908 Technische Hogeschool, Delft (Netherlands). Dept. of Geodesy.

HOMOGENEOUS PLATE DEFORMATIONS ON A SPHERE AS MONITORED BY SATELLITE LASER RANGING (SLR) NETWORKS ANALYZED WITH THE MULTI-EPOCH METHOD Thesis

B. J. DUESMANN 1986 184 p

(ETN-87-99221) Avail: NTIS HC A09

An expression between parameters describing the form of a satellite laser ranging network at different epochs and (spherical) parameters describing a matching deformation for each plate was derived. The deformation, the network, the measurements, and the reference coordinate system should fulfil the following conditions: all network sites are visited twice at least; the coordinates are given in orthonormal coordinate systems with corresponding covariance matrices; all network sites are known in one orthonormal reference coordinate system with a known absolute positioning; the deformation of a plate is small, homogeneous, and time-independent; and the size of each plate is limited. ESA

04

GEOLOGY AND MINERAL RESOURCES

Includes mineral deposits, petroleum deposits, spectral properties of rocks, geological exploration, and lithology.

A87-20689*

VOLCANOLOGY FROM SPACE - USING LANDSAT THEMATIC MAPPER DATA IN THE CENTRAL ANDES

P. W. FRANCIS and R. MCALLISTER EOS (ISSN 0096-3941), vol. 67, April 8, 1986, p. 170, 171.

(Contract NASW-4066; NAS5-28759)

The use of the Landsat thematic mapper to identify potentially active Andean volcanos and to study the history of individual volcanos is discussed. A thematic mapper image of the 6150-m-high Socompa volcano is presented and it is noted that TM data have played a valuable role in tracking debris streams in the avalanche derived from the different parts of the original volcanic edifice. The consequences of Landsat commercialization are considered. K.K.

A87-23782

ROCK TYPE DISCRIMINATION WITH AI-BASED TEXTURE ANALYSIS ALGORITHMS

SHIN-Y HSU (New York, State University, Binghamton, NY) IN: American Congress on Surveying and Mapping and American Society for Photogrammetry and Remote Sensing, Annual Convention, Washington, DC, Mar. 16-21, 1986, Technical Papers. Volume 4. Falls Church, VA, American Congress on Surveying and Mapping and American Society for Photogrammetry and Remote Sensing, 1986, p. 169-178. USAF-DARPA-sponsored research. refs

The goal of this study was to test whether it was possible to extract granite with Landsat MSS data in the arid regions of the United States. The test site for the experiments was the Duffer Peak Quadrangle, NV. The image processing methods examined include both supervised and unsupervised classification techniques. The training sets were independently selected by researchers associated with the U.S. Geological Survey. The results indicate that a combination of supervised and unsupervised classification methods can accurately delineate the boundary of the granite with a reasonable understanding that the Landsat sensed only the surficial material rather than the bedrock. From these experiments, it is reasonable to conclude that granite in arid regions can be extracted within a reasonable level of accuracy from Landsat MSS data. The decision maps from such automated analysis should be interpreted as a generalization of surficial material rather than the bedrock of the area. Author

A87-24274

GEOLOGICAL NATURE OF EARLY PRECAMBRIAN FORMATIONS (CONSIDERING THE EXAMPLE OF THE ANABAR SHIELD) [O GEOLOGICHESKOI PRIRODE RANNEDOKEM-BRIISKIKH OBRAZOVANII /NA PRIMERE ANABARSKOGO SHCHITA]

A. A. KUZNETSOV (Vsesoiuznyi Nauchno-Issledovatel'skii Geologicheskii Institut, Leningrad, USSR) Akademiia Nauk SSSR, Doklady (ISSN 0002-3264), vol. 290, no. 5, 1986, p. 1179-1183. In Russian. refs

The primordial nature of the catarchean-early Proterozoic crystalline formations making up the Anabar shield is analyzed on the basis of a variety of data, including Landsat observations. The shield is found to have a layered structure and a massively stratified rhythmic texture, consisting of geometrically regular layer-horizons, from several centimeters to several dozens of meters thick. B.J.

A87-24380

ANALYSIS OF CORRELATIONS BETWEEN STRUCTURAL ELEMENTS DETECTED ON SPACE IMAGES AND METALLOGENIC ZONES [OTSENKA KORRELIATSIONNYKH SVIAZEI MEZHDU STRUKTURNYMI ELEMENTAMI, VYIAVLENNYMI PO KOSMICHESKIM SNIMKAM, I METALLOGENICHESKIMI ZONAMI]

M. A. ARTAMONOV, V. M. MORALEV, D. G. RIKHTER, and O. G. SHEREMET (Proizvodstvennoe Geologicheskoe Ob'edinenie Aerogeologiya; AN SSSR, Institut Litosfery, Moscow, USSR) Issledovanie Zemli iz Kosmosa (ISSN 0205-9614), July-Aug. 1986, p. 42-50. In Russian. refs

Structural features recognized on space images and identified on a 1:5,000,000 space-geological map were correlated with locations of metallogenic zones in the northeastern Transbaikalian region, shown on a 1:2,500,000 metallogenic map. Two to three highly informative indicators were found for four out of the total six metallogenic zone types. These four zones are characterized by high coefficients of uniformity, defined as the degree of similarity between the lineament network on the reference sites and on the rest of the study area. I.S.

A87-24381

INTEGRATION OF SPACE-GEOLOGICAL AND GEOPHYSICAL METHODS IN REGIONAL AND LOCAL PREDICTIONS OF TECTONIC STRUCTURES IN THE CASPIAN DEPRESSION [KOMPLEKSIROVANIE KOSMOGEOLOGICHESKIKH I GEOFIZICHESKIKH METODOV PRI REGIONAL'NOM I LOKAL'NOM PROGNOZIROVANII TEKTONICHESKIKH STRUKTUR V PRIKASPIISKOI VPADINE]

V. IA. VOROBEV (Nizhne-Volzhskii Nauchno-Issledovatel'skii Institut Geologii i Geofiziki, Saratov, USSR) Issledovanie Zemli iz Kosmosa (ISSN 0205-9614), July-Aug. 1986, p. 51-60. In Russian. refs

A87-24382

IDENTIFICATION OF RECLAIMED LANDSCAPES OF BELORUSSIA FROM SPACE IMAGES [INDIKATSIIA MELIORIRUEMYKH LANDSHAFTOV BELORUSSII PO KOSMICHESKIM SNIMKAM]

V. I. MIKHAILOV (Belorusskii Politekhnikeskii Institut, Minsk, Belorussian SSR), V. N. GUBIN (Belorusskii Nauchno-Issledovatel'skii Geologorazvedochnyi Institut, Minsk, Belorussian SSR), and A. A. MAKAREVICH (Tsentral'nyi Nauchno-Issledovatel'skii Institut Kompleksnogo Ispol'zovaniia Vodnykh Resursov, Minsk, Belorussian SSR) Issledovanie Zemli iz Kosmosa (ISSN 0205-9614), July-Aug. 1986, p. 61-67. In Russian. refs

A87-24383

USE OF SPACE IMAGERY AND GEOPHYSICAL DATA IN METALLOGENIC PREDICTION STUDIES IN CENTRAL KYZYLKUM [ISPOL'ZOVANIE KOSMICHESKIKH SNIMKOV I GEOFIZICHESKIKH DANNYKH PRI PROGNOZNO-METALLOGENICHESKIKH ISSLEDOVANIIAKH V TSENTRAL'NYKH KYZYLKUMAKH]

G. V. GALPEROV, V. E. BOGATYREV, and A. V. PERTSOV (Proizvodstvennoe Geologicheskoe Ob'edinenie Aerogeologiya, Leningrad, USSR) Issledovanie Zemli iz Kosmosa (ISSN 0205-9614), July-Aug. 1986, p. 68-74. In Russian. refs

A87-24384

LINEMENTS OF EASTERN CUBA - GEOLOGICAL INTERPRETATION OF AERIAL AND SPACE IMAGERY [LINEAMENTY VOSTOKA KUBY - OPYT GEOLOGICHESKOI ITERPRETATSII AERO- I KOSMICHESKIKH IZOBRAZHENII]

V. I. MAKAROV, V. G. TRIFONOV, G. I. VOLCHKOVA, F. FORMEL, K. BREZHNIANSKII (AN SSSR, Geologicheskii Institut, Moscow, USSR; Academia de Ciencias de Cuba, Instituto de Geologia y Paleontologia, Havana, Cuba) et al. Issledovanie Zemli iz Kosmosa (ISSN 0205-9614), July-Aug. 1986, p. 75-85. In Russian. refs

A87-24866

STRUCTURE OF THE KERGUELEN PLATEAU PROVINCE FROM SEASAT ALTIMETRY AND SEISMIC REFLECTION DATA

MILLARD F. COFFIN, HUGH L. DAVIES (Bureau of Mineral Resources, Geology and Geophysics, Canberra, Australia), and WILLIAM F. HAXBY (Lamont-Doherty Geological Observatory, Palisades, NY) Nature (ISSN 0028-0836), vol. 324, Nov. 13, 1986, p. 134-136. refs

The results of a new analysis of the Kerguelen Plateau province's structure employing both Seasat and newly acquired multichannel seismic data for ground truth are reported. The northern sector is characterized by volcanism and a sedimentary basin; the southern sector by a broad anticlinal arch, major faulting, and a sedimentary basin; and the eastern sector by abyssal basin and bounding ridge. The three sectors argue for a more complex tectonic evolution of the feature than has been previously proposed. C.D.

A87-25588* Arkansas Univ., Fayetteville.

PRELIMINARY ANALYSES OF SIR-B RADAR DATA FOR RECENT HAWAII LAVA FLOWS

V. H. KAUPP, B. A. DERRYBERRY, H. C. MACDONALD (Arkansas, University, Fayetteville), L. R. GADDIS, P. J. MOUGINIS-MARK (Hawaii Institute of Geophysics, Honolulu) et al. Remote Sensing of Environment (ISSN 0034-4257), vol. 20, Dec. 1986, p. 283-290. refs

(Contract JPL-956925)

The Shuttle Imaging Radar (SIR-B) experiment acquired two L-band (23 cm wavelength) radar images (at about 28 and 48 deg incidence angles) over the Kilauea Volcano area of southeastern Hawaii. Geologic analysis of these data indicates that, although aa lava flows and pyroclastic deposits can be discriminated, pahoehoe lava flows are not readily distinguished from surrounding low return materials. Preliminary analysis of data extracted from isolated flows indicates that flow type (i.e., aa or pahoehoe) and relative age can be determined from their basic statistics and illumination angle. Author

A87-25890

EARTH SENSING - NEW TOOLS ENABLE SCIENTISTS TO GAIN INSIGHT INTO THE STRUCTURE OF OUR PLANET'S SURFACE

DAVID S. MEYER Commercial Space (ISSN 8756-4831), vol. 2, Fall 1986, p. 70, 71, 73.

The uses of a thematic mapper (TM) and imaging spectrometer to identify and map the earth's composition are evaluated. The TM detects mineral composition by measuring reflected solar radiation and the imaging spectrometer can directly identify and map minerals. The applications of the TM to the study of the Meatiq in the Eastern Desert of Egypt and of the TM and imaging spectrometer to the analysis of the Wind River Basin in Wyoming are described. The development of an expert system to interpret imaging spectrometer data is proposed and advances in image spectrometry are discussed. I.F.

A87-26532

METHODS OF GEOLOGICAL INTERPRETATION OF LINEAMENTS OF PLATFORM AREAS (WITH REFERENCE TO USTIURT) [PRIEMY GEOLOGICHESKOI INTERPRETATSII LINEAMENOV PLATFORMENNYKH TERRITORII /NA PRIMERE USTIURTA/]

M. I. BURLESHIN (Proizvodstvenno-Geologicheskoe Ob'edinenie Gidrospeitsgeologii, Moscow, USSR) Issledovanie Zemli iz Kosmosa (ISSN 0205-9614), Sept.-Oct. 1986, p. 26-36. In Russian. refs

Two approaches are suggested for geological interpretation of lineaments on satellite images. One, the geodynamic approach, is based on the analysis of geometrical characteristics of lineaments that vary with the geodynamic conditions. The geometric parameters analyzed in this approach include the lineament length, direction, and distribution density; the analysis includes examination of the relationship of the lineaments with plicative structures, systematic displacements by the lineaments of tectonic structures, and the characteristic features of the lineament pattern. The second approach to lineament interpretation, the landscape approach, relies entirely on the comparison of topographic characteristics of the lineaments. The use of each approach is illustrated by geological interpretation of the lineaments on the territory of the Ustiurt plateau. I.S.

A87-26533

THE PRINCIPLES AND PROCEDURES OF MODELING ORE-RELATED OBJECTS IN PREDICTIVE METALLOGENIC INVESTIGATIONS (USING SATELLITE-BORNE DATA) [PRINTSIPY I METODIKA MODELIROVANIIA RUDNYKH OB'EKTOV PRI PROGNOZNO-METALLOGENICHESKIKH ISSLEDOVANIIAKH /S ISPOL'ZOVANIEM KOSMICHESKOI INFORMATSII/]

M. A. BELOBORODOV and V. S. KOGEN (Proizvodstvennoe Geologicheskoe Ob'edinenie Aerogeologii, Moscow, USSR) Issledovanie Zemli iz Kosmosa (ISSN 0205-9614), Sept.-Oct. 1986, p. 37-43. In Russian. refs

Two classes of models for representing ore-related objects are described, along with the relevant implementation algorithms. One model class, the 'type model', represents an ordered description of the combination of the most typical features included in the model regardless of their occurrence outside the limits of an ore object. The other model type, the 'optimal model', is based on an ordered description of unique ore-related features selected from the features of the entire analyzed area, taking into account the distribution of the characteristics possessing predictive features outside known ore objects. The use of these model types is illustrated by developing ore cluster models from satellite-borne and field geological data. I.S.

A87-26534

QUANTITATIVE PROCESSING PROCEDURES AND THE INFORMATION CONTENT OF SPACE IMAGERY IN PREDICTIONS OF STRUCTURAL INHOMOGENEITIES OF THE SEDIMENTARY COVER [KOLICHESTVENNYE METODY OBRABOTKI I INFORMATIVNOST' KOSMICHESKIKH SNIMKOV PRI PROGNOZIROVANII STRUKTURNYKH NEODNORODNOSTEI OSADOCHNOGO CHEKHLA]

V. IA. VOROBEV and V. A. BASHMAKOV (Nizhne-Volzhskii Nauchno-Issledovatel'skii Institut Geologii i Geofiziki, Saratov, USSR) Issledovanie Zemli iz Kosmosa (ISSN 0205-9614), Sept.-Oct. 1986, p. 44-54. In Russian. refs

The steps of a quantitative processing scheme designed for obtaining predictive geological information from space photographs are described. Use of information-bearing indicators in developing a geological and geophysical model that represents the geology of a target is discussed. As an application example, the predictive value of space photography is demonstrated for the area of the Caspian Depression. I.S.

A87-28508

INVESTIGATION OF SPECTRAL CORRELATIONS OF VEGETATION GROWING ON DIFFERENT TYPES OF GEOLOGICAL STRUCTURES [ISSLEDOVANIE SPEKTRAL'NYKH KORRELIATSIONNYKH SVIAZEI RASTITEL'NYKH OBRAZOVANII, PROIZRASTAIUSHCHIKH NA RAZLICHNYKH GEOLOGICHESKIKH STRUKTURAKH]

N. P. LAVROVA, I. V. ALMAZOV, R. I. FIMIN, and V. N. OVECHKIN (Moskovskii Institut Inzhenerov Geodezii, Aerofotos'emki i Kartografii, Moscow, USSR) Geodeziia i Aerofotos'emka (ISSN 0536-101X), no. 4, 1986, p. 88-93. In Russian.

The paper describes a technique for determining correlations between the spectral brightness structure of the underlying surface and its geological properties on the basis of the statistical processing of aerial-photography data. The possibility of determining the petroleum content of a geological structure on the basis of brightness measurements is noted. Experimental results are presented. B.J.

A87-29010

A COMPARATIVE STUDY OF LINEAMENT ANALYSIS FROM DIFFERENT REMOTE SENSING IMAGERY OVER AREAS IN THE BENUE VALLEY AND JOS PLATEAU NIGERIA

B. N. KOOPMANS (International Institute for Aerospace Survey and Earth Sciences, Enschede, Netherlands) International Journal of Remote Sensing (ISSN 0143-1161), vol. 7, Dec. 1986, p. 1763-1771. refs

A comparison is made between lineament analyses made from side-looking radar (SLAR) imagery, Landsat and aerial photographs from an area on the Lamurde anticline (Benue Valley) and from an area of ring dyke complexes (Jos Plateau), Nigeria. Fault lineaments are, in general, well expressed on side-looking airborne radar with the exception of those lineaments orientated parallel or subparallel to the radar look direction. Look direction and radar incidence angle influence lineament detectability. Specifically the lineaments oriented perpendicular to the sun azimuth direction on the Landsat image were over-represented. Landsat, Slar and aerial photographs can be used in a complementary way; the first two for reconnaissance-type surveys and lineament analysis, the third for detailed surveying. Author

A87-29011

AN ANALYSIS OF GEOLOGIC LINEAMENTS SEEN ON LANDSAT MSS IMAGERY

A. J. PARSONS and R. J. YEARLEY (Keele, University, England) International Journal of Remote Sensing (ISSN 0143-1161), vol. 7, Dec. 1986, p. 1773-1782. refs

Lineament maps drawn from several Landsat images of a part of north Wales and western England display considerable variation in the number of lineaments identified. Analysis of the maps shows that it is not the case that maps with fewer lineaments are simply subsets of those with many lineaments. Rather, each map contains a high proportion of lineaments that are unique to it. Despite these differences, the same preferred lineament orientation is identified from almost all maps. These results imply that all available Landsat imagery may usefully contribute to a lineament analysis, little value may be placed on the density of lineaments seen on any one image and preferred lineament orientation is relatively easy to identify. It is concluded that guarded use may be made of lineament analysis in geology. Lineament maps may be employed to suggest hypotheses rather than to test them. Author

A87-30126

DISCRIMINATION OF ALTERED BASALTIC ROCKS IN THE SOUTHWESTERN UNITED STATES BY ANALYSIS OF LANDSAT THEMATIC MAPPER DATA

PHILIP A. DAVIS, PAT S. CHAVEZ, JR. (USGS, Flagstaff, AZ), and GRAYDON L. BERLIN (Northern Arizona University, Flagstaff, AZ) Photogrammetric Engineering and Remote Sensing (ISSN 0099-1112), vol. 53, Jan. 1987, p. 45-55. refs

Landsat Thematic Mapper image data were analyzed to determine their ability to discriminate red cone basalts from gray flow basalts and sedimentary country rocks for three volcanic fields in the southwestern United States. Analyses of all of the possible three-band combinations of the six nonthermal bands indicate that the combination of bands 1, 4, and 5 best discriminates among these materials. The color-composite image of these three bands unambiguously discriminates 89 percent of the mapped red volcanic cones in the three volcanic fields. Mineralogic and chemical analyses of collected samples indicate that discrimination is facilitated by the presence of hematite as a major mineral phase in the red cone basalts (hematite is only a minor mineral phase in the gray flow basalts and red sedimentary rocks). Discrimination between red cone basalts and red sedimentary rocks is aided by the presence of large quantities of carbonate, sulfate, and clay minerals in the sedimentary rocks. Author

A87-30884* California Univ., Los Angeles.

GEOPHYSICAL REMOTE SENSING

ROBERT L. MCPHERRON (California, University, Los Angeles) IN: Space science and applications: Progress and potential. New York, IEEE Press, 1986, p. 133-142. refs (Contract NGL-05-007-004)

The types of remote sensing images which have applications in geophysical studies are reviewed. Features of the Shuttle Imaging Radar, a synthetic aperture radar, are described and a sample image is provided to illustrate the capabilities for mapping large-scale geological structure. A combined Landsat-Seasat image is shown to yield data on crustal composition. Sea surface topographic features that result from gravitational effects are demonstrated to be amenable to characterization with another Seasat instrument, a radar altimeter. Magsat data allow identification of magnetic perturbations produced by crustal magnetization. Finally, auroral imagery gathered with the Atmospheric Dynamics Explorer are presented which show that the effects of particles bombarding the atmosphere can be detected at UV wavelengths. M.S.K.

N87-17117*# Arizona State Univ., Tempe. Dept. of Geology.

THERMAL IMAGING SPECTROSCOPY IN THE KELSO-BAKER REGION, CALIFORNIA

PHILIP R. CHRISTENSEN, MICHAEL C. MALIN, DONALD L. ANDERSON, and LINDA L. JARAMILLO In JPL, California Inst. of Technology The TIMS Data User's Workshop p 25-28 1 Nov. 1986

Avail: NTIS HC A05/MF A01 CSCL 14E

The ability of the Thermal Infrared Multispectral Scanner (TIMS) data to identify rock composition using thermal-infrared spectroscopy was assessed. A region was selected with a wide range of rock and soil types in an arid environment, and the spectra acquired by TIMS was compared to laboratory spectra of collected samples. A TIMS image was acquired of the Kelso-Baker region in the Mojave desert of California at a surface resolution of approximately 7 m. This image was then used to map the areal extent of each geologic component. The TIMS data provided an excellent means for discriminating and mapping rocks of very similar mineralogy. These findings suggest that thermal-infrared spectroscopy can provide a powerful tool for identifying and mapping rock composition on the Earth and other terrestrial planets. B.G.

N87-17118*# Jet Propulsion Lab., California Inst. of Tech., Pasadena. Geology Group.

LITHOLOGIC MAPPING OF SILICATE ROCKS USING TIMS

A. R. GILLESPIE In its The TIMS Data User's Workshop p 29-44 1 Nov. 1986

Avail: NTIS HC A05/MF A01 CSCL 08B

Common rock-forming minerals have thermal infrared spectral features that are measured in the laboratory to infer composition. An airborne Daedalus scanner (TIMS) that collects six channels of thermal infrared radiance data (8 to 12 microns), may be used to measure these same features for rock identification. Previously, false-color composite pictures made from channels 1, 3, and 5 and emittance spectra for small areas on these images were used to make lithologic maps. Central wavelength, standard deviation, and amplitude of normal curves regressed on the emittance spectra are related to compositional information for crystalline igneous silicate rocks. As expected, the central wavelength varies systematically with silica content and with modal quartz content. Standard deviation is less sensitive to compositional changes, but large values may result from mixed admixture of vegetation. Compression of the six TIMS channels to three image channels made from the regressed parameters may be effective in improving geologic mapping from TIMS data, and these synthetic images may form a basis for the remote assessment of rock composition. Author

N87-17119*# Nevada Univ., Reno. Dept. of Geological Sciences.

DETECTION AND MAPPING OF VOLCANIC ROCK ASSEMBLAGES AND ASSOCIATED HYDROTHERMAL ALTERATION WITH THERMAL INFRARED MULTIBAND SCANNER (TIMS) DATA COMSTOCK LODGE MINING DISTRICT, VIRGINIA CITY, NEVADA

JAMES V. TARANIK, AMY HUTSINPILLER, and MARCUS BORENGASSER *In* JPL, California Inst. of Technology The TIMS Data User's Workshop p 45-47 1 Nov. 1986
Avail: NTIS HC A05/MF A01 CSCL 08K

Thermal Infrared Multispectral Scanner (TIMS) data were acquired over the Virginia City area on September 12, 1984. The data were acquired at approximately 1130 hours local time (1723 IRIG). The TIMS data were analyzed using both photointerpretation and digital processing techniques. Karhuen-Loeve transformations were utilized to display variations in radiant spectral emittance. The TIMS image data were compared with color infrared metric camera photography, LANDSAT Thematic Mapper (TM) data, and key areas were photographed in the field. B.G.

N87-17120*# Geological Survey, Denver, Colo.
SIMULATION MODELING AND PRELIMINARY ANALYSIS OF TIMS DATA FROM THE CARLIN AREA AND THE NORTHERN GRAPEVINE MOUNTAINS, NEVADA

KEN WATSON, SUSANNE HUMMER-MILLER, and FRED A. KRUSE *In* JPL, California Inst. of Technology The TIMS Data User's Workshop p 48-49 1 Nov. 1986
Avail: NTIS HC A05/MF A01 CSCL 08B

A theoretical radiance model was employed together with laboratory data on a suite of igneous rock to evaluate various algorithms for processing Thermal Infrared Multispectral Scanner (TIMS) data. Two aspects of the general problem were examined: extraction of emissivity information from the observed TIMS radiance data, and how to use emissivity data in a way that is geologically meaningful. The four algorithms were evaluated for appropriate band combinations of TIMS data acquired on both day and night overflights of the Tuscarora Mountains, including the Carlin gold deposit, in north-central Nevada. Analysis of a color composited PC decorrelated image (Bands 3, 4, 5--blue/green/red) of the Northern Grapevine Mountains, Nevada, area showed some useful correlation with the regional geology. The thermal infrared region provides fundamental spectral information that can be used to discriminate the major rock types occurring on the Earth's surface. B.G.

N87-17121*# Jet Propulsion Lab., California Inst. of Tech., Pasadena.

APPLICATION OF TIMS DATA IN STRATIGRAPHIC ANALYSIS
H. R. LANG *In* its The TIMS Data User's Workshop p 50-52 1 Nov. 1986

Avail: NTIS HC A05/MF A01 CSCL 08B

An in-progress study demonstrates the utility of Thermal Infrared Multispectral Scanner (TIMS) data for unraveling the stratigraphic sequence of a western interior, North American foreland basin. The TIMS data can be used to determine the stratigraphic distribution of minerals that are diagnostic of specific depositional distribution. The thematic mapper (TM) and TIMS data were acquired in the Wind River/Bighorn area of central Wyoming in November 1982, and July 1983, respectively. Combined image processing, photogeologic, and spectral analysis methods were used to: map strata; construct stratigraphic columns; correlate data; and identify mineralogical facies. Author

N87-17125*# Forest Service, Atlanta, Ga.
LOCATING SUBSURFACE GRAVEL WITH THERMAL IMAGERY

DOUGLAS E. SCHOLEN, WILLIAM H. CLERKE, and DOUGLAS E. LUEPKE *In* JPL, California Inst. of Technology The TIMS Data User's Workshop p 59 1 Nov. 1986
Avail: NTIS HC A05/MF A01 CSCL 08G

A method was discussed for using 6 band thermal imagery to locate subsurface gravel deposits in vegetated areas. Geologic

history is reviewed to select potential areas of study. An overflight was made using a thermal scanner. The data were processed with a computerized system to delineate areas showing a quartz signature radiated by a gravel deposit. The method was developed during a search for gravel on National Forest land in Louisiana. Processed data from thermal imagery was compared with known gravel deposits and exploratory drill hole logs. A high correlation was noted for a wide range of deposits, from commercial pits to trace deposits only a foot thick. Overburden at these sites varied from zero to sixty feet, near the maximum annual penetration by the thermal wave. It was concluded that the method can be used to locate buried gravel deposits and that more time and effort are needed to verify the usefulness for developing gravel pits adjacent to proposed construction sites. Author

N87-17128*# Army Engineer Waterways Experiment Station, Vicksburg, Miss. Geotechnical Lab.

THE RED RIVER VALLEY ARCHEOLOGICAL PROJECT Abstract Only

JACK BENNETT, LAWSON SMITH, and MARK LAUSTRUP (Nebraska Univ., Omaha) *In* JPL, California Inst. of Technology The TIMS Data User's Workshop p 62 1 Nov. 1986
Avail: NTIS HC A05/MF A01 CSCL 08H

The Red River Valley Archeology Project is a long-term effort involving numerous individuals and institutions engaged in archeological investigations in the Texas and Oklahoma portions of the Red River Valley. To date the focus of the project was on site location. The project acquired both Thermal Infrared Multispectral Scanner (TIMS), TMS, and color infrared photographs over a significant portion of the project area in an effort to define signatures for archeological sites and to assist in the detailed geomorphological mapping of the flood plain. Preliminary analysis of acquired data indicates that both the TIMS and TMS can make a substantial contribution to landform definition, the identification of cultural resources, and to the clarification of site-landform correlations in this riverine environment. Author

N87-17129*# National Aeronautics and Space Administration, Goddard Space Flight Center, Greenbelt, Md.

THE PHYSICAL BASIS FOR SPECTRAL VARIATIONS IN THERMAL INFRARED EMITTANCE OF SILICATES AND APPLICATION TO REMOTE SENSING

LOUIS S. WALTER *In* JPL, California Inst. of Technology The TIMS Data User's Workshop p 63-64 1 Nov. 1986
Avail: NTIS HC A05/MF A01 CSCL 08G

The use of infrared spectroscopy for the remote characterization of planetary surfaces has received attention due to efforts in the investigation of these bodies from space. In the 8 to 14 micron region, a depression in the emittance spectra of rocks (sometimes called reststrahlen) is related to the fundamental stretching vibrations of Si-O bonds and shifts in the locations of this feature are ascribed to variations in rock composition. Thus, it should be possible to investigate, quantify, and model the relationships of reststrahlen spectral band location through silicate mineralogical composition to rock classification. This concept will be tested first through the use of laboratory-acquired data on the infrared spectra and mineralogy of selected mineral and rock samples. As a suitable classification model is developed, it will be tested through overflights of appropriate rock outcrops using the Thermal Infrared Multispectral Scanner (TIMS). B.G.

N87-17130*# Jet Propulsion Lab., California Inst. of Tech., Pasadena.

INFRARED SPECTROSCOPY FOR GEOLOGIC INTERPRETATION OF TIMS DATA

MARY JANE BARTHOLOMEW *In* its The TIMS Data User's Workshop p 65-66 1 Nov. 1986
Avail: NTIS HC A05/MF A01 CSCL 08G

The Portable Field Emission Spectrometer (PFES) was designed to collect meaningful spectra in the field under climatic, thermal, and sky conditions that approximate those at the time of the overflight. The specifications and procedures of PFES are discussed. Laboratory reflectance measurements of rocks and

04 GEOLOGY AND MINERAL RESOURCES

minerals were examined for the purpose of interpreting Thermal Infrared Multispectral Scanner (TIMS) data. The capability is currently being developed to perform direct laboratory measurement of the normal spectral radiance of Earth surface materials at low temperatures (20 to 30 C) at the Jet Propulsion Laboratory. B.G.

N87-17133*# Jet Propulsion Lab., California Inst. of Tech., Pasadena.

A GEOLOGIC ATLAS OF TIMS DATA

ELSA ABBOTT *In its* The TIMS Data User's Workshop p 74-75 1 Nov. 1986

Avail: NTIS HC A05/MF A01 CSCL 05B

In the three years since the first data were taken, it was well demonstrated that the Thermal Infrared Multispectral Scanner (TIMS), properly used, can be a most valuable tool for the geologist. Compilation of the TIMS data into a geological atlas was felt to be useful. Several data sets were extensively studied to establish TIMS as a geologic tool and to explore the optimum enhancement techniques. It was found that a decorrelation stretch of bands 1, 3, and 5 enhance the data to a form that is very useful and this enhancement will be used in the geologic atlas along with an accompanying geologic map and description. Many data sets are well published and familiar to TIMS users, but there are some sets that, for lack of time and funds, were not thoroughly studied or published. A short description of these least studied sets of data is presented. The images presented along with the many previously studied and published TIMS images constitute an enormously useful set of information for the geologist in the 8 to 10 micron range. B.G.

N87-17134*# Geological Survey, Reston, Va.

AIRBORNE THERMAL INFRARED MULTISPECTRAL SCANNER (TIMS) IMAGES OVER DISSEMINATED GOLD DEPOSITS, OSGOOD MOUNTAINS, HUMBOLDT COUNTY, NEVADA

M. DENNIS KROHN *In JPL*, California Inst. of Technology The TIMS Data User's Workshop (date) p 76-78 1 Nov. 1986

Avail: NTIS HC A05/MF A01 CSCL 08G

The U.S. Geological Survey (USGS) acquired airborne Thermal Infrared Multispectral Scanner (TIMS) images over several disseminated gold deposits in northern Nevada in 1983. The aerial surveys were flown to determine whether TIMS data could depict jasperoids (siliceous replacement bodies) associated with the gold deposits. The TIMS data were collected over the Pinson and Getchell Mines in the Osgood Mountains, the Carlin, Maggie Creek, Bootstrap, and other mines in the Tuscarora Mountains, and the Jerritt Canyon Mine in the Independence Mountains. The TIMS data seem to be a useful supplement to conventional geochemical exploration for disseminated gold deposits in the western United States. Siliceous outcrops are readily separable in the TIMS image from other types of host rocks. Different forms of silicification are not readily separable, yet, due to limitations of spatial resolution and spectral dynamic range. Features associated with the disseminated gold deposits, such as the large intrusive bodies and fault structures, are also resolvable on TIMS data. Inclusion of high-resolution thermal inertia data would be a useful supplement to the TIMS data. B.G.

N87-17136*# Cornell Univ., Ithaca, N.Y. Dept. of Geological Sciences.

TECTONIC GEOMORPHOLOGY OF THE ANDES WITH SIR-A AND SIR-B

ARTHUR L. BLOOM and ERIC J. FIELDING *In JPL* The Second Spaceborne Imaging Radar Symposium p 5-10 1 Dec. 1986

Avail: NTIS HC A10/MF A01 CSCL 08G

Data taken from SIR-A and SIR-B (Shuttle Imaging Radar) crossed all of the principal geomorphic provinces of the central Andes between 17 and 34 S latitude. In conjunction with Thematic Mapping images and photographs from hand-held cameras as well as from the Large Format Camera that was flown with SIR-B, the radar images give an excellent sampling of Andean geomorphology. In particular, the radar images show new details of volcanic rocks and landforms of late Cenozoic age in the Puna, and the exhumed

surfaces of tilted blocks of Precambrian crystalline basement in the Sierras Pampeanas. E.R.

N87-17137*# Chevron Oil Field Research Co., La Habra, Calif.

SPACE SHUTTLE RADAR IMAGES OF INDONESIA

FLOYD F. SABINS and JOHN P. FORD (Jet Propulsion Lab., California Inst. of Tech., Pasadena) *In JPL* The Second Spaceborne Imaging Radar Symposium p 11-16 1 Dec. 1986

Avail: NTIS HC A10/MF A01 CSCL 17I

Sabins (1983) interpreted Shuttle Imaging Radar (SIR)-A images of Indonesia; Sabins and Ford (1985) interpreted SIR-B images. These investigations had the following major results: (1) major lithologic assemblages are recognizable by their terrain characteristics in the SIR images, and (2) both local and regional geologic structures are mappable. These results are summarized.

Author

N87-17138*# Massachusetts Inst. of Tech., Cambridge. Earth Resources Lab.

DELINEATION OF FAULT ZONES USING IMAGING RADAR

M. N. TOKSOZ, L. GULEN, M. PRANGE, J. MATARESE, G. H. PETTENGILL, and P. G. FORD *In JPL* The Second Spaceborne Imaging Radar Symposium p 17-24 1 Dec. 1986

Avail: NTIS HC A10/MF A01 CSCL 08G

The assessment of earthquake hazards and mineral and oil potential of a given region requires a detailed knowledge of geological structure, including the configuration of faults. Delineation of faults is traditionally based on three types of data: (1) seismicity data, which shows the location and magnitude of earthquake activity; (2) field mapping, which in remote areas is typically incomplete and of insufficient accuracy; and (3) remote sensing, including LANDSAT images and high altitude photography. Recently, high resolution radar images of tectonically active regions have been obtained by SEASAT and Shuttle Imaging Radar (SIR-A and SIR-B) systems. These radar images are sensitive to terrain slope variations and emphasize the topographic signatures of fault zones. Techniques were developed for using the radar data in conjunction with the traditional types of data to delineate major faults in well-known test sites, and to extend interpretation techniques to remote areas. Author

N87-17139*# Geological Survey, Flagstaff, Ariz.

THE MEGAGEOMORPHOLOGY OF THE RADAR RIVERS OF THE EASTERN SAHARA

JOHN F. MCCAULEY, CAROL S. BREED, and GERALD G. SCHABER *In JPL* The Second Spaceborne Imaging Radar Symposium p 25-36 1 Dec. 1986

Avail: NTIS HC A10/MF A01 CSCL 08H

The Eastern Sahara is devoid of surface drainage; this unusual characteristic distinguishes its morphology from that of most other desert regions where running water dominates landscape development. A map derived from SIR-A/B and LANDSAT images and the literature, shows the major presently known paleodrainages in the Eastern Sahara. This compilation permits consideration of the key questions: Where did the radar rivers come from and where did they go? Analysis of SIR-A data led McCauley et al. to suggest that the radar rivers, because of their southwestward trends, once flowed into the Chad basin. This key North African feature is a regional structural low formed in the Early Cretaceous in response to initial opening of the South Atlantic. The problem of the origin of headwaters for the radar rivers was less tractable. The idea that the source areas of the radar rivers might originally have been the same as those later captured by the Nile was proposed tentatively. A more extensive review of the Cenozoic tectonic history of North Africa reveals no reason now to suppose that the Central African tributaries of the present Nile were ever connected to the large alluvial valleys in southwestern Egypt and northwestern Sudan, formed in the Early Cretaceous in response to initial opening of the South Atlantic. The problem of the origin of headwaters for the radar rivers was less tractable. The idea that the source areas of the radar rivers might originally have been the same as those (The Ethiopian Highlands) later captured by the Nile was proposed tentatively. A more extensive review of

the Cenozoic tectonic history of North Africa reveals no reason now to support that the Central African tributaries of the present Nile were ever connected to the large alluvial valleys in southwestern Egypt and northwestern Sudan. E.R.

N87-17140*# Jet Propulsion Lab., California Inst. of Tech., Pasadena.

GEOLOGICAL APPLICATIONS OF MULTIPOLARIZATION SAR DATA

DIANE L. EVANS *In its* The Second Spaceborne Imaging Radar Symposium p 36-41 1 Dec. 1986

Avail: NTIS HC A10/MF A01 CSCL 08G

Spaceborne Synthetic Aperture Radar (SAR) data acquired by SEASAT and the Shuttle Imaging Radar (SIR-A/B) operating at L-band with HH polarization were found to be useful in conjunction with other sensors for lithologic discrimination in arid environments with limited vegetation cover. In order to assess the utility of more advanced sensors for geologic research and define the unique contributions each sensor makes, remote sensing data were collected over the Deadman Butte area of the Wind River Basin, Wyoming. The Wind River Basin is an asymmetric sedimentary basin in central Wyoming created during the early Eocene Laramide orogeny. The stratigraphic section of the Deadman Butte study area, which was measured by Woodward is made up of Paleozoic and Mesozoic marine shales, siltstones, limestones, and sandstones. Sensor systems included LANDSAT 4 Thematic Mapper (TM), Thermal Infrared Multispectral Scanner (TIMS) and the Multipolarization, L-band airborne SAR, a prototype for the next Shuttle Imaging Radar (SIR-C). Sensor parameters are given. Author

N87-17146*# Jet Propulsion Lab., California Inst. of Tech., Pasadena.

A SCANNING RADAR ALTIMETER FOR MAPPING CONTINENTAL TOPOGRAPHY

T. H. DIXON *In its* The Second Spaceborne Imaging Radar Symposium p 84-88 1 Dec. 1986

Avail: NTIS HC A10/MF A01 CSCL 08B

Topographic information constitutes a fundamental data set for the Earth sciences. In the geological and geophysical sciences, topography combined with gravitational information provides an important constraint on the structure and rheologic properties of the crust and lithosphere. Detailed topography data can also be used to map offsets associated with faulting and to reveal the effects of tectonic deformation. In the polar regions, elevation data form a crucial but as yet largely unavailable resource for studying ice sheet mass balance and ice flow dynamics. The vast Antarctic ice sheet is the largest fresh water reservoir on Earth and is an important influence on ocean circulation and global climate. However, our knowledge of its stability is so limited that we cannot even specify whether the Antarctic ice sheet is growing or shrinking. It is clear that there is need for high quality global topography data. A summary of potential applications with their resolution requirements is shown. Author

N87-17232# Centre for Earth Science Studies, Trivandrum (India).

SIGNIFICANCE OF SPACE IMAGE, AIR PHOTO AND DRAINAGE LINEARS IN RELATION TO WEST COAST TECTONICS, INDIA

V. RAGHAVAN and D. CHANDRASEKHARAM (Centre for Water Resources Development and Management, Calicut, India) *In* ESA Proceedings of the 1986 International Geoscience and Remote Sensing Symposium (IGARSS '86) on Remote Sensing: Today's Solutions for Tomorrow's Information Needs, Volume 1 p 425-429 Aug. 1986

Avail: NTIS HC A99/MF E03; ESA, Paris, France, 3 volume set \$90 Member States, AU, CN, and NO (+20% others)

Lineament patterns over northern Kerala along the western continental margin of India (WCMI) were analyzed in conjunction with the structural, geochronological, and geological data to understand the structural and geomorphic evolution of WCMI. The NNW and ENE sets are subparallel to the basic dyke swarms in the region. Regional structural framework reveals that N-S

compressive stresses produced the NNW lineaments whereas the ENE trends represent younger tensional fractures developed due to near E-W compression. These fractures were periodically reactivated. Predominant air photo linears represent joints developed due to neotectonic stresses. Drainage development in the region is structurally controlled. Neotectonism involving vertical upliftment is suggested. ESA

N87-17233# University of North-Eastern Hill, Shillong (India). School of Environmental Sciences.

STRUCTURAL AND GEOMORPHIC EVOLUTION OF MEGHALAYA PLATEAU, INDIA ON LANDSAT IMAGERY

R. K. RAI *In* ESA Proceedings of the 1986 International Geoscience and Remote Sensing Symposium (IGARSS '86) on Remote Sensing: Today's Solutions for Tomorrow's Information Needs, Volume 1 p 431-435 Aug. 1986

Avail: NTIS HC A99/MF E03; ESA, Paris, France, 3 volume set \$90 Member States, AU, CN, and NO (+20% others)

The remote areas of North East Region of India were studied by LANDSAT imagery to analyze geological, structural, and geomorphological characteristics. The potential of LANDSAT imagery for structural and geomorphic evolution studies of Meghalaya Plateau is shown. Results indicate that rivers adapted their courses to regional structure and lineaments. All the major lineaments run in SW-NE direction. Field evidence such as deep gorges, waterfalls, river terraces, and breaks in slopes indicate that the plateau presents multicyclic surfaces at different altitudes. ESA

N87-17234# Karlsruhe Univ. (West Germany). Inst. fuer Photogrammetrie und Topographie.

HYDROGEOLOGICAL RESEARCH IN PELOPONNESUS (GREECE) KARST AREA BY SUPPORT AND COMPLETION OF LANDSAT-THEMATIC DATA

H. KAUFMANN, B. REICHAERT, and H. HOETZL *In* ESA Proceedings of the 1986 International Geoscience and Remote Sensing Symposium (IGARSS '86) on Remote Sensing: Today's Solutions for Tomorrow's Information Needs, Volume 1 p 437-441 Aug. 1986

Avail: NTIS HC A99/MF E03; ESA, Paris, France, 3 volume set \$90 Member States, AU, CN, and NO (+20% others)

Karst drainage from Peloponnesian catchment areas to springs at the coast, and possible pathways to win the fresh water before its submarine discharge were investigated, using high resolution satellite data to support and complement hydrogeological research. The derived fracture pattern, separated into strike-slip faults and joints by field check, and combined with known karst cavities and tracer experiments, gives results for possible underground pathways of the water. By use of a special band combination of the reflective data, the recharge area is subdivided into several categories. Several submarine springs near the coast are detected by the thermal band of the LANDSAT Thematic Mapper. ESA

N87-17235# Centre for Earth Science Studies, Trivandrum (India).

COMPUTER-AIDED ANALYSIS OF LANDSAT DATA FOR MAPPING GEOLOGIC AND GEOMORPHIC FEATURES, NORTH BOMBAY, INDIA

V. RAGHAVAN, S. M. TARIQUE (Aligarh Muslim Univ., India), and A. T. PEDROFERNANDES (Directorate of Mines and Industries, Panjim, India) *In* ESA Proceedings of the 1986 International Geoscience and Remote Sensing Symposium (IGARSS '86) on Remote Sensing: Today's Solutions for Tomorrow's Information Needs, Volume 1 p 443-447 Aug. 1986

Avail: NTIS HC A99/MF E03; ESA, Paris, France, 3 volume set \$90 Member States, AU, CN, and NO (+20% others)

Geologic and geomorphic information extraction from remotely sensed data using visual and computer aided techniques were attempted for a test area in North Bombay. Visual interpretations of LANDSAT images offer a limited possibility to demarcate terrain units. Computer aided analysis discriminates nine distinct spectral classes that correspond to various geomorphic/geologic units in the area. A combination of visual and computer aided techniques

04 GEOLOGY AND MINERAL RESOURCES

in addition to field data enables the preparation of thematic maps. ESA

N87-17236# Geological Survey of India, Jaipur. Photogeology and Remote Sensing Div.

COMPARATIVE STUDY OF LANDSAT MSS, SALLYUT-7 (TERRA) AND RADAR (SIR-A) IMAGES FOR GEOLOGICAL AND GEOMORPHOLOGICAL APPLICATIONS: A CASE STUDY FROM RAJASTHAN AND GUJARAT, INDIA

P. C. BAKLIWAL *In* ESA Proceedings of the 1986 International Geoscience and Remote Sensing Symposium (IGARSS '86) on Remote Sensing: Today's Solutions for Tomorrow's Information Needs, Volume 1 p 449-452 Aug. 1986
Avail: NTIS HC A99/MF E03; ESA, Paris, France, 3 volume set \$90 Member States, AU, CN, and NO (+20% others)

Rajasthan and Gujarat provinces of India were surveyed using the MKF-6 multispectral and KATE-140 stereo space photographs collected during TERRA experiment and SIR-A radar data acquired during the flight of Columbia Space Shuttle on Nov. 12, 1981. A comparative evaluation of these data for geological applications indicates that lithological discrimination is possible from SIR-A due to differential surface roughness and from KATE-140 due to stereo vision. Structural elements on SIR-A and KATE-140 are better interpreted. Radar data is most suitable for different surface covers and thus provides better details for geomorphic mapping. It is also found that MKF-6 and LANDSAT MSS data provide better data on geomorphology in decreasing order; KATE-140 provides altitude variations and is, therefore, most helpful in pediplain areas. ESA

N87-17242# Stanford Univ., Calif. Dept. of Applied Sciences. **INTERRELATIONSHIP BETWEEN FIELD SPECTRA AND AIRBORNE MSS SYSTEMS IN THE SINGATSE RANGE, (YERINGTON) NEVADA**

R. J. P. LYON *In* ESA Proceedings of the 1986 International Geoscience and Remote Sensing Symposium (IGARSS '86) on Remote Sensing: Today's Solutions for Tomorrow's Information Needs, Volume 1 p 481-484 Aug. 1986
Avail: NTIS HC A99/MF E03; ESA, Paris, France, 3 volume set \$90 Member States, AU, CN, and NO (+20% others)

Two stages of Singatse Range (Nevada) classical hydrothermal alterations of the felsic rock minerals to clays and other hydrous-bearing materials were mapped: early hypogene were associated with the Jurassic porphyry dike intrusion, and later geothermal (Jurassic/Cretaceous), associated with the circulation of meteoritic waters beneath the cogenetic volcanic pile. The whole rock mass of the Singatse Range was rotated 70 degW, so that what was once vertical is now flat-lying exposed over the 6Km of outcrop trending 290 deg (ESE-WNW) across the range. Due to the long thin nature of the economically-interesting target (hydrothermal alteration) aircraft flights were flown as parallel lines with this 290 deg trend. Spectral absorptions due to clay minerals in the hydrothermally-altered rocks can be seen readily in band-ratio imagery, from LANDSAT TM, TMS, and AIS digital data sets. Comparable spectral evidence can be seen in data from repeated flights over the same terrain, ground spectral measurements confirm the types of O-H bearing minerals seen in the flight data. ESA

N87-17243# Consiglio Nazionale delle Ricerche, Frascati (Italy). Ist. Astrofisica.

INTEGRATED ANALYSIS OF GEOLOGICAL AND REMOTE SENSING DATA AIMED AT MINERAL DEPOSITS DETECTION IN THE MONAPO AREA (NORTHERN MOZAMBIQUE)

M. POSCOLIERI, M. LORENZINI, G. ONORATI, and S. SALVI *In* ESA Proceedings of the 1986 International Geoscience and Remote Sensing Symposium (IGARSS '86) on Remote Sensing: Today's Solutions for Tomorrow's Information Needs, Volume 1 p 485-490 Aug. 1986

Avail: NTIS HC A99/MF E03; ESA, Paris, France, 3 volume set \$90 Member States, AU, CN, and NO (+20% others)

Geophysical, geological, geomorphological, and LANDSAT spectral data, concerning the Monapo Klippe area (Northern

Mozambique) were retrieved for ore bodies research. Variables were analyzed through an approach that allows the user to integrate different sources of digital data and to infer the relationships among them, using display, mapping, and statistical analysis. On the basis of the interpretation of the relationships among multisource data, geological structures indicating mineral interest zones were sought. The importance of circular structures and lineaments swarms for the emplacement of pegmatites and mineralized bodies was assessed. A hypothesis concerning mutual relationships among late Precambrian tectonic episodes was formulated for the study area. ESA

N87-17244# Stockholm Univ. (Sweden). Dept. of Physical Geography.

A STATISTICAL APPROACH TO SELECT THE OPTIMAL WAVELENGTH BANDS FOR SEPARATING ROCKS IN THE WAVELENGTH REGION 0.4 TO 2.3 MICRONS

K. WESTER and B. LUNDEN *In* ESA Proceedings of the 1986 International Geoscience and Remote Sensing Symposium (IGARSS '86) on Remote Sensing: Today's Solutions for Tomorrow's Information Needs, Volume 1 p 491-494 Aug. 1986

Avail: NTIS HC A99/MF E03; ESA, Paris, France, 3 volume set \$90 Member States, AU, CN, and NO (+20% others)

The use of laboratory measured spectral signatures for separation of rock types is considered. Spectral reflectances of different rock types (acid, semiacid, and basic) were measured in the laboratory using a reflectometer. The laboratory measured spectra provide a useful basis for determining the separability and the best wavelength regions for discrimination of the rock types. For the analysis, eight bands were used, LANDSAT Thematic Mapper bands plus two more bands in the near infrared. The used algorithm, a discriminant analysis for computer based comparisons of the different rock types, is described. The spectral signatures, the ranking for the best bands, combinations of bands, and the classification accuracy are discussed. ESA

N87-17246* # Dartmouth Coll., Hanover, N.H. Dept. of Earth Sciences.

DISCRIMINATION OF LITHOLOGIC UNITS USING GEOBOTANICAL AND LANDSAT TM SPECTRAL DATA

R. W. BIRNIE and N. J. DEFEO *In* ESA Proceedings of the 1986 International Geoscience and Remote Sensing Symposium (IGARSS '86) on Remote Sensing: Today's Solutions for Tomorrow's Information Needs, Volume 1 p 503-506 Aug. 1986

(Contract NASW-4049; JPL-956937)

Avail: NTIS HC A99/MF E03; ESA, Paris, France, 3 volume set \$90 Member States, AU, CN, and NO (+20% others) CSCL 08B

Thematic Mapper (TM) spectral data were correlated with lithologic units, geobotanical forest associations, and geomorphic site parameters in the Ridge and Valley Province of Pennsylvania. Both the TM and forest association data can be divided into four groups based on their lithology (sandstone or shale) and geomorphic aspect (north or south facing). In this clastic sedimentary terrane, geobotanical associations are useful indicators of lithology and these different geobotanical associations are detectable in LANDSAT TM data. ESA

N87-17247# Karlsruhe Univ. (West Germany). Inst. fuer Photogrammetrie und Topographie.

RESULTS OF TECTONIC AND SPECTRAL INVESTIGATIONS ALONG THE WADI ARABA FAULT IN JORDAN USING SPECIAL PROCESSED THEMATIC MAPPING (TM) DATA

H. KAUFMAN *In* ESA Proceedings of the 1986 International Geoscience and Remote Sensing Symposium (IGARSS '86) on Remote Sensing: Today's Solutions for Tomorrow's Information Needs, Volume 1 p 507-512 Aug. 1986

Avail: NTIS HC A99/MF E03; ESA, Paris, France, 3 volume set \$90 Member States, AU, CN, and NO (+20% others)

Tectonic and lithological investigations carried out in the Wadi Araba-Jordan graben area were supported by use of

LANDSAT/Thematic Mapper data. A processing concept was developed to satisfy the requirements for several user groups. Use of the data sets to complete supraregional tectonic research is discussed. The applicability of the processed data for registration of hydrothermal alteration minerals is demonstrated. The detection of an Fe-deposit is illustrated. ESA

N87-17248# Geological Survey of Canada, Ottawa (Ontario). Mineral Resources Div.

INTEGRATION OF SURFICIAL GEOCHEMISTRY AND LANDSAT IMAGERY TO DISCOVER SKARN TUNGSTEN DEPOSITS USING IMAGE ANALYSIS TECHNIQUES

S. ARANOFF (Dipix Systems Ltd., Ottawa, Ontario), W. GOODFELLOW, G. F. BONHAM-CARTER, and D. J. ELLWOOD /in ESA Proceedings of the 1986 International Geoscience and Remote Sensing Symposium (IGARSS '86) on Remote Sensing: Today's Solutions for Tomorrow's Information Needs, Volume 1 p 513-520 Aug. 1986

(CONTRIB-19586) Avail: NTIS HC A99/MF E03; ESA, Paris, France, 3 volume set \$90 Member States, AU, CN, and NO (+20% others)

A deposit model, LANDSAT imagery, and surficial geochemistry were used to develop a procedure for locating tungsten mineralization associated with shallowly buried intrusions. Image analysis techniques were used to develop a co-occurrence index, which was used to identify promising exploration targets. ESA

N87-17293# Manitoba Univ., Winnipeg. Dept. of Geophysics.
APPLICATION OF 2-D HILBERT TRANSFORM IN THE INTERPRETATION OF REMOTELY SENSED POTENTIAL FIELD DATA

W. MOON and A. USHAH /in ESA Proceedings of the 1986 International Geoscience and Remote Sensing Symposium (IGARSS '86) on Remote Sensing: Today's Solutions for Tomorrow's Information Needs, Volume 2 p 777-781 Aug. 1986

(Contract NSERC-A-7400)

Avail: NTIS HC A17/MF A01; ESA, Paris, France, 3 volume set \$90 Member States, AU, CN, and NO (+20% others)

The relationships between the 2-D Hilbert transform and 3-D potential field data are studied and the application of these relations in geological remote sensing is investigated. In the overburden covered area, direct mapping of geological formations using LANDSAT or other short wavelength remote sensing data are not possible and it becomes necessary to use other available data sets. The most readily available geophysical data are the potential field data sets and the 2-D Hilbert transform method was tested and applied to digital potential field data sets to compute the first and second vertical derivatives. Results show that the method speeds up the processing, and that the vertical derivatives convincingly identify the subsurface geological boundaries. ESA

N87-17294# Centre d'Etude Spatiale des Rayonnements, Toulouse (France).

COMPUTER-AIDED INTERPRETATION OF COMPLEX GEOLOGICAL PATTERNS IN REMOTE SENSING

G. FLOUZAT and K. MOUEDDENE /in ESA Proceedings of the 1986 International Geoscience and Remote Sensing Symposium (IGARSS '86) on Remote Sensing: Today's Solutions for Tomorrow's Information Needs, Volume 2 p 783-786 Aug. 1986

Avail: NTIS HC A17/MF A01; ESA, Paris, France, 3 volume set \$90 Member States, AU, CN, and NO (+20% others) CSCL 09B

A framework for aiding geological interpretation of remote sensing imagery, based on mathematical morphology for analyzing classified images is outlined. The case of a geologic fold is used to show ensemblist and structuring methodologies. In the first case, the direction anticline is known. The extraction of the connected components representing the folding uses this hypothesis. In the second case, the searched information is the main direction. The phenomenon characterization must be protected from the disturbance caused by the orientation of other relief elements.

The entities which indicate the complex form studied are the sites of relatively strong slope. They correspond to forests and umbra areas. Therefore, the processing begins by searching the low reflectance pixels. A radiometric treatment based on a classification is the first step of the sequence. But artificial textures can be generated and then must be eliminated. Morphologic filtering is applied at the different channels before classification, to increase compactness of the obtained connected components. ESA

N87-17348*# Jet Propulsion Lab., California Inst. of Tech., Pasadena.

ON THE RELATIONSHIP BETWEEN AGE OF LAVA FLOWS AND RADAR BACKSCATTERING

R. G. BLOM, P. COOLEY, and L. R. SCHENCK /in ESA Proceedings of the 1986 International Geoscience and Remote Sensing Symposium (IGARSS '86) on Remote Sensing: Today's Solutions for Tomorrow's Information Needs, Volume 2 p 1119-1127 Aug. 1986

Avail: NTIS HC A17/MF A01; ESA, Paris, France, 3 volume set \$90 Member States, AU, CN, and NO (+20% others) CSCL 20N

The observation that older lava flows have lower backscatter in radar images is assessed with multiwavelength/polarization scatterometer data with incidence angles from 15 to 50 deg. Backscatter decreases over time because surface roughness decreases due to infilling with dust and mechanical weathering of the rocks. Pahoehoe lavas in the Snake River Plain with ages of 2.1, 7.4, and 12.0 K yr are best separated with 2.25 cm wavelength data. Blocky obsidian flows at Medicine Lake Highland and Newberry Volcano with ages of 0.9, 1.1 and 1.4 K yr are best separated with 6.3 cm wavelength data. Two Pleistocene flows at the Snake River Plain are best separated with 19.0 cm wavelength data. Incidence angles from 20 to 35 deg are best. These data indicate it may be possible to separate lava flows into eruptive periods using calibrated multiwavelength radar backscatter data. ESA

N87-17418*# Purdue Univ., West Lafayette, Ind. Dept. of Earth and Atmospheric Sciences.

IMPROVING THE GEOLOGICAL INTERPRETATION OF MAGNETIC AND GRAVITY SATELLITE ANOMALIES Final Report, 1 Apr. 1985 - 31 Nov. 1986

WILLIAM J. HINZE, LAWRENCE W. BRAILE, and RALPH R. B. VONFRESE (Ohio State Univ., Columbus) Jan. 1987 124 p

(Contract NAGW-736)

(NASA-CR-180149; NAS 1.26:180149) Avail: NTIS HC A06/MF A01 CSCL 08G

Quantitative analysis of the geologic component of observed satellite magnetic and gravity fields requires accurate isolation of the geologic component of the observations, theoretically sound and viable inversion techniques, and integration of collateral, constraining geologic and geophysical data. A number of significant contributions were made which make quantitative analysis more accurate. These include procedures for: screening and processing orbital data for lithospheric signals based on signal repeatability and wavelength analysis; producing accurate gridded anomaly values at constant elevations from the orbital data by three-dimensional least squares collocation; increasing the stability of equivalent point source inversion and criteria for the selection of the optimum damping parameter; enhancing inversion techniques through an iterative procedure based on the superposition theorem of potential fields; and modeling efficiently regional-scale lithospheric sources of satellite magnetic anomalies. In addition, these techniques were utilized to investigate regional anomaly sources of North and South America and India and to provide constraints to continental reconstruction. Since the inception of this research study, eleven papers were presented with associated published abstracts, three theses were completed, four papers were published or accepted for publication, and an additional manuscript was submitted for publication. Author

N87-18139*# National Aeronautics and Space Administration. Goddard Space Flight Center, Greenbelt, Md.
GEOMORPHOLOGY FROM SPACE: A GLOBAL OVERVIEW OF REGIONAL LANDFORMS
 NICHOLAS M. SHORT, ed. and ROBERT W. BLAIR, JR., ed. (Fort Lewis A&M Coll., Durango, Colo.) 1986 737 p Original contains color illustrations
 (NASA-SP-486; NAS 1.21:486; LC-86-17974) Avail: SOD HC \$41.00 as 033-000-00994-1; NTIS MF E03 CSCL 08E

This book, Geomorphology from Space: A Global Overview of Regional Landforms, was published by NASA STIF as a successor to the two earlier works on the same subject: Mission to Earth: LANDSAT views the Earth, and ERTS-1: A New Window on Our Planet. The purpose of the book is threefold: first, to serve as a stimulant in rekindling interest in descriptive geomorphology and landforms analysis at the regional scale; second, to introduce the community of geologists, geographers, and others who analyze the Earth's surficial forms to the practical value of space-acquired remotely sensed data in carrying out their research and applications; and third, to foster more scientific collaboration between geomorphologists who are studying the Earth's landforms and astrogeologists who analyze landforms on other planets and moons in the solar system, thereby strengthening the growing field of comparative planetology. F.M.R.

N87-18190# Freie Univ., Berlin (West Germany). Inst. of Applied Geology and Remote Sensing.
LANDSAT-MSS REMOTE SENSING AND SATELLITE CARTOGRAPHY: AN INTEGRATED APPROACH TO THE PREPARATION OF A NEW GEOLOGICAL MAP OF EGYPT AT A SCALE OF 1:500 000

F. K. LIST, B. MEISSNER (Technische Hochschule, Berlin, West Germany), and G. POEHLMANN /in ESA Proceedings of the 1986 International Geoscience and Remote Sensing Symposium (IGARSS '86) on Remote Sensing: Today's Solutions for Tomorrow's Information Needs, Volume 3 p 1503-1510 Aug. 1986 Sponsored by the Deutsches Forschungsgemeinschaft Avail: NTIS HC A21/MF A01; ESA, Paris, France, 3 volume set \$90 Member States, AU, CN, and NO (+20% others)

A project to cover the entire territory of Egypt by a 1:500 000 geological map with a high degree of geometric accuracy and geologic reliability was started. LANDSAT-MSS data served as a geometrically corrected map base after digital correction and mosaicing with the aid of Transit satellite points determined in the field, and as a means for geologic interpretation. Computer enhanced color composites were produced and interpreted. As an intermediate stage, a working sheet series of the entire area, comprising 80 sheets at a scale of 1:250 000, was printed to serve as a base for geologic and topographic interpretation.

ESA

N87-18255*# Nevada Univ., Reno. Dept. of Geological Sciences.

NATURE AND ORIGIN OF MINERAL COATINGS ON VOLCANIC ROCKS OF THE BLACK MOUNTAIN, STONEWALL MOUNTAIN, AND KANE SPRINGS, WASH VOLCANIC CENTERS, SOUTHERN NEVADA Semiannual Progress Report, Jul. 1986 - Jan. 1987
 JAMES V. TARANIK, DONALD C. NOBLE, LIANG C. HSU, and DAVID M. SPATZ Jan. 1987 75 p
 (Contract NAS5-28765)
 (NASA-CR-180183; NAS 1.26:180183) Avail: NTIS HC A04/MF A01 CSCL 08M

LANDSAT Thematic Mapper imagery was evaluated over 3 Tertiary calderas in southern Nevada. Each volcanic center derived from a highly evolved silici magmatic system represented today by well exposed diverse lithologies. Distinctive imagery contrast between some of the late ash flows and earlier units follows from the high relative reflectance in longer wavelength bands (bands 5 and 7) of the former. Enhancement techniques provide color composite images which highlight some of the units in remarkable color contrast. Inasmuch as coatings on the tuffs are incompletely developed and apparently largely dependent spectrally on rock properties independent of petrochemistry, it is felt that the

distinctive imagery characteristics are more a function of primary lithologic or petrochemical properties. Any given outcrop is backdrop for a variety of cover types, of which coatings, at various stages of maturity, are one. Petrographic and X-ray diffraction analysis of the outer air-interface zone of coatings reveal they are composed chiefly of amorphous compounds, probably with varying proportions of iron and manganese. Observations support an origin for some outer (air-interface) coating constituents exogenous to the underlying host. Author

N87-18256*# Jet Propulsion Lab., California Inst. of Tech., Pasadena.

KINEMATICS AT THE INTERSECTION OF THE GARLOCK AND DEATH VALLEY FAULT ZONES, CALIFORNIA: INTEGRATION OF TM DATA AND FIELD STUDIES Progress Report, Jan. 1986 - Jan. 1987

MICHAEL ABRAMS, KEN VEROSUB (California Univ., Davis), TONY FINNERTY, and ROLAND BRADY (Fresno State Univ., Calif.) 15 Jan. 1987 10 p Sponsored by NASA (NASA-CR-180182; NAS 1.26:180182; LANDSAT-TM-019) Avail: NTIS HC A02/MF A01 CSCL 08G

The Garlock and Death Valley fault zones in SE California are two active strike-slip faults coming together on the east side of the Avawatz Mtns. The kinematics of this intersection, and the possible continuation of either fault zone, are being investigated using a combination of field mapping, and processing and interpretation of remotely sensed image data. Regional and local relationships are derivable from Thematic Mapper data (30 m resolution), including discrimination and relative age dating of alluvial fans, bedrock mapping, and fault mapping. Aircraft data provide higher spatial resolution over more limited areas. Hypotheses being considered are: (1) the Garlock fault extends east of the intersection; (2) the Garlock fault terminates at the intersection and the Death Valley fault continues southeastward; and (3) the Garlock fault has been offset right laterally by the Death Valley fault which continues to the southeast. Preliminary work indicates that the first hypothesis is invalid. From kinematic considerations, image analysis, and field work the third hypothesis is favored. The projected continuation of the Death Valley zone defines the boundary between the Mojave crustal block and the Basin and Range block. Author

N87-18910*# Lunar and Planetary Inst., Houston, Tex.
THEMATIC MAPPER STUDIES OF CENTRAL ANDEAN VOLCANOES Progress Report

PETER W. FRANCIS Jan. 1987 17 p

(Contract NAS5-28759)
 (NASA-CR-180252; NAS 1.26:180252) Avail: NTIS HC A02/MF A01 CSCL 08K

A series of false color composite images covering the volcanic cordillera was written. Each image is 45 km (1536 x 1536 pixels) and was constructed using bands 7, 4, and 2 of the Thematic Mapper (TM) data. Approximately 100 images were prepared to date. A set of LANDSAT Multispectral Scanner (MSS) images was used in conjunction with the TM hardcopy to compile a computer data base of all volcanic structure in the Central Andean province. Over 500 individual structures were identified. About 75 major volcanoes were identified as active, or potentially active. A pilot study was begun combining Shuttle Imaging Radar (SIR) data with TM for a test area in north Chile and Bolivia. B.G.

N87-18915# Department of Energy, Morgantown, W. Va. Energy Technology Center.

PROCEEDINGS OF THE SECOND WORKSHOP ON REMOTE SENSING/LINEAMENT APPLICATIONS FOR ENERGY EXTRACTION

C. A. KOMAR, ed. Jul. 1986 143 p Symposium held at Morgantown, W. Va., 23 Apr. 1986
 (DE86-006613; DOE/METC-86-6039; CONF-860244) Avail: NTIS HC A07/MF A01

The Second Workshop on Remote Sensing/Lineament Applications for Energy Extraction was held April 23 to 24, 1986, at the Ramada Inn in Morgantown, West Virginia, and was

sponsored and hosted by the US Department of Energy (DOE), Office of Fossil Energy, Morgantown Energy Technology Center. This annual meeting provides a forum for the exchange of information and was attended by 82 individuals who represented industry, private consulting firms, and DOE. Nine papers were presented at the meeting; participants in a panel discussion and an open discussion reviewed and analyzed the information presented. The proceedings have been reproduced from camera-ready manuscripts furnished by the authors. The papers have not been refereed, nor have they been extensively edited. All papers have been processed for inclusion in the Energy Data Base. DOE

N87-19788# Instituto de Pesquisas Espaciais, Sao Jose dos Campos (Brazil).

REMOTE SENSING APPLIED TO BASIC GEOLOGICAL SURVEYS: A METHODOLOGICAL APPROACH FOR THE NORTHEAST REGION M.S. Thesis [SENSORIAMENTO REMOTO APLICADO A LEVANTAMENTOS GEOLOGICOS BASICOS: UMA ABORDAGEM METODOLOGICAL PARA A REGIAO NORDESTE]

EDGAR DASILVAFAGUNDESFILHO Nov. 1986 107 p In PORTUGUESE; ENGLISH summary (INPE-4041-TDL/246) Avail: NTIS HC A06/MF A01

Geologists studied the necessity of retaking Basic Geology Surveys in Brazil, the contribution of remote sensing in these surveys in Northeast Brazil is studied. The discussion of information extraction techniques from images, based on a proper methodology which, once applied to the semi-arid environment of the Northeast, allowed the mapping of an area of 850 sq km at 1:100,000 scale, depicted the valuable contribution of remote sensing for geological mapping when properly used. The mapped area lies in the Serido Region, being composed by metasediment and metavolcanics of the Caico Complex, as well as by granitic bodies intruded into the supracrustals. Lithologic discriminations and structural features, including new data yet unknown, showed that integrated analyses of varied products of remote sensing, encompassing different techniques of image processing, can give important contribution to the regional geological cartography or even to the semidetall level. Author

N87-19796# Pacific Northwest Labs., Richland, Wash.
SURFACE REFLECTANCE CORRECTION AND STEREO ENHANCEMENT OF LANDSAT THEMATIC MAPPER IMAGERY FOR STRUCTURAL GEOLOGIC EXPLORATION

R. L. THIESSEN (Washington State Univ., Pullman), L. K. JOHNSON, H. P. FOOTE, and J. R. ELIASON Nov. 1986 12 p Presented at the 5th Thematic Conference on Remote Sensing for Exploration Geology, Reno, Nev., 29 Sep. 1986 (Contract DE-AC06-76RL-01830) (DE87-003095; PNL-SA-13832; CONF-8609200-1) Avail: NTIS HC A02/MF A01

Structural remote sensing analysis techniques for exploration have focussed on mapping of crustal fracture zones which can provide pathways for mineralization as well as permeability for movement and/or accumulation of oil, gas, and geothermal fluids. These analyses have relied heavily on manual lineament analysis of enhanced imagery. These image products contain shadow effects that preferentially enhance or suppress lineaments. This study was conducted to evaluate a digital technique for surface reflectance correction for shadows and subsequent stereo enhancement to provide shadow corrected stereo models for structural geologic exploration. Image products were produced from digital LANDSAT Thematic Mapper (TM) data and a digital elevation model (DEM). The Paiute Ridge quadrangle, Nevada was selected as a test area for the analysis. LANDSAT TM data were registered to the DEM and processed to reduce topographic shadowing effects. A Minnaert reflectance model was used to approximate the topographic lighting effects. This reflectance model provided quantitative evaluation of each pixel in the image and was directly used to create a shadow image. These reflectance values were utilized to remove shadow effects from the TM data to produce

the corrected surface reflectance. The DEM was used to stereo enhance the shadow corrected TM image. Fracture orientations determined from the original TM and shadow images show similar bias resulting from solar illumination. This bias was not present in the results from the shadow corrected and the corrected stereopair images, with the best correlation to the trends observed in the field data given by the latter. DOE

05

OCEANOGRAPHY AND MARINE RESOURCES

Includes sea-surface temperature, ocean bottom surveying imagery, drift rates, sea ice and icebergs, sea state, fish location.

A87-20204*# National Aeronautics and Space Administration. Goddard Space Flight Center, Greenbelt, Md.

CHLOROPHYLL PIGMENT CONCENTRATION USING SPECTRAL CURVATURE ALGORITHMS - AN EVALUATION OF PRESENT AND PROPOSED SATELLITE OCEAN COLOR SENSOR BANDS

FRANK E. HOGE (NASA, Goddard Space Flight Center, Greenbelt, MD) and ROBERT N. SWIFT (EG & G Washington Analytical Services Center, Inc., Pocomoke City, MD) Applied Optics (ISSN 0003-6935), vol. 25, Oct. 15, 1986, p. 3677-3682. NASA-supported research. refs

During the past several years symmetric three-band (460-, 490-, 520-nm) spectral curvature algorithm (SCA) has demonstrated rather accurate determination of chlorophyll pigment concentration using low-altitude airborne ocean color data. It is shown herein that the in-water asymmetric SCA, when applied to certain recently proposed OCI (NOAA-K and SPOT-3) and OCM (ERS-1) satellite ocean color bands, can adequately recover chlorophyll-like pigments. These airborne findings suggest that the proposed new ocean color sensor bands are in general satisfactorily, but not necessarily optimally, positioned to allow space evaluation of the SCA using high-precision atmospherically corrected satellite radiances. The pigment concentration recovery is not as good when existing Coastal Zone Color Scanner bands are used in the SCA. The in-water asymmetric SCA chlorophyll pigment recovery evaluations were performed using (1) airborne laser-induced chlorophyll fluorescence and (2) concurrent passive upwelled radiances. Data from a separate ocean color sensor aboard the aircraft were further used to validate the findings. Author

A87-20350

OPTICAL AND RADAR OBSERVATIONS OF THE NONLINEAR INTERACTION OF GRAVITY WAVES [NABLIUDENIE NELINEINOGO VZAIMODEISTVIA GRAVITATSIONNYKH VOLN OPTICHESKIMI I RADIOLOKATSIONNYMI METODAMI]

V. A. GRUSHIN, V. I. RAIZER, A. V. SMIRNOV, and V. S. ETKIN (AN SSSR, Institut Kosmicheskikh Issledovaniy, Moscow, USSR) Akademiia Nauk SSSR, Doklady (ISSN 0002-3264), vol. 290, no. 2, 1986, p. 458-462. In Russian. refs

New experimental data are presented on the spatial variability of the low-frequency ocean wave spectrum under conditions of a nonstationary wind field. In particular, a series of normalized Wiener spectra of the optical images of various sea conditions are presented along with the Wiener spectra of the radar images of very high (gale) sea. The possible mechanism of the formation of the low-frequency spectra of the waves is examined with reference to the results of the Fourier transform processing of the observational data. V.L.

A87-20520

DATA SENSITIVITIES OF SEA ICE DRIFT AND OCEAN STRESS IN NORTH ATLANTIC HIGH LATITUDES

JOHN E. WALSH, BECKY ROSS (Illinois, University, Urbana), DAVID W. PLUMMER, GERALD F. HERMAN, and WILLIAM H. RAYMOND (Wisconsin, University, Madison) *Journal of Geophysical Research* (ISSN 0148-0227), vol. 91, Oct. 15, 1986, p. 11,657-11,675. refs

(Contract NSF DPP-81-18563; NSF DPP-81-19155)

The effects of various data sources on surface stress and sea ice drift in North Atlantic high latitudes are investigated. Drifting buoy reports, surface marine observations, and Tiros-N satellite temperature retrievals for the period between February 25-March 7, 1979 are examined using limited area objective analyses. The planetary boundary layer model of Brown (1981) was employed to compute surface stress from objective analyses of the meteorological data and the sea ice model of Hibler (1979) was utilized for sea ice simulations. The data reveal that the buoy/marine and satellite data can produce significant differences in regional fields of surface stress and ice velocity. It is observed that the buoy/marine data have a greater effect on stress fields than satellite data and objective analyses are degraded by deletion of one or more data types. I.F.

A87-20524* Texas Univ., Austin.

ACCURATE MEASUREMENT OF MEAN SEA LEVEL CHANGES BY ALTIMETRIC SATELLITES

G. H. BORN, B. D. TAPLEY, J. C. RIES (Texas, University, Austin), and R. H. STEWART (California Institute of Technology, Jet Propulsion Laboratory, Pasadena; California, University, La Jolla) *Journal of Geophysical Research* (ISSN 0148-0227), vol. 91, Oct. 15, 1986, p. 11,775-11,782. NASA-supported research. refs

A technique for monitoring changes in global mean sea levels using altimeter data from a well-tracked satellite is examined. The usefulness of this technique is evaluated by analyzing Seasat altimeter data obtained during July-September 1978. The effects of orbit errors, geoid errors, sampling intervals, tides, and atmosphere refraction on the calculation of the mean sea level are investigated. The data reveal that the stability of an altimeter can be determined with an accuracy of \pm or $-$ 7 cm using globally averaged sea surface height measurements. The application of this procedure to the US/French Ocean Topography Experiment is discussed. I.F.

A87-20687*# National Aeronautics and Space Administration. Goddard Space Flight Center, Greenbelt, Md.

VARIABILITY OF THE PRODUCTIVE HABITAT IN THE EASTERN EQUATORIAL PACIFIC

GENE CARL FELDMAN (NASA, Goddard Space Flight Center, Greenbelt, MD) *EOS* (ISSN 0096-3941), vol. 67, March 4, 1986, p. 106-108. refs

It is shown that satellite ocean color data can be used to define the spatial extent of the region of enhanced biological production (the productive habitat) in the eastern equatorial Pacific. The degree of interannual variability in the areal extent of the productive habitat and in the estimated primary production of the region is determined. Frequency distributions of satellite-derived pigment concentrations are used to determine whether major changes in phytoplankton biomass have taken place from one period to the next. K.K.

A87-20692

COMPARISON BETWEEN SATELLITE IMAGE ADVECTIVE VELOCITIES, DYNAMIC TOPOGRAPHY, AND SURFACE DRIFTER TRAJECTORIES

W. J. EMERY, A. C. THOMAS, M. J. COLLINS (British Columbia, University, Vancouver, Canada), W. R. CRAWFORD, and D. L. MACKAS (Institute of Ocean Sciences, Sidney, Canada) *EOS* (ISSN 0096-3941), vol. 67, June 3, 1986, p. 498, 499. Research supported by the Department of Fisheries and Oceans and NSERC. refs

An objective technique for the calculation of advective surface velocities from sequential satellite images is presented.

Comparisons are made between these image-derived advective velocities and simultaneous measures of the near-surface flow by shallow drogued drifting buoys and 15/110-dB dynamic topography from CTD casts. The dominant feature in all cases is a cyclonic eddy. The good agreement found between these independent measurements of surface velocity suggests that image-derived advective velocities may provide useful representations of the surface current. K.K.

A87-20769

A NEW SEMI-EMPIRICAL SEA SPECTRUM FOR ESTIMATING THE SCATTERING COEFFICIENT

A. SARKAR and R. KUMAR (Indian Space Research Organization, Meteorology and Oceanography Div., Ahmedabad, India) *International Journal of Remote Sensing* (ISSN 0143-1161), vol. 7, Oct. 1986, p. 1369-1375. refs

A large database comprising Seasat-A satellite scatterometer measurements and quasi-concurrent high-quality sea-wind data, as represented by Britt and Schroeder (1984) in the form of a multivariate regression, has been used to tune the overall magnitude of the assumed sea spectrum by inverting the two-scale scattering theory. Scattering coefficient values computed for the derived spectrum have been compared with those computed for the spectrum suggested by Fung and Lee (1982), and an improvement is found in the surface wind-scattering coefficient relationship as verified by comparisons with the independent AAFE RADSCAT data set. Author

A87-20770

CORRELATION BETWEEN TIME- AND DEPTH-RESOLVED SIMULATED LIDAR SIGNALS

A. PUNJABI (Hampton University, VA) *International Journal of Remote Sensing* (ISSN 0143-1161), vol. 7, Oct. 1986, p. 1377-1382. refs

In this letter, the results from the analysis of the runs of SALMON code (Punjabi and Venable, 1984) are presented. One important result is that the effective attenuation coefficient at excitation wavelength shows a maximum correlation between depth-resolved and time-resolved signals for variable field of view and variable chlorophyll concentration. The effective attenuation coefficients are related as $C(z,L) = \text{about } Z_c(t,L)$. It is also found that the effective velocity of Raman photons decreases as the chlorophyll concentration increases. The incremental Raman normalized fluorescence signal as a function of depth lags behind the one as a function of time. Author

A87-20956*# National Aeronautics and Space Administration. Goddard Space Flight Center, Greenbelt, Md.

SIMULTANEOUS OCEAN CROSS SECTION AND RAINFALL MEASUREMENTS FROM SPACE WITH A NADIR-LOOKING RADAR

ROBERT MENEGHINI (NASA, Goddard Space Flight Center, Greenbelt, MD) and DAVID ATLAS (Maryland, University, College Park) *Journal of Atmospheric and Oceanic Technology* (ISSN 0739-0572), vol. 3, Sept. 1986, p. 400-413. refs
(Contract NAG5-542)

In the case of a nadir-looking spaceborne or aircraft radar in the presence of rain, the return power corresponding to secondary surface scattering may provide information on the properties of the surface and the precipitation. The object of the study is to evaluate a method for determining simultaneously the rainfall rate and the backscattering coefficient of the surface. The method is based upon the mirror-reflected power, which corresponds to the portion of the incident power scattered from the surface to the precipitation, intercepted by the precipitation, and again returned to the surface where it is scattered a final time back to the antenna. Author

A87-21367

THE APPLICATION OF GEODETIC RADIO INTERFEROMETRIC SURVEYING TO THE MONITORING OF SEA-LEVEL

W. E. CARTER, D. S. ROBERTSON (NOAA, National Ocean Service, Rockville, MD), T. E. PYLE, and J. DIAMANTE (NOAA, Office of Oceanic and Atmospheric Research, Rockville, MD) *Geophysical Journal* (ISSN 0016-8009), vol. 87, Oct. 1986, p. 3-13. refs

The use of VLBI and GPS observations for geodetic surveying is described. The capabilities and functions of the VLBI and the GPS are discussed. The application of the techniques to the calculation of the vertical rates of motion of tide gauges is examined and examples are provided. Consideration is given to polar motion and changes in length of day. I.F.

A87-22041

EQUATORIAL INDIAN OCEAN EVAPORATION ESTIMATES FROM OPERATIONAL METEOROLOGICAL SATELLITES AND SOME INFERENCES IN THE CONTEXT OF MONSOON ONSET AND ACTIVITY

BABY SIMON and PRANAV S. DESAI (Indian Space Research Organization, Space Applications Centre, Ahmedabad, India) *Boundary-Layer Meteorology* (ISSN 0006-8314), vol. 37, no. 1-2, Oct. 1986, p. 37-52. refs

A87-23362

THE EFFECT OF HURRICANE GLORIA ON SEA SURFACE TEMPERATURE PATTERNS

WILLIAM G. PICHEL, ROBERT A. WARNER, BARBARA A. BANKS (NOAA, National Environmental Satellite, Data, and Information Service, Washington, DC), and CRAIG S. NELSON (NOAA, National Meteorological Center, Washington, DC) IN: Conference on Satellite Meteorology/Remote Sensing and Applications, 2nd, Williamsburg, VA, May 13-16, 1986. Preprints. Boston, MA, American Meteorological Society, 1986, p. 178-182. refs

A87-23391* Jet Propulsion Lab., California Inst. of Tech., Pasadena.

MONTH-TO-MONTH VARIABILITY OF OCEAN-ATMOSPHERE LATENT HEAT FLUX AS OBSERVED FROM THE NIMBUS MICROWAVE RADIOMETER

W. TIMOTHY LIU (California Institute of Technology, Jet Propulsion Laboratory, Pasadena) IN: Conference on Satellite Meteorology/Remote Sensing and Applications, 2nd, Williamsburg, VA, May 13-16, 1986. Preprints. Boston, MA, American Meteorological Society, 1986, p. 328-332. NASA-supported research. refs

Comparison with in situ measurements shows that the Nimbus/Scanning Multichannel Microwave Radiometer is useful in describing the month-to-month variability of the latent heat flux 'LE' and related parameters during the 1982-1983 El Nino event. The spaceborne measured monthly mean LE was found to be within 30 W/sq m of those derived from ship reports. Absolute accuracy could not be determined, though satellite measurements could extrapolate information on the LE both in space and in time. R.R.

A87-23717

AN OBJECTIVE METHOD FOR COMPUTING ADVECTIVE SURFACE VELOCITIES FROM SEQUENTIAL INFRARED SATELLITE IMAGES

W. J. EMERY, A. C. THOMAS, M. J. COLLINS (British Columbia University, Vancouver, Canada), W. R. CRAWFORD, and D. L. MACKAS (Institute of Ocean Sciences, Sidney, Canada) *Journal of Geophysical Research* (ISSN 0148-0227), vol. 91, Nov. 15, 1986, p. 12865-12878. NSERC-supported research. refs

Using cross correlations between sequential infrared satellite images, an objective technique is developed to compute advective sea surface velocities. Cross correlations are computed in 32 x 32 pixel search (second image) and 22 x 22 template (first image) windows from gradients of sea surface temperature computed from the satellite images. Velocity vectors, computed from sequential images of the British Columbia coastal ocean, generally appear coherent and consistent with the seasonal surface current in the

region. During periods of strong wind forcing, as indicated by maps of sea level pressure, the image advective velocities are stronger and more coherent spatially and appear to cross surface temperature gradients; when winds are weaker, the advective velocities correspond better with the infrared temperature patterns, suggesting the increased contribution of the geostrophic current to the surface flow. Velocities determined from coincident, near-surface drogued (5-10 m) buoys, positioned every half hour by internal LORAN-C units in mid-June, show excellent agreement with the image advective velocities. In addition, conductivity, temperature, and depth (CTD) measurements (taken during the buoy tracking) confirm the homogeneity of the upper 10 m, and CTD-derived geostrophic currents are consistent with both buoy and sequential image displacement velocities. Author

A87-23718#

A SATELLITE TIME SERIES OF SEA SURFACE TEMPERATURES IN THE EASTERN EQUATORIAL PACIFIC OCEAN, 1982-1986

RICHARD LEGECKIS (NOAA, National Environmental Satellite Data Information Service, Washington, DC) *Journal of Geophysical Research* (ISSN 0148-0227), vol. 91, Nov. 15, 1986, p. 12879-12886. NOAA-supported research. refs

A87-23719

MESOSCALE HYDROGRAPHIC VARIABILITY IN THE VICINITY OF POINTS CONCEPTION AND ARGUELLO DURING APRIL-MAY 1983 - THE OPUS 1983 EXPERIMENT

LARRY P. ATKINSON (Old Dominion University, Norfolk, VA), KENNETH H. BRINK (Woods Hole Oceanographic Institution, MA), RUSS E. DAVIS (California, University, La Jolla), BURTON H. JONES (Southern California, University, Los Angeles), THERESA PALUSZKIEWICZ (Oregon State University, Corvallis) et al. *Journal of Geophysical Research* (ISSN 0148-0227), vol. 91, Nov. 15, 1986, p. 12899-12918. refs
(Contract NSF OCE-85-11526; NSF OCE-85-06468; NSF OCE-82-13872; NSF OCE-85-07438; NSF OCE-82-13456)

A87-23720* California Univ., La Jolla.

TEMPERATURE-PLANT PIGMENT-OPTICAL RELATIONS IN A RECURRENT OFFSHORE MESOSCALE EDDY NEAR POINT CONCEPTION, CALIFORNIA

JAMES J. SIMPSON, JOSE PELAEZ, LOREN R. HAURY, DAVID WIESENHANN (California, University, La Jolla), and CHESTER J. KOBLINSKY (NASA, Goddard Space Flight Center, Greenbelt, MD) *Journal of Geophysical Research* (ISSN 0148-0227), vol. 91, Nov. 15, 1986, p. 12919-12936. Research supported by the University of California and NASA. refs
(Contract N00014-86-K-0752)
(AD-A176666)

The temperature-plant pigment-optical structure of a mesoscale anticyclonic eddy consistently found in shipboard surveys and satellite-sensed data several hundred kilometers southwest of Point Conception, CA, is described on three different time scales (100-day mesoscale, annual, and several-year). The satellite coastal zone color scanner (CZCS) ocean color imagery detected the near-surface chlorophyll structure of the eddy, but in situ optical and plant pigment data suggest that such imagery does not provide a good estimate of the integrated chlorophyll field of the eddy. The temperature and plant pigment boundaries of the eddy, as determined from two-dimensional gradients of advanced very high resolution radiometer (AVHRR) and CZCS imagery, do not coincide spatially. This and in situ temperature, plant pigment, and optical structure provide additional evidence that some eddy systems in the California Current are not isolated vortex systems but rather continuously entrain waters of nonlocal origin laterally into their upper layers. Within the California Current a ratio of AVHRR/CZCS data is useful for separating inshore from oceanic water masses and following their surface entrainment by offshore vortices. The historical 28-year California Cooperative Oceanic Fisheries Investigations data for the Point Conception region of the California Current and remotely sensed data over this region show that the Point Conception eddy is a recurrent feature in the offshore

California Current. Moreover, the available data provide evidence that a large number of warm-core mesoscale eddies occur simultaneously in a transition zone between coastal and oceanic regimes, that these features recur at preferred locations within the transition zone, and that this family of eddies should impose a significant offshore boundary condition on the flow of the California Current. Author

A87-23721* California Univ., La Jolla.
BIOLOGICAL CONSEQUENCES OF A RECURRENT EDDY OFF POINT CONCEPTION, CALIFORNIA

LOREN R. HAURY, JAMES J. SIMPSON, JOSE PELAEZ, DAVID WISENHAHN (California, University, La Jolla), and CHESTER J. KOBLINSKY (NASA, Goddard Space Flight Center, Greenbelt, MD) *Journal of Geophysical Research* (ISSN 0148-0227), vol. 91, Nov. 15, 1986, p. 12937-12956. Research supported by the University of California and NASA. refs
 (Contract N00014-86-K-0752)

The biological effects on three different time scales (100-day mesoscale, annual, and several-year) of a mesoscale anticyclonic eddy consistently found in shipboard surveys and satellite-sensed data several hundred kilometers southwest of Point Conception, CA, are described. A detailed shipboard study of the eddy in January 1981 found a complex system of fronts in surface chlorophyll at the northern edge of the eddy; microplankton and zooplankton distributions were strongly affected by entrainment processes at the surface and, apparently, at depth. Concurrent satellite coastal zone color scanner ocean color images show agreement with the general surface characteristics of the eddy chlorophyll field but do not reflect features deeper than about 25 m, including the contribution of the deep chlorophyll maximum to the integrated chlorophyll values. Satellite data for the period October 1980 through October 1981 and shipboard data from California Cooperative Oceanic Fisheries Investigations (CalCOFI) for December 1980 to July 1981 show the continued presence of the eddy in the sea surface temperature and color field and in the distributions of surface chlorophyll and zooplankton displacement volume. A review of the CalCOFI survey results from 1949 to the present time demonstrates the recurrent nature of the eddy system on a year-to-year basis. The eddy system appears to have a significant effect on the distribution of both oceanic and nearshore organisms. Offshore transport of coastal species occurs in the form of large entrained plumes or filaments. Author

A87-23722* California Univ., La Jolla.
SPACE AND TIME VARIABILITY OF THE SURFACE COLOR FIELD IN THE NORTHERN ADRIATIC SEA

VITTORIO BARALE (California, University, La Jolla), CHARLES R. MCCLAIN (NASA, Goddard Space Flight Center, Greenbelt, MD), and PAOLA MALANOTTE-RIZZOLI (MIT, Cambridge, MA) *Journal of Geophysical Research* (ISSN 0148-0227), vol. 91, Nov. 15, 1986, p. 12957-12974. refs
 (Contract NAG5-583; NAG5-587)

A time series of coastal zone color scanner images for the years 1979 and 1980 was used to observe the spatial and temporal variability of bio-optical processes and circulation patterns of the northern Adriatic Sea on monthly, seasonal, and interannual scales. The chlorophyll-like pigment concentrations derived from satellite data exhibited a high correlation with sea truth measurements performed during seven surveys in the summer of both years. Comparison of the mean pigment fields indicates a general increase in concentration values and larger scales of coastal features from 1979 to 1980. This variability may be linked to the different patterns of nutrient influx due to coastal runoff in the 2 years. The distribution of surface features is consistent with the general cyclonic circulation pattern. The pigment heterogeneity appears to be governed by fluctuations of freshwater discharge, while the dominant wind fields do not appear to have important direct effects. The Po River presents a plume spreading predominantly in a southeastern direction, with scales positively correlated with its outflow. The spatial scales of the western coastal layer, in contrast, are negatively correlated with this outflow and the plume scales. Both

results are consistent with, and may be rationalized by, recent theoretical and experimental results involving a dynamical balance between nonlinear advection and bottom friction, with alternate predominance of one of the two effects. Author

A87-23725
MEASUREMENT OF MICROWAVE BACKSCATTERING SIGNATURES OF THE OCEAN SURFACE USING X BAND AND K(A) BAND AIRBORNE SCATTEROMETERS

HARUNOBU MASUKO (Bremen, Universitaet, West Germany), KENICHI OKAMOTO (Ministry of Posts and Telecommunications, Radio Research Laboratory, Kashima, Japan), MASANOBU SHIMADA (National Space Development Agency, Tsukuba Space Center, Japan), and SHUNTARO NIWA (Resources Remote Sensing System, Technology Research Association, Tokyo, Japan) *Journal of Geophysical Research* (ISSN 0148-0227), vol. 91, Nov. 15, 1986, p. 13065-13083. refs

An airborne microwave scatterometer-radiometer system operated in X band and K(a) band was applied to the observations of microwave backscattering signatures of the ocean. The normalized radar cross sections $\Delta \exp 0$ were measured as combined functions of microwave frequency (10.00 GHz and 34.43 GHz), polarization (HH and VV), incident angle (0-70 deg), azimuth angle (0-360 deg), and wind speed (3.2-17.2 m/s). The azimuth anisotropic signatures for K(a) band are confirmed to be similar to those for X band, and the wind speed dependences are analyzed for each azimuth angle, polarization, and incident angle. For each parameter the behaviors of $\Delta \exp 0$ for microwave frequencies is shown as compared with the results obtained by other experiments and theories. The effective reflection coefficient, the mean square surface slope, and the two-dimensional wave number spectrum of the short surface waves are estimated from the microwave scattering signatures. Author

A87-23834
THE USE OF REMOTE SENSING IN ESTIMATING BIOMASS OF FISH TREE AREAS IN THE RICHARD B. RUSSELL LAKE

WILLIAM A. SHAIN and RICHARD K. MYERS (Clemson University, SC) IN: American Congress on Surveying and Mapping and American Society for Photogrammetry and Remote Sensing, Annual Convention, Washington, DC, Mar. 16-21, 1986, Technical Papers. Volume 5. Falls Church, VA, American Congress on Surveying and Mapping and American Society for Photogrammetry and Remote Sensing, 1986, p. 297-301. refs

A87-24374
VERTICAL STRUCTURE OF THE TEMPERATURE FIELD ABOVE THE NORTH ATLANTIC [O VERTIKAL'NOI STRUKTURE POLIA TEMPERATURNY NAD SEVERNOI ATLANTIKOI]

V. A. VASILEV and M. A. TRUBINA IN: Aviation and satellite climatology. Moscow, Gidrometeoizdat, 1985, p. 132-142. In Russian. refs

A87-24376
THE RESULTS OF SEA-SURFACE TEMPERATURE DETERMINATIONS FROM IR AND MICROWAVE MEASUREMENTS ABOARD THE COSMOS-1151 SATELLITE [REZUL'TATY OPREDELENIYA TEMPERATURNY POVERKHNOSTI OKEANA PO IZMERENIIM IZLUCHENIYA V IK- I SVCH-DIAPAZONAKH SPECTRA SO SPUTNIKA 'KOSMOS-1151']

A. K. GORODETSKII, B. G. KUTUZA, M. S. MALKEVICH, and B. Z. PETRENKO (AN SSSR, Institut Kosmicheskikh Issledovaniy and Institut Radiotekhniki i Elektroniki, Moscow, USSR) *Issledovanie Zemli iz Kosmosa* (ISSN 0205-9614), July-Aug. 1986, p. 3-10. In Russian. refs

Sea-surface temperatures (SSTs) of 28 areas of the Atlantic Ocean were determined in the periods of January 21-28 and April 8-14, 1980 by means of IR (in the 11.1-micron range) and microwave (3.2-cm) measurements aboard the Cosmos-1151 satellite. It is shown that the SSTs determined from the angular distributions of the 11.1-micron outgoing radiation, combined with concurrently measured polarizations in the 3.2-cm region, permit

reliable recognition of areas with an IR SST error and those with anomalous values of SSTs as well. Compared with the SST data obtained by ships, the temperatures derived from satellite IR and microwave data were found to exhibit a persistent shift by 1-2 K. I.S.

A87-24377

EXACT DETERMINATION OF WAVE PARAMETERS FROM THE RESULTS OF FOURIER ANALYSIS OF SEA-SURFACE RADAR IMAGERY [TOCHNOE OPREDELENIE PARAMETROV VOLN PO DANNYM FUR'E ANALIZA RADIOIZOBRAZHENII MORSKOI POVERKHNOSTI]

IU. V. BULATOV, K. I. VOLIAK, and V. V. PANENKO (AN SSSR, Institut Obshchei Fiziki, Moscow, USSR; Simferopol'skii Gosudarstvennyi Universitet, Simferopol', Ukrainian SSR) *Issledovanie Zemli iz Kosmosa* (ISSN 0205-9614), July-Aug. 1986, p. 11-20. In Russian. refs

Side-looking radar images of sea waves were obtained over the Black Sea at several probing azimuths, and the values of the direction and the length of the wave vector were obtained by using coherent optical analysis of the wave images. Methods were developed for the correction of these parameters by accounting for the motions of the radar with respect to the waves and for the turns of the radar antenna. After applying these corrections, the accuracy of the directly determined sea-wave propagation direction and wave vector length improved almost twofold. The accuracy obtained was 2 and 5 deg, respectively. I.S.

A87-24379

POSSIBILITIES OF USING SATELLITE DATA FOR COMPUTATIONS OF THE OCEAN/ATMOSPHERE HEAT EXCHANGE IN THE NEWFOUNDLAND ENERGY-ACTIVE OCEAN ZONE IN WINTER [VOZMOZHNOСТИ ISPOL'ZOVANIIA DANNYKH ISZ DLIA RASCHETOV TEPLOOBMENA MEZHDUOKEANOM I ATMOSFEROI V N'IUFAUNDLENSKOI EAZO V ZIMNII PERIOD]

D. G. RZHEPLINSKII and N. N. SHVYRKOV (Vsesoiuznyi Nauchno-Issledovatel'skii Institut Morskogo Rybnogo Khoziaistva i Okeanografii, Moscow, USSR) *Issledovanie Zemli iz Kosmosa* (ISSN 0205-9614), July-Aug. 1986, p. 32-41. In Russian.

The ocean/atmosphere heat-exchange data obtained, in the winter season of 1983-1984, by ships within the Newfoundland energy-active Gulf Stream 'delta' are analyzed and compared with the concurrently obtained satellite scanner images. Synoptic hydrometeorological situations typical for the winter season are inferred from the images, and the characteristic ocean/atmosphere heat-exchange energy rates are estimated. The feasibility of using satellite data obtained in the winter season for rapid analysis of heat-exchange processes in the Newfoundland energy-active ocean zone is discussed. I.S.

A87-24748

WIND-WAVE RELATIONSHIP FROM SEASAT RADAR ALTIMETER DATA

P. C. PANDEY, R. M. GAIROLA, and B. S. GOHIL (Indian Space Research Organization, Space Application Centre, Ahmedabad, India) *Boundary-Layer Meteorology* (ISSN 0006-8314), vol. 37, Nov. 1986, p. 263-269. refs

The paper presents a nonlinear relationship between ocean surface wind at 10 m height (U10) and significant wave height of wind-generated gravity waves, $(H1/3)_{gw}$, over the open oceans using Seasat radar altimeter data. The data represent a variety of fetches, durations and strength of winds. Concurrent measurement of significant wave height, $(H1/3)$, which may contain a measure of swell and U10 obtained from the processed geophysical data record of the Seasat radar altimeter were used in the analysis. The total wave energy, $E(alt)$, characterized by altimeter $H1/3$ measurements was compared with the energy of a fully developed sea, $E(fd)$ derived from U10 measurements using the Pierson-Moskowitz model. The criteria $E(alt)$ less than equal to $E(fd)$ was used in data selection to minimize the influence of swell. $H(1/3)_{gw}$ thus obtained was used in a regression in terms of U10 in a second-degree polynomial. Verification with independent

radar altimeter data confirmed the validity of the proposed wind-wave model, which could be used for operational wave forecasting. Author

A87-25534#

OZONE IN THE BOUNDARY LAYER OF THE EQUATORIAL PACIFIC OCEAN

STEPHEN R. PIOTROWICZ, DEBORAH A. BORAN, and CHARLES J. FISCHER (NOAA, Atlantic Oceanographic and Meteorological Laboratory, Miami, FL) *Journal of Geophysical Research* (ISSN 0148-0227), vol. 91, Nov. 20, 1986, p. 13113-13119. refs

Shipboard (about 7 m) ozone measurements made in the equatorial Pacific Ocean between 20 deg N and 17 deg S and 140-160 deg W confirm the existence of a distinct ozone minimum in the vicinity of the equator in the late spring, its decline in the summer, and its absence in autumn. This minimum could not be correlated with high biological activity in surface waters. Coincident aircraft measurements of ozone from near sea surface (50-100 m) to 2 km in altitude were made along 150 deg W at stations at 10 deg N, and 0 deg, 5 deg and 12 deg S in May-June 1984. Aircraft data identified the existence of a distinct ozone maximum between the lifting condensation level (LCL) or cloud base, Z(b), and the trade wind inversion, with ozone mixing ratios amounting to 2-2.5 times the ozone levels in the well-mixed subcloud layer. A gradient of decreasing ozone with decreasing altitude extended from the LCL or Z(b) to the near-surface superadiabatic region but did not include it. Author

A87-25543

ATMOSPHERIC CHARACTERISTICS OF THE EQUATORIAL PACIFIC DURING THE 1982-1983 EL NINO, DEDUCED FROM SATELLITE AND AIRCRAFT OBSERVATIONS

OSWALDO GARCIA (NOAA, Environmental Research Laboratories, Boulder, CO), SIRI JODHA SINGH KHALSA, and ELLEN J. STEINER (Cooperative Institute for Research in Environmental Sciences, Boulder, CO) *Journal of Geophysical Research* (ISSN 0148-0227), vol. 91, Nov. 20, 1986, p. 13217-13231. NOAA-supported research. refs

A87-25787* Wisconsin Univ., Madison.

A CASE STUDY OF GWE SATELLITE DATA IMPACT ON GLA ASSIMILATION ANALYSES OF TWO OCEAN CYCLONES

R. G. GALLIMORE and D. R. JOHNSON (Wisconsin, University, Madison) *Monthly Weather Review* (ISSN 0027-0644), vol. 114, Nov. 1986, p. 2016-2032. refs

(Contract NAG5-81)
The effects of the Global Weather Experiment (GWE) data obtained on January 18-20, 1979 on Goddard Laboratory for Atmospheres assimilation analyses of simultaneous cyclones in the western Pacific and Atlantic oceans are examined. The ability of satellite data within assimilation models to determine the baroclinic structures of developing extratropical cyclones is evaluated. The impact of the satellite data on the amplitude and phase of the temperature structure within the storm domain, potential energy, and baroclinic growth rate is studied. The GWE data are compared with Data Systems Test results. It is noted that it is necessary to characterize satellite effects on the baroclinic structure of cyclone waves which degrade numerical weather predictions of cyclogenesis. I.F.

A87-25797* Washington Univ., Seattle.

OCEAN SURFACE PRESSURE FIELDS FROM SATELLITE-SENSED WINDS

ROBERT A. BROWN and GAD LEVY (Washington, University, Seattle) *Monthly Weather Review* (ISSN 0027-0644), vol. 114, Nov. 1986, p. 2197-2206. refs

(Contract NAGW-679)
The University of Washington's planetary boundary layer model is inverted to use remotely sensed satellite scatterometer-derived surface winds as input to calculate maritime surface pressure fields. The analysis of three different synoptic storm situations is performed using the model and is then compared to conventional National Weather Service analyses. Agreement is good. Isolation

of the PBL secondary flow, stratification and thermal wind effects in the model revealed that each may be significant under certain conditions. However, the model shows sensitivity to the thermodynamic features only in a general sense and even a neutral stratification solution gives a good approximation. The high density of the scatterometer data produces mesoscale (hundreds of kilometers) dynamic details, which cannot be confirmed by conventional data at this stage. Author

A87-26531

SPATIAL-STATISTICAL CHARACTERISTICS OF SEA SURFACE FOAM FIELDS (FROM OPTICAL SOUNDING DATA) [PROSTRANSTVENNO-STATISTICHESKIE KHARAKTERISTIKI PENNYKH POLEI NA MORSKOI POVERKHNOSTI /PO DANNYM OPTICHESKOGO ZONDIROVANIIA/]

I. V. POKROVSKAIA and E. A. SHARKOV (AN SSSR, Institut Kosmicheskikh Issledovaniy, Moscow, USSR) *Issledovanie Zemli iz Kosmosa* (ISSN 0205-9614), Sept.-Oct. 1986, p. 18-25. In Russian. refs

Statistically processed aerial photographs of a rough zone of Caspian Sea on October 31, 1981 were used to obtain experimental distributions of the spatial density of foam formations. The density distributions were found to vary from binomial (in the 0.03725 sq km frame) to Gaussian (1.49 sq km frame). It was found that samples of the spatial density field were linearly uncorrelated in any of their orientation relative to the general wave direction. I.S.

A87-26970

THE COASTAL ZONE COLOR SCANNER VIEWS THE BISMARCK SEA

E. WOLANSKI (Australian Institute of Marine Science, Townsville, Australia), D. J. CARPENTER (Australian National University, Canberra, Australia), and G. L. PICKARD (Australian Institute of Marine Science, Townsville, Australia; British Columbia, University, Vancouver, Canada) *Annales Geophysicae, Series B - Terrestrial and Planetary Physics* (ISSN 0755-0685), vol. 4, Feb. 1986, p. 55-62. refs

Coastal Zone Color Scanner images of the Bismarck Sea, obtained by the Nimbus-7 satellite in mid-September 1979, are described and interpreted to understand the likely near surface physical oceanographic phenomena occurring at the time. An atmospheric correction procedure was applied to eliminate the possibility of features being due to local aerosol variation, and an attempt at deriving a chlorophyll distribution image was made. Relative sea surface temperatures accurate to about 0.5 C were obtained. The long wakes and fronts noted, up to 300 km long and oriented roughly north-south, are suggested to be evidence of atmosphere-ocean interaction downwind of mountains and high islands. R.R.

A87-27545#

CLASSIFICATION OF SEA ICE TYPES WITH SINGLE-BAND (33.6 GHZ) AIRBORNE PASSIVE MICROWAVE IMAGERY

DUANE T. EPPLER, L. DENNIS FARMER, ALAN W. LOHANICK (U.S. Navy, Naval Ocean Research and Development Activity, Bay St. Louis, MS), and MERVYN HOOVER (U.S. Navy, Naval Weapons Center, China Lake, CA) *Journal of Geophysical Research* (ISSN 0148-0227), vol. 91, Sept. 15, 1986, p. 10661-10695. Navy-supported research. refs

During March 1983 extensive high-quality airborne passive Ka band (33.6 GHz) microwave imagery and coincident high-resolution aerial photography were obtained of ice along a 378-km flight line in the Beaufort Sea. Analysis of these data suggests that four classes of winter surfaces can be distinguished solely on the basis of 33.6-GHz brightness temperature: open water, frazil, old ice, and young/first-year ice. New ice (excluding frazil) and nilas display brightness temperatures that overlap the range of temperatures characteristic of old ice and, to a lesser extent, young/first-year ice. Scenes in which a new ice or nilas are present in appreciable amounts are subject to substantial errors in classification if static measures of Ka band radiometric brightness temperature alone are considered. Textural characteristics of nilas and new ice,

however, differ significantly from textural features characteristic of other ice types and probably can be used with brightness temperature data to classify ice type in high-resolution single-band microwave images. In any case, open water is radiometrically the coldest surface observed in any scene. Lack of overlap between brightness temperatures characteristic of other surfaces indicates that estimates of the areal extent of open water based on only 33.6-GHz brightness temperatures are accurate. Author

A87-27546*# National Aeronautics and Space Administration. Goddard Space Flight Center, Greenbelt, Md.

LARGE-SCALE SHORT-PERIOD SEA ICE ATMOSPHERE INTERACTION

ROBERT F. CAHALAN (NASA, Goddard Space Flight Center, Greenbelt, MD) and LONG S. CHIU (NASA, Goddard Space Flight Center, Greenbelt; Applied Research Corp., Landover, MD) *Journal of Geophysical Research* (ISSN 0148-0227), vol. 91, Sept. 15, 1986, p. 10709-10717. refs

Changes in the microwave brightness temperature measured by the Electrically Scanning Microwave Radiometer (ESMR) flown on board the Nimbus V satellite reveal large-scale sea ice fluctuations in the Antarctic marginal ice zone. These ice margin fluctuations are predominantly wave numbers 1-4, with phase speeds of about 3 m/s independent of wave number. The spatial pattern and eastward advection of the sea ice anomalies match those of the atmospheric sea level pressure, and are consistent with sea ice displacement due to surface wind stress. Examination of the outgoing longwave radiation indicates that suppression of high clouds in regions of increased sea ice increases the radiative cooling which contributes to maintaining the ice. Data from three winter seasons indicate about a one-third probability of occurrence of this large scale high frequency sea ice atmosphere interaction during any given 2-week period in winter. Author

A87-27547

AUTOMATED EXTRACTION OF PACK ICE MOTION FROM ADVANCED VERY HIGH RESOLUTION RADIOMETER IMAGERY

R. M. NINNIS, W. J. EMERY, and M. J. COLLINS (British Columbia, University, Vancouver, Canada) *Journal of Geophysical Research* (ISSN 0148-0227), vol. 91, Sept. 15, 1986, p. 10725-10734. refs

Multiple subarea cross correlations have been computed from visible, advanced very high resolution radiometer images of the Beaufort Sea in an automated technique to detect pack ice motion. The computational method is an application of the well-known matched filter and consists of subdividing the first image into a set of subareas and correlating each reference subarea against the appropriate region of the second image. The correlation functions are processed to determine a set of local maxima which define end point vectors of ice displacements from the subarea centers. Resulting velocities agree well with estimates of ice movement obtained by manually measuring invariant ice feature displacements. The velocity fields show the spatial structures of ice motion over scales of 100-500 km with a high degree of pattern consistency and agreement with simple surface wind driving. Author

A87-27848* Oregon State Univ., Corvallis.

FURTHER DEVELOPMENT OF AN IMPROVED ALTIMETER WIND SPEED ALGORITHM

DUDLEY B. CHELTON (Oregon State University, Corvallis) and FRANK J. WENTZ (Remote Sensing Systems, Sausalito, CA) *Journal of Geophysical Research* (ISSN 0148-0227), vol. 91, Dec. 15, 1986, p. 14250-14260. refs
(Contract NAGW-730; NASW-4046)

A previous altimeter wind speed retrieval algorithm was developed on the basis of wind speeds in the limited range from about 4 to 14 m/s. In this paper, a new approach which gives a wind speed model function applicable over the range 0 to 21 m/s is used. The method is based on comparing 50 km along-track averages of the altimeter normalized radar cross section measurements with neighboring off-nadir scatterometer wind speed measurements. The scatterometer winds are constructed from 100

km binned measurements of radar cross section and are located approximately 200 km from the satellite subtrack. The new model function agrees very well with earlier versions up to wind speeds of 14 m/s, but differs significantly at higher wind speeds. The relevance of these results to the Geosat altimeter launched in March 1985 is discussed. Author

A87-27891* R Scan Corp., Minneapolis, Minn.
FORECASTING SEA BREEZE THUNDERSTORMS AT THE KENNEDY SPACE CENTER USING THE PROGNOSTIC THREE-DIMENSIONAL MESOSCALE MODEL (P 3DM)
 WALTER A. LYONS, JEROME A. SCHUH (R-SCAN Corp., Minneapolis, MN), ROGER A. PIELKE, and MOTI M. SEGAL (ASTeR, Inc., Fort Collins, CO) IN: Conference on Weather Forecasting and Analysis, 11th, Kansas City, MO, June 17-20, 1986, Preprints. Boston, MA, American Meteorological Society, 1986, p. 389-396. refs
 (Contract NAS10-11142)

A Prognostic Three-Dimensional Model (P3DM) to produce 1- to 12-hr predictions of sea breeze convective (SBC) storms at KSC is described. The P3DM was developed to account for a scale of about 10 km, interactions between surface heat and moisture fluxes, boundary layer convergence, the movement of moisture into cloud formation zones, and alterations in the convective potential in the lower levels of the atmosphere during the diurnal cycle. Initialized with wind, temperature, specific humidity and local water temperature data, the model allows for the distortion of the boundary layer moisture and thermal fields by sea breeze conditions. The results of three simulations of events leading to the onset of SBC storms are presented to demonstrate the model's capabilities, and techniques which may enhance the accuracy of the predictions are discussed. M.S.K.

A87-28437#
DEVELOPMENT AND EXPERIMENT OF AIRBORNE MICROWAVE RAIN-SCATTEROMETER/RADIOMETER SYSTEM.IV - MICROWAVE BACK-SCATTERING EXPERIMENT OF OCEAN SURFACE

HARUNOBU MASUKO, KENICHI OKAMOTO, HIDEYUKI INOMATA, MASANOBU SHIMADA, HIROYOSHI YAMADA et al. Radio Research Laboratory, Review (ISSN 0033-801X), vol. 32, June 1986, p. 127-138. In Japanese, with abstract in English. refs

An airborne microwave scatterometer/radiometer system was used to observe microwave backscattering signatures of the ocean. The normalized radar cross sections (NRCS) were measured as combined functions of microwave frequency (10.00 GHz and 34.43 GHz), polarization (HH and VV), incident angle (0-70 deg), azimuth angle (0-360 deg), and wind speed (3.2-17.2 m/sec). The azimuth anisotropic signatures at 34.43 GHz were similar to those at 10.00 GHz. The wind speed dependences were analyzed for each azimuth angle, polarization and incident angle. The behavior of NRCS for microwave frequencies are compared with the results obtained by other studies. Some parameters of the ocean surface, such as the effective reflection coefficient, the mean-square surface slope, and the wave-number spectrum of the short surface waves are estimated from the microwave scattering signatures. Author

A87-28509
INTERPRETATION CHARACTERISTICS OF SPACE PHOTOGRAPHS OF SEA COASTS WITH WIND-INDUCED SURGES [OSOBENOSTI DESHIFRIROVANIJA KOSMICHEKIKH SNIMKOV MORSKIKH POBEREZHIJ SO SGONNO-NAGONNYMI IAVLENIAMIJ]

T. V. VERESHCHAKA (Moskovskii Institut Inzhenerov Geodezii, Aerofotos'emki i Kartografii, Moscow, USSR), G. F. KRASNOZHON, and I. E. KURBATOVA (AN SSSR, Institut Vodnykh Problem, Moscow, USSR) Geodeziia i Aerofotos'emka (ISSN 0536-101X), no. 4, 1986, p. 93-97. In Russian. refs

A method for interpreting satellite photographs of sea coasts with wind-induced surges is described, and results are presented for the North Caspian. Indirect indicators are examined which are significant in connection with the investigation of shoreline changes,

flood zones, and other phenomena affecting agriculture and biomass in the coastal region. B.J.

A87-29014
DISTRIBUTION AND BIOMASS OF FUCUS VESICULOSUS L. NEAR A COOLING-WATER EFFLUENT FROM A NUCLEAR POWER PLANT IN THE BALTIC SEA ESTIMATED BY AERIAL PHOTOGRAPHY
 GORAN BOBERG, BJORN GANNING, and KARL YTTERBORN, H. (Stockholms Universitet, Stockholm, Sweden) International Journal of Remote Sensing (ISSN 0143-1161), vol. 7, Dec. 1986, p. 1797-1807. refs

A87-29015
A RADAR OCEAN IMAGING MODEL FOR SMALL TO MODERATE INCIDENCE ANGLES
 DENNIS HOLLIDAY, GAETAN ST-CYR, and NANCY E. WOODS (R & D Associates, Marina del Rey, CA) International Journal of Remote Sensing (ISSN 0143-1161), vol. 7, Dec. 1986, p. 1809-1834. refs

Based on a first-principles scattering theory applicable to small to moderate incidence angles, a new imaging model for ocean features is proposed. In contrast to the Alpers and Hennings Bragg-based model, the new model incorporates the full ocean wave spectrum, utilizes Hughes' suggested spectral decay rate formula and contains no adjustable parameters. For typical ocean currents, the new model predicts realistic values for L-band cross section modulations and comparable L-band and X-band cross section modulations. These latter results are shown to be due to backscatter from ocean waves that are significantly longer than the Bragg resonant wave. By comparison the Bragg-based imaging model is shown to predict that X-band modulations will be at least one order of magnitude weaker than L-band modulations. Author

A87-29019
ON THE USE OF SYNTHETIC 12-MICRON DATA IN A SPLIT-WINDOW RETRIEVAL OF SEA SURFACE TEMPERATURE FROM AVHRR MEASUREMENTS
 P. J. MINNETT (NATO, Saclant Anti-Submarine Warfare Research Center, La Spezia, Italy) International Journal of Remote Sensing (ISSN 0143-1161), vol. 7, Dec. 1986, p. 1887-1891. refs
 (Contract CEC-STI-022-J-C)

A87-30143* California Univ., Los Angeles.
TIDAL HEATING IN AN INTERNAL OCEAN MODEL OF EUROPA
 M. N. ROSS and G. SCHUBERT (California, University, Los Angeles) Nature (ISSN 0028-0836), vol. 325, Jan. 8, 1987, p. 133, 134. refs
 (Contract NSG-7315)

Results are reported from computations of tidal heating processes in a realistic three-layer Europa model featuring an elastic ice lithosphere, an underlying inviscid water layer, and an elastic silicate core. The volumic density of the outer two layers were 940 and 1000, respectively, while the European mean density was 3030 kg/cu m and the total depth of the water layers was 100 km. Calculations of various thermal distributions in the liquid layer, heated tidally by the core, indicate that a decoupled ice lithosphere would be distorted by 23 m at the sub-jovian point, which would correspond with a Love number of 0.26. The tidal heating scenario does not explain the observed recent cracking of Europa's surface, unless the satellite also recently had a significantly more eccentric orbit. M.S.K.

A87-30146

SHEDDING OF AN AGULHAS RING OBSERVED AT SEA

J. R. E. LUTJEHARMS (Council for Scientific and Industrial Research, National Research Institute for Oceanology, Stellenbosch, Republic of South Africa) and A. L. GORDON (Lamont-Doherty Geological Observatory, Palisades, NY) *Nature* (ISSN 0028-0836), vol. 325, Jan. 8, 1987, p. 138-140. Research supported by the Foundation for Research Development. refs (Contract N00014-84-C-0132)

The Agulhas current flowing northerly into the Atlantic along the southern African coast has the largest volume of water, about 130 million cu m/sec, of any current in the Southern Hemisphere. Meteosat II thermal IR imagery, at 10.5-12.5 microns, of the current in November 1983 showed that the current shed vortex rings as the current encountered Antarctic surface waters. The evolution of the features and the path of the current, supported by surface buoy tracks, is traced over several days. The data indicated that the ring changed from an elliptical to a more stable, circular shape, and had a uniform temperature of about 10 C to a depth of at least 100 m. The ring eventually moved into the south Atlantic and is estimated to contribute up to 7 pct of the energy contributed by the wind to the basin. M.S.K.

A87-30883

OCEAN REMOTE SENSING

ROBERT L. BERNSTEIN (California, University, La Jolla) and PAYSON R. STEVENS IN: *Space science and applications: Progress and potential*. New York, IEEE Press, 1986, p. 123-131. refs

The areas in which spaceborne remote sensing of the oceans are ready to move from the demonstration project phase to routine utilization are surveyed. Seasat scatterometry furnished data for mapping global ocean current and surface wind patterns. Radar altimetry provides 10 cm accuracy for monitoring the sea surface height to map the vertical distribution of ocean thermal storage. Both passive and active microwave sensors have proven useful for mapping sea ice formation and movement, with active sensors providing 25 m resolution and global orbits allowing tracking ice movement over a 3 day period. Coastal Zone Color Scanner images have identified the boundaries between plankton-heavy regions and open ocean, data which permits fishing fleets to locate the interface where preferred fish schools swim. Landsat imagery has also allowed tracking the drift and dispersion of municipal waste dumped into the ocean. M.S.K.

A87-30900

THE QUANTITATIVE USE OF AIRBORNE THEMATIC MAPPER THERMAL INFRARED DATA

R. D. CALLISON, P. BLAKE, and J. M. ANDERSON (Dundee, University, Scotland) *International Journal of Remote Sensing* (ISSN 0143-1161), vol. 8, Jan. 1987, p. 113-126. refs

Daedalus Airborne Thematic Mapper (ATM) data, obtained between 12.14 GMT and 13.44 GMT on June 19, 1984 as part of the Natural Environment Research Council's Airborne MSS-84 campaign, have been used to calculate sea surface temperatures in the western English Channel. Quantitative analyses of the thermal infrared data are discussed with particular reference to boat trials and eddy structures. A method to calculate brightness temperatures and their associated errors is also discussed along with a review of two atmospheric correction procedures for the estimation of sea surface temperatures from thermal infrared data. An apparent asymmetry in the thermal infrared data is considered in the context of the atmospheric correction model used. Results show that the asymmetry can be compensated by using an effective scanner tilt angle. Author

A87-30923* National Oceanic and Atmospheric Administration, Seattle, Wash.

EQUATORIAL LONG-WAVE CHARACTERISTICS DETERMINED FROM SATELLITE SEA SURFACE TEMPERATURE AND IN SITU DATA

PATRICIA E. PULLEN (NOAA, Pacific Marine Environmental Laboratory, Seattle, WA), ROBERT L. BERNSTEIN (SeaSpace, San Diego, CA), and DAVID HALPERN (California Institute of Technology, Jet Propulsion Laboratory, Pasadena) *Journal of Geophysical Research* (ISSN 0148-0227), vol. 92, Jan. 15, 1987, p. 742-748. NOAA-supported research. refs

SST maps and imagery derived from the NOAA 6 satellite AVHRR for June and July 1981 in the eastern tropical Pacific portray the wavelike structure of the cool water along the equator from 93 deg W to 125 deg W. Cusped waves of approximately 1000-km zonal wavelength and 25-day period propagated westward with a phase speed of 40 km/day. The observed meridional extent between the crest and trough of the waves is about 300 km. Details in the imagery show cooler water at the cusps advected north and then east with the north equatorial countercurrent (NECC), consistent with the suggestion of a series of anticyclonic eddies occupying the shear zone between the NECC and the westward flowing south equatorial current. Absolute SST estimates from the AVHRR data agree to within 0.6 C with shipboard data taken along 110 deg W between 5 deg N and 5 deg S. The wavelike structures in the SST maps are also in agreement at the surface with a vertical expendable bathythermograph temperature section made along the equator between 93 deg W and 125 deg W, which shows the phase of the waves tilting westward with increasing depth over the upper 75 m. Such a phase shift, if it extended 100-200 km meridionally in either direction from the equator, would be associated with an equatorward flux of heat. Similar phase shifts appear in temperature time series at depths of 20 and 50 m, from a mooring at 0-deg 33-min N, 110-deg 30-min W. Near-surface currents measured at this and a second mooring on the equator at 109-deg 40-min W indicate a regular pattern of northward advection when wave cusps pass them, followed by southwest flow during the passage of wave troughs, again consistent with an equatorward flux of heat, as well as with earlier theoretical and drift buoy findings. Author

A87-30925

ISLAND WAKES AND HEADLAND EDDIES - A COMPARISON BETWEEN REMOTELY SENSED DATA AND LABORATORY EXPERIMENTS

CHARITHA PATTIARATCHI, ALEC JAMES, and MICHAEL COLLINS (Swansea, University College, Wales) *Journal of Geophysical Research* (ISSN 0148-0227), vol. 92, Jan. 15, 1987, p. 783-794. NERC-supported research. refs

Island wakes and headland eddies in coastal waters are identified from spaceborne and airborne remotely sensed imagery in the visible wavelengths. The imagery were obtained for the Bristol and English channels, United Kingdom, which are characterized by high tidal currents and levels of turbidity. Suspended matter in the surface waters is used as a passive tracer for the flow features. Scaling parameters (e.g., the Reynolds, Ekman, and Rossby numbers), obtained from the depth-averaged equation of motion, are presented, based upon information on oceanographic conditions at the times of the overpasses. The parameters are compared with data obtained from laboratory model investigations, presented by other experimenters in the published literature. The remotely sensed data demonstrate that in coastal waters with nonuniform obstacles and bathymetry, for a given Ekman number, the flow regimes occur at a lower Rossby number than might be expected from laboratory experiments. In the absence of a method for the accurate determination of the horizontal eddy viscosity, hence the Reynolds number, it is concluded that an 'island wake parameter' (Wolanski et al., 1984) should be adopted to describe such features in coastal waters. Author

N87-15652# GKSS-Forschungszentrum Geesthacht (West Germany). Inst. fuer Physik.

MULTIANGLE OR MULTIWAVELENGTH TECHNIQUE FOR REMOTE SENSING OF SEA SURFACE TEMPERATURE

WALTER MEYER (Kiel Univ., West Germany) and HARTMUT GRASSL *In* Ludwig-Maximilians-Universitaet Satellite Measurements of Radiation Budget of the Earth (3rd Symposium) p 155-162 Jul. 1986

Avail: NTIS HC A09/MF A01; Fachinformationszentrum, Karlsruhe, West Germany DM 37

The multiangle and multiwavelength techniques for sea surface temperature (SST) estimation were compared, using channels 4 and 5 of the Advanced Very High Resolution Radiometer/2 (AVHRR/2) on NOAA-7 centered at 10.8 and 12.0 microns, respectively, for the split window and the multiple angle approach. The influence of horizontal inhomogeneity, modeled by thin, almost invisible cirrus clouds, on the multiangle method was also examined. Results show no improvement in determining SST from measurements at two angles or by combining a two wavelength and a two angle technique at present radiometer noise levels. The influence of almost invisible, thin cirrus clouds on the conical scan is drastic. Normally distributed cirrus clouds (optical thickness between 0 and 0.02) add 0.8 K to the mean total error, reaching 1.31 K for polluted skies. Only direct comparison between the measurements of the Along Track Scanning Radiometer and the AVHRR/2 can decide which technique is best. ESA

N87-15989# Joint Publications Research Service, Arlington, Va. **DEVELOPMENT, STATUS, PROSPECTS OF MARINE OBSERVATION SATELLITE**

KOHEI ARAI *In its* Japan report: Science and Technology (JPRS-JST-86-018) p 25-40 2 Jul. 1986 Transl. into ENGLISH from Kaiyo Kagaku (Tokyo, Japan), Aug. 1985 p 510-516
Avail: NTIS HC A05/MF A01

The purpose for the development of the Marine Observation Satellite No 1 (MOS-1), the first Japanese Earth observation satellite, its present condition, future plans, systems, observational principles, and possibilities for observation are discussed. Author

N87-16384# Texas Univ., Austin. Center for Space Research. **NROSS (NAVY REMOTE OCEAN SENSING SYSTEM) TRACKING NETWORK ANALYSIS**

B. D. TAPLEY, J. C. RIES, and C. RAJASENAN 1986 19 p (Contract N00014-85-K-2034)
(AD-A172132) Avail: NTIS HC A02/MF A01 CSCL 04B

One of the main objectives of the NROSS mission is the daily production of mesoscale feature maps of selected ocean areas. The NROSS payload will include a SEASAT-class altimeter for the production of these maps and a scatterometer to measure wind speed and direction over the oceans. These wind measurements will be used in conjunction with the precision altimetry from TOPEX to examine the relationship between ocean circulation and winds. The authors conclude that the applicability of a particular tracking network would appear to depend strongly on orbit accuracy requirements. One- to two-meter radial orbit accuracies are fairly easily obtained with current gravity models and almost any tracking scenario if the arcs are long enough. However, if more accurate orbits are required, either the arcs must be shortened to reduce dynamical model error effects, the gravity models must be improved significantly, or some postlaunch gravity tuning is necessary. The latter technique can be successfully employed only if the tracking is fairly global, or geographically correlated errors will occur in the resulting geopotential field. In this case all the permanent sites and possibly many of the portable sites may be required. The same is true if the arcs are merely shortened, since there must be enough well distributed data to average out measurement model errors. Thus only the denser tracking networks are likely to provide radial orbit accuracies significantly below the 1 meter level. GRA

N87-16492*# National Aeronautics and Space Administration. Langley Research Center, Hampton, Va.

ARCHIVAL OF SEASAT-A SATELLITE SCATTEROMETER DATA MERGED WITH IN SITU DATA AT SELECTED, ILLUMINATED SITES OVER THE OCEAN

LYLE C. SCHROEDER and JON L. SWEET (PRC Kentron, Inc., Hampton, Va.) Feb. 1987 21 p (NASA-TM-87736; L-16156; NAS 1.15:87736) Avail: NTIS HC A02/MF A01 CSCL 08J

A large data base of Seasat-A Satellite Scatterometer (SASS) measurements merged with high-quality surface-truth wind, wave, and temperature data has been documented. The data base was developed for all times when selected in situ measurement sites were within the SASS footprint. Data were obtained from 42 sites located in the coastal waters of North America, Australia, Western Europe, and Japan and were assembled by correlating the SASS and surface-truth measurements in both time and distance. These data have been archived on a set of nine-track 6250 bpi ASCII coded magnetic tapes, which are available from the National Technical Information Service. Author

N87-16493# Naval Academy, Annapolis, Md. **ANALYSIS OF SURFACE PATTERNS OVER COBB SEAMOUNT USING SYNTHETIC-APERTURE RADAR IMAGERY Final Report, 1985 - 1986**

CLARK B. FREISE 27 May 1986 64 p (AD-A171670; USNA-TSPR-136) Avail: NTIS HC A04/MF A01 CSCL 17I

Anomalies in surface wave patterns observed on SEASAT Synthetic-Aperture Radar (SAR) imagery over Cobb Seamount are examined. These anomalies are the surface expression of currents interacting with the seamount. The wavelength of the imaged surface patterns are extracted with advanced SAR digital image processing techniques. Nine of the ten detected wavelengths match the expected spectral wavelength envelope of the internal waves that are calculated using oceanographic data. The results show that the wavelengths of the surface pattern imaged are actually the surface manifestation of internal waves on a subsurface density interface. The internal waves are created by current flow over and around Cobb Seamount disturbing the density interface. Author (GRA)

N87-17147*# Johns Hopkins Univ., Laurel, Md. Applied Physics Lab.

HYDRODYNAMICS OF INTERNAL SOLITONS AND A COMPARISON OF SIR-A AND SIR-B DATA WITH OCEAN MEASUREMENTS

J. R. APEL, R. F. GASPAROVIC, and D. R. THOMPSON *In* JPL The Second Spaceborne Imaging Radar Symposium p 91-102 1 Dec. 1986

Avail: NTIS HC A10/MF A01 CSCL 08H

Large internal solitary waves have been observed by Shuttle SIR-A and SIR-B at locations in the Andaman Sea and the New York Bight. Satellite imagery and oceanographic measurements are used in conjunction with hydrodynamic interaction and electromagnetic scattering models to estimate the expected SAR image intensity modulations associated with the internal waves. There is reasonable agreement between the predicted and observed internal wave signatures. Author

N87-17149*# Johns Hopkins Univ., Laurel, Md. Applied Physics Lab.

OPERATIONAL WAVE FORECASTING WITH SPACEBORNE SAR: PROSPECTS AND PITFALLS

R. C. BEAL *In* JPL The Second Spaceborne Imaging Radar Symposium p 107-113 1 Dec. 1986

Avail: NTIS HC A10/MF A01 CSCL 08C

Measurements collected in the Shuttle Imaging Radar (SIR-B) Extreme Waves Experiment confirm the ability of Synthetic Aperture Radar (SAR) to yield useful estimates of wave directional energy spectra over global scales, at least for shuttle altitudes. However, azimuth fall-off effects tend to become severe for wavelengths shorter than about 100 m in most sea states. Moreover, the azimuth

05 OCEANOGRAPHY AND MARINE RESOURCES

fall-off problem becomes increasingly severe as the platform altitude increases beyond 300 km. The most viable solution to the global wave measurements problem may be a low altitude spacecraft containing a combination of both the SAR and the Radar Ocean Wave Spectrometry (ROWS). Such a combination could have a synergy which yield global spectral estimates superior to those of either instrument singly employed. Author

N87-17150*# Environmental Research Inst. of Michigan, Ann Arbor. Radar Science Lab.

IMAGING RADAR CONTRIBUTIONS TO A MAJOR AIR-SEA-ICE INTERACTION STUDY IN THE GREENLAND SEA

ROBERT A. SHUCHMAN /in JPL The Second Spaceborne Imaging Radar Symposium p 114-118 1 Dec. 1986
Avail: NTIS HC A10/MF A01 CSCL 08C

By virtue of the Synthetic Aperture Radar (SAR's) imaging capabilities, such as all-weather imaging, relatively high resolution, and large dynamic range of backscatter from SAR ice and open ocean, information on the important marginal ice zone (MIZ) parameters can be derived from the SAR data. Information on ice edge location and location of ice-edge eddies, for example, can be obtained directly from examination of the imagery as can detection of ocean fronts and internal waves. With machine-assisted manual image analysis, estimates of ice concentration, floe size distributions, and ice field motion can also be derived. Full digital analysis, however, is required to obtain gravity wave spectral information and backscatter statistics for ice type discrimination and automated ice concentration algorithms. Author

N87-17151*# Washington Univ., Seattle. Applied Physics Lab.
OBSERVING THE POLAR OCEANS WITH SPACEBORNE RADAR

DREW ROTHROCK /in JPL The Second Spaceborne Imaging Radar Symposium p 119-122 1 Dec. 1986
Avail: NTIS HC A10/MF A01 CSCL 08C

The application of spaceborne imaging radar data to polar oceanography and sea ice is explored. Several problems come to mind which are presently ripe with ideas and models, but are in need of new data, SAR data, for any progress to be made. These are the study of the ice mass balance, the ice momentum balance, and the circulation of the Arctic Ocean. These problems are described along with the data which is applicable to them and can be extracted from SAR imagery. Some uses are discussed of these data to explore mesoscale processes which affect the oceans and ice cover. Author

N87-17166# National Space Development Agency, Tokyo (Japan). Earth Observation Center.

SOME RESULTS OF MARINE OBSERVATION SATELLITE (MOS-1) AIRBORNE VERIFICATION EXPERIMENT MULTISPECTRAL ELECTRONIC SELF SCANNING RADIOMETER (MESSR)

K. MAEDA, M. KOJIMA, and Y. AZUMA /in ESA Proceedings of the 1986 International Geoscience and Remote Sensing Symposium (IGARSS '86) on Remote Sensing: Today's Solutions for Tomorrow's Information Needs, Volume 1 p 15-20 Aug. 1986

Avail: NTIS HC A99/MF E03; ESA, Paris, France, 3 volume set \$90 Member States, AU, CN, and NO (+20% others)

In order to develop distortion correction methods for Marine Observation Satellite-1 (MOS-1) data and the evaluation methods for Earth observation system, airborne verification experiments using three airborne sensors equivalent in performance to MOS-1 sensors were conducted. A multispectral electronic self-scanning radiometer (MESSR) developed by modifying the engineering model of MOS-1 MESSR, which is capable of observing in visible and near-infrared wavelengths with CCD detector elements was tested in an airborne configuration. Results will be used in the spaceborne verification. ESA

N87-17184*# Environmental Research Inst. of Michigan, Ann Arbor. Radar Science Lab.

AN INTER-SENSOR COMPARISON OF THE MICROWAVE SIGNATURES OF ARCTIC SEA ICE

R. G. ONSTOTT /in ESA Proceedings of the 1986 International Geoscience and Remote Sensing Symposium (IGARSS '86) on Remote Sensing: Today's Solutions for Tomorrow's Information Needs, Volume 1 p 117-120 Aug. 1986
(Contract NAGW-334; N000-14-81-C-0295; N000-14-83-C-0404; N000-14-85-K-0200)

Avail: NTIS HC A99/MF E03; ESA, Paris, France, 3 volume set \$90 Member States, AU, CN, and NO (+20% others) CSCL 08L

Active and passive microwave and physical properties of Arctic sea ice in the marginal ice zone were measured during the summer. Results of an intercomparison of data acquired by an aircraft synthetic aperture radar, a passive microwave imager and a helicopter-mounted scatterometer indicate that early-to-mid summer sea ice microwave signatures are dominated by snowpack characteristics. Measurements show that the greatest contrast between thin first-year and multiyear sea ice occurs when operating actively between 5 and 10 GHz. Significant information about the state of melt of snow and ice is contained in the active and passive microwave signatures. ESA

N87-17185*# National Aeronautics and Space Administration. Goddard Space Flight Center, Greenbelt, Md.

ACTIVE/PASSIVE MICROWAVE SENSOR COMPARISON OF MIZ-ICE CONCENTRATION ESTIMATES

B. A. BURNS (Environmental Research Inst. of Michigan, Ann Arbor), D. J. CAVALIERI, and M. R. KELLER (Naval Research Lab., Washington, D. C.) /in ESA Proceedings of the 1986 International Geoscience and Remote Sensing Symposium (IGARSS '86) on Remote Sensing: Today's Solutions for Tomorrow's Information Needs, Volume 1 p 121-125 Aug. 1986

Avail: NTIS HC A99/MF E03; ESA, Paris, France, 3 volume set \$90 Member States, AU, CN, and NO (+20% others) CSCL 08L

Active and passive microwave data collected during the 1984 summer Marginal Ice Zone Experiment in the Fram Strait (MIZEX 84) are used to compare ice concentration estimates derived from synthetic aperture radar (SAR) data to those obtained from passive microwave imagery at several frequencies. The comparison is carried out to evaluate SAR performance against the more established passive microwave technique, and to investigate discrepancies in terms of how ice surface conditions, imaging geometry, and choice of algorithm parameters affect each sensor. Active and passive estimates of ice concentration agree on average to within 12%. Estimates from the multichannel passive microwave data show best agreement with the SAR estimates because the multichannel algorithm effectively accounts for the range in ice floe brightness temperatures observed in the MIZ. ESA

N87-17186*# Stanford Univ., Calif. STAR Lab.
AUTOMATED REMOTE SENSING OF SEA ICE USING SYNTHETIC APERTURE RADAR

J. F. VESECKY, R. SAMADANI, M. P. SMITH, J. M. DAIDA, and R. N. BRACEWELL /in ESA Proceedings of the 1986 International Geoscience and Remote Sensing Symposium (IGARSS '86) on Remote Sensing: Today's Solutions for Tomorrow's Information Needs, Volume 1 p 127-132 Aug. 1986 Sponsored by NASA and ONR

Avail: NTIS HC A99/MF E03; ESA, Paris, France, 3 volume set \$90 Member States, AU, CN, and NO (+20% others) CSCL 08J

Two techniques for automated sea ice tracking: image pyramids (hierarchical correlation) and feature tracking were applied to a pair of SEASAT SAR sea ice images. The results compare well with each other and manually tracked estimates of the ice velocity field. Refinement of the image pyramid technique should include removal of a small number of erroneous velocity vectors using constraints dependent on correlation coefficient, near neighbor

velocities, and velocity gradients. Estimates of sea ice velocity are successfully obtained over limited areas using the boundary segment tracking technique. Refinement of the feature tracking technique should include use of pressure ridge features, constrained search, and relaxation techniques. ESA

N87-17189# Canada Centre for Remote Sensing, Ottawa (Ontario). RADARSAT Project Office.

AN OVERVIEW OF OPERATIONAL SAR DATA COLLECTION AND DISSEMINATION PLANS FOR ERS-1 ICE DATA IN CANADA

L. MCNUTT and T. MULLANE (Atmospheric Environment Service, Ottawa, Ontario) *In* ESA Proceedings of the 1986 International Geoscience and Remote Sensing Symposium (IGARSS '86) on Remote Sensing: Today's Solutions for Tomorrow's Information Needs, Volume 1 p 147-152 Aug. 1986
 Avail: NTIS HC A99/MF E03; ESA, Paris, France, 3 volume set \$90 Member States, AU, CN, and NO (+20% others)

The ERS-1 and RADARSAT automated ice information system is described. This Ice Data Integration and Analysis System (IDIAS) will receive data from several sources, including satellite, aircraft, and ship reports, and integrate these onto a standard base map for production of ice forecast products. The satellite data will be received via the station in Gatineau, Quebec and the aircraft data will be downlinked to line-of-sight stations in the Arctic and retransmitted to Ottawa via the Anik-D satellite. The plans for ERS-1 data reception at Gatineau, data integration and product generation from the IDIAS system, and Canadian plans for operational demonstrations of the end-to-end information system within the ERS-1 timeframe are discussed. ESA

N87-17190# European Space Agency, Paris (France).

OVERVIEW AND STATUS OF THE ERS-1 PROGRAM

G. DUCHOSSOIS *In its* Proceedings of the 1986 International Geoscience and Remote Sensing Symposium (IGARSS '86) on Remote Sensing: Today's Solutions for Tomorrow's Information Needs, Volume 1 p 155-159 Aug. 1986
 Avail: NTIS HC A99/MF E03; ESA, Paris, France, 3 volume set \$90 Member States, AU, CN, and NO (+20% others)

The ERS-1 satellite system, and the ground segment configuration selected to allow global oceanic mission and delivery of standard products to users within 3 hr from observation are presented. Key features of the ERS-1 program, and information on the Announcement of Opportunity issued to solicit proposals for science investigations and application demonstrations are outlined. ESA

N87-17213*# City Coll. of the City Univ. of New York
VERIFICATION RESULTS FOR A TWO-SCALE MODEL OF MICROWAVE BACKSCATTER FROM THE SEA SURFACE

W. J. PIERSON, JR. and M. A. DONELAN (National Water Research Inst., Burlington, Ontario) *In* ESA Proceedings of the 1986 International Geoscience and Remote Sensing Symposium (IGARSS '86) on Remote Sensing: Today's Solutions for Tomorrow's Information Needs, Volume 1 p 297-302 Aug. 1986

(Contract NAGW-690)
 Avail: NTIS HC A99/MF E03; ESA, Paris, France, 3 volume set \$90 Member States, AU, CN, and NO (+20% others) CSCL 08C

The backscatter model of Donelan and Pierson (1986) was adjusted to fit Ku-Band at 13.9 GHz. Data from L to Ka-band are used to test the model. In general, there is no power law. When the wind drops below certain threshold speeds there may be no detectable Bragg backscatter. Saturation may occur at high winds. Results from the Seasat-SASS are used to substantiate the predictions of the model. Suggestions for experiments for determining the overall validity of the model are made. ESA

N87-17215# Physics and Electronics Lab. TNO, The Hague (Netherlands).

C AND KU-BAND SCATTEROMETER RESULTS FROM THE SCATMOD INTERNAL WAVE EXPERIMENT

D. VANHALSEMA, A. L. GRAY (Canada Centre for Remote Sensing, Ottawa, Ontario) 03(Defence Research Establishment Pacific, Victoria, British Columbia), S. J. HUGHES, and B. A. HUGHES *In* ESA Proceedings of the 1986 International Geoscience and Remote Sensing Symposium (IGARSS '86) on Remote Sensing: Today's Solutions for Tomorrow's Information Needs, Volume 1 p 311-317 Aug. 1986 Sponsored by a Canadian Defence Research Fellowship

Avail: NTIS HC A99/MF E03; ESA, Paris, France, 3 volume set \$90 Member States, AU, CN, and NO (+20% others)

Microwave backscatter values were obtained every 12.5 m by aircraft for incidence angles between 17 and 53 deg for 10 internal wave groups in Georgia Strait. Simultaneously, surface measurements (wave slopes, surface current, position, wind) were made. Under all conditions encountered during the 6 day experiment, internal-wave-induced backscatter modulations were measured. The magnitude of the modulations depends strongly on the wind speed. At low wind speed (1.5 to 2 m/sec) high contrasts (20 dB) are observed. At intermediate higher wind speed (6 m/sec) the modulations are much smaller (2 dB) and only weakly dependent on incidence angle. The average contrast in the Ku-band is 1 dB larger than in the C-band. When the magnitude of the modulations is plotted against the first order Bragg wavenumber, a distinct discontinuity occurs at the transition point between C and Ku-band. ESA

N87-17217# Kansas Univ. Center for Research, Inc., Lawrence. Radar Systems and Remote Sensing Lab.

TOWER-BASED BROADBAND BACKSCATTERING MEASUREMENTS FROM THE OCEAN SURFACE IN THE NORTH SEA

A. H. CHAUDRY, S. P. GOGINENI, and R. K. MOORE *In* ESA Proceedings of the 1986 International Geoscience and Remote Sensing Symposium (IGARSS '86) on Remote Sensing: Today's Solutions for Tomorrow's Information Needs, Volume 1 p 327-335 Aug. 1986

Avail: NTIS HC A99/MF E03; ESA, Paris, France, 3 volume set \$90 Member States, AU, CN, and NO (+20% others)

Broadband radar backscatter measurements were made in the North Sea, from aircraft and from a tower. Vertically and horizontally polarized radar backscattering measurements from the tower at C, X and Ku-bands, for the incidence angle range of 18 to 70 deg, wind speed range of 3 to 25 m/sec, and antenna look directions of upwind, downwind, and crosswind were made. Wind scatterometry and modulation-transfer-function (MTF) results are compared with those obtained from aircraft measurements and previous observations. Tower measurements compare well with the aircraft measurements in contradiction to results that showed higher scattering coefficient for the tower than for the aircraft. The magnitude of the crosswind MTF is higher than that for upwind. Location of the maximum scattering on the long ocean wave is obtained by the phase of the MTF and by the cross correlation lag of the radar power return and the long wave height. ESA

N87-17219# Environmental Research Inst. of Michigan, Ann Arbor. Radar Science Lab.

GEOPHYSICS OF THE MARGINAL ICE ZONE FROM SAR

R. A. SCHUCHMAN, B. A. BURNS, C. G. CARUTHERS, J. D. LYDEN, E. SVENDSEN (Bergen Univ., Norway), O. M. JOHANNESSEN, T. OLAUSSEN, and J. A. JOHANNESSEN *In* ESA Proceedings of the 1986 International Geoscience and Remote Sensing Symposium (IGARSS '86) on Remote Sensing: Today's Solutions for Tomorrow's Information Needs, Volume 1 p 345-351 Aug. 1986

(Contract N000-14-81-C-0295; N000-14-83-C-0404)
 Avail: NTIS HC A99/MF E03; ESA, Paris, France, 3 volume set \$90 Member States, AU, CN, and NO (+20% others)

Marginal Ice Zone (MIZ) sequential high resolution aircraft Synthetic Aperture Radar (SAR) images from a region in the Fram

Strait north of 78 N were analyzed. Changes in ice concentration, floe size distribution, and ice edge position, as well as eddy location and floe motion derived from multitemporal SAR images are investigated in terms of ocean surface current, wind fields and the bathymetry of the region. The SAR observations show that the MIZ ice cover is highly variable and exhibits rapid dynamic and thermodynamic responses. At the ice edge, during light to moderate wind conditions, the ice drift mirrors the ocean circulation. Radar derived ice kinematics also provide information on ocean eddies beneath the ice in the interior of the MIZ. ESA

N87-17221# Technical Univ. of Denmark, Lyngby. Inst. of Electromagnetics.

SEA ICE IN THE GREENLAND SEA OBSERVED BY THE NIMBUS-7 SCANNING MULTICHANNEL MICROWAVE RADIOMETER (SMMR)

P. SLOTH and L. T. PEDERSEN *In* ESA Proceedings of the 1986 International Geoscience and Remote Sensing Symposium (IGARSS '86) on Remote Sensing: Today's Solutions for Tomorrow's Information Needs, Volume 1 p 357-361 Aug. 1986 Sponsored by the Technical Univ. of Denmark, the Danish Space Research Committee, the Commission for Scientific Research, Greenland, and IBM Denmark
Avail: NTIS HC A99/MF E03; ESA, Paris, France, 3 volume set \$90 Member States, AU, CN, and NO (+20% others)

Using a simple model for the relation between microwave radiances and sea ice concentration, the ice cover in the Greenland Sea was investigated. Analysis of a time series of data from the NIMBUS-7 Scanning Microwave Radiometer suggests a theory for the formation of the ice cover phenomenon Odden, a large tongue of ice in the Greenland Sea. A cellular circulation on the shelf driven by strong winds from the north is proposed as the driving mechanism behind the melting of ice along the shelf slope. ESA

N87-17222# Columbia Univ., Palisades, N.Y. Lamont-Doherty Geological Observatory.

SAR ICE FLOE KINEMATICS AND CORRELATION WITH MESOSCALE OCEANIC STRUCTURE WITHIN THE MARGINAL ICE ZONE

T. O. MANLEY, R. A. SHUCHMAN (Environmental Research Inst. of Michigan, Ann Arbor.), and B. A. BURNS *In* ESA Proceeding of the 1986 International Geoscience and Remote Sensing Symposium (IGARSS '86) on Remote Sensing: Today's Solutions for Tomorrow's Information Needs, Volume 1 p 363-366 Aug. 1986

(Contract N00014-85-C-0132; N00014-81-C-0259; N00014-83-C-0404)

Avail: NTIS HC A99/MF E03; ESA, Paris, France, 3 volume set \$90 Member States, AU, CN, and NO (+20% others)

Synthetic aperture radar images collected over the same geographic area and over fairly short periods of time were used to prepare ice floe kinematic (floe trajectory) diagrams which show a positive correlation with a subice mesoscale frontal feature. The subice mesoscale feature is confirmed using helicopter-based oceanographic conductivity, temperature, density profiles and neutrally-buoyant sofar drifting floats. ESA

N87-17259# Atmospheric Environment Service, Downsview (Ontario).

APPLICATION OF THE SEASAT SCATTEROMETER TO OBSERVATIONS OF WIND SPEED AND DIRECTION AND ARCTIC ICE/WATER BOUNDARIES

S. PETERHERYCH, A. F. DAVIES, and G. MUTTIT *In* ESA Proceedings of the 1986 International Geoscience and Remote Sensing Symposium (IGARSS '86) on Remote Sensing: Today's Solutions for Tomorrow's Information Needs, Volume 1 p 585-588 Aug. 1986

Avail: NTIS HC A99/MF E03; ESA, Paris, France, 3 volume set \$90 Member States, AU, CN, and NO (+20% others)

Using conventional marine, land, and undealiased scatterometer data, a streamline analysis, a surface pressure analysis, and an Arctic ice-water boundary analysis were prepared. A low pressure center located near the coast in the Gulf of Alaska produced high

winds as far west as the Chukchi Sea (70 N, 180 W) northward to 75 N and eastward to Victoria Island (110 W). Surface ship and land data is used to assist the selection of the correct wind direction. A streamline and MSL pressure analysis are prepared. Undealiased Seasat data are used to identify the ice/water boundary. ESA

N87-17295# Defence Research Establishment Pacific, Victoria (British Columbia).

ESTIMATION OF INTERNAL WAVE CURRENTS FROM SAR AND INFRARED SCATTEROMETER IMAGERY

S. J. HUGHES and B. A. HUGHES *In* ESA Proceedings of the 1986 International Geoscience and Remote Sensing Symposium (IGARSS '86) on Remote Sensing: Today's Solutions for Tomorrow's Information Needs, Volume 2 p 789-794 Aug. 1986
Avail: NTIS HC A17/MF A01; ESA, Paris, France, 3 volume set \$90 Member States, AU, CN, and NO (+20% others)

Models for estimating internal-wave surface currents from SAR and infrared scatterometer images of the ocean surface are presented. Selected SAR images were analyzed using linear hydrodynamic interaction theory and first-order hydrodynamic interaction theory and first-order Bragg scattering, and one IR scatterometer image was analyzed using a semi empirical slope-probability-density model. It is shown that surface features evident in the remote imagery correspond to fluctuations in the measured internal-wave surface current. For both models, it is assumed that the internal-wave current amplitude is much smaller than the propagation speed. Although the wave fields presented have current amplitudes which may be too large for a rigorous application of this linear approximation, the estimated currents compare well with the surface-truth measurements. ESA

N87-17296# Naval Ocean Research and Development Activity, Bay St. Louis, Miss.

OBSERVATIONS OF SURFACE CURRENTS AT NANTUCKET SHOALS AND IMPLICATIONS FOR RADAR IMAGING OF THE BOTTOM

P. SMITH *In* ESA Proceedings of the 1986 International Geoscience and Remote Sensing Symposium (IGARSS '86) on Remote Sensing: Today's Solutions for Tomorrow's Information Needs, Volume 2 p 795-800 Aug. 1986
Avail: NTIS HC A17/MF A01; ESA, Paris, France, 3 volume set \$90 Member States, AU, CN, and NO (+20% others)

Measurements of surface current over a submerged ridge on the Nantucket Shoals and implications for the straining of surface waves are discussed. A photogrammetric analysis of the waves over the ridges is compared with predicted wavelengths. Aerial photos of surface roughness reveal a transition in roughness congruent with a lineal light streak. Ship drift across the ridge crest discloses a rapid drop in surface velocity at the crest. The measured strain rate disagrees, substantially, with the predicted strain rate, assuming barotropic flow and employing 2-D mass conservation. Wave blocking and refraction is consistent with the observed surface current and roughness distributions. ESA

N87-17298# TRW Space Technology Labs., Redondo Beach, Calif.

SAR IMAGING OF BOTTOM TOPOGRAPHY IN THE OCEAN: RESULTS FROM AN IMPROVED MODEL

H. C. YUEN, D. R. CRAWFORD (Jet Propulsion Lab., California Inst. of Tech., Pasadena.), and P. G. SAFFMAN *In* ESA Proceedings of the 1986 International Geoscience and Remote Sensing Symposium (IGARSS '86) on Remote Sensing: Today's Solutions for Tomorrow's Information Needs, Volume 2 p 807-815 Aug. 1986

Avail: NTIS HC A17/MF A01; ESA, Paris, France, 3 volume set \$90 Member States, AU, CN, and NO (+20% others)

A two-space dimensional model, which is applicable to arbitrary bottom topography and wind, is applied to Seasat Revs. 762, 957, 1430, and 1473. The model includes the additional modulational effects of a long-wave field on the short Bragg waves, both in the presence of a variable current field and results compared to data. Modulations associated with other radar frequencies are

also calculated under Rev. 762 conditions. It is shown that when the long-wave field effects are included, signature strength does not decrease with increasing radar frequency. The percentage enhancement due to long waves ranges from 7% for L band to 850% for K band. ESA

N87-17299# Environmental Research Inst. of Michigan, Ann Arbor. Radar Science Lab.

AN IMPROVED METHOD FOR THE DETERMINATION OF WATER DEPTH FROM SURFACE WAVE REFRACTION PATTERNS

J. R. BENNETT *In* ESA Proceedings of the 1986 International Geoscience and Remote Sensing Symposium (IGARSS '86) on Remote Sensing: Today's Solutions for Tomorrow's Information Needs, Volume 2 p 813-817 Aug. 1986 (Contract N00014-84-C-2312)

Avail: NTIS HC A17/MF A01; ESA, Paris, France, 3 volume set \$90 Member States, AU, CN, and NO (+20% others)

A mathematical model for using wave refraction observations to determine water depth from a synthetic aperture radar is presented. The model assumes that the waves are long-crested and obey linear theory, that the currents are negligible, and that there is a single dominant frequency. In principle, under these assumptions, the wavenumber magnitude alone is sufficient to determine the depth using the dispersion relation. However, observations of wavelength and direction do not necessarily obey the basic assumptions which lead to this relation. Therefore, before determining the depth from the dispersion relation, the model filters the data so that it is consistent with the theory. The method is tested against Seasat data. Results include the analysis of the expected error in mapping the depth for a given error in wavelength and the development of an algorithm for objectively analyzing an observed field of wavelength and direction data. This analysis provides a physically consistent field of wavenumber components which is close to the original data but which also obeys the law of conservation of waves and Snell's law. ESA

N87-17333# Johns Hopkins Univ., Laurel, Md. Applied Physics Lab.

CHARACTERISTICS OF A VERY LOW ALTITUDE SPACECRAFT FOR COLLECTING GLOBAL DIRECTIONAL WAVE SPECTRA WITH SPACEBORNE SYNTHETIC APERTURE RADAR

R. C. BEAL *In* ESA Proceedings of the 1986 International Geoscience and Remote Sensing Symposium (IGARSS '86) on Remote Sensing: Today's Solutions for Tomorrow's Information Needs, Volume 2 p 1025-1029 Aug. 1986

Avail: NTIS HC A17/MF A01; ESA, Paris, France, 3 volume set \$90 Member States, AU, CN, and NO (+20% others)

To assess the importance of spacecraft altitude on SAR azimuth wave detectability in realistic seas, an empirically determined azimuth wavenumber limit was combined with typical winter wave climatological data. A cumulative probability of azimuth wave attenuation as a function of spacecraft altitude indicates that, for the winter North Atlantic, azimuth wave detection begins to degrade for a spacecraft altitude as low as 200 km. The degradation becomes substantial (greater than 30% probability) around 300 km, and is essentially complete (greater than 95% probability) at 600 km altitude and higher. The results indicate that spaceborne SAR's should be placed in orbits no higher than 275 km to yield useful directional wave spectra, and probably should be combined with a radar ocean wave spectrometer to be most effective. ESA

N87-17334# Johns Hopkins Univ., Laurel, Md. Applied Physics Lab.

THE SAR IMAGE MODULATION TRANSFER FUNCTION DERIVED FROM SIR-B IMAGE SPECTRA AND AIRBORNE MEASUREMENTS OF OCEAN WAVE HEIGHT SPECTRA

F. MONALDO *In* ESA Proceedings of the 1986 International Geoscience and Remote Sensing Symposium (IGARSS '86) on Remote Sensing: Today's Solutions for Tomorrow's Information Needs, Volume 2 p 1031-1035 Aug. 1986

Avail: NTIS HC A17/MF A01; ESA, Paris, France, 3 volume set \$90 Member States, AU, CN, and NO (+20% others)

Using a procedure to estimate ocean height-variance spectra from SAR imagery, imagery from the SIR-B experiment is used to estimate directional ocean wave spectra. Comparison of these spectra with independent airborne wave spectra estimates indicate that a SAR is capable of producing relative height-variance spectra. It is also capable of producing height-variance spectra in absolute units. ESA

N87-17335# Marconi Co. Ltd., Chelmsford (England).

SIR-B OBSERVATIONS OF OCEAN WAVES IN THE NE ATLANTIC

J. T. MACKLIN, R. A. CORDEY, and G. E. KEYTE *In* ESA Proceedings of the 1986 International Geoscience and Remote Sensing Symposium (IGARSS '86) on Remote Sensing: Today's Solutions for Tomorrow's Information Needs, Volume 2 p 1037-1041 Aug. 1986

Avail: NTIS HC A17/MF A01; ESA, Paris, France, 3 volume set \$90 Member States, AU, CN, and NO (+20% others)

Synthetic-aperture radar (SAR) imagery from Shuttle Imaging Radar was obtained over a deep-water site in the NE Atlantic Ocean. Wave spectra derived from 2 almost orthogonal passes, separated by 6 hr, were compared with simultaneous wave-buoy observations in order to test the predictions of wave-imaging theories. Although azimuth-traveling waves were detected in the second pass, the discrepancy between the SAR and buoy wave spectra is almost an order of magnitude. It is suggested that the velocity-bunching mechanism predicted for azimuth-traveling waves is incorrectly described by the theories. ESA

N87-17336*# Johns Hopkins Univ., Laurel, Md. Applied Physics Lab.

DERIVING TWO-DIMENSIONAL OCEAN WAVE SPECTRA AND SURFACE HEIGHT MAPS FROM THE SHUTTLE IMAGING RADAR (SIR-B)

D. G. TILLEY *In* ESA Proceedings of the 1986 International Geoscience and Remote Sensing Symposium (IGARSS '86) on Remote Sensing: Today's Solutions for Tomorrow's Information Needs, Volume 2 p 1043-1049 Aug. 1986 Sponsored by NASA

Avail: NTIS HC A17/MF A01; ESA, Paris, France, 3 volume set \$90 Member States, AU, CN, and NO (+20% others) CSCL 08C

Directional ocean wave spectra were derived from Shuttle Imaging Radar (SIR-B) imagery in regions where nearly simultaneous aircraft-based measurements of the wave spectra were also available as part of the NASA Shuttle Mission 41G experiments. The SIR-B response to a coherently speckled scene is used to estimate the stationary system transfer function in the 15 even terms of an eighth-order two-dimensional polynomial. Surface elevation contours are assigned to SIR-B ocean scenes Fourier filtered using an empirical model of the modulation transfer function calibrated with independent measurements of wave height. The empirical measurements of the wave height distribution are illustrated for a variety of sea states. ESA

N87-17337# Johns Hopkins Univ., Laurel, Md. Applied Physics Lab.

SPATIAL EVOLUTION OF WAVE SPECTRA IN THE VICINITY OF THE AGULHAS CURRENT FROM SIR-B

D. E. IRVINE *In* ESA Proceedings of the 1986 International Geoscience and Remote Sensing Symposium (IGARSS '86) on Remote Sensing: Today's Solutions for Tomorrow's Information Needs, Volume 2 p 1051-1053 Aug. 1986

Avail: NTIS HC A17/MF A01; ESA, Paris, France, 3 volume set \$90 Member States, AU, CN, and NO (+20% others)

The SIR-B Agulhas (Southern Africa) experiment studied the propagation of swell across a major current as a test of technique and to understand the swell-related background to the Giant Wave problem. Image spectra, interpreted as wave spectra, show two distinct wave systems. One, evidently heading upstream, is tentatively identified as a trapped wave. ESA

N87-17338# Environmental Research Inst. of Michigan, Ann Arbor. Radar Science Lab.

CHARACTERISATION OF INTERNAL WAVE SURFACE PATTERNS ON AIRBORNE SAR IMAGERY

E. S. KASISCHKE *In* ESA Proceedings of the 1986 International Geoscience and Remote Sensing Symposium (IGARSS '86) on Remote Sensing: Today's Solutions for Tomorrow's Information Needs, Volume 2 p 1055-1060 Aug. 1986

(Contract N00014-81-C-0692)

Avail: NTIS HC A17/MF A01; ESA, Paris, France, 3 volume set \$90 Member States, AU, CN, and NO (+20% others)

Techniques to characterize the signatures of surface patterns associated with oceanic internal waves which appear on X and L-band, airborne SAR imagery collected during the SAR international wave imaging experiment (SARSEX) are presented. This data set shows that commonly-held conceptions concerning SAR detection of internal waves may need reevaluation. The SAR clearly images azimuth-traveling waves during SARSEX, and in some cases the X-band internal wave signature was stronger than the L-band signature. ESA

N87-17341# Universite Catholique de Louvain (Belgium). Lab. de Telecommunications et d'Hyperfrequences.

A TWO-STEP ALGORITHM FOR THE SEPARATE RETRIEVAL OF OCEAN SURFACE AND ATMOSPHERIC PARAMETERS FROM MICROWAVE RADIOMETERS

A. GUISSARD, P. SOBIESKI, and A. M. GUILLAUME *In* ESA Proceedings of the 1986 International Geoscience and Remote Sensing Symposium (IGARSS '86) on Remote Sensing: Today's Solutions for Tomorrow's Information Needs, Volume 2 p 1077-1082 Aug. 1986

Avail: NTIS HC A17/MF A01; ESA, Paris, France, 3 volume set \$90 Member States, AU, CN, and NO (+20% others)

An algorithm for passive microwave remote sensing of the ocean through the atmosphere is proposed. It is based on a contracted form of the radiative transfer equation and on an iterative two-step procedure, such that the extraction of the sea surface parameters and of the atmospheric parameters can be performed separately to a first approximation. Tests on synthetic measurements show that the algorithm is stable, converges rapidly, is independent of the first guess, and works properly in the presence of realistic instrumental errors. The method applies to a rough open sea and will be extended to include foam effects. ESA

N87-17342# Helsinki Univ. of Technology, Espoo (Finland). Radio Lab.

RETRIEVAL OF NEAR-SURFACE WIND SPEED IN THE BALTIC SEA FROM NIMBUS-7 SCANNING MULTICHANNEL MICROWAVE RADIOMETER (SMMR) OBSERVATIONS

M. HALLIKAINEN, T. TOLMUNEN, and P. TALMOLA *In* ESA Proceedings of the 1986 International Geoscience and Remote Sensing Symposium (IGARSS '86) on Remote Sensing: Today's Solutions for Tomorrow's Information Needs, Volume 2 p 1083-1088 Aug. 1986

Avail: NTIS HC A17/MF A01; ESA, Paris, France, 3 volume set \$90 Member States, AU, CN, and NO (+20% others)

Retrieval of near-surface wind speed in semienclosed seas from NIMBUS-7 Scanning Multichannel Microwave Radiometer (SMMR) data was investigated. The effects of antenna sidelobes over land and those of wind direction were assessed. The feasibility of all SMMR frequencies and polarizations to wind speed retrieval was tested. The effect of daily precipitation and integrated water vapor to the retrieval accuracy was studied. Based on the least squares method, a first-order polynomial was formed to calculate the brightness temperature from the wind speed at each SMMR frequency and polarization. The correlation coefficient between the brightness temperature and wind speed was calculated in each case. ESA

N87-17343# Helsinki Univ. of Technology, Espoo (Finland). Radio Lab.

SEA ICE STUDIES IN THE BALTIC SEA USING SATELLITE MICROWAVE RADIOMETER DATA

M. HALLIKAINEN and P.-V. MIKKOLA *In* ESA Proceedings of the 1986 International Geoscience and Remote Sensing Symposium (IGARSS '86) on Remote Sensing: Today's Solutions for Tomorrow's Information Needs, Volume 2 p 1089-1094 Aug. 1986

Avail: NTIS HC A17/MF A01; ESA, Paris, France, 3 volume set \$90 Member States, AU, CN, and NO (+20% others)

Data from NIMBUS-7 Scanning Multichannel Microwave Radiometer for Winter 1978 to 1979 were used to develop algorithms for retrieval of sea-ice concentration. Due to the small width of the Baltic Sea, only 18 GHz and 37 GHz data could be employed. Comparison of the algorithms indicates that the 37-GHz algorithm is much more sensitive to the properties of the snow cover upon the ice, including the liquid water content, snow depth, and snow grain size. ESA

N87-17367# Science Research Council, Chilton (England). Rutherford Appleton Lab.

GATHERING AND PROCESSING A COMPARATIVE DATA SET FOR THE CALIBRATION AND VALIDATION OF ERS-1 DATA PRODUCTS; PREPARATORY WORK AT THE UK-ERS-DC

REDVERS JOHN POWELL *In* ESA Proceedings of an ESA Workshop on ERS-1 Wind and Wave Calibration p 27-30 Sep. 1986

Avail: NTIS HC A11/MF A01

It is suggested that the main European effort to validate the wind and wave data products of ERS-1 should be concentrated in the North-East Atlantic and Norwegian sea. Also, that conventional oceanographic data gathering techniques using ships and buoys should be augmented with permanently deployed and well validated master stations and airborne instrumentation. The need to site such stations and altimeter transponders on the ground track argues strongly for the early selection of the location of the ground tracks associated with the initial three-day repeat orbit and for ensuring that any higher repeat cycle is a multiple of three. Work on this subject at the UK-ERS data center is described. ESA

N87-17369# Institute of Oceanographic Sciences, Wormley (England).

REQUIREMENTS AND CONSTRAINTS IN THE CALIBRATION AND VALIDATION OF ERS-1 WIND AND WAVE PARAMETERS

TREVOR H. GUYMER *In* ESA Proceedings of an ESA Workshop on ERS-1 Wind and Wave Calibration p 37-43 Sep. 1986
Avail: NTIS HC A11/MF A01

Calibration and validation of ERS-1 wind and wave parameters are discussed using the experience of other oceanographic satellite missions. Major limitations of past efforts appear to be: the limited number of comparisons with near-coincident in-situ platforms, the small dynamic ranges encountered, and the introduction of regional biases by calibrations that were heavily weighted to midlatitude, summertime conditions. On the basis of a study of climatological statistics, suitable locations for measuring high wind and wave conditions are suggested. ESA

N87-17370# Centre Oceanologique de Bretagne, Brest (France). Antenne CREO.

EVALUATION OF THE DIFFERENT PARAMETERS IN LONG'S C-BAND MODEL

ALAIN CAVANIE, JOELLE DEMURGER, and PASCAL LECOMTE *In* ESA Proceedings of an ESA Workshop on ERS-1 Wind and Wave Calibration p 47-51 Sep. 1986
Avail: NTIS HC A11/MF A01

Scatterometer measurements over the ocean were analyzed and a model for sigma-zero (S) as a function of wind speed, wind direction relative to the beam direction, and incidence angle was derived for ERS-1. Because ERS-1 is yaw-steered: in the space of 00 values of the forward, rear, and central, antennas (S_1 , S_2 , S_3), the surface of solutions is symmetric with respect to the plan $S_1 = S_2$. The ratios S_1/S_2 or S_2/S_1 reach 2 distinct maxima for a given wind speed. Two independent methods of calibration of parameters in the C-Band model, using only the wind speed furnished by meteorological fields are obtained. Such methods could be applied to pretune the scatterometer in its first months of flight, investigate regional variations, and monitor possible evolutions in the instrument's behavior. ESA

N87-17371# Meteorological Office, Bracknell (England).

THE USE OF NUMERICAL WIND AND WAVE MODELS TO PROVIDE AREAL AND TEMPORAL EXTENSION TO INSTRUMENT CALIBRATION AND VALIDATION OF REMOTELY SENSED DATA

PETER E. FRANCIS *In* ESA Proceedings of an ESA Workshop on ERS-1 Wind and Wave Calibration p 53-55 Sep. 1986
Avail: NTIS HC A11/MF A01

A scheme to use satellite derived ocean surface data in environmental sciences is outlined. The scheme involves comparisons between satellite data and ground based measurements, between ground based measurements and numerical models, and between numerical models and satellite data. Each comparison yields vital information, e.g., primary retrieval algorithms, model validation, extension of satellite data validation beyond the regions of surface based networks. Examples of performance characteristics and output products of the UK Meteorological Office global atmospheric and sea state models are given. ESA

N87-17372*# Jet Propulsion Lab., California Inst. of Tech., Pasadena. NASA Scatterometer Project.

SATELLITE SCATTEROMETER COMPARISONS WITH SURFACE MEASUREMENTS: TECHNIQUES AND SEASAT RESULTS

MICHAEL H. FREILICH *In* ESA Proceedings of an ESA Workshop on ERS-1 Wind and Wave Calibration p 57-62 Sep. 1986
Sponsored by NASA
Avail: NTIS HC A11/MF A01 CSCL 08C

A method by which satellite and surface measurements can be compared in order to validate satellite wind observations is presented. The regression method requires knowledge of the expected differences (due to atmospheric variability and differing averaging) between perfect satellite and perfect buoy

measurements. A model for estimating these differences is described. The regression method is applied to comparisons between Seasat Scatterometer (SASS) and U.S. National Data Buoy Office buoy data. Comparisons indicating a dependence of SASS accuracy on sea-surface temperature are summarized.

ESA

N87-17373# GKSS-Forschungszentrum Geesthacht (West Germany).

COMPARISON CONCEPT OF SATELLITE DERIVED WIND AND WAVE DATA WITH GROUND TRUTH

WOLFGANG KOCH and R. RAMSEIER *In* ESA Proceedings of an ESA Workshop on ERS-1 Wind and Wave Calibration p 63-68 Sep. 1986

Avail: NTIS HC A11/MF A01

To demonstrate the capabilities of numerical models for the calibration of satellite derived pressure, wind, and wave-fields, results from numerical simulations are shown and compared to measurements and SMMR-data from NIMBUS 7. The proposed calibration procedure relies on numerical simulation models which themselves are quantitatively calibrated with regionally representative measurements. ESA

N87-17374# Institute of Oceanographic Sciences, Wormley (England).

VALIDATION OF ERS-1 WIND DATA USING OBSERVATIONS FROM RESEARCH AND VOLUNTARY OBSERVING SHIPS

PETER K. TAYLOR *In* ESA Proceedings of an ESA Workshop on ERS-1 Wind and Wave Calibration p 69-75 Sep. 1986

Avail: NTIS HC A11/MF A01

A method for validation of ERS-1 wind measurements using observations from the Voluntary Observing Ships (VOS) is proposed. The data are available from most ocean regions allowing validation over a wide range of conditions. Although the observations are individually of poor quality, data from the North Sea is used to demonstrate that, where sufficient observations exist, a mean value averaged over 1 month and a few hundred kilometers should be accurate to 1m/sec or better. For absolute calibration a subset of the VOS would be used. For these ships, the wind errors due to poor anemometer exposure must be determined. Results obtained by mounting a high mast in ships' bows are encouraging. ESA

N87-17376# Royal Netherlands Meteorological Inst., De Bilt.

THE ACCURACY AND AVAILABILITY OF OPERATIONAL MARINE SURFACE WIND DATA FOR ERS-1 SENSOR CALIBRATION AND VALIDATION FROM FIXED PLATFORMS AND FREE DRIFTING BUOYS

WIEBE A. OOST *In* ESA Proceedings of an ESA Workshop on ERS-1 Wind and Wave Calibration p 85-86 Sep. 1986

Avail: NTIS HC A11/MF A01

Problems when using wind data from oil or gas production platforms and a proposal for a calibration experiment, using drifting buoys are outlined. The problems with platforms are discussed on the basis of studies on the K13-A platform in the southern North Sea. Drifting buoys being the most cost-effective platforms to obtain data from the high seas, a suggestion is made to deploy a group of drifters measuring wind and, possibly, waves. This could be done by cooperation with the COST-43 organization, which maintains drifting buoy programs in 2 areas. ESA

N87-17377# Centre Oceanologique de Bretagne, Brest (France).

USING BUOYS AND SHIPS TO CALIBRATE ERS-1 ALTIMETER AND SCATTEROMETER

ROBERT EZRATY *In* ESA Proceedings of an ESA Workshop on ERS-1 Wind and Wave Calibration p 91-97 Sep. 1986

Avail: NTIS HC A11/MF A01

Given the stated accuracy of ERS-1 sensors, the constraints to be dealt with using ships and buoys for a dedicated calibration experiment are discussed. Wave measuring buoys giving directional and non directional information are available to be used remotely in the open ocean. Wind measurements from ships can be

considered as a reference, if ship effects are properly taken into account. Sea tests of a spar buoy, measuring the wind vector at 4 m are being conducted. The importance of the continuity of wind data is stressed and has to be accounted for to plan the on-board electronics. The geometry of wave and wind buoy networks are different since the altimeter and scatterometer do not scan the same area. Network configurations are presented.

ESA

N87-17380*# National Aeronautics and Space Administration. Goddard Space Flight Center, Greenbelt, Md.

OCEANOGRAPHIC MEASUREMENT CAPABILITIES OF THE NASA P-3 AIRCRAFT

ERIK MOLLO-CHRISTENSEN, F. C. JACKSON, E. J. WALSH, and F. HOGE *In* ESA Proceedings of an ESA Workshop on ERS-1 Wind and Wave Calibration p 111-121 Sep. 1986

Avail: NTIS HC A11/MF A01 CSCL 04B

Instrumentation on NASA P3 aircraft available to provide ground truth for ERS-1 is described. The wave sensors include the 36 GHz Surface Contour Radar (SCR), the Ku-band Radar Ocean Wave Spectrometer (ROWS), and the Airborne Oceanographic Lidar. The other sensors include a C-band scatterometer, video camera, radiation thermometer, and AXRTs. The SCR and ROWS directional spectrum measurements are discussed. When planning for an underflight mission, the limited endurance of the aircraft (6 hr) and flight cost (2.7 K\$/hr) must be considered. The advantage of the redundancy afforded by the several wave instruments is another important consideration.

ESA

N87-17381# Johns Hopkins Univ., Laurel, Md. Applied Physics Lab.

A PROCEDURE FOR ESTIMATION OF TWO-DIMENSIONAL OCEAN HEIGHT-VARIANCE SPECTRA FROM SAR IMAGERY

FRANK MONALDO *In* ESA Proceedings of an ESA Workshop on ERS-1 Wind and Wave Calibration p 123-129 Sep. 1986

Avail: NTIS HC A11/MF A01

A step-by-step procedure to convert synthetic aperture radar (SAR) imagery into estimates of the ocean surface wave spectra is outlined. The procedure is based on a linearized version of a model to convert SAR image intensity spectra into either wave slope or height-variance spectra. The procedure is applied to SAR imagery from the SIR-B mission and shown to produce spectra which are highly correlated to two-dimensional spectra measured independently.

ESA

N87-17383# Science Research Council, Chilton (England). Rutherford Appleton Lab.

MEASUREMENT OF THE DIRECTIONAL SPECTRUM OF OCEAN WAVES USING A CONICALLY-SCANNING RADAR

ANDREW ROBERT BIRKS *In* ESA Proceedings of an ESA Workshop on ERS-1 Wind and Wave Calibration p 135-138 Sep. 1986

Avail: NTIS HC A11/MF A01

It is proposed to use a short-pulse radar altimeter, modified by the addition of a steerable antenna which can scan a cone about nadir, to measure the directional spectrum of ocean waves. The method can be used from either a satellite or aircraft; application from an aircraft is described, having in mind its use in the validation of satellite instruments. Near simultaneous measurements of significant wave height and of the directional wave spectrum are possible with the same instrument, enhancing the value of both measurements. Airborne measurements were made using a 13GHz radar during a campaign with the NASA CV-900 aircraft.

ESA

N87-17384*# Jet Propulsion Lab., California Inst. of Tech., Pasadena.

AN OVERVIEW OF THE NSCAT/N-ROSS PROGRAM

B. D. MARTIN, MICHAEL H. FREILICH, F. K. LI, and PHILLIP S. CALLAHAN *In* ESA Proceedings of an ESA Workshop on ERS-1 Wind and Wave Calibration p 143-149 Sep. 1986 Sponsored by NASA

Avail: NTIS HC A11/MF A01 CSCL 14B

The NASA Scatterometer (NSCAT) to fly on the U.S. Navy Remote Ocean Sensing System (N-ROSS) mission is presented. The overall N-ROSS mission, the NSCAT flight instrument and groundbased data processing/distribution system, and NASA-supported science and verification activities are described. The N-ROSS system is designed to provide measurements of near-surface wind, ocean topography, wave height, sea-surface temperature, and atmospheric water content over the global oceans. The NSCAT is an improved version of the Seasat scatterometer. It will measure near surface vector winds.

ESA

N87-17386# Massachusetts Univ., Amherst.

INTERSENSOR COMPARISONS FOR VALIDATION OF WIND SPEED MEASUREMENTS FROM ERS-1 ALTIMETER AND SCATTEROMETER

CALVIN SWIFT and N. M. MOGNARD *In* ESA Proceedings of an ESA Workshop on ERS-1 Wind and Wave Calibration p 157-164 Sep. 1986

Avail: NTIS HC A11/MF A01

Discrepancies in wind magnitude data from the three wind sensors on board Seasat, namely the radar altimeter, the scatterometer, and the scanning microwave multifrequency radiometer were analyzed on a global and regional scale for time periods varying from the entire 3-month Seasat period, to a monthly, and a 3-day time scale. The data are analyzed in the Southern Oceans where, during the Seasat lifetime, the highest sea state conditions were found. The algorithms used to process each data set are the official JPL Seasat algorithms. The results point to a more detailed verification activity for future satellite systems such as the SSM/I, NSCATT and the ERS-1 scatterometer.

ESA

N87-17389# Max-Planck-Inst. fuer Meteorologie, Hamburg (West Germany).

WAVE MODELING ACTIVITIES OF THE WAVE MODELING (WAM) GROUP RELEVANT TO ERS-1

KLAUS HASSELMANN *In* ESA Proceedings of an ESA Workshop on ERS-1 Wind and Wave Calibration p 173-175 Sep. 1986

Avail: NTIS HC A11/MF A01

A third generation wave model was developed and successfully tested in hindcast studies, in global and regional, deep and shallow water versions. The model will be applied to assimilate wind and wave data from ERS-1. The model will be embedded in a data assimilation system based on a global atmospheric circulation model together with the wave model. The availability of such an operational system at the time of the ERS-1 commissioning phase would greatly assist the calibration and validation of the ERS-1 wind and wave sensors.

ESA

N87-17390# Ministerio de Obras Publicas, Madrid (Spain). Direccion General de Puertos y Costas.

MARINE CLIMATE PROGRAM

JUAN JOSE CONDE, JOSIE ENRIQUE LUIS, and ADOLFO MARON *In* ESA Proceedings of an ESA Workshop on ERS-1 Wind and Wave Calibration p 177-179 Sep. 1986

Avail: NTIS HC A11/MF A01

Research on ocean wave forecasting, wave time series analysis, and flow propagation is summarized. A buoy network for the Spanish littoral is described.

ESA

N87-17391# Marconi Co. Ltd., Chelmsford (England). Remote Sensing Group.

A SCATTEROMETER RESEARCH PROGRAM

IAN A. WARD *In* ESA Proceedings of an ESA Workshop on ERS-1 Wind and Wave Calibration p 181-185 Sep. 1986
 Avail: NTIS HC A11/MF A01

A research program on SAR ocean surface scattering and imaging is outlined. It covers Bragg scattering, specular reflection, and wedge diffraction. Speckle statistics; bias to longer wavelengths in azimuthally traveling-waves; orbital and phase-velocities of swell waves; velocity-bunching; the degradation of azimuthal resolution; information from nonlinear imaging situations; and imaging theory to incorporate breaking-waves are covered. ESA

N87-17428# Danish Meteorological Inst., Copenhagen.
THE ICE CONDITIONS IN THE GREENLAND WATERS, 1980

JENS S. FABRICIUS 1986 167 p
 (REPT-551.467.3.068(988); ISBN-87-7478-275-4) Avail: NTIS HC A08/MF A01

During the period July to September 1980, the Danish Hydraulic Institute (DHI) made a series of special ice reconnaissances off East Greenland for the Greenland Geological Survey (GGU). Twelve monthly compiled charts followed by an annex (A through F) containing copies of all Danish ice reconnaissance charts, regionally arranged. The Danish Meteorological Institute (DMI) interpreted a series of satellite images. The charts from DHI/GGU and the satellite interpretations from DMI are added to this annual as appendix I and II. B.G.

N87-18158# Environmental Research Inst. of Michigan, Ann Arbor.

DETECTION OF BOTTOM-RELATED SURFACE PATTERNS ON VISIBLE SPECTRUM IMAGERY

E. S. KASISCHKE and F. J. TANIS *In* ESA Proceedings of the 1986 International Geoscience and Remote Sensing Symposium (IGARSS '86) on Remote Sensing: Today's Solutions for Tomorrow's Information Needs, Volume 3 p 1301-1306 Aug. 1986

(Contract N00014-84-C-2312)
 Avail: NTIS HC A21/MF A01; ESA, Paris, France, 3 volume set \$90 Member States, AU, CN, and NO (+20% others)

A model which predicts the total radiance from an ocean surface is used to investigate the observations of bottom-related surface patterns on visible spectrum imagery. An example of Large Format Camera Imagery from NW Australia is used to demonstrate the importance of viewing geometry for the detection of these features. A second example utilizing Thematic Mapper imagery illustrates that the observation of bottom-related surface patterns can be explained by changes in the rms slopes of the surface capillary and ultragravity waves. ESA

N87-18160# Johns Hopkins Univ., Laurel, Md. Applied Physics Lab.

A DESCRIPTION OF LARGE-SCALE VARIABILITY IN THE OCEAN USING THE DIFFUSE ATTENUATION COEFFICIENT

J. A. GIANNINI *In* ESA Proceedings of the 1986 International Geoscience and Remote Sensing Symposium (IGARSS '86) on Remote Sensing: Today's Solutions for Tomorrow's Information Needs, Volume 3 p 1313-1318 Aug. 1986

Avail: NTIS HC A21/MF A01; ESA, Paris, France, 3 volume set \$90 Member States, AU, CN, and NO (+20% others)

Coastal Zone Color Scanner (CZCS) data from NIMBUS-7 satellite are used to study the spatial and temporal variability of ocean color. The large-scale spatial variability (greater than 10 km) is examined using the diffuse attenuation coefficient (K) obtained from Level 2 processed CZCS imagery. Time series of the mean and variability of K from 1979 from the mid-Atlantic show an increase in the average K and correspondingly in average variability of 16% and 18%, respectively, over a 6 week period. Because of the very coarse spacing in time, this increase does not reflect the full extent of the peak bloom. Even more dramatic differences are observed when the statistics from different ocean global locations are compared. Additional data must be examined

to show a more detailed evolution of the bloom within 1979 and to describe the multi-year variability for different seasons. ESA

N87-18165# Ocean Surface Research, Boulder, Colo.
SEASAT MICROWAVE ALTIMETER MEASUREMENT OF THE OCEAN GRAVITY WAVE EQUILIBRIUM-RANGE SPECTRAL BEHAVIOR USING FULL-WAVE THEORY

D. E. BARRICK and E. BAHAR (Nebraska Univ., Lincoln) *In* ESA Proceedings of the 1986 International Geoscience and Remote Sensing Symposium (IGARSS '86) on Remote Sensing: Today's Solutions for Tomorrow's Information Needs, Volume 3 p 1345-1349 Aug. 1986

Avail: NTIS HC A21/MF A01; ESA, Paris, France, 3 volume set \$90 Member States, AU, CN, and NO (+20% others)

A spectral law for the equilibrium region of the waveheight spatial spectrum is derived from the SEASAT altimeter data set. Applicable to the open ocean under all conditions of wave development, the result is a K sup-3.86 power-law dependence rather than the classic-4. This spectral model is established using the specular-point result for backscatter supported by full-wave theory to determine the upper wavenumber limit for the slope spectrum. ESA

N87-18167# Hamburg Univ. (West Germany). Inst. fuer Organische Chemie.

ON THE DISCRIMINATION BETWEEN CRUDE OIL SPILLS AND MONOMOLECULAR SEA SLICKS BY AIRBORNE REMOTE SENSORS: TODAY'S POSSIBILITIES AND LIMITATIONS

H. HUEHNERFUSS, W. ALPERS (Bremen Univ., West Germany), O. FAEST (Swedish Space Corp., Solna), P. A. LANGE (Bundesanstalt fuer Wasserbau, Brunswick, West Germany), A. LOFFET (Belfotop P.v.b.a., Wommel, Belgium.), K. RICHTER (Deutsches Hydrographisches Inst., Hamburg, West Germany), R. C. SCHRIEL (Rijkswaterstaat, Rijswijk, Netherlands), N. SKOU (Technical Univ. of Denmark, Lyngby), and F. WITTE (Deutsche Forschungs- und Versuchsanstalt fuer Luft- und Raumfahrt, Oberpfaffenhofen, West Germany) *In* ESA Proceedings of the 1986 International Geoscience and Remote Sensing Symposium (IGARSS '86) on Remote Sensing: Today's Solutions for Tomorrow's Information Needs, Volume 3 p 1359-1364 Aug. 1986 Sponsored by the Joint Research Center of the European Community

Avail: NTIS HC A21/MF A01; ESA, Paris, France, 3 volume set \$90 Member States, AU, CN, and NO (+20% others)

The applicability of X-band real aperture radars (RAR) to the discrimination between crude oil spills and monomolecular sea slicks was investigated. The images obtained by five airborne RAR-systems, flown nearly simultaneously at various angles to the wind direction, were analyzed. The results from flights over four different types of oil spills (Ekofisk crude, chocolate mousse, heavy fuel oil, medium fuel oil) and three monomolecular sea slicks (oleyl alcohol, di-(thylenglycol)-mono-isostearyl ether, methyl oleate) show that the advantage of an imaging radar is its unequivocal potential for surveying large sea surfaces. However, RAR systems do not allow a discrimination between oil spills and sea slicks. Therefore, an airborne coastal patrol to identify oil spills reliably must utilize additional sensors. ESA

N87-18169# Deutsche Forschungs- und Versuchsanstalt fuer Luft- und Raumfahrt, Wesseling (West Germany). Inst. for Radio Frequency Technology.

OIL SLICK DETECTION WITH A SIDELOOKING AIRBORNE RADAR

F. WITTE *In* ESA Proceedings of the 1986 International Geoscience and Remote Sensing Symposium (IGARSS '86) on Remote Sensing: Today's Solutions for Tomorrow's Information Needs, Volume 3 p 1369-1374 Aug. 1986

Avail: NTIS HC A21/MF A01; ESA, Paris, France, 3 volume set \$90 Member States, AU, CN, and NO (+20% others)

An experimental inexpensive SLAR operating in X-band is described. It is used for generation of radar imagery from land and sea surfaces with spatial resolution similar to that of future satellite systems. Depending on the application, the SLAR is flown

in different aircraft such as the Cessna 207, Do28 or Do228. The SLAR was employed during the Archimedes 2 project (oil slick detection, qualification and classification in the North Sea). The data collected show the good ability of the SLAR to detect thin oil slicks, 1 micron or less, on the water's surface. The observed shapes of the slicks are similar to those obtained from a UV and IR sensor. ESA

N87-18170# Deutsche Forschungs- und Versuchsanstalt fuer Luft- und Raumfahrt, Oberpfaffenhofen (West Germany). Inst. for Radio Frequency Technology.

CONTRIBUTIONS TO OIL SPILL DETECTION AND ANALYSIS WITH RADAR AND MICROWAVE RADIOMETRY, RESULTS OF THE ARCHIMEDES 2 CAMPAIGN

K. GRUENER, N. BARTSCH, F. WITTE, H. SCHREIBER, and W. KEYDEL *In* ESA Proceedings of the 1986 International Geoscience and Remote Sensing Symposium (IGARSS '86) on Remote Sensing: Today's Solutions for Tomorrow's Information Needs, Volume 3 p 1375-1380 Aug. 1986

Avail: NTIS HC A21/MF A01; ESA, Paris, France, 3 volume set \$90 Member States, AU, CN, and NO (+20% others)

Oil spill detection with an X-band SLAR, a primitive L-band SAR, and 5 microwave radiometers (1.3 GHz, 32 GHz, 90 GHz) is summarized. The SLAR and the radiometer were installed and flown in the same aircraft. All microwave sensors demonstrate their ability to be used within an oil pollution detection and clearance system. However, especially for the use of microwave radiometry, a sufficient geometrical resolution has to be used in order to estimate thickness and volume of spilled oil with sufficient accuracy. Statistical evaluation methods should be investigated in more detail for radar and for microwave radiometry. It seems possible that the higher statistical moments contain more detailed signature information on the chemical and geometrical quality of observed surface pollution. ESA

N87-18181# INTERA Environmental Consultants Ltd., Calgary (Alberta).

STAR-VUE: A TACTICAL ICE NAVIGATION WORKSTATION

R. T. LOWRY, S. D. THORNTON, and G. MCAVOY *In* ESA Proceedings of the 1986 International Geoscience and Remote Sensing Symposium (IGARSS '86) on Remote Sensing: Today's Solutions for Tomorrow's Information Needs, Volume 3 p 1443-1448 Aug. 1986

Avail: NTIS HC A21/MF A01; ESA, Paris, France, 3 volume set \$90 Member States, AU, CN, and NO (+20% others)

Downlinks to carry airborne SLAR and SAR data to vessels in Arctic ice fields were developed. Data transmitted from the aircraft are automatically recorded on disk. The system allows the recall of current or previous radar imagery for display on a high resolution monitor. With the aid of a trackball, any section of the main image may be displayed in an expanded form. The selected partial display may be output to a hardcopy device if a permanent record is required. The trackball controls all operations, thus no keyboard operations are required. The system is intended to be used by a person with no previous exposure to computer systems. ESA

N87-18199# Manitoba Univ., Winnipeg. Dept. of Earth Sciences.

STUDY OF OCEAN BOTTOM COUPLING PROCESS USING SATELLITE ALTIMETER DATA

W. MOON, R. TANG (Texaco Canada Resources Ltd., Calgary, Alberta), and B. H. CHOI (Sung Kyun Kwan Univ., Suwon, South Korea) *In* ESA Proceedings of the 1986 International Geoscience and Remote Sensing Symposium (IGARSS '86) on Remote Sensing: Today's Solutions for Tomorrow's Information Needs, Volume 3 p 1555-1561 Aug. 1986

(Contract NSERC-A-7400)

Avail: NTIS HC A21/MF A01; ESA, Paris, France, 3 volume set \$90 Member States, AU, CN, and NO (+20% others)

The ocean bottom friction law is investigated in the Hudson Bay area of Canada and East China Sea through numerical modeling and correlation of the computed results with Seasat altimeter data. Interactive hydrodynamic modeling is applied in

the analysis of the sea surface elevation observed by the Seasat altimeter. Meteorological forcing function is derived by a 2-D grid governed by a set of meteorological relations over the study areas. Since the ocean tides in the study areas introduce large spatial and periodic height variation, the major tidal constituents are included in the computation. Other corrections such as body tide, loading tide, and steric variation of the ocean surface are also included in the processing. The linear bottom friction coefficient estimated over the Hudson Bay area water body is 0.24 cm/sec and the quadratic coupling coefficient over the Hudson Bay area of Canada and East China Sea is 0.0024. ESA

N87-18283# World Climate Programme, Geneva (Switzerland). **REPORT OF THE FOURTH SESSION OF THE JSC/CCCO TROPICAL OCEAN GLOBAL ATMOSPHERE (TOGA) SCIENTIFIC STEERING GROUP**

Jul. 1986 40 p Session held in New Delhi, India, 10-14 Feb. 1986

(WCP-120; WMO/TD-129; ETN-87-98901) Avail: NTIS MF A01; print copy available from WMO, Geneva, Switzerland

Observational and data processing activities required for the Tropical Ocean Global Atmosphere (TOGA) program of the WMO were discussed. Surface winds and interface fluxes; requirements for TOGA process studies; and modeling for TOGA were considered. ESA

N87-18293*# Alaska Univ., Anchorage.

INFLUENCE OF THE YUKON RIVER ON THE BERING SEA Annual Progress Report

K. DEAN and C. P. MCROY Oct. 1986 15 p Original contains color illustrations

(Contract NAS5-28769)

(NASA-CR-180065; NAS 1.26:180065) Avail: NTIS HC A02/MF A01 CSCL 08C

The purpose is to use satellite data to study relationships between discharge of the Yukon River to currents and biologic productivity in the northern Bering Sea. Amended specific objectives are: to develop thermal, sediment and chlorophyll surface maps using thematic mapping (TM) data of the discharge of the Yukon River and the Alaska Coastal Current during the ice free season; to develop a historical model of the distribution of the Yukon River discharge and the Alaska Coastal Current using LANDSAT multispectral scanner (MMS) and NOAA satellite imagery; and to use high resolution TM data to define the surface dynamics of the front between the Alaska Coastal Current and the Bering Shelf/Anadyr Current. LANDSAT MSS and TM, and Advanced Very High Resolution Radiometer (AVHRR) data were recorded during the 1985 ice-free period. The satellite data coincided with shipboard measurements acquired by Inner Self Transfer and Recycling scientists. Circumstances were such, that on July 5 and July 22, all three sensors recorded data that has been registered to a common map projection and map base, then contrast stretched, color composited, and density sliced. Author

N87-18295# Naval Ocean Research and Development Activity, Bay St. Louis, Miss.

THE IMPACT OF SATELLITE INFRARED SEA SURFACE TEMPERATURES ON FNOC (FLEET NUMERICAL OCEANOGRAPHY CENTER) OCEAN THERMAL ANALYSES Final Report

JEFFREY D. HAWKINS, JOHN M. HARDING, JUANITA R. CHASE, R. M. CLANCY, and BONITA L. SAMUELS Jun. 1986 44 p

(AD-A173333; NORDA-142) Avail: NTIS HC A03/MF A01 CSCL 08J

The Navy's global operational domain and system performance criteria place strict requirements on specifying sea surface temperatures (SST) and ocean thermal structure on many space and time scales. As in situ observations of the ocean's temperature field are sparse and are often inaccurate, the Navy and other oceanographers have increasingly relied on remotely sensed data to fill gaps. Infrared imagery from polar orbiting and geostationary satellites was first used from qualitative standpoint to locate strong ocean frontal areas. Over the last 5 years, the Navy has included quantitative satellite measurements as an integral part of their

SST data base. These multichannel sea surface temperatures (MCSST), 50,000 to 100,000 per day, far outweigh the spatial and temporal coverage of all in situ reports combined. The MCSST data provide the Expanded Ocean Thermal Structure analysis with highly accurate reports that span the globe. This study reveals that MCSST data significantly add to the mesoscale fronts and eddies mapping effort by tightening up strong frontal gradients and reducing the impact of noisy ship data. Higher resolution analyses are also seen to greatly aid in correctly delineating sharp ocean mesoscale features, as well as take advantages of the MCSST's 8 km by 8 km resolution. GRA

N87-18298# Naval Polar Oceanography Center, Washington, D.C.

EASTERN-WESTERN ARCTIC SEA ICE ANALYSIS, 1985

Nov. 1986 110 p

(AD-A173972; RR-12) Avail: NTIS HC A06/MF A01 CSCL 08L

This publication is the twelfth in a continuing yearly series of Arctic sea ice atlases prepared in the Joint Ice Center at the Naval Polar Oceanography Center, Suitland. The atlas contains weekly charts depicting Northern Hemisphere and Great Lakes ice conditions and extents. The information presented was prepared under operational time constraints principally from satellite imagery supplemented by conventional observations. GRA

N87-18913# Jet Propulsion Lab., California Inst. of Tech., Pasadena.

INVESTIGATION OF PHYSICS OF SYNTHETIC APERTURE RADAR IN OCEAN REMOTE SENSING TOWARD 84/86 FIELD EXPERIMENT. VOLUME 1: DATA SUMMARY AND EARLY RESULTS Interim Report, Sep. 1984 - May 1985

OMAR H. SHEMDIN May 1986 160 p

(AD-A174197) Avail: NTIS HC A08/MF A01 CSCL 17I

The mechanisms responsible for SAR imaging of the ocean surface are not adequately understood at present. Conflicting hypotheses have been proposed that remain without valid proof, because of lack of adequate data sets to test these hypotheses. The influence of environmental parameters has prevented extending relationships that were demonstrated under one set of conditions to another beyond the range used in formulating the relationships. GRA

N87-18931# Rhode Island Univ., Kingston. Graduate School for Oceanography.

ARCTIC HAZE: NATURAL OR POLLUTION? Progress Report

KENNETH A. RAHN and DOUGLAS H. LOWENTHAL 1 Nov. 1986 159 p

(AD-A174025) Avail: NTIS HC A08/MF A01 CSCL 04B

A 3-year program of continued research on Arctic haze is planned. The research builds on the accomplishments of the past three years and extends them, with particular emphasis on strengthening the new elemental tracer system, attempting to determine the history of Arctic haze by analyzing the Russian/Norwegian ice core from Nordauslandet, and analyzing aircraft samples from the AGASP II aircraft experiment of spring 1986. The tracer system will be improved in at least three ways: its statistical aspects will be refined, innovative ways of deriving signatures from hard-to-sample areas will be explored, and the tracer power of several noble metals will be determined. From the Nordauslandet core, as many as 100 to 200 samples will be analyzed for trace elements with our new technique developed under DOE sponsorship: we hope to use the results to write both the modern history of Arctic haze and the history of the various regions contributing to it. An extensive set of aircraft samples from AGASP II will be analyzed for trace elements and compared with the results of other investigators. GRA

N87-18961# Office of Naval Research, Arlington, Va.
PHYSICAL OCEANOGRAPHY PROGRAM SCIENCE ABSTRACTS Annual Report, for Period Ending FY85

THOMAS SPENCE 1 Apr. 1986 143 p

(AD-A174019) Avail: NTIS HC A07/MF A01 CSCL 08C

This report presents a summary of work sponsored by the Physical Oceanography Program, ONR, Environmental Sciences Directorate, covering the FY85 period. It includes brief descriptions of research for about 110 physical oceanography projects, and a bibliography containing publications in FY85 supported by the program. GRA

N87-18963# Naval Postgraduate School, Monterey, Calif.
THE RELATIONSHIP BETWEEN MARINE AEROSOL OPTICAL DEPTH AND SATELLITE-SENSED SEA SURFACE TEMPERATURE M.S. Thesis

SUSAN K. RUNCO Jun. 1986 77 p

(AD-A174337) Avail: NTIS HC A05/MF A01 CSCL 17E

Multichannel sea surface temperatures (MCSST) computed from NOAA 7 AVHRR channels 4 and 5 are compared to sea surface temperatures measured by an aircraft radiometer (PRT-5). This data set was collected in Fall, 1982 off the southern Californian coast. The MCSST was warmer by 0.82 degrees in the area aerosol effects did not offset increasing radiance due to vertically warming air temperature. As aerosols were able to offset the temperature contribution to radiance, the difference between MCSST and PRT-5 SST measurements decreased. Aerosol effects on infrared radiance were qualitatively examined using an atmospheric transmittance model (LOWTRAN 6). Comparing the model and PRT-5 results indicates that below the marine boundary layer, high aerosol extinction caused significant cooling. Above the boundary layer, aerosols scattered and emitted energy, generally decreasing the measured radiance. The emission moderated the decrease by increasing the radiance slightly. GRA

N87-18966# Office of Naval Research, Arlington, Va. Ocean Sciences Div.

INVESTIGATION OF PHYSICS OF SYNTHETIC APERTURE RADAR IN OCEAN REMOTE SENSING TOWARD 84/86 FIELD EXPERIMENT. VOLUME 2: CONTRIBUTIONS OF INDIVIDUAL INVESTIGATORS Interim Report

OMAR H. SHEMDIN May 1986 195 p

(AD-A174527) Avail: NTIS HC A09/MF A01 CSCL 17I

Surface Gravity Wave Measurements; Development and Utilization of a Surface Energy Measurement System in Toward 84/85; Wave Follower Measurements During Toward 84/85; The Propagation of Short Surface Waves on Longer Gravity Waves; Toward Meteorology Measurements; Processing of JPL SAR Frame; Azimuthal Waves on 31 October 1984; SAR Imagery Simulated From Two Scale Radar Wave Probe Return; and Sample Predictions and Simulations of SAR Ocean Imagery are presented. GRA

N87-18970# Institute of Oceanographic Sciences, Wormley (England).

SEASOAR CTD SURVEYS DURING FASINEX

R. T. POLLARD, J. F. READ, and J. SMITHERS 1986 108 p

(IOS-230; ETN-87-99137) Avail: NTIS HC A06/MF A01

During the Frontal Air Sea Interaction Experiment (FASINEX) 5 SeaSoar runs were carried out, including a creeping line ahead survey of a 120 km x 160 km box spanning the main FASINEX front, a single box 30 km x 90 km circumnavigated 4 times in 3.75 days, and several circuits of the FASINEX mooring array, to measure CTD in the North Atlantic. Track plots using a mixture of Loran and GPS were constructed in near-real-time. ESA

N87-18971# National Oceanic and Atmospheric Administration, Washington, D. C. National Environmental Data Referral Service.
SATELLITE REMOTE SENSING OF THE MARINE ENVIRONMENT: LITERATURE AND DATA SOURCES
 G. BARTON, B. ROBERTS, and E. RICCIO Jul. 1986 245 p
 (PB86-245446; NEDRES-5) Avail: NTIS HC A11/MF A01
 CSCL 08A

The joint NEDRES/NALIS publication presents bibliographic and data source information pertinent to remote sensing of the marine environment. Satellite oceanography has made a major contribution to knowledge of the oceans on a global scale. The bibliographic data bases searched for the publication were NALIS, NTIS, ASFA and MGA. The environmental data directory searched was NEDRES. GRA

N87-19877*# Alaska Univ., Anchorage.
INFLUENCE OF THE YUKON RIVER ON THE BERING SEA Semiannual Progress Report
 K. DEAN and C. P. MCROY Mar. 1987 15 p Original
 contains color illustrations
 (Contract NAS5-28769)
 (NASA-CR-180356; NAS 1.26:180356) Avail: NTIS HC A02/MF
 A01 CSCL 08C

The distribution of near-surface, turbid water, discharged by the Yukon River, was studied based on analysis of satellite imagery. The interannual analyses indicates that the net flow of near-surface, turbid water is northward of the delta across the entrance to Norton Sound. Only turbid water to the east enters Norton Sound and consists of 25% of the total area. Approximately 10% of the water circulates into the sound along the southern coast and is lost to view in the vicinity of Unalakleet. Suspended sediments transported by this southern circulation are primarily deposited along the southern coast. Three distinct zones within the turbid water were identified based on relative brightness levels. These zones appear to be primarily related to differences in suspended-sediment concentrations and position of the sediments in the water column. The extent of turbid water varies seasonally. It is most extensive June through October even though discharge of the Yukon River decreases substantially after July. B.G.

N87-19879# Naval Research Lab., Washington, D. C.
COMPARISON OF OCEAN TIDE MODELS WITH SATELLITE ALTIMETER DATA Final Report, Jan. 1985 - Jul. 1986
 L. W. CHOY and M. GRUNES 14 Nov. 1986 23 p
 (AD-A174698; NRL-MR-5866) Avail: NTIS HC A02/MF A01
 CSCL 08C

Ocean tides are noise to those who wish to construct the ocean geoid using satellite altimeter data. Precise modeling of the ocean tides will help improve the geoid modeling accuracy. This report studies whether altimeter data itself can be used to assess various tide models. The Schwiderski Global Tide Model and the Kuo Pacific Ocean tide model were examined using SEASAT altimeter data in the Gulf of Alaska and South Pacific region. The NSWC Ocean Tide Model contains nine harmonic partial tides of the semi-diurnal, diurnal, and long-period species. The model includes effects of tide-generated terrestrial and oceanic mass perturbations. The Kuo model is a Pacific Ocean total tide model with earth tide corrections. The method employed here cannot as yet be used to study the long wavelength component of tides removed by the quadratic fits, and only height differences along near-repeat sub-satellite tracks can be studied; if the altimeter repeat ground tracks do not overlap exactly, geoidal variations can not be completely removed by simple subtraction. The precision of satellite altimetry also places a limit on the accuracy with which one can safely assess the error of a tide model. Within these limitations, the feasibility of using altimeter data to assess tide models has been successfully demonstrated. GRA

HYDROLOGY AND WATER MANAGEMENT

Includes snow cover and water runoff in rivers and glaciers, saline intrusion, drainage analysis, geomorphology of river basins, land uses, and estuarine studies.

A87-20765
SNOW SURVEY FROM METEOROLOGICAL SATELLITE IMAGES IN THE QILIAN MOUNTAIN BASIN IN NORTHWEST CHINA

Z. K. LIU (University of Science and Technology of China, Hefei, People's Republic of China), S. Y. ZHENG, and Q. Z. ZENG (Chinese Academy of Sciences, Lanzhou Institute of Glaciology and Cryopedology, People's Republic of China) International Journal of Remote Sensing (ISSN 0143-1161), vol. 7, Oct. 1986, p. 1335-1340.

A87-20951
A THERMAL DEVICE FOR AIRCRAFT MEASUREMENT OF THE SOLID WATER CONTENT OF CLOUDS

W. D. KING and D. E. TURVEY (CSIRO, Cloud Physics Laboratory, Sydney, Australia) Journal of Atmospheric and Oceanic Technology (ISSN 0739-0572), vol. 3, Sept. 1986, p. 356-362. refs

A constant temperature probe for the measurement of solid water content of clouds is described. The probe is operated at a temperature of 25 C, and is designed to collect and melt ice particles that impact in an open half-cylinder, the amount of power supplied to the probe being related to the solid water content through its dimensions, etc. Comparisons in a small wind tunnel with values derived from weightings of oil-coated slides suggests that the probe is accurate to about 50 percent, while data from two different aircraft indicate that it performs reliably under flight conditions. Author

A87-23361
REMOTELY SENSED ALBEDO OF SNOW-COVERED LANDS
 DAVID A. ROBINSON (Lamont-Doherty Geological Observatory, Palisades, NY) IN: Conference on Satellite Meteorology/Remote Sensing and Applications, 2nd, Williamsburg, VA, May 13-16, 1986, Preprints. Boston, MA, American Meteorological Society, 1986, p. 173-176. refs

(Contract NSF ATM-83-18676; AF-AFOSR-86-0053)
 Using remotely-sensed aircraft and satellite data, examples of clear-sky albedo variations of both fresh and aging snow cover are examined. The variations observed were found to be caused by variations in the type and density of vegetation, and the depth, physical properties, and continuity of the snowpack. Thus, to retrieve information on a snow-covered region, an interactive analysis of satellite data on an image processor must be performed by an observer familiar with the area. I.S.

A87-23370
SATELLITE RAINFALL RETRIEVAL BY LOGISTIC REGRESSION

LONG S. CHIU (Applied Research Corp., Landover, MD) and BENJAMIN KEDEM (Maryland, University, College Park) IN: Conference on Satellite Meteorology/Remote Sensing and Applications, 2nd, Williamsburg, VA, May 13-16, 1986, Preprints. Boston, MA, American Meteorological Society, 1986, p. 224-227. refs

A model using logistic regression in which a likelihood function is maximized is described for use in rainfall estimation. The model output is the distribution of rainrate categories from which standard errors can be estimated, and the significance of the covariates can be easily tested. The logistic model is demonstrated with the example of Gate phase I data for a scenario for which observations of microwave temperature and fractional rain area are available. R.R.

A87-23374

REMOTE SENSING OF HYDROLOGICAL VARIABLES FROM THE DMSP MICROWAVE MISSION SENSORS

R. G. ISAACS, Y.-Q. JIN, G. DEBLONDE, R. D. WORSHAM, and L. D. KAPLAN (Atmospheric and Environmental Research, Inc., Cambridge, MA) IN: Conference on Satellite Meteorology/Remote Sensing and Applications, 2nd, Williamsburg, VA, May 13-16, 1986, Preprints. Boston, MA, American Meteorological Society, 1986, p. 243-248. refs

(Contract F19628-83-C-0027; F19628-84-C-0134)

Characteristics of three meteorological sensors (the SSM/I microwave imager, SSM/T microwave temperature sounder, and SSM/T-2 millimeter wave moisture sounder) of the Defense Meteorological Satellite Program (DMSP) spacecraft of the 1990s are described. Using simulated sensor data, unified retrieval techniques are developed for obtaining water vapor profiles, precipitation, integrated water vapor, cloud liquid water, soil moisture, and surface type. The DMSP microwave mission sensor package is shown to be effective in retrieving these quantities, especially when a multispectral approach is taken. I.S.

A87-23414

ANNUAL AND INTERANNUAL VARIABILITY IN LARGE-SCALE CONVECTION OVER THE EASTERN PACIFIC AND TROPICAL SOUTH AMERICA

PHILLIP A. ARKIN (NOAA, Climate Analysis Center, Washington, DC) IN: Conference on Satellite Meteorology/Remote Sensing and Applications, 2nd, Williamsburg, VA, May 13-16, 1986, Preprints. Boston, MA, American Meteorological Society, 1986, p. 479-484. refs

A87-23699

ANTARCTICA - MEASURING GLACIER VELOCITY FROM SATELLITE IMAGES

B. K. LUCCHITTA and H. M. FERGUSON (USGS, Flagstaff, AZ) Science (ISSN 0036-8075), vol. 234, Nov. 28, 1986, p. 1105-1108. refs

Many Landsat images of Antarctica show distinctive flow and crevasse features in the floating part of ice streams and outlet glaciers immediately below their grounding zones. Some of the features, which move with the glacier or ice stream, remain visible over many years and thus allow time-lapse measurements of ice velocities. Measurements taken from Landsat images of features on Byrd Glacier agree well with detailed ground and aerial observations. The satellite-image technique thus offers a rapid and cost-effective method of obtaining average velocities, to a first order of accuracy, of many ice streams and outlet glaciers near their termini. Author

A87-23808

SATELLITE OBSERVATIONS OF SNOW COVERED AREA IN THE HIGH ATLAS MOUNTAINS OF MOROCCO

JAMES P. VERDIN (Wright Water Engineers, Inc., Denver, CO) IN: American Congress on Surveying and Mapping and American Society for Photogrammetry and Remote Sensing, Annual Convention, Washington, DC, Mar. 16-21, 1986, Technical Papers. Volume 4. Falls Church, VA, American Congress on Surveying and Mapping and American Society for Photogrammetry and Remote Sensing, 1986, p. 500-510.

A87-23815

PRE-ASSESSMENT FOR LARGE SCALE CIVIL ENGINEERING PROJECTS BY INTEGRATED ANALYSIS WITH THE DATA NUMERICAL TOPOGRAPHY AND REMOTE SENSING

TAICHI OSHIMA, ATSUSHI RIKIMARU (Hosei University, Tokyo, Japan), YOUICHI KATO (Pasco Corp., Tokyo, Japan), and MASAHARU NAKAMURA IN: American Congress on Surveying and Mapping and American Society for Photogrammetry and Remote Sensing, Annual Convention, Washington, DC, Mar. 16-21, 1986, Technical Papers. Volume 5. Falls Church, VA, American Congress on Surveying and Mapping and American Society for Photogrammetry and Remote Sensing, 1986, p. 44-52.

A87-23824

THE UTILITY OF THEMATIC MAPPER DATA FOR TEMPERATURE MAPPING IN THE GREAT LAKES

RICHARD G. LATHROP, JR. and THOMAS M. LILLESAND (Wisconsin, University, Madison) IN: American Congress on Surveying and Mapping and American Society for Photogrammetry and Remote Sensing, Annual Convention, Washington, DC, Mar. 16-21, 1986, Technical Papers. Volume 5. Falls Church, VA, American Congress on Surveying and Mapping and American Society for Photogrammetry and Remote Sensing, 1986, p. 151-161. Research supported by the University of Wisconsin. refs

(Contract NOAA-NA-800AAD00086)

The use of Landsat-5 TM thermal IR data to measure and map surface water temperatures in the Great Lakes is studied. Empirical and theoretical modeling approaches for calibrating the TM are described; the calibration was performed using TM data obtained on July 18, 1984 over the Chicago-South Lake Michigan region. The surface water temperature data derived with the quadratic model, cubic model, lookup table, and empirical model are examined and compared. It is observed that all the models effectively estimated the water temperatures and that the cubic model provided a better prediction of the surface reference data than the quadratic or empirical models. I.F.

A87-23825

LANDSAT THEMATIC MAPPER DATA ANALYSIS WITHIN THE SUWANNEE RIVER BASIN

PATRICK F. ECHOLS, BYRON E. RUTH, DOUGLAS M. JORDAN, and JANET D. DEGNER (Florida, University, Gainesville) IN: American Congress on Surveying and Mapping and American Society for Photogrammetry and Remote Sensing, Annual Convention, Washington, DC, Mar. 16-21, 1986, Technical Papers. Volume 5. Falls Church, VA, American Congress on Surveying and Mapping and American Society for Photogrammetry and Remote Sensing, 1986, p. 162-171. refs

The application of Landsat TM data to land cover classification, delineation of floodplain boundaries, and interpretation of geomorphologic features is evaluated. Landsat-4 TM data for the Suwannee River Basin in Florida are analyzed using image processing software. The initial classification using bands 2, 3, 5, and 7 yielded 16 land cover classes from the 24 spectral classes and the second analysis using bands 1, 3, 4, 6, and 7 produced only 14 land cover classes. The difference in produced land cover classes is attributed to the poor performance of band 6; causes of the poor performance of band 6 are discussed. It is also observed that the TM permits delineation of smaller features than the MSS data and there is good correlation between the vegetation and floodplain boundary. I.F.

A87-23826

REMOTE SENSING OF AQUATIC MACROPHYTE DISTRIBUTION IN UPPER LAKE MARION

JOHN R. JENSEN and BRUCE A. DAVIS (South Carolina, University, Columbia) IN: American Congress on Surveying and Mapping and American Society for Photogrammetry and Remote Sensing, Annual Convention, Washington, DC, Mar. 16-21, 1986, Technical Papers. Volume 5. Falls Church, VA, American Congress on Surveying and Mapping and American Society for Photogrammetry and Remote Sensing, 1986, p. 181-189.

This study investigates the utility of the Landsat Thematic Mapper sensor system as a source of information on aquatic macrophytes. Analysis of data acquired on May 14th and July 17th, 1984 discriminated predominantly submersed and emersed aquatic vegetation from other land cover classes. Furthermore, innovative extension of spectral clusters resulted in a land cover classification of 41,000 acres in the upper reaches of Lake Marion. Author

A87-23831

LANDSAT THEMATIC MAPPER IMAGES FOR HYDROLOGIC LAND USE AND COVER

L. J. TROLIER, W. R. PHILIPSON, and W. D. PHILPOT (Cornell University, Ithaca, NY) IN: American Congress on Surveying and Mapping and American Society for Photogrammetry and Remote Sensing, Annual Convention, Washington, DC, Mar. 16-21, 1986, Technical Papers. Volume 5. Falls Church, VA, American Congress on Surveying and Mapping and American Society for Photogrammetry and Remote Sensing, 1986, p. 269-278. Research supported by the Department of the Interior. refs

A Landsat Thematic Mapper (TM) image of Rochester, N.Y., was visually and digitally analyzed to determine how well 22 hydrologically important land use and cover classes could be identified. Visual interpretations at a scale of 1:70,000 recognized 16 of the classes, while digital classification with a maximum likelihood classifier recognized nine classes with a very high degree of confidence. Bands 3, 4 and 5 provided most of the information for both visual and digital analyses, and would be a sufficient subset of the seven TM bands for either method. Greater land use detail was interpretable through visual analysis because spatial characteristics were included, while the digital analysis recognized more general classes, representing mostly cover differences.

Author

A87-25746

VISUALIZATION BY AERIAL THERMOGRAPHY OF HYDRODYNAMIC EXCHANGES BETWEEN THE WATER TABLE, STREAMS AND GRAVEL PITS IN THE RHINE PLAIN NORTH OF STRASBOURG [VISUALIZATION, PAR THERMOGRAPHIE AERIENNE, DES ECHANGES HYDRODYNAMIQUES ENTRE LA NAPPE PHREATIQUE, LES COURS D'EAU ET LES GRAVIERES DANS LA PLAINE DU RHIN AU NORD DE STRASBOURG]

ANDRE DURBEC (Ecole Nationale des Ingenieurs des Travaux Ruraux et des Techniques Sanitaires, Strasbourg, France), PAUL MUNTZER, and LOTHAIRE ZILLIOX (Strasbourg I, Universite, France) Societe Francaise de Photogrammetrie et de Teledetection, Bulletin (ISSN 0244-6014), no. 102, 1986, p. 25-36. In French. refs

A87-26537

USE OF DECIMETER WAVES IN STUDIES OF WATER BODIES BY METHODS OF MICROWAVE RADIOMETRY [OB ISPOL'ZOVANII DIAPAZONA DETSIMETROVYKH VOLN DLIA ISSLEDOVANIIA AKVATORII METODAMI SVCH-RADIOMETRII]

A. G. GRANKOV and A. M. SHUTKO (AN SSSR, Institut Radiotekhniki i Elektroniki, Moscow, USSR) Issledovanie Zemli iz Kosmosa (ISSN 0205-9614), Sept.-Oct. 1986, p. 78-89. In Russian. refs

The determination of the temperature and salinity of water bodies from remote sensing data on the microwave (30-100 cm) emission from the water surface is described. The analysis takes into account the state of the water surface, including foam, wave formations, and oil film features. Approximate corrections are calculated to estimate the contributions of cosmic radio emission and emission from (or absorption by) the ionosphere at these wavelengths. I.S.

A87-27883

DETECTING AND FORECASTING WESTERN REGION FLASH FLOODS USING GOES IMAGERY AND CONVENTIONAL DATA

LEROY E. SPAYD, JR. (NOAA, National Weather Service, Camp Springs, MD) IN: Conference on Weather Forecasting and Analysis, 11th, Kansas City, MO, June 17-20, 1986, Preprints. Boston, MA, American Meteorological Society, 1986, p. 315-320. refs

A87-28436#

DEVELOPMENT AND EXPERIMENT OF AIRBORNE MICROWAVE RAIN-SCATTEROMETER/RADIOMETER SYSTEM. III - RAIN MEASUREMENT AND ITS DATA ANALYSIS

MASAHARU FUJITA, KENICHI OKAMOTO, HARUNOBU MASUKO, SHIN YOSHIKADO, and KENJI NAKAMURA Radio Research Laboratory, Review (ISSN 0033-801X), vol. 32, June 1986, p. 107-125. In Japanese, with abstract in English. refs

An algorithm for estimating the rain rate using data from dual-frequency radar is presented, along with the results of a simulation of its performance. Rain rate is determined by comparing the power of the radar echoes backscattered from the ocean surface with predicted attenuation. A radiative transfer equation is employed to equate the antenna temperature to the rain rate profile sensed with a scatterometer. Account is taken of the effects of the sea surface temperature on the backscattered signal. The excess antenna temperature at 10 GHz is demonstrated to be proportional to the path-integrated rain rate. M.S.K.

A87-29013

DRAINAGE CHANNEL NETWORK OF THE ARCACHON BASIN USING THEMATIC MAPPER DATA OBTAINED AT HIGH TIDE [RESEAU DES CHENAUX DU BASIN D'ARCACHON ETABLI PAR DES DONNEES THEMATIC MAPPER ACQUISES AHAUTE MAREE]

LI WANG (Ecole Normale Superieure, Montrouge, France) and DONG-CHEN HE (Institut National des Sciences de l'Univers, Paris, France) International Journal of Remote Sensing (ISSN 0143-1161), vol. 7, Dec. 1986, p. 1789-1795. In French. refs

An attempt was made to produce a drainage channel network chart of the Arcachon Basin (on the French west coast), by using unsupervised classification of Landsat-5 Thematic Mapper data acquired while the basin was completely covered with water. This study shows that satellite data supply information about submarine topography, making it possible to study underwater geomorphology at a certain depth with the data furnished by satellite. Author

A87-30899

MAPPING OF WATER QUALITY IN COASTAL WATERS USING AIRBORNE THEMATIC MAPPER DATA

J. C. RIMMER, M. B. COLLINS, and C. B. PATTIARATCHI (Swansea, University College, Wales) International Journal of Remote Sensing (ISSN 0143-1161), vol. 8, Jan. 1987, p. 85-102. NERC-supported research. refs

ATM data from the Swansea Bay, England are utilized in the regression analysis for suspended sediment concentration, mean grain size of material in suspension, surface salinity, and chlorophyll a. Thematic maps of water quality distributions in the embayment are developed by applying the derived regression equations to the remotely sensed data. The thematic maps for the various parameters are compared to sea-truth data; it is observed that the data correlate well. It is concluded that remote sensing is a useful technique for mapping surface water quality in coastal regions. I.F.

N87-15547# University Coll., Dublin (Ireland). Dept. of Civil Engineering.

HYDROLOGIC MODELS OF LAND SURFACE PROCESSES

JAMES C. I. DOOGE In ESA Proceedings of an International Satellite Land-Surface Climatology Project (ISLSCP) Conference p 3-16 May 1986

Avail: NTIS HC A99/MF A01

The role of soil moisture in climate modeling, particularly those aspects to which remote sensing can make a significant contribution, is reviewed. The main features of models of soil water storage and movement at the microscale of a representative local volume, the mesoscale of an experimental plot, and the macroscale of a catchment are summarized. Soil moisture modeling in general circulation models is discussed, together with uses of remote sensing in the improvement of such techniques. ESA

N87-15569# Meteorological Office, Bracknell (England).
REMOTE SENSING IDENTIFIED IN CLIMATE MODEL EXPERIMENTS WITH HYDROLOGICAL AND ALBEDO CHANGES IN THE SAHEL

P. R. ROWNTREE and A. B. SANGSTER /In ESA Proceedings of an International Satellite Land-Surface Climatology Project (ISLSCP) Conference p 175-183 May 1986
 Avail: NTIS HC A99/MF A01

Mechanisms by which changes in the land surface may affect climate in lower latitudes are discussed and general circulation model experiments are reviewed. Albedo and surface moisture availability appear to be the most important factors. Results of experiments designed to assess the effects on rainfall of variations in model land surface properties in the Sahel, such as could follow from a loss of vegetation in the region are presented. These changes led to decreases in rainfall of similar magnitude to those observed during the Sahel drought of the last 15 to 20 yr. However there is only a little quantitative information readily available for assessing whether such changes have actually occurred. There is a need for regular satellite monitoring of relevant land surface characteristics with extension as far into the past as possible.

ESA

N87-15587# Reading Univ. (England). Dept. of Meteorology.
RAINFALL ESTIMATION OVER THE SAHEL USING METEOSAT THERMAL INFRA-RED DATA

G. DUGDALE and J. R. MILFORD /In ESA Proceedings of an International Satellite Land-Surface Climatology Project (ISLSCP) Conference p 315-319 May 1986 Sponsored by UK Overseas Development Agency and the European Economic Community
 Avail: NTIS HC A99/MF A01

Objective methods for estimating rainfall from West African squall lines were devised. The nature of the phenomenon requires frequent IR imagery to be used. Large area mean rainfall or small area long period means may be estimated from the size and duration of storms in the area. Rainfall in limited areas (one to four pixels) from individual events requires an objective method for estimating the time varying vigor of the convective system. Rainfall estimations for periods of 30 and 10 days over the Republic of Niger show encouraging results in discriminating areas having significantly less or more than the mean for the zone.

ESA

N87-15588# Mullard Space Science Lab., Dorking (England).
THE PROSPECTS FOR HYDROLOGICAL MEASUREMENTS USING ERS-1

M. A. J. GUZKOWSKA, I. M. MASON, C. G. RAPLEY, and F. A. STREET-PERROTT (Oxford Univ., England) /In ESA Proceedings of an International Satellite Land-Surface Climatology Project (ISLSCP) Conference p 321-326 May 1986 Sponsored by UK Science and Engineering Research Council
 Avail: NTIS HC A99/MF A01

The prospects for using the Radar Altimeter (RA) and the Along Track Scanning Radiometer (ATSR) on ERS-1, for the joint measurement of lake levels and lake areas were assessed. SEASAT return waveforms over Great Salt Lake (USA) illustrate the use of the RA. It is estimated that with a repeat track of 35 days the RA could measure up to 200 closed lakes and 500 open lakes of over 100 sq km on a global scale. The ATSR has virtually complete global coverage. These measurements would be quality-controlled, accurate, self-consistent and have a high time resolution.

ESA

N87-15609# Reading Univ. (England). Dept. of Meteorology.
HYDROLOGICAL STUDIES IN NIGER

I. D. FLITCROFT, G. DUGDALE, and J. R. MILFORD /In ESA Proceedings of an International Satellite Land-Surface Climatology Project (ISLSCP) Conference p 455-459 May 1986 Sponsored by UK Overseas Development Agency and the European Economic Community
 Avail: NTIS HC A99/MF A01

A data set for the development and validation of algorithms relating Meteosat data to components of the water budget in the Niger was collected. Field measurements show that evaporation

from bare soils in these regions is mainly controlled by the depth of the upper layer of dry soil. A useful approximation to the daily evaporation rate can be obtained from a simple relationship between the evaporation and the time since the previous rainfall. Rainfall estimation from satellites must be calibrated against rain gage measurements. The rapid decrease in correlation between rainfalls with increasing grid separation is significant for the interpretation of rain gage and satellite rainfall measurements. Spatial variability in IR radiances must be taken into account where comparing observed surface temperatures with those deduced from Meteosat.

ESA

N87-15611# Instituut voor Cultuurtechniek en Waterhuishouding, Wageningen (Netherlands).

GROUND WATER-FED LAKES IN THE LIBYAN DESERT: THEIR VARYING AREA AS OBSERVED BY MEANS OF LANDSAT-MSS DATA

H. KUIPERS and M. MENETI /In ESA Proceedings of an International Satellite Land-Surface Climatology Project (ISLSCP) Conference p 467-471 May 1986
 Avail: NTIS HC A99/MF A01

Five LANDSAT-MSS images acquired between November 1975 and September 1978 were used to study the temporal variability of the area of 3 small groundwater-fed lakes in the Idehan Awbari, Libya. The hydrological role of the lakes is described. Mean reflectance of a small image window enclosing each lake is taken as a measure of the lake area. To obtain the mean surface reflectance applying to the spectral region 0.4 to 1.1 microns, radiometric and geometric corrections are applied. Results show that oscillations of the lake area occur which would not be predicted on the basis of current hydrological wisdom applying to this region.

ESA

N87-15626# Environmental Analysis and Remote Sensing, Delft (Netherlands).

GROUP AGROMET MONITORING PROJECT (GAMP) METHODOLOGY INTEGRATED MAPPING OF RAINFALL, EVAPOTRANSPIRATION, GERMINATION, BIOMASS DEVELOPMENT AND THERMAL INERTIA, BASED ON METEOSAT AND CONVENTIONAL METEOROLOGICAL DATA

A. ROSEMA /In ESA Proceedings of an International Satellite Land-Surface Climatology Project (ISLSCP) Conference p 549-557 May 1986 Original contains color illustrations
 Avail: NTIS HC A99/MF A01

Satellite and conventional meteorological data were integrated to achieve space and time continuous mapping and monitoring of rainfall, evapotranspiration, germination dynamics, and biomass development. Rainfall, evapotranspiration, and biomass mapping results demonstrate the feasibility of the methodology to extend existing sources of agro and hydrometeorological information. The accuracy of rainfall mapping, based on METEOSAT cloud information, is 30%. The accuracy of evapotranspiration mapping, based on METEOSAT ground information, is 0.5 mm (10%). Germination and biomass mapping are based on the latter data. End of season biomass results compare well with field observations. The mapping and analysis of thermal inertia demonstrates the potential of evaluating soil water infiltration immediately after rainfall.

ESA

N87-15632# INAP, Paris (France).
HYDROLOGICAL ATMOSPHERIC PILOT EXPERIMENT (HAPEX) HYDROLOGY BUDGET MODELING (MOBILHY): OUTLINE OF THE PROGRAM

ANDREE TUZET /In Ludwig-Maximilians-Universitaet Satellite Measurements of Radiation Budget of the Earth (3rd Symposium) p 19-23 Jul. 1986
 Avail: NTIS HC A09/MF A01; Fachinformationszentrum, Karlsruhe, West Germany DM 37

An experiment to improve understanding of land surface processes at scales from 100m to 100km; test parameterization schemes used in general circulation models; and aid to the interpretation of remote sensing data is outlined. The strategy is based on an instrumented network with a grid size of the order of

06 HYDROLOGY AND WATER MANAGEMENT

10 x 10 km on a total domain of the order of 100 x 100 km. The network includes surface, subsurface, and atmospheric measurements. The network data are completed by airborne data to extrapolate to larger scales the local measurements, and to get calibrating data for the satellite remote sensing measurements. The experiments are followed by a numerical simulation of the mesoscale atmospheric flow above the domain. ESA

N87-16382# Instituto de Pesquisas Espaciais, Sao Jose dos Campos (Brazil).

APPLICATION OF REMOTE SENSING IN HYDROLOGY AND WATER RESOURCES [APLICACOES DE SENSORIAMENTO REMOTO EM HIDROLOGIA E RECURSOS HIDRICOS]

EVLYN MARCIA LEAO DE NOVO Sep. 1986 14 p In PORTUGUESE Submitted for publication (INPE-3986-PRE/991) Avail: NTIS HC A02/MF A01

Possible remote sensing data applications in the areas of hydrology and water resources are discussed. The principal field of activity and the electromagnetic spectrum band most used are analyzed first with research in the available bibliography. Also supplied are some examples of orbital data used to monitor water resources monitors as developed at INPE/MCT. Author

N87-16383*# California Univ., Berkeley. Dept. of Forestry and Resource Management.

DEVELOPMENT OF EOS-AIDED PROCEDURES FOR THE DETERMINATION OF THE WATER BALANCE OF HYDROLOGIC BUDGET OF A LARGE WATERSHED Semiannual Progress Report, 1 Aug. - 31 Dec. 1986

RUSSELL G. CONGALTON, RANDALL W. THOMAS, and PAUL J. ZINKE 31 Dec. 1986 15 p (Contract NAGW-881) (NASA-CR-180118; NAS 1.26:180118) Avail: NTIS HC A02/MF A01 CSCL 08H

Work focused on the acquisition of remotely sensed data for the 1985 to 1986 hydrologic year; continuation of the field measurement program; continued acquisition and construction of passive microwave remote sensing instruments; a compilation of data necessary for an initial water balance computation; and participation with the EOS Simultaneity Team in reviewing the Feather River watershed as a possible site for a simultaneity experiment. B.G.

N87-16386# Air Force Geophysics Lab., Hanscom AFB, Mass. **AN EXTENSION OF THE SPLIT WINDOW TECHNIQUE FOR THE RETRIEVAL OF PRECIPITABLE WATER**

THOMAS J. KLEESPIES and LARRY M. MCMILLIN 3 Oct. 1986 5 p (AD-A173008; AFGL-TR-86-0201) Avail: NTIS HC A02/MF A01 CSCL 17H

The split window technique has been demonstrated to be a viable method of removing effects of atmospheric attenuation in order to make a more accurate estimate of surface properties. This technique has also been used to estimate low level water vapor fields. In this paper we make an extension to the split window technique such that it is possible to estimate total precipitable water. The essence of the split window technique is making observations of the earth in two differentially absorbing windows. We extend this technique by making observations in the split window under conditions where the atmospheric contribution to the upwelling radiance is essentially invariant, but the surface contribution changes markedly. Under these conditions it is possible to write a set of simultaneous equations and solve them for the transmittance of the split window, and from that deduce the quantity of the primary absorber, water. The conditions under which this extension is valid basically fall under two categories; that of variation in time, and that of variation in space. Consecutive observations of a land surface from a geosynchronous satellite during the heating cycle of the day would be one example. Another would be observations from either a geosynchronous or polar orbiting satellite of immediately adjacent land and water surfaces with contrasting skin temperatures. GRA

N87-17223# Environmental Research Inst. of Michigan, Ann Arbor.

ANALYSIS OF MULTICHANNEL SAR DATA OF SPITSBERGEN

B. A. BURNS, R. SHUCHMAN, C. MATZLER (Bern Univ., Switzerland), and J. DOWDESWELL (Scott Polar Research Inst., Cambridge, England) In ESA Proceedings of the 1986 International Geoscience and Remote Sensing Symposium (IGARSS '86) on Remote Sensing: Today's Solutions for Tomorrow's Information Needs, Volume 1 p 367-371 Aug. 1986

Avail: NTIS HC A99/MF E03; ESA, Paris, France, 3 volume set \$90 Member States, AU, CN, and NO (+20% others)

Multitemporal aircraft SAR images obtained over Spitsbergen in summer are used to illustrate the application of SAR data to identification and monitoring of features of glaciological interest. Snow cover on bare ground, on glaciers, and on moraines, as well as ice cover on lakes, can be clearly identified. Monitoring the up-glacier retreat of the snowline is also possible. This discrimination is based on relative backscatter signatures, and is shown to depend on the frequency and polarization of the radar wave. Other features such as terminal moraines are discriminated on the basis of topographic expression, which is enhanced with stereo images. ESA

N87-17264# Helsinki Univ. of Technology, Espoo (Finland). Radio Lab.

DEVELOPPEMENT OF ALGORITHMS TO RETRIEVE THE WATER EQUIVALENT OF SNOW COVER FROM SATELLITE MICROWAVE RADIOMETER DATA

M. HALLIKAINEN and P. JOLMA In ESA Proceedings of the 1986 International Geoscience and Remote Sensing Symposium (IGARSS '86) on Remote Sensing: Today's Solutions for Tomorrow's Information Needs, Volume 1 p 611-616 Aug. 1986

Avail: NTIS HC A99/MF E03; ESA, Paris, France, 3 volume set \$90 Member States, AU, CN, and NO (+20% others)

Algorithms to retrieve the water equivalent of snow cover from NIMBUS-7 scanning Multichannel Microwave Radiometer for winters 1978-79 through 1981-82 were tested. Using the best algorithm, the microwave response to snow water equivalent was examined. Substantial short-term and long-term (annual) variations are observed in the response, due to the thermal history of snow. First-order regression lines were fitted to each winter's data. ESA

N87-17314# Toba Merchant Marine Coll. (Japan).

ESTIMATION OF MAXIMUM SNOW VOLUME DISTRIBUTION USING NOAA-AVHRR DATA

S. TAKEUCHI, K. TAKEDA, H. OCHIAI, and T. SEKI In ESA Proceedings of the 1986 International Geoscience and Remote Sensing Symposium (IGARSS '86) on Remote Sensing: Today's Solutions for Tomorrow's Information Needs, Volume 2 p 909-914 Aug. 1986

Avail: NTIS HC A17/MF A01; ESA, Paris, France, 3 volume set \$90 Member States, AU, CN, and NO (+20% others)

Snow volume was represented as snow water equivalent value at the maximum stage obtained by combining the extraction of snow-nonsnow boundary mesh from AVHRR images and the degree day method. The maximum snow water equivalent at a certain snow boundary mesh is calculated by the degree day method using daily average air temperature data of the nearest neighbor weather station. The estimated snow water equivalent values are extended to maps covering the whole area of north-east Japan. Case studies show the usefulness of satellite data for yearly monitoring of snow volume distribution which extends over several tens of thousands of square kilometers. ESA

N87-17317# Zurich Univ. (Switzerland). Dept. of Geography.
**TOWARDS SNOWMELT RUNOFF FORECAST USING
 LANDSAT-MSS AND NOAA/AVHRR DATA**

M. F. BAUMGARTNER, K. SEIDEL (Eidgenoessische Technische Hochschule, Zurich, Switzerland), and J. MARTINEC (Eidgenoessisches Inst. fuer Schnee- und Lawinenforschung, Weissfluhjoch/Davos, Switzerland) *In* ESA Proceedings of the 1986 International Geoscience and Remote Sensing Symposium (IGARSS '86) on Remote Sensing: Today's Solutions for Tomorrow's Information Needs, Volume 2 p 925-928 Aug. 1986

Avail: NTIS HC A17/MF A01; ESA, Paris, France, 3 volume set \$90 Member States, AU, CN, and NO (+20% others)

Digital snow cover mapping by NOAA/AVHRR to assist snowmelt runoff forecasting from LANDSAT MSS data is discussed. It is shown how remote sensing information from LANDSAT-MSS and NOAA/AVHRR supplement each other. When using coarse spatial sensor resolution, special attention to the area, topography, and amount of snow coverage must be paid. ESA

N87-17319# Oslo Univ. (Norway). Dept. of Geography.
**A CLIMATOLOGICAL-HYDROLOGICAL STUDY OF LAKE ICE
 IN THE SOUTHWESTERN MOUNTAIN AREA IN NORWAY BY
 USE OF SATELLITE SENSING**

J. E. SKORVE *In* ESA Proceedings of the 1986 International Geoscience and Remote Sensing Symposium (IGARSS '86) on Remote Sensing: Today's Solutions for Tomorrow's Information Needs, Volume 2 p 933-938 Aug. 1986

Avail: NTIS HC A17/MF A01; ESA, Paris, France, 3 volume set \$90 Member States, AU, CN, and NO (+20% others)

Snow and lake ice melting in a 63,000 sqkm area of the southwestern mountains in Norway was studied by use of cloudfree LANDSAT imagery obtained during the period 1975-83. Results confirm the utility of satellite imagery for water management in remote areas, and confirm that snow cover is the single most important parameter in lake ice melting. ESA

N87-17340*# Minnesota Univ., Minneapolis. Dept. of Physics
 and Astronomy.

**MICROWAVE RADIANCES FROM HORIZONTALLY FINITE
 PRECIPITATING CLOUDS CONTAINING ICE AND LIQUID
 HYDROMETEORS**

C. KUMMEROW and J. A. WEINMAN (Wisconsin Univ., Madison) *In* ESA Proceedings of the 1986 International Geoscience and Remote Sensing Symposium (IGARSS '86) on Remote Sensing: Today's Solutions for Tomorrow's Information Needs, Volume 2 p 1069-1075 Aug. 1986

(Contract NAG5-580; N00014-86-K-2001)

Avail: NTIS HC A17/MF A01; ESA, Paris, France, 3 volume set \$90 Member States, AU, CN, and NO (+20% others) CSCL 04B

Microwave radiances that would be measured from satellite borne radiometers were computed as a function of rainfall rates from horizontally finite precipitating clouds containing ice and liquid hydrometeors capped by a layer of nonprecipitating ice that covers the remainder of the footprint. Ice at the top of the precipitating clouds depresses the brightness temperatures which depend on rainfall rates because the ice hydrometeor concentrations are assumed to be related to the rainfall rates at the cloud base. It is also found that the brightness temperatures of footprints partially covered by precipitation cells are a nonlinear function of the rainfall rate averaged over the footprint. Thus the average brightness temperatures depend on the peak rainfall rates and the size of the precipitating cloud. ESA

N87-18159# Oulu Univ. (Finland). Dept. of Astronomy.
**REMOTE SENSING OF SHALLOW WATER AREAS WITH
 REFERENCE TO ENVIRONMENTAL AND MULTITEMPORAL
 MONITORING OF THE HAILUOTO AREA, FINLAND**

J. RAITALA and H. JANTUNEN *In* ESA Proceedings of the 1986 International Geoscience and Remote Sensing Symposium (IGARSS '86) on Remote Sensing: Today's Solutions for Tomorrow's Information Needs, Volume 3 p 1307-1311 Aug. 1986

Avail: NTIS HC A21/MF A01; ESA, Paris, France, 3 volume set \$90 Member States, AU, CN, and NO (+20% others)

Multispectral LANDSAT images were used to study the area near Hailuoto Island (Finland) where traffic links to the mainland are being considered. The hydrolittoral unit classification depends on the changes in water depth and quality and bottom soil in addition to the growing units on a scale of one or more hectares. Open water classes are affected by water vegetation near shores. The LANDSAT classification agrees well with depth measurements in the hydrolittoral of the Hailuoto area for a depth of 0 to 2.5 m, but in deeper water the classification is not so clear. The use of satellite data before a decision is made is of limited value since political and economic factors are more influential than objective assessments of environmental parameters. ESA

N87-18172# North Carolina State Coll., Raleigh. Computer
 Graphics Center.

**MODELLING OF ESTUARINE CHLOROPHYLL-A FROM AN
 AIRBORNE SCANNER**

S. KHORRAM, G. P. CATTS, J. E. CLOERN, and A. W. KNIGHT *In* ESA Proceedings of the 1986 International Geoscience and Remote Sensing Symposium (IGARSS '86) on Remote Sensing: Today's Solutions for Tomorrow's Information Needs, Volume 3 p 1387-1396 Aug. 1986 Sponsored in cooperation with the California State Resources Agency and Geological Survey (Contract NOAA-NA80AA-D-00120; PROJ. R/CZ-68)

Avail: NTIS HC A21/MF A01; ESA, Paris, France, 3 volume set \$90 Member States, AU, CN, and NO (+20% others)

The applicability and consistency of a model reflecting relationship between digital spectral data and estuarine chlorophyll-A concentrations were examined. The approach involved collection and laboratory analysis of water quality samples, simultaneous acquisition of airborne multispectral scanner data, and selection of channels and their ratios. Results include prediction of chlorophyll-A for two dates composed of high and low freshwater inflow conditions based on the same wavelength channels and their ratios. ESA

N87-18200# Mullard Space Science Lab., Dorking (England).
**SATELLITE ALTIMETER MEASUREMENTS OVER LAND AND
 INLAND WATER**

M. A. J. GUZKOWSKA, C. G. RAPLEY, and I. M. MASON *In* ESA Proceedings of the 1986 International Geoscience and Remote Sensing Symposium (IGARSS '86) on Remote Sensing: Today's Solutions for Tomorrow's Information Needs, Volume 3 p 1563-1568 Aug. 1986

Avail: NTIS HC A21/MF A01; ESA, Paris, France, 3 volume set \$90 Member States, AU, CN, and NO (+20% others)

The applicability of satellite altimetry to profiling terrain and inland waters was assessed using Seasat data. The data reveal ocean-like returns from lakes, providing direct estimates of surface height, surface waveheight and surface backscatter coefficient, quasi-specular returns from several surface types, giving accurate elevation measurements over areas as small as 180m in diameter, and complex returns with features which correspond to specific surface features. Once retracked, the ocean-like and quasi-specular waveforms can be used to carry out precise and accurate terrain profiling. The minimum range and along-track location of features within the complex returns may also be found. Given accurate independent elevation measurements, such data could be used to calibrate the altimeter range estimates. ESA

N87-19799# Rijkswaterstaat, The Hague (Netherlands).
EVALUATION OF REMOTE SENSING RESULTS FOR THE BENEFIT OF WATER QUALITY RESEARCH ON THE NORTH SEA [EVALUATIE RESULTATEN VAN REMOTE SENSING TBV WATERKWALITEITSONDERZOEK OP DE NOORDZEE]

ALPHEN PETERS Jan. 1986 21 p In DUTCH
(NZ-R-86.15; ETN-87-99215) Avail: NTIS HC A02/MF A01

The results of the application of remote sensing techniques to water quality studies were evaluated from the point of view of the user. The operational applicability of satellites is presently insufficient for routine observations due to the relatively low passing frequency of suitable systems in combination with the high frequency of unsuitable weather conditions. The present systems, based on passive techniques, provide data on a limited number of water quality parameters, and have an insufficient accuracy. The character of the data (accuracy, parameters) does not justify the cost for data acquisition and data processing. It is proposed to use satellite images for the qualitative study of large scale processes. The flexibility of systems onboard aircraft is promising for project-like research. The research should be more directed toward the application of active remote sensing techniques (lasers).
ESA

07

DATA PROCESSING AND DISTRIBUTION SYSTEMS

Includes film processing, computer technology, satellite and aircraft hardware, and imagery.

A87-20683

SPOT DATA DISTRIBUTION

PAUL ARCHER (Nigel Press Associates, Edenbridge, England) Spaceflight (ISSN 0038-6340), vol. 28, Sept.-Oct. 1986, p. 362-364.

The French Spot satellite, launched in February 1986 to provide the first remote sensing on a commercial basis, is discussed. Program requests from clients to acquire data according to specified parameters are received and evaluated for feasibility. Urgent requests can be programmed within three to eight hours. Other applications of Spot include a global Systematic Surveying program carried out with reference to 181 homogeneous climate zones. A computerized catalogue system maintains an inventory of all images received.
R.R.

A87-20768

ILLUSTRATION OF THE INFLUENCE OF SHADOWING ON HIGH LATITUDE INFORMATION DERIVED FROM SATELLITE IMAGERY

K. MCGUFFIE and A. HENDERSON-SELLERS (Liverpool, University, England) International Journal of Remote Sensing (ISSN 0143-1161), vol. 7, Oct. 1986, p. 1359-1365. refs

Two separate types of contamination by shadowing have been identified following an analysis of two Thematic Mapper scenes from the Arctic. The well-established effect of orographic shadowing is particularly important for cryospheric surfaces. Cirrus clouds, often very difficult to identify by automated techniques, also cast shadows which decrease the radiances detected from snow and ice surfaces. These effects are illustrated here in relation to snow mapping algorithms.
Author

A87-21095

EXPLOITATION OF THE SPOT SYSTEM

G. CALHES (CNES, Toulouse, France) and Y. TREMPAT (SPOT Image, S.A.; CNES, Toulouse, France) Geocarto International, no. 3, 1986, p. 15-23.

After briefly describing the organizational structure, the paper describes the different components of the SPOT ground system, which include the Mission and Operations Control Center in charge

of controlling all the exploitation operations, the Space Imagery Receiving Station which collects the raw data from the satellite telemetry, and the Space Imagery Rectification Center, which performs the preprocessing of these data into the standard products to be offered to the customers. Indications are given regarding the capacity of the system in terms of the number of images which it can acquire and process per year and per receiving station, as a function of their latitude.
Author

A87-23348* National Environmental Satellite Service, Madison, Wis.

VERIFICATION OF SMALL-SCALE WATER VAPOR FEATURES IN VAS IMAGERY USING HIGH RESOLUTION MAMS IMAGERY

PAUL W. MENZEL (NOAA, National Environmental Satellite, Data, and Information Service, Madison, WI), GARY JEDLOVEC (Cooperative Institute for Meteorological Satellite Studies, Madison, WI), and GREGORY WILSON (NASA, Marshall Space Flight Center, Huntsville, AL) IN: Conference on Satellite Meteorology/Remote Sensing and Applications, 2nd, Williamsburg, VA, May 13-16, 1986, Preprints. Boston, MA, American Meteorological Society, 1986, p. 108-113. NASA-supported research.

The Multispectral Atmospheric Mapping Sensor (MAMS), a modification of NASA's Airborne Thematic Mapper, is described, and radiances from the MAMS and the VISSR Atmospheric Sounder (VAS) are compared which were collected simultaneously on May 18, 1985. Thermal emission from the earth atmosphere system in eight visible and three infrared spectral bands (12.3, 11.2 and 6.5 microns) are measured by the MAMS at up to 50 m horizontal resolution, and the infrared bands are similar to three of the VAS infrared bands. Similar radiometric performance was found for the two systems, though the MAMS showed somewhat less attenuation from water vapor than VAS because its spectral bands are shifted to shorter wavelengths away from the absorption band center.
R.R.

A87-23784

COMPOSITE/PROGRESSIVE SAMPLING - A PROGRAM PACKAGE FOR COMPUTER SUPPORTED COLLECTION OF DTM DATA

K. TEMPFLI (International Institute for Aerial Survey and Earth Sciences, Enschede, Netherlands) IN: American Congress on Surveying and Mapping and American Society for Photogrammetry and Remote Sensing, Annual Convention, Washington, DC, Mar. 16-21, 1986, Technical Papers. Volume 4. Falls Church, VA, American Congress on Surveying and Mapping and American Society for Photogrammetry and Remote Sensing, 1986, p. 202-209. refs

Composite sampling, which unifies selective sampling and progressive sampling, is a method of photogrammetric data collection for digital terrain models, especially for large scale applications. Distinct terrain surface features are selected and digitized with manual control. These 'skeleton data' are utilized in the second step where an incomplete grid is measured with semiautomatic control. The grid density is progressively adapted to the variations in terrain relief. Initial coarse sampling is followed by data analysis in near real-time, which permits synthesis for finer sampling. After numerous performance studies on the prototype system, which was built at ITC around a computer-supported analog instrument, a program package was developed which is presently operational on the Kern DSR analytical plotters. The paper outlines data collection by selective and progressive sampling and conditioning of data for further use. Characteristics of composite sampling with respect to efficiency of the process and quality of the data are indicated.
Author

A87-23785

DIGITAL IMAGE MATCHING TECHNIQUES FOR STANDARD PHOTOGRAMMETRIC APPLICATIONS

WOLFGANG FOERSTNER (Stuttgart, Universitaet, West Germany) IN: American Congress on Surveying and Mapping and American Society for Photogrammetry and Remote Sensing, Annual Convention, Washington, DC, Mar. 16-21, 1986, Technical Papers. Volume 4 . Falls Church, VA, American Congress on Surveying and Mapping and American Society for Photogrammetry and Remote Sensing, 1986, p. 210-219. refs

The paper presents digital image matching techniques for standard applications in photogrammetry, such as aerial triangulation, orthophotomapping or data acquisition for digital surface models. The properties of feature based algorithms for computational stereo are discussed. They consist of three steps: (1) selecting appropriate features in the images, as corners, edges, dark or light spots, using an interest operator; (2) finding corresponding points in the images using a matching procedure, leading to three-dimensional-coordinates of points in object space; and (3) interpolation between these points based on a mathematical model of the surface. This concept, being standard in nonphotogrammetric stereo vision systems contrasts to gray level based correlation techniques and profile-oriented or grid-oriented data acquisition methods common in photogrammetry. The paper shows that the methods can be applied for point transfer in aerial triangulation and high precision measurement of digital surface models, especially if one uses an analytical plotter extended by digital cameras. Empirical tests demonstrate that the accuracy obtained with computational stereo is comparable to that reached by the human operator allowing a practical implementation of the methods in the near future. Author

A87-23787

THE PRODUCTION OF ORTHOPHOGRAPHS BY DIGITAL IMAGE PROCESSING TECHNIQUES

LEONARD GAYDOS, LYMAN LADNER, RICHARD CHAMPION, and DAVID HOOPER (USGS, Menlo Park, CA) IN: American Congress on Surveying and Mapping and American Society for Photogrammetry and Remote Sensing, Annual Convention, Washington, DC, Mar. 16-21, 1986, Technical Papers. Volume 4 . Falls Church, VA, American Congress on Surveying and Mapping and American Society for Photogrammetry and Remote Sensing, 1986, p. 241-249. refs

A method for rectifying an aerial photograph using completely digital techniques has been developed. A digital image created by scanning an aerial photograph using a microdensitometer and a digital elevation model of the same area are used as input to the process that rectifies the photograph in two major steps, one operating on 30-m digital elevation model cells and one operating on individual image pixels. The resulting rectified digital image shows promise for a number of applications. New photographs taken over an area in need of map revision could be rectified first, then interpreted using digital image processing software and interactive display hardware. Image processing could also be applied to the data to create customized orthophotographs to enhance features of interest to scientists or resource managers. Author

A87-23788

ACCURATE DETERMINATION OF ELLIPSE CENTERS IN DIGITAL IMAGERY

GUOPING ZHOU (Kern Instruments, Inc., Brewster, NY) IN: American Congress on Surveying and Mapping and American Society for Photogrammetry and Remote Sensing, Annual Convention, Washington, DC, Mar. 16-21, 1986, Technical Papers. Volume 4 . Falls Church, VA, American Congress on Surveying and Mapping and American Society for Photogrammetry and Remote Sensing, 1986, p. 256-264. refs

An algorithm has been developed to determine the coordinates of the center of an ellipse to the accuracy of a few hundredths of a pixel. A bright ellipse surrounded by a dark background can be considered to consist of a number of rectangular pulses when the image is scanned along the row or column directions. Each pulse

is formed by two steps in the opposite directions, and the edge location of each step can be accurately calculated to a subpixel value by using the moment preservation method. Theoretically, the midpoint between the two edge locations for pulses along the same scanning direction should fall in a diameter. The diameters, which cross pulse midpoints along two scan directions respectively, can be determined by least square fitting, and their intersection is the center of the ellipse. For noisy images, median filtering can be applied to the individual pulse before the edge location is found. Errors, using this method, tested with a large number of simulated ellipses, were less than 0.05 pixels. Author

A87-23790

THE DATA DILEMMA - HOW TO PROPERLY CONSTRUCT AND UTILIZE AERIAL PHOTO VOLUME TABLES

JAMES SMITH, MARY BLEIER, and RICHARD ODERWALD (Virginia Polytechnic Institute and State University, Blacksburg) IN: American Congress on Surveying and Mapping and American Society for Photogrammetry and Remote Sensing, Annual Convention, Washington, DC, Mar. 16-21, 1986, Technical Papers. Volume 4 . Falls Church, VA, American Congress on Surveying and Mapping and American Society for Photogrammetry and Remote Sensing, 1986, p. 286-293. refs

A persistent problem in the development and application of aerial photo volume tables has been the need to choose between ground and photo measured data in table construction. Certain statistical assumptions have led to the common belief that ground measured information is the only valid choice. This contention was empirically examined for a previously published data set, and some surprising results were discovered. Bias and precision of stand alone volume predictions from aerial photography were indeed affected by the type of data used, but not necessarily in the manner expected. Practical recommendations for developing and utilizing aerial photo volume tables in a statistically valid manner are presented. Author

A87-23791

AN INFORMATION PROCESSING SYSTEM FOR INTEGRATION OF DATA FROM REMOTE SENSORS, AERIAL PHOTOGRAPHS AND EXISTING MAPS

BELUR V. DASARATHY (Intergraph Corp., Huntsville, AL) IN: American Congress on Surveying and Mapping and American Society for Photogrammetry and Remote Sensing, Annual Convention, Washington, DC, Mar. 16-21, 1986, Technical Papers. Volume 4 . Falls Church, VA, American Congress on Surveying and Mapping and American Society for Photogrammetry and Remote Sensing, 1986, p. 294-302.

A composite image and graphics display/processing system is described which integrates into a common image data base data obtained from different sources. Data from aerial photographs and existing hard copy sources are converted to digital form via monochromatic or color scanning using optical scanners. Spectral and processing tools permit matching, scaling, and aligning of the data from different sources, facilitating the integration of newly acquired information with prior information in the form of hard copy maps. The integrated raster and vector domain capabilities enhance the ease of performing change detection and update of the relevant data base. Operations such as rectification, spectral normalization and feathering are also possible. R.R.

A87-23793

CAPABILITIES FOR SOURCE ASSESSMENT

JOHN A. KEARNEY and JAMES R. MULLER (Synectics Corp., Rome, NY) IN: American Congress on Surveying and Mapping and American Society for Photogrammetry and Remote Sensing, Annual Convention, Washington, DC, Mar. 16-21, 1986, Technical Papers. Volume 4 . Falls Church, VA, American Congress on Surveying and Mapping and American Society for Photogrammetry and Remote Sensing, 1986, p. 324-333. (Contract F30602-82-C-0148)

The capabilities of the Source Assessment System for examining and evaluating imagery and/or cartographic source material for the production of cartographic products, are discussed.

The system includes formatted textual data entry, extensive error checking, and viewing capabilities such as real-time video and digital modes, and a roam/zoom function. Gray scale, color, and pseudocolor display enhancements are discussed, and the use of split screen, superposition, and graphic overlay, facilitate visual comparison and change detection. Data entry capabilities include both soft copy graphic data for entering feature attributes, and textual data entry to provide descriptive information. Output capabilities include reports, hard copy graphics and digital data files. R.R.

A87-23795

CLASSIFICATION OF MULTIDATE THEMATIC MAPPER DATA

MICHAEL W. SNYDER and MICHAEL H. STORY (Science Applications Research, Lanham, MD) IN: American Congress on Surveying and Mapping and American Society for Photogrammetry and Remote Sensing, Annual Convention, Washington, DC, Mar. 16-21, 1986, Technical Papers. Volume 4 . Falls Church, VA, American Congress on Surveying and Mapping and American Society for Photogrammetry and Remote Sensing, 1986, p. 360-369. refs

Five level II land cover classifications of Thematic Mapper data were compared. Three of these classifications used single dates: March, July, and November, and two used the combination of all three dates. One of the combined date images was reduced in resolution to 60 M. Each method was classified using the same unsupervised clustering algorithm. Comparing these classifications in terms of accuracy showed that swamp, pasture/grassland, and mixed forest were most accurately identified in March; water, marsh, bare soil, coniferous trees, and clearcut areas were most accurately identified in July; and deciduous trees and cropland were most accurately identified in November. There was no significant difference in accuracy between the full and reduced resolution classifications. Author

A87-23796

THE EFFECT OF TRAINING DATA VARIABILITY ON CLASSIFICATION ACCURACY

MICHAEL H. STORY (Science Applications Research, Lanham, MD) and JAMES B. CAMPBELL (Virginia Polytechnic Institute and State University, Blacksburg) IN: American Congress on Surveying and Mapping and American Society for Photogrammetry and Remote Sensing, Annual Convention, Washington, DC, Mar. 16-21, 1986, Technical Papers. Volume 4 . Falls Church, VA, American Congress on Surveying and Mapping and American Society for Photogrammetry and Remote Sensing, 1986, p. 370-379. refs

The effects of different levels of variance in the training statistics upon the accuracy of digital classifiers are investigated. Four classification algorithms were applied to three digital images using various combinations of spectral classes for training data, and the resulting classifications were digitally compared to a reference image to measure accuracy. When spectral subclasses are combined into land cover classes, it is found that the minimum distance and parallelipiped techniques produced significantly less accurate results, while the Bayesian techniques produced more accurate results. Results also indicate that the Bayesian techniques were more robust than the others when the training data was varied. R.R.

A87-23798

PERFORMANCE OF SELECTED SPATIAL DOMAIN EDGE DETECTION ALGORITHMS FOR EARTH RESOURCES APPLICATION

WILLIAM R. BERGEN, PAUL R. THIES, and FRANK L. SCARPACE (Wisconsin, University, Madison) IN: American Congress on Surveying and Mapping and American Society for Photogrammetry and Remote Sensing, Annual Convention, Washington, DC, Mar. 16-21, 1986, Technical Papers. Volume 4 . Falls Church, VA, American Congress on Surveying and Mapping and American Society for Photogrammetry and Remote Sensing, 1986, p. 388-397. refs

Many spatial edge detection techniques have been developed and attempts have been made to compare their performance.

However, little has been reported which involve spatially complex images. At the Environmental Remote Sensing Center, University of Wisconsin-Madison, a comprehensive comparison of twenty common spatial edge detection algorithms was conducted on an IBM PC-AT microcomputer. The performance of four of the algorithms is discussed with reference to one low noise and two complex earth resource scenes. It was found that some commonly used techniques have questionable utility for earth resource type images and that careful selection and comparison of various window size and weighting function combinations are necessary to achieve optimal results. A possible method for window size selection is described. Author

A87-23800

A COGNITIVE MEASURE OF TEXTURE IN IMAGERY

MICHAEL E. HODGSON and ROBERT E. LLOYD (South Carolina, University, Columbia) IN: American Congress on Surveying and Mapping and American Society for Photogrammetry and Remote Sensing, Annual Convention, Washington, DC, Mar. 16-21, 1986, Technical Papers. Volume 4 . Falls Church, VA, American Congress on Surveying and Mapping and American Society for Photogrammetry and Remote Sensing, 1986, p. 407-416. refs

Texture, the frequency and arrangement of tones in an image, is one of the fundamental features (along with tone, shape context, etc.) used in the visual image interpretation process. Various authors have proposed over 30 quantitative measures of texture in imagery to use in automated pattern recognition procedures. However, it is unknown whether the proposed measures of texture model the photo interpreter's cognitive measure. For artificial intelligence implementations, the need to emulate the interpreter's cognitive response to texture becomes very important. This paper presents a method for measuring the cognitive response to texture in imagery. Ten subimages extracted from digitized panchromatic aerial photography were used in an experiment with subjects to measure the dissimilarities in texture among the subimages. Multidimensional scaling was used to convert the dissimilarity estimates to a configuration of perceived texture measurements along a single dimension. A number of the previously proposed quantitative measures of texture were then compared to the cognitive measures. Author

A87-23802

PHOTOMETRIC FUNCTIONS, REFLECTANCE MAP - TWO TECHNIQUES FOR DETERMINING SURFACE SHAPE AND ORIENTATION FROM IMAGE INTENSITY

KHALEEL IBRAHEM JASSEM and JAMES P. SCHERZ (Wisconsin, University, Madison) IN: American Congress on Surveying and Mapping and American Society for Photogrammetry and Remote Sensing, Annual Convention, Washington, DC, Mar. 16-21, 1986, Technical Papers. Volume 4 . Falls Church, VA, American Congress on Surveying and Mapping and American Society for Photogrammetry and Remote Sensing, 1986, p. 427-434. refs

Photometric function is a technique using image intensity as a means to obtain slope of a surface from a single photograph. The backbone theory of the technique is that the reflected light intensity from a surface is a function of the surface shape and orientation. The idea was first introduced in the late fifties to map part of the lunar surface. That was the first and the last attempt to use such a method for mapping purposes. In the mid-seventies, Horn (1975) introduced the idea of using a reflectance map to obtain shapes from its shadow. This paper presents the concepts of both photometric function and reflectance maps and their potential applications as well as the possibility of modifying them for mapping purposes. Author

A87-23805* National Aeronautics and Space Administration. Goddard Space Flight Center, Greenbelt, Md.

POLYSITE - AN INTERACTIVE PACKAGE FOR THE SELECTION AND REFINEMENT OF LANDSAT IMAGE TRAINING SITES

MARILYN J. P. MACK (NASA, Goddard Space Flight Center, Greenbelt, MD) IN: American Congress on Surveying and Mapping and American Society for Photogrammetry and Remote Sensing, Annual Convention, Washington, DC, Mar. 16-21, 1986, Technical Papers. Volume 4 . Falls Church, VA, American Congress on Surveying and Mapping and American Society for Photogrammetry and Remote Sensing, 1986, p. 466-475. refs

A versatile multifunction package, POLYSITE, developed for Goddard's Land Analysis System, is described which simplifies the process of interactively selecting and correcting the sites used to study Landsat TM and MSS images. Image switching between the zoomed and nonzoomed image, color and shape cursor change and location display, and bit plane erase or color change, are global functions which are active at all times. Local functions possibly include manipulation of intensive study areas, new site definition, mensuration, and new image copying. The program is illustrated with the example of a full TM maser scene of metropolitan Washington, DC. R.R.

A87-23809
CARTOGRAPHIC ANALYSIS OF REMOTE SENSING DATA THROUGH LANDSAT MOSAIC SCALING

A. A. NAVARRO (Gabun-Paracale Mining Co., Inc., Manila, Philippines) IN: American Congress on Surveying and Mapping and American Society for Photogrammetry and Remote Sensing, Annual Convention, Washington, DC, Mar. 16-21, 1986, Technical Papers. Volume 4 . Falls Church, VA, American Congress on Surveying and Mapping and American Society for Photogrammetry and Remote Sensing, 1986, p. 511-519.

The use of Landsat controlled mosaics for ratioing and rectification is discussed, and it is suggested that both controlled and uncontrolled photomosaics are valuable tools for mineral resource inventory, analysis and monitoring. It is suggested that the use of radar mosaics will be enhanced by the mass production of mosaics at a scale of 1:250,000 and by the combined usage of ERTS-1 and radar flight strips. A formulation for the relationship between swath width, depression angle, and height above terrain is derived. R.R.

A87-23827* Vexcel Corp., Boulder, Colo.

SPACE SHUTTLE RADARGRAMMETRY RESULTS

F. LEBERL, G. DOMIK (Vexcel Corp., Boulder, CO), J. RAGGAM (Graz, Universitaet, Austria), J. CIMINO, and M. KOBRICK (California Institute of Technology, Jet Propulsion Laboratory, Pasadena) IN: American Congress on Surveying and Mapping and American Society for Photogrammetry and Remote Sensing, Annual Convention, Washington, DC, Mar. 16-21, 1986, Technical Papers. Volume 5 . Falls Church, VA, American Congress on Surveying and Mapping and American Society for Photogrammetry and Remote Sensing, 1986, p. 198-201; Abridged. Research supported by Vexcel Corp. refs (Contract NAS7-100)

Preliminary results on the radargrammetric processing of SIR-A and SIR-B data are presented. Radargrammetric processing was applied to images of the Trinity National Forest in Northern California, the islands of Cephalonia, Ithaka, and Sardegna, Mt. Shasta, and Cordón La Grasa, Argentina. The preliminary processing of the SIR-A and SIR-B data has produced digital elevation models, stereo models, and a contour map. I.F.

A87-24542
ATLAS OF GEO-SCIENCE ANALYSES OF LANDSAT IMAGERY IN CHINA

SHUPENG CHEN, ED. (Chinese Academy of Sciences, Institute of Geography; National Remote Sensing Center, Beijing, People's Republic of China) Beijing, Science Press, 1986, 234 p. No individual items are abstracted in this volume.

The atlas contains Landsat MSS images of China's surface obtained during 1975-1978 as well as illustrations and explanations

revealing the information bearing capability of Landsat imagery. Topics include land cover and land use, hydrological dynamical phenomena, the regional characteristics of landform, and the lineaments of geological structures. A reference map of China is also provided. K.K.

A87-25249
THE USE OF SPACE PHOTOGRAPHY TO CREATE AND RENEW SMALL-SCALE MAPS [ISPOL'ZOVANIE KOSMICHESKOI FOTOS'EMKI DLIA SOZDANIIA I OBNOVLENIIA MELKOMASSHTABNYKH KART]

L. K. ZATONSKII Geodeziia i Kartografiia (ISSN 0016-7126), Aug. 1986, p. 29-33. In Russian. refs

A87-25587
EFFECT OF SURFACE PROPERTIES ON THE NARROW TO BROADBAND SPECTRAL RELATIONSHIP IN CLEAR SKY SATELLITE OBSERVATIONS

R. T. PINKER and J. A. EWING (Maryland, University, College Park) Remote Sensing of Environment (ISSN 0034-4257), vol. 20, Dec. 1986, p. 267-282. refs (Contract NOAA-NA-84AAH00026)

Several computational experiments have been conducted to estimate the difference between clear sky spectral narrowband (0.5-0.7 microns) and broadband (0.3-2.5 microns) planetary albedo for three cases of wavelength-independent surface albedo and four cases of surface wavelength-dependent (snow, dry sand, meadow, water) albedo. The spectral interval of (0.5-0.7 microns) was selected to approximate the bulk of the VISSR visible channel on the GOES satellites and Channel 1 of the AVHRR on the NOAA operational satellites. Different atmospheric conditions and solar zenith angles have been simulated. It was demonstrated that the relationship between the spectral narrowband and broadband planetary albedo depends primarily on the assumptions made about the magnitude and wavelength dependence of the surface albedo and less on the atmospheric conditions. Future attempts to parametrize the conversion from narrowband to broadband spectral observations should account for the surface type. Author

A87-26540
METHOD FOR COMPUTING THE PERIODICITY OF A REMOTE-SENSING SURVEY [METODIKA RASCHETA PERIODICHNOSTI OBZORA, OSUSHCHESTVIAEMOGO SISTEIMO IPRZ]

V. K. SAULSKII Issledovanie Zemli iz Kosmosa (ISSN 0205-9614), Sept.-Oct. 1986, p. 103-112. In Russian.

A method is presented for calculating the effective periodicity of a survey of an earth surface zone by a system of satellites making observations on both the sunlit and the shaded side of the earth. The method consists of computer-aided sequential construction of multisatellite charts, using a system of vector equations. The method can be applied to complex satellite systems with as many as 100 satellites. I.S.

A87-29430
SPOT IMAGE AND COMMERCIALISATION OF REMOTE SENSING DATA

GERARD BRACHET (SPOT IMAGE, Toulouse, France) IN: Space commerce '86; Proceedings of the International Conference and Exhibition on the Commercial and Industrial Uses of Outer Space, Montreux, Switzerland, June 16-20, 1986 . Geneva, Interavia Publishing Group, 1986, p. 360-363.

The early operational performance of the SPOT satellite and its image distribution system are summarized. SPOT was injected into an 832 km circular orbit on Feb. 22, 1986 and began transmitting pictures the first day. Operational checkouts were completed by the end of April and by June 60,000 images had been transmitted for storage and distribution by SPOT IMAGE, a government/private company. The images are also distributed through contracting agencies in over 40 countries, and six countries have contracted for direct reception of SPOT images. The main applications thus far have been land use surveying and monitoring.

A second, identical SPOT satellite will be launched in either 1987 or 1988. Improvements planned for the SPOT 3 and 4 satellites are discussed briefly. M.S.K.

A87-29499
A COMPARATIVE TEST OF PHOTOGRAMMETRICALLY SAMPLED DIGITAL ELEVATION MODELS

KENNERT TORLEGARD, ANDERS OSTMAN, and RALF LINDGREN (Kungl. Tekniska Hogskolan, Stockholm, Sweden) *Photogrammetria* (ISSN 0031-8663), vol. 41, Oct. 1986, p. 1-16.

Results are presented from tests comparing the techniques and accuracy of several digital terrain elevation models. The studies covered the relationships among the methods of sampling, the features of the approximation function for the elevations, and the accuracy of elevations derived with the respective digital elevation models (DEM). The DEMs were tested using data from two sets of aerial photographs of farmland, rugged granite bedrock, forests, urban areas, steep and rugged mountains, hills of moderate height, and smooth terrain. Ground truth data were used to validate the DEM projections. The tests revealed standard error factors of 0.2-0.4 per mile in flying height over level terrain, increasing to about 1-2 per mile in hilly terrain. The percentage of errors in the DEMs tested was around 0.5 percent. The photogrammetrists queried were found to understate the error bounds of the projections. M.S.K.

A87-30127
TERRAIN ANALYSIS FROM DIGITAL PATTERNS IN GEOMORPHOMETRY AND LANDSAT MSS SPECTRAL RESPONSE

STEVEN E. FRANKLIN (Newfoundland, Memorial University, Saint John's, Canada) *Photogrammetric Engineering and Remote Sensing* (ISSN 0099-1112), vol. 53, Jan. 1987, p. 59-65. refs (Contract NSERC-A-8454)

Digital Landsat multispectral images are used with elevation model variables in high relief terrain analysis. An integrated terrain map from conventional photomorphometric methods (based on aerial photointerpretation) is compared with the results of digital processing methods. The objective is to show that there will be a reasonable correspondence between the analogue and digital mappings, and that digital data and methods offer significant advantages in terms of survey reliability, accuracy, and repeatability. Digital patterns in spectral response and geomorphometry are shown to capture those attributes of the surface necessary for classification of landscape units. Classification of the MSS digital patterns showed up to 46 percent agreement with photomorphometric survey methods. Agreement rose up to 75 percent as the MSS data were augmented with the geomorphometric patterns. Maps produced using this enhanced discrimination technique are 70 percent accurate when the classes are weighted by area and compared to the photointerpretation on a pixel-by-pixel basis at field-checked test areas. Greater overall interpretation accuracy might have been obtained with more precise digital class description, greater rigor in the conventional survey, or both.

Author

N87-15590# Centre de Developpement des Techniques Avancees, Alger-Gare (Algeria).

THE FUNDAMENTAL PROBLEMS FOR THE ENERGY BALANCE STUDY BY SATELLITE IMAGERY

A. ABDELLAOUI *In* ESA Proceedings of an International Satellite Land-Surface Climatology Project (ISLSCP) Conference p 335-338 May 1986

Avail: NTIS HC A99/MF A01

Models for studying the energy balance at the soil-atmosphere interface are reviewed. Problems to be solved for their application at a regional scale include expression of the dynamic resistances, combination of climatological measurements with satellite data, significance of the output parameters, and using the different scales for the input data. Solutions to problems concerning climatological parameters and the spatial extension of models are outlined.

ESA

N87-15625# Centre National de la Recherche Scientifique, Strasbourg (France). Groupement Scientifique de Teledetection Spatiale.

DESIGN OF A DATA BASE SYSTEM FOR INFERRING LAND SURFACE PARAMETERS AND FLUXES FROM SATELLITE RADIANCES

L. ASFAR (IBM France S. A., Paris), A. ASEM (IBM France S. A., Paris), F. BECKER, P. Y. DESCHAMPS (Centre National d'Etudes Spatiales, Toulouse, France), P. DEFRAIPONT, D. HO (IBM France S. A., Paris), J. L. MERCIER, E. OLORY-HECHINGER, P. OLORY (IBM France S. A., Paris), M. RAFFY et al. *In* ESA Proceedings of an International Satellite Land-Surface Climatology Project (ISLSCP) Conference p 541-548 May 1986 Sponsored by CNRS, CNES, and IBM

Avail: NTIS HC A99/MF A01

A data base system which handles as automatically as possible the satellite images and necessary input data used to study time and space variations of climate processes was designed. The general scheme to infer latent and sensible heat fluxes, ground fluxes, and thermal inertia includes calibration, atmospheric corrections, navigation (geometric corrections) and the models which lead to the requested land surface parameters and fluxes from relocated and renormalized radiances. ESA

N87-16388# Army Engineer Topographic Labs., Fort Belvoir, Va.

SPARSE AREA STEREO MATCHING EXPERIMENT

MICHAEL A. CROMBIE Jul. 1986 34 p (AD-A173601; ETL-0424) Avail: NTIS HC A03/MF A01 CSCL 08B

The algorithm used in this experiment is considered by many to be state-of-the-art for calculating x-parallax over rural regions. Even so, its output must be refined in sparse areas in order to meet accuracy requirements. The major result of this experiment showed that x-parallax should be measured from digital imagery containing no more than 10 lone pairs per millimeter. The objective of this report is to find ways to improve the output of the X-parallax front-end processor without using information from other front-end processors, and without drastically revising the algorithm. Two approaches were tested, namely to provide to the processor image data most suitable for rural type matching and to use similar yet less demanding procedures in difficult areas. In the first case, stereo matching was performed with digital pictures containing up to 10 lp/mm of information, and in the second case large correlation windows were used on difficult points. The latter approach was performed with another DIAL program designed to measure corresponding points in a pass point mode. GRA

N87-16963# Centre National d'Etudes Spatiales, Toulouse (France). Radar Dept.

VARAN-S RADAR IMAGE INTERPRETATION

N. LANNELONGUE 30 Aug. 1986 8 p (CNES-CT/DRT/TIT/RL-54-T; ETN-87-98806) Avail: NTIS HC A02/MF A01

Images taken by the VARAN-S side-looking airborne radar were interpreted. During an Arctic campaign a set of data was collected using the VARAN-S. An image covering a 15 km x 24 km zone is presented with a classification of 6 classes. The interpretation is preliminary but seems very promising to obtain quantitative data in an operational way with ERS. ESA

N87-17116*# Jet Propulsion Lab., California Inst. of Tech., Pasadena. Geology Group.

ENHANCEMENT OF TIME IMAGES FOR PHOTINTERPRETATION

A. R. GILLESPIE *In* its The TIMS Data User's Workshop p 12-24 1 Nov. 1986

Avail: NTIS HC A05/MF A01 CSCL 14E

The Thermal Infrared Multispectral Scanner (TIMS) images consist of six channels of data acquired in bands between 8 and 12 microns, thus they contain information about both temperature and emittance. Scene temperatures are controlled by reflectivity of the surface, but also by its geometry with respect to the Sun,

time of day, and other factors unrelated to composition. Emittance is dependent upon composition alone. Thus the photointerpreter may wish to enhance emittance information selectively. Because thermal emittances in real scenes vary but little, image data tend to be highly correlated along channels. Special image processing is required to make this information available for the photointerpreter. Processing includes noise removal, construction of model emittance images, and construction of false-color pictures enhanced by decorrelation techniques. Author

N87-17131*# Jet Propulsion Lab., California Inst. of Tech., Pasadena.

CALCULATION OF DAY AND NIGHT EMITTANCE VALUES

ANNE B. KAHLE *In its* The TIMS Data User's Workshop p 67-70 1 Nov. 1986

Avail: NTIS HC A05/MF A01 CSCL 04A

In July 1983, the Thermal Infrared Multispectral Scanner (TIMS) was flown over Death Valley, California on both a midday and predawn flight within a two-day period. The availability of calibrated digital data permitted the calculation of day and night surface temperature and surface spectral emittance. Image processing of the data included panorama correction and calibration to radiance using the on-board black bodies and the measured spectral response of each channel. Scene-dependent isolated-point noise due to bit drops, was located by its relatively discontinuous values and replaced by the average of the surrounding data values. A method was developed in order to separate the spectral and temperature information contained in the TIMS data. Night and day data sets were processed. The TIMS is unique in allowing collection of both spectral emittance and thermal information in digital format with the same airborne scanner. For the first time it was possible to produce day and night emittance images of the same area, coregistered. These data add to an understanding of the physical basis for the discrimination of difference in surface materials afforded by TIMS. Author

N87-17135*# Jet Propulsion Lab., California Inst. of Tech., Pasadena.

THE SECOND SPACEBORNE IMAGING RADAR SYMPOSIUM

1 Dec. 1986 223 p Symposium held in Pasadena, Calif., 28-30 Apr. 1986

(Contract NAS7-918)

(NASA-CR-180131; JPL-PUB-86-26; NAS 1.26:180131) Avail: NTIS HC A10/MF A01 CSCL 05B

Summaries of the papers presented at the Second Spaceborne Imaging Radar Symposium are presented. The purpose of the symposium was to present an overview of recent developments in the different scientific and technological fields related to spaceborne imaging radars and to present future international plans.

N87-17159*# New South Wales Univ., Kensington (Australia). Centre for Remote Sensing.

RADAR SIGNATURE DETERMINATION: TRENDS AND LIMITATIONS

J. A. RICHARDS *In* JPL The Second Spaceborne Imaging Radar Symposium p 184-190 1 Dec. 1986

Avail: NTIS HC A10/MF A01 CSCL 17I

Modelling studies, as means for assessing what could be called radar signatures, are a part of two radar remote sensing research programs with which the author is affiliated. First, at the University of New South Wales, assessment of SIR-B data is being undertaken for a number of purposes including its value in arid land geomorphological and geological studies, forest and crop assessment, and mapping. A number of early results have been reported, however modelling aspects are still at an early stage. Secondly, the author recently spent 6 months working on SIR-B invertible forest canopy modelling in the Department of Geography at the University of California, Santa Barbara. Results from this work are outlined. Author

N87-17164# Michigan Univ., Ann Arbor. Inst. of Environmental Research.

COMPONENTS AND COMPARISONS OF POTENTIAL INFORMATION FROM SEVERAL IMAGING SATELLITES

A. MALILA *In* ESA Proceedings of the 1986 International Geoscience and Remote Sensing Symposium (IGARSS '86) on Remote Sensing: Today's Solutions for Tomorrow's Information Needs, Volume 1 p 3-8 Aug. 1986

Avail: NTIS HC A99/MF E03; ESA, Paris, France, 3 volume set \$90 Member States, AU, CN, and NO (+20% others)

An approach for measuring and comparing the potential information content of multispectral image data, based on sensor system specifications is developed. The method extends beyond the spectral and spatial domains to include the temporal domain, and adds a measure of the information in spatial registration. The total potential information of LANDSAT Thematic Mapper data is found to be the greatest of the systems analyzed, and that of the geostationary Visible Infrared Spin Scan Radiometer (VISSR) the least. Polar-orbiting Advanced Very High Resolution Radiometer (AVHRR) and Coastal Zone Color Scanner (CZCS) meteorological systems with wide-angle coverage, moderate spatial resolution, and five or six spectral bands rank below the TM but above the LANDSAT MSS and SPOT HRV which are comparable to each other. ESA

N87-17172# Institut Geographique National, Paris (France).

MONITORING OF LARGE PHENOMENA IN DEVELOPING COUNTRIES THROUGH SATELLITE IMAGERY

L. GUYOT *In* ESA Proceedings of the 1986 International Geoscience and Remote Sensing Symposium (IGARSS '86) on Remote Sensing: Today's Solutions for Tomorrow's Information Needs, Volume 1 p 49-51 Aug. 1986

Avail: NTIS HC A99/MF E03; ESA, Paris, France, 3 volume set \$90 Member States, AU, CN, and NO (+20% others)

Inter-annual comparisons between satellite images showing the effects of slowly evolving phenomena such as forest degradation or desert spreading, and intra-annual comparisons between images showing the flooding conditions over large areas are discussed. Trampling and overgrazing around a borehole, and monitoring of Niger river throughout a flooding season are described. ESA

N87-17174# Zurich Univ. (Switzerland). Dept. of Geography.

SRI LANKA'S SOLUTION TO LAND USE MAPPING AND MONITORING FOR THIRD WORLD COUNTRIES DEVELOPMENT

K. I. ITTEN, S. D. F. C. NANAYAKKARA (Center for Remote Sensing, Colombo, Sri Lanka), H. S. JAYATILAKA, M. BICHSEL, G. SCHNEIDER, and R. HEUMBEL *In* ESA Proceedings of the 1986 International Geoscience and Remote Sensing Symposium (IGARSS '86) on Remote Sensing: Today's Solutions for Tomorrow's Information Needs, Volume 1 p 57-61 Aug. 1986

Avail: NTIS HC A99/MF E03; ESA, Paris, France, 3 volume set \$90 Member States, AU, CN, and NO (+20% others)

Airphoto interpretation with digitally corrected and enhanced LANDSAT MSS imagery was used for land use mapping in Sri Lanka in the scale of 1:1,000,000. Thematic masking procedures starting from the single classes from the land use map, result in an easy assessment of per class changes, with newly acquired satellite imagery. Thus inventorying the land use and monitoring its changes have become an operational national task of the Center for Remote Sensing of the Sri Lanka Survey Department. ESA

N87-17176# Software Sciences Ltd., Farnborough (England).

THE DESIGN OF AN INTERNATIONAL DATA CENTRE FOR REMOTE SENSING

D. R. SLOGGETT *In* ESA Proceedings of the 1986 International Geoscience and Remote Sensing Symposium (IGARSS '86) on Remote Sensing: Today's Solutions for Tomorrow's Information Needs, Volume 1 p 67-71 Aug. 1986

Avail: NTIS HC A99/MF E03; ESA, Paris, France, 3 volume set \$90 Member States, AU, CN, and NO (+20% others)

An architecture for a worldwide infrastructure to enable effective research, commercial, and national exploitation of remote sensing

data is presented. A modular approach that caters to the needs of many different countries and application areas relevant to those countries is envisaged. The work being conducted in the UK to set up a national infrastructure forms a useful basis for other countries to work from as a baseline. The concept requires work to provide a worldwide infrastructure for monitoring all aspects of the environment, and the effects of mankind and nature upon our world. ESA

N87-17203# Stanford Univ., Calif. Dept. of Applied Earth Science.

A KNOWLEDGE-BASED SOFTWARE ENVIRONMENT FOR THE ANALYSIS OF SPECTRORADIOMETER DATA

H. R. GOETTING and R. J. P. LYON /In ESA Proceedings of the 1986 International Geoscience and Remote Sensing Symposium (IGARSS '86) on Remote Sensing: Today's Solutions for Tomorrow's Information Needs, Volume 1 p 235-238 Aug. 1986

Avail: NTIS HC A99/MF E03; ESA, Paris, France, 3 volume set \$90 Member States, AU, CN, and NO (+20% others)

A mineral identification expert system for the interpretation of symbolic features extracted from numerical data by sequential heuristic classification is described. Solutions for a given classification become data for the next classification step. In this way the expert system is used to merge numerical data with (symbolic) knowledge. The prototype expert system distinguishes between various spectral features in mineral samples by interpreting waveforms from a spectroradiometer. ESA

N87-17206# Flinders Univ., Bedford Park (Australia). Dept. of Environment and Planning.

THE FRS-68010: A NEW CONCEPT FOR THE ACQUISITION AND ANALYSIS OF NOAA HRPT DATA

M. WEGENER /In ESA Proceedings of the 1986 International Geoscience and Remote Sensing Symposium (IGARSS '86) on Remote Sensing: Today's Solutions for Tomorrow's Information Needs, Volume 1 p 253-258 Aug. 1986

Avail: NTIS HC A99/MF E03; ESA, Paris, France, 3 volume set \$90 Member States, AU, CN, and NO (+20% others)

A concept for a NOAA ground station using an array of yagis instead of tracking antennas is presented. This inexpensive antenna configuration guarantees a sufficient signal to noise ratio for the reliable acquisition of HRPT data of the South Australian coastal waters between 32-36 S and 134-141 E. Data processing is performed by a microprocessor system based on the Motorola 68010. Due to the software being written in C and assembly language, basic image processing operations can be performed in 1 sec. Part of the FRS-68010 is a video display processor storing 4 images of 576 by 448 pixels. The image format is reconfigurable by software yielding up to 64 smaller images which can be represented as a loop movie. ESA

N87-17207# Instituto Nacional de Meteorologia e Geofisica, Lisbon (Portugal).

DIGITAL SATELLITE IMAGERY ACQUISITION AND PROCESSING

R. ALMEIDA, I. GOMES, L. PESSANHA, and C. TAVARES /In ESA Proceedings of the 1986 International Geoscience and Remote Sensing Symposium (IGARSS '86) on Remote Sensing: Today's Solutions for Tomorrow's Information Needs, Volume 1 p 259-263 Aug. 1986

Avail: NTIS HC A99/MF E03; ESA, Paris, France, 3 volume set \$90 Member States, AU, CN, and NO (+20% others)

The equipment and organization of a satellite imagery ground station are described. Research concerning calibration, IR radiance to temperature conversion, normalization of VIS image data, geometric corrections, pseudocolor table generation, image enhancement, and classification is summarized. ESA

N87-17211# Analytic Sciences Corp., Reading, Mass.
EXTRACTING SURFACE FEATURES IN MULTISPECTRAL IMAGERY

M. J. CARLOTTO /In ESA Proceedings of the 1986 International Geoscience and Remote Sensing Symposium (IGARSS '86) on Remote Sensing: Today's Solutions for Tomorrow's Information Needs, Volume 1 p 283-288 Aug. 1986

Avail: NTIS HC A99/MF E03; ESA, Paris, France, 3 volume set \$90 Member States, AU, CN, and NO (+20% others)

A method for recognizing surface features in multispectral imagery is described. First, the surface material composition (SMC) is inferred using a combination of spectral shape and histogram analysis techniques. A symbolic description is then computed in which each connected area in the SMC map is represented by a node in a graph structure. Surface features are represented by a set of constraints over groupings of connected areas (nodes in the graph structure) in the form of rules. Examples illustrating the extraction of selected surface feature classes from LANDSAT Thematic Mapper imagery are included. ESA

N87-17229# Canada Centre for Remote Sensing, Ottawa (Ontario).

CANADIAN PLANS FOR OPERATIONAL DEMONSTRATIONS OF SATELLITE IMAGING RADAR APPLICATIONS

E. LANGHAM, S. PARASHAR, N. DENYER, L. MCNUTT, V. R. SLANEY, R. BROWN, N. FREEMAN, and T. MULLANE (Atmospheric Environment Service, Ottawa, Ontario) /In ESA Proceedings of the 1986 International Geoscience and Remote Sensing Symposium (IGARSS '86) on Remote Sensing: Today's Solutions for Tomorrow's Information Needs, Volume 1 p 405-409 Aug. 1986

Avail: NTIS HC A99/MF E03; ESA, Paris, France, 3 volume set \$90 Member States, AU, CN, and NO (+20% others)

Canadian objectives for the utilization of data from ERS-1, particularly SAR image data, for ocean, ice, and land and resources monitoring are presented. The ERS-1 data will allow suitable preparations and readiness of data handling systems and user capability for exploiting data from Canadian RADARSAT satellite. These efforts will receive support from a radar program based on ground-based and airborne scatterometers, airborne SAR, and data processing and analysis systems. ESA

N87-17239# Vexcell Corp., Boulder, Colo.
USING SECONDARY IMAGE PRODUCTS TO AID IN UNDERSTANDING AND INTERPRETATION OF RADAR IMAGERY

G. DOMIK and F. LEBERL /In ESA Proceedings of the 1986 International Geoscience and Remote Sensing Symposium (IGARSS '86) on Remote Sensing: Today's Solutions for Tomorrow's Information Needs, Volume 1 p 467-468 Aug. 1986 Sponsored by ESA

Avail: NTIS HC A99/MF E03; ESA, Paris, France, 3 volume set \$90 Member States, AU, CN, and NO (+20% others)

Radargrammetric exploitation of radar images as single images, stereo pairs, images combined with collateral data to form multisensor data sets, and as time series was reviewed. Secondary image products (ortho images, stereo ortho images, slope-effect reduced images, simulated radar images, and false color presentations using image products and synergetic data sets) were designed to satisfy the needs to analyze, predict, and extract information from radar images by bringing the original image closer to the investigator. ESA

N87-17245# Arkansas Univ., Fayetteville. Dept. of Electrical Engineering.

HAWAIIAN LAVA FLOWS AND SIR-B RESULTS

B. A. DERRYBERRY, W. P. WAITE, V. H. KAUPP, H. C. MACDONALD, L. R. GADDIS (Hawaii Inst. of Geophysics, Honolulu.), and P. MOUGINIS-MARK *In* ESA Proceedings of the 1986 International Geoscience and Remote Sensing Symposium (IGARSS '86) on Remote Sensing: Today's Solutions for Tomorrow's Information Needs, Volume 1 p 497-501 Aug. 1986

Avail: NTIS HC A99/MF E03; ESA, Paris, France, 3 volume set \$90 Member States, AU, CN, and NO (+20% others)

Analysis of SIR-B data is applied to the estimation of sigma zero for basaltic lava flows, the sea, and tropical rain forest. Aerial photo data, ground truth observations, and surface roughness measurements are included. Empirical and theoretical electromagnetic scattering models for sigma zero are considered, allowing that the radar return may not be limited to a simple surface scattering problem. A relative calibration model for the SIR-B data based upon ancillary information about the sea state around Hawaii is proposed. ESA

N87-17249# Kanazawa Inst. of Tech. (Japan).

BITEMPORAL ANALYSIS OF THEMATIC MAPPER DATA FOR LAND COVER CLASSIFICATION

S. UENO, T. KUSAKA, and Y. KAWATA *In* ESA Proceedings of the 1986 International Geoscience and Remote Sensing Symposium (IGARSS '86) on Remote Sensing: Today's Solutions for Tomorrow's Information Needs, Volume 1 p 523-528 Aug. 1986

(Contract JAP-MIN-OF-ED-60129032)

Avail: NTIS HC A99/MF E03; ESA, Paris, France, 3 volume set \$90 Member States, AU, CN, and NO (+20% others)

Time-sequential analysis of LANDSAT-5 Thematic Mapper (TM) data was performed for diverse land-cover types in Kanazawa area, Takayama district, Japan. The subscene of TM data in the study site covering 800x800 pixels of 25 m span was extracted from the full scene data. After preprocessing, the gray levels in TM data were classified by the Gaussian Maximum Likelihood classifier, allowing for feature selection. The classification procedure was compared for two seasons, i.e., August and October, in terms of the atmospheric reflectance, and the statistical quantities of the gray levels. Results show that atmospheric reflectance is effective for the bitemporal analysis of TM data for land cover classification. ESA

N87-17251# IBM Japan. Tokyo Scientific Center.

EVALUATION OF LANDSAT 5 THEMATIC MAPPING (TM) DATA FOR IMAGE CLUSTERING AND CLASSIFICATION

M. IOKA and M. KODA *In* ESA Proceedings of the 1986 International Geoscience and Remote Sensing Symposium (IGARSS '86) on Remote Sensing: Today's Solutions for Tomorrow's Information Needs, Volume 1 p 535-540 Aug. 1986

Avail: NTIS HC A99/MF E03; ESA, Paris, France, 3 volume set \$90 Member States, AU, CN, and NO (+20% others)

Analysis and evaluation on the quality of the LANDSAT-5 Thematic Mapper (TM) data for multispectral image clustering and classification are performed. Data used is the TM test data of Tokyo metropolitan area (Path-107; Row-035) dated November 4, 1984. Map-precision geometric correction is performed and the TM data are resampled to 30 m pixel spacing. Statistical characteristics of seven TM bands are analyzed, then information content is evaluated based on the clustering and supervised image classification. For routine land-cover classification, a concept of training data file is proposed and generated to assure the stability of the classification processes. The results are quantitatively compared with the ground truth data with 10 m spatial accuracy. Results confirm that the classification accuracy can be increased with the improvement of ground resolution of the satellite image data in general. ESA

N87-17255# Analytic Sciences Corp., Reading, Mass.

A SYNERGISTIC APPROACH FOR MULTISPECTRAL IMAGE RESTORATION USING REFERENCE IMAGERY

V. T. TOM *In* ESA Proceedings of the 1986 International Geoscience and Remote Sensing Symposium (IGARSS '86) on Remote Sensing: Today's Solutions for Tomorrow's Information Needs, Volume 1 p 559-564 Aug. 1986

Avail: NTIS HC A99/MF E03; ESA, Paris, France, 3 volume set \$90 Member States, AU, CN, and NO (+20% others)

A synergistic image restoration approach, based on a local multichannel least-squares (LS) modeling technique, is demonstrated on multispectral satellite imagery. This approach differs from more traditional global enhancement techniques by effectively exploiting the local correlation properties of multispectral imagery in order to spatially enhance or reduce noise in individual component images. The LS technique optimally estimates the input image using other spectral bands or image sources as local reference data. The procedure is applied to spatially enhance LANDSAT-D MSS and SPOT multispectral data and to reduce noise levels in LANDSAT-D TM data. ESA

N87-17267# Zurich Univ. (Switzerland). Dept. of Geography.

MERGING SPACEBORNE IMAGE DATA OF OPTICAL AND MICROWAVE SENSORS

D. R. NUESCH, E. H. MEIER, D. K. BLAETTLER, K. CH. GRAF, and F. M. HOLECZ *In* ESA Proceedings of the 1986 International Geoscience and Remote Sensing Symposium (IGARSS '86) on Remote Sensing: Today's Solutions for Tomorrow's Information Needs, Volume 1 p 633-637 Aug. 1986

Avail: NTIS HC A99/MF E03; ESA, Paris, France, 3 volume set \$90 Member States, AU, CN, and NO (+20% others)

Seasat SAR images and LANDSAT TM images were merged with high accuracy by a pixel-to-map transformation. The spatial resolution of 1 pixel was limited to 100 m, due to the grid size of the digital terrain model (DTM) required for the SAR image rectification. Accuracy depends on the grid size of the DTM which should be as fine meshed as possible, preferably on the order of the spatial resolution capability of the sensor being used. Results demonstrate that missing information or incomplete data from optical sensors, due for instance to clouds during the overflight, can be completed by data from microwave sensors. It is suggested that images with clouds taken by photographic cameras could be restored after being scanned by a raster device scanner. The procedure could also be applied to meteorological satellite images. ESA

N87-17269# INTERA Environmental Consultants Ltd., Calgary (Alberta).

DIGITAL TERRAIN MAPPING WITH STAR-1 SAR DATA

J. B. MERCER, R. T. LOWRY, F. LEBERL (Vexcell Corp., Boulder, Colo.), and G. DOMIK *In* ESA Proceedings of the 1986 International Geoscience and Remote Sensing Symposium (IGARSS '86) on Remote Sensing: Today's Solutions for Tomorrow's Information Needs, Volume 1 p 645-650 Aug. 1986

Avail: NTIS HC A99/MF E03; ESA, Paris, France, 3 volume set \$90 Member States, AU, CN, and NO (+20% others)

A program to assess the capability of deriving Digital Terrain Mapping (DTM) products from STAR-1 data, an airborne, digital SAR is outlined. A 500 sq km area was flown over varied terrain, and the resultant stereo images were analyzed on an analytical plotter. The DTM thus derived was used to rectify the imagery. Contour plots and an ortho-photo-like radar image were derived at a scale of 1:50,000. An error analysis was performed indicating that rms elevation errors less than 30 m can be achieved in a production environment. ESA

N87-17274# Bern Univ. (Switzerland). Inst. of Geography.
**ATMOSPHERIC CORRECTIONS OF NOAA-AVHRR DATA
 VERIFICATION OF DIFFERENT METHODS BY GROUND TRUTH
 MEASUREMENTS**

G. NEJEDLY *In* ESA Proceedings of the 1986 International Geoscience and Remote Sensing Symposium (IGARSS '86) on Remote Sensing: Today's Solutions for Tomorrow's Information Needs, Volume 1 p 677-682 Aug. 1986 Sponsored by the Swiss National Science Foundation
 Avail: NTIS HC A99/MF E03; ESA, Paris, France, 3 volume set \$90 Member States, AU, CN, and NO (+20% others)

Satellite data and precision radiation thermometer radiation temperature measurements carried out from low-altitude airplanes over land and water surfaces were compared. The WINDOW radiation transfer model and several split-window algorithms are tested for their suitability to eliminate the atmospheric effect. It is shown that, if meteorological soundings are available, the influence of the atmosphere can be minimized by using the WINDOW model. For water temperature retrievals over Switzerland, a split-window algorithm is computed using satellite data and compared to published algorithms. ESA

N87-17327# Purdue Univ., West Lafayette, Ind. School of Electrical Engineering.

PARAMETER SPACE TECHNIQUES FOR IMAGE REGISTRATION

P. ANUTA and C. MCGILLEM *In* ESA Proceedings of the 1986 International Geoscience and Remote Sensing Symposium (IGARSS '86) on Remote Sensing: Today's Solutions for Tomorrow's Information Needs, Volume 2 p 989-994 Aug. 1986
 (Contract NSF ECS-82-15539)

Avail: NTIS HC A17/MF A01; ESA, Paris, France, 3 volume set \$90 Member States, AU, CN, and NO (+20% others)

Three methods using parameter space analysis for image registration are compared. The first is a direct correlation of gray tone image patches. The second is a correlation of edge images derived from the image pair to be registered. The third is the parameter space method in which intersecting line segments are located in the two images. The methods are also tested on LANDSAT multispectral scanner and thematic mapper imagery. It is shown that the performance of the three methods is roughly equivalent for high signal-to-noise ratios but that the parameter space method is more robust at low ratios. ESA

N87-17332# Indiana State Univ., Terre Haute.
**IRSAP: AN IMPROVED APPROACH IN PROCESSING
 REMOTELY SENSED DATA**

M. P. BISHOP, K. LULLA, and P. MAUSEL *In* ESA Proceedings of the 1986 International Geoscience and Remote Sensing Symposium (IGARSS '86) on Remote Sensing: Today's Solutions for Tomorrow's Information Needs, Volume 2 p 1017-1021 Aug. 1986

Avail: NTIS HC A17/MF A01; ESA, Paris, France, 3 volume set \$90 Member States, AU, CN, and NO (+20% others)

A software accessing package named Interactive Remote Sensing Applications Package (IRSAP) was developed to rectify lack of interaction between software which when used together promotes synergism, flexibility, and efficiency for complex analyses in remote sensing/geographical information systems applications. The IRSAP software system is modular in design with menu driven architecture. The software system allows for easy integration of new application programs and software modules with existing system software. Its implementation allows users to process remotely sensed data in one processing environment even when accessing other software packages. Consequently, users need not contact programming staff in order to access other software packages, or have previous computer science background in order to process remotely sensed data. ESA

N87-17362# Deutsche Forschungs- und Versuchsanstalt fuer Luft- und Raumfahrt, Oberpfaffenhofen (West Germany). Inst. fuer Hochfrequenztechnik.

**X-SAR EXTENDS THE FREQUENCY RANGE OF SHUTTLE
 IMAGING RADAR**

W. KEYDEL *In* ESA Proceedings of the 1986 International Geoscience and Remote Sensing Symposium (IGARSS '86) on Remote Sensing: Today's Solutions for Tomorrow's Information Needs, Volume 2 p 1207-1212 Aug. 1986

Avail: NTIS HC A17/MF A01; ESA, Paris, France, 3 volume set \$90 Member States, AU, CN, and NO (+20% others)

The X-SAR/SIR-C mission is introduced. The mission will be a multifrequency SAR with multipolarization capability. The X-SAR to SIR-C addition extends the frequency range of the whole mission to the upper frequency limit existing today due to physical and technological limits. The experiments cover worldwide very many test areas under the same geometrical, atmospheric and radar technical conditions. The X-SAR development and its application together with SIR-C will strongly impact the future of microwave sensing development with respect to planned future activities like polar platforms, the advanced ERS-1, and the space station. ESA

N87-18155# Klagenfurt Univ. (Austria). Inst. of Geography.
**LAND SURFACE MODELS AS COLLATERAL DATA IN
 SATELLITE IMAGE INTERPRETATION**

M. SEGER and P. MANDL *In* ESA Proceedings of the 1986 International Geoscience and Remote Sensing Symposium (IGARSS '86) on Remote Sensing: Today's Solutions for Tomorrow's Information Needs, Volume 3 p 1281-1286 Aug. 1986

Avail: NTIS HC A21/MF A01; ESA, Paris, France, 3 volume set \$90 Member States, AU, CN, and NO (+20% others)

An analytic scheme for the human interpretation process of satellite images is proposed. Two types of collateral data are used: ecological and socioeconomic (land use) systems and models; and the differentiation of the real space (topographic and thematic informations of the study area). A system of photo pattern features and a system of land surface classes are combined into an interpretation key. This process is optimized by a multiple feasibility checking, concerning interpretation principles as well as the selection of land surface classes oriented to the aim of the regional study. The decision process is described as the application of interpretation rules to delineate and to name photo pattern areas, using also spatial collateral data. An ecologically oriented land surface map was compiled. The categories of collateral knowledge for the interpretation could also be a structural base for expert systems. ESA

N87-18157# Digim (1983), Inc. Montreal (Quebec).
SPATIAL REMOTE SENSING TO LAND MANAGEMENT

G. ROCHON, T. TOUTIN, S. R. HAJA, and A. LECLERC *In* ESA Proceedings of the 1986 International Geoscience and Remote Sensing Symposium (IGARSS '86) on Remote Sensing: Today's Solutions for Tomorrow's Information Needs, Volume 3 p 1291-1296 Aug. 1986

Avail: NTIS HC A21/MF A01; ESA, Paris, France, 3 volume set \$90 Member States, AU, CN, and NO (+20% others)

The development of highly automated methods and software for use with high-resolution SPOT satellite imagery and GPS data to obtain digital elevation models (DEM), topographic maps, and basic data for map revision at scales of 1:50 000 and smaller is discussed. Reduction of production costs in the order of 50% for base maps and 75% for ortho-images and DEMs, and reduction in production delays are expected. The system will offer the possibility of integration of the digital products with remote sensing images from other sources and geographic information systems. ESA

N87-18176# National Space Development Agency, Ibaraki (Japan). Earth Observation Center.

OUTLINE OF SAR-850 DATA PROCESSING METHOD IN JAPAN

K. MAEDA and Y. AZUMA *In* ESA Proceedings of the 1986 International Geoscience and Remote Sensing Symposium '86 on Remote Sensing: Today's Solutions for Tomorrow's Information Needs, Volume 3 p 1413-1418 Aug. 1986

Avail: NTIS HC A21/MF A01; ESA, Paris, France, 3 volume set \$90 Member States, AU, CN, and NO (+20% others)

A SAR data digital processing method for the Japanese Earth Resources Satellite 1 was developed. By using autofocusing in the azimuth and range direction, smear in the output image is the smallest possible. Selective multilook function by spatial filters is employed to produce the desired number of look images from a single look image. Resolution simulation function is employed to simulate spaceborne SAR data. It is possible to cancel and restart processing at any step. It is easy to define the size of processed image and change processing parameter. It is possible to input raw SAR data of either CCRS format or ERIM format for CCT. Output SAR image CCT is CCRS format based upon world standard superstructure used for LANDSAT MSS/TM. ESA

N87-18177# Dornier-Werke G.m.b.H., Friedrichshafen (West Germany).

DIGITAL REALTIME SAR PROCESSOR FOR C- AND X-BAND APPLICATIONS

R. SCHOTTER *In* ESA Proceedings of the 1986 International Geoscience and Remote Sensing Symposium (IGARSS '86) on Remote Sensing: Today's Solutions for Tomorrow's Information Needs, Volume 3 p 1419-1423 Aug. 1986

Avail: NTIS HC A21/MF A01; ESA, Paris, France, 3 volume set \$90 Member States, AU, CN, and NO (+20% others)

A flexible hardware concept to handle high speed image processing tasks is applied to a real time SAR-processor covering C-band ERS-1 as well as X-band radar data. The SPECAN-algorithm used in the processor breadboard, the basic hardware processing modules, and its performance data are described including storage unit, FIR filter correlator, complex multiplication, fast Fourier transformation, and pipeline controller. The performance data show that high speed image processing can be implemented at low power consumption and small volume. Due to the universal concept cost can also be kept down for this class of processing task. ESA

N87-18179# Toshiba Research and Development Center, Kawasaki (Japan). Electronics and Telecommunication Group.

HIGH SPEED IMAGE PROCESSING SYSTEM BASED ON THE CUSTOM VLSI FOR DIGITAL SIGNAL PROCESSING (DSP)

M. KUBO, K. Horiguchi, Y. Kuniyasu, S. Horii, E. OSAKI, Y. OSHIMA, K. HIROSHIMA, N. NAKAYAMA, and K. SUZUKI *In* ESA Proceedings of the 1986 International Geoscience and Remote Sensing Symposium (IGARSS '86) on Remote Sensing: Today's Solutions for Tomorrow's Information Needs, Volume 3 p 1433-1436 Aug. 1986

Avail: NTIS HC A21/MF A01; ESA, Paris, France, 3 volume set \$90 Member States, AU, CN, and NO (+20% others)

A 16 bit VLSI including a 32 bit multiplier was designed for a SAR image processing system to minimize the error of the summing of the products. The image processing system consists of the data memories, interface circuits, the VLSI's, and the vision processing system. The complex fast Fourier transformation on 1024 points was done in 2 millisecc with 1 VLSI. Tests reveal that this system is suitable for the image reconstruction of SAR as well as for the processing of the images taken optical sensors. ESA

N87-18182# Deutsche Forschungs- und Versuchsanstalt fuer Luft- und Raumfahrt, Oberpfaffenhofen (West Germany).

SOUTHERN PANTANAL MATOGROSSENSE (SOUTH AMERICA) OF MODULAR OPTOELECTRONIC MULTISPECTRAL SCANNER (MOMS) DATA, PRELIMINARY RESULTS

M. HAUCK, K. HILLER, and H. KUX (Instituto de Pesquisas Espaciais, Sao Jose dos Campos, Brazil) *In* ESA Proceedings of the 1986 International Geoscience and Remote Sensing Symposium (IGARSS '86) on Remote Sensing: Today's Solutions for Tomorrow's Information Needs, Volume 3 p 1451-1456 Aug. 1986

Avail: NTIS HC A21/MF A01; ESA, Paris, France, 3 volume set \$90 Member States, AU, CN, and NO (+20% others)

Corresponding data sets from MOMS and LANDSAT TM of parts of the Pantanal Matogrossense (South America) were investigated. The area displays open water bodies as well as dense vegetation of different types. Results of data evaluation show that TM data allow excellent identification of water bodies; MOMS data are superior with respect to the diversification of subtle differences in density and type of forested areas. ESA

N87-18188# Eidgenoessische Technische Hochschule, Zurich (Switzerland).

POINT POSITIONING AND MAPPING WITH LARGE FORMAT CAMERA DATA

A. GRUEN and E. SPIESS *In* ESA Proceedings of the 1986 International Geoscience and Remote Sensing Symposium (IGARSS '86) on Remote Sensing: Today's Solutions for Tomorrow's Information Needs, Volume 3 p 1485-1494 Aug. 1986

Avail: NTIS HC A21/MF A01; ESA, Paris, France, 3 volume set \$90 Member States, AU, CN, and NO (+20% others)

Large Format Camera (LFC) positioning accuracy is explored for planimetry and height with respect to strip triangulation and single stereomodel processing. Identification and interpretation of map features, and the map updating capabilities are analyzed in relation to the map standards of a topographic map 1:100 000. Experiences with digital terrain model generation and orthophoto production are reported. Results show that LFC photographs are superior to all other civilian space imaging systems in terms of spatial resolution, geometric integrity, area coverage, and price. ESA

N87-18189# Ludwig-Maximilians-Universitaet, Munich (West Germany). Inst. fuer Geographie.

ANALYSIS OF LARGE FORMAT CAMERA IMAGES FROM THE BLACK HILLS, USA, FOR TOPOGRAPHIC AND THEMATIC MAPPING

K. R. DIETZ *In* ESA Proceedings of the 1986 International Geoscience and Remote Sensing Symposium (IGARSS '86) on Remote Sensing: Today's Solutions for Tomorrow's Information Needs, Volume 3 p 1495-1501 Aug. 1986

Avail: NTIS HC A21/MF A01; ESA, Paris, France, 3 volume set \$90 Member States, AU, CN, and NO (+20% others)

Large Format Camera (LFC) photos from the Black Hills, taken during Space Shuttle Mission 41-G, were analyzed with regard to their suitability for topographic and thematic mapping. The images were compared with Metric Camera (MC) photos from the same area. The analysis was accompanied by field work. The use of high resolution film, forward motion compensation, as well as better illumination conditions and base-height ratios of the LFC photos give a distinct improvement compared to the MC data. The LFC images seem suitable for mapping on the scale of 1:100,000, if supported by ground truth. Due to the moderate image quality provided by the EROS Data Center, the production of maps on the scale of 1:50,000 does not seem possible. ESA

N87-18191# Centro Studi ed Applicazioni in Tecnologie Avanzate, Bari (Italy).

UMUS: A PROJECT FOR USAGE OF LANDSAT MSS AND ANCILLARY DATA IN LAND COVER MAPPING OF LARGE AREAS IN SOUTHERN ITALY

C. CAROPPO, V. DIGENNARO, and G. PASQUARIELLO *In* ESA Proceedings of the 1986 International Geoscience and Remote Sensing Symposium (IGARSS '86) on Remote Sensing: Today's Solutions for Tomorrow's Information Needs, Volume 3 p 1511-1516 Aug. 1986

Avail: NTIS HC A21/MF A01; ESA, Paris, France, 3 volume set \$90 Member States, AU, CN, and NO (+20% others)

The problem of producing a land use map at 1:200,000 scale and at a 1-II level by using LANDSAT MSS data in a geographical context characterized by spatially complex vegetation and terrain are considered. The procedure is based on the integration of multitemporal satellite images with conventional data (digital terrain model, aerial photos, and existing agricultural inventory data). Management of integrated data sets, the method for sample areas selection, and the use of prior probabilities in the classification process are emphasized. The final map is presented and its accuracy quoted. ESA

N87-18192# Kanazawa Inst. of Tech. (Japan).

AUTOMATIC UPDATE PROCEDURE OF THE DIGITIZED LAND USE MAP USING LANDSAT TM DATA

T. KUSAKA, Y. KAWATA, and S. UENO *In* ESA Proceedings of the 1986 International Geoscience and Remote Sensing Symposium (IGARSS '86) on Remote Sensing: Today's Solutions for Tomorrow's Information Needs, Volume 3 p 1517-1519 Aug. 1986

Avail: NTIS HC A21/MF A01; ESA, Paris, France, 3 volume set \$90 Member States, AU, CN, and NO (+20% others)

The updating procedure of the existing land use map using LANDSAT-5 Thematic Mapper (TM) data is described. The colored land use map at a scale of 1:25,000 was digitized, making use of the raster scanning device. In order to get up-to-date information on land use and land cover types, LANDSAT TM data was classified. The optimum categories in the updating procedure were determined from the detailed interpretation of the classified TM image and the digitized map image. Candidates of the optimum categories are rice fields, urban area, and orchard. ESA

N87-18194# Freiburg Univ. (West Germany). Inst. of Physical Geography.

DEDUCTION OF A SYNTHETIC BIOCLIMATOLOGICAL MAP BY MEANS OF REMOTE SENSING DATA AND A DIGITAL TERRAIN MODEL USING A CORRELATION APPROACH

G. MENZ *In* ESA Proceedings of the 1986 International Geoscience and Remote Sensing Symposium (IGARSS '86) on Remote Sensing: Today's Solutions for Tomorrow's Information Needs, Volume 3 p 1525-1529 Aug. 1986

Avail: NTIS HC A21/MF A01; ESA, Paris, France, 3 volume set \$90 Member States, AU, CN, and NO (+20% others)

It is argued that a synthetic bioclimatological map can be developed from remote sensing data and a digital terrain model stored in a geographic information system. This map is created through statistical procedures resulting in so-called stochastic models. Through this method, classical bioclimatological maps can be gathered with high significance. ESA

N87-18212# MacDonald, Dettwiler and Associates Ltd., Richmond (British Columbia).

RESOLVING THE DOPPLER AMBIGUITY FOR SPACEBORNE SYNTHETIC APERTURE RADAR

I. G. CUMMING, P. F. KAVANAGH, and M. R. ITO (British Columbia Univ., Vancouver) *In* ESA Proceedings of the 1986 International Geoscience and Remote Sensing Symposium (IGARSS '86) on Remote Sensing: Today's Solutions for Tomorrow's Information Needs, Volume 3 p 1639-1643 Aug. 1986 Sponsored by MacDonald Dettwiler, SPAR Aerospace and the Radar Project Office

Avail: NTIS HC A21/MF A01; ESA, Paris, France, 3 volume set \$90 Member States, AU, CN, and NO (+20% others)

A method for estimating the Doppler centroid directly from the received radar data, during the image formation process, is presented. It is based on measuring the range displacement between individual looks, using image correlation techniques. The algorithm was programmed into the GSAR processor, and encouraging test results obtained. ESA

N87-19787# Instituto de Pesquisas Espaciais, Sao Jose dos Campos (Brazil).

EVALUATION OF LANDSAT 4 MSS DATA FOR GEOMORPHOLOGICAL MAPPING IN THE SEMIARID ENVIRONMENT FOR REGIONAL PLANNING PURPOSES: AN INTEGRATED APPROACH (STUDY SITE, THE JUAZEIRO REGION) M.S. Thesis [AVALIACAO DE DADOS DO MSS-LANDSAT-4 PARA O MAPEAMENTO GEOMORFOLOGICO NO SEMI-ARIDO COMO SUPORTE AO PLANEJAMENTO REGIONAL: UMA ABORDAGEM INTEGRADA (AREA-TESTE REGIAO DE JUAZEIRO-BA)]

TERESA GALLOTTIFLORENZANO Sep. 1986 194 p *In* PORTUGUESE; ENGLISH summary (INPE-3984-TDL/236) Avail: NTIS HC A09/MF A01

The utilization of LANDSAT-MSS data is evaluated for geomorphological mapping at 1:100 scale in a semiarid environment for regional planning purposes. An integrated mapping approach was used. The study site is located in northern Bahia State and covers nearly 800 sq. km. An integrated method of qualitative nature, based on the CSIRO system, was used together with an analysis of quantitative parameters: morphometric indexes calculated from topographic maps and soil physicochemical data. The remote sensing products used were panchromatic aerial photography at 1:70 and LANDSAT-MSS data of both dry and wet seasons. The digital data were enhanced and classified using a nonsupervised classification algorithm. A map with geomorphological units was drawn using aerial photography. This map was used afterwards as a basis for the evaluation of LANDSAT-MSS data. The geomorphological units were characterized according to their lithology, geomorphology, soils, vegetation, land use and the environmental morphodynamic type. A great amount of information was obtained from the visual analysis of LANDSAT-MSS data, specially when using the contrast stretched color composite. Author

N87-19792# Instituto de Pesquisas Espaciais, Sao Jose dos Campos (Brazil).

METHODOLOGY FOR THE ELABORATION OF THEMATIC MAPS UTILIZING LANDSAT-TM DATA M.S. Thesis [METODOLOGIA PARA A CONFECCAO DE MAPAS TEMATICOS UTILIZANDO DADOS T.M.-LANDSAT]

LUIS ANTONIO DEANDRADE May 1986 133 p *In* PORTUGUESE; ENGLISH summary (INPE-3893-TDL/225) Avail: NTIS HC A07/MF A01

A methodology for the elaboration of thematic maps for military use in the scale of 1:100,000 is developed. Techniques of digital processing and visual analysis of remote sensing images were used. The thematic mapper sensor of the LANDSAT Satellite was employed and the selected area of study was Formosa (GO). The analysis of the spectral, spatial and temporal attributes of digital and photographic paper images of the LANDSAT Thematic Mapper helped by ancillary data and ground observations of surface characteristics constitute the framework. Four thematic products

are developed depending on the availability of pedology, topography, geology, and potential agricultural use data. A comparison among them as well as with a standard product was done aiming at military applications. The principal contribution is to make possible the use of thematic maps through satellite images as well as to allow a constant updating of existing maps. Author

08

INSTRUMENTATION AND SENSORS

Includes data acquisition and camera systems and remote sensors.

A87-19647* Reading Univ. (England).

INSTRUMENTATION FOR OPTICAL REMOTE SENSING FROM SPACE; PROCEEDINGS OF THE MEETING, CANNES, FRANCE, NOVEMBER 27-29, 1985

JOHN S. SEELEY, ED. (Reading, University, England), JOHN W. LEAR, ED., SIDNEY L. RUSSAK, ED. (Martin Marietta Corp., Denver, CO), and ANDRE MONFILS, ED. (Liege, Universite, Belgium) Meeting organized by SPIE and Association Nationale de la Recherche Technique; Sponsored by CNES, NASA, ESA, et al. Bellingham, WA, Society of Photo-Optical Instrumentation Engineers (SPIE Proceedings. Volume 589), 1986, 258 p. For individual items see A87-19648 to A87-19676. (SPIE-589)

Papers are presented on such topics as the development of the Imaging Spectrometer for Shuttle and space platform applications; the in-flight calibration of pushbroom remote sensing instruments for the SPOT program; buttable detector arrays for 1.55-1.7 micron imaging; the design of the Improved Stratospheric and Mesospheric Sounder on the Upper Atmosphere Research Satellite; and SAGE II design and in-orbit performance. Consideration is also given to the Shuttle Imaging Radar-B/C instruments; the Venus Radar Mapper multimode radar system design; various ISO instruments (ISOCAM, ISOPHOT, and SWS and LWS); and instrumentation for the Space Infrared Telescope Facility. B.J.

A87-19652

IN FLIGHT CALIBRATION OF PUSH BROOM REMOTE SENSING INSTRUMENTS

JEAN-PIERRE DESHAYES (CNES, Toulouse, France) IN: Instrumentation for optical remote sensing from space; Proceedings of the Meeting, Cannes, France, November 27-29, 1985 Bellingham, WA, Society of Photo-Optical Instrumentation Engineers, 1986, p. 54-59.

The calibration procedures and onboard calibration devices for the SPOT system are described. Tests show that the specification of 10 percent for absolute calibration accuracy and 3 percent for interband calibration accuracy should be satisfied, and better performance is expected. Attention is given to the HRV calibration. B.J.

A87-19655

IMPROVED MULTISPECTRAL EARTH IMAGING FROM SPACE USING ELECTRONIC IMAGE ALIGNMENT

A. J. MORD (Ball Corp., Ball Aerospace Systems Div., Boulder, CO) IN: Instrumentation for optical remote sensing from space; Proceedings of the Meeting, Cannes, France, November 27-29, 1985. Bellingham, WA, Society of Photo-Optical Instrumentation Engineers, 1986, p. 72-80. refs

A scheme for simplifying the design of CCD-based multispectral pushbroom scanners is presented. A new type of real-time signal processor permits registration of the images in the various spectral bands to + or - 0.1 pixel even though the system is mechanically aligned to only + or - 8 pixels. This permits design flexibility and cost reduction in the sensor optical system. The same signal processing can also correct for earth rotation skew and platform

attitude errors at the same time, thereby simplifying the archiving and use of the data. An operational land observing system design that uses these ideas is described. Author

A87-19660

THE ALONG TRACK SCANNING RADIOMETER (ATSR) FOR ERS1

J. DELDERFIELD, D. T. LLEWELLYN-JONES (SERC, Rutherford Appleton Laboratory, Didcot, England), R. BERNARD, Y. DE JAVEL (Centre de Recherches en Physique de l'Environnement Terrestre et Planetaire, Issy-les-Moulineaux, France), E. J. WILLIAMSON (Oxford University, England) et al. IN: Instrumentation for optical remote sensing from space; Proceedings of the Meeting, Cannes, France, November 27-29, 1985. Bellingham, WA, Society of Photo-Optical Instrumentation Engineers, 1986, p. 114-120. refs

The ATSR is an infrared imaging radiometer which has been selected to fly aboard the ESA Remote Sensing Satellite No. 1 (ERS1) with the specific objective of accurately determining global Sea Surface Temperature (SST). Novel features, including the technique of 'along track' scanning, a closed Stirling cycle cooler, and the precision on-board blackbodies are described. Instrument subsystems are identified and their design trade-offs discussed. Author

A87-20672

EVALUATION OF THE MID-INFRARED (1.45 TO 2.0 MICRONS) WITH A BLACK-AND-WHITE INFRARED VIDEO CAMERA

J. H. EVERITT, D. E. ESCOBAR, P. R. NIXON (USDA, Agricultural Research Service, Weslaco, TX), C. H. BLAZQUEZ (Florida, University, Lake Alfred), and M. A. HUSSEY (Texas A & M University, Weslaco) Photogrammetric Engineering and Remote Sensing (ISSN 0099-1112), vol. 52, Oct. 1986, p. 1655-1660. refs

A 0.9-2.2-micron sensitive B&W IR video camera, filtered to record radiation in the 1.45-2.0-micron water absorption region, was evaluated as a potential tool for remote-sensing. Imagery obtained in the laboratory of *Peperomia obtusifolia* A. Dietr. leaves successfully demonstrated the influence of its unusual internal leaf structure on its 1.45-2.0-micron absorption. Ground-based field video recordings of the succulent prickly pear (*Opuntia lindheimeri* Engelm.) showed the influence of its high water content on its 1.45-2.0-micron absorption. The camera provided acceptable airborne imagery that detected severely drought-stressed grass from lightly stressed grass. These results demonstrated that a video camera with sensitivity at 1.45-2.0 microns has considerable potential as an applied remote-sensing tool. Author

A87-20795

PROPOSED DESIGN OF AN IMAGING SPECTROPOLARIMETER/PHOTOMETER FOR REMOTE SENSING OF EARTH RESOURCES

WALTER G. EGAN (Lamont-Doherty Geological Observatory, Palisades, NY) Optical Engineering (ISSN 0091-3286), vol. 25, Oct. 1986, p. 1155-1159. refs

A design is presented for an imaging spectropolarimeter/photometer based on the Landsat multispectral scanner (MSS) for the wavelength range of 0.5 to 1.1 microns. The proposed scanner has essentially the same wavelength sensitivity, field of view, and scanning parameters of the original MSS except for the duplication of sensing and data systems for the determination of the amount of plane polarization. A unique nonpolarizing (i.e., polarization-compensated) scanning system is described, as well as a nonpolarizing beam splitter. Author

A87-20961*# National Aeronautics and Space Administration. Goddard Space Flight Center, Greenbelt, Md.
INSTRUMENT CHARACTERIZATION FOR THE DETECTION OF LONG-TERM CHANGES IN STRATOSPHERIC OZONE - AN ANALYSIS OF THE SBUV/2 RADIOMETER

J. E. FREDERICK, D. F. HEATH (NASA, Goddard Space Flight Center, Greenbelt, MD), and R. P. CEBULA (SASC Technologies, Inc., Hyattsville, MD) *Journal of Atmospheric and Oceanic Technology* (ISSN 0739-0572), vol. 3, Sept. 1986, p. 472-480. NASA-supported research.

The scientific objective of unambiguously detecting subtle global trends in upper stratospheric ozone requires that one maintains a thorough understanding of the satellite-based remote sensors intended for this task. The instrument now in use for long term ozone monitoring is the SBUV/2 being flown on NOAA operational satellites. A critical activity in the data interpretation involves separating small changes in measurement sensitivity from true atmospheric variability. By defining the specific issues that must be addressed and presenting results derived early in the mission of the first SBUV/2 flight model, this work serves as a guide to the instrument investigations that are essential in the attempt to detect long-term changes in the ozone layer. Author

A87-21094
THE SPOT SATELLITES - FROM SPOT 1 TO SPOT 4

M. COURTOIS and M. TRAZET (CNES, Paris, France) *Geocarto International*, no. 3, 1986, p. 4-14.

Starting with SPOT 1, the paper describes successively its sun-synchronous orbit, the 2 identical imaging instruments, and the other subsystems such as the onboard tape recorders, the telemetry package, the stabilization equipment, etc. Special emphasis is given to the technological innovations, in SPOTs 1 and 2, with respect to the first-generation satellites represented by the three first spacecraft of the Landsat series. The paper then details the improvements carried out on the design of the 3rd and 4th models. Author

A87-22025
THE SEU RISK ASSESSMENT OF Z80A, 8086 AND 80C86 MICROPROCESSORS INTENDED FOR USE IN A LOW ALTITUDE POLAR ORBIT

R. HARBOE-SORENSEN, L. ADAMS, E. J. DALY, C. SANSONE (ESA, European Space Research and Technology Centre, Noordwijk, Netherlands), D. MAPPER (Atomic Energy Research Establishment, Harwell, England) et al. (IEEE, DNA, Sandia National Laboratories, and NASA, 1986 Annual Conference on Nuclear and Space Radiation Effects, 23rd, Providence, RI, July 21-23, 1986) *IEEE Transactions on Nuclear Science* (ISSN 0018-9499), vol. NS-33, Dec. 1986, pt. 1, p. 1626-1631. refs

This paper presents the results of a test and analysis program carried out in support of an Earth Resources Satellite project in order to provide a quantitative SEU risk assessment for certain microprocessor based subsystems. The key features of the program were the low cost and comparative simplicity of the test techniques which, nevertheless, provided sufficient data for a quantitative risk assessment using the CREME suite of programs. Author

A87-22476#
EFFECTS OF A DOWNSTREAM DISTURBANCE ON THE STRUCTURE OF A TURBULENT PLANE MIXING LAYER

M. M. KOCHESFAHANI and P. E. DIMOTAKIS (California Institute of Technology, Pasadena) *AIAA, Aerospace Sciences Meeting*, 25th, Reno, NV, Jan. 12-15, 1987. 8 p. Research supported by the California Institute of Technology. refs
 (Contract AF-AFOSR-84-0120)
 (AIAA PAPER 87-0197)

The responses of the mixing layer in the regions upstream and downstream of a two-dimensional disturbance are studied using flow visualization and laser Doppler velocimetry. The disturbance is generated by a two-dimensional pitching airfoil located downstream of the splitter plate trailing edge. It is observed that at low forcing frequencies the region upstream of the disturbance is unaffected and the shear layer growth rate downstream is

increased; for high forcing frequencies the flow structure in the upstream region is modified and the growth rate in the downstream area is unchanged. It is proposed that a coupling mechanism may cause these changes in the shear layer. I.F.

A87-22556*# Jet Propulsion Lab., California Inst. of Tech., Pasadena.

EARTH OBSERVING SYSTEM - THE EARTH RESEARCH SYSTEM OF THE 1990'S

JAMES E. GRAF (California Institute of Technology, Jet Propulsion Laboratory, Pasadena) *AIAA, Aerospace Sciences Meeting*, 25th, Reno, NV, Jan. 12-15, 1987. 14 p. NASA-supported research. refs

(AIAA PAPER 87-0320)

The Earth Observing Systems' objective of comprehensively studying the earth's change leads to an array of technological and implementational challenges. Included in those challenges are in the in-orbit maintenance of fifty instruments through periodic servicing and the development of an international ground information system which permits rapid access to high quality data. The paper describes these challenges and also discusses potential contributions from international and USA agencies, mission design and payload groupings strategies, as well as design approaches to the spacecraft itself. Author

A87-23390
NIMBUS-7 SMMR MULTISPECTRAL PASSIVE MICROWAVE CORRELATIONS WITH AN ANTECEDENT PRECIPITATION INDEX

GREGORY D. WILKE (USAF, Global Weather Central, Offutt AFB, NE) and MARSHALL J. MCFARLAND (Texas A & M University, College Station) *IN: Conference on Satellite Meteorology/Remote Sensing and Applications*, 2nd, Williamsburg, VA, May 13-16, 1986, Preprints. Boston, MA, American Meteorological Society, 1986, p. 322-327. refs

A correlation analysis between Nimbus 7 Scanning Multichannel Microwave Radiometer passive microwave brightness temperatures (from between October 1978 and November 1979) and an antecedent precipitation index, API, (calculated from precipitation observations) was performed to infer surface soil moisture. Three transformations of vertical and horizontal components of the polarized brightness temperatures were used to represent various aspects of terrain, vegetation, and atmospheric conditions. Results indicate that the polarization difference transform had the highest correlation coefficient with the API, though the values were insignificantly different from the other transform values indicating that any one of the transforms could be used to estimate the API over bare soil without the need for an additional surface temperature estimate. R.R.

A87-23419* National Aeronautics and Space Administration. Goddard Space Flight Center, Greenbelt, Md.

IDEAS FOR A FUTURE EARTH OBSERVING SYSTEM FROM GEOSYNCHRONOUS ORBIT

WILLIAM E. SHENK, FORREST HALL, WAYNE ESAIAS, MARVIN MAXWELL (NASA, Goddard Space Flight Center, Greenbelt, MD), VERNER E. SUOMI (Wisconsin, University, Madison), and FRITZ VON BUN (NASA, Office of Space Science and Applications, Washington, DC) *IN: Conference on Satellite Meteorology/Remote Sensing and Applications*, 2nd, Williamsburg, VA, May 13-16, 1986, Preprints. Boston, MA, American Meteorological Society, 1986, p. 508-513. refs

Uses for the proposed geosynchronous platform are described. The geosynchronous satellite could provide good spatial and temporal resolution, a large field-of-view, easier calibration, stereography, and data relay. The limitations of the platform are discussed. The applications of the geosynchronous platform to meteorology, earth surveying, and oceanography are examined. I.F.

A87-23546* National Aeronautics and Space Administration. Langley Research Center, Hampton, Va.

SAM II MEASUREMENTS OF ANTARCTIC PSC'S AND AEROSOLS

M. P. MCCORMICK (NASA, Langley Research Center, Hampton, VA) and C. R. TREPTE (SASC Technologies, Inc., Hampton, VA) Geophysical Research Letters (Supplement) (ISSN 0094-8276), vol. 13, Nov. 1986, p. 1276-1279. refs
(Contract NAS7-17022)

Measurements by the SAM II satellite instrument show that polar stratospheric clouds (PSC's) are a regular feature of the austral winter season in either nonvolcanically or volcanically disturbed periods. The tops of these clouds are observed above 20 km in early winter and descend in altitude over the course of the season to heights near 15 km in mid September. Typically, PSC's persist in the lowest stratospheric altitudes throughout September. Subsequently, October always represents a relative annual minimum in aerosol extinction above 15 km and in stratospheric column amount. In addition, volcanically produced aerosols in Antarctica peaked in early 1983 and, if linearly related to ozone losses, are probably not a contributing factor to the continued loss of total ozone in the Antarctic spring in 1984 and 1985. Author

A87-23650

MULTILENS CAMERAS FOR HIGH VELOCITY/LOW ALTITUDE PHOTORECONNAISSANCE

GUENTHER DREYER (Carl Zeiss, Oberkochen, West Germany) Optical Engineering (ISSN 0091-3286), vol. 25, Nov. 1986, p. 1253-1260.

After an outline of the fundamentals of the multilens array combined with focal plane shutter and angle-correct forward motion compensation, the KS-153A Trilens and Pentalens arrays are described. Then the special ground resolution capability of the multilens camera is compared to that of the tricamera fan, and the geometric imaging capability is compared to that of the panoramic scan camera. Author

A87-23786

AIRBORNE LASER PROFILING AND MAPPING SYSTEMS COME OF AGE

JOSEPH JEPSKY (Associated Controls and Communications, Inc., Cambridge, MA) IN: American Congress on Surveying and Mapping and American Society for Photogrammetry and Remote Sensing, Annual Convention, Washington, DC, Mar. 16-21, 1986, Technical Papers. Volume 4. Falls Church, VA, American Congress on Surveying and Mapping and American Society for Photogrammetry and Remote Sensing, 1986, p. 229-238.

The design and operational characteristics of the high and low altitude ACCI PRAM IV systems, using both pulsed gallium arsenide and Nd:YAG laser profilers for mapping, surveying, photogrammetric control, and Digital Terrain Modeling, are discussed. Data outputs are provided in standard RS-232, IEEE488, parallel binary and analog formats, and timing data is generated in an appropriate format for integration of the laser profiler with all inertial navigation or microwave positioning systems and camera systems. The 10-15 nanosecond pulsewidth of all transceivers permits the penetration of heavy jungle foliage or rain forest. R.R.

A87-23804

CONTROL EXTENSION UTILIZING LARGE FORMAT CAMERA IMAGERY

LAURENCE NEWTON and EUGENE DERENYI (New Brunswick, University, Fredericton, Canada) IN: American Congress on Surveying and Mapping and American Society for Photogrammetry and Remote Sensing, Annual Convention, Washington, DC, Mar. 16-21, 1986, Technical Papers. Volume 4. Falls Church, VA, American Congress on Surveying and Mapping and American Society for Photogrammetry and Remote Sensing, 1986, p. 456-465. Research supported by the Department of Energy, Mines, and Resources of Canada. refs

Investigations were conducted into the accuracy obtainable for control extension utilizing Large Format Camera (LFC) imagery taken from the Space Shuttle. Using ground-control data the locations of approximately 120 ground-control points were identified on a strip of nine photographs taken during orbit 38 of Space Shuttle mission 41G, October 1984. The strip, of approximate scale 1:790,000 extends over a 500-km track in Saskatchewan, Canada. The ground control points were established using inertial survey systems, and are typically located adjacent to road intersections. Image coordinates were observed in an OMI AP-2C analytical plotter. The following computations were carried out: (1) image refinement (including use of observed reseau); (2) analytical model formation; (3) independent model aerotriangulation using program PAT-M-43; (4) bundle aerotriangulation using GEBAT; and (5) space resection of single images, and subsequent reprojection of check-point image coordinates. The accuracy of derived ground coordinates was evaluated by comparing computed and known ground positions. Conclusions are drawn on the performance of the LFC imagery as a means of control extension. Author

A87-24385

AN ANALYSIS OF THE POTENTIAL OF SATELLITE-BORNE BISTATIC RADAR SENSING OF THE EARTH [ANALIZ VOZMOZHNOSTEI BISTATICHESKOI RADIOLOKATSII ZEMLI S ISZ]

A. I. KUCHERIAVENKOV, O. E. MILEKHIN, and A. G. PAVELEV (AN SSSR, Institut Radiotekhniki i Elektroniki, Moscow, USSR) Issledovanie Zemli iz Kosmosa (ISSN 0205-9614), July-Aug. 1986, p. 86-94. In Russian. refs

The potential of bistatic radar sensing of the earth surface from geostationary and low-orbit satellites were analyzed. It is shown that large-scale surface slopes appreciably affect the position of the midband frequency of the radar-echo Doppler spectrum, while the reflection coefficient significantly depends on soil permittivity. The possibility of using radar sensing for measuring the height of sea waves was evaluated, and the effect of the wind speed on the shape of the mean Doppler spectrum was estimated. I.S.

A87-24778* National Aeronautics and Space Administration. Goddard Space Flight Center, Greenbelt, Md.

CHARACTERISTICS OF MAXIMUM-VALUE COMPOSITE IMAGES FROM TEMPORAL AVHRR DATA

BRENT N. HOLBEN (NASA, Goddard Space Flight Center, Greenbelt, MD) International Journal of Remote Sensing (ISSN 0143-1161), vol. 7, Nov. 1986, p. 1417-1434. refs

Red and near-infrared satellite data from the Advanced Very High Resolution Radiometer sensor have been processed over several days and combined to produce spatially continuous cloud-free imagery over large areas with sufficient temporal resolution to study green-vegetation dynamics. The technique minimizes cloud contamination, reduces directional reflectance and off-nadir viewing effects, minimizes sun-angle and shadow effects, and minimizes aerosol and water-vapor effects. The improvement is highly dependent on the state of the atmosphere, surface-cover type, and the viewing and illumination geometry of the sun, target and sensor. An example from southern Africa showed an increase of 40 percent from individual image values to the final composite image. Limitations associated with the technique are discussed, and recommendations are given to improve this approach. Author

A87-26098

SATELLITE REMOTE SENSING OF METEOROLOGICAL PARAMETERS FOR GLOBAL NUMERICAL WEATHER PREDICTION

R. G. ISAACS, R. N. HOFFMAN, and L. D. KAPLAN (Atmospheric and Environmental Research, Inc., Cambridge, MA) Reviews of Geophysics (ISSN 8755-1209), vol. 24, Nov. 1986, p. 701-743. refs

(Contract F19628-83-C-0027; F19628-84-C-0134; F19628-86-C-0141)

Current methods for the retrieval of temperature- and moisture-related variables from satellite observations and the use of these methods in global numerical weather prediction (NWP) are discussed. Consideration is given to satellite sensors and their spectral regions, the inverse and forward retrieval methods, and data analysis. Other retrievable meteorological parameters which may be used for NWP are examined; these include winds at the surface and cloud drift winds aloft, as well as other surface properties, such as soil moisture, surface albedo, snow cover, and surface temperature and fluxes. I.S.

A87-27872

OBSERVATIONS AND ANALYSIS OF A POLAR LOW OVER THE GREAT LAKES REGION

JOHN R. SMART (NOAA, Environmental Research Laboratories, Boulder, CO) and FREDERICK H. CARR (Oklahoma, University, Norman) IN: Conference on Weather Forecasting and Analysis, 11th, Kansas City, MO, June 17-20, 1986, Preprints. Boston, MA, American Meteorological Society, 1986, p. 188-193. refs

The evolution of a polar low which developed over the Great Lakes between April 8-9, 1985 is traced. The low was associated with heavy snowfall and record low temperatures in the region. The genesis and formation of the clouds into a comma and its subsequent growth and intensification are described. Sample satellite visible and IR images, geopotential isopleth, wind maps and rawinsonde data are provided for the central states during various stages of the storm. The images and maps led to the identification of the cause of the storm as intrusion of weakly stratified polar air beneath a mid-tropospheric frontal zone. M.S.K.

A87-27882* National Oceanic and Atmospheric Administration, Fort Collins, Colo.

SATELLITE CONTRIBUTIONS TO CONVECTIVE SCALE WEATHER ANALYSIS AND FORECASTING

JAMES F. W. PURDOM (NOAA, Satellite Applications Laboratory; Colorado State University, Fort Collins) IN: Conference on Weather Forecasting and Analysis, 11th, Kansas City, MO, June 17-20, 1986, Preprints. Boston, MA, American Meteorological Society, 1986, p. 295-314. refs

(Contract NAGW-504; NOAA-NA-85RAH05045; NOAA-NA-84AAH00020; NOAA-NA-84AAD00017)

Severe weather phenomena which are amenable to remote sensing by satellite instruments and having resolution fine enough to discern mesoscale features are described. GOES satellites acquire imagery with 1 km resolution in the visible band and 8 km at IR wavelengths. Animation of the images allows tracking the evolution and motions of clouds, which are the prime indicators of convective activity. Sample satellite imagery of sea, lake and river breezes which reveal differential heating processes, the effect of early morning cloud cover, thunderstorm outflow processes, and mesoscale convective systems are provided. Techniques for analyzing the satellite data to predict the onset of severe weather are discussed. M.S.K.

A87-27999#

RESULTS OF AN AIRBORNE SYNTHETIC-APERTURE RADAR (SAR) EXPERIMENT OVER A SIR-B (SHUTTLE IMAGING RADAR) TEST SITE IN GERMANY

A. SIEBER and W. NOACK (DFVLR, Oberpfaffenhofen, West Germany) ESA Journal (ISSN 0379-2285), vol. 10, no. 3, 1986, p. 291-310. refs

Results are reported from airborne calibration tests of an SIR-B system as part of the development program for the operational European Remote Sensing Satellite (ERS-1) program. Fifteen corner deflectors were deployed at various sites which were imaged in X- and S-bands in a high-resolution mode during 23 overflights at altitudes from 20,000-22,000 ft AGL. Design and performance details of the SAR-590 dual-polarization system employed are presented, along with the data analysis procedures which were applied. Several examples are provided of imagery obtained to demonstrate the usefulness of linear polarization scans for monitoring man-made objects. M.S.K.

A87-29431

CURRENT ACHIEVEMENTS AND FUTURE PROJECTS/USEFUL APPLICATIONS OF WEATHER SATELLITES AND FUTURE REMOTE SENSING

ROSS N. WILLIAMS (Ocean Data Systems, Inc., Rockville, MD) IN: Space commerce '86; Proceedings of the International Conference and Exhibition on the Commercial and Industrial Uses of Outer Space, Montreux, Switzerland, June 16-20, 1986. Geneva, Interavia Publishing Group, 1986, p. 367-371.

The capabilities of weather/remote sensing satellites are explored. Two NOAA satellites fly polar orbits while GOES spacecraft in GEO collect visible and IR images of cloud and weather systems. The satellites measure the vertical temperature and moisture structure of atmosphere, the sea surface temperature and topography, and the solar input, as well as broadcast data in real-time or stored modes, collect data from ocean-going ships, buoys and remote data collection platforms, and relay distress signals from aircraft and ships. Future satellites will also carry scatterometers, SARs, low frequency microwave radiometers, enhanced precision altimeters and advanced microwave sounding units. Uses of the data for weather prediction and monitoring, locating fish schools for commercial fishing, planning shipping and aircraft routes, improving the safety of ships around offshore platforms, performing hydrographic surveys, and as an agricultural aid are discussed. M.S.K.

A87-29849* Jet Propulsion Lab., California Inst. of Tech., Pasadena.

IMAGING RADAR POLARIMETRY FROM WAVE SYNTHESIS

HOWARD A. ZEBKER, JAKOB J. VAN ZYL, and DANIEL N. HELD (California Institute of Technology, Jet Propulsion Laboratory, Pasadena) Journal of Geophysical Research (ISSN 0148-0227), vol. 91, Jan. 10, 1987, p. 683-701. refs

A new approach is reported to the measurement of the complete polarization signature of each resolution element in an image implemented with an airborne synthetic aperture radar system. Signals recorded on one data pass from orthogonal linearly polarized antennas are utilized. The signals are combined in a data processor to synthesize any desired combination of transmit and receive polarizations. The technique permits measurement of the complex, multichannel reflectivity of a scene on a single aircraft pass and to late reprocess the data to provide multiple image maps, with each representing the backscattered energy from the scene measured with a different combination of observational transmit and receive polarizations. The resulting polarization signature measurements indicate optimum polarizations for observations of certain classes of objects and give insight into the identification of dominant scattering mechanisms for each kind of object. The mathematical model for polarization synthesis is summarized, and some theoretical polarization measurements are illustrated for several types of targets. The overall radar system implementation is described in detail. Some analyses of data acquired on three aircraft flights are presented. The technique

has been applied to mapping and differentiation of lava flows and to differentiation of forested and clear-cut areas. D.H.

A87-30885

WEATHER AND ATMOSPHERE REMOTE SENSING

S. ICHTIAQUE RASOOL (Ecole Normale Supérieure, Paris, France) IN: Space science and applications: Progress and potential. New York, IEEE Press, 1986, p. 143-150. refs

Remotely sensed meteorological images, the first having been obtained by Tiros 1 in 1960, provide global maps of weather systems, which may travel about 500 km/day. Numerical forecast can theoretically be accurate out to 14 days, i.e., the time span in which small eddies evolve into large-scale weather patterns. Lower atmosphere temperature and wind data are critical for weather predictions, with the accuracy of length of the prediction being dependent on the density of accurate data. The GARP experiment revealed the need for more accurate temperature data than currently available if prediction accuracy is to improve. A summary is presented of ongoing efforts to monitor the global sea surface temperature, atmospheric dust and volcanic aerosols, snow and ice cover extents and amounts, evapotranspiration, and the atmospheric content of anthropogenic CO₂ in order to improve the chances of predicting long-term climatic changes. M.S.K.

A87-30895

THE INTERACTIVE EFFECT OF SPATIAL RESOLUTION AND DEGREE OF INTERNAL VARIABILITY WITHIN LAND-COVER TYPES ON CLASSIFICATION ACCURACIES

JANIS L. CUSHNIE (Reading, University, England) International Journal of Remote Sensing (ISSN 0143-1161), vol. 8, Jan. 1987, p. 15-29. refs

(Contract NERC-F60/G6/03)

A study is made to assess the effect of spatial resolution on the degree of internal variability within land-cover classes and then to examine how this within-class variance affects classification accuracy. Airborne Multispectral Scanner data flown at 5 m resolution are degraded to simulate 10 and 20 m data. Classification accuracies within internally homogeneous classes are found to be high at all spatial resolutions. In contrast, classification accuracies of land-cover types characterized by a high degree of internal variability or scene noise improve by up to 20 per cent as spatial resolution is coarsened because the proportion of scene noise is reduced. A further improvement in classification can be achieved by smoothing the imagery prior to classification using various spatial filters. The extent of this improvement was found to be as much as 25 percent depending on the type of spatial filter used, the window size of the filter, the spatial resolution of the data and the land-cover type being classified. Author

A87-31139*# National Aeronautics and Space Administration. Langley Research Center, Hampton, Va.

SPACE SHUTTLE CLOUD DETECTION AND EARTH FEATURE CLASSIFICATION EXPERIMENT

W. E. SIVERTSON, JR. (NASA, Langley Research Center, Hampton, VA) Sensors Expo, Chicago, IL, Sept. 16-19, 1986, Paper. 8 p. refs

The Feature Identification and Location Experiment (FILE) that is being designed for the detection and classification of four primary earth features (water, vegetation, bare land, and the clouds-snow-ice class) is described. Consideration is given to the FILE classification technology concept and the FILE instrument, which will use two solid-state CCD cameras operating at 0.65 and 0.85-micron center frequency wavelengths, with the camera outputs being functions of the earth surface material radiance. The classification is based on camera output radiance ratio values. The preliminary analysis of the data collected on the STS 41-G mission is discussed. The results demonstrated the suitability of using the two-channel-ratio detection technology and a simple ($y = mx$) algorithm to autonomously classify the four earth surface features. The technology is especially attractive as a cloud sensor, where, in advance of or during a mission, a threshold value for cloud cover percentage can be programmed and/or adaptively modified for use in the control of other remote sensors. I.S.

N87-15242 Indian Space Research Organization, Ahmedabad. Space Application Centre.

INDIAN REMOTE SENSING PROGRAM

P. D. BHAVSAR /in DFVLR Colloquium about Joint Projects within the DFVLR/ISRO Cooperation p 21-27 Jul. 1986
Avail: DFVLR, Cologne, West Germany DM 46

The history of Indian remote sensing research is outlined. Participation in LANDSAT and NOAA is summarized. The design and production of sensors and the Bhaskara satellites are described. Satellite utilization in agriculture, geology, and Earth resources is outlined. International remote sensing projects are mentioned. ESA

N87-15573*# National Aeronautics and Space Administration. Goddard Space Flight Center, Greenbelt, Md.

REMOTE SENSING OF LAND-SURFACE TEMPERATURE FROM HIRS/MSU DATA

M. T. CHAHINE (Jet Propulsion Lab., California Inst. of Tech., Pasadena), R. HASKINS, J. SUSSKIND, and D. REUTER /in ESA Proceedings of an International Satellite Land-Surface Climatology Project (ISLSCP) Conference p 215-223 May 1986
Original contains color illustrations
Avail: NTIS HC A99/MF A01 CSCL 04B

A relaxation algorithm which permits meteorological parameters to be obtained from satellite data, without a priori assumptions about the properties of the other unknowns in the field of view, was developed. Atmospheric temperature profiles, atmospheric humidity, cloud cover, cloud top height, cloud top temperature, sea-surface temperature, land-surface temperature, snow cover, and ice cover are derived. Simultaneous determination of atmospheric and surface thermal structure and the cloud distribution provides information on heat sources and sinks, storage rates, and transport phenomena in the atmosphere. Such information is critical in determining the driving mechanisms for motions in the atmosphere and oceans and in improving numerical weather prediction. ESA

N87-15594*# Arizona Univ., Tucson. Optical Sciences Center.
VARIATIONS IN IN-FLIGHT ABSOLUTE RADIOMETRIC CALIBRATION

PHILIP N. SLATER /in ESA Proceedings of an International Satellite Land-Surface Climatology Project (ISLSCP) Conference p 357-363 May 1986 Sponsored by NASA
Avail: NTIS HC A99/MF A01 CSCL 08C

Variations in the in-flight absolute radiometric calibration of the Coastal Zone Color Scanner and the Thematic Mapper (TM) are reviewed. At short wavelengths, the sensors show a gradual reduction in response, while in the mid-IR the TM shows oscillatory variations. One set of measurements made at White Sands, New Mexico shows anomalous results in TM bands 2 and 4. The results of a reflectance-based and a radiance-based calibration method at White Sands are described. An analysis of the radiance-based method shows the value of such measurements from helicopter altitudes for calibration. ESA

N87-15624# Marmara Research Inst., Gebze (Turkey).
REMOTE SENSING ACTIVITIES IN TURKEY: POSSIBLE CONTRIBUTIONS TO CLIMATE STUDIES

F. INCE /in ESA Proceedings of an International Satellite Land-Surface Climatology Project (ISLSCP) Conference p 539-540 May 1986

Avail: NTIS HC A99/MF A01

Remote sensing institutions and activities in Turkey are listed. Climate related data collection needs are stressed, especially at the Euphrates Basin where several thousand square kilometers of land will be either inundated or turned into irrigated areas in 10 to 20 yr. ESA

N87-15628# Instituut voor Cultuurtechniek en Waterhuishouding, Wageningen (Netherlands).

FUTURE EUROPEAN PLANS IN THE FRAMEWORK OF THE INTERNATIONAL SATELLITE LAND SURFACE CLIMATOLOGY PROJECT (ISLSCP)

M. MENENTI and F. BECKER (Centre National de la Recherche Scientifique, Strasbourg, France) /n ESA Proceedings of an International Satellite Land-Surface Climatology Project (ISLSCP) Conference p 563-566 May 1986
Avail: NTIS HC A99/MF A01

Steps which led to a stable organizational framework of European participation in the International Satellite Land Surface Climatology Project are summarized. The objectives of the joint European experimental program are described, along with the criteria applied to the planning of the field experiments. It is emphasized that field experiments are necessary under different climatic conditions. A main shortcoming of algorithms to extract surface properties from satellite data is their dependence on climate, because of the simplifying assumptions involved. An inventory of field experiments and geographic areas; scientific goals; relevance for applications; and coordination and integration are outlined. ESA

N87-15660*# Texas Univ., Austin. Center for Space Research. **UNDERSEA VOLCANO PRODUCTION VERSUS LITHOSPHERIC STRENGTH FROM SATELLITE ALTIMETRY Semiannual Research Progress/Status Report, 1 Jun. - 31 Nov. 1986**

B. D. TAPLEY and D. T. SANDWELL 20 Jan. 1986 8 p
(Contract NAG5-787)
(NASA-CR-179984; NAS 1.26:179984) Avail: NTIS HC A02/MF A01 CSCL 08K

All seamount signatures apparent in the SEASAT altimeter profiles were located and digitized. In addition to locating the seamount signatures, their amplitudes were also estimated. The second phase consisted of determining what basic characteristics of a seamount can be extracted from a single vertical deflection profile. Seven seamounts that had both good bathymetric coverage and good satellite altimeter coverage were used to test a simple flexural model. A method was developed to combine satellite altimeter profiles from several different satellites to construct a detailed and accurate geoid. B.G.

N87-15669*# Pennsylvania State Univ., University Park. Dept. of Meteorology.

UTILIZATION OF SATELLITE DATA IN MESOSCALE MODELING OF SEVERE WEATHER Final Report

THOMAS T. WARNER 20 Jan. 1987 5 p
(Contract NSG-5205)
(NASA-CR-179917; NAS 1.26:179917) Avail: NTIS HC A02/MF A01 CSCL 04B

The Visible Infrared Spin Scan Radiometer Atmospheric Sounder (VAS) data were used to model the 36 hour cyclogenesis period over the Pacific Ocean. Various combinations of VAS data, conventional radiosonde data, and gridded data from the National Weather Service global analysis were used in successive-correction and variational objective-analysis procedures. The Penn State/NCAR mesoscale model was used to test the impact of the VAS data on a 12 hour forecast of convective precipitation in the midwestern U.S. B.G.

N87-16387# SRI International Corp., Menlo Park, Calif. Atmospheric Science Center.

DEVELOPMENT AND DEMONSTRATION OF ALARM (AIRBORNE LIDAR AGENT REMOTE MONITOR) Final Report

EDWARD E. UTHE, BRUCE M. MORLEY, and NORM B. NIELSEN Aug. 1986 125 p
(Contract DAAG29-82-K-0175)
(AD-A172886; ARO-18954.2-GS) Avail: NTIS HC A06/MF A01 CSCL 17H

An airborne wavelength-tunable CO₂ differential absorption lidar (DIAL) capable of making simultaneous measurements of atmospheric backscatter and surface-reflected energy has been developed and tested in a series of experiments. A data base of

surface returns for a flight track that passed over ocean, farmland, urban, forest and grassland surfaces was collected for various lidar wavelengths and wavelength separations. The data show that highest correlation between two-wavelength surface returns occurs over land surfaces and the highest decorrelation over ocean surfaces-the DIAL sensitivity for detection of chemical agents based on surface returns is significantly better over land than ocean areas. The data also show that the highest decorrelation is associated with the highest reflectivity surfaces of ocean and urban areas, probably a result of specular reflection. The correlation of surface returns decreases with increasing wavelength separation over land areas but is nearly independent of wavelength separation over ocean areas. The airborne DIAL system was demonstrated for mapping the cross-plume gas concentration distribution resulting from a near-surface release of SF₆. A new Fourier analysis method was used to improve single pulse-pair signal-to-noise ratios.

GRA

N87-17110*# Jet Propulsion Lab., California Inst. of Tech., Pasadena.

EVALUATION OF GEOPHYSICAL PARAMETERS MEASURED BY THE NIMBUS-7 MICROWAVE RADIOMETER FOR THE TOGA HEAT EXCHANGE PROJECT

W. TIMOTHY LIU and DONALD R. MOCK 1 Dec. 1986 26 p
(Contract NAS7-918)
(NASA-CR-180151; JPL-PUB-86-50; NAS 1.26:180151) Avail: NTIS HC A03/MF A01 CSCL 08E

The data distributed by the National Space Science Data Center on the Geophysical parameters of precipitable water, sea surface temperature, and surface-level wind speed, measured by the Scanning Multichannel Microwave Radiometer (SMMR) on Nimbus-7, are evaluated with in situ measurements between Jan. 1980 and Oct. 1983 over the tropical oceans. In tracking annual cycles and the 1982-83 E1 Nino/Southern Oscillation episode, the radiometer measurements are coherent with sea surface temperatures and surface-level wind speeds measured at equatorial buoys and with precipitable water derived from radiosonde soundings at tropical island stations. However, there are differences between SMMR and in situ measurements. Corrections based on radiosonde and ship data were derived supplementing correction formulae suggested in the databook. This study is the initial evaluation of the data for quantitative description of the 1982-83 E1 Nino/Southern Oscillation episode. It paves the way for determination of the ocean-atmosphere moisture and latent heat exchanges, a priority of the Tropical Ocean and Global Atmosphere (TOGA) Heat Exchange Program. Author

N87-17111*# Jet Propulsion Lab., California Inst. of Tech., Pasadena.

THE TIMS DATA USER'S WORKSHOP

ANNE B. KAHLE, ed. and ELSA ABBOTT, ed. 1 Nov. 1986 96 p
Workshop held in Bay Saint Louis, Miss., 18-19 Jun. 1985; sponsored by NASA NSTL Original contains color illustrations (Contract NAS7-918)
(NASA-CR-180130; JPL-PUB-86-38; NAS 1.26:180130) Avail: NTIS HC A05/MF A01 CSCL 08E

A workshop was held to bring together all users of data from NASA's airborne Thermal Infrared Multispectral Scanner (TIMS). The purpose was to allow users to compare results, data processing algorithms, and problems encountered; to update the users on the latest instrument changes and idiosyncracies, including distribution of the TIMS investigation guide; to inform the users of the wide range of problems that are currently being tackled by other TIMS investigators; to explore ways to expand the user community; to discuss current areas where more basic research is required; and to discuss the future directions of NASA's thermal infrared remote sensing programs. Also discussed were: geology, land use, archeology; and data processing and noise research.

N87-17112*# Daedalus Enterprises, Inc., Ann Arbor, Mich.

THE TIMS INSTRUMENT

CHUCK STANICH *In* JPL, California Inst. of Technology The TIMS Data User's Workshop p 5-7 1 Nov. 1986
 Avail: NTIS HC A05/MF A01 CSCL 14B

The scan head and spectrometer of the Thermal Infrared Multispectral Scanner (TIMS) are mounted in the unpressurized tail cone of a NASA/NSTL Learjet and operated through a hole cut through the skin. Design criteria are discussed. The digitized field of view is described. The functions of the scan head and spectrometer are examined. B.G.

N87-17113*# Jet Propulsion Lab., California Inst. of Tech., Pasadena.

THE TIMS INVESTIGATOR'S GUIDE

FRANK D. PALLUCONI *In its* The TIMS Data User's Workshop p 8 1 Nov. 1986

Avail: NTIS HC A05/MF A01 CSCL 14B

The Thermal Infrared Multispectral Scanner (TIMS) is a NASA aircraft scanner providing six-channel spectral capability in the thermal infrared region of the electromagnetic spectrum. Operating in the thermal infrared atmospheric window region (8 to 12 microns) with a sensitivity of approximately 0.1 C, TIMS may be used whenever an accurate measurement of spectral radiance or brightness temperature is needed. The purpose of the TIMS Investigator's Guide is to provide in one location, enough information about TIMS that potential investigators can decide whether or not it would provide measurements useful in their research program and to provide a new user of TIMS data sufficient information to begin analysis. B.G.

N87-17114*# National Aeronautics and Space Administration. Earth Resources Lab., Bay St. Louis, Miss.

ESTIMATION OF ABSOLUTE WATER SURFACE TEMPERATURE BASED ON ATMOSPHERICALLY CORRECTED THERMAL INFRARED MULTISPECTRAL SCANNER DIGITAL DATA

JAMES E. ANDERSON *In* JPL, California Inst. of Technology The TIMS Data User's Workshop p 9-10 1 Nov. 1986

Avail: NTIS HC A05/MF A01 CSCL 05B

Airborne remote sensing systems, as well as those on board Earth orbiting satellites, sample electromagnetic energy in discrete wavelength regions and convert the total energy sampled into data suitable for processing by digital computers. In general, however, the total amount of energy reaching a sensor system located at some distance from the target is composed not only of target related energy, but, in addition, contains a contribution originating from the atmosphere itself. Thus, some method must be devised for removing or at least minimizing the effects of the atmosphere. The LOWTRAN-6 Program was designed to estimate atmospheric transmittance and radiance for a given atmospheric path at moderate spectral resolution over an operational wavelength region from 0.25 to 28.5 microns. In order to compute the Thermal Infrared Multispectral Scanner (TIMS) digital values which were recorded in the absence of the atmosphere, the parameters derived from LOWTRAN-6 are used in a correction equation. The TIMS data were collected at 1:00 a.m. local time on November 21, 1983, over a recirculating cooling pond for a power plant in southeastern Mississippi. The TIMS data were analyzed before and after atmospheric corrections were applied using a band ratioing model to compute the absolute surface temperature of various points on the power plant cooling pond. The summarized results clearly demonstrate the desirability of applying atmospheric corrections. B.G.

N87-17115*# National Aeronautics and Space Administration. Earth Resources Lab., Bay St. Louis, Miss.

ATMOSPHERIC CORRECTION OF TIMS DATA

DOUG RICKMAN *In* JPL, California Inst. of Technology The TIMS Data User's Workshop p 11 1 Nov. 1986

Avail: NTIS HC A05/MF A01 CSCL 14B

The Thermal Infrared Multispectral Scanner (TIMS) is a unique sensor for two reasons, it is multispectral in the thermal-infrared

and it has on board, active calibration sources. The existence of the calibration permits the recorded DN's to be converted unambiguously to absolute energy units. However, to relate the data to energy originating from a target on the ground it is necessary to remove the atmospheric contribution to the signal, specifically its transmittance and emittance. These can be obtained fairly easily by use of the atmospheric model provided by LOWTRAN-6 and the data from the U.S. Weather Service network of bidaily radiosondes. Using these data with the TIMS responsivity curves an equation can be obtained which permits the unambiguous correction of the TIMS data for the atmosphere. Author

N87-17141*# Jet Propulsion Lab., California Inst. of Tech., Pasadena.

SPACEBORNE IMAGING RADAR RESEARCH IN THE 90'S

CHARLES ELACHI *In its* The Second Spaceborne Imaging Radar Symposium p 45-55 1 Dec. 1986

Avail: NTIS HC A10/MF A01 CSCL 171

The imaging radar experiments on SEASAT and on the space shuttle (SIR-A and SIR-B) have led to a wide interest in the use of spaceborne imaging radars in Earth and planetary sciences. The radar sensors provide unique and complimentary information to what is acquired with visible and infrared imagers. This includes subsurface imaging in arid regions, all weather observation of ocean surface dynamic phenomena, structural mapping, soil moisture mapping, stereo imaging and resulting topographic mapping. However, experiments up to now have exploited only a very limited range of the generic capability of radar sensors. With planned sensor developments in the late 80's and early 90's, a quantum jump will be made in our ability to fully exploit the potential of these sensors. These developments include: multiparameter research sensors such as SIR-C and X-SAR, long-term and global monitoring sensors such as ERS-1, JERS-1, EOS, Radarsat, GLORI and the spaceborne sounder, planetary mapping sensors such as the Magellan and Cassini/Titan mappers, topographic three-dimensional imagers such as the scanning radar altimeter and three-dimensional rain mapping. These sensors and their associated research are briefly described. Author

N87-17145*# Jet Propulsion Lab., California Inst. of Tech., Pasadena.

PRESENT STATUS OF JAPANESE ERS-1 PROJECT

YASUFUMI ISHIWADA and YOSHIKI NEMOTO *In its* The Second Spaceborne Imaging Radar Symposium p 79-83 1 Dec. 1986

Avail: NTIS HC A10/MF A01 CSCL 22B

Earth Resources Satellite 1 (ERS-1) will be launched in the FY 1990 with the H-1 rocket from Tanegashima Space Center. ERS-1 will seek to firmly establish remote sensing technologies from space by using synthetic aperture radar and optical sensors, as well as primarily exploring for non-renewable resources and also monitoring for land use, agriculture, forestry, fishery, conservation of environment, prevention of disasters, and surveillance of coastal regions. ERS-1 is a joint project in which the main responsibility for the development of the mission equipment is assumed by the Agency of Industrial Science and Technology, MITI, and the Technology Research Association of Resources Remote Sensing System, while that for the satellite itself and launching rocket is assumed by the Science and Technology Agency (STA) and the National Space Development Agency (NASDA). In relation to this project, users have maintained a close working relationship with the manufacturers after submitting their requirements in 1984 on the specifications of the mission equipments. This missions parameters are outlined. Author

N87-17157*# Jet Propulsion Lab., California Inst. of Tech., Pasadena.

MULTIPLE INCIDENCE ANGLE SIR-B EXPERIMENT OVER ARGENTINA

JOBEA CIMINO, DAREN CASEY, STEPHEN WALL, ALDO BRANDANI (Consejo Nacional de Investigaciones Cientificas y Tecnicas, Mar del Plata, Argentina), GITTA DOMIK (Vexcell Corp., Boulder, Colo.), and FRANZ LEBERL *In its* The Second Spaceborne Imaging Radar Symposium p 165-173 1 Dec. 1986
 Avail: NTIS HC A10/MF A01 CSCL 08B

The Shuttle Imaging Radar (SIR-B), the second synthetic aperture radar (SAR) to fly aboard a shuttle, was launched on October 5, 1984. One of the primary goals of the SIR-B experiment was to use multiple incidence angle radar images to distinguish different terrain types through the use of their characteristic backscatter curves. This goal was accomplished in several locations including the Chubut Province of southern Argentina. Four descending image acquisitions were collected providing a multiple incidence angle image set. The data were first used to assess stereo-radargrammetric techniques. A digital elevation model was produced using the optimum pair of multiple incidence angle images. This model was then used to determine the local incidence angle of each picture element to generate curves of relative brightness vs. incidence angle. Secondary image products were also generated using the multi-angle data. The results of this work indicate that: (1) various forest species and various structures of a single species may be discriminated using multiple incidence angle radar imagery, and (2) it is essential to consider the variation in backscatter due to a variable incidence angle when analyzing and comparing data collected at varying frequencies and polarizations. Author

N87-17163# European Space Agency, Paris (France).
PROCEEDINGS OF THE 1986 INTERNATIONAL GEOSCIENCE AND REMOTE SENSING SYMPOSIUM (IGARSS '86) ON REMOTE SENSING: TODAY'S SOLUTIONS FOR TOMORROW'S INFORMATION NEEDS, VOLUME 1

T. D. GUYENNE, ed. and J. J. HUNT, ed. Aug. 1986 752 p
 Symposium held in Zurich, Switzerland, 8-11 Sep. 1986; sponsored by NASA, IEEE Geoscience and Remote Sensing Society, ESA, EARSeL, NOAA, CNES, DFVLR, Swiss Academy of Sciences, the Swiss Association for Space Technology, Contraves Ltd., et al. (ESA-SP-254-VOL-1; IEEE-86CH2268-1-VOL-1; LC-86-80109-VOL-1; ISSN-0379-6566; ETN-87-98535) Avail: NTIS HC A99/MF E03; ESA, Paris, France, 3 volume set \$90 Member States, AU, CN, and NO (+20% others)

New instruments with enormous information gathering abilities are being planned to provide data from all parts of the spectrum. New data processing and storage hardware, combined with fundamental advances in information systems concepts and algorithms are awaiting the research efforts to mold them for special use. Some topics covered in the proceedings are: Optical and infrared remote sensing systems; information transfer and Third World development; wave target interaction mechanisms; microwave remote sensing of sea ice; ERS-1 sensor performance, calibration, and data validation; geophysics; imaging spectrometry; image analysis systems; ocean radar scattering; marginal ice zone remote sensing; geomorphology; SAR applications; geology; multispectral image analysis; ocean wind scatterometry; passive microwave sensing; radar mapping and land use; meteorology and atmospheric sounding; and radar instrumentation.

ESA

N87-17167# Messerschmitt-Boelkow-Blohm G.m.b.H., Munich (West Germany).

THE STEREO-PUSHBROOM SCANNER SYSTEM DIGITAL PHOTOGRAMMETRY SYSTEM (DPS) AND ITS ACCURACY

O. HOFMANN *In* ESA Proceedings of the 1986 International Geoscience and Remote Sensing Symposium (IGARSS '86) on Remote Sensing: Today's Solutions for Tomorrow's Information Needs, Volume 1 p 21-28 Aug. 1986

Avail: NTIS HC A99/MF E03; ESA, Paris, France, 3 volume set \$90 Member States, AU, CN, and NO (+20% others)

A digital stereo-scanner with three line sensor arrays working on the pushbroom principle and a suitable, rigorous compilation process was developed. It delivers the orientation data of the camera in selectable update points along the flight path of aircraft, spacecraft, or missiles, the three-dimensional coordinates of the digital elevation model, ortho and stereo-orthophotos, digital elements for line maps, and rectified multispectral images. By computer simulated operational models, the influence of the camera and flight parameters on the accuracy of the models were tested. Results show high stability and nearly constant accuracy over an entire strip model. ESA

N87-17169# European Space Agency. European Space Research and Technology Center, ESTEC, Noordwijk (Netherlands).

CONCEPT OF A FUTURE MULTISPECTRAL THERMAL INFRARED (TIR) PUSHBROOM MISSION FOR EARTH OBSERVATION FROM SPACE

M. RAST and M. L. REYNOLDS *In its* Proceedings of the 1986 International Geoscience and Remote Sensing Symposium (IGARSS '86) on Remote Sensing: Today's Solutions for Tomorrow's Information Needs, Volume 1 p 33-37 Aug. 1986

Avail: NTIS HC A99/MF E03; ESA, Paris, France, 3 volume set \$90 Member States, AU, CN, and NO (+20% others)

Mission requirements and instrument specifications for a multispectral thermal infrared pushbroom imager for land observation and coastal and inland water applications are outlined. Applications to vegetation, agriculture, and forestry; water resources; geosciences; and environmental monitoring are described. ESA

N87-17192# European Space Agency. European Space Research and Technology Center, ESTEC, Noordwijk (Netherlands).

THE ESA APPROACH FOR ERS-1 SENSOR CALIBRATION AND PERFORMANCE VERIFICATION

J. LOUET *In its* Proceedings of the 1986 International Geoscience and Remote Sensing Symposium (IGARSS '86) on Remote Sensing: Today's Solutions for Tomorrow's Information Needs, Volume 1 p 167-174 Aug. 1986

Avail: NTIS HC A99/MF E03; ESA, Paris, France, 3 volume set \$90 Member States, AU, CN, and NO (+20% others)

The approach taken for validation and calibration of the ERS-1 mission is outlined. A clear distinction is made between the engineering and geophysical performances of the mission. The pre and post-launch activities required to calibrate the ERS-1 system and validate the geophysical performances are described. ESA

N87-17194# European Space Agency. European Space Research and Technology Center, ESTEC, Noordwijk (Netherlands).

ERS-1 RADAR ALTIMETER: PERFORMANCE, CALIBRATION AND DATA VALIDATION

C. R. FRANCIS *In its* Proceedings of the 1986 International Geoscience and Remote Sensing Symposium (IGARSS '86) on Remote Sensing: Today's Solutions for Tomorrow's Information Needs, Volume 1 p 181-184 Aug. 1986

Avail: NTIS HC A99/MF E03; ESA, Paris, France, 3 volume set \$90 Member States, AU, CN, and NO (+20% others)

Key characteristics of the ERS-1 radar altimeter and of the overall measurement system are described. Operating modes include ocean and ice. Calibration is based on ground test and

simulation data and onboard, independent measures. Performance will be established once the hardware implementation is complete. The altimeter is not sensitive to yaw, but a roll tilt mode used when calibrating the wind scatterometer leads to loss of altimeter data. Science data are tape recorded and telemetered in a high speed dump in real time to ground stations. ESA

N87-17195# Mullard Space Science Lab., Dorking (England).
AN AUTOMATIC TRACKING MODE SWITCHING ALGORITHM FOR THE ERS-1 ALTIMETER

D. J. WINGHAM *In* ESA Proceedings of the 1986 International Geoscience and Remote Sensing Symposium (IGARSS '86) on Remote Sensing: Today's Solutions for Tomorrow's Information Needs, Volume 1 p 185-190 Aug. 1986
 (Contract ESTEC-6375/85-NL-BI)

Avail: NTIS HC A99/MF E03; ESA, Paris, France, 3 volume set \$90 Member States, AU, CN, and NO (+20% others)

A tracking system which switches automatically the ERS-1 radio altimeter tracking mode and the range window width is described. The system estimates the shape of the return, which may be used to control the instrument gain and determine if the return is sufficiently ocean-like for the use of an ocean specific error algorithm; and it provides a linear height error algorithm for a wide variety of return shapes, which permits the height error to be open or close the range window. The linear height error substantially improves the tracking performance in areas where the range to the surface is varying rapidly. Simulated performance over a variety of geographical surfaces, in particular the ocean, sea ice and ice shelves, and simulations of the altimeter and of the normal incidence radar returns from these surfaces are described. By combining these two, it is possible to assess the performance of the control system over these surfaces. The examples are deliberately chosen as worst case possibilities, and it is clear that the system offers a great increase in coverage over any previous system. ESA

N87-17202*# Jet Propulsion Lab., California Inst. of Tech., Pasadena.

IMAGING SPECTROMETRY: AIRCRAFT AND SPACE PROGRAM

M. J. ABRAMS *In* ESA Proceedings of the 1986 International Geoscience and Remote Sensing Symposium (IGARSS '86) on Remote Sensing: Today's Solutions for Tomorrow's Information Needs, Volume 1 p 231-234 Aug. 1986

Avail: NTIS HC A99/MF E03; ESA, Paris, France, 3 volume set \$90 Member States, AU, CN, and NO (+20% others) CSDL 08B

Imaging spectrometry for the remote sensing of the Earth is introduced. Reflected solar energy from the surface is dispersed in a spectrometer and used to form up to 200 registered spectral images. Each pixel has associated with it sufficient information for the reconstruction of a complete reflectance spectrum. The technique allows the diagnostic narrow band spectral features that are characteristic of many surface materials to be used to identify those materials. These spectral features are typically 20 to 40 nm wide; spectral imaging systems which acquire data in contiguous 10 nm bands therefore have sufficient resolution for direct identification of those materials with diagnostic spectral bands. ESA

N87-17204*# Jet Propulsion Lab., California Inst. of Tech., Pasadena.

ANALYSIS OF AIS RADIOMETRY AT MONO LAKE, CALIFORNIA

J. E. CONEL, S. L. ADAMS, R. E. ALLEY, G. L. HOOVER, and S. SCHULTZ *In* ESA Proceedings of the 1986 International Geoscience and Remote Sensing Symposium (IGARSS '86) on Remote Sensing: Today's Solutions for Tomorrow's Information Needs, Volume 1 p 239-244 Aug. 1986

Avail: NTIS HC A99/MF E03; ESA, Paris, France, 3 volume set \$90 Member States, AU, CN, and NO (+20% others) CSDL 08B

Airborne imaging spectrometer (AIS) data were studied to establish absolute instrumental calibration and to provide atmospheric corrections. Good agreement is found between calculated and measured radiances for uniform surface targets (beaches), but simulations of atmospheric properties with LOWTRAN lead to unreasonably low values of atmospheric precipitable water. Absorptions from CO₂ are not detected in the AIS data, but are strongly present in the LOWTRAN model. The apparent low contrast of all atmospheric absorption bands leads to a study of contamination from overlapping spectral orders in the AIS data. The suspected contamination is shown unambiguously to be present beyond 1500 nm. The magnitude remains uncertain. Spectral band filling at 1400 nm cannot be accounted for by order mixing because of the 800 nm blocking filter used. Rough corrections for short wavelength mode observations might be possible if an after-the-fact radiometric calibration of the instrument can be developed. ESA

N87-17205*# Operations Research, Inc., Rockville, Md.
THE SEQUENTIAL FILTER IMAGING RADIOMETER (SFIR), A NEW INSTRUMENT CONFIGURATION FOR EARTH OBSERVATIONS

M. S. MAXWELL *In* ESA Proceedings of the 1986 International Geoscience and Remote Sensing Symposium (IGARSS '86) on Remote Sensing: Today's Solutions for Tomorrow's Information Needs, Volume 1 p 245-250 Aug. 1986
 (Contract NAS5-28057)

Avail: NTIS HC A99/MF E03; ESA, Paris, France, 3 volume set \$90 Member States, AU, CN, and NO (+20% others) CSDL 14B

The sequential filter imaging radiometer (SFIR) concept is presented, contrasted with other sensor configurations, and its strengths and weaknesses discussed. In a pushbroom SFIR the optics images the scene onto a long, narrow area array. The length of the array defines the field of view. The spectral defining filters are sequentially placed over the full array, a sample of data for that band taken, and then the next filter placed in front of the array. All of the filters are placed over the array in the time that it takes the image of the scene to advance the array width. Thus the entire scene is observed in each band. Advantages of the SFIR are: spectral bands can be broad, narrow or overlap; it is easy to improve signal to noise ratio; and it is simple to make bands polarized. Its main disadvantage is that it requires more detectors than other instrument configurations. ESA

N87-17224# European Space Agency. European Space Research and Technology Center, ESTEC, Noordwijk (Netherlands).

ERS-1 FAST DELIVERY PROCESSING AND PRODUCTS

J. P. GUIGNARD *In* its Proceedings of the 1986 International Geoscience and Remote Sensing Symposium (IGARSS '86) on Remote Sensing: Today's Solutions for Tomorrow's Information Needs, Volume 1 p 375-379 Aug. 1986

Avail: NTIS HC A99/MF E03; ESA, Paris, France, 3 volume set \$90 Member States, AU, CN, and NO (+20% others)

The ERS-1 satellite SAR image mode and wave mode products, scatterometer products, and altimeter products are listed. Ground station organization and facilities are described. ESA

N87-17260*# National Aeronautics and Space Administration. Goddard Space Flight Center, Greenbelt, Md.

THE ELECTRONICALLY STEERED THINNED ARRAY RADIOMETER (ESTAR)

C. T. SWIFT (Massachusetts Univ., Amherst), C. RUF, A. TANNER, and D. LEVINE *In* ESA Proceedings of the 1986 International Geoscience and Remote Sensing Symposium (IGARSS '86) on Remote Sensing: Today's Solutions for Tomorrow's Information Needs, Volume 1 p 591-593 Aug. 1986

Avail: NTIS HC A99/MF E03; ESA, Paris, France, 3 volume set \$90 Member States, AU, CN, and NO (+20% others) CSDL 14B

The concept of a thinned array radiometer is described as an alternate to large filled apertures to achieve high resolution imaging from space. The serious limitations of conventional mechanical scanning systems and the practical problems associated with a multiple receiver pushbroom system that utilizes a large antenna are discussed. The thinned array is developed in terms of aperture synthesis techniques used in radio astronomy. Examples of thinned array configurations are presented, and future directions are discussed. ESA

N87-17277# Naval Research Lab., Washington, D. C. Space Systems and Technology Div.

APPLICATION OF SPACEBORNE DISTRIBUTED APERTURE/COHERENT ARRAY PROCESSING (SDA/CAP) TECHNOLOGY TO ACTIVE AND PASSIVE MICROWAVE REMOTE SENSING

M. S. KAPLAN *In* ESA Proceedings of the 1986 International Geoscience and Remote Sensing Symposium (IGARSS '86) on Remote Sensing: Today's Solutions for Tomorrow's Information Needs, Volume 1 p 697-701 Aug. 1986

Avail: NTIS HC A99/MF E03; ESA, Paris, France, 3 volume set \$90 Member States, AU, CN, and NO (+20% others)

Application of spaceborne distributed aperture/coherent array processing (SDA/CAP) to environmental remote sensing missions is discussed. This technology differs from conventional monostatic remote sensing approaches in that sensor elements are distributed among many space platforms. It is possible to coherently combine the inputs from many receiving spacecraft in order to form a very large distributed aperture, thousands of kilometers in size. This enormous effective aperture size can provide nanoradian resolution in the microwave region of the spectrum. Relative spacecraft phase measurement accuracies on the order of a fraction of a wavelength are required to support the technology. Spacecraft relative position and time measurement via hydrogen maser time references on each spacecraft and laser ranging between spacecraft is proposed. Intersatellite laser ranging technology needs to be developed to support the application of SDA/CAP techniques for advanced space environmental remote sensor systems. ESA

N87-17278# Kansas Univ. Center for Research, Inc., Lawrence. Radar Systems and Remote Sensing Lab.

SOME TRADE-OFFS IN MODEST-RESOLUTION RADARS FOR SPACE

R. K. MOORE *In* ESA Proceedings of the 1986 International Geoscience and Remote Sensing Symposium (IGARSS '86) on Remote Sensing: Today's Solutions for Tomorrow's Information Needs, Volume 1 p 703-708 Aug. 1986

Avail: NTIS HC A99/MF E03; ESA, Paris, France, 3 volume set \$90 Member States, AU, CN, and NO (+20% others)

It is argued that radars may be added easily to radiometers to provide a synergistic capability, while providing improved resolution within the radiometer footprint with little additional power. Modest-resolution radars without radiometers are so much simpler than focussed SARs that they can provide useful alternatives where image resolution need not be fine, such as geologic exploration, soil-moisture measurement, and mapping ocean features other than wave spectra. Modest-resolution radar systems often require transmitter power of only milliwatts; under some conditions the power required is less than that of the local oscillator of the accompanying radiometer receiver. The lowest power requirement

is for forward-looking radars that achieve modest resolution in the along-track direction by Doppler filtering. ESA

N87-17279# Jet Propulsion Lab., California Inst. of Tech., Pasadena.

IMAGING RADAR POLARIMETRY FROM WAVE SYNTHESIS

H. A. ZEBKER, J. J. VANZYL, and D. N. HELD *In* ESA Proceedings of the 1986 International Geoscience and Remote Sensing Symposium (IGARSS '86) on Remote Sensing: Today's Solutions for Tomorrow's Information Needs, Volume 1 p 709-713 Aug. 1986

Avail: NTIS HC A99/MF E03; ESA, Paris, France, 3 volume set \$90 Member States, AU, CN, and NO (+20% others)

It is shown that it is possible to measure the complete scattering matrix of an object using data acquired on a single aircraft pass, and combine the signals later in the data processor to generate radar images corresponding to any desired combination of transmit and receive polarization. Various scattering models predict different dependence on polarization state of received power from an object. The imaging polarimeter permits determination of this dependence, the polarization signature, of each point in a radar image. Comparison of predictions and observational data reveals scattering mechanisms for each area of interest. Backscatter from the ocean is highly polarized and well-modeled by Bragg scattering, while scattering from trees in a city park possesses a considerable unpolarized component. Urban regions exhibit the characteristics expected from dihedral corner reflectors, and their polarization signatures are quite different from the on-bounce Bragg model. ESA

N87-17283# European Space Agency, Paris (France).

PROCEEDINGS OF THE 1986 INTERNATIONAL GEOSCIENCE AND REMOTE SENSING SYMPOSIUM (IGARSS '86) ON REMOTE SENSING: TODAY'S SOLUTIONS FOR TOMORROW'S INFORMATION NEEDS, VOLUME 2

T. D. GUYENNE, ed. and J. J. HUNT, ed. Aug. 1986 388 p Symposium held in Zurich, Switzerland, 8-11 Sep. 1986; sponsored by NASA, ESA, EARSeL NOAA, CNES, DFVLR, Swiss Academy of Sciences, Swiss Association for Space Technology, Contraves Ltd., Dornier-Werke GmbH, Intern. Union of Radio Science, et al. (ESA-SP-254-VOL-2; IEEE-86CH2268-1-VOL-2; LC-86-80109-VOL-2; ISSN-0379-6566; ETN-87-98536) Avail:

NTIS HC A17/MF A01; ESA, Paris, France, 3 volume set \$90 Member States, AU, CN, and NO (+20% others)

Remote sensing applications to agriculture; image processing methodology; active microwave sensing of the ocean; passive microwave sensing of vegetation and soils; radar forestry; hydrology; imaging radar missions; SAR observation of ocean waves; land analysis with optical sensors; and SAR system considerations were discussed. ESA

N87-17320# Stuttgart Univ. (West Germany). Inst. fuer Navigation.

FUTURE USER REQUIREMENTS AND REQUIRED TECHNOLOGICAL DEVELOPMENTS OF SPACEBORNE SYNTHETIC APERTURE RADARS

PH. HARTL and H. M. BRAUN (Dornier-Werke G.m.b.H., Friedrichshafen, West Germany) *In* ESA Proceedings of the 1986 International Geoscience and Remote Sensing Symposium (IGARSS '86) on Remote Sensing: Today's Solutions for Tomorrow's Information Needs, Volume 2 p 941-946 Aug. 1986

Avail: NTIS HC A17/MF A01; ESA, Paris, France, 3 volume set \$90 Member States, AU, CN, and NO (+20% others)

The ERS-1 and SIR-C SAR systems are introduced. Attempts to meet future user requirements by developing a long antenna, wide swath SAR and a multimode SAR are reviewed. Trends in SAR antennas, high power amplifiers, and real time SAR processing are discussed. ESA

N87-17324# INTERA Environmental Consultants Ltd., Ottawa (Ontario).

THERMAL INFRARED REMOTE SENSING: ONE OF TODAY'S SOLUTIONS

J. P. TRACEY and G. R. LAWRENCE *In* ESA Proceedings of the 1986 International Geoscience and Remote Sensing Symposium (IGARSS '86) on Remote Sensing: Today's Solutions for Tomorrow's Information Needs, Volume 2 p 967-973 Aug. 1986

Avail: NTIS HC A17/MF A01; ESA, Paris, France, 3 volume set \$90 Member States, AU, CN, and NO (+20% others)

Airborne thermal infrared linescanning programs for environmental and engineering applications are summarized. Individual airborne thermal surveys are discussed with pertinent logistics described for each. Thermal infrared imagery for specific applications is included. It is shown how operational thermal imaging linescanning programs are utilized to satisfy the requirements of resource and utility managers. ESA

N87-17325# Tokyo Univ. (Japan).

MODELS FOR TEMPERATURE ESTIMATION FROM REMOTELY SENSED THERMAL IR DATA

S. FUJIMURA and T. YOKOTA *In* ESA Proceedings of the 1986 International Geoscience and Remote Sensing Symposium (IGARSS '86) on Remote Sensing: Today's Solutions for Tomorrow's Information Needs, Volume 2 p 975-980 Aug. 1986

Avail: NTIS HC A17/MF A01; ESA, Paris, France, 3 volume set \$90 Member States, AU, CN, and NO (+20% others)

The accuracy of the temperatures estimated from remotely sensed thermal IR data was evaluated by comparison with ground measurements. A relation between them is derived from a simple physical model, on which the evaluation should be based. The atmosphere is represented by a thin layer with a transmittance and an effective temperature. Four kinds of models slightly modified from one to another are considered. The regression coefficients obtained through regression analysis by taking the estimated temperature as dependent variable, and the measured one as independent variable are discussed. It is shown for all the models that the regression coefficient should be less than 1. Most of actual data taken over the sea satisfy this relation. ESA

N87-17329# Kanazawa Univ. (Japan).

RADIOMETRIC CORRECTION METHOD WHICH REMOVES BOTH ATMOSPHERIC AND TOPOGRAPHIC EFFECTS FROM THE LANDSAT-MSS DATA

Y. KAWATA, S. UENO, and T. KUSAKA *In* ESA Proceedings of the 1986 International Geoscience and Remote Sensing Symposium (IGARSS '86) on Remote Sensing: Today's Solutions for Tomorrow's Information Needs, Volume 2 p 1001-1004 Aug. 1986

Avail: NTIS HC A17/MF A01; ESA, Paris, France, 3 volume set \$90 Member States, AU, CN, and NO (+20% others)

A radiometric correction method which can remove atmospheric and topographic effects from rugged terrain image data remotely sensed by LANDSAT was applied to a mountainous test site where digital terrain data is available. The values of necessary atmospheric parameters, such as the optical thickness, the single scattering albedo, and the turbidity factor of the atmosphere were derived from LOWTRAN 5 Code in the evaluation of scattering and transmission functions. Lambert's law of reflection on the ground surface is assumed. Results are satisfactory. ESA

N87-17353# Kombinet VEB Carl Zeiss, Jena (East Germany).

OPTICAL VISUAL EVALUATION AND INTERPRETATION OF REMOTE SENSING DATA

W. MARCKWARDT *In* ESA Proceedings of the 1986 International Geoscience and Remote Sensing Symposium (IGARSS '86) on Remote Sensing: Today's Solutions for Tomorrow's Information Needs, Volume 2 p 1155-1159 Aug. 1986

Avail: NTIS HC A17/MF A01; ESA, Paris, France, 3 volume set \$90 Member States, AU, CN, and NO (+20% others)

A photographic system for satellite-borne remote sensing is described. The multispectral camera operates with 6 parallelly aligned normal-angle lenses of 125 mm focal length and 6 separate cassettes for 70 mm film. The film frames have the format 81 mm x 56 mm with the longer side being transverse to the flight direction. A narrow-band interference filter is attached to each lens (centroid wavelengths 480, 540, 600, 660, 720, 840 nm). At 250 km altitude, the camera supplies photographs at the scale 1:2,000,000 covering an area of 160 km x 110 km and allowing a detail recognizability of 10 to 25 m. Ground processing is achieved by instruments for multispectral projection, stereoscopic viewing and superposition, and optical-mechanical rectification. ESA

N87-17358# National Space Development Agency, Ibaraki (Japan).

A SATELLITE-BORNE SAR TRANSMITTER AND RECEIVER

M. FUKAI, K. NISHIKAWA, I. IZUMI, T. TSUJI, H. KONDO, H. KASHIHARA, H. NISHINO, K. TANAKA, Y. HISADA, and Y. ITOH *In* ESA Proceedings of the 1986 International Geoscience and Remote Sensing Symposium (IGARSS '86) on Remote Sensing: Today's Solutions for Tomorrow's Information Needs, Volume 2 p 1187-1192 Aug. 1986

Avail: NTIS HC A17/MF A01; ESA, Paris, France, 3 volume set \$90 Member States, AU, CN, and NO (+20% others)

A SAR transmitter-receiver for Earth observations from space was designed for the Japanese Earth Resources Satellite-1. Thermal vacuum and vibration tests were executed on critical components, i.e., the oscillator, the high power amplifier, the power supply for the high power amplifier, and the chirp pulse generator. Results prove that the thermal and structural design is satisfactory. Subsystem designs were verified by evaluating the SAR R and D model. ESA

N87-17360# National Space Development Agency, Ibaraki (Japan). Tsukuba Space Center.

PULSE COMPRESSION TEST RESULTS OF THE SAR TRANSMITTER AND RECEIVER

K. TANAKA, H. SHINOHARA, H. NISHINO, H. KASHIHARA, K. NISHIKAWA, Y. HISADA, and Y. ITOH *In* ESA Proceedings of the 1986 International Geoscience and Remote Sensing Symposium (IGARSS '86) on Remote Sensing: Today's Solutions for Tomorrow's Information Needs, Volume 2 p 1195-1200 Aug. 1986

Avail: NTIS HC A17/MF A01; ESA, Paris, France, 3 volume set \$90 Member States, AU, CN, and NO (+20% others)

The pulse compression test principle and the test results on the breadboard model of the spaceborne SAR for the Japanese Earth Resources Satellite 1 are summarized. Using their own transmitter chirp pulse as the test signal for the transmitter-receiver, the resultant receiver output pulses are digitized and recorded by high density digital tape recorder then processed by the ideal matched-filter. The usefulness of the pulse compression test method for evaluation of the SAR transmitter-receiver in view of range focusing capability is emphasized. A pulse compression ratio greater than 392 is obtained. ESA

N87-17363# European Space Agency, Paris (France).
PROCEEDINGS OF AN ESA WORKSHOP ON ERS-1 WIND AND WAVE CALIBRATION

J. J. HUNT, ed. Noordwijk, Netherlands Sep. 1986 240 p
 Workshop held in Schliersee, West Germany, 2-6 Jun. 1986; sponsored by ESA
 (ESA-SP-262; ISSN-0072-6566; ETN-87-98836) Avail: NTIS HC A11/MF A01

Classification of ERS-1 wind and wave measurements; wind and wave models; surface and airborne measurements to calibrate the ERS-1 instruments; and planned and on-going climate and oceanographic programs were discussed.

ESA

N87-17364# European Space Agency. European Space Research and Technology Center, ESTEC, Noordwijk (Netherlands).

ERS-1 MISSION CONSTRAINTS RELATED TO WIND AND WAVE CALIBRATION

JACQUES LOUET *In its* Proceedings of an ESA Workshop on ERS-1 Wind and Wave Calibration p 3-10 Sep. 1986
 Avail: NTIS HC A11/MF A01

The approach taken for validation and calibration of the ERS-1 mission is outlined. A clear distinction is made between the engineering and geophysical performances of the mission. The pre and post-launch activities required to calibrate the ERS-1 system and validate the geophysical performance are described.

ESA

N87-17379# Canada Centre for Remote Sensing, Ottawa (Ontario).

CANADA CENTER FOR REMOTE SENSING (CCRS) CONVAIR 580 RESULTS RELEVANT TO ERS-1 WIND AND WAVE CALIBRATION

NELSON G. FREEMAN, A. L. GRAY, R. K. HAWKINS, and C. E. LIVINGSTONE *In* ESA Proceedings of an ESA Workshop on ERS-1 Wind and Wave Calibration p 101-109 Sep. 1986
 Avail: NTIS HC A11/MF A01

Results from Convaire 580 wind and wave measurement campaigns are presented to demonstrate the usefulness of such an airborne microwave research facility for ERS-1 dedicated calibration and validation experiments. Scatterometer measurements from the PROMESS campaigns show that C-band sensitivity for wind speeds (2 to 12 m/sec) is 70% to 80% of the Ku-band sensitivity. It is also shown that the ERS-1 active microwave image mode should be able to detect surface oil as a 5 to 7 dB drop in scattering cross section when observed at 23 deg incidence angle. Ship targets, however, may be lost in the sea clutter for wind speeds greater than 8m/sec. Results from the Cape Sable SAR wave imaging experiments indicate that airborne SAR can be used to investigate the effect of R/V scaling and look direction on azimuthal falloff in SAR derived directional wave spectra.

ESA

N87-17382# Meteorological Office, Bracknell (England).
THE USE OF AIRCRAFT FOR WIND SCATTEROMETER CALIBRATION

DAVID OFFILER *In* ESA Proceedings of an ESA Workshop on ERS-1 Wind and Wave Calibration p 131-134 Sep. 1986
 Avail: NTIS HC A11/MF A01

The use of a Hercules aircraft to assist in the calibration and verification of ERS wind scatterometer products is proposed. The capabilities of this aircraft and its advantages are described, and compared to other sources of calibration data.

ESA

N87-17387# Commonwealth Scientific and Industrial Research Organization, Aspendale (Australia). Div. of Atmospheric Research.

AUSTRALIAN VALIDATION PLANS FOR ERS-1

IAN J. BARTON *In* ESA Proceedings of an ESA Workshop on ERS-1 Wind and Wave Calibration p 165-168 Sep. 1986
 Avail: NTIS HC A11/MF A01

Australian calibration/validation plans for the instruments carried on the ERS-1 satellite are described. A large experiment is planned for 1990 in the tropical waters to the north-east of the continent. Although the prime concern of this experiment is the validation of the along track scanning radiometer in tropical areas there will be side programs involving the validation of the products from the microwave instrumentation. Extended comparison between measurements from two HF radars (one ground-wave and one sky-wave) and the ERS-1 data will also be attempted. Other studies planned relate to the calibration and general use of data both over land and ocean surfaces and in Antarctica.

ESA

N87-17410 Florida State Univ., Tallahassee.

VARIABILITY IN THE EARTH RADIATION BUDGET AS DETERMINED FROM THE NIMBUS ERB EXPERIMENTS Ph.D. Thesis

PHILIP EDWARD ARDANUY 1986 344 p
 Avail: Univ. Microfilms Order No. DA8619135

Data taken by the Earth Radiation Budget (ERB) experiment on board the Nimbus-6 and Nimbus-7 satellites is examined. The goal is an understanding of the bounds of variability of the radiation budget components. This variability is examined on daily, monthly, and annual time scales. An in-flight characterization of the instrument was performed, and a set of calibration adjustments for the Nimbus-7 ERB was developed that enabled interannual climate studies to be made. A technique for the transfer of this calibration to the Nimbus-6 ERB experiment was derived that enables the creation of a decadal joint ERB data set. Error bars for the data set were established. The radiation budget component (albedo and longwave emission) responses to the 1982 eruptions of the El Chichon volcano were examined. Based on the observations, an understanding of the global distribution, evolution, and persistence of the resultant aerosol cloud was achieved. The evolution of the major 1982/1983 ENSO event was monitored for the first time by broadband radiometers. Quasi-stationary, planetary-scale tropical and midlatitude teleconnection patterns are shown to emerge as the event reaches its peak intensity. The onset, intensification, and withdrawal of drought over Indonesia, Australia, the Pacific Ocean island chains, and the Amazon River Valley was monitored based on inferred irrotational, three-dimensional flow fields. Anomalous subsidence, forced by the ENSO episode was noted over all drought regions.

Dissert. Abstr.

N87-18142# European Space Agency, Paris (France).

PROCEEDINGS OF THE 1986 INTERNATIONAL GEOSCIENCE AND REMOTE SENSING SYMPOSIUM (IGARSS '86) ON REMOTE SENSING: TODAY'S SOLUTIONS FOR TOMORROW'S INFORMATION NEEDS, VOLUME 3

T. D. GUYENNE, ed. and J. J. HUNT, ed. Noordwijk, Netherlands Aug. 1986 491 p Symposium held in Zurich, Switzerland, 8-11 Sep. 1986; sponsored by NASA, ESA, EARSeL, NOAA, CNES, DFVLR, Swiss Academy of Sciences, Swiss Assoc. for Space Technology, Contraves Ltd., Dornier-Werke GmbH, International Union of Radio Science, et al.
 (ESA-SP-254-VOL-3; IEEE-86CH2268-VOL-3; LC-86-80109; ISSN-0379-6566; ETN-87-98537) Avail: NTIS HC A21/MF A01; ESA, Paris, France, 3 volume set \$90 Member States, AU, CN, and NO (+20% others)

Remote sensing of soils; geographic information systems; oceanography; altimetry; oil pollution monitoring; stress detection in forestry and vegetation; SAR processing; vegetation and land use; mapping; and laser induced fluorescence were discussed.

ESA

N87-18161# Johns Hopkins Univ., Laurel, Md. Applied Physics Lab.

DEVELOPMENT IN RADAR ALTIMETRY: THE NAVY GEOSAT MISSION

C. C. KILGUS and J. L. MACARTHUR *In* ESA Proceedings of the 1986 International Geoscience and Remote Sensing Symposium (IGARSS '86) on Remote Sensing: Today's Solutions for Tomorrow's Information Needs, Volume 3 p 1321-1326 Aug. 1986

(Contract N00024-86-PR-69506)

Avail: NTIS HC A21/MF A01; ESA, Paris, France, 3 volume set \$90 Member States, AU, CN, and NO (+20% others)

The Geosat radar altimeter and its data set are described. The Geosat radar altimeter is identical to the SEASAT-A altimeter in terms of the mechanical, thermal, and electrical interfaces. Changes were made primarily to support an 18-month mission goal. These include use of a 20-W long-life TWT amplifier and, for improved radiation tolerance, an 8085 microprocessor. Other changes include substitutions for parts no longer available and revised firmware tracking algorithms for reduced height noise. It measures altitude: 3.5 cm for 2-m significant wave height; significant wave height: 10% of significant wave height or 0.5 m; and wind speed: 1.8 m/sec over the range 1 to 18 m/sec. ESA

N87-18164# Mullard Space Science Lab., Dorking (England).
NEW TECHNIQUES IN SATELLITE ALTIMETER TRACKING SYSTEMS

D. J. WINGHAM, C. G. RAPLEY, and H. GRIFFITHS (University Coll., London, England) *In* ESA Proceedings of the 1986 International Geoscience and Remote Sensing Symposium (IGARSS '86) on Remote Sensing: Today's Solutions for Tomorrow's Information Needs, Volume 3 p 1339-1344 Aug. 1986

(Contract ESTEC-6079/84-NL-PB(SC))

Avail: NTIS HC A21/MF A01; ESA, Paris, France, 3 volume set \$90 Member States, AU, CN, and NO (+20% others)

A satellite radar altimeter tracking algorithm was designed to permit robust tracking of topographic surfaces without compromising the accuracy or precision of the altimeter over the ocean. The altimeter was applied to the SEASAT system. It generates a pulse shape independent linear height error and a pulse shape dependent gain error. The algorithm has acceptable performance in the presence of fading and thermal noise. ESA

N87-18178# Deutsche Forschungs- und Versuchsanstalt fuer Luft- und Raumfahrt, Oberpfaffenhofen (West Germany).

INTELLIGENT SAR PROCESSOR (ISAR), A NEW CONCEPT FOR HIGH THROUGHPUT AND HIGH PRECISION DIGITAL SAR PROCESSING

W. NOACK, A. POPELLA, and M. PICH *In* ESA Proceedings of the 1986 International Geoscience and Remote Sensing Symposium (IGARSS '86) on Remote Sensing: Today's Solutions for Tomorrow's Information Needs, Volume 3 p 1425-1432 Aug. 1986

Avail: NTIS HC A21/MF A01; ESA, Paris, France, 3 volume set \$90 Member States, AU, CN, and NO (+20% others)

The ISAR knowledge-based digital SAR processor for ERS-1 is presented. All central parts of the software system are managed by the expert system running on the Knowledge Engineering Workstation (KEW). The KEW controls the whole production process by receiving production, orders from the processing and archiving facility; configuring the production process; supervising the correlation sequence; and supporting the operator in all decision processes. The specified processing time of 30 min for a standard bulk product is possible using an ST-100 array processor, and considerable speed up is possible. ESA

N87-18180# Canada Centre for Remote Sensing, Ottawa (Ontario).

A VERY FAST SYNTHETIC-APERTURE RADAR SIGNAL PROCESSOR FOR ERS-1 AND RADARSAT

M. R. VANT and P. GEORGE (MacDonald, Dettwiler and Associates Ltd., Richmond, British Columbia) *In* ESA Proceedings of the 1986 International Geoscience and Remote Sensing Symposium (IGARSS '86) on Remote Sensing: Today's Solutions for Tomorrow's Information Needs, Volume 3 p 1437-1442 Aug. 1986

Avail: NTIS HC A21/MF A01; ESA, Paris, France, 3 volume set \$90 Member States, AU, CN, and NO (+20% others)

A SAR signal processor being developed for the Canadian ERS-1 ground station, capable of processing data from the Radarsat, ERS-1, SEASAT, and Japanese ERS-1 SAR satellites is described. The processing speed is projected to be 1/46 real-time rate for the production of either 6-look ERS-1 images or 4-look Radarsat images. For SEASAT 1/3 swath, 4-look images the rate will be slower, 1/74 real-time rate. ESA

N87-18197# Chalmers Univ. of Technology, Goeteborg (Sweden). Dept. of Radio and Space Science.

ATMOSPHERIC WATER VAPOR CORRECTIONS FOR ALTIMETRY MEASUREMENTS

J. ASKNE, G. ELGERED, and H. NORDIUS *In* ESA Proceedings of the 1986 International Geoscience and Remote Sensing Symposium (IGARSS '86) on Remote Sensing: Today's Solutions for Tomorrow's Information Needs, Volume 3 p 1543-1548 Aug. 1986 Sponsored by ESA and the Swedish Board for Space-Activities

Avail: NTIS HC A21/MF A01; ESA, Paris, France, 3 volume set \$90 Member States, AU, CN, and NO (+20% others)

Two methods to estimate path delay based on atmospheric modeling were developed. One uses a closed form model of the atmosphere where two parameters describe typical variations of temperature and humidity with height. The other employs discretized atmospheric profiles derived from radiosonde statistics and surface data. Methods for delay estimation by water vapor radiometry were also developed. The methods are compared with radiosonde data. Root mean square errors range from 3.9 cm for the closed form model to 0.77 cm for the best water vapor radiometry algorithm. The use of water vapor estimates from meteorological satellites and possibilities to improve these are discussed. ESA

N87-18219# Indian Space Research Organization, Ahmedabad. Space Applications Centre.

RETRIEVAL AND GLOBAL COMPARISON OF OCEANIC WINDS FROM SEASAT RADIOMETER, SCATTEROMETER AND ALTIMETER

P. C. PANDEY *In* ESA Proceedings of the 1986 International Geoscience and Remote Sensing Symposium (IGARSS '86) on Remote Sensing: Today's Solutions for Tomorrow's Information Needs, Volume 3 p 1677-1681 Aug. 1986

Avail: NTIS HC A21/MF A01; ESA, Paris, France, 3 volume set \$90 Member States, AU, CN, and NO (+20% others)

Wind speed was retrieved using different channel combinations of SEASAT Scanning Multichannel Microwave Radiometer data. Comparison with high quality in situ observations obtained during Joint Air-Sea Interaction Experiment gives an rms difference of better than + or - 2 m/sec. Global maps of oceanic winds were generated and compared with maps obtained from scatterometer and altimeter derived winds. The three sensors depict general features of wind distribution but differ quantitatively over certain latitude belts. ESA

N87-18221*# Rochester Inst. of Tech., N. Y.
RADIOMETRIC ANALYSIS OF THE LONGWAVE INFRARED CHANNEL OF THE THEMATIC MAPPER ON LANDSAT 4 AND 5 Digital Imaging and Remote Sensing Lab.
 JOHN R. SCHOTT, WILLIAM J. VOLCHOK, and JOSEPH D. BIEGEL 1986 85 p
 (Contract NAS5-27323)
 (NASA-CR-180180; NAS 1.26:180180; RIT/DIRS-86/87-51-112)
 Avail: NTIS HC A05/MF A01 CSCL 14B

The first objective was to evaluate the postlaunch radiometric calibration of the LANDSAT Thematic Mapper (TM) band 6 data. The second objective was to determine to what extent surface temperatures could be computed from the TM and 6 data using atmospheric propagation models. To accomplish this, ground truth data were compared to a single TM-4 band 6 data set. This comparison indicated satisfactory agreement over a narrow temperature range. The atmospheric propagation model (modified LOWTRAN 5A) was used to predict surface temperature values based on the radiance at the spacecraft. The aircraft data were calibrated using a multi-altitude profile calibration technique which had been extensively tested in previous studies. This aircraft calibration permitted measurement of surface temperatures based on the radiance reaching the aircraft. When these temperature values are evaluated, an error in the satellite's ability to predict surface temperatures can be estimated. This study indicated that by carefully accounting for various sensor calibration and atmospheric propagation effects, and expected error (1 standard deviation) in surface temperature would be 0.9 K. This assumes no error in surface emissivity and no sampling error due to target location. These results indicate that the satellite calibration is within nominal limits to within this study's ability to measure error.

Author

N87-18697*# Jet Propulsion Lab., California Inst. of Tech., Pasadena.

SHUTTLE IMAGING RADAR-C SCIENCE PLAN

1 Sep. 1986 180 p Original contains color illustrations
 (Contract NAS7-918)
 (NASA-CR-180241; JPL-PUB-86-29; NAS 1.26:180241) Avail:
 NTIS HC A09/MF A01 CSCL 17I

The Shuttle Imaging Radar-C (SIR-C) mission will yield new and advanced scientific studies of the Earth. SIR-C will be the first instrument to simultaneously acquire images at L-band and C-band with HH, VV, HV, or VH polarizations, as well as images of the phase difference between HH and VV polarizations. These data will be digitally encoded and recorded using onboard high-density digital tape recorders and will later be digitally processed into images using the JPL Advanced Digital SAR Processor. SIR-C geologic studies include cold-region geomorphology, fluvial geomorphology, rock weathering and erosional processes, tectonics and geologic boundaries, geobotany, and radar stereogrammetry. Hydrology investigations cover arid, humid, wetland, snow-covered, and high-latitude regions. Additionally, SIR-C will provide the data to identify and map vegetation types, interpret landscape patterns and processes, assess the biophysical properties of plant canopies, and determine the degree of radar penetration of plant canopies. In oceanography, SIR-C will provide the information necessary to: forecast ocean directional wave spectra; better understand internal wave-current interactions; study the relationship of ocean-bottom features to surface expressions and the correlation of wind signatures to radar backscatter; and detect current-system boundaries, oceanic fronts, and mesoscale eddies. And, as the first spaceborne SAR with multi-frequency, multipolarization imaging capabilities, whole new areas of glaciology will be opened for study when SIR-C is flown in a polar orbit.

Author

GENERAL

Includes economic analysis.

A87-20682

SPACE REMOTE SENSING

JOHN MCELROY (Earth Observation Satellite Co., New York) Spaceflight (ISSN 0038-6340), vol. 28, Sept.-Oct. 1986, p. 358-360.

A review of the U.S. Land Remote Sensing Programme (Landsat) from the Launch of ERTS in 1972 through the program's transfer to the private sector in 1985 is presented. The spacecraft design chosen by EOSAT for the future Landsats 6 and 7 is the OMNISTAR long life platform which will provide flexible design for Shuttle launch, retrieval and in-orbit refurbishment and component replacements. The platform contains instruments and subsystems designed for a minimum of five years in-orbit life. Applications include bathymetry, meteorology, and oceanography. R.R.

A87-25531

PARTNERSHIPS IN REMOTE SENSING - A THEME WITH SOME EXAMPLES

WILLIAM P. BISHOP (NOAA, National Environmental Satellite, Data, and Information Service, Washington, DC) Space Policy (ISSN 0265-9646), vol. 2, Nov. 1986, p. 322-341. refs

This article reviews the revolution in remote sensing which has taken place over the past 25 years. This revolution could not have occurred without the closest cooperation among government agencies, industry and academia. International cooperation is shown to be essential in carrying out the bold missions planned for the next decade. The article reviews the history of the NASA-NOAA relationship, and the history of international partnerships with emphasis on development of the operational Metsat system. The government-industry partnership is also reviewed, with case studies to examine the evolution of Metsat sensor design, Landsat commercialization, and the NOAA Administrator's new initiative to facilitate development of a commercial Ocean Color Instrument. Government interaction with academia, in the form of National Science Foundation programs and government-university 'cooperative institutes', is reviewed. The author concludes by showing how plans for integrating research and operations on Space Station platforms can only succeed through an alliance of all the remote-sensing players. Author

A87-27452

SOVIET REMOTE SENSING

K. IA. KONDRATEV and IU. P. KIENKO (Academy of Sciences, Remote Sensing Institute, USSR) Space (ISSN 0267-954X), vol. 2, Dec. 1986-Feb. 1987, p. 11-15.

Initial Soviet progress in satellite earth imaging systems was in applications for meteorology, climatology, and oceanography. Subsequent systems were dedicated to hydrologic and geologic mapping missions, chiefly through thematic mapper instrumentation. A new emphasis is being put on linking global earth resources monitoring systems and moving remote sensing systems from experimental to operational status. Sample images of the U.S.S.R. are provided, noting recent attempts to integrate the remote sensing functions of Kosmos and Meteor satellites, the Mir and Salyut space stations, airborne, fixed and mobile ground and sea stations. A chief goal of current remote sensing is exploration for mineral deposits. M.S.K.

**A87-29433
BUSINESS APPROACH TO EARTH OBSERVATION
APPLICATIONS**

BRUNO RATTI (Telespazio S.p.A., Rome, Italy) IN: Space commerce '86; Proceedings of the International Conference and Exhibition on the Commercial and Industrial Uses of Outer Space, Montreux, Switzerland, June 16-20, 1986. Geneva, Interavia Publishing Group, 1986, p. 381-386.

The business side of commercial remote sensing operations is examined. Satellite sensors can collect data on resources, e.g., mineralogical or agricultural, and atmospheric and oceanic processes, e.g., climate and currents. It is easier to assign a value to measurements of tangible resources than to intangible factors such as the environment, although all resource monitoring is useful, and in many cases necessary, due to rapid population growth, on the global, regional and local scales. Graphic techniques are defined for assessing the economic feasibility of establishing and operating a remote sensing system, manufacturing sensors, or operating in the presence or competition. No fully commercial remote sensing operation now exists; both EOSAT and SPOT rely heavily on various forms of subsidies from the U.S. and French governments, respectively. M.S.K.

**A87-30876
SPACE SCIENCE AND APPLICATIONS: PROGRESS AND
POTENTIAL**

JOHN H. MCELROY, ED. (Hughes Aircraft Co., Space and Communications Group, Los Angeles, CA) New York, IEEE Press, 1986, 270 p. For individual items see A87-30877 to A87-30893.

The evolution, growth, goals and applications of space technologies and capabilities are explored in depth. Experimentation using manned and unmanned spacecraft, Skylab, and the Shuttle to explore sun-earth relations, phenomena and planetary bodies in the solar system, observe and measure astrophysical phenomena, and perform life sciences studies are described. The applications, data collected, and future systems for remote sensing of the earth are summarized. Past, present, and future studies of and industrial scale performance of processing materials in space are examined, with emphasis on NASA efforts to foster commercial development in this area. Finally, the evolution and capabilities of the technologies, designs, and applications of satellites communications systems for data transfer, navigation, telephony, television broadcasts, etc., is traced. The impacts the Space Station and related systems will have on current and future operational space systems are also explored. M.S.K.

**A87-30881
REMOTE SENSING FROM SPACE - AN OVERVIEW**

RALPH BERNSTEIN (IBM Scientific Center, Palo Alto, CA) IN: Space science and applications: Progress and potential. New York, IEEE Press, 1986, p. 71-76.

Current and future capabilities and applications of space-based remote sensing of the earth are described. A brief history of remote sensing is also presented, starting from Aristotle's camera obscura 2300 yr in the past. Research to date on space-based imaging has concentrated on sensor development and preprocessing techniques. Future research will target information extraction, understanding and modeling. The capabilities of the Landsat series of spacecraft and the SPOT are reviewed, noting a move toward merging the sensors with digital processing technology, and toward partially automated image processing capabilities which will ameliorate present labor-intensive analysis and processing procedures. One option that is described is to include on-board selection of packaged algorithms for image processing. The human role will become that of applying sophisticated phenomenon models to information from massive databases. M.S.K.

N87-16662# Executive Office of the President, Washington, D.C.

**AERONAUTICS AND SPACE REPORT OF THE PRESIDENT:
1985 ACTIVITIES**

1986 132 p
Avail: NTIS HC A07/MF A01

The achievements of aeronautics and space programs in the United States for 1985 are summarized in the areas of communications; Earth atmosphere, environment, and resources; space science; space transportation; commercial use of space; space tracking and data systems; space station; and aeronautics and space research and technology. The achievements of each of the following organizations are described: National Aeronautics and Space Administration, Department of Defense, Department of Commerce, Department of Energy, Department of the Interior, Department of Agriculture, Federal Communications Commission, Department of Transportation, Environmental Protection Agency, National Science Foundation, Smithsonian Institution, Department of State, Arms Control and Disarmament Agency, and United States Information Agency. Appendices provide historical information on launches, satellites, manned and unmanned spacecraft, and federal budgets for aeronautical and astronautical activities. J.P.B.

N87-17170# Florida International Univ., Miami. Dept. of International Business.

**THE TRANSFER OF REMOTE SENSING TECHNOLOGY TO
DEVELOPING COUNTRIES: A SURVEY OF EXPERTS IN THE
FIELD**

C. SPECTER *In* ESA Proceedings of the 1986 International Geoscience and Remote Sensing Symposium (IGARSS '86) on Remote Sensing: Today's Solutions for Tomorrow's Information Needs, Volume 1 p 41-44 Aug. 1986
Avail: NTIS HC A99/MF E03; ESA, Paris, France, 3 volume set \$90 Member States, AU, CN, and NO (+20% others)

The transfer of LANDSAT-related remote sensing technology from the United States to developing countries was examined. A questionnaire was sent to experts in the field of remote sensing technology to determine what they perceived as the major barriers to remote sensing technology transfer (RSTT). Useable questionnaire responses were received from 618 professionals in 63 countries. Responses of participants representing developed countries, developing countries, and international organizations were compared in order to identify similarities and differences in their perceptions of the RSTT barriers. Of the eight major barriers identified, five are related to economics. Participants tend to perceive the withdrawal of the U.S. government from management of the LANDSAT system, the lack of knowledge about application of remote sensing technology among government decision-makers in developing countries, and the lack of personnel experienced in using computer compatible tapes as major RSTT barriers. ESA

N87-17177# Earth Observation Satellite Co., Va.
**COMMERCIAL OPPORTUNITIES IN EARTH OBSERVATION
FROM SPACE**

C. P. WILLIAMS *In* ESA Proceedings of the 1986 International Geoscience and Remote Sensing Symposium (IGARSS '86) on Remote Sensing: Today's Solutions for Tomorrow's Information Needs, Volume 1 p 73-76 Aug. 1986
Avail: NTIS HC A99/MF E03; ESA, Paris, France, 3 volume set \$90 Member States, AU, CN, and NO (+20% others)

Land and ocean remote sensing programs are listed. The LANDSAT and SPOT instruments are described. Commercial prospects for the 21st century are considered. ESA

09 GENERAL

N87-18152# Geological Survey, Reston, Va.

THE USE OF SPACE TECHNOLOGY IN FEDERALLY FUNDED LAND PROCESSES RESEARCH IN THE UNITED STATES

G. A. THORLEY and R. MCARDLE (Department of Agriculture, Washington, D.C.) /n ESA Proceedings of the 1986 International Geoscience and Remote Sensing Symposium (IGARSS '86) on Remote Sensing: Today's Solutions for Tomorrow's Information Needs, Volume 3 p 1267-1272 Aug. 1986

Avail: NTIS HC A21/MF A01; ESA, Paris, France, 3 volume set \$90 Member States, AU, CN, and NO (+20% others)

The use of space technology in federally funded Earth science research in the United States was reviewed. Government departments and independent agencies, representing the primary Earth science research agencies in the Federal government, participated in the review: NASA, NOAA, Department of the Interior, Department of Agriculture, Department of Energy, U.S. Army Corps of Engineers, Agency for International Development, National Science Foundation, and Environmental Protection Agency. The review indicates that, while there is considerable overlap in the legislated missions of the Earth science agencies, most of the space-related land processes research is complementary. ESA

N87-18227# Instituto Nacional de Tecnica Aeroespacial, Madrid (Spain). Dept. de Avionica y Electrooptica.

REMOTE SENSING LABORATORY [LABORATORIO DE TELEDETECCION]

RITA BARCALA MONTEJANO and JESUS GUTIERREZDELACAMARAARA 1986 19 p In SPANISH; ENGLISH summary

(ETN-87-98850) Avail: NTIS HC A02/MF A01

Operational ground support of remote sensing from satellites or aircraft is described. The laboratory facilities are detailed. The activities include flight coordination, film and quick look processing, densitometry, scanner data conversion to computer compatible tape, image processing and analysis, and developing of new applications. ESA

N87-18907*# California Univ., Santa Barbara. Information Sciences Research Group.

REMOTE SENSING INFORMATION SCIENCES RESEARCH GROUP, YEAR FOUR

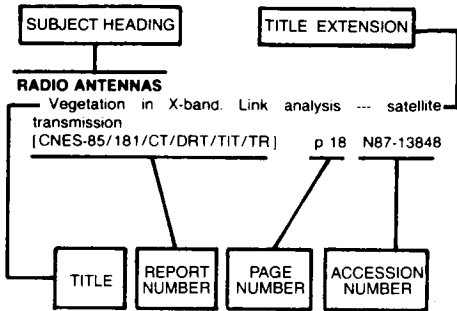
JOHN E. ESTES, TERENCE SMITH, and JEFFREY L. STAR 1 Jan. 1987 140 p

(Contract NAGW-455)

(NASA-CR-180198; NAS 1.26:180198) Avail: NTIS HC A07/MF A01 CSCL 05B

The needs of the remote sensing research and application community which will be served by the Earth Observing System (EOS) and space station, including associated polar and co-orbiting platforms are examined. Research conducted was used to extend and expand existing remote sensing research activities in the areas of georeferenced information systems, machine assisted information extraction from image data, artificial intelligence, and vegetation analysis and modeling. Projects are discussed in detail. B.G.

Typical Subject Index Listing



The subject heading is a key to the subject content of the document. The title is used to provide a description of the subject matter. When the title is insufficiently descriptive of the document content, the title extension is added, separated from the title by three hyphens. The (NASA or AIAA) accession number and the page number are included in each entry to assist the user in locating the abstract in the abstract section. If applicable, a report number is also included as an aid in identifying the document. Under any one subject heading, the accession numbers are arranged in sequence with the AIAA accession numbers appearing first.

A

ABSORPTION SPECTRA

Interrelationship between field spectra and airborne MSS systems in the Singatse range, (Yerington) Nevada --- multispectral scanner (MSS) mineral exploration p 34 N87-17242

ABSTRACTS

Physical oceanography program science abstracts [AD-A174019] p 55 N87-18961

ACCURACY

The effect of training data variability on classification accuracy p 64 A87-23796

ADRIATIC SEA

Space and time variability of the surface color field in the northern Adriatic Sea p 40 A87-23722

ADVECTION

The effect of local advection on the inference of soil moisture from thermal infrared radiances p 3 A87-23388

An objective method for computing advective surface velocities from sequential infrared satellite images p 39 A87-23717

AERIAL PHOTOGRAPHY

Optical and radar observations of the nonlinear interaction of gravity waves p 37 A87-20350

An initial evaluation of two digital airborne imagers for surveying spruce budworm defoliation p 1 A87-20671

Experimental results in soil moisture mapping using IR thermography p 2 A87-21246

Accuracy of population estimation from medium-scale aerial photography p 24 A87-23777

The production of orthophotographs by digital image processing techniques p 63 A87-23787

The data dilemma - How to properly construct and utilize aerial photo volume tables p 63 A87-23790

An information processing system for integration of data from remote sensors, aerial photographs and existing maps p 63 A87-23791

Estimation of density in young pine plantations using 35mm aerial photography p 5 A87-23819

Lineaments of eastern Cuba - Geological interpretation of aerial and space imagery p 28 A87-24384

A photographic technique for studying reflection indicatrices of vegetation cover p 5 A87-24388

The spectral reflectance of stands of Norway spruce and Scotch pine, measured from a helicopter p 7 A87-25586

Assessment of grassland phytomass with airborne video imagery p 8 A87-25590

Visualization by aerial thermography of hydrodynamic exchanges between the water table, streams and gravel pits in the Rhine plain north of Strasbourg p 58 A87-25746

Spatial-statistical characteristics of sea surface foam fields (from optical sounding data) p 42 A87-26531

Estimating pre-harvest production of maize in Kenya using large-scale aerial photography and radiometry p 9 A87-29004

Estimating and mapping grass cover and biomass from low-level photographic sampling p 9 A87-29005

Classification of reflectance on colour infrared aerial photographs and sub-tropical salt-marsh vegetation types p 10 A87-29012

Distribution and biomass of *Fucus vesiculosus* L. near a cooling-water effluent from a nuclear power plant in the Baltic Sea estimated by aerial photography p 43 A87-29014

Preliminary measurements of leaf spectral reflectance in the 8-14-micron p 10 A87-29018

A comparative test of photogrammetrically sampled digital elevation models p 66 A87-29499

Terrain analysis from digital patterns in geomorphometry and Landsat MSS spectral response p 66 A87-30127

Microcomputer-assisted video image analysis of lodging in winter wheat p 10 A87-30130

Spectral separation of moorland vegetation in airborne Thematic Mapper data p 10 A87-30897

Significance of space image, air photo and drainage linears in relation to west coast tectonics, India p 33 N87-17232

The use of remote sensing (including aerial photographs) to devise cost-effective methods for soil conservation in the Kocaeli Peninsula, Turkey p 20 N87-18149

First step in the use of remote sensing for regional mapping of soil organization data: Application in Brittany (France) and French Guiana p 23 N87-18193

AERIAL RECONNAISSANCE

Multilens cameras for high velocity/low altitude photoreconnaissance p 75 A87-23650

The ice conditions in the Greenland waters, 1980 [REPT-551.467.3.068(988)] p 53 N87-17428

AERONAUTICAL ENGINEERING

Aeronautics and space report of the President: 1985 activities p 87 N87-16662

AEROSOLS

SAM II measurements of Antarctic PSC's and aerosols --- Stratospheric Aerosol Measurement satellite - Polar Stratospheric Clouds p 75 A87-23546

Weather and atmosphere remote sensing p 77 A87-30885

Variability in the Earth radiation budget as determined from the Nimbus ERB experiments p 84 N87-17410

Arctic haze: Natural or pollution? [AD-A174025] p 55 N87-18931

The relationship between marine aerosol optical depth and satellite-sensed sea surface temperature [AD-A174337] p 55 N87-18963

AEROSPACE ENGINEERING

Aeronautics and space report of the President: 1985 activities p 87 N87-16662

AEROSPACE SCIENCES

Space science and applications: Progress and potential p 87 A87-30876

AFRICA

Monitoring East African vegetation using AVHRR data p 6 A87-24781

Monitoring the grasslands of the Sahel 1984-1985 p 7 A87-24787

Growing period and drought early warning in Africa using satellite data p 7 A87-24788

Assessment of ecological conditions associated with the 1980/81 desert locust plague upsurge in West Africa using environmental satellite data p 7 A87-24789

Rainfall estimation over the Sahel using Meteosat thermal infra-red data p 59 N87-15587

Observations of the seasonal variability of soil moisture and vegetation cover over Africa using satellite microwave radiometry p 12 N87-15593

AGRICULTURE

Thermography - Principles and application in the Oost-Gelderland remote sensing study project p 3 A87-21247

Agricultural remote sensing in South Carolina - A study of crop identification capabilities utilizing Landsat data p 4 A87-23806

Landsat Thematic Mapper digital information content for agricultural environments p 5 A87-23830

Identification of forest and agricultural edges using Landsat Thematic Mapper data - Preliminary results p 5 A87-23832

Mapping of agricultural lands in the USSR p 11 N87-15507

Modelisation of evapotranspiration and soil available water over an agricultural region applicable for remote sensing p 12 N87-15554

Use of remote sensing application for agricultural expansion into semi-arid areas of Kenya p 13 N87-15607

Applications of TIMS data in agricultural areas and related atmospheric considerations p 15 N87-17124

Comparison of Thematic Mapper (TM) and SPOT simulation data for agricultural applications in south west Germany p 16 N87-17165

Extraction of the backscatter coefficient of agricultural fields from an airborne SAR image p 16 N87-17265

Applications of remote sensing in the US Department of Agriculture p 17 N87-17285

Bare soil measurements with the Delft University Scatterometer (DUTSCAT) system (L-band) [REPT-64-220-86-T-1LH] p 24 N87-19797

AGRISTARS PROJECT

An overview of remote sensing agricultural applications in North America: Past, present and future p 17 N87-17284

AIR LAND INTERACTIONS

The Coastal Zone Color Scanner views the Bismarck Sea p 42 A87-26970

The fundamental problems for the energy balance study by satellite imagery p 66 N87-15590

AIR POLLUTION

Ozone formation in pollutant plumes: A reactive plume model with arbitrary crosswind resolution [PB86-236973] p 26 N87-18246

Arctic haze: Natural or pollution? [AD-A174025] p 55 N87-18931

AIR SAMPLING

Arctic haze: Natural or pollution? [AD-A174025] p 55 N87-18931

AIR SEA ICE INTERACTIONS

Large-scale short-period sea ice atmosphere interaction p 42 A87-27546

Imaging radar contributions to a major air-sea-ice interaction study in the Greenland Sea p 46 N87-17150

Application of the Seasat scatterometer to observations of wind speed and direction and Arctic ice/water boundaries p 48 N87-17259

AIR WATER INTERACTIONS

Optical and radar observations of the nonlinear interaction of gravity waves p 37 A87-20350

Data sensitivities of sea ice drift and ocean stress in North Atlantic high latitudes p 38 A87-20520

The effect of Hurricane Gloria on sea surface temperature patterns p 39 A87-23362

Month-to-month variability of ocean-atmosphere latent heat flux as observed from the Nimbus microwave radiometer p 39 A87-23391

Possibilities of using satellite data for computations of the ocean/atmosphere heat exchange in the Newfoundland energy-active ocean zone in winter p 41 A87-24379

SUBJECT

- Wind-wave relationship from Seasat radar altimeter data p 41 A87-24748
 Interpretation characteristics of space photographs of sea coasts with wind-induced surges p 43 A87-28509
- Report of the Fourth Session of the JSC/CCCO Tropical Ocean Global Atmosphere (TOGA) Scientific Steering Group [WCP-120] p 54 A87-18283
 Physical oceanography program science abstracts [AD-A174019] p 55 A87-18961
 SeaSoar CTD surveys during FASINEX --- Conductivity Temperature Depth (CTD); Frontal Air Sea Interaction Experiment (FASINEX) p 55 A87-18970
- AIRBORNE EQUIPMENT**
 A thermal device for aircraft measurement of the solid water content of clouds p 56 A87-20951
 Verification of small-scale water vapor features in VAS imagery using high resolution MAMS imagery --- VISSR Atmospheric Sounder - Multispectral Atmospheric Mapping Sensor p 62 A87-23348
 Aircraft and satellite thermographic systems for wildfire mapping and assessment [AIAA PAPER 87-0187] p 7 A87-24933
 Imaging radar polarimetry from wave synthesis p 76 A87-29849
 Thermal infrared remote sensing: One of today's solutions p 83 A87-17324
 Characterisation of internal wave surface patterns on airborne SAR imagery p 50 A87-17338
 The use of thermal airborne remote sensing for soil identification: A case study in Limousin (France) p 20 A87-18146
 On the discrimination between crude oil spills and monomolecular sea slicks by airborne remote sensors: Today's possibilities and limitations p 53 A87-18167
 Modelling of estuarine chlorophyll-A from an airborne scanner p 61 A87-18172
 STAR-VUE: A tactical ice navigation workstation p 54 A87-18181
 The processing of and information extraction from airborne SLAR data [NLR-MP-86004-U] p 23 A87-18919
- AIRBORNE LASERS**
 Chlorophyll pigment concentration using spectral curvature algorithms - An evaluation of present and proposed satellite ocean color sensor bands p 37 A87-20204
 Airborne laser profiling and mapping systems come of age p 75 A87-23786
- AIRBORNE/SPACEBORNE COMPUTERS**
 The SEU risk assessment of Z80A, 8086 and 80C86 microprocessors intended for use in a low altitude polar orbit p 74 A87-22025
- AIRCRAFT INSTRUMENTS**
 Development and experiment of airborne microwave rain-scatterometer/radiometer system. III - Rain measurement and its data analysis p 58 A87-28436
 Development and experiment of airborne microwave rain-scatterometer/radiometer system. IV - Microwave back-scattering experiment of ocean surface p 43 A87-28437
- AIRFOILS**
 Effects of a downstream disturbance on the structure of a turbulent plane mixing layer [AIAA PAPER 87-0197] p 74 A87-22476
- ALASKA**
 Influence of the Yukon River on the Bering Sea [NASA-CR-180356] p 56 A87-19877
- ALBEDO**
 Remotely sensed albedo of snow-covered lands p 56 A87-23361
- ALGAE**
 Distribution and biomass of *Fucus vesiculosus* L. near a cooling-water effluent from a nuclear power plant in the Baltic Sea estimated by aerial photography p 43 A87-29014
- ALGORITHMS**
 Further development of an improved altimeter wind speed algorithm p 42 A87-27848
 Sparse area stereo matching experiment [AD-A173601] p 66 A87-16388
 Simulation modeling and preliminary analysis of TIMS data from the Carin area and the northern Grapevine Mountains, Nevada p 31 A87-17120
 An automatic tracking mode switching algorithm for the ERS-1 altimeter p 81 A87-17195
 Developpement of algorithms to retrieve the water equivalent of snow cover from satellite microwave radiometer data p 60 A87-17264
 A two-step algorithm for the separate retrieval of ocean surface and atmospheric parameters from microwave radiometers p 50 A87-17341
 Basic research for the geodynamics program [NASA-CR-180137] p 27 A87-17415
- New techniques in satellite altimeter tracking systems p 85 A87-18164
- ALPS MOUNTAINS (EUROPE)**
 Snow cover recession in an Alpine ecological system p 18 A87-17316
- ALTIMETERS**
 Further development of an improved altimeter wind speed algorithm p 42 A87-27848
- ANALOG TO DIGITAL CONVERTERS**
 Integrating vector and satellite data to evaluate the adequacy of a grain silo network p 21 A87-18156
- ANDES MOUNTAINS (SOUTH AMERICA)**
 Tectonic geomorphology of the Andes with SIR-A and SIR-B p 32 A87-17136
 Thematic mapper studies of central Andean volcanoes [NASA-CR-180252] p 36 A87-18910
- ANNUAL VARIATIONS**
 Annual and interannual variability in large-scale convection over the eastern Pacific and tropical South America p 57 A87-23414
 Observations of the seasonal variability of soil moisture and vegetation cover over Africa using satellite microwave radiometry p 12 A87-15593
 Monitoring of large phenomena in developing countries through satellite imagery p 67 A87-17172
 Eastern-Western Arctic Sea Ice Analysis, 1985 [AD-A173972] p 55 A87-18298
- ANOMALIES**
 Improvement of the Earth's gravity field from terrestrial and satellite data [NASA-CR-180139] p 27 A87-17416
- ANTARCTIC REGIONS**
 SAM II measurements of Antarctic PSC's and aerosols --- Stratospheric Aerosol Measurement satellite - Polar Stratospheric Clouds p 75 A87-23546
 Antarctica - Measuring glacier velocity from satellite images p 57 A87-23699
 Large-scale short-period sea ice atmosphere interaction p 42 A87-27546
- ANTENNA ARRAYS**
 The Electronically Steered Thinned Array Radiometer (ESTAR) p 82 A87-17260
- ANTENNA DESIGN**
 The FRS-68010: A new concept for the acquisition and analysis of NOAA HRPT data p 68 A87-17206
 The Electronically Steered Thinned Array Radiometer (ESTAR) p 82 A87-17260
- APPLICATIONS PROGRAMS (COMPUTERS)**
 IRSAP: An improved approach in processing remotely sensed data --- Interactive Remote Sensing Applications Package (IRSAP) p 70 A87-17332
- AQUATIC PLANTS**
 Remote sensing of aquatic macrophyte distribution in upper Lake Marion p 57 A87-23826
- ARCHAEOLOGY**
 The Red River Valley archeological project p 31 A87-17128
- ARCTIC OCEAN**
 Observing the polar oceans with spaceborne radar p 46 A87-17151
 An inter-sensor comparison of the microwave signatures of Arctic sea ice p 46 A87-17184
 Active/passive microwave sensor comparison of MIZ-ice concentration estimates --- Marginal Ice Zone (MIZ) p 46 A87-17185
 Sea ice in the Greenland sea observed by the Nimbus-7 Scanning Multichannel Microwave Radiometer (SMMR) p 48 A87-17221
 Application of the Seasat scatterometer to observations of wind speed and direction and Arctic ice/water boundaries p 48 A87-17259
- ARGENTINA**
 Multiple incidence angle SIR-B experiment over Argentina p 80 A87-17157
- ARID LANDS**
 Spectral brightness and surface soil characteristics in an arid Mediterranean region (southern Tunisia) p 2 A87-21242
 The thematic mapper - A new tool for soil mapping in arid areas p 2 A87-21243
 Processing thematic mapper data for mapping in Tunisia p 2 A87-21244
 An application of thematic mapper data in Tunisia - Estimation of daily amplitude in near-surface soil temperature and discrimination of hypersaline soils p 2 A87-21245
 Calibration of Landsat data for sparsely vegetated semi-arid rangelands p 9 A87-29008
 Preliminary analysis of SPOT HRV multispectral products of an arid environment p 10 A87-29017
 The use of aerial remote sensing in a case study of desertification: Quixaba-PE [INPE-3963-PRE/980] p 11 A87-15519
 Rainfall estimation over the Sahel using Meteosat thermal infra-red data p 59 A87-15587
- Use of remote sensing application for agricultural expansion into semi-arid areas of Kenya p 13 A87-15607
 Surface albedo change in arid regions in the Sudan p 13 A87-15615
 Spatial analysis of the dynamics of an ecosystem by multistage remote sensing in Kenya p 16 A87-17173
 Assessment of soil degradation in an arid region using remote sensing p 20 A87-18148
- ARTIFICIAL INTELLIGENCE**
 Rock type discrimination with AI-based texture analysis algorithms p 28 A87-23782
- ARTIFICIAL SATELLITES**
 Aeronautics and space report of the President: 1985 activities p 87 A87-16662
- ASTRONOMICAL COORDINATES**
 The use of Doppler observations to obtain initial geodetic data and to derive plumbline deviations and quasi-geoid heights p 27 A87-28504
- ATLANTIC OCEAN**
 Data sensitivities of sea ice drift and ocean stress in North Atlantic high latitudes p 38 A87-20520
 Vertical structure of the temperature field above the North Atlantic p 40 A87-24374
 Shedding of an Agulhas ring observed at sea p 44 A87-30146
- ATMOSPHERIC ATTENUATION**
 An extension of the split window technique for the retrieval of precipitable water [AD-A173008] p 60 A87-16386
 Analysis of AIS radiometry at Mono Lake, California --- Airborne Imaging Spectrometer (AIS) p 81 A87-17204
 Radiometric analysis of the longwave infrared channel of the Thematic Mapper on LANDSAT 4 and 5 [NASA-CR-180180] p 86 A87-18221
- ATMOSPHERIC BOUNDARY LAYER**
 Ozone in the boundary layer of the equatorial Pacific Ocean p 41 A87-25534
- ATMOSPHERIC CIRCULATION**
 Atmospheric characteristics of the equatorial Pacific during the 1982-1983 El Nino, deduced from satellite and aircraft observations p 41 A87-25543
 Observations and analysis of a polar low over the Great Lakes region p 76 A87-27872
 NROSS (Navy Remote Ocean Sensing System) tracking network analysis [AD-A172132] p 45 A87-16384
- ATMOSPHERIC COMPOSITION**
 SAM II measurements of Antarctic PSC's and aerosols --- Stratospheric Aerosol Measurement satellite - Polar Stratospheric Clouds p 75 A87-23546
- ATMOSPHERIC CORRECTION**
 Estimation of absolute water surface temperature based on atmospherically corrected thermal infrared multispectral scanner digital data p 79 A87-17114
 Atmospheric correction of TIMS data p 79 A87-17115
- ATMOSPHERIC EFFECTS**
 Estimation of surface albedo using satellite data. A simple formulation for atmospheric effects p 25 A87-15579
 Applications of TIMS data in agricultural areas and related atmospheric considerations p 15 A87-17124
 Atmospheric corrections of NOAA-AVHRR data verification of different methods by ground truth measurements p 70 A87-17274
 Radiometric correction method which removes both atmospheric and topographic effects from the LANDSAT-MSS data p 83 A87-17329
 A two-step algorithm for the separate retrieval of ocean surface and atmospheric parameters from microwave radiometers p 50 A87-17341
- ATMOSPHERIC HEAT BUDGET**
 Evaluation of geophysical parameters measured by the Nimbus-7 microwave radiometer for the TOGA Heat Exchange Project [NASA-CR-180151] p 78 A87-17110
- ATMOSPHERIC MODELS**
 Atmospheric characteristics of the equatorial Pacific during the 1982-1983 El Nino, deduced from satellite and aircraft observations p 41 A87-25543
 Forecasting sea breeze thunderstorms at the Kennedy Space Center using the Prognostic Three-Dimensional Mesoscale Model (P 3DM) p 43 A87-27891
 Modélisation of evapotranspiration and soil available water over an agricultural region applicable for remote sensing p 12 A87-15554
 Remote sensing identified in climate model experiments with hydrological and albedo changes in the Sahel p 59 A87-15569
 The fundamental problems for the energy balance study by satellite imagery p 66 A87-15590
 Hydrological Atmospheric Pilot Experiment (HAPEX) hydrology budget modeling (MOBILHY): Outline of the program p 59 A87-15632

- Atmospheric correction of TIMS data
p 79 N87-17115
- Applications of TIMS data in agricultural areas and related atmospheric considerations p 15 N87-17124
- Atmospheric water vapor corrections for altimetry measurements p 85 N87-18197
- Ozone formation in pollutant plumes: A reactive plume model with arbitrary crosswind resolution [PB86-236973] p 26 N87-18246
- ATMOSPHERIC MOISTURE**
Atmospheric water vapor corrections for altimetry measurements p 85 N87-18197
- ATMOSPHERIC OPTICS**
Analysis of AIS radiometry at Mono Lake, California --- Airborne Imaging Spectrometer (AIS) p 81 N87-17204
- ATMOSPHERIC SOUNDING**
Verification of small-scale water vapor features in VAS imagery using high resolution MAMS imagery --- VISSR Atmospheric Sounder - Multispectral Atmospheric Mapping Sensor p 62 A87-23348
- Utilization of satellite data in mesoscale modeling of severe weather [NASA-CR-179917] p 78 N87-15669
- Proceedings of the 1986 International Geoscience and Remote Sensing Symposium (IGARSS '86) on Remote Sensing: Today's Solutions for Tomorrow's Information Needs, volume 1 [ESA-SP-254-VOL-1] p 80 N87-17163
- Proceedings of the 1986 International Geoscience and Remote Sensing Symposium (IGARSS '86) on Remote Sensing: Today's Solutions for Tomorrow's Information Needs, volume 2 [ESA-SP-254-VOL-2] p 82 N87-17283
- ATMOSPHERIC TEMPERATURE**
Vertical structure of the temperature field above the North Atlantic p 40 A87-24374
- ATMOSPHERIC WINDOWS**
On the use of synthetic 12-micron data in a split-window retrieval of sea surface temperature from AVHRR measurements p 43 A87-29019
- An extension of the split window technique for the retrieval of precipitable water [AD-A173008] p 60 N87-16386
- ATTENUATION COEFFICIENTS**
A description of large-scale variability in the ocean using the diffuse attenuation coefficient p 53 N87-18160
- B**
- BACKSCATTERING**
Theoretical approach to radar backscattering of soils p 3 A87-21250
- Measurement of microwave backscattering signatures of the ocean surface using X band and K(a) band airborne scatterometers p 40 A87-23725
- Microwave backscattering from a layer of randomly oriented discs with application to scattering from vegetation p 8 A87-28316
- Radar signature determination: Trends and limitations p 67 N87-17159
- Verification results for a two-scale model of microwave backscatter from the sea surface p 47 N87-17213
- Tower-based broadband backscattering measurements from the ocean surface in the North Sea p 47 N87-17217
- Extraction of the backscatter coefficient of agricultural fields from an airborne SAR image p 16 N87-17265
- Evaluating roughness models of radar backscatter p 19 N87-17344
- On the relationship between age of lava flows and radar backscattering p 35 N87-17348
- BALTIC SEA**
Retrieval of near-surface wind speed in the Baltic Sea from NIMBUS-7 Scanning Multichannel Microwave Radiometer (SMMR) observations p 50 N87-17342
- Sea ice studies in the Baltic Sea using satellite microwave radiometer data p 50 N87-17343
- BARLEY**
Analysis of the spatial structure of Synthetic Aperture Radar (SAR) imagery for a better separability of cereal crops, wheat and barley p 17 N87-17287
- BAROCLINIC INSTABILITY**
A case study of GWE satellite data impact on GLA assimilation analyses of two ocean cyclones p 41 A87-25787
- BARREN LAND**
Ground radiometry and airborne multispectral survey of bare soils p 10 A87-30894
- Remote sensing of structurally complex semi-natural vegetation - An example from heathland p 10 A87-30896
- Spectral separation of moorland vegetation in airborne Thematic Mapper data p 10 A87-30897
- Remote sensing identified in climate model experiments with hydrological and albedo changes in the Sahel p 59 N87-15569
- Vegetation index models for the assessment of vegetation in marginal areas p 12 N87-15584
- BASALT**
Discrimination of altered basaltic rocks in the southwestern United States by analysis of Landsat Thematic Mapper data p 30 A87-30126
- BATHYMETERS**
Observations of surface currents at Nantucket Shoals and implications for radar imaging of the bottom p 48 N87-17296
- BEARING (DIRECTION)**
Measurement of the directional spectrum of ocean waves using a conically-scanning radar p 52 N87-17383
- BEAUFORT SEA (NORTH AMERICA)**
Classification of sea ice types with single-band (33.6 GHz) airborne passive microwave imagery p 42 A87-27545
- BEDROCK**
Geological nature of early Precambrian formations (considering the example of the Anabar shield) p 28 A87-24274
- BERING SEA**
Influence of the Yukon River on the Bering Sea [NASA-CR-180065] p 54 N87-18293
- Influence of the Yukon River on the Bering Sea [NASA-CR-180356] p 56 N87-19877
- BIBLIOGRAPHIES**
Physical oceanography program science abstracts [AD-A174019] p 55 N87-18961
- BIOLOGICAL EFFECTS**
Biological consequences of a recurrent eddy off Point Conception, California p 40 A87-23721
- BIOMASS**
The use of remote sensing in estimating biomass of fish tree areas in the Richard B. Russell Lake p 40 A87-23834
- Assessment of grassland phytomass with airborne video imagery p 8 A87-25590
- Estimating and mapping grass cover and biomass from low-level photographic sampling p 9 A87-29005
- Distribution and biomass of *Fucus vesiculosus* L. near a cooling-water effluent from a nuclear power plant in the Baltic Sea estimated by aerial photography p 43 A87-29014
- Group Agromet Monitoring Project (GAMP) methodology integrated mapping of rainfall, evapotranspiration, germination, biomass development and thermal inertia, based on Meteosat and conventional meteorological data p 59 N87-15626
- Description of a methodology for biomass change mapping with the use of LANDSAT TM data p 22 N87-18186
- BIOMETEOROLOGY**
Deduction of a synthetic bioclimatological map by means of remote sensing data and a digital terrain model using a correlation approach p 72 N87-18194
- BIRDS**
Using Landsat to assess tropical forest habitat for migratory birds in the Yucatan Peninsula p 4 A87-23807
- BLACK AND WHITE PHOTOGRAPHY**
Evaluation of the mid-infrared (1.45 to 2.0 microns) with a black-and-white infrared video camera p 73 A87-20672
- BOTANY**
Moorland plant community recognition using Landsat MSS data p 7 A87-25589
- BOTSWANA**
Satellite remote sensing of rangelands in Botswana. I - Landsat MSS and herbaceous vegetation p 7 A87-24785
- BRAZIL**
The use of aerial remote sensing in a case study of desertification: Quixaba-PE [INPE-3963-PRE/980] p 11 N87-15519
- Application of remote sensing in hydrology and water resources [INPE-3986-PRE/991] p 60 N87-16382
- BRIDGES (STRUCTURES)**
Remote sensing of shallow water areas with reference to environmental and multitemporal monitoring of the Hailuoto area, Finland p 61 N87-18159
- BRIGHTNESS TEMPERATURE**
The TIMS investigator's guide p 79 N87-17113
- Microwave radiances from horizontally finite precipitating clouds containing ice and liquid hydrometeors p 61 N87-17340
- BUOYS**
The accuracy and availability of operational marine surface wind data for ERS-1 sensor calibration and validation from fixed platforms and free drifting buoys p 51 N87-17376
- Using buoys and ships to calibrate ERS-1 altimeter and scatterometer p 51 N87-17377
- C**
- C BAND**
C and Ku-band scatterometer results from the SCATMOD internal wave experiment p 47 N87-17215
- Evaluation of the different parameters in Long's C-band model --- for ERS-1 scatterometer p 51 N87-17370
- C-130 AIRCRAFT**
The use of aircraft for wind scatterometer calibration --- ERS-1 scatterometer p 84 N87-17382
- CADASTRAL MAPPING**
Mapping of agricultural lands in the USSR p 11 N87-15507
- CALIBRATING**
In flight calibration of push broom remote sensing instruments p 73 A87-19652
- Mobile very long baseline interferometry and Global Positioning System measurement of vertical crustal motion p 26 A87-21931
- Variations in in-flight absolute radiometric calibration --- satellite remote sensors p 77 N87-15594
- Atmospheric correction of TIMS data p 79 N87-17115
- SIR-B measurements and modeling of vegetation p 15 N87-17160
- The ESA approach for ERS-1 sensor calibration and performance verification p 80 N87-17192
- ERS-1 radar altimeter: Performance, calibration and data validation p 80 N87-17194
- Analysis of AIS radiometry at Mono Lake, California --- Airborne Imaging Spectrometer (AIS) p 81 N87-17204
- Extraction of the backscatter coefficient of agricultural fields from an airborne SAR image p 16 N87-17265
- Proceedings of an ESA Workshop on ERS-1 Wind and Wave Calibration [ESA-SP-262] p 84 N87-17363
- ERS-1 mission constraints related to wind and wave calibration p 84 N87-17364
- Gathering and processing a comparative data set for the calibration and validation of ERS-1 data products; preparatory work at the UK-ERS-DC --- Data Center (DC) p 50 N87-17367
- Requirements and constraints in the calibration and validation of ERS-1 wind and wave parameters p 51 N87-17369
- The use of numerical wind and wave models to provide areal and temporal extension to instrument calibration and validation of remotely sensed data --- satellite data p 51 N87-17371
- The accuracy and availability of operational marine surface wind data for ERS-1 sensor calibration and validation from fixed platforms and free drifting buoys p 51 N87-17376
- Using buoys and ships to calibrate ERS-1 altimeter and scatterometer p 51 N87-17377
- Canada Center for Remote Sensing (CCRS) Convair 580 results relevant to ERS-1 wind and wave calibration p 84 N87-17379
- The use of aircraft for wind scatterometer calibration --- ERS-1 scatterometer p 84 N87-17382
- Australian validation plans for ERS-1 p 84 N87-17387
- Variability in the Earth radiation budget as determined from the Nimbus ERB experiments p 84 N87-17410
- Radiometric analysis of the longwave infrared channel of the Thematic Mapper on LANDSAT 4 and 5 [NASA-CR-180180] p 86 N87-18221
- CALIFORNIA**
Thermal imaging spectroscopy in the Kelso-Baker Region, California p 30 N87-17117
- The application of remotely sensed data to pedologic and geomorphic mapping on alluvial fan and playa surfaces in Saline Valley, California p 15 N87-17127
- Application of Thermal Infrared Multiband Scanner (TIMS) data to mapping of Plutonic and stratified rock and assemblages in accreted terrains of the Northern Sierra, California p 15 N87-17132
- CAMERAS**
Evaluation of the mid-infrared (1.45 to 2.0 microns) with a black-and-white infrared video camera p 73 A87-20672
- Control extension utilizing Large Format Camera imagery p 75 A87-23804
- CANADIAN SPACE PROGRAM**
Canadian plans for operational demonstrations of satellite imaging radar applications --- ERS-1 p 68 N87-17229

CANOPIES (VEGETATION)

CANOPIES (VEGETATION)

- Estimation of canopy parameters for inhomogeneous vegetation canopies from reflectance data. II - Estimation of leaf area index and percentage of ground cover for row canopies p 1 A87-20761
- Phenological effects on grass canopy/spectral relationships p 4 A87-23818
- Diurnal-seasonal light interception, leaf area index, and vegetation index interrelations in a wheat canopy - A case study p 5 A87-23822
- A photographic technique for studying reflection indicatrices of vegetation cover p 5 A87-24388
- Investigation of spectral correlations of vegetation growing on different types of geological structures p 29 A87-28508
- Estimating and mapping grass cover and biomass from low-level photographic sampling p 9 A87-29005
- Estimation of vegetation cover at subpixel resolution using LANDSAT data [NASA-CR-177077] p 11 N87-15514
- Canopy reflectance modeling in a tropical wooded grassland [NASA-CR-180097] p 11 N87-15518
- Vegetation index models for the assessment of vegetation in marginal areas p 12 N87-15584
- Investigation of forest canopy temperatures recorded by the thermal infrared multispectral scanner at H. J. Andrews Experimental Forest p 14 N87-17123
- Applications of TIMS data in agricultural areas and related atmospheric considerations p 15 N87-17124
- TIMS data applications in Nebraska p 15 N87-17126
- Analysis of multiple incidence angle SIR-B data for determining forest stand characteristics p 15 N87-17156
- Assessing grass canopy condition and growth from combined optical-microwave measurements p 17 N87-17286
- L to X-band scatter and emission measurements of vegetation p 19 N87-17347
- Canopy hot-spot as crop identifier [DE86-011258] p 19 N87-17395
- Influence of canopy shadow on stress detection in coniferous forests using LANDSAT data p 21 N87-18173
- Relationship between tree density, leaf area index, soil metal content, and LANDSAT MSS canopy radiance values p 21 N87-18174
- Forest cover analysis using SIR-B data p 23 N87-18220
- Off-nadir optical remote sensing from satellites for vegetation identification [DE86-012387] p 23 N87-18916
- CARBON DIOXIDE LASERS**
- Development and demonstration of ALARM (Airborne Lidar Agent Remote Monitor) [AD-A172886] p 78 N87-16387
- CARIBBEAN REGION**
- Vegetation change and desertification in the Caribbean p 14 N87-15619
- CELESTIAL GEODESY**
- The use of Doppler observations to obtain initial geodetic data and to derive plumbline deviations and quasi-geoid heights p 27 A87-28504
- CENTROIDS**
- Resolving the Doppler ambiguity for spaceborne synthetic aperture radar p 72 N87-18212
- CHANGE DETECTION**
- Accurate measurement of mean sea level changes by altimetric satellites p 38 A87-20524
- Instrument characterization for the detection of long-term changes in stratospheric ozone - An analysis of the SBUV/2 radiometer p 74 A87-20961
- CHARGE COUPLED DEVICES**
- Improved multispectral earth imaging from space using electronic image alignment p 73 A87-19655
- CHEMICAL ANALYSIS**
- Discrimination of altered basaltic rocks in the southwestern United States by analysis of Landsat Thematic Mapper data p 30 A87-30126
- CHEMICAL COMPOSITION**
- Lithologic mapping of silicate rocks using TIMS p 30 N87-17118
- The physical basis for spectral variations in thermal infrared emittance of silicates and application to remote sensing p 31 N87-17129
- Relationship between tree density, leaf area index, soil metal content, and LANDSAT MSS canopy radiance values p 21 N87-18174
- Nature and origin of mineral coatings on volcanic rocks of the Black Mountain, Stonewall Mountain, and Kane Springs, Wash volcanic centers, Southern Nevada [NASA-CR-180183] p 36 N87-18255
- CHILE**
- Thematic mapper studies of central Andean volcanoes [NASA-CR-180252] p 36 N87-18910

CHINA

- Atlas of geo-science analyses of Landsat imagery in China --- Book p 65 A87-24542

CHLOROPHYLLS

- Chlorophyll pigment concentration using spectral curvature algorithms - An evaluation of present and proposed satellite ocean color sensor bands p 37 A87-20204
- Biological consequences of a recurrent eddy off Point Conception, California p 40 A87-23721
- Modelling of estuarine chlorophyll-A from an airborne scanner p 61 N87-18172
- Laser-induced chlorophyll-A fluorescence of terrestrial plants p 23 N87-18207

CITIES

- Accuracy of population estimation from medium-scale aerial photography p 24 A87-23777
- Detection of new urban build-up in Ardmore and McAlester, Oklahoma using Landsat MSS data p 25 A87-23829
- Utility of AVHRR channels 3 and 4 in land-cover mapping p 9 A87-28388

CLASSIFICATIONS

- Classification of multitemporal Thematic Mapper data p 64 A87-23795
- The effect of training data variability on classification accuracy p 64 A87-23796
- An iterative Landsat-MSS classification methodology for soil survey p 3 A87-23797
- The interactive effect of spatial resolution and degree of internal variability within land-cover types on classification accuracies p 77 A87-30895
- The physical basis for spectral variations in thermal infrared emittance of silicates and application to remote sensing p 31 N87-17129
- Multispectral classification of microwave remote sensing images --- SAR crop identification p 16 N87-17238
- A statistical approach to select the optimal wavelength bands for separating rocks in the wavelength region 0.4 to 2.3 microns p 34 N87-17244
- Evaluation of LANDSAT 5 Thematic Mapping (TM) data for image clustering and classification p 69 N87-17251
- Classification of forest and surface types by satellite microwave radiometry p 18 N87-17305

CLIMATE

- Land surface climatic variables monitored by NOAA-AVHRR satellites p 4 A87-23811
- Evaluation of climate relevant land surface characteristics from remote sensing p 12 N87-15572
- Remote sensing activities in Turkey: Possible contributions to climate studies p 77 N87-15624
- Future European plans in the framework of the International Satellite Land Surface Climatology Project (ISLSCP) p 78 N87-15628
- The first International Satellite Land Surface Climatology Project (ISLSCP) Field Experiment - FIFE p 14 N87-15629
- An overview of the implementation of the World Climate Research program p 26 N87-17388

CLIMATOLOGY

- Satellite rainfall retrieval by logistic regression p 56 A87-23370
- Use of topographic and climatological models in a geographical data base to improve Landsat MSS classification for Olympic National Park p 25 A87-30128
- Weather and atmosphere remote sensing p 77 A87-30885
- Imaging radar contributions to a major air-sea-ice interaction study in the Greenland Sea p 46 N87-17150

CLOSED ECOLOGICAL SYSTEMS

- Snow cover recession in an Alpine ecological system p 18 N87-17316

CLOUD GLACIATION

- Microwave radiances from horizontally finite precipitating clouds containing ice and liquid hydrometeors p 61 N87-17340

CLOUD PHYSICS

- A thermal device for aircraft measurement of the solid water content of clouds p 56 A87-20951
- SAM II measurements of Antarctic PSC's and aerosols --- Stratospheric Aerosol Measurement satellite - Polar Stratospheric Clouds p 75 A87-23546

CLOUD SEEDING

- Satellite observations of snow covered area in the High Atlas Mountains of Morocco p 57 A87-23808

CLOUDS (METEOROLOGY)

- Microwave radiances from horizontally finite precipitating clouds containing ice and liquid hydrometeors p 61 N87-17340

CLUSTER ANALYSIS

- Evaluation of LANDSAT 5 Thematic Mapping (TM) data for image clustering and classification p 69 N87-17251

- Spectral characteristics and the extent of paleosols of the Palouse formation [NASA-CR-180357] p 24 N87-19826

COASTAL CURRENTS

- Temperature-plant pigment-optical relations in a recurrent offshore mesoscale eddy near Point Conception, California [AD-A176666] p 39 A87-23720
- Biological consequences of a recurrent eddy off Point Conception, California p 40 A87-23721
- Space and time variability of the surface color field in the northern Adriatic Sea p 40 A87-23722

COASTAL WATER

- Drainage channel network of the Arcachon Basin using Thematic Mapper data obtained at high tide p 58 A87-29013
- Mapping of water quality in coastal waters using Airborne Thematic Mapper data p 58 A87-30899
- Island wakes and headland eddies - A comparison between remotely sensed data and laboratory experiments p 44 A87-30925

COASTAL ZONE COLOR SCANNER

- Chlorophyll pigment concentration using spectral curvature algorithms - An evaluation of present and proposed satellite ocean color sensor bands p 37 A87-20204
- Space and time variability of the surface color field in the northern Adriatic Sea p 40 A87-23722
- The Coastal Zone Color Scanner views the Bismarck Sea p 42 A87-26970
- Ocean remote sensing p 44 A87-30883
- Variations in in-flight absolute radiometric calibration --- satellite remote sensors p 77 N87-15594
- A description of large-scale variability in the ocean using the diffuse attenuation coefficient p 53 N87-18160

COASTS

- Interpretation characteristics of space photographs of sea coasts with wind-induced surges p 43 A87-28509
- The ice conditions in the Greenland waters, 1980 [REPT-551.467.3.068(988)] p 53 N87-17428

COATINGS

- Nature and origin of mineral coatings on volcanic rocks of the Black Mountain, Stonewall Mountain, and Kane Springs, Wash volcanic centers, Southern Nevada [NASA-CR-180183] p 36 N87-18255

COEFFICIENT OF FRICTION

- Study of ocean bottom coupling process using satellite altimeter data p 54 N87-18199

COHERENT RADAR

- Application of Spaceborne Distributed Aperture/Coherent Array Processing (SDA/CAP) technology to active and passive microwave remote sensing p 82 N87-17277

COLOR INFRARED PHOTOGRAPHY

- Classification of reflectance on colour infrared aerial photographs and sub-tropical salt-marsh vegetation types p 10 A87-29012

COLORADO

- Modeling energy flow and nutrient cycling in natural semiarid grassland ecosystems with the aid of thematic mapper data [NASA-CR-179903] p 11 N87-15517

COMMERCIAL SPACECRAFT

- SPOT IMAGE and commercialisation of remote sensing data p 65 A87-29430

COMPUTER AIDED MAPPING

- Computer-aided analysis of LANDSAT data for mapping geologic and geomorphic features, North Bombay, India p 33 N87-17235
- Computer-aided interpretation of complex geological patterns in remote sensing p 35 N87-17294
- Marrying geocoded image data with other types of geographic information in a PC environment --- forestry p 21 N87-18154
- Spatial remote sensing to land management --- SPOT/GPS p 70 N87-18157

COMPUTER GRAPHICS

- Marrying geocoded image data with other types of geographic information in a PC environment --- forestry p 21 N87-18154

COMPUTER PROGRAMS

- Composite/progressive sampling - A program package for computer supported collection of DTM data --- Digital Terrain Models p 62 A87-23784

COMPUTER SYSTEMS DESIGN

- The design of an international data centre for remote sensing p 67 N87-17176
- A knowledge-based software environment for the analysis of spectroradiometer data --- mineral identification p 68 N87-17203
- Intelligent SAR Processor (ISAR), a new concept for high throughput and high precision digital SAR processing p 85 N87-18178
- STAR-VUE: A tactical ice navigation workstation p 54 N87-18181

COMPUTER TECHNIQUES

- Method for computing the periodicity of a remote-sensing survey p 65 A87-26540
 Microcomputer-assisted video image analysis of lodging in winter wheat p 10 A87-30130

COMPUTERIZED SIMULATION

- Development and experiment of airborne microwave rain-scatterometer/radiometer system. III - Rain measurement and its data analysis p 58 A87-28436
 A comparative test of photogrammetrically sampled digital elevation models p 66 A87-29499

CONFERENCES

- Instrumentation for optical remote sensing from space; Proceedings of the Meeting, Cannes, France, November 27-29, 1985 [SPIE-589] p 73 A87-19647
 American Congress on Surveying and Mapping and American Society for Photogrammetry and Remote Sensing, Annual Convention, Washington, DC, Mar. 16-21, 1986, Technical Papers. Volume 5 - Remote Sensing p 4 A87-23810
 Space science and applications: Progress and potential p 87 A87-30876
 The TIMS Data User's Workshop [NASA-CR-180130] p 78 A87-17111
 Proceedings of the 1986 International Geoscience and Remote Sensing Symposium (IGARSS '86) on Remote Sensing: Today's Solutions for Tomorrow's Information Needs, volume 1 p 80 A87-17163
 Proceedings of the 1986 International Geoscience and Remote Sensing Symposium (IGARSS '86) on Remote Sensing: Today's Solutions for Tomorrow's Information Needs, volume 2 p 82 A87-17283
 Proceedings of an ESA Workshop on ERS-1 Wind and Wave Calibration [ESA-SP-262] p 84 A87-17363
 Proceedings of the 1986 International Geoscience and Remote Sensing Symposium (IGARSS '86) on Remote Sensing: Today's Solutions for Tomorrow's Information Needs, volume 3 [ESA-SP-254-VOL-3] p 84 A87-18142

CONICAL SCANNING

- Measurement of the directional spectrum of ocean waves using a conically-scanning radar p 52 A87-17383

CONIFERS

- Thematic mapper analysis of coniferous forest structure and composition p 1 A87-20762
 Assessing forest decline in coniferous forests of Vermont using NS-001 Thematic Mapper Simulator data p 1 A87-20763
 The data dilemma - How to properly construct and utilize aerial photo volume tables p 63 A87-23790
 An assessment of evapotranspirational water losses in a Sierran Mixed Conifer forest using remotely sensed data p 4 A87-23816
 Estimation of density in young pine plantations using 35mm aerial photography p 5 A87-23819
 The spectral reflectance of stands of Norway spruce and Scotch pine, measured from a helicopter p 7 A87-25586
 Influence of canopy shadow on stress detection in coniferous forests using LANDSAT data p 21 A87-18173
 Relationship between tree density, leaf area index, soil metal content, and LANDSAT MSS canopy radiance values p 21 A87-18174

CONVECTION CLOUDS

- Annual and interannual variability in large-scale convection over the eastern Pacific and tropical South America p 57 A87-23414

CONVECTIVE FLOW

- Satellite contributions to convective scale weather analysis and forecasting p 76 A87-27882

CORN

- Estimating pre-harvest production of maize in Kenya using large-scale aerial photography and radiometry p 9 A87-29004

CORRECTION

- Surface reflectance correction and stereo enhancement of LANDSAT thematic mapper imagery for structural geologic exploration [DE87-003095] p 37 A87-19796

COSMOS SATELLITES

- The results of sea-surface temperature determinations from IR and microwave measurements aboard the Cosmos-1151 satellite p 40 A87-24376

COST EFFECTIVENESS

- Utility of remote sensing data in renewable resource sample survey p 18 A87-17289

COUPLING

- Study of ocean bottom coupling process using satellite altimeter data p 54 A87-18199

CROP GROWTH

- Modeling energy flow and nutrient cycling in natural semiarid grassland ecosystems with the aid of thematic mapper data [NASA-CR-179903] p 11 A87-15517
 An integrated system to assess agricultural productivity --- satellite imagery p 14 A87-15621
 Assessing grass canopy condition and growth from combined optical-microwave measurements p 17 A87-17286
 L to X-band scatter and emission measurements of vegetation p 19 A87-17347

CROP IDENTIFICATION

- Agricultural remote sensing in South Carolina - A study of crop identification capabilities utilizing Landsat data p 4 A87-23806
 Estimating pre-harvest production of maize in Kenya using large-scale aerial photography and radiometry p 9 A87-29004
 Comparison of some classification methods on a test site (Kiskore, Hungary) - Separability as a measure of accuracy p 9 A87-29006
 Multispectral classification of microwave remote sensing images --- SAR crop identification p 16 A87-17238
 The influence of resampling method and multitemporal LANDSAT imagery on crop classification accuracy in the United Kingdom p 16 A87-17250
 The processing of and information extraction from airborne SLAR data [NLR-MP-86004-U] p 23 A87-18919
 Agricultural crop estimates using information gathered by remote sensing satellites, as well as ground data, through samples of geographic layers [INPE-4102-RPE/534] p 24 A87-19786

CROP INVENTORIES

- Diurnal-seasonal light interception, leaf area index, and vegetation index interrelations in a wheat canopy - A case study p 5 A87-23822
 Vegetable crop inventory with Landsat TM data p 5 A87-23833
 Rural land use inventory and mapping in the Ardeche area (France) using multitemporal Thematic Mapping (TM) data p 19 A87-17350
 An integrated data bank for agricultural productivity by remote sensing p 21 A87-18153
 Integrating vector and satellite data to evaluate the adequacy of a grain silo network p 21 A87-18156
 Agricultural crop estimates using information gathered by remote sensing satellites, as well as ground data, through samples of geographic layers [INPE-4102-RPE/534] p 24 A87-19786
 CANASATE: Sugar cane mapping by satellite, area 3 [INPE-4068-RPE/526] p 24 A87-19790

CROP VIGOR

- Automation of thematic processing of space images in evaluating crop condition p 8 A87-26539
 Microcomputer-assisted video image analysis of lodging in winter wheat p 10 A87-30130
 An integrated system to assess agricultural productivity --- satellite imagery p 14 A87-15621
 An integrated data bank for agricultural productivity by remote sensing p 21 A87-18153

CROPS

- Remote sensing of the state of crops and soils p 1 A87-20758

CRUSTAL FRACTURES

- Basic research for the geodynamics program [NASA-CR-180137] p 27 A87-17415

CULTIVATION

- Remote sensing applications in the study of land use and soils of aeolian cover of the western part of Haryana State, India p 22 A87-18187

CYCLONES

- A case study of GWE satellite data impact on GLA assimilation analyses of two ocean cyclones p 41 A87-25787
 Observations and analysis of a polar low over the Great Lakes region p 76 A87-27872

D

DAMAGE ASSESSMENT

- Assessing forest decline in coniferous forests of Vermont using NS-001 Thematic Mapper Simulator data p 1 A87-20763
 Use of TMS/TM data for mapping of forest decline damage in the northeastern United States --- Thematic Mapper Simulator (TMS) Thematic Mapper (TM) p 22 A87-18175

DATA ACQUISITION

- Equatorial Indian Ocean evaporation estimates from operational meteorological satellites and some inferences in the context of monsoon onset and activity p 39 A87-22041

- Monitoring vegetation in the Mali Sahel during summer 1984 p 6 A87-24784
 Hydrological studies in Niger p 59 A87-15609
 Atmospheric correction of TIMS data p 79 A87-17115

- Detection and mapping of volcanic rock assemblages and associated hydrothermal alteration with Thermal Infrared Multiband Scanner (TIMS) data Comstock Lode Mining District, Virginia City, Nevada p 31 A87-17119
 Investigation of forest canopy temperatures recorded by the thermal infrared multispectral scanner at H. J. Andrews Experimental Forest p 14 A87-17123
 TIMS data applications in Nebraska p 15 A87-17126

- A geologic atlas of TIMS data p 32 A87-17133
 The FRS-68010: A new concept for the acquisition and analysis of NOAA HRPT data p 68 A87-17206
 Digital satellite imagery acquisition and processing p 68 A87-17207

DATA BASE MANAGEMENT SYSTEMS

- Design of a data base system for inferring land surface parameters and fluxes from satellite radiances p 66 A87-15625

DATA BASES

- A geologic atlas of TIMS data p 32 A87-17133
 The design of an international data centre for remote sensing p 67 A87-17176
 Gathering and processing a comparative data set for the calibration and validation of ERS-1 data products; preparatory work at the UK-ERS-DC --- Data Center (DC) p 50 A87-17367
 Improvement of the Earth's gravity field from terrestrial and satellite data [NASA-CR-180139] p 27 A87-17416
 An integrated data bank for agricultural productivity by remote sensing p 21 A87-18153
 The impact of satellite infrared sea surface temperatures on FNOC (Fleet Numerical Oceanography Center) ocean thermal analyses [AD-A173333] p 54 A87-18295

DATA CORRELATION

- Correlation between time- and depth-resolved simulated lidar signals --- for estimating phytoplankton distribution p 38 A87-20770

DATA MANAGEMENT

- An overview of operational SAR data collection and dissemination plans for ERS-1 ice data in Canada p 47 A87-17189
 Remote Sensing Information Sciences Research Group, year four [NASA-CR-180198] p 88 A87-18907

DATA PROCESSING

- IRSAP: An improved approach in processing remotely sensed data --- Interactive Remote Sensing Applications Package (IRSAP) p 70 A87-17332
 Outline of SAR-850 data processing method in Japan --- ERS-1 (NASDA) p 71 A87-18176

DATA SAMPLING

- Composite/progressive sampling - A program package for computer supported collection of DTM data --- Digital Terrain Models p 62 A87-23784
 A comparative test of photogrammetrically sampled digital elevation models p 66 A87-29499
 The influence of resampling method and multitemporal LANDSAT imagery on crop classification accuracy in the United Kingdom p 16 A87-17250
 Utility of remote sensing data in renewable resource sample survey p 18 A87-17289

DATA SYSTEMS

- Gathering and processing a comparative data set for the calibration and validation of ERS-1 data products; preparatory work at the UK-ERS-DC --- Data Center (DC) p 50 A87-17367

DEATH VALLEY (CA)

- Kinematics at the intersection of the Garlock and Death Valley fault zones, California: Integration of TM data and field studies [NASA-CR-180182] p 36 A87-18256

DECIDUOUS TREES

- Fruit tree inventory with Landsat Thematic Mapper data p 8 A87-28387

DECIMETER WAVES

- Use of decimeter waves in studies of water bodies by methods of microwave radiometry p 58 A87-26537

DECISION MAKING

- Remote sensing of shallow water areas with reference to environmental and multitemporal monitoring of the Hailuoto area, Finland p 61 A87-18159

DEFORESTATION

- The application of LANDSAT imagery for land cover assessment --- Thailand p 13 A87-15614
 Monitoring of large phenomena in developing countries through satellite imagery p 67 A87-17172

DEFORMATION

DEFORMATION

Homogeneous plate deformations on a sphere as monitored by Satellite Laser Ranging (SLR) networks analyzed with the multi-epoch method [ETN-87-99221] p 27 N87-18908

DENSITY MEASUREMENT

Estimation of density in young pine plantations using 35mm aerial photography p 5 A87-23819

DEPTH

SeaSoar CTD surveys during FASINEX --- Conductivity Temperature Depth (CTD); Frontal Air Sea Interaction Experiment (FASINEX) [IOS-230] p 55 N87-18970

DEPTH MEASUREMENT

An improved method for the determination of water depth from surface wave refraction patterns --- SAR imagery p 49 N87-17249

DESERTIFICATION

The use of aerial remote sensing in a case study of desertification: Quixaba-PE [INPE-3963-PRE/980] p 11 N87-15519
Remote sensing identified in climate model experiments with hydrological and albedo changes in the Sahel p 59 N87-15569

Desertification monitoring: Remotely sensed data for drought impact studies in the Sudan p 12 N87-15604
Regional studies with satellite data in Africa on the desertification of the Sudan-Sahel belt in Nigeria p 13 N87-15605

Vegetation change and desertification in the Caribbean p 14 N87-15619

Monitoring of large phenomena in developing countries through satellite imagery p 67 N87-17172
Spatial analysis of the dynamics of an ecosystem by multistage remote sensing in Kenya p 16 N87-17173

DESERTS

Assessment of ecological conditions associated with the 1980/81 desert locust plague upsurge in West Africa using environmental satellite data p 7 A87-24789
Monitoring sediment transfer processes on the desert margin [NASA-CR-180181] p 23 N87-18222

DETECTION

Monitoring sediment transfer processes on the desert margin [NASA-CR-180181] p 23 N87-18222

DEVELOPING NATIONS

Remote sensing options for soil survey in developing countries p 2 A87-21239
Sri Lanka's solution to land use mapping and monitoring for Third World countries development p 67 N87-17174

DIELECTRICS

Microwave backscattering from a layer of randomly oriented discs with application to scattering from vegetation p 8 A87-28316

DIGITAL DATA

Composite/progressive sampling - A program package for computer supported collection of DTM data --- Digital Terrain Models p 62 A87-23784

Digital image matching techniques for standard photogrammetric applications p 63 A87-23785

The production of orthophotographs by digital image processing techniques p 63 A87-23787

The effect of training data variability on classification accuracy p 64 A87-23796

Landsat Thematic Mapper digital information content for agricultural environments p 5 A87-23830

Terrain analysis from digital patterns in geomorphometry and Landsat MSS spectral response p 66 A87-30127

Sparse area stereo matching experiment [AD-A173601] p 66 N87-16388

Digital satellite imagery acquisition and processing p 68 N87-17207

Soil degradation evaluation by digital image processing p 20 N87-18147

DIGITAL RADAR SYSTEMS

Digital terrain mapping with STAR-1 SAR data p 69 N87-17269

DIGITAL TECHNIQUES

The production of orthophotographs by digital image processing techniques p 63 A87-23787

Accurate determination of ellipse centers in digital imagery p 63 A87-23788

Classification of multistage Thematic Mapper data p 64 A87-23795

Performance of selected spatial domain edge detection algorithms for earth resources application p 64 A87-23798

Detection and mapping of volcanic rock assemblages and associated hydrothermal alteration with Thermal Infrared Multiband Scanner (TIMS) data Comstock Lode Mining District, Virginia City, Nevada p 31 N87-17119

Applications of TIMS data in agricultural areas and related atmospheric considerations p 15 N87-17124

Calculation of day and night emittance values p 67 N87-17131

Application of Thermal Infrared Multiband Scanner (TIMS) data to mapping of Plutonic and stratified rock and assemblages in accreted terrains of the Northern Sierra, California p 15 N87-17132

DISCRIMINANT ANALYSIS (STATISTICS)

A statistical approach to select the optimal wavelength bands for separating rocks in the wavelength region 0.4 to 2.3 microns p 34 N87-17244

DMSP SATELLITES

Remote sensing of hydrological variables from the DMSP microwave mission sensors p 57 A87-23374

DOPPLER EFFECT

The use of Doppler observations to obtain initial geodetic data and to derive plumbline deviations and quasi-geoid heights p 27 A87-28504

Resolving the Doppler ambiguity for spaceborne synthetic aperture radar p 72 N87-18212

Preliminary evaluation of Doppler-determined pole positions computed using world geodetic system 1984 [AD-A173467] p 27 N87-18225

DOWNLINKING

STAR-VUE: A tactical ice navigation workstation p 54 N87-18181

DRAINAGE

Towards snowmelt runoff forecast using LANDSAT-MSS and NOAA/AVHRR data p 61 N87-17317

DRAINAGE PATTERNS

Drainage channel network of the Arcachon Basin using Thematic Mapper data obtained at high tide p 58 A87-29013

The megageomorphology of the radar rivers of the eastern Sahara p 32 N87-17139

Significance of space image, air photo and drainage linears in relation to west coast tectonics, India p 33 N87-17232

Hydrogeological research in Peloponnesus (Greece) Karst area by support and completion of LANDSAT-thematic data p 33 N87-17234

DROUGHT

Reflections on drought - Ethiopia 1983-1984 p 6 A87-24780

Growing period and drought early warning in Africa using satellite data p 7 A87-24788

Desertification monitoring: Remotely sensed data for drought impact studies in the Sudan p 12 N87-15604

Regional studies with satellite data in Africa on the desertification of the Sudan-Sahel belt in Nigeria p 13 N87-15605

Variability in the Earth radiation budget as determined from the Nimbus ERB experiments p 84 N87-17410

DUNES

Remote sensing applications in the study of land use and soils of aeolian cover of the western part of Haryana State, India p 22 N87-18187

E

EARTH (PLANET)

Improvement of the Earth's gravity field from terrestrial and satellite data [NASA-CR-180139] p 27 N87-17416

EARTH ALBEDO

Effect of surface properties on the narrow to broadband spectral relationship in clear sky satellite observations p 65 A87-25587

Remote sensing identified in climate model experiments with hydrological and albedo changes in the Sahel p 59 N87-15569

Estimation of surface albedo using satellite data. A simple formulation for atmospheric effects p 25 N87-15579

Surface albedo change in arid regions in the Sudan p 13 N87-15615

EARTH ATMOSPHERE

Report of the Fourth Session of the JSC/CCCO Tropical Ocean Global Atmosphere (TOGA) Scientific Steering Group [WCP-120] p 54 N87-18283

Arctic haze: Natural or pollution? [AD-A174025] p 55 N87-18931

EARTH CORE

The earth's C21 and S21 gravity coefficients and the rotation of the core p 27 A87-29977

EARTH CRUST

Mobile very long baseline interferometry and Global Positioning System measurement of vertical crustal motion p 26 A87-21931

A scanning radar altimeter for mapping continental topography p 33 N87-17146

EARTH MOVEMENTS

Mobile very long baseline interferometry and Global Positioning System measurement of vertical crustal motion p 26 A87-21931

EARTH OBSERVATIONS (FROM SPACE)

Instrumentation for optical remote sensing from space; Proceedings of the Meeting, Cannes, France, November 27-29, 1985 p 73 A87-19647

[SPIE-589] Improved multispectral earth imaging from space using electronic image alignment p 73 A87-19655

Accurate measurement of mean sea level changes by altimetric satellites p 38 A87-20524

Space remote sensing p 86 A87-20682

Spot data distribution --- selling satellite images p 62 A87-20683

Earth Observing System - The earth research system of the 1990's p 74 A87-22556

[AIAA PAPER 87-0320] Ideas for a future earth observing system from geosynchronous orbit p 74 A87-23419

An analysis of the potential of satellite-borne bistatic radar sensing of the earth p 75 A87-24385

Satellite remote sensing of rangelands in Botswana. II - NOAA AVHRR and herbaceous vegetation p 7 A87-24786

Partnerships in remote sensing - A theme with some examples p 86 A87-25531

Earth sensing - New tools enable scientists to gain insight into the structure of our planet's surface p 29 A87-25890

Soviet remote sensing p 86 A87-27452

Fruit tree inventory with Landsat Thematic Mapper data p 8 A87-28387

Utility of AVHRR channels 3 and 4 in land-cover mapping p 9 A87-28388

The shape of the earth in the space age p 26 A87-28442

Business approach to earth observation applications p 87 A87-29433

Remote sensing from space - An overview p 87 A87-30881

Land applications for remote sensing from space p 25 A87-30882

Space Shuttle cloud detection and earth feature classification experiment p 77 A87-31139

Development, status, prospects of marine observation satellite p 45 N87-15989

Concept of a future multispectral Thermal Infrared (TIR) pushbroom mission for Earth observation from space p 80 N87-17169

Commercial opportunities in Earth observation from space p 87 N87-17177

The Sequential Filter Imaging Radiometer (SFIR), a new instrument configuration for Earth observations p 81 N87-17205

The Electronically Steered Thinned Array Radiometer (ESTAR) p 82 N87-17260

X-SAR extends the frequency range of Shuttle Imaging Radar p 70 N87-17362

The use of space technology in federally funded land processes research in the United States p 88 N87-18152

Commercial opportunities in Earth observation from space p 87 N87-17177

The Sequential Filter Imaging Radiometer (SFIR), a new instrument configuration for Earth observations p 81 N87-17205

The Electronically Steered Thinned Array Radiometer (ESTAR) p 82 N87-17260

X-SAR extends the frequency range of Shuttle Imaging Radar p 70 N87-17362

The use of space technology in federally funded land processes research in the United States p 88 N87-18152

Commercial opportunities in Earth observation from space p 87 N87-17177

The Sequential Filter Imaging Radiometer (SFIR), a new instrument configuration for Earth observations p 81 N87-17205

The Electronically Steered Thinned Array Radiometer (ESTAR) p 82 N87-17260

X-SAR extends the frequency range of Shuttle Imaging Radar p 70 N87-17362

The use of space technology in federally funded land processes research in the United States p 88 N87-18152

Commercial opportunities in Earth observation from space p 87 N87-17177

The Sequential Filter Imaging Radiometer (SFIR), a new instrument configuration for Earth observations p 81 N87-17205

The Electronically Steered Thinned Array Radiometer (ESTAR) p 82 N87-17260

X-SAR extends the frequency range of Shuttle Imaging Radar p 70 N87-17362

The use of space technology in federally funded land processes research in the United States p 88 N87-18152

Commercial opportunities in Earth observation from space p 87 N87-17177

The Sequential Filter Imaging Radiometer (SFIR), a new instrument configuration for Earth observations p 81 N87-17205

The Electronically Steered Thinned Array Radiometer (ESTAR) p 82 N87-17260

X-SAR extends the frequency range of Shuttle Imaging Radar p 70 N87-17362

The use of space technology in federally funded land processes research in the United States p 88 N87-18152

Commercial opportunities in Earth observation from space p 87 N87-17177

The Sequential Filter Imaging Radiometer (SFIR), a new instrument configuration for Earth observations p 81 N87-17205

The Electronically Steered Thinned Array Radiometer (ESTAR) p 82 N87-17260

X-SAR extends the frequency range of Shuttle Imaging Radar p 70 N87-17362

The use of space technology in federally funded land processes research in the United States p 88 N87-18152

- Shuttle imaging radar-C science plan
[NASA-CR-180241] p 86 N87-18697
- EARTH RESOURCES PROGRAM**
An overview of remote sensing agricultural applications in North America: Past, present and future p 17 N87-17284
- EARTH ROTATION**
The earth's C21 and S21 gravity coefficients and the rotation of the core p 27 N87-29977
Basic research for the geodynamics program [NASA-CR-180137] p 27 N87-17415
- EARTH SURFACE**
Land surface climatic variables monitored by NOAA-AVHRR satellites p 4 N87-23811
The use of space photography to create and renew small-scale maps p 65 N87-25249
Effect of surface properties on the narrow to broadband spectral relationship in clear sky satellite observations p 65 N87-25587
Earth sensing - New tools enable scientists to gain insight into the structure of our planet's surface p 29 N87-25890
Determination of the properties of a plowed soil layer from multispectral space imagery p 8 N87-26536
Hydrologic models of land surface processes --- soil moisture p 58 N87-15547
Evaluation of climate relevant land surface characteristics from remote sensing p 12 N87-15572
Remote sensing of land-surface temperature from HIRS/MSU data --- High Resolution Infrared Sounder/Microwave Sounding Unit (HIRS/MSU) p 77 N87-15573
Estimation of surface albedo using satellite data. A simple formulation for atmospheric effects p 25 N87-15579
Design of a data base system for inferring land surface parameters and fluxes from satellite radiances p 66 N87-15625
Future European plans in the framework of the International Satellite Land Surface Climatology Project (ISLSCP) p 78 N87-15628
The first International Satellite Land Surface Climatology Project (ISLSCP) Field Experiment - FIFE p 14 N87-15629
An extension of the split window technique for the retrieval of precipitable water [AD-A173008] p 60 N87-16386
Infrared spectroscopy for geologic interpretation of TIMS data p 31 N87-17130
Extracting surface features in multispectral imagery p 68 N87-17211
Dielectric and surface parameters related to microwave scatter and emission properties p 16 N87-17262
Classification of forest and surface types by satellite microwave radiometry p 18 N87-17305
- EARTH TIDES**
Comparison of ocean tide models with satellite altimeter data [AD-A174698] p 56 N87-19879
- EARTHQUAKES**
Delineation of fault zones using imaging radar p 32 N87-17138
- ECOLOGY**
Assessment of ecological conditions associated with the 1980/81 desert locust plague upsurge in West Africa using environmental satellite data p 7 N87-24789
- ECOSYSTEMS**
Modeling energy flow and nutrient cycling in natural semiarid grassland ecosystems with the aid of thematic mapper data [NASA-CR-179903] p 11 N87-15517
Monitoring vegetation recovery patterns on Mount St. Helens using thermal infrared multispectral data p 14 N87-17122
- EDGES**
Performance of selected spatial domain edge detection algorithms for earth resources application p 64 N87-23798
- EDUCATION**
The transfer of remote sensing technology to developing countries: A survey of experts in the field p 87 N87-17170
- EFFLUENTS**
Distribution and biomass of *Fucus vesiculosus* L. near a cooling-water effluent from a nuclear power plant in the Baltic Sea estimated by aerial photography p 43 N87-29014
- EGYPT**
Assessment of wind and fluvial action by using LANDSAT-MSS color composites in the lower Nile Valley (Egypt) p 13 N87-15612
LANDSAT-MSS remote sensing and satellite cartography: An integrated approach to the preparation of a new geological map of Egypt at a scale of 1:500 000 p 36 N87-18190
- EL NINO**
Atmospheric characteristics of the equatorial Pacific during the 1982-1983 El Nino, deduced from satellite and aircraft observations p 41 N87-25543
- ELECTROMAGNETIC RADIATION**
Application of remote sensing in hydrology and water resources [INPE-3986-PRE/991] p 60 N87-16382
- ELECTROMAGNETIC SCATTERING**
Hydrodynamics of internal solitons and a comparison of SIR-A and SIR-B data with ocean measurements p 45 N87-17147
- EMITTANCE**
Enhancement of time images for photointerpretation p 66 N87-17116
Lithologic mapping of silicate rocks using TIMS p 30 N87-17118
The Red River Valley archeological project p 31 N87-17128
The physical basis for spectral variations in thermal infrared emittance of silicates and application to remote sensing p 31 N87-17129
Infrared spectroscopy for geologic interpretation of TIMS data p 31 N87-17130
- ENERGY BUDGETS**
The fundamental problems for the energy balance study by satellite imagery p 66 N87-15590
- ENERGY SPECTRA**
Operational wave forecasting with spaceborne SAR: Prospects and pitfalls p 45 N87-17149
- ENVIRONMENT EFFECTS**
Evaluation of climate relevant land surface characteristics from remote sensing p 12 N87-15572
The use of remote sensing techniques in the study of vegetation recovery after fire in Mediterranean countries (a preliminary study) p 14 N87-15623
Environmental modification of metropolitan areas through satellite images: Study of urban design in the tropics p 25 N87-17175
Use of TMS/TM data for mapping of forest decline damage in the northeastern United States --- Thematic Mapper Simulator (TMS) Thematic Mapper (TM) p 22 N87-18175
- ENVIRONMENT MANAGEMENT**
Monitoring land use changes in Sri Lanka for land use planning using a geographic information system and satellite imagery p 26 N87-18151
- ENVIRONMENTAL ENGINEERING**
The use of remote sensing (including aerial photographs) to devise cost-effective methods for soil conservation in the Kocaeli Peninsula, Turkey p 20 N87-18149
- ENVIRONMENTAL MONITORING**
Forest fire monitoring using the NOAA satellite series p 3 N87-23360
Remote detection of forest damage p 8 N87-26197
Impact of environmental variables on spectral signatures acquired by the Landsat Thematic Mapper p 9 N87-29003
Calibration of Landsat data for sparsely vegetated semi-arid rangelands p 9 N87-29008
Current achievements and future projects/useful applications of weather satellites and future remote sensing p 76 N87-29431
Proceedings of the 1986 International Geoscience and Remote Sensing Symposium (IGARSS '86) on Remote Sensing: Today's Solutions for Tomorrow's Information Needs, volume 1 p 80 N87-17163
Monitoring of large phenomena in developing countries through satellite imagery p 67 N87-17172
Sri Lanka's solution to land use mapping and monitoring for Third World countries development p 67 N87-17174
The design of an international data centre for remote sensing p 67 N87-17176
Application of Spaceborne Distributed Aperture/Coherent Array Processing (SDA/CAP) technology to active and passive microwave remote sensing p 82 N87-17277
Proceedings of the 1986 International Geoscience and Remote Sensing Symposium (IGARSS '86) on Remote Sensing: Today's Solutions for Tomorrow's Information Needs, volume 2 p 82 N87-17283
[ESA-SP-254-VOL-2] p 82 N87-17283
The use of numerical wind and wave models to provide areal and temporal extension to instrument calibration and validation of remotely sensed data --- satellite data p 51 N87-17371
Monitoring land use changes in Sri Lanka for land use planning using a geographic information system and satellite imagery p 26 N87-18151
Remote sensing of shallow water areas with reference to environmental and multitemporal monitoring of the Hailuotu area, Finland p 61 N87-18159
- EQUATORIAL REGIONS**
Variability of the productive habitat in the eastern equatorial Pacific p 38 N87-20687
Equatorial Indian Ocean evaporation estimates from operational meteorological satellites and some inferences in the context of monsoon onset and activity p 39 N87-22041
Ozone in the boundary layer of the equatorial Pacific Ocean p 41 N87-25534
Atmospheric characteristics of the equatorial Pacific during the 1982-1983 El Nino, deduced from satellite and aircraft observations p 41 N87-25543
Equatorial long-wave characteristics determined from satellite sea surface temperature and in situ data p 44 N87-30923
- EQUIPMENT SPECIFICATIONS**
The TIMS instrument p 79 N87-17112
- ERROR ANALYSIS**
The effect of measurement error and confusion from vegetation on passive microwave estimates of soil moisture p 18 N87-17304
Atmospheric water vapor corrections for altimetry measurements p 85 N87-18197
- ERRORS**
Variability in the Earth radiation budget as determined from the Nimbus ERB experiments p 84 N87-17410
- ERS-1 (ESA SATELLITE)**
The SEU risk assessment of Z80A, 80B6 and 80C86 microprocessors intended for use in a low altitude polar orbit p 74 N87-22025
The prospects for hydrological measurements using ERS-1 --- lakes p 59 N87-15588
An overview of operational SAR data collection and dissemination plans for ERS-1 ice data in Canada p 47 N87-17189
Overview and status of the ERS-1 program p 47 N87-17190
The ESA approach for ERS-1 sensor calibration and performance verification p 80 N87-17192
ERS-1 radar altimeter: Performance, calibration and data validation p 80 N87-17194
An automatic tracking mode switching algorithm for the ERS-1 altimeter p 81 N87-17195
ERS-1 fast delivery processing and products p 81 N87-17224
Canadian plans for operational demonstrations of satellite imaging radar applications --- ERS-1 p 68 N87-17229
Future user requirements and required technological developments of spaceborne synthetic aperture radars p 82 N87-17320
Proceedings of an ESA Workshop on ERS-1 Wind and Wave Calibration [ESA-SP-262] p 84 N87-17363
ERS-1 mission constraints related to wind and wave calibration p 84 N87-17364
Gathering and processing a comparative data set for the calibration and validation of ERS-1 data products; preparatory work at the UK-ERS-DC --- Data Center (DC) p 50 N87-17367
Requirements and constraints in the calibration and validation of ERS-1 wind and wave parameters p 51 N87-17369
Evaluation of the different parameters in Long's C-band model --- for ERS-1 scatterometer p 51 N87-17370
Validation of ERS-1 wind data using observations from research and voluntary observing ships p 51 N87-17374
The accuracy and availability of operational marine surface wind data for ERS-1 sensor calibration and validation from fixed platforms and free drifting buoys p 51 N87-17376
Using buoys and ships to calibrate ERS-1 altimeter and scatterometer p 51 N87-17377
Canada Center for Remote Sensing (CCRS) Convoir 580 results relevant to ERS-1 wind and wave calibration p 84 N87-17379
Oceanographic measurement capabilities of the NASA P-3 aircraft --- ERS-1 mission p 52 N87-17380
The use of aircraft for wind scatterometer calibration --- ERS-1 scatterometer p 84 N87-17382
Intersensor comparisons for validation of wind speed measurements from ERS-1 altimeter and scatterometer --- Seasat p 52 N87-17386
Australian validation plans for ERS-1 p 84 N87-17387
Wave modeling activities of the Wave Modeling (WAM) group relevant to ERS-1 p 52 N87-17389
Intelligent SAR Processor (ISAR), a new concept for high throughput and high precision digital SAR processing p 85 N87-18178
A very fast synthetic-aperture radar signal processor for ERS-1 and Radarsat p 85 N87-18180
- ESA SPACECRAFT**
The Along Track Scanning Radiometer (ATSR) for ERS1 p 73 N87-19660

ESTIMATING

Estimation of vegetation cover at subpixel resolution using LANDSAT data [NASA-CR-177077] p 11 N87-15514

ESTUARIES

Drainage channel network of the Arcachon Basin using Thematic Mapper data obtained at high tide p 58 A87-29013
Modelling of estuarine chlorophyll-A from an airborne scanner p 61 N87-18172

ETHIOPIA

Reflections on drought - Ethiopia 1983-1984 p 6 A87-24780

EUROPA

Tidal heating in an internal ocean model of Europa p 43 A87-30143

EUROPE

Satellite-derived vegetation index over Europe p 12 N87-15583

EUROPEAN SPACE PROGRAMS

Future European plans in the framework of the International Satellite Land Surface Climatology Project (ISLSCP) p 78 N87-15628

EVAPORATION RATE

Equatorial Indian Ocean evaporation estimates from operational meteorological satellites and some inferences in the context of monsoon onset and activity p 39 A87-22041

EVAPOTRANSPIRATION

Thermography - Principles and application in the Oost-Gelderland remote sensing study project p 3 A87-21247

An assessment of evapotranspirational water losses in a Sierran Mixed Conifer forest using remotely sensed data p 4 A87-23816

Modelisation of evapotranspiration and soil available water over an agricultural region applicable for remote sensing p 12 N87-15554

Contribution of passive microwave remote sensing in soil moisture and evapotranspiration measurements p 12 N87-15589

Group Agromet Monitoring Project (GAMP) methodology integrated mapping of rainfall, evapotranspiration, germination, biomass development and thermal inertia, based on Meteosat and conventional meteorological data p 59 N87-15626

EXPERIMENT DESIGN

The first International Satellite Land Surface Climatology Project (ISLSCP) Field Experiment - FIFE p 14 N87-15629

Hydrological Atmospheric Pilot Experiment (HAPEX) hydrology budget modeling (MOBILHY): Outline of the program p 59 N87-15632

X-SAR extends the frequency range of Shuttle Imaging Radar p 70 N87-17362

Shuttle imaging radar-C science plan [NASA-CR-180241] p 86 N87-18697

EXPERT SYSTEMS

A knowledge-based software environment for the analysis of spectroradiometer data --- mineral identification p 68 N87-17203

F**FARM CROPS**

Automation of thematic processing of space images in evaluating crop condition p 8 A87-26539

Canopy hot-spot as crop identifier [DE86-011258] p 19 N87-17395

The processing of and information extraction from airborne SLAR data [NLR-MP-86004-U] p 23 N87-18919

FARMLANDS

Comparison of some classification methods on a test site (Kiskore, Hungary) - Separability as a measure of accuracy p 9 A87-29006

Calibration of normalized vegetation index against pasture growth --- NOAA-7 data p 12 N87-15585

Evaluating roughness models of radar backscatter p 19 N87-17344

FEDERAL BUDGETS

The use of space technology in federally funded land processes research in the United States p 88 N87-18152

FILTER WHEEL INFRARED SPECTROMETERS

The Sequential Filter Imaging Radiometer (SFIR), a new instrument configuration for Earth observations p 81 N87-17205

FINLAND

Remote sensing of shallow water areas with reference to environmental and multitemporal monitoring of the Hailuoto area, Finland p 61 N87-18159

FIRE DAMAGE

The use of remote sensing techniques in the study of vegetation recovery after fire in mediterranean countries (a preliminary study) p 14 N87-15623

FISHES

The use of remote sensing in estimating biomass of fish tree areas in the Richard B. Russell Lake p 40 A87-23834

FLIGHT PATHS

Investigation of physics of synthetic aperture radar in ocean remote sensing TOWARD 84/86 field experiment. Volume 2: Contributions of individual investigators [AD-A174527] p 55 N87-18966

FLIGHT TESTS

Results of an airborne synthetic-aperture radar (SAR) experiment over a SIR-B (Shuttle Imaging Radar) test site in Germany p 76 A87-27999

Variations in in-flight absolute radiometric calibration --- satellite remote sensors p 77 N87-15594

Some results of Marine Observation Satellite (MOS-1) airborne verification experiment Multispectral Electronic Self Scanning Radiometer (MESSR) p 46 N87-17166

Canada Center for Remote Sensing (CCRS) Convoir 580 results relevant to ERS-1 wind and wave calibration p 84 N87-17379

FLOOD DAMAGE

The use of remote sensing in estimating biomass of fish tree areas in the Richard B. Russell Lake p 40 A87-23834

FLOOD PREDICTIONS

Detecting and forecasting western region flash floods using GOES imagery and conventional data p 58 A87-27883

FLOW DISTORTION

Effects of a downstream disturbance on the structure of a turbulent plane mixing layer [AIAA PAPER 87-0197] p 74 A87-22476

FOREST FIRE DETECTION

Forest fire monitoring using the NOAA satellite series p 3 A87-23360

FOREST FIRES

Aircraft and satellite thermographic systems for wildfire mapping and assessment [AIAA PAPER 87-0187] p 7 A87-24933

FOREST MANAGEMENT

An assessment of evapotranspirational water losses in a Sierran Mixed Conifer forest using remotely sensed data p 4 A87-23816

Microwave remote sensing: Its applications and limitations in operational tasks of land use inventory and forest management p 17 N87-17266

Classification of forest and surface types by satellite microwave radiometry p 18 N87-17305

SAR imagery for forest management p 18 N87-17313

Influence of canopy shadow on stress detection in coniferous forests using LANDSAT data p 21 N87-18173

Interpreting forest and grassland biome productivity utilizing nested scales of image resolution and biogeographical analysis [NASA-CR-180213] p 23 N87-18912

FORESTS

Thematic mapper analysis of coniferous forest structure and composition p 1 A87-20762

Assessing forest decline in coniferous forests of Vermont using NS-001 Thematic Mapper Simulator data p 1 A87-20763

Estimation of density in young pine plantations using 35mm aerial photography p 5 A87-23819

Identification of forest and agricultural edges using Landsat Thematic Mapper data - Preliminary results p 5 A87-23832

Remote detection of forest damage p 8 A87-26197

The development of procedures for forest interpretation from texture-selective images p 8 A87-26535

Utility of AVHRR channels 3 and 4 in land-cover mapping p 9 A87-28388

Canopy reflectance modeling in a tropical wooded grassland [NASA-CR-180097] p 11 N87-15518

AVHRR and MSS data based vegetation indices studies over Indian sites --- NOAA radiometer (AVHRR) LANDSAT multispectral scanner (MSS) p 14 N87-15622

Investigation of forest canopy temperatures recorded by the thermal infrared multispectral scanner at H. J. Andrews Experimental Forest p 14 N87-17123

Locating subsurface gravel with thermal imagery p 31 N87-17125

Analysis of multiple incidence angle SIR-B data for determining forest stand characteristics p 15 N87-17156

Multiple incidence angle SIR-B experiment over Argentina p 80 N87-17157

Comparison of Thematic Mapper (TM) and SPOT simulation data for agricultural applications in south west Germany p 16 N87-17165

Viewing angle corrections of airborne multispectral scanner data acquired over forested surfaces p 17 N87-17273

Classification of forest and surface types by satellite microwave radiometry p 18 N87-17305

LANDSAT-5 Thematic Mapping (TM) data applications to land use classification on around the Bosphorus area, Turkey p 19 N87-17351

Marrying geocoded image data with other types of geographic information in a PC environment --- forestry p 21 N87-18154

Use of TMS/TM data for mapping of forest decline damage in the northeastern United States --- Thematic Mapper Simulator (TMS) Thematic Mapper (TM) p 22 N87-18175

Multitemporal analysis of the phenological stage of vegetation using TM-data in the Southern Black Forest (West Germany) p 22 N87-18184

Forest cover analysis using SIR-B data p 23 N87-18220

FORMATIONS

Proceedings of the Second Workshop on Remote Sensing/Lineament Applications for Energy Extraction [DE86-006613] p 36 N87-18915

FOURIER ANALYSIS

Exact determination of wave parameters from the results of Fourier analysis of sea-surface radar imagery p 41 A87-24377

FRANCE

Rural land use inventory and mapping in the Ardeche area (France) using multitemporal Thematic Mapping (TM) data p 19 N87-17350

G**GEOBOTANY**

Discrimination of lithologic units using geobotanical and LANDSAT TM spectral data p 34 N87-17246

GEOCHEMISTRY

Integration of surficial geochemistry and LANDSAT imagery to discover skarn tungsten deposits using image analysis techniques [CONTRIB-19586] p 35 N87-17248

GEOCHRONOLOGY

On the relationship between age of lava flows and radar backscattering p 35 N87-17348

GEODESY

Mobile very long baseline interferometry and Global Positioning System measurement of vertical crustal motion p 26 A87-21931

The shape of the earth in the space age p 26 A87-28442

Homogeneous plate deformations on a sphere as monitored by Satellite Laser Ranging (SLR) networks analyzed with the multi-epoch method [ETN-87-99221] p 27 N87-18908

GEODETTIC SATELLITES

The shape of the earth in the space age p 26 A87-28442

GEODETTIC SURVEYS

The application of geodetic radio interferometric surveying to the monitoring of sea-level p 39 A87-21367

The shape of the earth in the space age p 26 A87-28442

The use of Doppler observations to obtain initial geodetic data and to derive plumbline deviations and quasi-geoid heights p 27 A87-28504

GEOYNAMICS

The application of geodetic radio interferometric surveying to the monitoring of sea-level p 39 A87-21367

The earth's C21 and S21 gravity coefficients and the rotation of the core p 27 A87-29977

Basic research for the geodynamics program [NASA-CR-180137] p 27 N87-17415

GEOGRAPHIC INFORMATION SYSTEMS

Techniques for deriving land use information from Landsat data through the use of a geographic information system p 24 A87-23828

Use of topographic and climatological models in a geographical data base to improve Landsat MSS classification for Olympic National Park p 25 A87-30128

GEOGRAPHY

Atlas of geo-science analyses of Landsat imagery in China --- Book p 65 A87-24542

GEOIDS

The use of Doppler observations to obtain initial geodetic data and to derive plumbline deviations and quasi-geoid heights p 27 A87-28504

- Undersea volcano production versus lithospheric strength from satellite altimetry [NASA-CR-179984] p 78 N87-15660
- Improvement of the Earth's gravity field from terrestrial and satellite data [NASA-CR-180139] p 27 N87-17416
- Comparison of ocean tide models with satellite altimeter data [AD-A174698] p 56 N87-19879
- GEOLOGICAL FAULTS**
- Delineation of fault zones using imaging radar p 32 N87-17138
- The megageomorphology of the radar rivers of the eastern Sahara p 32 N87-17139
- A scanning radar altimeter for mapping continental topography p 33 N87-17146
- Kinematics at the intersection of the Garlock and Death Valley fault zones, California: Integration of TM data and field studies [NASA-CR-180182] p 36 N87-18256
- GEOLOGICAL SURVEYS**
- Integration of space-geological and geophysical methods in regional and local predictions of tectonic structures in the Caspian depression p 28 A87-24381
- Identification of reclaimed landscapes of Belorussia from space images p 28 A87-24382
- Use of space imagery and geophysical data in metallogenic prediction studies in central Kyzylkum p 28 A87-24383
- Lineaments of eastern Cuba - Geological interpretation of aerial and space imagery p 28 A87-24384
- Structure of the Kerguelen Plateau province from Seasat altimetry and seismic reflection data p 28 A87-24866
- Quantitative processing procedures and the information content of space imagery in predictions of structural inhomogeneities of the sedimentary cover p 29 A87-26534
- Investigation of spectral correlations of vegetation growing on different types of geological structures p 29 A87-28508
- A comparative study of lineament analysis from different remote sensing imagery over areas in the Benue Valley and Jos Plateau Nigeria p 30 A87-29010
- Geophysical remote sensing p 30 A87-30884
- Structural and geomorphic evolution of Meghalaya plateau, India on LANDSAT imagery p 33 N87-17233
- Hydrogeological research in Peloponnesus (Greece) Karst area by support and completion of LANDSAT-thematic data p 33 N87-17234
- Computer-aided analysis of LANDSAT data for mapping geologic and geomorphic features, North Bombay, India p 33 N87-17235
- Comparative study of LANDSAT MSS, Salyut-7 (TERRA) and radar (SIR-A) images for geological and geomorphological applications: A case study from Rajasthan and Gujarat, India p 34 N87-17236
- Interrelationship between field spectra and airborne MSS systems in the Singatse range, (Yerington) Nevada --- multispectral scanner (MSS) mineral exploration p 34 N87-17242
- Integrated analysis of geological and remote sensing data aimed at mineral deposits detection in the Monapo area (northern Mozambique) p 34 N87-17243
- Application of 2-D Hilbert transform in the interpretation of remotely sensed potential field data --- geology p 35 N87-17293
- Computer-aided interpretation of complex geological patterns in remote sensing p 35 N87-17294
- Proceedings of the Second Workshop on Remote Sensing/Lineament Applications for Energy Extraction [DE86-006613] p 36 N87-18915
- Remote sensing applied to basic geological surveys: A methodological approach for the northeast region [INPE-4041-TDL/246] p 37 N87-19788
- Surface reflectance correction and stereo enhancement of LANDSAT thematic mapper imagery for structural geologic exploration [DE87-003095] p 37 N87-19796
- GEOLOGY**
- Infrared spectroscopy for geologic interpretation of TMS data p 31 N87-17130
- A geologic atlas of TMS data p 32 N87-17133
- GEOMETRICAL OPTICS**
- Microwave backscattering from a layer of randomly oriented discs with application to scattering from vegetation p 8 A87-28316
- GEOMORPHOLOGY**
- Geological nature of early Precambrian formations (considering the example of the Anabar shield) p 28 A87-24274
- Use of space imagery and geophysical data in metallogenic prediction studies in central Kyzylkum p 28 A87-24383
- Terrain analysis from digital patterns in geomorphometry and Landsat MSS spectral response p 66 A87-30127
- The application of remotely sensed data to pedologic and geomorphic mapping on alluvial fan and playa surfaces in Saline Valley, California p 15 N87-17127
- The Red River Valley archeological project p 31 N87-17128
- Tectonic geomorphology of the Andes with SIR-A and SIR-B p 32 N87-17136
- Space shuttle radar images of Indonesia p 32 N87-17137
- Delineation of fault zones using imaging radar p 32 N87-17138
- The megageomorphology of the radar rivers of the eastern Sahara p 32 N87-17139
- Structural and geomorphic evolution of Meghalaya plateau, India on LANDSAT imagery p 33 N87-17233
- Computer-aided analysis of LANDSAT data for mapping geologic and geomorphic features, North Bombay, India p 33 N87-17235
- Comparative study of LANDSAT MSS, Salyut-7 (TERRA) and radar (SIR-A) images for geological and geomorphological applications: A case study from Rajasthan and Gujarat, India p 34 N87-17236
- Geomorphology from space: A global overview of regional landforms [NASA-SP-486] p 36 N87-18139
- Monitoring sediment transfer processes on the desert margin [NASA-CR-180181] p 23 N87-18222
- Evaluation of LANDSAT 4 MSS data for geomorphological mapping in the semiarid environment for regional planning purposes: An integrated approach (study site, the Juazeiro region) [INPE-3984-TDL/236] p 72 N87-19787
- GEOPHYSICAL SATELLITES**
- Evaluation of geophysical parameters measured by the Nimbus-7 microwave radiometer for the TOGA Heat Exchange Project [NASA-CR-180151] p 78 N87-17110
- GEOPHYSICS**
- Integration of space-geological and geophysical methods in regional and local predictions of tectonic structures in the Caspian depression p 28 A87-24381
- Geophysical remote sensing p 30 A87-30884
- Improving the geological interpretation of magnetic and gravity satellite anomalies [NASA-CR-180149] p 35 N87-17418
- GEOPOTENTIAL**
- The earth's C21 and S21 gravity coefficients and the rotation of the core p 27 A87-29977
- GEOSYNCHRONOUS ORBITS**
- Ideas for a future earth observing system from geosynchronous orbit p 74 A87-23419
- GEOTHERMAL ENERGY EXTRACTION**
- Proceedings of the Second Workshop on Remote Sensing/Lineament Applications for Energy Extraction [DE86-006613] p 36 N87-18915
- GERMINATION**
- Group Agromet Monitoring Project (GAMP) methodology integrated mapping of rainfall, evapotranspiration, germination, biomass development and thermal inertia, based on Meteosat and conventional meteorological data p 59 N87-15626
- GLACIAL DRIFT**
- Antarctica - Measuring glacier velocity from satellite images p 57 A87-23699
- GLACIOLOGY**
- Analysis of multichannel SAR data of Spitsbergen --- glaciology p 60 N87-17223
- GLOBAL POSITIONING SYSTEM**
- Mobile very long baseline interferometry and Global Positioning System measurement of vertical crustal motion p 26 A87-21931
- Spatial remote sensing to land management --- SPOT/GPS p 70 N87-18157
- GOLD**
- Airborne Thermal Infrared Multispectral Scanner (TIMS) images over disseminated gold deposits, Osgood Mountains, Humboldt County, Nevada p 32 N87-17134
- GRAINS (FOOD)**
- Integrating vector and satellite data to evaluate the adequacy of a grain silo network p 21 N87-18156
- GRANITE**
- Rock type discrimination with AI-based texture analysis algorithms p 28 A87-23782
- GRASSES**
- Phenological effects on grass canopy/spectral relationships p 4 A87-23818
- Estimating and mapping grass cover and biomass from low-level photographic sampling p 9 A87-29005
- GRASSLANDS**
- Machine processing of Landsat data for soil survey - The Benue Valley savanna case study p 1 A87-20759
- Monitoring the grasslands of the Sahel using NOAA AVHRR data Niger 1983 p 6 A87-24782
- Rainfall and vegetation monitoring in the Savanna Zone of the Democratic Republic of Sudan using the NOAA Advanced Very High Resolution Radiometer p 6 A87-24783
- Monitoring the grasslands of the Sahel 1984-1985 p 7 A87-24787
- Assessment of grassland phytomass with airborne video imagery p 8 A87-25590
- Airborne MSS data to estimate GLAI --- Green Leaf Area Index p 11 A87-30898
- Canopy reflectance modeling in a tropical wooded grassland [NASA-CR-180097] p 11 N87-15518
- Calibration of normalized vegetation index against pasture growth --- NOAA-7 data p 12 N87-15585
- Assessing grass canopy condition and growth from combined optical-microwave measurements p 17 N87-17286
- Multitemporal analysis of the phenological stage of vegetation using TM-data in the Southern Black Forest (West Germany) p 22 N87-18184
- GRAVELS**
- Visualization by aerial thermography of hydrodynamic exchanges between the water table, streams and gravel pits in the Rhine plain north of Strasbourg p 58 A87-25746
- Locating subsurface gravel with thermal imagery p 31 N87-17125
- GRAVITATIONAL FIELDS**
- Improvement of the Earth's gravity field from terrestrial and satellite data [NASA-CR-180139] p 27 N87-17416
- GRAVITY ANOMALIES**
- Improving the geological interpretation of magnetic and gravity satellite anomalies [NASA-CR-180149] p 35 N87-17418
- GRAVITY WAVES**
- Optical and radar observations of the nonlinear interaction of gravity waves p 37 A87-20350
- Wind-wave relationship from Seasat radar altimeter data p 41 A87-24748
- SEASAT microwave altimeter measurement of the ocean gravity wave equilibrium-range spectral behavior using full-wave theory p 53 N87-18165
- GRAZING**
- Spatial analysis of the dynamics of an ecosystem by multistage remote sensing in Kenya p 16 N87-17173
- GREAT LAKES (NORTH AMERICA)**
- The utility of Thematic Mapper data for temperature mapping in the Great Lakes p 57 A87-23824
- GREECE**
- The use of remote sensing techniques in the study of vegetation recovery after fire in mediterranean countries (a preliminary study) p 14 N87-15623
- Hydrogeological research in Peloponnesus (Greece) Karst area by support and completion of LANDSAT-thematic data p 33 N87-17234
- GREENLAND**
- The ice conditions in the Greenland waters, 1980 [REPT-551.467.3.068(988)] p 53 N87-17428
- GROUND STATIONS**
- The FRS-68010: A new concept for the acquisition and analysis of NOAA HRPT data p 68 N87-17206
- Digital satellite imagery acquisition and processing p 68 N87-17207
- Remote Sensing Laboratory [ETN-87-98850] p 88 N87-18227
- GROUND TRUTH**
- NMR instrument for soil moisture ground-truth data collection p 2 A87-21240
- Extraction of areas infested by pine bark beetle using Landsat MSS data p 10 A87-30129
- Ground radiometry and airborne multispectral survey of bare soils p 10 A87-30894
- Archival of Seasat-A satellite scatterometer data merged with in situ data at selected, illuminated sites over the ocean [NASA-TM-87736] p 45 N87-16492
- Atmospheric corrections of NOAA-AVHRR data verification of different methods by ground truth measurements p 70 N87-17274
- Comparison concept of satellite derived wind and wave data with ground truth p 51 N87-17373
- Oceanographic measurement capabilities of the NASA P-3 aircraft --- ERS-1 mission p 52 N87-17380
- GROUND WATER**
- Development of EOS-aided procedures for the determination of the water balance of hydrologic budget of a large watershed [NASA-CR-180118] p 60 N87-16388

H

HABITATS

- Using Landsat to assess tropical forest habitat for migratory birds in the Yucatan Peninsula p 4 A87-23807

HAWAII

- Hawaiian lava flows and SIR-B results p 69 N87-17245

HAZARDS

- Application of remote sensing in the study of the soil hazards of Haryana State, India p 20 N87-18150

HAZE

- Arctic haze: Natural or pollution? [AD-A174025] p 55 N87-18931

HEAT FLUX

- Month-to-month variability of ocean-atmosphere latent heat flux as observed from the Nimbus microwave radiometer p 39 A87-23391
Modelisation of evapotranspiration and soil available water over an agricultural region applicable for remote sensing p 12 N87-15554
Thermal inertia and soil fluxes by remote sensing p 20 N87-18143

HEAT ISLANDS

- Environmental modification of metropolitan areas through satellite images: Study of urban design in the tropics p 25 N87-17175

HEAT TRANSFER

- Possibilities of using satellite data for computations of the ocean/atmosphere heat exchange in the Newfoundland energy-active ocean zone in winter p 41 A87-24379

HEATING

- Tidal heating in an internal ocean model of Europa p 43 A87-30143

HIGH SPEED CAMERAS

- Multilens cameras for high velocity/low altitude photoreconnaissance p 75 A87-23650

HILBERT TRANSFORMATION

- Application of 2-D Hilbert transform in the interpretation of remotely sensed potential field data --- geology p 35 N87-17293

HUMAN PERFORMANCE

- A cognitive measure of texture in imagery p 64 A87-23800
Land surface models as collateral data in satellite image interpretation p 70 N87-18155

HURRICANES

- The effect of Hurricane Gloria on sea surface temperature patterns p 39 A87-23362

HYDRODYNAMIC COEFFICIENTS

- Study of ocean bottom coupling process using satellite altimeter data p 54 N87-18199

HYDRODYNAMICS

- Visualization by aerial thermography of hydrodynamic exchanges between the water table, streams and gravel pits in the Rhine plain north of Strasbourg p 58 A87-25746
Hydrodynamics of internal solitons and a comparison of SIR-A and SIR-B data with ocean measurements p 45 N87-17147

HYDROGEOLOGY

- Hydrogeological research in Peloponnesus (Greece) Karst area by support and completion of LANDSAT-thematic data p 33 N87-17234

HYDROGRAPHY

- Mesoscale hydrographic variability in the vicinity of Points Conception and Arguello during April-May 1983 - The OPUS 1983 experiment p 39 A87-23719

HYDROLOGY

- Remote sensing of hydrological variables from the DMSP microwave mission sensors p 57 A87-23374
Landsat Thematic Mapper images for hydrologic land use and cover p 58 A87-23831
Visualization by aerial thermography of hydrodynamic exchanges between the water table, streams and gravel pits in the Rhine plain north of Strasbourg p 58 A87-25746
Use of decimeter waves in studies of water bodies by methods of microwave radiometry p 58 A87-26537
Hydrological studies in Niger p 59 N87-15609
Application of remote sensing in hydrology and water resources [INPE-3986-PRE/991] p 60 N87-16382
Development of EOS-aided procedures for the determination of the water balance of hydrologic budget of a large watershed [NASA-CR-180118] p 60 N87-16383

HYDROLOGY MODELS

- Hydrologic models of land surface processes --- soil moisture p 58 N87-15547
Remote sensing identified in climate model experiments with hydrological and albedo changes in the Sahel p 59 N87-15569

- Hydrological Atmospheric Pilot Experiment (HAPEX) hydrology budget modeling (MOBILHY): Outline of the program p 59 N87-15632

HYDROMETEOROLOGY

- Remote sensing of hydrological variables from the DMSP microwave mission sensors p 57 A87-23374
Microwave radiances from horizontally finite precipitating clouds containing ice and liquid hydrometeors p 61 N87-17340

I

ICE

- A thermal device for aircraft measurement of the solid water content of clouds p 56 A87-20951
The ice conditions in the Greenland waters, 1980 [REPT-551.467.3.068(988)] p 53 N87-17428
Arctic haze: Natural or pollution? [AD-A174025] p 55 N87-18931

ICE ENVIRONMENTS

- Imaging radar contributions to a major air-sea-ice interaction study in the Greenland Sea p 46 N87-17150
Observing the polar oceans with spaceborne radar p 46 N87-17151

ICE FLOES

- SAR ice floe kinematics and correlation with mesoscale oceanic structure within the marginal ice zone p 48 N87-17222

ICE MAPPING

- Automated remote sensing of sea ice using synthetic aperture radar p 46 N87-17186
An overview of operational SAR data collection and dissemination plans for ERS-1 ice data in Canada p 47 N87-17189
Geophysics of the marginal ice zone from SAR p 47 N87-17219

ICE NUCLEI

- Microwave radiances from horizontally finite precipitating clouds containing ice and liquid hydrometeors p 61 N87-17340

ICE REPORTING

- STAR-VUE: A tactical ice navigation workstation p 54 N87-18181

IDENTIFYING

- Vegetation identification and variability in the Tahoua area, Nigeria --- LANDSAT thematic mapper p 13 N87-15610

- A knowledge-based software environment for the analysis of spectroradiometer data --- mineral identification p 68 N87-17203

IMAGE ANALYSIS

- Machine processing of Landsat data for soil survey - The Benue Valley savanna case study p 1 A87-20759
Illustration of the influence of shadowing on high latitude information derived from satellite imagery p 62 A87-20768

- Capabilities for source assessment --- in cartography p 63 A87-23793

- Classification of multirate Thematic Mapper data p 64 A87-23795

- A cognitive measure of texture in imagery p 64 A87-23800

- Photometric functions, reflectance map - Two techniques for determining surface shape and orientation from image intensity p 64 A87-23802

- Pre-assessment for large scale civil engineering projects by integrated analysis with the data numerical topography and remote sensing p 57 A87-23815

- Landsat Thematic Mapper data analysis within the Suwannee River Basin p 57 A87-23825

- Exact determination of wave parameters from the results of Fourier analysis of sea-surface radar imagery p 41 A87-24377

- Methods of geological interpretation of lineaments of platform areas (with reference to Ustiurt) p 29 A87-26532

- The principles and procedures of modeling ore-related objects in predictive metallogenic investigations (using satellite-borne data) p 29 A87-26533

- Extraction of areas infested by pine bark beetle using Landsat MSS data p 10 A87-30129

- Microcomputer-assisted video image analysis of lodging in winter wheat p 10 A87-30130

- Comparison of Thematic Mapper (TM) and SPOT simulation data for agricultural applications in south west Germany p 16 N87-17165

- Extracting surface features in multispectral imagery p 68 N87-17211

- Using secondary image products to aid in understanding and interpretation of radar imagery p 68 N87-17239

- Integration of surficial geochemistry and LANDSAT imagery to discover skarn tungsten deposits using image analysis techniques [CONTRIB-19586] p 35 N87-17248

- The influence of resampling method and multitemporal LANDSAT imagery on crop classification accuracy in the United Kingdom p 16 N87-17250

- Analysis of the spatial structure of Synthetic Aperture Radar (SAR) imagery for a better separability of cereal crops, wheat and barley p 17 N87-17287

- Computer-aided interpretation of complex geological patterns in remote sensing p 35 N87-17294

- Parameter space techniques for image registration p 70 N87-17327

- Land surface models as collateral data in satellite image interpretation p 70 N87-18155

- Nature and origin of mineral coatings on volcanic rocks of the Black Mountain, Stonewall Mountain, and Kane Springs, Wash volcanic centers, Southern Nevada [NASA-CR-180183] p 36 N87-18255

- Remote sensing applied to basic geological surveys: A methodological approach for the northeast region [INPE-4041-TDL/246] p 37 N87-19788

- Spectral characteristics and the extent of paleosols of the Palouse formation p 24 N87-19826

- Influence of the Yukon River on the Bering Sea [NASA-CR-180356] p 56 N87-19877

- IMAGE ENHANCEMENT

- A synergistic approach for multispectral image restoration using reference imagery p 69 N87-17255

- Merging spaceborne image data of optical and microwave sensors p 69 N87-17267

- IMAGE MOTION COMPENSATION

- Multilens cameras for high velocity/low altitude photoreconnaissance p 75 A87-23650

- IMAGE PROCESSING

- Processing thematic mapper data for mapping in Tunisia p 2 A87-21244

- Rock type discrimination with AI-based texture analysis algorithms p 28 A87-23782

- Digital image matching techniques for standard photogrammetric applications p 63 A87-23785

- The production of orthophotographs by digital image processing techniques p 63 A87-23787

- Accurate determination of ellipse centers in digital imagery p 63 A87-23788

- An information processing system for integration of data from remote sensors, aerial photographs and existing maps p 63 A87-23791

- Space Shuttle radargrammetry results p 65 A87-23827

- Automation of thematic processing of space images in evaluating crop condition p 8 A87-26539

- Space Shuttle cloud detection and earth feature classification experiment p 77 A87-31139

- Sparse area stereo matching experiment [AD-A173601] p 66 N87-16388

- Enhancement of time images for photointerpretation p 66 N87-17116

- Detection and mapping of volcanic rock assemblages and associated hydrothermal alteration with Thermal Infrared Multiband Scanner (TIMS) data Comstock Lode Mining District, Virginia City, Nevada p 31 N87-17119

- Application of TIMS data in stratigraphic analysis p 31 N87-17121

- Calculation of day and night emittance values p 67 N87-17131

- SIR-B measurements and modeling of vegetation p 15 N87-17160

- Digital satellite imagery acquisition and processing p 68 N87-17207

- Extracting surface features in multispectral imagery p 68 N87-17211

- ERS-1 fast delivery processing and products p 81 N87-17224

- Multispectral classification of microwave remote sensing images --- SAR crop identification p 16 N87-17238

- Using secondary image products to aid in understanding and interpretation of radar imagery p 68 N87-17239

- Application of 2-D Hilbert transform in the interpretation of remotely sensed potential field data --- geology p 35 N87-17293

- Computer-aided interpretation of complex geological patterns in remote sensing p 35 N87-17294

- Parameter space techniques for image registration p 70 N87-17327

- Optical visual evaluation and interpretation of remote sensing data p 83 N87-17353

- A procedure for estimation of two-dimensional ocean height-variance spectra from SAR imagery p 52 N87-17381

- Soil degradation evaluation by digital image processing p 20 N87-18147

- Integrating vector and satellite data to evaluate the adequacy of a grain silo network p 21 N87-18156

- Digital realtime SAR processor for C- and X-band applications p 71 N87-18177

- Intelligent SAR Processor (ISAR), a new concept for high throughput and high precision SAR processing p 85 N87-18178
- High speed image processing system based on the custom VLSI for Digital Signal Processing (DSP) --- SAR imagery p 71 N87-18179
- Vegetation and soils information contained in transformed Thematic Mapper data p 22 N87-18185
- Description of a methodology for biomass change mapping with the use of LANDSAT TM data p 22 N87-18186
- Resolving the Doppler ambiguity for spaceborne synthetic aperture radar p 72 N87-18212
- Remote Sensing Information Sciences Research Group, year four [NASA-CR-180198] p 88 N87-18907
- Surface reflectance correction and stereo enhancement of LANDSAT thematic mapper imagery for structural geologic exploration [DE87-003095] p 37 N87-19796
- IMAGE RECONSTRUCTION**
- A synergistic approach for multispectral image restoration using reference imagery p 69 N87-17255
- Merging spaceborne image data of optical and microwave sensors p 69 N87-17267
- IMAGE RESOLUTION**
- Point positioning and mapping with Large Format Camera data p 71 N87-18188
- IMAGERY**
- Monitoring sediment transfer processes on the desert margin [NASA-CR-180181] p 23 N87-18222
- Nature and origin of mineral coatings on volcanic rocks of the Black Mountain, Stonewall Mountain, and Kane Springs, Wash volcanic centers, Southern Nevada [NASA-CR-180183] p 36 N87-18255
- IMAGES**
- VARAN-S radar image interpretation [CNES-CT/DRT/TIT/RL-54-T] p 66 N87-16963
- IMAGING RADAR**
- The Second Spaceborne Imaging Radar Symposium [NASA-CR-180131] p 67 N87-17135
- Delineation of fault zones using imaging radar p 32 N87-17138
- Spaceborne imaging radar research in the 90's p 79 N87-17141
- Imaging radar contributions to a major air-sea-ice interaction study in the Greenland Sea p 46 N87-17150
- Observing the polar oceans with spaceborne radar p 46 N87-17151
- Imaging radar polarimetry from wave synthesis p 82 N87-17279
- On the discrimination between crude oil spills and monomolecular sea slicks by airborne remote sensors: Today's possibilities and limitations p 53 N87-18167
- Oil slick detection with a sidelooking airborne radar p 53 N87-18169
- IMAGING TECHNIQUES**
- Locating subsurface gravel with thermal imagery p 31 N87-17125
- Imaging spectrometry: Aircraft and space program p 81 N87-17202
- The Sequential Filter Imaging Radiometer (SFIR), a new instrument configuration for Earth observations p 81 N87-17205
- Thematic mapper studies of central Andean volcanoes [NASA-CR-180252] p 36 N87-18910
- INCIDENCE**
- Multiple incidence angle SIR-B experiment over Argentina p 80 N87-17157
- INCIDENT RADIATION**
- A radar ocean imaging model for small to moderate incidence angles p 43 A87-29015
- INDEXES (RATIOS)**
- Satellite-derived vegetation index over Europe p 12 N87-15583
- INDIA**
- AVHRR and MSS data based vegetation indices studies over Indian sites --- NOAA radiometer (AVHRR) LANDSAT multispectral scanner (MSS) p 14 N87-15622
- Significance of space image, air photo and drainage linears in relation to west coast tectonics, India p 33 N87-17232
- Structural and geomorphic evolution of Meghalaya plateau, India on LANDSAT imagery p 33 N87-17233
- Application of remote sensing in the study of the soil hazards of Haryana State, India p 20 N87-18150
- Remote sensing applications in the study of land use and soils of aeolian cover of the western part of Haryana State, India p 22 N87-18187
- INDIAN OCEAN**
- Equatorial Indian Ocean evaporation estimates from operational meteorological satellites and some inferences in the context of monsoon onset and activity p 39 A87-22041
- Spatial evolution of wave spectra in the vicinity of the Agulhas current from SIR-B p 50 N87-17337
- INDIAN SPACE PROGRAM**
- Indian remote sensing program p 77 N87-15242
- INDIAN SPACECRAFT**
- Indian remote sensing program p 77 N87-15242
- INDONESIA**
- Space shuttle radar images of Indonesia p 32 N87-17137
- INERTIA**
- Thermal inertia and soil fluxes by remote sensing p 20 N87-18143
- INFESTATION**
- An initial evaluation of two digital airborne imagers for surveying spruce budworm defoliation p 1 A87-20671
- Assessment of ecological conditions associated with the 1980/81 desert locust plague upsurge in West Africa using environmental satellite data p 7 A87-24789
- Extraction of areas infested by pine bark beetle using Landsat MSS data p 10 A87-30129
- INFORMATION SYSTEMS**
- Monitoring land use changes in Sri Lanka for land use planning using a geographic information system and satellite imagery p 26 N87-18151
- INFORMATION THEORY**
- Components and comparisons of potential information from several imaging satellites p 67 N87-17164
- INFRARED IMAGERY**
- Evaluation of the mid-infrared (1.45 to 2.0 microns) with a black-and-white infrared video camera p 73 A87-20672
- Experimental results in soil moisture mapping using IR thermography p 2 A87-21246
- Timely thermal infrared data acquisition for soil survey in humid temperature environments p 3 A87-21249
- An objective method for computing advective surface velocities from sequential infrared satellite images p 39 A87-23717
- The quantitative use of airborne Thematic Mapper thermal infrared data p 44 A87-30900
- Rainfall estimation over the Sahel using Meteosat thermal infra-red data p 59 N87-15587
- Concept of a future multispectral Thermal Infrared (TIR) pushbroom mission for Earth observation from space p 80 N87-17169
- Estimation of internal wave currents from SAR and infrared scatterometer imagery p 48 N87-17295
- Thermal infrared remote sensing: One of today's solutions p 83 N87-17324
- Off-nadir optical remote sensing from satellites for vegetation identification p 22 N87-18183
- The impact of satellite infrared sea surface temperatures on FNOCC (Fleet Numerical Oceanography Center) ocean thermal analyses [AD-A173333] p 54 N87-18295
- INFRARED RADAR**
- Spaceborne imaging radar research in the 90's p 79 N87-17141
- INFRARED RADIATION**
- The effect of local advection on the inference of soil moisture from thermal infrared radiances p 3 A87-23388
- Radiometric analysis of the longwave infrared channel of the Thematic Mapper on LANDSAT 4 and 5 [NASA-CR-180180] p 86 N87-18221
- INFRARED RADIOMETERS**
- The Along Track Scanning Radiometer (ATSR) for ERS1 p 73 A87-19660
- Verification of small-scale water vapor features in VAS imagery using high resolution MAMS imagery --- VISSR Atmospheric Sounder - Multispectral Atmospheric Mapping Sensor p 62 A87-23348
- Soil moisture estimates from satellite infrared temperatures and their relation to surface measurements p 3 A87-23389
- Characteristics of maximum-value composite images from temporal AVHRR data p 75 A87-24778
- Estimating pre-harvest production of maize in Kenya using large-scale aerial photography and radiometry p 9 A87-29004
- On the use of synthetic 12-micron data in a split-window retrieval of sea surface temperature from AVHRR measurements p 43 A87-29019
- Contribution of passive microwave remote sensing in soil moisture and evapotranspiration measurements p 12 N87-15589
- INFRARED SCANNERS**
- The Along Track Scanning Radiometer (ATSR) for ERS1 p 73 A87-19660
- The TIMS Data User's Workshop [NASA-CR-180130] p 78 N87-17111
- The TIMS instrument p 79 N87-17112
- Models for temperature estimation from remotely sensed thermal IR data p 83 N87-17325
- The use of thermal airborne remote sensing for soil identification: A case study in Limousin (France) p 20 N87-18146
- INLAND WATERS**
- Satellite altimeter measurements over land and inland water p 61 N87-18200
- INTERNAL WAVES**
- Analysis of surface patterns over Cobb Seamount using synthetic-aperture radar imagery [AD-A171670] p 45 N87-16493
- Hydrodynamics of internal solitons and a comparison of SIR-A and SIR-B data with ocean measurements p 45 N87-17147
- C and Ku-band scatterometer results from the SCATTMOD internal wave experiment p 47 N87-17215
- Estimation of internal wave currents from SAR and infrared scatterometer imagery p 48 N87-17295
- Characterisation of internal wave surface patterns on airborne SAR imagery p 50 N87-17338
- INVENTORIES**
- Microwave remote sensing: Its applications and limitations in operational tasks of land use inventory and forest management p 17 N87-17266
- INVERSIONS**
- Improving the geological interpretation of magnetic and gravity satellite anomalies [NASA-CR-180149] p 35 N87-17418
- IRAN**
- Discrimination of land features using LANDSAT false colour composite in N Iran p 19 N87-17352
- ISLANDS**
- Island wakes and headland eddies - A comparison between remotely sensed data and laboratory experiments p 44 A87-30925
- ISRO**
- Indian remote sensing program p 77 N87-15242
- ITERATIVE SOLUTION**
- An iterative Landsat-MSS classification methodology for soil survey p 3 A87-23797
- J**
- JAPANESE SPACE PROGRAM**
- Present status of Japanese ERS-1 Project p 79 N87-17145
- A satellite-borne SAR transmitter and receiver p 83 N87-17358
- Pulse compression test results of the SAR transmitter and receiver --- satellite-borne SAR p 83 N87-17360
- JAPANESE SPACECRAFT**
- Development, status, prospects of marine observation satellite p 45 N87-15989
- Outline of SAR-850 data processing method in Japan --- ERS-1 (NASDA) p 71 N87-18176
- JORDAN**
- Results of tectonic and spectral investigations along the Wadi Araba fault in Jordan using special processed Thematic Mapping (TM) data p 34 N87-17247
- K**
- KARST**
- Hydrogeological research in Peloponnesus (Greece) Karst area by support and completion of LANDSAT-thematic data p 33 N87-17234
- KENYA**
- Use of remote sensing application for agricultural expansion into semi-arid areas of Kenya p 13 N87-15607
- KINEMATICS**
- SAR ice floe kinematics and correlation with mesoscale oceanic structure within the marginal ice zone p 48 N87-17222
- Kinematics at the intersection of the Garlock and Death Valley fault zones, California: Integration of TM data and field studies [NASA-CR-180182] p 36 N87-18256
- L**
- LABORATORY EQUIPMENT**
- Remote Sensing Laboratory [ETN-87-98850] p 88 N87-18227
- LAKE ICE**
- A climatological-hydrological study of lake ice in the southwestern mountain area in Norway by use of satellite sensing p 61 N87-17319
- LAKES**
- Remote sensing of aquatic macrophyte distribution in upper Lake Marion p 57 A87-23826
- The use of remote sensing in estimating biomass of fish tree areas in the Richard B. Russell Lake p 40 A87-23834

- The prospects for hydrological measurements using ERS-1 --- lakes p 59 N87-15588
Ground water-fed lakes in the Libyan desert: Their varying area as observed by means of LANDSAT-MSS data p 59 N87-15611
Analysis of AIS radiometry at Mono Lake, California --- Airborne Imaging Spectrometer (AIS) p 81 N87-17204
- LAND**
Hydrologic models of land surface processes --- soil moisture p 58 N87-15547
Evaluation of climate relevant land surface characteristics from remote sensing p 12 N87-15572
Design of a data base system for inferring land surface parameters and fluxes from satellite radiances p 66 N87-15625
Future European plans in the framework of the International Satellite Land Surface Climatology Project (ISLSCP) p 78 N87-15628
The first International Satellite Land Surface Climatology Project (ISLSCP) Field Experiment - FIFE p 14 N87-15629
The use of space technology in federally funded land processes research in the United States p 88 N87-18152
- LAND ICE**
Sea ice in the Greenland sea observed by the Nimbus-7 Scanning Multichannel Microwave Radiometer (SMMR) p 48 N87-17221
- LAND MANAGEMENT**
Spatial remote sensing to land management --- SPOT/GPS p 70 N87-18157
- LAND MOBILE SATELLITE SERVICE**
Tree attenuation at 869 MHz derived from remotely piloted aircraft measurements p 9 A87-28414
- LAND USE**
Techniques for deriving land use information from Landsat data through the use of a geographic information system p 24 A87-23828
Landsat Thematic Mapper images for hydrologic land use and cover p 58 A87-23831
Land applications for remote sensing from space p 25 A87-30882
The interactive effect of spatial resolution and degree of internal variability within land-cover types on classification accuracies p 77 A87-30895
The use of aerial remote sensing in a case study of desertification: Quixaba-PE [INPE-3963-PRE/980] p 11 N87-15519
Regional studies with satellite data in Africa on the desertification of the Sudan-Sahel belt in Nigeria p 13 N87-15605
The application of LANDSAT imagery for land cover assessment --- Thailand p 13 N87-15614
Sri Lanka's solution to land use mapping and monitoring for Third World countries development p 67 N87-17174
Bitemporal analysis of Thematic Mapper data for land cover classification p 69 N87-17249
Monitoring land use changes in Sri Lanka for land use planning using a geographic information system and satellite imagery p 26 N87-18151
Land surface models as collateral data in satellite image interpretation p 70 N87-18155
Southern Pantanal Matogrossense (South America) of Modular Optoelectronic Multispectral Scanner (MOMS) data, preliminary results p 71 N87-18182
Remote sensing applications in the study of land use and soils of aeolian cover of the western part of Haryana State, India p 22 N87-18187
UMUS: A project for usage of LANDSAT MSS and ancillary data in land cover mapping of large areas in southern Italy p 72 N87-18191
Automatic update procedure of the digitized land use map using LANDSAT TM data p 72 N87-18192
CANASATE: Sugar cane mapping by satellite, area 3 [INPE-4068-RPE/526] p 24 N87-19790
- LANDFORMS**
Geomorphology from space: A global overview of regional landforms [NASA-SP-486] p 36 N87-18139
- LANDSAT SATELLITES**
Space remote sensing p 86 A87-20682
Machine processing of Landsat data for soil survey - The Benue Valley savanna case study p 1 A87-20759
Spectral brightness and surface soil characteristics in an arid Mediterranean region (southern Tunisia) p 2 A87-21242
The thematic mapper - A new tool for soil mapping in arid areas p 2 A87-21243
Processing thematic mapper data for mapping in Tunisia p 2 A87-21244
An iterative Landsat-MSS classification methodology for soil survey p 3 A87-23797
POLYSITE - An interactive package for the selection and refinement of Landsat image training sites p 65 A87-23805
- Agricultural remote sensing in South Carolina - A study of crop identification capabilities utilizing Landsat data p 4 A87-23806
Using Landsat to assess tropical forest habitat for migratory birds in the Yucatan Peninsula p 4 A87-23807
Cartographic analysis of remote sensing data through Landsat mosaic scaling p 65 A87-23809
Landsat Thematic Mapper data analysis within the Suwannee River Basin p 57 A87-23825
Techniques for deriving land use information from Landsat data through the use of a geographic information system p 24 A87-23828
Detection of new urban build-up in Ardmore and McAlester, Oklahoma using Landsat MSS data p 25 A87-23829
Landsat Thematic Mapper digital information content for agricultural environments p 5 A87-23830
Landsat Thematic Mapper images for hydrologic land use and cover p 58 A87-23831
Vegetable crop inventory with Landsat TM data p 5 A87-23833
Atlas of geo-science analyses of Landsat imagery in China --- Book p 65 A87-24542
Satellite remote sensing of rangelands in Botswana. I - Landsat MSS and herbaceous vegetation p 7 A87-24785
Moorland plant community recognition using Landsat MSS data p 7 A87-25589
Fruit tree inventory with Landsat Thematic Mapper data p 8 A87-28387
Impact of environmental variables on spectral signatures acquired by the Landsat Thematic Mapper p 9 A87-29003
An analysis of geologic lineaments seen on Landsat MSS imagery p 30 A87-29011
Discrimination of altered basaltic rocks in the southwestern United States by analysis of Landsat Thematic Mapper data p 30 A87-30126
Use of topographic and climatological models in a geographical data base to improve Landsat MSS classification for Olympic National Park p 25 A87-30128
Extraction of areas infested by pine bark beetle using Landsat MSS data p 10 A87-30129
Land applications for remote sensing from space p 25 A87-30882
Ocean remote sensing p 44 A87-30883
Geophysical remote sensing p 30 A87-30884
Estimation of surface albedo using satellite data. A simple formulation for atmospheric effects p 25 N87-15579
Vegetation index models for the assessment of vegetation in marginal areas p 12 N87-15584
Vegetation identification and variability in the Tahoua area, Nigeria --- LANDSAT thematic mapper p 13 N87-15610
Ground water-fed lakes in the Libyan desert: Their varying area as observed by means of LANDSAT-MSS data p 59 N87-15611
Assessment of wind and fluvial action by using LANDSAT-MSS color composites in the lower Nile Valley (Egypt) p 13 N87-15612
The application of LANDSAT imagery for land cover assessment --- Thailand p 13 N87-15614
AVHRR and MSS data based vegetation indices studies over Indian sites --- NOAA radiometer (AVHRR) LANDSAT multispectral scanner (MSS) p 14 N87-15622
Comparison of Thematic Mapper (TM) and SPOT simulation data for agricultural applications in south west Germany p 16 N87-17165
The transfer of remote sensing technology to developing countries: A survey of experts in the field p 87 N87-17170
Structural and geomorphic evolution of Meghalaya plateau, India on LANDSAT imagery p 33 N87-17233
Hydrogeological research in Peloponnesus (Greece) Karst area by support and completion of LANDSAT-thematic data p 33 N87-17234
Computer-aided analysis of LANDSAT data for mapping geologic and geomorphic features, North Bombay, India p 33 N87-17235
Comparative study of LANDSAT MSS, Salyut-7 (TERRA) and radar (SIR-A) images for geological and geomorphological applications: A case study from Rajasthan and Gujarat, India p 34 N87-17236
Discrimination of lithologic units using geobotanical and LANDSAT TM spectral data p 34 N87-17246
Results of tectonic and spectral investigations along the Wadi Araba fault in Jordan using special processed Thematic Mapping (TM) data p 34 N87-17247
Integration of surficial geochemistry and LANDSAT imagery to discover skarn tungsten deposits using image analysis techniques [CONTRIB-19586] p 35 N87-17248
- The influence of resampling method and multitemporal LANDSAT imagery on crop classification accuracy in the United Kingdom p 16 N87-17250
Towards snowmelt runoff forecast using LANDSAT-MSS and NOAA/AVHRR data p 61 N87-17317
Radiometric correction method which removes both atmospheric and topographic effects from the LANDSAT-MSS data p 83 N87-17329
Discrimination of land features using LANDSAT false colour composite in N Iran p 19 N87-17352
Influence of canopy shadow on stress detection in coniferous forests using LANDSAT data p 21 N87-18173
Relationship between tree density, leaf area index, soil metal content, and LANDSAT MSS canopy radiance values p 21 N87-18174
Use of TMS/TM data for mapping of forest decline damage in the northeastern United States --- Thematic Mapper Simulator (TMS) Thematic Mapper (TM) p 22 N87-18175
Vegetation and soils information contained in transformed Thematic Mapper data p 22 N87-18185
Description of a methodology for biomass change mapping with the use of LANDSAT TM data p 22 N87-18186
Remote sensing applications in the study of land use and soils of aeolian cover of the western part of Haryana State, India p 22 N87-18187
LANDSAT-MSS remote sensing and satellite cartography: An integrated approach to the preparation of a new geological map of Egypt at a scale of 1:500 000 p 36 N87-18190
UMUS: A project for usage of LANDSAT MSS and ancillary data in land cover mapping of large areas in southern Italy p 72 N87-18191
Monitoring sediment transfer processes on the desert margin [NASA-CR-180181] p 23 N87-18222
Methodology for the elaboration of thematic maps utilizing LANDSAT-TM data [INPE-3893-TDL/225] p 72 N87-19792
- LANDSAT 4**
Identification of forest and agricultural edges using Landsat Thematic Mapper data - Preliminary results p 5 A87-23832
Radiometric analysis of the longwave infrared channel of the Thematic Mapper on LANDSAT 4 and 5 [NASA-CR-180180] p 86 N87-18221
Evaluation of LANDSAT 4 MSS data for geomorphological mapping in the semiarid environment for regional planning purposes: An integrated approach (study site, the Juazeiro region) [INPE-3984-TDL/236] p 72 N87-19787
- LANDSAT 5**
Bitemporal analysis of Thematic Mapper data for land cover classification p 69 N87-17249
Evaluation of LANDSAT 5 Thematic Mapping (TM) data for image clustering and classification p 69 N87-17251
Rural land use inventory and mapping in the Ardeche area (France) using multitemporal Thematic Mapping (TM) data p 19 N87-17350
LANDSAT-5 Thematic Mapping (TM) data applications to land use classification on around the Bosphorus area, Turkey p 19 N87-17351
Automatic update procedure of the digitized land use map using LANDSAT TM data p 72 N87-18192
Radiometric analysis of the longwave infrared channel of the Thematic Mapper on LANDSAT 4 and 5 [NASA-CR-180180] p 86 N87-18221
- LARGE AREA CROP INVENTORY EXPERIMENT**
An overview of remote sensing agricultural applications in North America: Past, present and future p 17 N87-17284
- LASER APPLICATIONS**
Airborne laser profiling and mapping systems come of age p 75 A87-23786
- LASER INDUCED FLUORESCENCE**
Chlorophyll pigment concentration using spectral curvature algorithms - An evaluation of present and proposed satellite ocean color sensor bands p 37 A87-20204
Proceedings of the 1986 International Geoscience and Remote Sensing Symposium (IGARSS '86) on Remote Sensing: Today's Solutions for Tomorrow's Information Needs, volume 3 [ESA-SP-254-VOL-3] p 84 N87-18142
Laser-induced chlorophyll-A fluorescence of terrestrial plants p 23 N87-18207
- LASER RANGE FINDERS**
Homogeneous plate deformations on a sphere as monitored by Satellite Laser Ranging (SLR) networks analyzed with the multi-epoch method [ETN-87-99221] p 27 N87-18908

LATENT HEAT

Month-to-month variability of ocean-atmosphere latent heat flux as observed from the Nimbus microwave radiometer p 39 A87-23391

LAVA

Preliminary analyses of SIB-B radar data for recent Hawaii lava flows p 29 A87-25588

Hawaiian lava flows and SIR-B results p 69 N87-17245

On the relationship between age of lava flows and radar backscattering p 35 N87-17348

LEAST SQUARES METHOD

A synergistic approach for multispectral image restoration using reference imagery p 69 N87-17255

LEAVES

Estimation of canopy parameters for inhomogeneous vegetation canopies from reflectance data. II - Estimation of leaf area index and percentage of ground cover for row canopies p 1 A87-20761

Diurnal-seasonal light interception, leaf area index, and vegetation index interrelations in a wheat canopy - A case study p 5 A87-23822

Satellite remote sensing of primary production p 6 A87-24777

Preliminary measurements of leaf spectral reflectance in the 8-14/micron p 10 A87-29018

Airborne MSS data to estimate GLAI --- Green Leaf Area Index p 11 A87-30898

LIBYA

Ground water-fed lakes in the Libyan desert: Their varying area as observed by means of LANDSAT-MSS data p 59 N87-15611

LIBYAN DESERT

Ground water-fed lakes in the Libyan desert: Their varying area as observed by means of LANDSAT-MSS data p 59 N87-15611

LIGHT SCATTERING

Radar signature determination: Trends and limitations p 67 N87-17159

LIMNOLOGY

The utility of Thematic Mapper data for temperature mapping in the Great Lakes p 57 A87-23824

Remote sensing of aquatic macrophyte distribution in upper Lake Marion p 57 A87-23826

LITHOLOGY

Lithologic mapping of silicate rocks using TIMS p 30 N87-17118

Application of TIMS data in stratigraphic analysis p 31 N87-17121

A geologic atlas of TIMS data p 32 N87-17133

Space shuttle radar images of Indonesia p 32 N87-17137

Geological applications of multipolarization SAR data p 33 N87-17140

Discrimination of lithologic units using geobotanical and LANDSAT TM spectral data p 34 N87-17246

Results of tectonic and spectral investigations along the Wadi Araba fault in Jordan using special processed Thematic Mapping (TM) data p 34 N87-17247

Nature and origin of mineral coatings on volcanic rocks of the Black Mountain, Stonewall Mountain, and Kane Springs, Wash volcanic centers, Southern Nevada [NASA-CR-180183] p 36 N87-18255

LITHOSPHERE

Improving the geological interpretation of magnetic and gravity satellite anomalies [NASA-CR-180149] p 35 N87-17418

LOCUSTS

Assessment of ecological conditions associated with the 1980/81 desert locust plague upsurge in West Africa using environmental satellite data p 7 A87-24789

LOGISTICS MANAGEMENT

Integrating vector and satellite data to evaluate the adequacy of a grain silo network p 21 N87-18156

LONG TERM EFFECTS

Instrument characterization for the detection of long-term changes in stratospheric ozone - An analysis of the SBUV/2 radiometer p 74 A87-20961

LOUISIANA

Locating subsurface gravel with thermal imagery p 31 N87-17125

LOW ALTITUDE

Multisens cameras for high velocity/low altitude photoreconnaissance p 75 A87-23650

Characteristics of a very low altitude spacecraft for collecting global directional wave spectra with spaceborne synthetic aperture radar p 49 N87-17333

LUMINOUS INTENSITY

Photometric functions, reflectance map - Two techniques for determining surface shape and orientation from image intensity p 64 A87-23802

M**MAGMA**

Nature and origin of mineral coatings on volcanic rocks of the Black Mountain, Stonewall Mountain, and Kane Springs, Wash volcanic centers, Southern Nevada [NASA-CR-180183] p 36 N87-18255

MAGNETIC ANOMALIES

Improving the geological interpretation of magnetic and gravity satellite anomalies [NASA-CR-180149] p 35 N87-17418

MALI

Monitoring vegetation in the Mali Sahel during summer 1984 p 6 A87-24784

MAN ENVIRONMENT INTERACTIONS

The use of aerial remote sensing in a case study of desertification: Quixaba-PE [INPE-3963-PRE/980] p 11 N87-15519

Desertification monitoring: Remotely sensed data for drought impact studies in the Sudan p 12 N87-15604

Spatial analysis of the dynamics of an ecosystem by multistage remote sensing in Kenya p 16 N87-17173

Environmental modification of metropolitan areas through satellite images: Study of urban design in the tropics p 25 N87-17175

MANNED SPACE FLIGHT

Aeronautics and space report of the President: 1985 activities p 87 N87-16662

MANNED SPACECRAFT

Aeronautics and space report of the President: 1985 activities p 87 N87-16662

MAPPING

Airborne laser profiling and mapping systems come of age p 75 A87-23786

Microwave remote sensing: Its applications and limitations in operational tasks of land use inventory and forest management p 17 N87-17266

Digital terrain mapping with STAR-1 SAR data p 69 N87-17269

The ice conditions in the Greenland waters, 1980 [REPT-551.467.3.068(988)] p 53 N87-17428

MAPS

NROSS (Navy Remote Ocean Sensing System) tracking network analysis [AD-A172132] p 45 N87-16384

MARINE BIOLOGY

Variability of the productive habitat in the eastern equatorial Pacific p 38 A87-20687

MARINE ENVIRONMENTS

Ozone in the boundary layer of the equatorial Pacific Ocean p 41 A87-25534

Distribution and biomass of *Fucus vesiculosus* L. near a cooling-water effluent from a nuclear power plant in the Baltic Sea estimated by aerial photography p 43 A87-29014

NROSS (Navy Remote Ocean Sensing System) tracking network analysis [AD-A172132] p 45 N87-16384

The relationship between marine aerosol optical depth and satellite-sensed sea surface temperature [AD-A174337] p 55 N87-18963

Satellite remote sensing of the marine environment: Literature and data sources [PB86-245446] p 56 N87-18971

MARINE METEOROLOGY

The effect of Hurricane Gloria on sea surface temperature patterns p 39 A87-23362

Month-to-month variability of ocean-atmosphere latent heat flux as observed from the Nimbus microwave radiometer p 39 A87-23391

Annual and interannual variability in large-scale convection over the eastern Pacific and tropical South America p 57 A87-23414

Vertical structure of the temperature field above the North Atlantic p 40 A87-24374

Atmospheric characteristics of the equatorial Pacific during the 1982-1983 El Nino, deduced from satellite and aircraft observations p 41 A87-25543

A case study of GWE satellite data impact on GLA assimilation analyses of two ocean cyclones [AD-A174337] p 41 A87-25787

NROSS (Navy Remote Ocean Sensing System) tracking network analysis [AD-A172132] p 45 N87-16384

Archival of Seasat-A satellite scatterometer data merged with in situ data at selected, illuminated sites over the ocean [NASA-TM-87736] p 45 N87-16492

Marine climate program p 52 N87-17390

The relationship between marine aerosol optical depth and satellite-sensed sea surface temperature [AD-A174337] p 55 N87-18963

MARITIME SATELLITES

Development, status, prospects of marine observation satellite p 45 N87-15989

Some results of Marine Observation Satellite (MOS-1) airborne verification experiment Multispectral Electronic Self Scanning Radiometer (MESSR) p 46 N87-17166

Development in radar altimetry: The Navy Geosat mission p 85 N87-18161

Study of ocean bottom coupling process using satellite altimeter data p 54 N87-18199

MARSHLANDS

Classification of reflectance on colour infrared aerial photographs and sub-tropical salt-marsh vegetation types p 10 A87-29012

MASS TRANSFER

Monitoring sediment transfer processes on the desert margin [NASA-CR-180181] p 23 N87-18222

MATCHING

Digital image matching techniques for standard photogrammetric applications p 63 A87-23785

MATHEMATICAL MODELS

Estimation of absolute water surface temperature based on atmospherically corrected thermal infrared multispectral scanner digital data p 79 N87-17114

Simulation modeling and preliminary analysis of TIMS data from the Carlin area and the northern Grapevine Mountains, Nevada p 31 N87-17120

Verification results for a two-scale model of microwave backscatter from the sea surface p 47 N87-17213

SAR imaging of bottom topography in the ocean: Results from an improved model p 48 N87-17298

Evaluating roughness models of radar backscatter p 19 N87-17344

Canopy hot-spot as crop identifier [DE86-011258] p 19 N87-17395

Improving the geological interpretation of magnetic and gravity satellite anomalies [NASA-CR-180149] p 35 N87-17418

Deduction of a synthetic bioclimatological map by means of remote sensing data and a digital terrain model using a correlation approach p 72 N87-18194

Comparison of ocean tide models with satellite altimeter data [AD-A174698] p 56 N87-19879

MAXIMUM LIKELIHOOD ESTIMATES

Satellite rainfall retrieval by logistic regression p 56 A87-23370

MEGALOPOLISES

Environmental modification of metropolitan areas through satellite images: Study of urban design in the tropics p 25 N87-17175

MELTING

Snow cover recession in an Alpine ecological system p 18 N87-17316

Towards snowmelt runoff forecast using LANDSAT-MSS and NOAA/AVHRR data p 61 N87-17317

A climatological-hydrological study of lake ice in the southwestern mountain area in Norway by use of satellite sensing p 61 N87-17319

MESOMETEOROLOGY

Forecasting sea breeze thunderstorms at the Kennedy Space Center using the Prognostic Three-Dimensional Mesoscale Model (P 3DM) p 43 A87-27891

MESOSCALE PHENOMENA

Mesoscale hydrographic variability in the vicinity of Points Conception and Arguello during April-May 1983 - The OPUS 1983 experiment p 39 A87-23719

Temperature-plant pigment-optical relations in a recurrent offshore mesoscale eddy near Point Conception, California [AD-A176666] p 39 A87-23720

Ocean surface pressure fields from satellite-sensed winds p 41 A87-25797

Utilization of satellite data in mesoscale modeling of severe weather [NASA-CR-179917] p 78 N87-15669

SAR ice floe kinematics and correlation with mesoscale oceanic structure within the marginal ice zone p 48 N87-17222

METALS

Analysis of correlations between structural elements detected on space images and metallogenic zones p 28 A87-24380

Use of space imagery and geophysical data in metallogenic prediction studies in central Kyzylkum p 28 A87-24383

METEOROLOGICAL FLIGHT

Canada Center for Remote Sensing (CCRS) Convair 580 results relevant to ERS-1 wind and wave calibration p 84 N87-17379

Oceanographic measurement capabilities of the NASA P-3 aircraft --- ERS-1 mission p 52 N87-17380

The use of aircraft for wind scatterometer calibration --- ERS-1 scatterometer p 84 N87-17382

METEOROLOGICAL PARAMETERS

Remote sensing of hydrological variables from the DMSP microwave mission sensors p 57 A87-23374

- Satellite remote sensing of meteorological parameters for global numerical weather prediction p 76 A87-26098
- Remote sensing of land-surface temperature from HIRS/MSU data --- High Resolution Infrared Sounder/Microwave Sounding Unit (HIRS/MSU) p 77 N87-15573
- A two-step algorithm for the separate retrieval of ocean surface and atmospheric parameters from microwave radiometers p 50 N87-17341
- METEOROLOGICAL RADAR**
- Imaging radar contributions to a major air-sea-ice interaction study in the Greenland Sea p 46 N87-17150
- METEOROLOGICAL SATELLITES**
- Satellite remote sensing of meteorological parameters for global numerical weather prediction p 76 A87-26098
- Satellite contributions to convective scale weather analysis and forecasting p 76 A87-27882
- Current achievements and future projects/useful applications of weather satellites and future remote sensing p 76 A87-29431
- Future European plans in the framework of the International Satellite Land Surface Climatology Project (ISLSCP) p 78 N87-15628
- Atmospheric water vapor corrections for altimetry measurements p 85 N87-18197
- METEOROLOGICAL SERVICES**
- Detecting and forecasting western region flash floods using GOES imagery and conventional data p 58 A87-27883
- METEOSAT SATELLITE**
- Rainfall estimation over the Sahel using Meteosat thermal infra-red data p 59 N87-15587
- Group Agromet Monitoring Project (GAMP) methodology integrated mapping of rainfall, evapotranspiration, germination, biomass development and thermal inertia, based on Meteosat and conventional meteorological data p 59 N87-15626
- MICROCOMPUTERS**
- Microcomputer-assisted video image analysis of lodging in winter wheat p 10 A87-30130
- MICROPROCESSORS**
- The SEU risk assessment of Z80A, 8086 and 80C86 microprocessors intended for use in a low altitude polar orbit p 74 A87-22025
- MICROWAVE ATTENUATION**
- Tree attenuation at 869 MHz derived from remotely piloted aircraft measurements p 9 A87-28414
- MICROWAVE EMISSION**
- Dielectric and surface parameters related to microwave scatter and emission properties p 16 N87-17262
- Microwave radiances from horizontally finite precipitating clouds containing ice and liquid hydrometeors p 61 N87-17340
- L to X-band scatter and emission measurements of vegetation p 19 N87-17347
- MICROWAVE IMAGERY**
- Classification of sea ice types with single-band (33.6 GHz) airborne passive microwave imagery p 42 A87-27545
- The processing of and information extraction from airborne SLAR data [NLR-MP-86004-U] p 23 N87-18919
- MICROWAVE RADIOMETERS**
- Nimbus-7 SMMR multispectral passive microwave correlations with an antecedent precipitation index p 74 A87-23390
- Month-to-month variability of ocean-atmosphere latent heat flux as observed from the Nimbus microwave radiometer p 39 A87-23391
- Use of decimeter waves in studies of water bodies by methods of microwave radiometry p 58 A87-26537
- Further development of an improved altimeter wind speed algorithm p 42 A87-27848
- Development and experiment of airborne microwave rain-scatterometer/radiometer system. III - Rain measurement and its data analysis p 58 A87-28436
- Development and experiment of airborne microwave rain-scatterometer/radiometer system. IV - Microwave back-scattering experiment of ocean surface p 43 A87-28437
- Contribution of passive microwave remote sensing in soil moisture and evapotranspiration measurements p 12 N87-15589
- Observations of the seasonal variability of soil moisture and vegetation cover over Africa using satellite microwave radiometry p 12 N87-15593
- Evaluation of geophysical parameters measured by the Nimbus-7 microwave radiometer for the TOGA Heat Exchange Project [NASA-CR-180151] p 78 N87-17110
- Sea ice in the Greenland sea observed by the Nimbus-7 Scanning Multichannel Microwave Radiometer (SMMR) p 48 N87-17221
- The Electronically Steered Thinned Array Radiometer (ESTAR) p 82 N87-17260
- Development of algorithms to retrieve the water equivalent of snow cover from satellite microwave radiometer data p 60 N87-17264
- Atmospheric corrections of NOAA-AVHRR data verification of different methods by ground truth measurements p 70 N87-17274
- Classification of forest and surface types by satellite microwave radiometry p 18 N87-17305
- Estimation of maximum snow volume distribution using NOAA-AVHRR data p 60 N87-17314
- A two-step algorithm for the separate retrieval of ocean surface and atmospheric parameters from microwave radiometers p 50 N87-17341
- Retrieval of near-surface wind speed in the Baltic Sea from NIMBUS-7 Scanning Multichannel Microwave Radiometer (SMMR) observations p 50 N87-17342
- Sea ice studies in the Baltic Sea using satellite microwave radiometer data p 50 N87-17343
- Intersensor comparisons for validation of wind speed measurements from ERS-1 altimeter and scatterometer --- Seasat p 52 N87-17386
- Contributions to oil spill detection and analysis with radar and microwave radiometry, results of the Archimedes 2 campaign p 54 N87-18170
- Retrieval and global comparison of oceanic winds from SEASAT radiometer, scatterometer and altimeter p 85 N87-18219
- MICROWAVE SCATTERING**
- Measurement of microwave backscattering signatures of the ocean surface using X band and K(a) band airborne scatterometers p 40 A87-23725
- Microwave backscattering from a layer of randomly oriented discs with application to scattering from vegetation p 8 A87-28316
- Development and experiment of airborne microwave rain-scatterometer/radiometer system. III - Rain measurement and its data analysis p 58 A87-28436
- Development and experiment of airborne microwave rain-scatterometer/radiometer system. IV - Microwave back-scattering experiment of ocean surface p 43 A87-28437
- Verification results for a two-scale model of microwave backscatter from the sea surface p 47 N87-17213
- C and Ku-band scatterometer results from the SCATTMOD internal wave experiment p 47 N87-17215
- Dielectric and surface parameters related to microwave scatter and emission properties p 16 N87-17262
- L to X-band scatter and emission measurements of vegetation p 19 N87-17347
- SEASAT microwave altimeter measurement of the ocean gravity wave equilibrium-range spectral behavior using full-wave theory p 53 N87-18165
- MICROWAVE SENSORS**
- Remote sensing of hydrological variables from the DMSP microwave mission sensors p 57 A87-23374
- Assessing grass canopy condition and growth from combined optical-microwave measurements p 17 N87-17286
- MICROWAVE SOUNDING**
- An inter-sensor comparison of the microwave signatures of Arctic sea ice p 46 N87-17184
- Active/passive microwave sensor comparison of MIZ-ice concentration estimates --- Marginal Ice Zone (MIZ) p 46 N87-17185
- MIGRATION**
- Using Landsat to assess tropical forest habitat for migratory birds in the Yucatan Peninsula p 4 A87-23807
- MINERAL EXPLORATION**
- Analysis of correlations between structural elements detected on space images and metallogenic zones p 28 A87-24380
- Use of space imagery and geophysical data in metallogenic prediction studies in central Kyzylkum p 28 A87-24383
- Airborne Thermal Infrared Multispectral Scanner (TIMS) images over disseminated gold deposits, Osgood Mountains, Humboldt County, Nevada p 32 N87-17134
- Interrelationship between field spectra and airborne MSS systems in the Singatse range, (Yerington) Nevada --- multispectral scanner (MSS) mineral exploration p 34 N87-17242
- Integrated analysis of geological and remote sensing data aimed at mineral deposits detection in the Monapo area (northern Mozambique) p 34 N87-17243
- Integration of surficial geochemistry and LANDSAT imagery to discover skarn tungsten deposits using image analysis techniques [CONTRIB-19586] p 35 N87-17248
- MINERALOGY**
- The principles and procedures of modeling ore-related objects in predictive metallogenic investigations (using satellite-borne data) p 29 A87-26533
- Discrimination of altered basaltic rocks in the southwestern United States by analysis of Landsat Thematic Mapper data p 30 A87-30126
- MINERALS**
- Application of TIMS data in stratigraphic analysis p 31 N87-17121
- A knowledge-based software environment for the analysis of spectroradiometer data --- mineral identification p 68 N87-17203
- MISSION PLANNING**
- Present statue of Japanese ERS-1 Project p 79 N87-17145
- MODELS**
- Canopy reflectance modeling in a tropical wooded grassland [NASA-CR-180097] p 11 N87-15518
- MODULATION TRANSFER FUNCTION**
- The SAR image modulation transfer function derived from SIR-B image spectra and airborne measurements of ocean wave height spectra p 49 N87-17334
- MOISTURE CONTENT**
- A thermal device for aircraft measurement of the solid water content of clouds p 56 A87-20951
- Modeling energy flow and nutrient cycling in natural semiarid grassland ecosystems with the aid of thematic mapper data [NASA-CR-179903] p 11 N87-15517
- Development of algorithms to retrieve the water equivalent of snow cover from satellite microwave radiometer data p 60 N87-17264
- Estimation of maximum snow volume distribution using NOAA-AVHRR data p 60 N87-17314
- MONOMOLECULAR FILMS**
- On the discrimination between crude oil spills and monomolecular sea slicks by airborne remote sensors: Today's possibilities and limitations p 53 N87-18167
- MONSOONS**
- Equatorial Indian Ocean evaporation estimates from operational meteorological satellites and some inferences in the context of monsoon onset and activity p 39 A87-22041
- MONTE CARLO METHOD**
- Canopy hot-spot as crop identifier [DE86-011258] p 19 N87-17395
- MORPHOLOGY**
- Computer-aided interpretation of complex geological patterns in remote sensing p 35 N87-17294
- MOZAICS**
- Cartographic analysis of remote sensing data through Landsat mosaic scaling p 65 A87-23809
- MOUNTAINS**
- Satellite observations of snow covered area in the High Atlas Mountains of Morocco p 57 A87-23808
- Airborne Thermal Infrared Multispectral Scanner (TIMS) images over disseminated gold deposits, Osgood Mountains, Humboldt County, Nevada p 32 N87-17134
- Multitemporal analysis of the phenological stage of vegetation using TM-data in the Southern Black Forest (West Germany) p 22 N87-18184
- MOZAMBIQUE**
- Integrated analysis of geological and remote sensing data aimed at mineral deposits detection in the Monapo area (northern Mozambique) p 34 N87-17243
- MULTISPECTRAL BAND CAMERAS**
- Optical visual evaluation and interpretation of remote sensing data p 83 N87-17353
- MULTISPECTRAL BAND SCANNERS**
- Improved multispectral earth imaging from space using electronic image alignment p 73 A87-19655
- Proposed design of an imaging spectropolarimeter/photometer for remote sensing of earth resources p 73 A87-20795
- Verification of small-scale water vapor features in VAS imagery using high resolution MAMS imagery --- VISSR Atmospheric Sounder - Multispectral Atmospheric Mapping Sensor p 62 A87-23348
- An iterative Landsat-MSS classification methodology for soil survey p 3 A87-23797
- Moorland plant community recognition using Landsat MSS data p 7 A87-25589
- Terrain analysis from digital patterns in geomorphometry and Landsat MSS spectral response p 66 A87-30127
- Use of topographic and climatological models in a geographical data base to improve Landsat MSS classification for Olympic National Park p 25 A87-30128
- Extraction of areas infested by pine bark beetle using Landsat MSS data p 10 A87-30129
- Land applications for remote sensing from space p 25 A87-30882

SUBJECT INDEX

Ground radiometry and airborne multispectral survey of bare soils p 10 A87-30894

The interactive effect of spatial resolution and degree of internal variability within land-cover types on classification accuracies p 77 A87-30895

Airborne MSS data to estimate GLAI --- Green Leaf Area Index p 11 A87-30898

Ground water-fed lakes in the Libyan desert: Their varying area as observed by means of LANDSAT-MSS data p 59 N87-15611

The TIMS Data User's Workshop [NASA-CR-180130] p 78 N87-17111

The TIMS instrument p 79 N87-17112

Concept of a future multispectral Thermal Infrared (TIR) pushbroom mission for Earth observation from space p 80 N87-17169

Imaging spectrometry: Aircraft and space program p 81 N87-17202

Extracting surface features in multispectral imagery p 68 N87-17211

Comparative study of LANDSAT MSS, Salyut-7 (TERRA) and radar (SIR-A) images for geological and geomorphological applications: A case study from Rajasthan and Gujarat, India p 34 N87-17236

Interrelationship between field spectra and airborne MSS systems in the Singatse range, (Yerington) Nevada --- multispectral scanner (MSS) mineral exploration p 34 N87-17242

The influence of resampling method and multitemporal LANDSAT imagery on crop classification accuracy in the United Kingdom p 16 N87-17250

A synergistic approach for multispectral image restoration using reference imagery p 69 N87-17255

Viewing angle corrections of airborne multispectral scanner data acquired over forested surfaces p 17 N87-17273

Radiometric correction method which removes both atmospheric and topographic effects from the LANDSAT-MSS data p 83 N87-17329

Discrimination of land features using LANDSAT false colour composite in N Iran p 19 N87-17352

Modelling of estuarine chlorophyll-A from an airborne scanner p 61 N87-18172

Relationship between tree density, leaf area index, soil metal content, and LANDSAT MSS canopy radiance values p 21 N87-18174

Southern Pantanal Matogrossense (South America) of Modular Optoelectronic Multispectral Scanner (MOMS) data, preliminary results p 71 N87-18182

Monitoring sediment transfer processes on the desert margin [NASA-CR-180181] p 23 N87-18222

Surface reflectance correction and stereo enhancement of LANDSAT thematic mapper imagery for structural geological exploration [DE87-003095] p 37 N87-19796

MULTISPECTRAL LINEAR ARRAYS

Improved multispectral earth imaging from space using electronic image alignment p 73 A87-19655

MULTISPECTRAL PHOTOGRAPHY

Determination of the properties of a plowed soil layer from multispectral space imagery p 8 A87-26536

Preliminary analysis of SPOT HRV multispectral products of an arid environment p 10 A87-29017

Components and comparisons of potential information from several imaging satellites p 67 N87-17164

LANDSAT-MSS remote sensing and satellite cartography: An integrated approach to the preparation of a new geological map of Egypt at a scale of 1:500 000 p 36 N87-18190

UMUS: A project for usage of LANDSAT MSS and ancillary data in land cover mapping of large areas in southern Italy p 72 N87-18191

Evaluation of LANDSAT 4 MSS data for geomorphological mapping in the semiarid environment for regional planning purposes: An integrated approach (study site, the Juazeiro region) [INPE-3984-TDL/236] p 72 N87-19787

MULTISTATIC RADAR

An analysis of the potential of satellite-borne bistatic radar sensing of the earth p 75 A87-24385

N

NASA PROGRAMS

Partnerships in remote sensing - A theme with some examples p 86 A87-25531

NASA SPACE PROGRAMS

Aeronautics and space report of the President: 1985 activities p 87 N87-16662

NATIONAL PARKS

Use of topographic and climatological models in a geographical data base to improve Landsat MSS classification for Olympic National Park p 25 A87-30128

NAVIGATION SATELLITES

Preliminary evaluation of Doppler-determined pole positions computed using world geodetic system 1984 [AD-A173467] p 27 N87-18225

NEVADA

Detection and mapping of volcanic rock assemblages and associated hydrothermal alteration with Thermal Infrared Multiband Scanner (TIMS) data Comstock Lode Mining District, Virginia City, Nevada p 31 N87-17119

Simulation modeling and preliminary analysis of TIMS data from the Carlin area and the northern Grapevine Mountains, Nevada p 31 N87-17120

TIMS data applications in Nebraska p 15 N87-17126

Airborne Thermal Infrared Multispectral Scanner (TIMS) images over disseminated gold deposits, Osgood Mountains, Humboldt County, Nevada p 32 N87-17134

Interrelationship between field spectra and airborne MSS systems in the Singatse range, (Yerington) Nevada --- multispectral scanner (MSS) mineral exploration p 34 N87-17242

NEW MEXICO

Estimation of vegetation cover at subpixel resolution using LANDSAT data [NASA-CR-177077] p 11 N87-15514

NIGER

Monitoring the grasslands of the Sahel using NOAA AVHRR data Niger 1983 p 6 A87-24782

Hydrological studies in Niger p 59 N87-15609

Vegetation identification and variability in the Tahoua area, Nigeria --- LANDSAT thematic mapper p 13 N87-15610

NIGERIA

Regional studies with satellite data in Africa on the desertification of the Sudan-Sahel belt in Nigeria p 13 N87-15605

NIMBUS SATELLITES

Month-to-month variability of ocean-atmosphere latent heat flux as observed from the Nimbus microwave radiometer p 39 A87-23391

NIMBUS 7 SATELLITE

Nimbus-7 SMMR multispectral passive microwave correlations with an antecedent precipitation index p 74 A87-23390

Observations of the seasonal variability of soil moisture and vegetation cover over Africa using satellite microwave radiometry p 12 N87-15593

Evaluation of geophysical parameters measured by the Nimbus-7 microwave radiometer for the TOGA Heat Exchange Project [NASA-CR-180151] p 78 N87-17110

Development of algorithms to retrieve the water equivalent of snow cover from satellite microwave radiometer data p 60 N87-17264

Classification of forest and surface types by satellite microwave radiometry p 18 N87-17305

Retrieval of near-surface wind speed in the Baltic Sea from NIMBUS-7 Scanning Multichannel Microwave Radiometer (SMMR) observations p 50 N87-17342

Sea ice studies in the Baltic Sea using satellite microwave radiometer data p 50 N87-17343

NOAA SATELLITES

Forest fire monitoring using the NOAA satellite series p 3 A87-23360

Land surface climatic variables monitored by NOAA-AVHRR satellites p 4 A87-23811

Monitoring the grasslands of the Sahel using NOAA AVHRR data Niger 1983 p 6 A87-24782

Rainfall and vegetation monitoring in the Savanna Zone of the Democratic Republic of Sudan using the NOAA Advanced Very High Resolution Radiometer p 6 A87-24783

Partnerships in remote sensing - A theme with some examples p 86 A87-25531

Utility of AVHRR channels 3 and 4 in land-cover mapping p 9 A87-28388

Remote sensing of land-surface temperature from HIRS/MSU data --- High Resolution Infrared Sounder/Microwave Sounding Unit (HIRS/MSU) p 77 N87-15573

Satellite-derived vegetation index over Europe p 12 N87-15583

AVHRR and MSS data based vegetation indices studies over Indian sites --- NOAA radiometer (AVHRR) LANDSAT multispectral scanner (MSS) p 14 N87-15622

The FRS-68010: A new concept for the acquisition and analysis of NOAA HRPT data p 68 N87-17206

Estimation of maximum snow volume distribution using NOAA-AVHRR data p 60 N87-17314

Towards snowmelt runoff forecast using LANDSAT-MSS and NOAA/AVHRR data p 61 N87-17317

NOAA 7 SATELLITE

Snow survey from meteorological satellite images in the Qilian Mountain Basin in northwest China p 56 A87-20765

OCEAN DATA ACQUISITIONS SYSTEMS

Satellite remote sensing of rangelands in Botswana. II - NOAA AVHRR and herbaceous vegetation p 7 A87-24786

Calibration of normalized vegetation index against pasture growth --- NOAA-7 data p 12 N87-15585

NORTH SEA

Evaluation of remote sensing results for the benefit of water quality research on the North Sea [NZ-R-86.15] p 62 N87-19799

NUCLEAR MAGNETIC RESONANCE

NMR instrument for soil moisture ground-truth data collection p 2 A87-21240

NUCLEAR POWER PLANTS

Distribution and biomass of Fucus vesiculosus L. near a cooling-water effluent from a nuclear power plant in the Baltic Sea estimated by aerial photography p 43 A87-29014

NUMERICAL WEATHER FORECASTING

Satellite remote sensing of meteorological parameters for global numerical weather prediction p 76 A87-26098

Forecasting sea breeze thunderstorms at the Kennedy Space Center using the Prognostic Three-Dimensional Mesoscale Model (P 3DM) p 43 A87-27891

Weather and atmosphere remote sensing p 77 A87-30885

NUTRIENTS

Modeling energy flow and nutrient cycling in natural semiarid grassland ecosystems with the aid of thematic mapper data [NASA-CR-179903] p 11 N87-15517

O

OCEAN BOTTOM

Observations of surface currents at Nantucket Shoals and implications for radar imaging of the bottom p 48 N87-17296

SAR imaging of bottom topography in the ocean: Results from an improved model p 48 N87-17298

Detection of bottom-related surface patterns on visible spectrum imagery --- ocean bottom p 53 N87-18158

Study of ocean bottom coupling process using satellite altimeter data p 54 N87-18199

OCEAN COLOR SCANNER

Space and time variability of the surface color field in the northern Adriatic Sea p 40 A87-23722

OCEAN CURRENTS

Comparison between satellite image advective velocities, dynamic topography, and surface drifter trajectories p 38 A87-20692

An objective method for computing advective surface velocities from sequential infrared satellite images p 39 A87-23717

Automated extraction of pack ice motion from advanced very high resolution radiometer imagery p 42 A87-27547

Shedding of an Agulhas ring observed at sea p 44 A87-30146

Analysis of surface patterns over Cobb Seamount using synthetic-aperture radar imagery [AD-A171670] p 45 N87-16493

Estimation of internal wave currents from SAR and infrared scatterometer imagery p 48 N87-17295

Observations of surface currents at Nantucket Shoals and implications for radar imaging of the bottom p 48 N87-17296

Spatial evolution of wave spectra in the vicinity of the Agulhas current from SIR-B p 50 N87-17337

Influence of the Yukon River on the Bering Sea [NASA-CR-180065] p 54 N87-18293

Physical oceanography program science abstracts [AD-A174019] p 55 N87-18961

OCEAN DATA ACQUISITIONS SYSTEMS

Correlation between time- and depth-resolved simulated lidar signals --- for estimating phytoplankton distribution p 38 A87-20770

NROSS (Navy Remote Ocean Sensing System) tracking network analysis [AD-A172132] p 45 N87-16384

Archival of Seasat-A satellite scatterometer data merged with in situ data at selected, illuminated sites over the ocean [NASA-TM-87736] p 45 N87-16492

Proceedings of the 1986 International Geoscience and Remote Sensing Symposium (IGARSS '86) on Remote Sensing: Today's Solutions for Tomorrow's Information Needs, volume 1 [ESA-SP-254-VOL-1] p 80 N87-17163

Proceedings of the 1986 International Geoscience and Remote Sensing Symposium (IGARSS '86) on Remote Sensing: Today's Solutions for Tomorrow's Information Needs, volume 2 [ESA-SP-254-VOL-2] p 82 N87-17283

- Characteristics of a very low altitude spacecraft for collecting global directional wave spectra with spaceborne synthetic aperture radar p 49 N87-17333
The accuracy and availability of operational marine surface wind data for ERS-1 sensor calibration and validation from fixed platforms and free drifting buoys p 51 N87-17376
- Oceanographic measurement capabilities of the NASA P-3 aircraft --- ERS-1 mission p 52 N87-17380
Development in radar altimetry: The Navy Geosat mission p 85 N87-18161
New techniques in satellite altimeter tracking systems p 85 N87-18164
- Satellite remote sensing of the marine environment: Literature and data sources [PB86-245446] p 56 N87-18971
- OCEAN DYNAMICS**
The Coastal Zone Color Scanner views the Bismarck Sea p 42 A87-26970
Shedding of an Agulhas ring observed at sea p 44 A87-30146
Island wakes and headland eddies - A comparison between remotely sensed data and laboratory experiments p 44 A87-30925
Operational wave forecasting with spaceborne SAR: Prospects and pitfalls p 45 N87-17149
SAR ice floe kinematics and correlation with mesoscale oceanic structure within the marginal ice zone p 48 N87-17222
Physical oceanography program science abstracts [AD-A174019] p 55 N87-18961
- OCEAN MODELS**
A radar ocean imaging model for small to moderate incidence angles p 43 A87-29015
Tidal heating in an internal ocean model of Europa p 43 A87-30143
Wave modeling activities of the Wave Modeling (WAM) group relevant to ERS-1 p 52 N87-17389
Marine climate program p 52 N87-17390
Comparison of ocean tide models with satellite altimeter data [AD-A174698] p 56 N87-19879
- OCEAN SURFACE**
A new semi-empirical sea spectrum for estimating the scattering coefficient p 38 A87-20769
Simultaneous ocean cross section and rainfall measurements from space with a nadir-looking radar p 38 A87-20956
Measurement of microwave backscattering signatures of the ocean surface using X band and Ka) band airborne scatterometers p 40 A87-23725
Exact determination of wave parameters from the results of Fourier analysis of sea-surface radar imagery p 41 A87-24377
Wind-wave relationship from Seasat radar altimeter data p 41 A87-24748
Ocean surface pressure fields from satellite-sensed winds p 41 A87-25797
Spatial-statistical characteristics of sea surface foam fields (from optical sounding data) p 42 A87-26531
Development and experiment of airborne microwave rain-scatterometer/radiometer system. IV - Microwave back-scattering experiment of ocean surface p 43 A87-28437
An automatic tracking mode switching algorithm for the ERS-1 altimeter p 81 N87-17195
Verification results for a two-scale model of microwave backscatter from the sea surface p 47 N87-17213
C and Ku-band scatterometer results from the SCATMOD internal wave experiment p 47 N87-17215
Tower-based broadband backscattering measurements from the ocean surface in the North Sea p 47 N87-17217
Estimation of internal wave currents from SAR and infrared scatterometer imagery p 48 N87-17295
Observations of surface currents at Nantucket Shoals and implications for radar imaging of the bottom p 48 N87-17296
The SAR image modulation transfer function derived from SIR-B image spectra and airborne measurements of ocean wave height spectra p 49 N87-17334
Deriving two-dimensional ocean wave spectra and surface height maps from the Shuttle Imaging Radar (SIR-B) p 49 N87-17336
Characterisation of internal wave surface patterns on airborne SAR imagery p 50 N87-17338
A two-step algorithm for the separate retrieval of ocean surface and atmospheric parameters from microwave radiometers p 50 N87-17341
Retrieval of near-surface wind speed in the Baltic Sea from NIMBUS-7 Scanning Multichannel Microwave Radiometer (SMMR) observations p 50 N87-17342
- The use of numerical wind and wave models to provide areal and temporal extension to instrument calibration and validation of remotely sensed data --- satellite data p 51 N87-17371
Satellite scatterometer comparisons with surface measurements: Techniques and Seasat results p 51 N87-17372
Validation of ERS-1 wind data using observations from research and voluntary observing ships p 51 N87-17374
The accuracy and availability of operational marine surface wind data for ERS-1 sensor calibration and validation from fixed platforms and free drifting buoys p 51 N87-17376
A procedure for estimation of two-dimensional ocean height-variance spectra from SAR imagery p 52 N87-17381
Measurement of the directional spectrum of ocean waves using a conically-scanning radar p 52 N87-17383
An overview of the NSCAT/N-ROSS program p 52 N87-17384
Intersensor comparisons for validation of wind speed measurements from ERS-1 altimeter and scatterometer --- Seasat p 52 N87-17386
A scatterometer research program p 53 N87-17391
Detection of bottom-related surface patterns on visible spectrum imagery --- ocean bottom p 53 N87-18158
SEASAT microwave altimeter measurement of the ocean gravity wave equilibrium-range spectral behavior using full-wave theory p 53 N87-18165
Study of ocean bottom coupling process using satellite altimeter data p 54 N87-18199
- OCEAN TEMPERATURE**
Temperature-plant pigment-optical relations in a recurrent offshore mesoscale eddy near Point Conception, California [AD-A176666] p 39 A87-23720
Possibilities of using satellite data for computations of the ocean/atmosphere heat exchange in the Newfoundland energy-active ocean zone in winter p 41 A87-24379
Tidal heating in an internal ocean model of Europa p 43 A87-30143
The impact of satellite infrared sea surface temperatures on FNOC (Fleet Numerical Oceanography Center) ocean thermal analyses p 54 N87-18295
SeaSoar CTD surveys during FASINEX --- Conductivity Temperature Depth (CTD); Frontal Air Sea Interaction Experiment (FASINEX) [IOS-230] p 55 N87-18970
- OCEANOGRAPHIC PARAMETERS**
Data sensitivities of sea ice drift and ocean stress in North Atlantic high latitudes p 38 A87-20520
A radar ocean imaging model for small to moderate incidence angles p 43 A87-29015
Ocean remote sensing p 44 A87-30883
The Second Spaceborne Imaging Radar Symposium [NASA-CR-180131] p 67 N87-17135
Hydrodynamics of internal solitons and a comparison of SIR-A and SIR-B data with ocean measurements p 45 N87-17147
A two-step algorithm for the separate retrieval of ocean surface and atmospheric parameters from microwave radiometers p 50 N87-17341
Gathering and processing a comparative data set for the calibration and validation of ERS-1 data products; preparatory work at the UK-ERS-DC --- Data Center (DC) p 50 N87-17367
Requirements and constraints in the calibration and validation of ERS-1 wind and wave parameters p 51 N87-17369
Evaluation of the different parameters in Long's C-band model --- for ERS-1 scatterometer p 51 N87-17370
A description of large-scale variability in the ocean using the diffuse attenuation coefficient p 53 N87-18160
Retrieval and global comparison of oceanic winds from SEASAT radiometer, scatterometer and altimeter p 85 N87-18219
Investigation of physics of synthetic aperture radar in ocean remote sensing TOWARD 84/86 field experiment. Volume 2: Contributions of individual investigators [AD-A174527] p 55 N87-18966
SeaSoar CTD surveys during FASINEX --- Conductivity Temperature Depth (CTD); Frontal Air Sea Interaction Experiment (FASINEX) [IOS-230] p 55 N87-18970
- OCEANOGRAPHY**
The TIMS Data User's Workshop [NASA-CR-180130] p 78 N87-17111
Proceedings of the 1986 International Geoscience and Remote Sensing Symposium (IGARSS '86) on Remote Sensing: Today's Solutions for Tomorrow's Information Needs, volume 3 [ESA-SP-254-VOL-3] p 84 N87-18142
- Report of the Fourth Session of the JSC/CCCO Tropical Ocean Global Atmosphere (TOGA) Scientific Steering Group [WCP-120] p 54 N87-18283
The impact of satellite infrared sea surface temperatures on FNOC (Fleet Numerical Oceanography Center) ocean thermal analyses p 54 N87-18295
Physical oceanography program science abstracts [AD-A174019] p 55 N87-18961
- OCEANS**
A case study of GWE satellite data impact on GLA assimilation analyses of two ocean cyclones p 41 A87-25787
Investigation of physics of synthetic aperture radar in ocean remote sensing toward 84/86 field experiment. Volume 1: Data summary and early results [AD-A174197] p 55 N87-18913
- OFFSHORE PLATFORMS**
Tower-based broadband backscattering measurements from the ocean surface in the North Sea p 47 N87-17217
The accuracy and availability of operational marine surface wind data for ERS-1 sensor calibration and validation from fixed platforms and free drifting buoys p 51 N87-17376
- OIL POLLUTION**
Proceedings of the 1986 International Geoscience and Remote Sensing Symposium (IGARSS '86) on Remote Sensing: Today's Solutions for Tomorrow's Information Needs, volume 3 [ESA-SP-254-VOL-3] p 84 N87-18142
On the discrimination between crude oil spills and monomolecular sea slicks by airborne remote sensors: Today's possibilities and limitations p 53 N87-18167
Contributions to oil spill detection and analysis with radar and microwave radiometry, results of the Archimedes 2 campaign p 54 N87-18170
- OIL SLICKS**
On the discrimination between crude oil spills and monomolecular sea slicks by airborne remote sensors: Today's possibilities and limitations p 53 N87-18167
Oil slick detection with a sidelooking airborne radar p 53 N87-18169
- OKLAHOMA**
The Red River Valley archeological project p 31 N87-17128
- OPTICAL EQUIPMENT**
Instrumentation for optical remote sensing from space; Proceedings of the Meeting, Cannes, France, November 27-29, 1985 [SPIE-589] p 73 A87-19647
- OPTICAL MEASURING INSTRUMENTS**
Present status of Japanese ERS-1 Project p 79 N87-17145
- OPTICAL RADAR**
Correlation between time- and depth-resolved simulated lidar signals --- for estimating phytoplankton distribution p 38 A87-20770
Development and demonstration of ALARM (Airborne Lidar Agent Remote Monitor) [AD-A172886] p 78 N87-16387
- OPTICAL SCANNERS**
Assessing grass canopy condition and growth from combined optical-microwave measurements p 17 N87-17286
Off-nadir optical remote sensing from satellites for vegetation identification p 22 N87-18183
- OPTIMIZATION**
Interpreting forest and grassland biome productivity utilizing nested scales of image resolution and biogeographical analysis [NASA-CR-180213] p 23 N87-18912
- ORBITAL SPACE STATIONS**
Remote Sensing Information Sciences Research Group, year four [NASA-CR-180198] p 88 N87-18907
- ORCHARDS**
Fruit tree inventory with Landsat Thematic Mapper data p 8 A87-28387
- OREGON**
Investigation of forest canopy temperatures recorded by the thermal infrared multispectral scanner at H. J. Andrews Experimental Forest p 14 N87-17123
- ORTHOGRAPHY**
The production of orthophotographs by digital image processing techniques p 63 A87-23787
- OZONE**
Ozone in the boundary layer of the equatorial Pacific Ocean p 41 A87-25534
Ozone formation in pollutant plumes: A reactive plume model with arbitrary crosswind resolution [PB86-236973] p 26 N87-18246

OZONOMETRY

Instrument characterization for the detection of long-term changes in stratospheric ozone - An analysis of the SBUV/2 radiometer p 74 A87-20961

P**P-3 AIRCRAFT**

Oceanographic measurement capabilities of the NASA P-3 aircraft --- ERS-1 mission p 52 N87-17380

PACIFIC OCEAN

Variability of the productive habitat in the eastern equatorial Pacific p 38 A87-20687
Annual and interannual variability in large-scale convection over the eastern Pacific and tropical South America p 57 A87-23414
A satellite time series of sea surface temperatures in the eastern equatorial Pacific Ocean, 1982-1986 p 39 A87-23718

Ozone in the boundary layer of the equatorial Pacific Ocean p 41 A87-25534

Atmospheric characteristics of the equatorial Pacific during the 1982-1983 El Nino, deduced from satellite and aircraft observations p 41 A87-25543

Influence of the Yukon River on the Bering Sea [NASA-CR-180065] p 54 N87-18293

PARAMETER IDENTIFICATION

An integrated system to assess agricultural productivity --- satellite imagery p 14 N87-15621

Design of a data base system for inferring land surface parameters and fluxes from satellite radiances p 66 N87-15625

The effect of measurement error and confusion from vegetation on passive microwave estimates of soil moisture p 18 N87-17304

PARAMETERIZATION

Toward a satellite system to monitor the spatial and temporal behavior of soil water content p 18 N87-17288

Parameter space techniques for image registration p 70 N87-17327

Evaluation of the different parameters in Long's C-band model --- for ERS-1 scatterometer p 51 N87-17370

PATTERN RECOGNITION

Accurate determination of ellipse centers in digital imagery p 63 A87-23788

Photometric functions, reflectance map - Two techniques for determining surface shape and orientation from image intensity p 64 A87-23802

Sparse area stereo matching experiment [AD-A173601] p 66 N87-16388

PATTERN REGISTRATION

Parameter space techniques for image registration p 70 N87-17327

PERFORMANCE PREDICTION

ERS-1 radar altimeter: Performance, calibration and data validation p 80 N87-17194

PERFORMANCE TESTS

A satellite-borne SAR transmitter and receiver p 83 N87-17358

Pulse compression test results of the SAR transmitter and receiver --- satellite-borne SAR p 83 N87-17360

PERMITTIVITY

Dielectric and surface parameters related to microwave scatter and emission properties p 16 N87-17262

PERSONAL COMPUTERS

Marrying geocoded image data with other types of geographic information in a PC environment --- forestry p 21 N87-18154

PETROGRAPHY

Nature and origin of mineral coatings on volcanic rocks of the Black Mountain, Stonewall Mountain, and Kane Springs, Wash volcanic centers, Southern Nevada [NASA-CR-180183] p 36 N87-18255

PHENOLOGY

Multitemporal analysis of the phenological stage of vegetation using TM-data in the Southern Black Forest (West Germany) p 22 N87-18184

PHOTO GEOLOGY

Analysis of correlations between structural elements detected on space images and metallogenic zones p 28 A87-24380

Use of space imagery and geophysical data in metallogenic prediction studies in central Kyzylkum p 28 A87-24383

Earth sensing - New tools enable scientists to gain insight into the structure of our planet's surface p 29 A87-25890

Methods of geological interpretation of lineaments of platform areas (with reference to Ustiurt) p 29 A87-26532

Quantitative processing procedures and the information content of space imagery in predictions of structural inhomogeneities of the sedimentary cover p 29 A87-26534

A comparative study of lineament analysis from different remote sensing imagery over areas in the Benue Valley and Jos Plateau Nigeria p 30 A87-29010

An analysis of geologic lineaments seen on Landsat MSS imagery p 30 A87-29011

Discrimination of altered basaltic rocks in the southwestern United States by analysis of Landsat Thematic Mapper data p 30 A87-30126

Geomorphology from space: A global overview of regional landforms [NASA-SP-486] p 36 N87-18139

Proceedings of the Second Workshop on Remote Sensing/Lineament Applications for Energy Extraction [DE86-006613] p 36 N87-18915

PHOTOGRAMMETRY

Composite/progressive sampling - A program package for computer supported collection of DTM data --- Digital Terrain Models p 62 A87-23784

Digital image matching techniques for standard photogrammetric applications p 63 A87-23785

American Congress on Surveying and Mapping and American Society for Photogrammetry and Remote Sensing, Annual Convention, Washington, DC, Mar. 16-21, 1986, Technical Papers. Volume 5 - Remote Sensing p 4 A87-23810

PHOTOINTERPRETATION

Space Shuttle radargrammetry results p 65 A87-23827

A comparative test of photogrammetrically sampled digital elevation models p 66 A87-29499

The stereo-pushbroom scanner system Digital Photogrammetry System (DPS) and its accuracy p 80 N87-17167

PHOTOINTERPRETATION

Soil science interpretation of photographs taken by Spacelab 1 p 2 A87-21241

Capabilities for source assessment --- in cartography p 63 A87-23793

A cognitive measure of texture in imagery p 64 A87-23800

Identification of reclaimed landscapes of Belorussia from space images p 28 A87-24382

Lineaments of eastern Cuba - Geological interpretation of aerial and space imagery p 28 A87-24384

The development of procedures for forest interpretation from texture-selective images p 8 A87-26535

Classification of sea ice types with single-band (33.6 GHz) airborne passive microwave imagery p 42 A87-27545

Interpretation characteristics of space photographs of sea coasts with wind-induced surges p 43 A87-28509

Comparison of some classification methods on a test site (Kiskore, Hungary) - Separability as a measure of accuracy p 9 A87-29006

Performance of Landsat-5 TM data in land-cover classification p 25 A87-29007

Classification of reflectance on colour infrared aerial photographs and sub-tropical salt-marsh vegetation types p 10 A87-29012

Terrain analysis from digital patterns in geomorphometry and Landsat MSS spectral response p 66 A87-30127

Enhancement of time images for photointerpretation p 66 N87-17116

Detection and mapping of volcanic rock assemblages and associated hydrothermal alteration with Thermal Infrared Multiband Scanner (TIMS) data Comstock Lode Mining District, Virginia City, Nevada p 31 N87-17119

Application of Thermal Infrared Multiband Scanner (TIMS) data to mapping of Plutonic and stratified rock and assemblages in accreted terrains of the Northern Sierra, California p 15 N87-17132

Land surface models as collateral data in satellite image interpretation p 70 N87-18155

Evaluation of LANDSAT 4 MSS data for geomorphological mapping in the semiarid environment for regional planning purposes: An integrated approach (study site, the Juazeiro region) [INPE-3984-TDL/236] p 72 N87-19787

Methodology for the elaboration of thematic maps utilizing LANDSAT-TM data [INPE-3893-TDL/225] p 72 N87-19792

PHOTOMAPPING

An information processing system for integration of data from remote sensors, aerial photographs and existing maps p 63 A87-23791

Capabilities for source assessment --- in cartography p 63 A87-23793

Photometric functions, reflectance map - Two techniques for determining surface shape and orientation from image intensity p 64 A87-23802

Cartographic analysis of remote sensing data through Landsat mosaic scaling p 65 A87-23809

American Congress on Surveying and Mapping and American Society for Photogrammetry and Remote Sensing, Annual Convention, Washington, DC, Mar. 16-21, 1986, Technical Papers. Volume 5 - Remote Sensing p 4 A87-23810

A photographic technique for studying reflection indicatrices of vegetation cover p 5 A87-24388

The use of space photography to create and renew small-scale maps p 65 A87-25249

Performance of Landsat-5 TM data in land-cover classification p 25 A87-29007

Point positioning and mapping with Large Format Camera data p 71 N87-18188

Analysis of Large Format Camera images from the Black Hills, USA, for topographic and thematic mapping p 71 N87-18189

LANDSAT-MSS remote sensing and satellite cartography: An integrated approach to the preparation of a new geological map of Egypt at a scale of 1:500 000 p 36 N87-18190

First step in the use of remote sensing for regional mapping of soil organization data: Application in Brittany (France) and French Guiana p 23 N87-18193

Remote sensing applied to basic geological surveys: A methodological approach for the northeast region [INPE-4041-TDL/246] p 37 N87-19788

CANASATE: Sugar cane mapping by satellite, area 3 [INPE-4068-RPE/526] p 24 N87-19790

Methodology for the elaboration of thematic maps utilizing LANDSAT-TM data [INPE-3893-TDL/225] p 72 N87-19792

PHOTOMETRY

Photometric functions, reflectance map - Two techniques for determining surface shape and orientation from image intensity p 64 A87-23802

PHOTORECONNAISSANCE

Multilens cameras for high velocity/low altitude photoreconnaissance p 75 A87-23650

PHOTOSYNTHESIS

Satellite remote sensing of primary production p 6 A87-24777

PHYTOPLANKTON

Variability of the productive habitat in the eastern equatorial Pacific p 38 A87-20687

Correlation between time- and depth-resolved simulated lidar signals --- for estimating phytoplankton distribution p 38 A87-20770

PLANETARY SURFACES

The physical basis for spectral variations in thermal infrared emittance of silicates and application to remote sensing p 31 N87-17129

PLANETARY WAVES

Equatorial long-wave characteristics determined from satellite sea surface temperature and in situ data p 44 A87-30923

PLANT STRESS

Remote detection of forest damage p 8 A87-26197

Proceedings of the 1986 International Geoscience and Remote Sensing Symposium (IGARSS '86) on Remote Sensing: Today's Solutions for Tomorrow's Information Needs, volume 3 [ESA-SP-254-VOL-3] p 84 N87-18142

Remote sensing of wetland plant stress p 21 N87-18171

Influence of canopy shadow on stress detection in coniferous forests using LANDSAT data p 21 N87-18173

PLANTS (BOTANY)

Satellite remote sensing of primary production p 6 A87-24777

Moorland plant community recognition using Landsat MSS data p 7 A87-25589

Laser-induced chlorophyll-A fluorescence of terrestrial plants p 23 N87-18207

PLATEAUS

Structure of the Kerguelen Plateau province from Seasat altimetry and seismic reflection data p 28 A87-24866

Methods of geological interpretation of lineaments of platform areas (with reference to Ustiurt) p 29 A87-26532

PLAYAS

Monitoring sediment transfer processes on the desert margin [NASA-CR-180181] p 23 N87-18222

PLUMES

Ozone formation in pollutant plumes: A reactive plume model with arbitrary crosswind resolution [PB86-236973] p 26 N87-18246

POLAR METEOROLOGY

Observations and analysis of a polar low over the Great Lakes region p 76 A87-27872

POLAR ORBITS

The SEU risk assessment of Z80A, 8086 and 80C86 microprocessors intended for use in a low altitude polar orbit p 74 A87-22025

POLAR REGIONS

Preliminary evaluation of Doppler-determined pole positions computed using world geodetic system 1984 [AD-A173467] p 27 N87-18225

POLAR REGIONS

Illustration of the influence of shadowing on high latitude information derived from satellite imagery p 62 A87-20768

Observing the polar oceans with spaceborne radar p 46 N87-17151

POLAR WANDERING (GEOLOGY)

The application of geodetic radio interferometric surveying to the monitoring of sea-level p 39 A87-21367

POLARIMETERS

Proposed design of an imaging spectropolarimeter/photometer for remote sensing of earth resources p 73 A87-20795
Imaging radar polarimetry from wave synthesis p 76 A87-29849

POLARIMETRY

Imaging radar polarimetry from wave synthesis p 82 N87-17279

POLLUTION MONITORING

Oil slick detection with a sidelooking airborne radar p 53 N87-18169

Contributions to oil spill detection and analysis with radar and microwave radiometry, results of the Archimedes 2 campaign p 54 N87-18170

POLLUTION TRANSPORT

Ozone formation in pollutant plumes: A reactive plume model with arbitrary crosswind resolution [PB86-236973] p 26 N87-18246

POLYSTATION DOPPLER TRACKING SYSTEM

NROSS (Navy Remote Ocean Sensing System) tracking network analysis [AD-A172132] p 45 N87-16384

POPULATIONS

Variability of the productive habitat in the eastern equatorial Pacific p 38 A87-20687
Accuracy of population estimation from medium-scale aerial photography p 24 A87-23777
Spatial analysis of the dynamics of an ecosystem by multistage remote sensing in Kenya p 16 N87-17173

POTENTIAL FIELDS

Application of 2-D Hilbert transform in the interpretation of remotely sensed potential field data --- geology p 35 N87-17293

POWER EFFICIENCY

Some trade-offs in modest-resolution radars for space p 82 N87-17278

PRECAMBRIAN PERIOD

Geological nature of early Precambrian formations (considering the example of the Anabar shield) p 28 A87-24274

PRECIPITATION (METEOROLOGY)

Nimbus-7 SMMR multispectral passive microwave correlations with an antecedent precipitation index p 74 A87-23390

PREDICTION ANALYSIS TECHNIQUES

Operational wave forecasting with spaceborne SAR: Prospects and pitfalls p 45 N87-17149

PRESSURE DISTRIBUTION

Ocean surface pressure fields from satellite-sensed winds p 41 A87-25797

PROJECT MANAGEMENT

Pre-assessment for large scale civil engineering projects by integrated analysis with the data numerical topography and remote sensing p 57 A87-23815

Future European plans in the framework of the International Satellite Land Surface Climatology Project (ISLSCP) p 78 N87-15628

Overview and status of the ERS-1 program p 47 N87-17190

Report of the Fourth Session of the JSC/CCCO Tropical Ocean Global Atmosphere (TOGA) Scientific Steering Group [WCP-120] p 54 N87-18283

PROVING

Australian validation plans for ERS-1 p 84 N87-17387

PULSE COMPRESSION

Pulse compression test results of the SAR transmitter and receiver --- satellite-borne SAR p 83 N87-17360

PUSHBROOM SENSOR MODES

In flight calibration of push broom remote sensing instruments p 73 A87-19652

The stereo-pushbroom scanner system Digital Photogrammetry System (DPS) and its accuracy p 80 N87-17167

Concept of a future multispectral Thermal Infrared (TIR) pushbroom mission for Earth observation from space p 80 N87-17169

The Sequential Filter Imaging Radiometer (SFIR), a new instrument configuration for Earth observations p 81 N87-17205

Q

QUALITY CONTROL

Evaluation of remote sensing results for the benefit of water quality research on the North Sea [NZ-R-86.15] p 62 N87-19799

R

RADAR CROSS SECTIONS

Measurement of microwave backscattering signatures of the ocean surface using X band and K(a) band airborne scatterometers p 40 A87-23725
Further development of an improved altimeter wind speed algorithm p 42 A87-27848

RADAR DATA

An overview of operational SAR data collection and dissemination plans for ERS-1 ice data in Canada p 47 N87-17189

Analysis of multichannel SAR data of Spitsbergen --- glaciology p 60 N87-17223

Outline of SAR-850 data processing method in Japan --- ERS-1 (NASDA) p 71 N87-18176

Digital realtime SAR processor for C- and X-band applications p 71 N87-18177

Intelligent SAR Processor (ISAR), a new concept for high throughput and high precision digital SAR processing p 85 N87-18178

STAR-VUE: A tactical ice navigation workstation p 54 N87-18181

RADAR GEOLOGY

The Second Spaceborne Imaging Radar Symposium [NASA-CR-180131] p 67 N87-17135

RADAR IMAGERY

Optical and radar observations of the nonlinear interaction of gravity waves p 37 A87-20350

Radar images for soil survey in England and Wales p 3 A87-21251

Space Shuttle radargrammetry results p 65 A87-23827

Exact determination of wave parameters from the results of Fourier analysis of sea-surface radar imagery p 41 A87-24377

An analysis of the potential of satellite-borne bistatic radar sensing of the earth p 75 A87-24385

Preliminary analyses of SIB-B radar data for recent Hawaii lava flows p 29 A87-25588

Results of an airborne synthetic-aperture radar (SAR) experiment over a SIR-B (Shuttle Imaging Radar) test site in Germany p 76 A87-27999

A radar ocean imaging model for small to moderate incidence angles p 43 A87-29015

Imaging radar polarimetry from wave synthesis p 76 A87-29849

Analysis of surface patterns over Cobb Seamount using synthetic-aperture radar imagery [AD-A171670] p 45 N87-16493

VARAN-S radar image interpretation [CNES-CT/DRT/TIT/RL-54-T] p 66 N87-16963

Analysis of multiple incidence angle SIR-B data for determining forest stand characteristics p 15 N87-17156

Radar signature determination: Trends and limitations p 67 N87-17159

SAR ice floe kinematics and correlation with mesoscale oceanic structure within the marginal ice zone p 48 N87-17222

Analysis of multichannel SAR data of Spitsbergen --- glaciology p 60 N87-17223

Canadian plans for operational demonstrations of satellite imaging radar applications --- ERS-1 p 68 N87-17229

Comparative study of LANDSAT MSS, Salyut-7 (TERRA) and radar (SIR-A) images for geological and geomorphological applications: A case study from Rajasthan and Gujarat, India p 34 N87-17236

Multispectral classification of microwave remote sensing images --- SAR crop identification p 16 N87-17238

Using secondary image products to aid in understanding and interpretation of radar imagery p 68 N87-17239

Extraction of the backscatter coefficient of agricultural fields from an airborne SAR image p 16 N87-17265

Microwave remote sensing: Its applications and limitations in operational tasks of land use inventory and forest management p 17 N87-17266

Analysis of the spatial structure of Synthetic Aperture Radar (SAR) imagery for a better separability of cereal crops, wheat and barley p 17 N87-17287

Estimation of internal wave currents from SAR and infrared scatterometer imagery p 48 N87-17295

Observations of surface currents at Nantucket Shoals and implications for radar imaging of the bottom p 48 N87-17296

SAR imaging of bottom topography in the ocean: Results from an improved model p 48 N87-17298

An improved method for the determination of water depth from surface wave refraction patterns --- SAR imagery p 49 N87-17299

SAR imagery for forest management p 18 N87-17313

The SAR image modulation transfer function derived from SIR-B image spectra and airborne measurements of ocean wave height spectra p 49 N87-17334

SIR-B observations of ocean waves in the NE Atlantic p 49 N87-17335

Deriving two-dimensional ocean wave spectra and surface height maps from the Shuttle Imaging Radar (SIR-B) p 49 N87-17336

Spatial evolution of wave spectra in the vicinity of the Agulhas current from SIR-B p 50 N87-17337

Characterisation of internal wave surface patterns on airborne SAR imagery p 50 N87-17338

X-SAR extends the frequency range of Shuttle Imaging Radar p 70 N87-17362

A procedure for estimation of two-dimensional ocean height-variance spectra from SAR imagery p 52 N87-17381

A scatterometer research program p 53 N87-17391

On the discrimination between crude oil spills and monomolecular sea slicks by airborne remote sensors: Today's possibilities and limitations p 53 N87-18167

Oil slick detection with a sidelooking airborne radar p 53 N87-18169

Contributions to oil spill detection and analysis with radar and microwave radiometry, results of the Archimedes 2 campaign p 54 N87-18170

Digital realtime SAR processor for C- and X-band applications p 71 N87-18177

High speed image processing system based on the custom VLSI for Digital Signal Processing (DSP) --- SAR imagery p 71 N87-18179

Resolving the Doppler ambiguity for spaceborne synthetic aperture radar p 72 N87-18212

Investigation of physics of synthetic aperture radar in ocean remote sensing toward 84/86 field experiment. Volume 1: Data summary and early results [AD-A174197] p 55 N87-18913

Investigation of physics of synthetic aperture radar in ocean remote sensing TOWARD 84/86 field experiment. Volume 2: Contributions of individual investigators [AD-A174527] p 55 N87-18966

RADAR MAPS

A scanning radar altimeter for mapping continental topography p 33 N87-17146

Deriving two-dimensional ocean wave spectra and surface height maps from the Shuttle Imaging Radar (SIR-B) p 49 N87-17336

Satellite altimeter measurements over land and inland water p 61 N87-18200

RADAR MEASUREMENT

Simultaneous ocean cross section and rainfall measurements from space with a nadir-looking radar p 38 A87-20956

Wind-wave relationship from Seasat radar altimeter data p 41 A87-24748

Tower-based broadband backscattering measurements from the ocean surface in the North Sea p 47 N87-17217

Geophysics of the marginal ice zone from SAR p 47 N87-17219

Deriving two-dimensional ocean wave spectra and surface height maps from the Shuttle Imaging Radar (SIR-B) p 49 N87-17336

L to X-band scatter and emission measurements of vegetation p 19 N87-17347

Measurement of the directional spectrum of ocean waves using a conically-scanning radar p 52 N87-17383

Bare soil measurements with the Delft University Scatterometer (DUTSCAT) system (L-band) [REPT-64-220-86-T-1LH] p 24 N87-19797

RADAR RECEIVERS

A satellite-borne SAR transmitter and receiver p 83 N87-17358

Pulse compression test results of the SAR transmitter and receiver --- satellite-borne SAR p 83 N87-17360

RADAR RESOLUTION

Some trade-offs in modest-resolution radars for space p 82 N87-17278

RADAR SCATTERING

Simultaneous ocean cross section and rainfall measurements from space with a nadir-looking radar p 38 A87-20956

Theoretical approach to radar backscattering of soils p 3 A87-21250

Hawaiian lava flows and SIR-B results p 69 N87-17245

Extraction of the backscatter coefficient of agricultural fields from an airborne SAR image p 16 N87-17265

Imaging radar polarimetry from wave synthesis p 82 N87-17279

- Evaluating roughness models of radar backscatter
p 19 N87-17344
- On the relationship between age of lava flows and radar backscattering p 35 N87-17348
- A scatterometer research program p 53 N87-17391
- RADAR SIGNATURES**
- Radar signature determination: Trends and limitations p 67 N87-17159
- An inter-sensor comparison of the microwave signatures of Arctic sea ice p 46 N87-17184
- RADAR TRACKING**
- Automated remote sensing of sea ice using synthetic aperture radar p 46 N87-17186
- An automatic tracking mode switching algorithm for the ERS-1 altimeter p 81 N87-17195
- RADAR TRANSMITTERS**
- A satellite-borne SAR transmitter and receiver p 83 N87-17358
- Pulse compression test results of the SAR transmitter and receiver --- satellite-borne SAR p 83 N87-17360
- RADARSAT**
- A very fast synthetic-aperture radar signal processor for ERS-1 and Radarsat p 85 N87-18180
- RADIANCE**
- Design of a data base system for inferring land surface parameters and fluxes from satellite radiances p 66 N87-15625
- The TIMS investigator's guide p 79 N87-17113
- Simulation modeling and preliminary analysis of TIMS data from the Carlin area and the northern Grapevine Mountains, Nevada p 31 N87-17120
- Infrared spectroscopy for geologic interpretation of TIMS data p 31 N87-17130
- Microwave radiances from horizontally finite precipitating clouds containing ice and liquid hydrometeors p 61 N87-17340
- Detection of bottom-related surface patterns on visible spectrum imagery --- ocean bottom p 53 N87-18158
- Relationship between tree density, leaf area index, soil metal content, and LANDSAT MSS canopy radiance values p 21 N87-18174
- RADIATION MEASURING INSTRUMENTS**
- Variability in the Earth radiation budget as determined from the Nimbus ERB experiments p 84 N87-17410
- RADIATIVE TRANSFER**
- On the use of synthetic 12-micron data in a split-window retrieval of sea surface temperature from AVHRR measurements p 43 A87-29019
- Estimation of vegetation cover at subpixel resolution using LANDSAT data [NASA-CR-177077] p 11 N87-15514
- Atmospheric corrections of NOAA-AVHRR data verification of different methods by ground truth measurements p 70 N87-17274
- The relationship between marine aerosol optical depth and satellite-sensed sea surface temperature [AD-A174337] p 55 N87-18963
- RADIO ALTIMETERS**
- Structure of the Kerguelen Plateau province from Seasat altimetry and seismic reflection data p 28 A87-24966
- ERS-1 radar altimeter: Performance, calibration and data validation p 80 N87-17194
- An automatic tracking mode switching algorithm for the ERS-1 altimeter p 81 N87-17195
- ERS-1 fast delivery processing and products p 81 N87-17224
- Using buoys and ships to calibrate ERS-1 altimeter and scatterometer p 51 N87-17377
- Measurement of the directional spectrum of ocean waves using a conically-scanning radar p 52 N87-17383
- Intersensor comparisons for validation of wind speed measurements from ERS-1 altimeter and scatterometer --- Seasat p 52 N87-17386
- Proceedings of the 1986 International Geoscience and Remote Sensing Symposium (IGARSS '86) on Remote Sensing: Today's Solutions for Tomorrow's Information Needs, volume 3 [ESA-SP-254-VOL-3] p 84 N87-18142
- Development in radar altimetry: The Navy Geosat mission p 85 N87-18161
- New techniques in satellite altimeter tracking systems p 85 N87-18164
- SEASAT microwave altimeter measurement of the ocean gravity wave equilibrium-range spectral behavior using full-wave theory p 53 N87-18165
- Atmospheric water vapor corrections for altimetry measurements p 85 N87-18197
- Study of ocean bottom coupling process using satellite altimeter data p 54 N87-18199
- Satellite altimeter measurements over land and inland water p 61 N87-18200
- Retrieval and global comparison of oceanic winds from SEASAT radiometer, scatterometer and altimeter p 85 N87-18219
- RADIO INTERFEROMETERS**
- The application of geodetic radio interferometric surveying to the monitoring of sea-level p 39 A87-21367
- RADIO PROBING**
- Use of decimeter waves in studies of water bodies by methods of microwave radiometry p 58 A87-26537
- RADIO WAVE REFRACTION**
- An improved method for the determination of water depth from surface wave refraction patterns --- SAR imagery p 49 N87-17299
- RADIOMETERS**
- Mobile very long baseline interferometry and Global Positioning System measurement of vertical crustal motion p 26 A87-21931
- Automated extraction of pack ice motion from advanced very high resolution radiometer imagery p 42 A87-27547
- Ground radiometry and airborne multispectral survey of bare soils p 10 A87-30894
- Some results of Marine Observation Satellite (MOS-1) airborne verification experiment Multispectral Electronic Self Scanning Radiometer (MESSR) p 46 N87-17166
- Analysis of AIS radiometry at Mono Lake, California --- Airborne Imaging Spectrometer (AIS) p 81 N87-17204
- The Sequential Filter Imaging Radiometer (SFIR), a new instrument configuration for Earth observations p 81 N87-17205
- RADIOMETRIC CORRECTION**
- Viewing angle corrections of airborne multispectral scanner data acquired over forested surfaces p 17 N87-17273
- Atmospheric corrections of NOAA-AVHRR data verification of different methods by ground truth measurements p 70 N87-17274
- Radiometric correction method which removes both atmospheric and topographic effects from the LANDSAT-MSS data p 83 N87-17329
- Radiometric analysis of the longwave infrared channel of the Thematic Mapper on LANDSAT 4 and 5 [NASA-CR-180180] p 86 N87-18221
- RADIOMETRIC RESOLUTION**
- Instrument characterization for the detection of long-term changes in stratospheric ozone - An analysis of the SBUV/2 radiometer p 74 A87-20961
- Automated extraction of pack ice motion from advanced very high resolution radiometer imagery p 42 A87-27547
- Analysis of AIS radiometry at Mono Lake, California --- Airborne Imaging Spectrometer (AIS) p 81 N87-17204
- RAIN**
- Simultaneous ocean cross section and rainfall measurements from space with a nadir-looking radar p 38 A87-20956
- Satellite rainfall retrieval by logistic regression p 56 A87-23370
- Annual and interannual variability in large-scale convection over the eastern Pacific and tropical South America p 57 A87-23414
- Rainfall and vegetation monitoring in the Savanna Zone of the Democratic Republic of Sudan using the NOAA Advanced Very High Resolution Radiometer p 6 A87-24783
- Development and experiment of airborne microwave rain-scatterometer/radiometer system. III - Rain measurement and its data analysis p 58 A87-28436
- Development and experiment of airborne microwave rain-scatterometer/radiometer system. IV - Microwave back-scattering experiment of ocean surface p 43 A87-28437
- Rainfall estimation over the Sahel using Meteosat thermal infra-red data p 59 N87-15587
- Group Agromet Monitoring Project (GAMP) methodology integrated mapping of rainfall, evapotranspiration, germination, biomass development and thermal inertia, based on Meteosat and conventional meteorological data p 59 N87-15626
- RAIN GAGES**
- Hydrological studies in Niger p 59 N87-15609
- RANGELANDS**
- Satellite remote sensing of rangelands in Botswana. I - Landsat MSS and herbaceous vegetation p 7 A87-24785
- Satellite remote sensing of rangelands in Botswana. II - NOAA AVHRR and herbaceous vegetation p 7 A87-24786
- Estimating and mapping grass cover and biomass from low-level photographic sampling p 9 A87-29005
- Calibration of Landsat data for sparsely vegetated semi-arid rangelands p 9 A87-29008
- REAL TIME OPERATION**
- Digital real-time SAR processor for C- and X-band applications p 71 N87-18177
- REFLECTANCE**
- Canopy reflectance modeling in a tropical wooded grassland [NASA-CR-180097] p 11 N87-15518
- Off-nadir optical remote sensing from satellites for vegetation identification [DE86-012387] p 23 N87-18916
- REFLECTED WAVES**
- Photometric functions, reflectance map - Two techniques for determining surface shape and orientation from image intensity p 64 A87-23802
- REGIONS**
- Geomorphology from space: A global overview of regional landforms [NASA-SP-486] p 36 N87-18139
- REGRESSION ANALYSIS**
- Satellite rainfall retrieval by logistic regression p 56 A87-23370
- Estimation of vegetation cover at subpixel resolution using LANDSAT data [NASA-CR-177077] p 11 N87-15514
- Estimation of absolute water surface temperature based on atmospherically corrected thermal infrared multispectral scanner digital data p 79 N87-17114
- Agricultural crop estimates using information gathered by remote sensing satellites, as well as ground data, through samples of geographic layers [INPE-4102-RPE/534] p 24 N87-19786
- RELIEF MAPS**
- Composite/progressive sampling - A program package for computer supported collection of DTM data --- Digital Terrain Models p 62 A87-23784
- Digital terrain mapping with STAR-1 SAR data p 69 N87-17269
- Analysis of Large Format Camera images from the Black Hills, USA, for topographic and thematic mapping p 71 N87-18189
- REMOTE SENSING**
- Instrumentation for optical remote sensing from space; Proceedings of the Meeting, Cannes, France, November 27-29, 1985 [SPIE-589] p 73 A87-19647
- In flight calibration of push broom remote sensing instruments p 73 A87-19652
- The Along Track Scanning Radiometer (ATSR) for ERS1 p 73 A87-19660
- Evaluation of the mid-infrared (1.45 to 2.0 microns) with a black-and-white infrared video camera p 73 A87-20672
- Space remote sensing p 86 A87-20682
- Remote sensing of the state of crops and soils p 1 A87-20758
- Estimation of canopy parameters for inhomogeneous vegetation canopies from reflectance data. II - Estimation of leaf area index and percentage of ground cover for row canopies p 1 A87-20761
- Assessing forest decline in coniferous forests of Vermont using NS-001 Thematic Mapper Simulator data p 1 A87-20763
- Correlation between time- and depth-resolved simulated lidar signals --- for estimating phytoplankton distribution p 38 A87-20770
- The SPOT satellites - From SPOT 1 to SPOT 4 p 74 A87-21094
- Remote sensing options for soil survey in developing countries p 2 A87-21239
- NMR instrument for soil moisture ground-truth data collection p 2 A87-21240
- Spectral brightness and surface soil characteristics in an arid Mediterranean region (southern Tunisia) p 2 A87-21242
- The thematic mapper - A new tool for soil mapping in arid areas p 2 A87-21243
- Experimental results in soil moisture mapping using IR thermography p 2 A87-21246
- Thermography - Principles and application in the Oost-Gelderland remote sensing study project p 3 A87-21247
- Timely thermal infrared data acquisition for soil survey in humid temperature environments p 3 A87-21249
- Theoretical approach to radar backscattering of soils p 3 A87-21250
- Radar images for soil survey in England and Wales p 3 A87-21251
- Forest fire monitoring using the NOAA satellite series p 3 A87-23360
- Remotely sensed albedo of snow-covered lands p 56 A87-23361
- Remote sensing of hydrological variables from the DMSP microwave mission sensors p 57 A87-23374
- Soil moisture estimates from satellite infrared temperatures and their relation to surface measurements p 3 A87-23389
- Nimbus-7 SMMR multispectral passive microwave correlations with an antecedent precipitation index p 74 A87-23390

- The data dilemma - How to properly construct and utilize aerial photo volume tables p 63 A87-23790
- An information processing system for integration of data from remote sensors, aerial photographs and existing maps p 63 A87-23791
- Performance of selected spatial domain edge detection algorithms for earth resources application p 64 A87-23798
- Control extension utilizing Large Format Camera imagery p 75 A87-23804
- Agricultural remote sensing in South Carolina - A study of crop identification capabilities utilizing Landsat data p 4 A87-23806
- Cartographic analysis of remote sensing data through Landsat mosaic scaling p 65 A87-23809
- American Congress on Surveying and Mapping and American Society for Photogrammetry and Remote Sensing, Annual Convention, Washington, DC, Mar. 16-21, 1986, Technical Papers. Volume 5 - Remote Sensing p 4 A87-23810
- Land surface climatic variables monitored by NOAA-AVHRR satellites p 4 A87-23811
- Pre-assessment for large scale civil engineering projects by integrated analysis with the data numerical topography and remote sensing p 57 A87-23815
- An assessment of evapotranspirational water losses in a Sierran Mixed Conifer forest using remotely sensed data p 4 A87-23816
- Phenological effects on grass canopy/spectral relationships p 4 A87-23818
- Remote sensing of aquatic macrophyte distribution in upper Lake Marion p 57 A87-23826
- Space Shuttle radargrammetry results p 65 A87-23827
- Techniques for deriving land use information from Landsat data through the use of a geographic information system p 24 A87-23828
- Landsat Thematic Mapper digital information content for agricultural environments p 5 A87-23830
- Identification of forest and agricultural edges using Landsat Thematic Mapper data - Preliminary results p 5 A87-23832
- The use of remote sensing in estimating biomass of fish tree areas in the Richard B. Russell Lake p 40 A87-23834
- An analysis of the potential of satellite-borne bistatic radar sensing of the earth p 75 A87-24385
- Atlas of geo-science analyses of Landsat imagery in China --- Book p 65 A87-24542
- Satellite remote sensing of primary production p 6 A87-24777
- Characteristics of maximum-value composite images from temporal AVHRR data p 75 A87-24778
- Analysis of the dynamics of African vegetation using the normalized difference vegetation index p 6 A87-24779
- Satellite remote sensing of rangelands in Botswana. I - Landsat MSS and herbaceous vegetation p 7 A87-24785
- Aircraft and satellite thermographic systems for wildfire mapping and assessment [AIAA PAPER 87-0187] p 7 A87-24933
- Partnerships in remote sensing - A theme with some examples p 86 A87-25531
- The spectral reflectance of stands of Norway spruce and Scotch pine, measured from a helicopter p 7 A87-25586
- Earth sensing - New tools enable scientists to gain insight into the structure of our planet's surface p 29 A87-25890
- Satellite remote sensing of meteorological parameters for global numerical weather prediction p 76 A87-26098
- Remote detection of forest damage p 8 A87-26197
- Spatial-statistical characteristics of sea surface foam fields (from optical sounding data) p 42 A87-26531
- The principles and procedures of modeling ore-related objects in predictive metallogenic investigations (using satellite-borne data) p 29 A87-26533
- The development of procedures for forest interpretation from texture-selective images p 8 A87-26535
- Automation of thematic processing of space images in evaluating crop condition p 8 A87-26539
- Method for computing the periodicity of a remote-sensing survey p 65 A87-26540
- Proposal of a remote sensing method for measuring soil moisture of bare soils in the frequency range 100 MHz-1 GHz p 8 A87-26974
- Soviet remote sensing p 86 A87-27452
- Microwave backscattering from a layer of randomly oriented discs with application to scattering from vegetation p 8 A87-28316
- Estimating pre-harvest production of maize in Kenya using large-scale aerial photography and radiometry p 9 A87-29004
- Comparison of some classification methods on a test site (Kiskore, Hungary) - Separability as a measure of accuracy p 9 A87-29006
- A comparative study of lineament analysis from different remote sensing imagery over areas in the Benue Valley and Jos Plateau Nigeria p 30 A87-29010
- SPOT IMAGE and commercialisation of remote sensing data p 65 A87-29430
- Current achievements and future projects/useful applications of weather satellites and future remote sensing p 76 A87-29431
- Business approach to earth observation applications p 87 A87-29433
- Remote sensing from space - An overview p 87 A87-30881
- Land applications for remote sensing from space p 25 A87-30882
- Ocean remote sensing p 44 A87-30883
- Geophysical remote sensing p 30 A87-30884
- Weather and atmosphere remote sensing p 77 A87-30885
- Ground radiometry and airborne multispectral survey of bare soils p 10 A87-30894
- The interactive effect of spatial resolution and degree of internal variability within land-cover types on classification accuracies p 77 A87-30895
- Remote sensing of structurally complex semi-natural vegetation - An example from heathland p 10 A87-30896
- Spectral separation of moorland vegetation in airborne Thematic Mapper data p 10 A87-30897
- Airborne MSS data to estimate GLAI --- Green Leaf Area Index p 11 A87-30898
- Mapping of water quality in coastal waters using Airborne Thematic Mapper data p 58 A87-30899
- The quantitative use of airborne Thematic Mapper thermal infrared data p 44 A87-30900
- Island wakes and headland eddies - A comparison between remotely sensed data and laboratory experiments p 44 A87-30925
- Indian remote sensing program p 77 A87-15242
- Estimation of vegetation cover at subpixel resolution using LANDSAT data [NASA-CR-177077] p 11 A87-15514
- Hydrologic models of land surface processes --- soil moisture p 58 A87-15547
- Modelisation of evapotranspiration and soil available water over an agricultural region applicable for remote sensing p 12 A87-15554
- Remote sensing identified in climate model experiments with hydrological and albedo changes in the Sahel p 59 A87-15569
- Evaluation of climate relevant land surface characteristics from remote sensing p 12 A87-15572
- Remote sensing of land-surface temperature from HIRS/MSU data --- High Resolution Infrared Sounder/Microwave Sounding Unit (HIRS/MSU) p 77 A87-15573
- The prospects for hydrological measurements using ERS-1 --- lakes p 59 A87-15588
- Contribution of passive microwave remote sensing in soil moisture and evapotranspiration measurements p 12 A87-15589
- Use of remote sensing application for agricultural expansion into semi-arid areas of Kenya p 13 A87-15607
- Hydrological studies in Niger p 59 A87-15609
- Ground water-fed lakes in the Libyan desert: Their varying area as observed by means of LANDSAT-MSS data p 59 A87-15611
- The use of remote sensing techniques in the study of vegetation recovery after fire in mediterranean countries (a preliminary study) p 14 A87-15623
- Remote sensing activities in Turkey: Possible contributions to climate studies p 77 A87-15624
- Multiangle or multiwavelength technique for remote sensing of sea surface temperature p 45 A87-15652
- The TIMS investigator's guide p 79 A87-17113
- Thermal imaging spectroscopy in the Kelso-Baker Region, California p 30 A87-17117
- Lithologic mapping of silicate rocks using TIMS p 30 A87-17118
- TIMS data applications in Nebraska p 15 A87-17126
- The application of remotely sensed data to pedologic and geomorphic mapping on alluvial fan and playa surfaces in Saline Valley, California p 15 A87-17127
- The Red River Valley archeological project p 31 A87-17128
- The physical basis for spectral variations in thermal infrared emittance of silicates and application to remote sensing p 31 A87-17129
- Proceedings of the 1986 International Geoscience and Remote Sensing Symposium (IGARSS '86) on Remote Sensing: Today's Solutions for Tomorrow's Information Needs, volume 1 [ESA-SP-254-VOL-1] p 80 A87-17163
- The transfer of remote sensing technology to developing countries: A survey of experts in the field p 87 A87-17170
- The design of an international data centre for remote sensing p 67 A87-17176
- Commercial opportunities in Earth observation from space p 87 A87-17177
- An inter-sensor comparison of the microwave signatures of Arctic sea ice p 46 A87-17184
- Automated remote sensing of sea ice using synthetic aperture radar p 46 A87-17186
- Overview and status of the ERS-1 program p 47 A87-17190
- Multispectral classification of microwave remote sensing images --- SAR crop identification p 16 A87-17238
- Integrated analysis of geological and remote sensing data aimed at mineral deposits detection in the Monapo area (northern Mozambique) p 34 A87-17243
- Microwave remote sensing: Its applications and limitations in operational tasks of land use inventory and forest management p 17 A87-17266
- Application of Spaceborne Distributed Aperture/Coherent Array Processing (SDA/CAP) technology to active and passive microwave remote sensing p 82 A87-17277
- Proceedings of the 1986 International Geoscience and Remote Sensing Symposium (IGARSS '86) on Remote Sensing: Today's Solutions for Tomorrow's Information Needs, volume 2 [ESA-SP-254-VOL-2] p 82 A87-17283
- An overview of remote sensing agricultural applications in North America: Past, present and future p 17 A87-17284
- Applications of remote sensing in the US Department of Agriculture p 17 A87-17285
- Assessing grass canopy condition and growth from combined optical-microwave measurements p 17 A87-17286
- Analysis of the spatial structure of Synthetic Aperture Radar (SAR) imagery for a better separability of cereal crops, wheat and barley p 17 A87-17287
- Toward a satellite system to monitor the spatial and temporal behavior of soil water content p 18 A87-17288
- Utility of remote sensing data in renewable resource sample survey p 18 A87-17289
- Application of 2-D Hilbert transform in the interpretation of remotely sensed potential field data --- geology p 35 A87-17293
- Computer-aided interpretation of complex geological patterns in remote sensing p 35 A87-17294
- The effect of measurement error and confusion from vegetation on passive microwave estimates of soil moisture p 18 A87-17304
- Towards snowmelt runoff forecast using LANDSAT-MSS and NOAA/AVHRR data p 61 A87-17317
- A climatological-hydrological study of lake ice in the southwestern mountain area in Norway by use of satellite sensing p 61 A87-17319
- Thermal infrared remote sensing: One of today's solutions p 83 A87-17324
- Models for temperature estimation from remotely sensed thermal IR data p 83 A87-17325
- Parameter space techniques for image registration p 70 A87-17327
- IRSAP: An improved approach in processing remotely sensed data --- Interactive Remote Sensing Applications Package (IRSAP) p 70 A87-17332
- Optical visual evaluation and interpretation of remote sensing data p 83 A87-17353
- The use of numerical wind and wave models to provide areal and temporal extension to instrument calibration and validation of remotely sensed data --- satellite data p 51 A87-17371
- Geomorphology from space: A global overview of regional landforms [NASA-SP-486] p 36 A87-18139
- Proceedings of the 1986 International Geoscience and Remote Sensing Symposium (IGARSS '86) on Remote Sensing: Today's Solutions for Tomorrow's Information Needs, volume 3 [ESA-SP-254-VOL-3] p 84 A87-18142
- Thermal inertia and soil fluxes by remote sensing p 20 A87-18143
- The use of thermal airborne remote sensing for soil identification: A case study in Limousin (France) p 20 A87-18146
- Assessment of soil degradation in an arid region using remote sensing p 20 A87-18148

- The use of remote sensing (including aerial photographs) to devise cost-effective methods for soil conservation in the Kocaeli Peninsula, Turkey p 20 N87-18149
- Application of remote sensing in the study of the soil hazards of Haryana State, India p 20 N87-18150
- The use of space technology in federally funded land processes research in the United States p 88 N87-18152
- An integrated data bank for agricultural productivity by remote sensing p 21 N87-18153
- Spatial remote sensing to land management --- SPOT/GPS p 70 N87-18157
- Remote sensing of shallow water areas with reference to environmental and multitemporal monitoring of the Hailuoto area, Finland p 61 N87-18159
- A description of large-scale variability in the ocean using the diffuse attenuation coefficient p 53 N87-18160
- Remote sensing of wetland plant stress p 21 N87-18171
- Modelling of estuarine chlorophyll-A from an airborne scanner p 61 N87-18172
- Off-nadir optical remote sensing from satellites for vegetation identification p 22 N87-18183
- Remote sensing applications in the study of land use and soils of aeolian cover of the western part of Haryana State, India p 22 N87-18187
- First step in the use of remote sensing for regional mapping of soil organization data: Application in Brittany (France) and French Guiana p 23 N87-18193
- Deduction of a synthetic bioclimatological map by means of remote sensing data and a digital terrain model using a correlation approach p 72 N87-18194
- Laser-induced chlorophyll-A fluorescence of terrestrial plants p 23 N87-18207
- Remote Sensing Laboratory [ETN-87-98850] p 88 N87-18227
- Influence of the Yukon River on the Bering Sea [NASA-CR-180065] p 54 N87-18293
- Shuttle imaging radar-C science plan [NASA-CR-180241] p 86 N87-18697
- Remote Sensing Information Sciences Research Group, year four [NASA-CR-180198] p 88 N87-18907
- Interpreting forest and grassland biome productivity utilizing nested scales of image resolution and biogeographical analysis [NASA-CR-180213] p 23 N87-18912
- Investigation of physics of synthetic aperture radar in ocean remote sensing toward 84/86 field experiment. Volume 1: Data summary and early results [AD-A174197] p 55 N87-18913
- Proceedings of the Second Workshop on Remote Sensing/Lineament Applications for Energy Extraction [DE86-006613] p 36 N87-18915
- Investigation of physics of synthetic aperture radar in ocean remote sensing TOWARD 84/86 field experiment. Volume 2: Contributions of individual investigators [AD-A174527] p 55 N87-18966
- Satellite remote sensing of the marine environment: Literature and data sources [PB86-245446] p 56 N87-18971
- Agricultural crop estimates using information gathered by remote sensing satellites, as well as ground data, through samples of geographic layers [INPE-4102-RPE/534] p 24 N87-19786
- Remote sensing applied to basic geological surveys: A methodological approach for the northeast region [INPE-4041-TDL/246] p 37 N87-19788
- Evaluation of remote sensing results for the benefit of water quality research on the North Sea [NZ-R-86.15] p 62 N87-19799
- REMOTE SENSORS**
- Proposed design of an imaging spectropolarimeter/photometer for remote sensing of earth resources p 73 A87-20795
- Airborne laser profiling and mapping systems come of age p 75 A87-23786
- Variations in in-flight absolute radiometric calibration --- satellite remote sensors p 77 N87-15594
- NROSS (Navy Remote Ocean Sensing System) tracking network analysis [AD-A172132] p 45 N87-16384
- An extension of the split window technique for the retrieval of precipitable water [AD-A173008] p 60 N87-16386
- Development and demonstration of ALARM (Airborne Lidar Agent Remote Monitor) [AD-A172886] p 78 N87-16387
- Proceedings of the 1986 International Geoscience and Remote Sensing Symposium (IGARSS '86) on Remote Sensing: Today's Solutions for Tomorrow's Information Needs, volume 1 [ESA-SP-254-VOL-1] p 80 N87-17163
- Active/passive microwave sensor comparison of MIZ-ice concentration estimates --- Marginal Ice Zone (MIZ) p 46 N87-17185
- The ESA approach for ERS-1 sensor calibration and performance verification p 80 N87-17192
- Proceedings of the 1986 International Geoscience and Remote Sensing Symposium (IGARSS' 86) on Remote Sensing: Today's Solutions for Tomorrow's Information Needs, volume 2 [ESA-SP-254-VOL-2] p 82 N87-17283
- ERS-1 mission constraints related to wind and wave calibration p 84 N87-17364
- On the discrimination between crude oil spills and monomolecular sea slicks by airborne remote sensors: Today's possibilities and limitations p 53 N87-18167
- REMOTELY PILOTED VEHICLES**
- Tree attenuation at 869 MHz derived from remotely piloted aircraft measurements p 9 A87-28414
- RESEARCH AND DEVELOPMENT**
- Aeronautics and space report of the President: 1985 activities p 87 N87-16662
- Remote Sensing Information Sciences Research Group, year four [NASA-CR-180198] p 88 N87-18907
- RESEARCH MANAGEMENT**
- An overview of the implementation of the World Climate Research program p 26 N87-17388
- Shuttle imaging radar-C science plan [NASA-CR-180241] p 86 N87-18697
- RESOURCES MANAGEMENT**
- Utility of remote sensing data in renewable resource sample survey p 18 N87-17289
- RIVER BASINS**
- Landsat Thematic Mapper data analysis within the Suwannee River Basin p 57 A87-23825
- Drainage channel network of the Arcachon Basin using Thematic Mapper data obtained at high tide p 58 A87-29013
- RIVERS**
- The megageomorphology of the radar rivers of the eastern Sahara p 32 N87-17139
- Influence of the Yukon River on the Bering Sea [NASA-CR-180065] p 54 N87-18293
- Influence of the Yukon River on the Bering Sea [NASA-CR-180356] p 56 N87-19877
- ROCKS**
- Rock type discrimination with AI-based texture analysis algorithms p 28 A87-23782
- Thermal imaging spectroscopy in the Kelso-Baker Region, California p 30 N87-17117
- Lithologic mapping of silicate rocks using TMS p 30 N87-17118
- Detection and mapping of volcanic rock assemblages and associated hydrothermal alteration with Thermal Infrared Multiband Scanner (TMS) data Comstock Lode Mining District, Virginia City, Nevada p 31 N87-17119
- Simulation modeling and preliminary analysis of TMS data from the Carlin area and the northern Grapevine Mountains, Nevada p 31 N87-17120
- Infrared spectroscopy for geologic interpretation of TMS data p 31 N87-17130
- Calculation of day and night emittance values p 67 N87-17131
- Application of Thermal Infrared Multiband Scanner (TMS) data to mapping of Plutonic and stratified rock and assemblages in accreted terrans of the Northern Sierra, California p 15 N87-17132
- A geologic atlas of TMS data p 32 N87-17133
- Space shuttle radar images of Indonesia p 32 N87-17137
- A statistical approach to select the optimal wavelength bands for separating rocks in the wavelength region 0.4 to 2.3 microns p 34 N87-17244
- Nature and origin of mineral coatings on volcanic rocks of the Black Mountain, Stonewall Mountain, and Kane Springs, Wash volcanic centers, Southern Nevada [NASA-CR-180183] p 36 N87-18255
- RURAL AREAS**
- Modelisation of evapotranspiration and soil available water over an agricultural region applicable for remote sensing p 12 N87-15554
- Sparse area stereo matching experiment [AD-A173601] p 66 N87-16388
- RURAL LAND USE**
- Mapping of agricultural lands in the USSR p 11 N87-15507
- Use of remote sensing application for agricultural expansion into semi-arid areas of Kenya p 13 N87-15607
- Monitoring of land-surface change in Sri Lanka p 13 N87-15618
- Microwave remote sensing: Its applications and limitations in operational tasks of land use inventory and forest management p 17 N87-17266
- Classification of forest and surface types by satellite microwave radiometry p 18 N87-17305
- Rural land use inventory and mapping in the Ardeche area (France) using multitemporal Thematic Mapping (TM) data p 19 N87-17350
- LANDSAT-5 Thematic Mapping (TM) data applications to land use classification on around the Bosphorus area, Turkey p 19 N87-17351
- Discrimination of land features using LANDSAT false colour composite in N Iran p 19 N87-17352
- S**
- S MATRIX THEORY**
- Imaging radar polarimetry from wave synthesis p 82 N87-17279
- SAHARA DESERT (AFRICA)**
- The megageomorphology of the radar rivers of the eastern Sahara p 32 N87-17139
- SALINITY**
- SeaSoar CTD surveys during FASINEX --- Conductivity Temperature Depth (CTD); Frontal Air Sea Interaction Experiment (FASINEX) [IOS-230] p 55 N87-18970
- SALYUT SPACE STATION**
- Comparative study of LANDSAT MSS, Salyut-7 (TERRA) and radar (SIR-A) images for geological and geomorphological applications: A case study from Rajasthan and Gujarat, India p 34 N87-17236
- SATELLITE ALTIMETRY**
- Accurate measurement of mean sea level changes by altimetric satellites p 38 A87-20524
- Wind-wave relationship from Seasat radar altimeter data p 41 A87-24748
- Structure of the Kerguelen Plateau province from Seasat altimetry and seismic reflection data p 28 A87-24866
- Undersea volcano production versus lithospheric strength from satellite altimetry [NASA-CR-179984] p 78 N87-15660
- A scanning radar altimeter for mapping continental topography p 33 N87-17146
- Comparison of ocean tide models with satellite altimeter data [AD-A174698] p 56 N87-19879
- SATELLITE DESIGN**
- Overview and status of the ERS-1 program p 47 N87-17190
- SATELLITE GROUND SUPPORT**
- Exploitation of the SPOT system p 62 A87-21095
- SATELLITE IMAGERY**
- Comparison between satellite image advective velocities, dynamic topography, and surface drifter trajectories p 38 A87-20692
- Snow survey from meteorological satellite images in the Qilian Mountain Basin in northwest China p 56 A87-20765
- Illustration of the influence of shadowing on high latitude information derived from satellite imagery p 62 A87-20768
- Spectral brightness and surface soil characteristics in an arid Mediterranean region (southern Tunisia) p 2 A87-21242
- Processing thematic mapper data for mapping in Tunisia p 2 A87-21244
- An application of thematic mapper data in Tunisia - Estimation of daily amplitude in near-surface soil temperature and discrimination of hypersaline soils p 2 A87-21245
- Forest fire monitoring using the NOAA satellite series p 3 A87-23360
- Antarctica - Measuring glacier velocity from satellite images p 57 A87-23699
- An objective method for computing advective surface velocities from sequential infrared satellite images p 39 A87-23717
- A satellite time series of sea surface temperatures in the eastern equatorial Pacific Ocean, 1982-1986 p 39 A87-23718
- Rock type discrimination with AI-based texture analysis algorithms p 28 A87-23782
- Classification of multirate Thematic Mapper data p 64 A87-23795
- The effect of training data variability on classification accuracy p 64 A87-23796
- An iterative Landsat-MSS classification methodology for soil survey p 3 A87-23797
- POLYSITE - An interactive package for the selection and refinement of Landsat image training sites p 65 A87-23805
- Agricultural remote sensing in South Carolina - A study of crop identification capabilities utilizing Landsat data p 4 A87-23806
- Using Landsat to assess tropical forest habitat for migratory birds in the Yucatan Peninsula p 4 A87-23807
- Satellite observations of snow covered area in the High Atlas Mountains of Morocco p 57 A87-23808
- Cartographic analysis of remote sensing data through Landsat mosaic scaling p 65 A87-23809

- Phenological effects on grass canopy/spectral relationships p 4 A87-23818
- Remote sensing of aquatic macrophyte distribution in upper Lake Marion p 57 A87-23826
- Techniques for deriving land use information from Landsat data through the use of a geographic information system p 24 A87-23828
- Detection of new urban build-up in Ardmore and McAlester, Oklahoma using Landsat MSS data p 25 A87-23829
- Landsat Thematic Mapper images for hydrologic land use and cover p 58 A87-23831
- Identification of forest and agricultural edges using Landsat Thematic Mapper data - Preliminary results p 5 A87-23832
- Vegetable crop inventory with Landsat TM data p 5 A87-23833
- Analysis of correlations between structural elements detected on space images and metallogenic zones p 28 A87-24380
- Integration of space-geological and geophysical methods in regional and local predictions of tectonic structures in the Caspian depression p 28 A87-24381
- Identification of reclaimed landscapes of Belorussia from space images p 28 A87-24382
- Use of space imagery and geophysical data in metallogenic prediction studies in central Kyzylkum p 28 A87-24383
- Lineaments of eastern Cuba - Geological interpretation of aerial and space imagery p 28 A87-24384
- An analysis of the potential of satellite-borne bistatic radar sensing of the earth p 75 A87-24385
- Atlas of geo-science analyses of Landsat imagery in China --- Book p 65 A87-24542
- Maximum normalized difference vegetation index images for sub-Saharan Africa for 1983-1985 p 6 A87-24776
- Characteristics of maximum-value composite images from temporal AVHRR data p 75 A87-24778
- Analysis of the dynamics of African vegetation using the normalized difference vegetation index p 6 A87-24779
- Reflections on drought - Ethiopia 1983-1984 p 6 A87-24780
- Moorland plant community recognition using Landsat MSS data p 7 A87-25589
- Quantitative processing procedures and the information content of space imagery in predictions of structural inhomogeneities of the sedimentary cover p 29 A87-26534
- Determination of the properties of a plowed soil layer from multispectral space imagery p 8 A87-26536
- Automation of thematic processing of space images in evaluating crop condition p 8 A87-26539
- Soviet remote sensing p 86 A87-27452
- Automated extraction of pack ice motion from advanced very high resolution radiometer imagery p 42 A87-27547
- Observations and analysis of a polar low over the Great Lakes region p 76 A87-27872
- Satellite contributions to convective scale weather analysis and forecasting p 76 A87-27882
- Detecting and forecasting western region flash floods using GOES imagery and conventional data p 58 A87-27883
- Interpretation characteristics of space photographs of sea coasts with wind-induced surges p 43 A87-28509
- Impact of environmental variables on spectral signatures acquired by the Landsat Thematic Mapper p 9 A87-29003
- Comparison of some classification methods on a test site (Kiskore, Hungary) - Separability as a measure of accuracy p 9 A87-29006
- Performance of Landsat-5 TM data in land-cover classification p 25 A87-29007
- Calibration of Landsat data for sparsely vegetated semi-arid rangelands p 9 A87-29008
- An analysis of geologic lineaments seen on Landsat MSS imagery p 30 A87-29011
- Drainage channel network of the Arcachon Basin using Thematic Mapper data obtained at high tide p 58 A87-29013
- Preliminary analysis of SPOT HRV multispectral products of an arid environment p 10 A87-29017
- On the use of synthetic 12-micron data in a split-window retrieval of sea surface temperature from AVHRR measurements p 43 A87-29019
- Business approach to earth observation applications p 87 A87-29433
- Terrain analysis from digital patterns in geomorphometry and Landsat MSS spectral response p 66 A87-30127
- Extraction of areas infested by pine bark beetle using Landsat MSS data p 10 A87-30129
- Land applications for remote sensing from space p 25 A87-30882
- Ocean remote sensing p 44 A87-30883
- Equatorial long-wave characteristics determined from satellite sea surface temperature and in situ data p 44 A87-30923
- Estimation of vegetation cover at subpixel resolution using Landsat data [NASA-CR-177077] p 11 N87-15514
- Modeling energy flow and nutrient cycling in natural semiarid grassland ecosystems with the aid of thematic mapper data p 11 N87-15517
- Rainfall estimation over the Sahel using Meteosat thermal infra-red data p 59 N87-15587
- The fundamental problems for the energy balance study by satellite imagery p 66 N87-15590
- Assessment of wind and fluvial action by using LANDSAT-MSS color composites in the lower Nile Valley (Egypt) p 13 N87-15612
- The application of LANDSAT imagery for land cover assessment --- Thailand p 13 N87-15614
- Surface albedo change in arid regions in the Sudan p 13 N87-15615
- Monitoring of land-surface change in Sri Lanka p 13 N87-15618
- An integrated system to assess agricultural productivity --- satellite imagery p 14 N87-15621
- AVHRR and MSS data based vegetation indices studies over Indian sites --- NOAA radiometer (AVHRR) LANDSAT multispectral scanner (MSS) p 14 N87-15622
- Application of remote sensing in hydrology and water resources [INPE-3986-PRE/991] p 60 N87-16382
- Proceedings of the 1986 International Geoscience and Remote Sensing Symposium (IGARSS '86) on Remote Sensing: Today's Solutions for Tomorrow's Information Needs, volume 1 [ESA-SP-254-VOL-1] p 80 N87-17163
- Components and comparisons of potential information from several imaging satellites p 67 N87-17164
- Comparison of Thematic Mapper (TM) and SPOT simulation data for agricultural applications in south west Germany p 16 N87-17165
- The stereo-pushbroom scanner system Digital Photogrammetry System (DPS) and its accuracy p 80 N87-17167
- Concept of a future multispectral Thermal Infrared (TIR) pushbroom mission for Earth observation from space p 80 N87-17169
- Monitoring of large phenomena in developing countries through satellite imagery p 67 N87-17172
- Spatial analysis of the dynamics of an ecosystem by multistage remote sensing in Kenya p 16 N87-17173
- Environmental modification of metropolitan areas through satellite images: Study of urban design in the tropics p 25 N87-17175
- Digital satellite imagery acquisition and processing p 68 N87-17207
- Extracting surface features in multispectral imagery p 68 N87-17211
- ERS-1 fast delivery processing and products p 81 N87-17224
- Canadian plans for operational demonstrations of satellite imaging radar applications --- ERS-1 p 68 N87-17229
- Significance of space image, air photo and drainage linears in relation to west coast tectonics, India p 33 N87-17232
- Structural and geomorphic evolution of Meghalaya plateau, India on LANDSAT imagery p 33 N87-17233
- Hydrogeological research in Peloponnesus (Greece) Karst area by support and completion of LANDSAT-thematic data p 33 N87-17234
- Discrimination of lithologic units using geobotanical and LANDSAT TM spectral data p 34 N87-17246
- The influence of resampling method and multitemporal LANDSAT imagery on crop classification accuracy in the United Kingdom p 16 N87-17250
- Evaluation of LANDSAT 5 Thematic Mapping (TM) data for image clustering and classification p 69 N87-17251
- A synergistic approach for multispectral image restoration using reference imagery p 69 N87-17255
- Merging spaceborne image data of optical and microwave sensors p 69 N87-17267
- Application of 2-D Hilbert transform in the interpretation of remotely sensed potential field data --- geology p 35 N87-17293
- Estimation of maximum snow volume distribution using NOAA-AVHRR data p 60 N87-17314
- A climatological-hydrological study of lake ice in the southwestern mountain area in Norway by use of satellite sensing p 61 N87-17319
- Radiometric correction method which removes both atmospheric and topographic effects from the LANDSAT-MSS data p 83 N87-17329
- Rural land use inventory and mapping in the Ardeche area (France) using multitemporal Thematic Mapping (TM) data p 19 N87-17350
- LANDSAT-5 Thematic Mapping (TM) data applications to land use classification on around the Bosphorus area, Turkey p 19 N87-17351
- Discrimination of land features using LANDSAT false colour composite in N Iran p 19 N87-17352
- Optical visual evaluation and interpretation of remote sensing data p 83 N87-17353
- Canada Center for Remote Sensing (CCRS) Conair 580 results relevant to ERS-1 wind and wave calibration p 84 N87-17379
- Canopy hot-spot as crop identifier [DE86-011258] p 19 N87-17395
- The ice conditions in the Greenland waters, 1980 [REPT-551.467.3.068(988)] p 53 N87-17428
- Soil degradation evaluation by digital image processing p 20 N87-18147
- Assessment of soil degradation in an arid region using remote sensing p 20 N87-18148
- The use of remote sensing (including aerial photographs) to devise cost-effective methods for soil conservation in the Kocaeli Peninsula, Turkey p 20 N87-18149
- Application of remote sensing in the study of the soil hazards of Haryana State, India p 20 N87-18150
- Monitoring land use changes in Sri Lanka for land use planning using a geographic information system and satellite imagery p 26 N87-18151
- Land surface models as collateral data in satellite image interpretation p 70 N87-18155
- Integrating vector and satellite data to evaluate the adequacy of a grain silo network p 21 N87-18156
- Detection of bottom-related surface patterns on visible spectrum imagery --- ocean bottom p 53 N87-18158
- Remote sensing of shallow water areas with reference to environmental and multitemporal monitoring of the Hailuoto area, Finland p 61 N87-18159
- Multitemporal analysis of the phenological stage of vegetation using TM-data in the Southern Black Forest (West Germany) p 22 N87-18184
- Remote sensing applications in the study of land use and soils of aeolian cover of the western part of Haryana State, India p 22 N87-18187
- Eastern-Western Arctic Sea Ice Analysis, 1985 [AD-A173972] p 55 N87-18298
- Evaluation of LANDSAT 4 MSS data for geomorphological mapping in the semiarid environment for regional planning purposes: An integrated approach (study site, the Juazeiro region) [INPE-3984-TDL/236] p 72 N87-19787
- CANASATE: Sugar cane mapping by satellite, area 3 [INPE-4068-RPE/526] p 24 N87-19790
- Methodology for the elaboration of thematic maps utilizing LANDSAT-TM data [INPE-3893-TDL/225] p 72 N87-19792
- Surface reflectance correction and stereo enhancement of LANDSAT thematic mapper imagery for structural geologic exploration [DE87-003095] p 37 N87-19796
- Influence of the Yukon River on the Bering Sea [NASA-CR-180356] p 56 N87-19877
- SATELLITE NETWORKS**
- Hydrological Atmospheric Pilot Experiment (HAPEX) hydrology budget modeling (MOBILHY): Outline of the program p 59 N87-15632
- Homogeneous plate deformations on a sphere as monitored by Satellite Laser Ranging (SLR) networks analyzed with the multi-epoch method [ETN-87-99221] p 27 N87-18908
- SATELLITE OBSERVATION**
- Volcanology from space - Using Landsat thematic mapper data in the central Andes p 27 A87-20689
- Thematic mapper analysis of coniferous forest structure and composition p 1 A87-20762
- Equatorial Indian Ocean evaporation estimates from operational meteorological satellites and some inferences in the context of monsoon onset and activity p 39 A87-22041
- Satellite rainfall retrieval by logistic regression p 56 A87-23370
- The effect of local advection on the inference of soil moisture from thermal infrared radiances p 3 A87-23388
- Soil moisture estimates from satellite infrared temperatures and their relation to surface measurements p 3 A87-23389
- Satellite remote sensing of primary production p 6 A87-24777
- Monitoring East African vegetation using AVHRR data p 6 A87-24781
- Monitoring the grasslands of the Sahel using NOAA AVHRR data Niger 1983 p 6 A87-24782

- Rainfall and vegetation monitoring in the Savanna Zone of the Democratic Republic of Sudan using the NOAA Advanced Very High Resolution Radiometer p 6 A87-24783
- Monitoring vegetation in the Mali Sahel during summer 1984 p 6 A87-24784
- Satellite remote sensing of rangelands in Botswana. I - Landsat MSS and herbaceous vegetation p 7 A87-24785
- Satellite remote sensing of rangelands in Botswana. II - NOAA AVHRR and herbaceous vegetation p 7 A87-24786
- Monitoring the grasslands of the Sahel 1984-1985 p 7 A87-24787
- Growing period and drought early warning in Africa using satellite data p 7 A87-24788
- Assessment of ecological conditions associated with the 1980/81 desert locust plague upsurge in West Africa using environmental satellite data p 7 A87-24789
- Effect of surface properties on the narrow to broadband spectral relationship in clear sky satellite observations p 65 A87-25587
- Ocean surface pressure fields from satellite-sensed winds p 41 A87-25797
- The Coastal Zone Color Scanner views the Bismarck Sea p 42 A87-26970
- Remote sensing of land-surface temperature from HIRS/MSU data --- High Resolution Infrared Sounder/Microwave Sounding Unit (HIRS/MSU) p 77 A87-15573
- Estimation of surface albedo using satellite data. A simple formulation for atmospheric effects p 25 A87-15579
- Satellite-derived vegetation index over Europe p 12 A87-15583
- Calibration of normalized vegetation index against pasture growth --- NOAA-7 data p 12 A87-15585
- Design of a data base system for inferring land surface parameters and fluxes from satellite radiances p 66 A87-15625
- The first International Satellite Land Surface Climatology Project (ISLSCP) Field Experiment - FIFE p 14 A87-15629
- Components and comparisons of potential information from several imaging satellites p 67 A87-17164
- Sea ice in the Greenland sea observed by the Nimbus-7 Scanning Multichannel Microwave Radiometer (SMMR) p 48 A87-17221
- The use of numerical wind and wave models to provide areal and temporal extension to instrument calibration and validation of remotely sensed data --- satellite data p 51 A87-17371
- Satellite scatterometer comparisons with surface measurements: Techniques and Seasat results p 51 A87-17372
- Comparison concept of satellite derived wind and wave data with ground truth p 51 A87-17373
- Off-nadir optical remote sensing from satellites for vegetation identification p 22 A87-18183
- Remote Sensing Laboratory [ETN-87-98850] p 88 A87-18227
- Off-nadir optical remote sensing from satellites for vegetation identification [DE86-012387] p 23 A87-18916
- Satellite remote sensing of the marine environment: Literature and data sources [PB86-245446] p 56 A87-18971
- Agricultural crop estimates using information gathered by remote sensing satellites, as well as ground data, through samples of geographic layers [INPE-4102-RPE/534] p 24 A87-19786
- Evaluation of remote sensing results for the benefit of water quality research on the North Sea [NZ-R-86.15] p 62 A87-19799
- SATELLITE SOUNDING**
- Ideas for a future earth observing system from geosynchronous orbit p 74 A87-23419
- SAM II measurements of Antarctic PSC's and aerosols --- Stratospheric Aerosol Measurement satellite - Polar Stratospheric Clouds p 75 A87-23546
- Vertical structure of the temperature field above the North Atlantic p 40 A87-24374
- The results of sea-surface temperature determinations from IR and microwave measurements aboard the Cosmos-1151 satellite p 40 A87-24376
- Possibilities of using satellite data for computations of the ocean/atmosphere heat exchange in the Newfoundland energy-active ocean zone in winter p 41 A87-24379
- Satellite remote sensing of meteorological parameters for global numerical weather prediction p 76 A87-26098
- Use of decimeter waves in studies of water bodies by methods of microwave radiometry p 58 A87-26537
- Method for computing the periodicity of a remote-sensing survey p 65 A87-26540
- Current achievements and future projects/useful applications of weather satellites and future remote sensing p 76 A87-29431
- SATELLITE SURFACES**
- Tidal heating in an internal ocean model of Europa p 43 A87-30143
- SATELLITE TRACKING**
- Basic research for the geodynamics program [NASA-CR-180137] p 27 A87-17415
- Improvement of the Earth's gravity field from terrestrial and satellite data [NASA-CR-180139] p 27 A87-17416
- New techniques in satellite altimeter tracking systems p 85 A87-18164
- SATELLITE-BORNE INSTRUMENTS**
- Instrumentation for optical remote sensing from space; Proceedings of the Meeting, Cannes, France, November 27-29, 1985 [SPIE-589] p 73 A87-19647
- Accurate measurement of mean sea level changes by altimetric satellites p 38 A87-20524
- Instrument characterization for the detection of long-term changes in stratospheric ozone - An analysis of the SBUV/2 radiometer p 74 A87-20961
- Month-to-month variability of ocean-atmosphere latent heat flux as observed from the Nimbus microwave radiometer p 39 A87-23391
- Aircraft and satellite thermographic systems for wildfire mapping and assessment [AIAA PAPER 87-0187] p 7 A87-24933
- Multiangle or multiwavelength technique for remote sensing of sea surface temperature p 45 A87-15652
- Some results of Marine Observation Satellite (MOS-1) airborne verification experiment Multispectral Electronic Self Scanning Radiometer (MESSR) p 46 A87-17166
- The stereo-pushbroom scanner system Digital Photogrammetry System (DPS) and its accuracy p 80 A87-17167
- Evaluation of LANDSAT 5 Thematic Mapping (TM) data for image clustering and classification p 69 A87-17251
- Proceedings of an ESA Workshop on ERS-1 Wind and Wave Calibration [ESA-SP-262] p 84 A87-17363
- The use of numerical wind and wave models to provide areal and temporal extension to instrument calibration and validation of remotely sensed data --- satellite data p 51 A87-17371
- An overview of the NSCAT/N-ROSS program p 52 A87-17384
- Australian validation plans for ERS-1 p 84 A87-17387
- Development in radar altimetry: The Navy Geosat mission p 85 A87-18161
- SATELLITE-BORNE PHOTOGRAPHY**
- Spot data distribution --- selling satellite images p 62 A87-20683
- Methods of geological interpretation of lineaments of platform areas (with reference to Ustiurt) p 29 A87-26532
- Optical visual evaluation and interpretation of remote sensing data p 83 A87-17353
- Geomorphology from space: A global overview of regional landforms [NASA-SP-486] p 36 A87-18139
- LANDSAT-MSS remote sensing and satellite cartography: An integrated approach to the preparation of a new geological map of Egypt at a scale of 1:500 000 p 36 A87-18190
- UMUS: A project for usage of LANDSAT MSS and ancillary data in land cover mapping of large areas in southern Italy p 72 A87-18191
- SATELLITE-BORNE RADAR**
- Simultaneous ocean cross section and rainfall measurements from space with a nadir-looking radar p 38 A87-20956
- Geological applications of multipolarization SAR data p 33 A87-17140
- Observing the polar oceans with spaceborne radar p 46 A87-17151
- Some trade-offs in modest-resolution radars for space p 82 A87-17278
- Future user requirements and required technological developments of spaceborne synthetic aperture radars p 82 A87-17320
- Characteristics of a very low altitude spacecraft for collecting global directional wave spectra with spaceborne synthetic aperture radar p 49 A87-17333
- A satellite-borne SAR transmitter and receiver p 83 A87-17358
- Pulse compression test results of the SAR transmitter and receiver --- satellite-borne SAR p 83 A87-17360
- Outline of SAR-850 data processing method in Japan --- ERS-1 (NASDA) p 71 A87-18176
- Satellite altimeter measurements over land and inland water p 61 A87-18200
- Resolving the Doppler ambiguity for spaceborne synthetic aperture radar p 72 A87-18212
- SCANNERS**
- The stereo-pushbroom scanner system Digital Photogrammetry System (DPS) and its accuracy p 80 A87-17167
- SCATTERING COEFFICIENTS**
- A new semi-empirical sea spectrum for estimating the scattering coefficient p 38 A87-20769
- Hawaiian lava flows and SIR-B results p 69 A87-17245
- Extraction of the backscatter coefficient of agricultural fields from an airborne SAR image p 16 A87-17265
- SCATTEROMETERS**
- Measurement of microwave backscattering signatures of the ocean surface using X band and K(a) band airborne scatterometers p 40 A87-23725
- Further development of an improved altimeter wind speed algorithm p 42 A87-27848
- Development and experiment of airborne microwave rain-scatterometer/radiometer system. III - Rain measurement and its data analysis p 58 A87-28436
- Development and experiment of airborne microwave rain-scatterometer/radiometer system. IV - Microwave back-scattering experiment of ocean surface p 43 A87-28437
- Archival of Seasat-A satellite scatterometer data merged with in situ data at selected, illuminated sites over the ocean [NASA-TM-87736] p 45 A87-16492
- ERS-1 fast delivery processing and products p 81 A87-17224
- Application of the Seasat scatterometer to observations of wind speed and direction and Arctic ice/water boundaries p 48 A87-17259
- Estimation of internal wave currents from SAR and infrared scatterometer imagery p 48 A87-17295
- Evaluation of the different parameters in Long's C-band model --- for ERS-1 scatterometer p 51 A87-17370
- Satellite scatterometer comparisons with surface measurements: Techniques and Seasat results p 51 A87-17372
- The accuracy and availability of operational marine surface wind data for ERS-1 sensor calibration and validation from fixed platforms and free drifting buoys p 51 A87-17376
- Using buoys and ships to calibrate ERS-1 altimeter and scatterometer p 51 A87-17377
- Canada Center for Remote Sensing (CCRS) Convair 580 results relevant to ERS-1 wind and wave calibration p 84 A87-17379
- The use of aircraft for wind scatterometer calibration --- ERS-1 scatterometer p 84 A87-17382
- An overview of the NSCAT/N-ROSS program p 52 A87-17384
- Intersensor comparisons for validation of wind speed measurements from ERS-1 altimeter and scatterometer --- Seasat p 52 A87-17386
- A scatterometer research program p 53 A87-17391
- Retrieval and global comparison of oceanic winds from SEASAT radiometer, scatterometer and altimeter p 85 A87-18219
- Bare soil measurements with the Delft University Scatterometer (DUTSCAT) system (L-band) [REPT-64-220-86-T-1LH] p 24 A87-19797
- SCENE ANALYSIS**
- Forest cover analysis using SIR-B data p 23 A87-18220
- SEA BREEZE**
- Forecasting sea breeze thunderstorms at the Kennedy Space Center using the Prognostic Three-Dimensional Mesoscale Model (P 3DM) p 43 A87-27891
- SEA ICE**
- Data sensitivities of sea ice drift and ocean stress in North Atlantic high latitudes p 38 A87-20520
- Classification of sea ice types with single-band (33.6 GHz) airborne passive microwave imagery p 42 A87-27545
- Automated extraction of pack ice motion from advanced very high resolution radiometer imagery p 42 A87-27547
- Observing the polar oceans with spaceborne radar p 46 A87-17151
- An inter-sensor comparison of the microwave signatures of Arctic sea ice p 46 A87-17184
- Active/passive microwave sensor comparison of MIZ-ice concentration estimates --- Marginal Ice Zone (MIZ) p 46 A87-17185
- Automated remote sensing of sea ice using synthetic aperture radar p 46 A87-17186
- Geophysics of the marginal ice zone from SAR p 47 A87-17219
- Sea ice in the Greenland sea observed by the Nimbus-7 Scanning Multichannel Microwave Radiometer (SMMR) p 48 A87-17221

- Sea ice studies in the Baltic Sea using satellite microwave radiometer data p 50 N87-17343
STAR-VUE: A tactical ice navigation workstation p 54 N87-18181
Eastern-Western Arctic Sea Ice Analysis, 1985 [AD-A173972] p 55 N87-18298
- SEA LEVEL**
Accurate measurement of mean sea level changes by altimetric satellites p 38 A87-20524
The application of geodetic radio interferometric surveying to the monitoring of sea-level p 39 A87-21367
- SEA ROUGHNESS**
Optical and radar observations of the nonlinear interaction of gravity waves p 37 A87-20350
Spatial-statistical characteristics of sea surface foam fields (from optical sounding data) p 42 A87-26531
- SEA SURFACE TEMPERATURE**
Comparison between satellite image advective velocities, dynamic topography, and surface drifter trajectories p 38 A87-20692
The effect of Hurricane Gloria on sea surface temperature patterns p 39 A87-23362
A satellite time series of sea surface temperatures in the eastern equatorial Pacific Ocean, 1982-1986 p 39 A87-23718
Mesoscale hydrographic variability in the vicinity of Points Conception and Arguello during April-May 1983 - The OPUS 1983 experiment p 39 A87-23719
The results of sea-surface temperature determinations from IR and microwave measurements aboard the Cosmos-1151 satellite p 40 A87-24376
On the use of synthetic 12-micron data in a split-window retrieval of sea surface temperature from AVHRR measurements p 43 A87-29019
Weather and atmosphere remote sensing p 77 A87-30885
The quantitative use of airborne Thematic Mapper thermal infrared data p 44 A87-30900
Equatorial long-wave characteristics determined from satellite sea surface temperature and in situ data p 44 A87-30923
Multiangle or multiwavelength technique for remote sensing of sea surface temperature p 45 N87-15652
Development, status, prospects of marine observation satellite p 45 N87-15989
The impact of satellite infrared sea surface temperatures on FNOC (Fleet Numerical Oceanography Center) ocean thermal analyses [AD-A173333] p 54 N87-18295
The relationship between marine aerosol optical depth and satellite-sensed sea surface temperature [AD-A174337] p 55 N87-18963
- SEA TRUTH**
Satellite scatterometer comparisons with surface measurements: Techniques and Seasat results p 51 N87-17372
Validation of ERS-1 wind data using observations from research and voluntary observing ships p 51 N87-17374
- SEAMOUNTS**
Undersea volcano production versus lithospheric strength from satellite altimetry [NASA-CR-179984] p 78 N87-15660
Analysis of surface patterns over Cobb Seamount using synthetic-aperture radar imagery [AD-A171670] p 45 N87-16493
- SEASAT PROGRAM**
Further development of an improved altimeter wind speed algorithm p 42 A87-27848
- SEASAT SATELLITES**
A new semi-empirical sea spectrum for estimating the scattering coefficient p 38 A87-20769
Wind-wave relationship from Seasat radar altimeter data p 41 A87-24748
Structure of the Kerguelen Plateau province from Seasat altimetry and seismic reflection data p 28 A87-24866
Ocean remote sensing p 44 A87-30883
Geophysical remote sensing p 30 A87-30884
Archival of Seasat-A satellite scatterometer data merged with in situ data at selected, illuminated sites over the ocean [NASA-TM-87736] p 45 N87-16492
Geological applications of multipolarization SAR data p 33 N87-17140
Application of the Seasat scatterometer to observations of wind speed and direction and Arctic ice/water boundaries p 48 N87-17259
Satellite scatterometer comparisons with surface measurements: Techniques and Seasat results p 51 N87-17372
Intersensor comparisons for validation of wind speed measurements from ERS-1 altimeter and scatterometer --- Seasat p 52 N87-17386
- SEASAT microwave altimeter measurement of the ocean gravity wave equilibrium-range spectral behavior using full-wave theory p 53 N87-18165
Retrieval and global comparison of oceanic winds from SEASAT radiometer, scatterometer and altimeter p 85 N87-18219
- SEDIMENTS**
Quantitative processing procedures and the information content of space imagery in predictions of structural inhomogeneities of the sedimentary cover p 29 A87-26534
Monitoring sediment transfer processes on the desert margin [NASA-CR-180181] p 23 N87-18222
- SEISMIC ENERGY**
Structure of the Kerguelen Plateau province from Seasat altimetry and seismic reflection data p 28 A87-24866
- SHADOWS**
Illustration of the influence of shadowing on high latitude information derived from satellite imagery p 62 A87-20768
Influence of canopy shadow on stress detection in coniferous forests using LANDSAT data p 21 N87-18173
- SHALLOW WATER**
Remote sensing of shallow water areas with reference to environmental and multitemporal monitoring of the Hailuoto area, Finland p 61 N87-18159
- SHEAR LAYERS**
Effects of a downstream disturbance on the structure of a turbulent plane mixing layer [AIAA PAPER 87-0197] p 74 A87-22476
- SHIPS**
Validation of ERS-1 wind data using observations from research and voluntary observing ships p 51 N87-17374
Using buoys and ships to calibrate ERS-1 altimeter and scatterometer p 51 N87-17377
STAR-VUE: A tactical ice navigation workstation p 54 N87-18181
- SHUTTLE IMAGING RADAR**
Space Shuttle radargrammetry results p 65 A87-23827
Preliminary analyses of SIB-B radar data for recent Hawaii lava flows p 29 A87-25588
Results of an airborne synthetic-aperture radar (SAR) experiment over a SIR-B (Shuttle Imaging Radar) test site in Germany p 76 A87-27999
Geophysical remote sensing p 30 A87-30884
The Second Spaceborne Imaging Radar Symposium [NASA-CR-180131] p 67 N87-17135
Tectonic geomorphology of the Andes with SIR-A and SIR-B p 32 N87-17136
Space shuttle radar images of Indonesia p 32 N87-17137
Delineation of fault zones using imaging radar p 32 N87-17138
The megageomorphology of the radar rivers of the eastern Sahara p 32 N87-17139
Geological applications of multipolarization SAR data p 33 N87-17140
Spaceborne imaging radar research in the 90's p 79 N87-17141
Hydrodynamics of internal solitons and a comparison of SIR-A and SIR-B data with ocean measurements p 45 N87-17147
Analysis of multiple incidence angle SIR-B data for determining forest stand characteristics p 15 N87-17156
Multiple incidence angle SIR-B experiment over Argentina p 80 N87-17157
Radar signature determination: Trends and limitations p 67 N87-17159
SIR-B measurements and modeling of vegetation p 15 N87-17160
Comparative study of LANDSAT MSS, Salyut-7 (TERRA) and radar (SIR-A) images for geological and geomorphological applications: A case study from Rajasthan and Gujarat, India p 34 N87-17236
Hawaiian lava flows and SIR-B results p 69 N87-17245
Future user requirements and required technological developments of spaceborne synthetic aperture radars p 82 N87-17320
The SAR image modulation transfer function derived from SIR-B image spectra and airborne measurements of ocean wave height spectra p 49 N87-17334
SIR-B observations of ocean waves in the NE Atlantic p 49 N87-17335
Deriving two-dimensional ocean wave spectra and surface height maps from the Shuttle Imaging Radar (SIR-B) p 49 N87-17336
Spatial evolution of wave spectra in the vicinity of the Agulhas current from SIR-B p 50 N87-17337
X-SAR extends the frequency range of Shuttle Imaging Radar p 70 N87-17362
- Forest cover analysis using SIR-B data p 23 N87-18220
Shuttle imaging radar-C science plan [NASA-CR-180241] p 86 N87-18697
- SIDE-LOOKING RADAR**
VARAN-S radar image interpretation [CNES-CT/DRT/TIT/RL-54-T] p 66 N87-16963
Oil slick detection with a sidelooking airborne radar p 53 N87-18169
STAR-VUE: A tactical ice navigation workstation p 54 N87-18181
The processing of and information extraction from airborne SLAR data [NLR-MP-86004-U] p 23 N87-18919
- SIGNAL PROCESSING**
A very fast synthetic-aperture radar signal processor for ERS-1 and Radarsat p 85 N87-18180
- SIGNAL TRANSMISSION**
Mobile very long baseline interferometry and Global Positioning System measurement of vertical crustal motion p 26 A87-21931
- SIGNATURE ANALYSIS**
Utility of AVHRR channels 3 and 4 in land-cover mapping p 9 A87-28388
A statistical approach to select the optimal wavelength bands for separating rocks in the wavelength region 0.4 to 2.3 microns p 34 N87-17244
- SIGNATURES**
Undersea volcano production versus lithospheric strength from satellite altimetry [NASA-CR-179984] p 78 N87-15660
Arctic haze: Natural or pollution? [AD-A174025] p 55 N87-18931
- SILICATES**
Lithologic mapping of silicate rocks using TIMS p 30 N87-17118
The Red River Valley archeological project p 31 N87-17128
The physical basis for spectral variations in thermal infrared emittance of silicates and application to remote sensing p 31 N87-17129
- SINGLE EVENT UPSETS**
The SEU risk assessment of Z80A, 8086 and 80C86 microprocessors intended for use in a low altitude polar orbit p 74 A87-22025
- SITE SELECTION**
POLYSITE - An interactive package for the selection and refinement of Landsat image training sites p 65 A87-23805
- SKY BRIGHTNESS**
Mobile very long baseline interferometry and Global Positioning System measurement of vertical crustal motion p 26 A87-21931
- SNOW**
Snow survey from meteorological satellite images in the Qilian Mountain Basin in northwest China p 56 A87-20765
- SNOW COVER**
Remotely sensed albedo of snow-covered lands p 56 A87-23361
Satellite observations of snow covered area in the High Atlas Mountains of Morocco p 57 A87-23808
Development of algorithms to retrieve the water equivalent of snow cover from satellite microwave radiometer data p 60 N87-17264
Estimation of maximum snow volume distribution using NOAA-AVHRR data p 60 N87-17314
Snow cover recession in an Alpine ecological system p 18 N87-17316
Towards snowmelt runoff forecast using LANDSAT-MSS and NOAA-AVHRR data p 61 N87-17317
A climatological-hydrological study of lake ice in the southwestern mountain area in Norway by use of satellite sensing p 61 N87-17319
- SOFTWARE ENGINEERING**
Basic research for the geodynamics program [NASA-CR-180137] p 27 N87-17415
- SOIL EROSION**
Assessment of wind and fluvial action by using LANDSAT-MSS color composites in the lower Nile Valley (Egypt) p 13 N87-15612
Soil degradation evaluation by digital image processing p 20 N87-18147
Assessment of soil degradation in an arid region using remote sensing p 20 N87-18148
The use of remote sensing (including aerial photographs) to devise cost-effective methods for soil conservation in the Kocaeli Peninsula, Turkey p 20 N87-18149
Application of remote sensing in the study of the soil hazards of Haryana State, India p 20 N87-18150
- SOIL MAPPING**
Remote sensing of the state of crops and soils p 1 A87-20758
Machine processing of Landsat data for soil survey - The Benue Valley savanna case study p 1 A87-20759

- Remote sensing options for soil survey in developing countries p 2 A87-21239
- The thematic mapper - A new tool for soil mapping in arid areas p 2 A87-21243
- An application of thematic mapper data in Tunisia - Estimation of daily amplitude in near-surface soil temperature and discrimination of hypersaline soils p 2 A87-21245
- Experimental results in soil moisture mapping using IR thermography p 2 A87-21246
- Radar images for soil survey in England and Wales p 3 A87-21251
- Determination of the properties of a plowed soil layer from multispectral space imagery p 8 A87-26536
- Proposal of a remote sensing method for measuring soil moisture of bare soils in the frequency range 100 MHz-1 GHz p 8 A87-26974
- The use of thermal airborne remote sensing for soil identification: A case study in Limousin (France) p 20 N87-18146
- Soil degradation evaluation by digital image processing p 20 N87-18147
- Assessment of soil degradation in an arid region using remote sensing p 20 N87-18148
- The use of remote sensing (including aerial photographs) to devise cost-effective methods for soil conservation in the Kocaeli Peninsula, Turkey p 20 N87-18149
- Application of remote sensing in the study of the soil hazards of Haryana State, India p 20 N87-18150
- Vegetation and soils information contained in transformed Thematic Mapper data p 22 N87-18185
- First step in the use of remote sensing for regional mapping of soil organization data: Application in Brittany (France) and French Guiana p 23 N87-18193
- SOIL MOISTURE**
- NMR instrument for soil moisture ground-truth data collection p 2 A87-21240
- Experimental results in soil moisture mapping using IR thermography p 2 A87-21246
- The effect of local advection on the inference of soil moisture from thermal infrared radiances p 3 A87-23388
- Soil moisture estimates from satellite infrared temperatures and their relation to surface measurements p 3 A87-23389
- Growing period and drought early warning in Africa using satellite data p 7 A87-24788
- Proposal of a remote sensing method for measuring soil moisture of bare soils in the frequency range 100 MHz-1 GHz p 8 A87-26974
- Hydrologic models of land surface processes --- soil moisture p 58 N87-15547
- Modellisation of evapotranspiration and soil available water over an agricultural region applicable for remote sensing p 12 N87-15554
- Contribution of passive microwave remote sensing in soil moisture and evapotranspiration measurements p 12 N87-15589
- SIR-B measurements and modeling of vegetation p 15 N87-17160
- Toward a satellite system to monitor the spatial and temporal behavior of soil water content p 18 N87-17288
- The effect of measurement error and confusion from vegetation on passive microwave estimates of soil moisture p 18 N87-17304
- SOIL SCIENCE**
- Soil science interpretation of photographs taken by Spacelab 1 p 2 A87-21241
- The application of remotely sensed data to pedologic and geomorphic mapping on alluvial fan and playa surfaces in Saline Valley, California p 15 N87-17127
- SOILS**
- Timely thermal infrared data acquisition for soil survey in humid temperature environments p 3 A87-21249
- Theoretical approach to radar backscattering of soils p 3 A87-21250
- An iterative Landsat-MSS classification methodology for soil survey p 3 A87-23797
- Ground radiometry and airborne multispectral survey of bare soils p 10 A87-30894
- Modeling energy flow and nutrient cycling in natural semiarid grassland ecosystems with the aid of thematic mapper data [NASA-CR-179903] p 11 N87-15517
- Development of EOS-aided procedures for the determination of the water balance of hydrologic budget of a large watershed [NASA-CR-180118] p 60 N87-16383
- Thermal imaging spectroscopy in the Kelso-Baker Region, California p 30 N87-17117
- TIMS data applications in Nebraska p 15 N87-17126
- Dielectric and surface parameters related to microwave scatter and emission properties p 16 N87-17262
- Proceedings of the 1986 International Geoscience and Remote Sensing Symposium (IGARSS '86) on Remote Sensing: Today's Solutions for Tomorrow's Information Needs, volume 3 [ESA-SP-254-VOL-3] p 84 N87-18142
- Thermal inertia and soil fluxes by remote sensing p 20 N87-18143
- The use of thermal airborne remote sensing for soil identification: A case study in Limousin (France) p 20 N87-18146
- Relationship between tree density, leaf area index, soil metal content, and LANDSAT MSS canopy radiance values p 21 N87-18174
- Remote sensing applications in the study of land use and soils of aeolian cover of the western part of Haryana State, India p 22 N87-18187
- Bare soil measurements with the Delft University Scatterometer (DUTSCAT) system (L-band) [REPT-64-220-86-T-1LH] p 24 N87-19797
- Spectral characteristics and the extent of paleosols of the Palouse formation [NASA-CR-180357] p 24 N87-19826
- SOLITARY WAVES**
- Hydrodynamics of internal solitons and a comparison of SIR-A and SIR-B data with ocean measurements p 45 N87-17147
- SOUTH DAKOTA**
- Modeling energy flow and nutrient cycling in natural semiarid grassland ecosystems with the aid of thematic mapper data [NASA-CR-179903] p 11 N87-15517
- SPACE BASED RADAR**
- Spaceborne imaging radar research in the 90's p 79 N87-17141
- SPACE COMMERCIALIZATION**
- Spot data distribution --- selling satellite images p 62 A87-20683
- SPOT IMAGE and commercialisation of remote sensing data p 65 A87-29430
- Business approach to earth observation applications p 87 A87-29433
- Commercial opportunities in Earth observation from space p 87 N87-17177
- SPACE FLIGHT**
- Aeronautics and space report of the President: 1985 activities p 87 N87-16662
- SPACE LAW**
- Partnerships in remote sensing - A theme with some examples p 86 A87-25531
- SPACE MISSIONS**
- Aeronautics and space report of the President: 1985 activities p 87 N87-16662
- SPACE PLATFORMS**
- Space remote sensing p 86 A87-20682
- Earth Observing System - The earth research system of the 1990's [AIAA PAPER 87-0320] p 74 A87-22556
- SPACE PROGRAMS**
- Aeronautics and space report of the President: 1985 activities p 87 N87-16662
- SPACE SHUTTLE MISSION 41-G**
- Analysis of Large Format Camera images from the Black Hills, USA, for topographic and thematic mapping p 71 N87-18189
- SPACE SHUTTLE PAYLOADS**
- Space Shuttle cloud detection and earth feature classification experiment p 77 A87-31139
- SPACEBORNE ASTRONOMY**
- Instrumentation for optical remote sensing from space; Proceedings of the Meeting, Cannes, France, November 27-29, 1985 [SPIE-589] p 73 A87-19647
- SPACEBORNE EXPERIMENTS**
- Space Shuttle cloud detection and earth feature classification experiment p 77 A87-31139
- X-SAR extends the frequency range of Shuttle Imaging Radar p 70 N87-17362
- Southern Pantanal Matogrossense (South America) of Modular Optoelectronic Multispectral Scanner (MOMS) data, preliminary results p 71 N87-18182
- SPACEBORNE PHOTOGRAPHY**
- Soil science interpretation of photographs taken by Spacelab 1 p 2 A87-21241
- Control extension utilizing Large Format Camera imagery p 75 A87-23804
- The use of space photography to create and renew small-scale maps p 65 A87-25249
- Point positioning and mapping with Large Format Camera data p 71 N87-18188
- Analysis of Large Format Camera images from the Black Hills, USA, for topographic and thematic mapping p 71 N87-18189
- SPACECRAFT INSTRUMENTS**
- Evaluation of geophysical parameters measured by the Nimbus-7 microwave radiometer for the TOGA Heat Exchange Project [NASA-CR-180151] p 78 N87-17110
- SPACELAB**
- Soil science interpretation of photographs taken by Spacelab 1 p 2 A87-21241
- SPATIAL DISTRIBUTION**
- Relationship between tree density, leaf area index, soil metal content, and LANDSAT MSS canopy radiance values p 21 N87-18174
- Spectral characteristics and the extent of paleosols of the Palouse formation [NASA-CR-180357] p 24 N87-19826
- SPATIAL RESOLUTION**
- The interactive effect of spatial resolution and degree of internal variability within land-cover types on classification accuracies p 77 A87-30895
- SPECTRAL BANDS**
- Chlorophyll pigment concentration using spectral curvature algorithms - An evaluation of present and proposed satellite ocean color sensor bands p 37 A87-20204
- Effect of surface properties on the narrow to broadband spectral relationship in clear sky satellite observations p 65 A87-25587
- SPECTRAL CORRELATION**
- Investigation of spectral correlations of vegetation growing on different types of geological structures p 29 A87-28508
- SPECTRAL EMISSION**
- Calculation of day and night emittance values p 67 N87-17131
- SPECTRAL METHODS**
- Thematic mapper analysis of coniferous forest structure and composition p 1 A87-20762
- SPECTRAL RECONNAISSANCE**
- Development and demonstration of ALARM (Airborne Lidar Agent Remote Monitor) [AD-A172886] p 78 N87-16387
- SPECTRAL REFLECTANCE**
- Estimation of canopy parameters for inhomogeneous vegetation canopies from reflectance data. II - Estimation of leaf area index and percentage of ground cover for row canopies p 1 A87-20761
- Phenological effects on grass canopy/spectral relationships p 4 A87-23818
- A photographic technique for studying reflection indicatrices of vegetation cover p 5 A87-24388
- The spectral reflectance of stands of Norway spruce and Scotch pine, measured from a helicopter p 7 A87-25586
- Classification of reflectance on colour infrared aerial photographs and sub-tropical salt-marsh vegetation types p 10 A87-29012
- Preliminary measurements of leaf spectral reflectance in the 8-14/micron p 10 A87-29018
- Estimation of vegetation cover at subpixel resolution using LANDSAT data [NASA-CR-177077] p 11 N87-15514
- Imaging spectrometry: Aircraft and space program p 81 N87-17202
- A statistical approach to select the optimal wavelength bands for separating rocks in the wavelength region 0.4 to 2.3 microns p 34 N87-17244
- Results of tectonic and spectral investigations along the Wadi Araba fault in Jordan using special processed Thematic Mapping (TM) data p 34 N87-17247
- Relationship between tree density, leaf area index, soil metal content, and LANDSAT MSS canopy radiance values p 21 N87-18174
- Surface reflectance correction and stereo enhancement of LANDSAT thematic mapper imagery for structural geologic exploration [DE87-003095] p 37 N87-19796
- SPECTRAL RESOLUTION**
- Estimation of vegetation cover at subpixel resolution using LANDSAT data [NASA-CR-177077] p 11 N87-15514
- SPECTRAL SIGNATURES**
- Estimation of canopy parameters for inhomogeneous vegetation canopies from reflectance data. II - Estimation of leaf area index and percentage of ground cover for row canopies p 1 A87-20761
- Impact of environmental variables on spectral signatures acquired by the Landsat Thematic Mapper p 9 A87-29003
- Interrelationship between field spectra and airborne MSS systems in the Singatse range, (Yerington) Nevada --- multispectral scanner (MSS) mineral exploration p 34 N87-17242
- A statistical approach to select the optimal wavelength bands for separating rocks in the wavelength region 0.4 to 2.3 microns p 34 N87-17244

Off-nadir optical remote sensing from satellites for vegetation identification [DE86-012387] p 23 N87-18916

SPECTROMETERS
Imaging spectrometry: Aircraft and space program p 81 N87-17202

SPECTROPHOTOMETERS
Proposed design of an imaging spectropolarimeter/photometer for remote sensing of earth resources p 73 A87-20795

SPECTRORADIOMETERS
A knowledge-based software environment for the analysis of spectroradiometer data --- mineral identification p 68 N87-17203

SPECTRUM ANALYSIS
Chlorophyll pigment concentration using spectral curvature algorithms - An evaluation of present and proposed satellite ocean color sensor bands p 37 A87-20204
Thermal imaging spectroscopy in the Kelso-Baker Region, California p 30 N87-17117
Simulation modeling and preliminary analysis of TIMS data from the Carlin area and the northern Grapevine Mountains, Nevada p 31 N87-17120
Application of TIMS data in stratigraphic analysis p 31 N87-17121
A statistical approach to select the optimal wavelength bands for separating rocks in the wavelength region 0.4 to 2.3 microns p 34 N87-17244

SPHERICAL HARMONICS
Improvement of the Earth's gravity field from terrestrial and satellite data [NASA-CR-180139] p 27 N87-17416

SPOT (FRENCH SATELLITE)
In flight calibration of push broom remote sensing instruments p 73 A87-19652
Space remote sensing p 86 A87-20682
Spot data distribution --- selling satellite images p 62 A87-20683
The SPOT satellites - From SPOT 1 to SPOT 4 p 74 A87-21094
Exploitation of the SPOT system p 62 A87-21095
Preliminary analysis of SPOT HRV multispectral products of an arid environment p 10 A87-29017
SPOT IMAGE and commercialisation of remote sensing data p 65 A87-29430
Spatial remote sensing to land management --- SPOT/GPS p 70 N87-18157

SRI LANKA
Monitoring of land-surface change in Sri Lanka p 13 N87-15618
Monitoring land use changes in Sri Lanka for land use planning using a geographic information system and satellite imagery p 26 N87-18151

STATISTICAL ANALYSIS
Spectral characteristics and the extent of paleosols of the Palouse formation [NASA-CR-180357] p 24 N87-19826

STEREOPHOTOGRAPHY
Control extension utilizing Large Format Camera imagery p 75 A87-23804
The stereo-pushbroom scanner system Digital Photogrammetry System (DPS) and its accuracy p 80 N87-17167

STEREOSCOPY
Accuracy of population estimation from medium-scale aerial photography p 24 A87-23777
Analysis of multichannel SAR data of Spitsbergen --- glaciology p 60 N87-17223

STORMS (METEOROLOGY)
Satellite contributions to convective scale weather analysis and forecasting p 76 A87-27882

STRATIFICATION
Geological nature of early Precambrian formations (considering the example of the Anabar shield) p 28 A87-24274

STRATIGRAPHY
Application of TIMS data in stratigraphic analysis p 31 N87-17121

STRATOSPHERE
Instrument characterization for the detection of long-term changes in stratospheric ozone - An analysis of the SBUV/2 radiometer p 74 A87-20961
SAM II measurements of Antarctic PSC's and aerosols --- Stratospheric Aerosol Measurement satellite - Polar Stratospheric Clouds p 75 A87-23546

STREAMS
Visualization by aerial thermography of hydrodynamic exchanges between the water table, streams and gravel pits in the Rhine plain north of Strasbourg p 58 A87-25746

STRUCTURAL BASINS
Integration of space-geological and geophysical methods in regional and local predictions of tectonic structures in the Caspian depression p 28 A87-24381

STRUCTURAL PROPERTIES (GEOLOGY)

Analysis of correlations between structural elements detected on space images and metallogenic zones p 28 A87-24380

Lineaments of eastern Cuba - Geological interpretation of aerial and space imagery p 28 A87-24384
Methods of geological interpretation of lineaments of platform areas (with reference to Ustiurt) p 29 A87-26532

A comparative study of lineament analysis from different remote sensing imagery over areas in the Benue Valley and Jos Plateau Nigeria p 30 A87-29010
An analysis of geologic lineaments seen on Landsat MSS imagery p 30 A87-29011
Airborne Thermal Infrared Multispectral Scanner (TIMS) images over disseminated gold deposits, Osgood Mountains, Humboldt County, Nevada p 32 N87-17134
Significance of space image, air photo and drainage linears in relation to west coast tectonics, India p 33 N87-17232
Structural and geomorphic evolution of Meghalaya plateau, India on LANDSAT imagery p 33 N87-17233

SUDAN
Rainfall and vegetation monitoring in the Savanna Zone of the Democratic Republic of Sudan using the NOAA Advanced Very High Resolution Radiometer p 6 A87-24783
Desertification monitoring: Remotely sensed data for drought impact studies in the Sudan p 12 N87-15604
Surface albedo change in arid regions in the Sudan p 13 N87-15615

SUGAR CANE
CANASATE: Sugar cane mapping by satellite, area 3 [INPE-4068-RPE/526] p 24 N87-19790

SUMMER
An inter-sensor comparison of the microwave signatures of Arctic sea ice p 46 N87-17184

SUPERHIGH FREQUENCIES
C and Ku-band scatterometer results from the SCATMOD internal wave experiment p 47 N87-17215
L to X-band scatter and emission measurements of vegetation p 19 N87-17347
X-SAR extends the frequency range of Shuttle Imaging Radar p 70 N87-17362

SURFACE PROPERTIES
Effect of surface properties on the narrow to broadband spectral relationship in clear sky satellite observations p 65 A87-25587
An extension of the split window technique for the retrieval of precipitable water [AD-A173008] p 60 N87-16386
Development and demonstration of ALARM (Airborne Lidar Agent Remote Monitor) [AD-A172886] p 78 N87-16387

SURFACE ROUGHNESS
Dielectric and surface parameters related to microwave scatter and emission properties p 16 N87-17262
Observations of surface currents at Nantucket Shoals and implications for radar imaging of the bottom p 48 N87-17296

SURFACE ROUGHNESS EFFECTS
Radiometric correction method which removes both atmospheric and topographic effects from the LANDSAT-MSS data p 83 N87-17329
Evaluating roughness models of radar backscatter p 19 N87-17344

SURFACE TEMPERATURE
An application of thematic mapper data in Tunisia - Estimation of daily amplitude in near-surface soil temperature and discrimination of hypersaline soils p 2 A87-21245
Timely thermal infrared data acquisition for soil survey in humid temperature environments p 3 A87-21249
Soil moisture estimates from satellite infrared temperatures and their relation to surface measurements p 3 A87-23389
Remote sensing of land-surface temperature from HIRS/MSU data --- High Resolution Infrared Sounder/Microwave Sounding Unit (HIRS/MSU) p 77 N87-15573
Estimation of absolute water surface temperature based on atmospherically corrected thermal infrared multispectral scanner digital data p 79 N87-17114
Enhancement of time images for photointerpretation p 66 N87-17116
Calculation of day and night emittance values p 67 N87-17131

SURFACE WAVES
Analysis of surface patterns over Cobb Seamount using synthetic-aperture radar imagery [AD-A171670] p 45 N87-16493
Observations of surface currents at Nantucket Shoals and implications for radar imaging of the bottom p 48 N87-17296

Investigation of physics of synthetic aperture radar in ocean remote sensing toward 84/86 field experiment. Volume 1: Data summary and early results [AD-A174197] p 55 N87-18913

SYNCHRONOUS SATELLITES
An extension of the split window technique for the retrieval of precipitable water [AD-A173008] p 60 N87-16386

SYNTHETIC APERTURE RADAR
Results of an airborne synthetic-aperture radar (SAR) experiment over a SIR-B (Shuttle Imaging Radar) test site in Germany p 76 A87-27999
Imaging radar polarimetry from wave synthesis p 76 A87-29849
Analysis of surface patterns over Cobb Seamount using synthetic-aperture radar imagery [AD-A171670] p 45 N87-16493
The Second Spaceborne Imaging Radar Symposium [NASA-CR-180131] p 67 N87-17135
Geological applications of multipolarization SAR data p 33 N87-17140
Present status of Japanese ERS-1 Project p 79 N87-17145
A scanning radar altimeter for mapping continental topography p 33 N87-17146
Operational wave forecasting with spaceborne SAR: Prospects and pitfalls p 45 N87-17149
Observing the polar oceans with spaceborne radar p 46 N87-17151
Analysis of multiple incidence angle SIR-B data for determining forest stand characteristics p 15 N87-17156
Multiple incidence angle SIR-B experiment over Argentina p 80 N87-17157
SIR-B measurements and modeling of vegetation p 15 N87-17160
Automated remote sensing of sea ice using synthetic aperture radar p 46 N87-17186
An overview of operational SAR data collection and dissemination plans for ERS-1 ice data in Canada p 47 N87-17189
Geophysics of the marginal ice zone from SAR p 47 N87-17219
SAR ice floe kinematics and correlation with mesoscale oceanic structure within the marginal ice zone p 48 N87-17222
Analysis of multichannel SAR data of Spitsbergen --- glaciology p 60 N87-17223
Canadian plans for operational demonstrations of satellite imaging radar applications --- ERS-1 p 68 N87-17229
Multispectral classification of microwave remote sensing images --- SAR crop identification p 16 N87-17238
Extraction of the backscatter coefficient of agricultural fields from an airborne SAR image p 16 N87-17265
Merging spaceborne image data of optical and microwave sensors p 69 N87-17267
Digital terrain mapping with STAR-1 SAR data p 69 N87-17269
Analysis of the spatial structure of Synthetic Aperture Radar (SAR) imagery for a better separability of cereal crops, wheat and barley p 17 N87-17287
Estimation of internal wave currents from SAR and infrared scatterometer imagery p 48 N87-17295
SAR imaging of bottom topography in the ocean: Results from an improved model p 48 N87-17298
An improved method for the determination of water depth from surface wave refraction patterns --- SAR imagery p 49 N87-17299
SAR imagery for forest management p 18 N87-17313
Future user requirements and required technological developments of spaceborne synthetic aperture radars p 82 N87-17320
Characteristics of a very low altitude spacecraft for collecting global directional wave spectra with spaceborne synthetic aperture radar p 49 N87-17333
The SAR image modulation transfer function derived from SIR-B image spectra and airborne measurements of ocean wave height spectra p 49 N87-17334
SIR-B observations of ocean waves in the NE Atlantic p 49 N87-17335
Characterisation of internal wave surface patterns on airborne SAR imagery p 50 N87-17338
A satellite-borne SAR transmitter and receiver p 83 N87-17358
Pulse compression test results of the SAR transmitter and receiver --- satellite-borne SAR p 83 N87-17360
X-SAR extends the frequency range of Shuttle Imaging Radar p 70 N87-17362
A procedure for estimation of two-dimensional ocean height-variance spectra from SAR imagery p 52 N87-17381
A scatterometer research program p 53 N87-17391

- Proceedings of the 1986 International Geoscience and Remote Sensing Symposium (IGARSS '86) on Remote Sensing: Today's Solutions for Tomorrow's Information Needs, volume 3
[ESA-SP-254-VOL-3] p 84 N87-18142
- Outline of SAR-850 data processing method in Japan --- ERS-1 (NASDA) p 71 N87-18176
- Digital realtime SAR processor for C- and X-band applications p 71 N87-18177
- Intelligent SAR Processor (ISAR), a new concept for high throughput and high precision digital SAR processing p 85 N87-18178
- High speed image processing system based on the custom VLSI for Digital Signal Processing (DSP) --- SAR imagery p 71 N87-18179
- A very fast synthetic-aperture radar signal processor for ERS-1 and Radarsat p 85 N87-18180
- STAR-VUE: A tactical ice navigation workstation p 54 N87-18181
- Resolving the Doppler ambiguity for spaceborne synthetic aperture radar p 72 N87-18212
- Shuttle imaging radar-C science plan [NASA-CR-180241] p 86 N87-18697
- Investigation of physics of synthetic aperture radar in ocean remote sensing toward 84/86 field experiment. Volume 1: Data summary and early results [AD-A174197] p 55 N87-18913
- Investigation of physics of synthetic aperture radar in ocean remote sensing TOWARD 84/86 field experiment. Volume 2: Contributions of individual investigators [AD-A174527] p 55 N87-18966
- SYNTHETIC APERTURES**
- Application of Spaceborne Distributed Aperture/Coherent Array Processing (SDA/CAP) technology to active and passive microwave remote sensing p 82 N87-17277
- SYNTHETIC ARRAYS**
- The Electronically Steered Thinned Array Radiometer (ESTAR) p 82 N87-17280
- Application of Spaceborne Distributed Aperture/Coherent Array Processing (SDA/CAP) technology to active and passive microwave remote sensing p 82 N87-17277
- T**
- TABLES (DATA)**
- The data dilemma - How to properly construct and utilize aerial photo volume tables p 63 A87-23790
- TECHNOLOGY ASSESSMENT**
- Space science and applications: Progress and potential p 87 A87-30876
- Remote sensing from space - An overview p 87 A87-30881
- The prospects for hydrological measurements using ERS-1 --- lakes p 59 N87-15588
- Components and comparisons of potential information from several imaging satellites p 67 N87-17164
- Comparative study of LANDSAT MSS, Salyut-7 (TERRA) and radar (SIR-A) images for geological and geomorphological applications: A case study from Rajasthan and Gujarat, India p 34 N87-17236
- Assessment of soil degradation in an arid region using remote sensing p 20 N87-18148
- On the discrimination between crude oil spills and monomolecular sea slicks by airborne remote sensors: Today's possibilities and limitations p 53 N87-18167
- Evaluation of remote sensing results for the benefit of water quality research on the North Sea [NZ-R-86.15] p 62 N87-19799
- TECHNOLOGY TRANSFER**
- The transfer of remote sensing technology to developing countries: A survey of experts in the field p 87 N87-17170
- TECHNOLOGY UTILIZATION**
- Exploitation of the SPOT system p 62 A87-21095
- Remote sensing options for soil survey in developing countries p 2 A87-21239
- The transfer of remote sensing technology to developing countries: A survey of experts in the field p 87 N87-17170
- Microwave remote sensing: Its applications and limitations in operational tasks of land use inventory and forest management p 17 N87-17266
- Applications of remote sensing in the US Department of Agriculture p 17 N87-17285
- Thermal infrared remote sensing: One of today's solutions p 83 N87-17324
- The use of remote sensing (including aerial photographs) to devise cost-effective methods for soil conservation in the Kocaeli Peninsula, Turkey p 20 N87-18149
- The use of space technology in federally funded land processes research in the United States p 88 N87-18152
- TECTONICS**
- Integration of space-geological and geophysical methods in regional and local predictions of tectonic structures in the Caspian depression p 28 A87-24381
- Tidal heating in an internal ocean model of Europa p 43 A87-30143
- Tectonic geomorphology of the Andes with SIR-A and SIR-B p 32 N87-17136
- Delineation of fault zones using imaging radar p 32 N87-17138
- Significance of space image, air photo and drainage linears in relation to west coast tectonics, India p 33 N87-17232
- Results of tectonic and spectral investigations along the Wadi Araba fault in Jordan using special processed Thematic Mapping (TM) data p 34 N87-17247
- TEMPERATURE MEASUREMENT**
- The results of sea-surface temperature determinations from IR and microwave measurements aboard the Cosmos-1151 satellite p 40 A87-24376
- On the use of synthetic 12-micron data in a split-window retrieval of sea surface temperature from AVHRR measurements p 43 A87-29019
- Multiangle or multiwavelength technique for remote sensing of sea surface temperature p 45 N87-15652
- Application of remote sensing in hydrology and water resources [INPE-3986-PRE/991] p 60 N87-16382
- Enhancement of time images for photointerpretation p 66 N87-17116
- Monitoring vegetation recovery patterns on Mount St. Helens using thermal infrared multispectral data p 14 N87-17122
- Investigation of forest canopy temperatures recorded by the thermal infrared multispectral scanner at H. J. Andrews Experimental Forest p 14 N87-17123
- Models for temperature estimation from remotely sensed thermal IR data p 83 N87-17325
- Thermal inertia and soil fluxes by remote sensing p 20 N87-18143
- Radiometric analysis of the longwave infrared channel of the Thematic Mapper on LANDSAT 4 and 5 [NASA-CR-180180] p 86 N87-18221
- TEMPERATURE PROBES**
- A thermal device for aircraft measurement of the solid water content of clouds p 56 A87-20951
- TERRAIN**
- Sparse area stereo matching experiment [AD-A173601] p 66 N87-16388
- Multiple incidence angle SIR-B experiment over Argentina p 80 N87-17157
- Digital terrain mapping with STAR-1 SAR data p 69 N87-17269
- Satellite altimeter measurements over land and inland water p 61 N87-18200
- TERRAIN ANALYSIS**
- Composite/progressive sampling - A program package for computer supported collection of DTM data --- Digital Terrain Models p 62 A87-23784
- A comparative test of photogrammetrically sampled digital elevation models p 66 A87-29499
- Imaging radar polarimetry from wave synthesis p 76 A87-29849
- Terrain analysis from digital patterns in geomorphometry and Landsat MSS spectral response p 66 A87-30127
- Deduction of a synthetic bioclimatological map by means of remote sensing data and a digital terrain model using a correlation approach p 72 N87-18194
- TEXAS**
- The Red River Valley archeological project p 31 N87-17128
- TEXTURES**
- Rock type discrimination with AI-based texture analysis algorithms p 28 A87-23782
- A cognitive measure of texture in imagery p 64 A87-23800
- THAILAND**
- The application of LANDSAT imagery for land cover assessment --- Thailand p 13 N87-15614
- THEMATIC MAPPING**
- Improved multispectral earth imaging from space using electronic image alignment p 73 A87-19655
- An initial evaluation of two digital airborne imagers for surveying spruce budworm defoliation p 1 A87-20671
- Volcanology from space - Using Landsat thematic mapper data in the central Andes p 27 A87-20689
- Thematic mapper analysis of coniferous forest structure and composition p 1 A87-20762
- Assessing forest decline in coniferous forests of Vermont using NS-001 Thematic Mapper Simulator data p 1 A87-20763
- The thematic mapper - A new tool for soil mapping in arid areas p 2 A87-21243
- Processing thematic mapper data for mapping in Tunisia p 2 A87-21244
- An application of thematic mapper data in Tunisia - Estimation of daily amplitude in near-surface soil temperature and discrimination of hypersaline soils p 2 A87-21245
- Classification of multivariate Thematic Mapper data p 64 A87-23795
- POLYSITE - An interactive package for the selection and refinement of Landsat image training sites p 65 A87-23805
- The utility of Thematic Mapper data for temperature mapping in the Great Lakes p 57 A87-23824
- Landsat Thematic Mapper data analysis within the Suwannee River Basin p 57 A87-23825
- Landsat Thematic Mapper digital information content for agricultural environments p 5 A87-23830
- Landsat Thematic Mapper images for hydrologic land use and cover p 58 A87-23831
- Vegetable crop inventory with Landsat TM data p 5 A87-23833
- Monitoring East African vegetation using AVHRR data p 6 A87-24781
- Monitoring the grasslands of the Sahel using NOAA AVHRR data Niger 1983 p 6 A87-24782
- Rainfall and vegetation monitoring in the Savanna Zone of the Democratic Republic of Sudan using the NOAA Advanced Very High Resolution Radiometer p 6 A87-24783
- Monitoring the grasslands of the Sahel 1984-1985 p 7 A87-24787
- Aircraft and satellite thermographic systems for wildfire mapping and assessment [AIAA PAPER 87-0187] p 7 A87-24933
- Automation of thematic processing of space images in evaluating crop condition p 8 A87-26539
- Fruit tree inventory with Landsat Thematic Mapper data p 8 A87-28387
- Impact of environmental variables on spectral signatures acquired by the Landsat Thematic Mapper p 9 A87-29003
- Performance of Landsat-5 TM data in land-cover classification p 25 A87-29007
- Drainage channel network of the Arcachon Basin using Thematic Mapper data obtained at high tide p 58 A87-29013
- Discrimination of altered basaltic rocks in the southwestern United States by analysis of Landsat Thematic Mapper data p 30 A87-30126
- Spectral separation of moorland vegetation in airborne Thematic Mapper data p 10 A87-30897
- Mapping of water quality in coastal waters using Airborne Thematic Mapper data p 58 A87-30899
- The quantitative use of airborne Thematic Mapper thermal infrared data p 44 A87-30900
- Mapping of agricultural lands in the USSR p 11 N87-15507
- Variations in in-flight absolute radiometric calibration --- satellite remote sensors p 77 N87-15594
- Vegetation identification and variability in the Tahoua area, Nigeria --- LANDSAT thematic mapper p 13 N87-15610
- Monitoring of land-surface change in Sri Lanka p 13 N87-15618
- Group Agromet Monitoring Project (GAMP) methodology integrated mapping of rainfall, evapotranspiration, germination, biomass development and thermal inertia, based on Meteosat and conventional meteorological data p 59 N87-15626
- Application of TIMS data in stratigraphic analysis p 31 N87-17121
- The application of remotely sensed data to pedologic and geomorphic mapping on alluvial fan and playa surfaces in Saline Valley, California p 15 N87-17127
- Tectonic geomorphology of the Andes with SIR-A and SIR-B p 32 N87-17136
- Analysis of multiple incidence angle SIR-B data for determining forest stand characteristics p 15 N87-17156
- Comparison of Thematic Mapper (TM) and SPOT simulation data for agricultural applications in south west Germany p 16 N87-17165
- Sri Lanka's solution to land use mapping and monitoring for Third World countries development p 67 N87-17174
- Hydrogeological research in Peloponnesus (Greece) Karst area by support and completion of LANDSAT-thematic data p 33 N87-17234
- Computer-aided analysis of LANDSAT data for mapping geologic and geomorphic features, North Bombay, India p 33 N87-17235
- Discrimination of lithologic units using geobotanical and LANDSAT TM spectral data p 34 N87-17246
- Results of tectonic and spectral investigations along the Wadi Araba fault in Jordan using special processed Thematic Mapping (TM) data p 34 N87-17247
- Bi-temporal analysis of Thematic Mapper data for land cover classification p 69 N87-17249

Evaluation of LANDSAT 5 Thematic Mapping (TM) data for image clustering and classification

p 69 N87-17251
Merging spaceborne image data of optical and microwave sensors p 69 N87-17267
Rural land use inventory and mapping in the Ardeche area (France) using multitemporal Thematic Mapping (TM) data p 19 N87-17350

LANDSAT-5 Thematic Mapping (TM) data applications to land use classification on around the Bosphorus area, Turkey p 19 N87-17351
Discrimination of land features using LANDSAT false colour composite in N Iran p 19 N87-17352
Monitoring land use changes in Sri Lanka for land use planning using a geographic information system and satellite imagery p 26 N87-18151
Use of TMS/TM data for mapping of forest decline damage in the northeastern United States --- Thematic Mapper Simulator (TMS) Thematic Mapper (TM) p 22 N87-18175

Southern Pantanal Matogrossense (South America) of Modular Optoelectronic Multispectral Scanner (MOMS) data, preliminary results p 71 N87-18182
Multitemporal analysis of the phenological stage of vegetation using TM-data in the Southern Black Forest (West Germany) p 22 N87-18184
Vegetation and soils information contained in transformed Thematic Mapper data p 22 N87-18185
Description of a methodology for biomass change mapping with the use of LANDSAT TM data p 22 N87-18186

Analysis of Large Format Camera images from the Black Hills, USA, for topographic and thematic mapping p 71 N87-18189

LANDSAT-MSS remote sensing and satellite cartography: An integrated approach to the preparation of a new geological map of Egypt at a scale of 1:500 000 p 36 N87-18190

UMUS: A project for usage of LANDSAT MSS and ancillary data in land cover mapping of large areas in southern Italy p 72 N87-18191

Automatic update procedure of the digitized land use map using LANDSAT TM data p 72 N87-18192
Radiometric analysis of the longwave infrared channel of the Thematic Mapper on LANDSAT 4 and 5 [NASA-CR-180180] p 86 N87-18221

Monitoring sediment transfer processes on the desert margin [NASA-CR-180181] p 23 N87-18222

Nature and origin of mineral coatings on volcanic rocks of the Black Mountain, Stonewall Mountain, and Kane Springs, Wash volcanic centers, Southern Nevada [NASA-CR-180183] p 36 N87-18255

Influence of the Yukon River on the Bering Sea [NASA-CR-180065] p 54 N87-18293

Thematic mapper studies of central Andean volcanoes [NASA-CR-180252] p 36 N87-18910

Interpreting forest and grassland biome productivity utilizing nested scales of image resolution and biogeographical analysis p 23 N87-18912

Evaluation of LANDSAT 4 MSS data for geomorphological mapping in the semiarid environment for regional planning purposes: An integrated approach (study site, the Juazeiro region) [INPE-3984-TDL/236] p 72 N87-19787

Methodology for the elaboration of thematic maps utilizing LANDSAT-TM data [INPE-3893-TDL/225] p 72 N87-19792

Spectral characteristics and the extent of paleosols of the Palouse formation [NASA-CR-180357] p 24 N87-19826

Influence of the Yukon River on the Bering Sea [NASA-CR-180356] p 56 N87-19877

THERMAL MAPPING
The TMS Data User's Workshop [NASA-CR-180130] p 78 N87-17111

The TMS instrument p 79 N87-17112
The TMS investigator's guide p 79 N87-17113

Estimation of absolute water surface temperature based on atmospherically corrected thermal infrared multispectral scanner digital data p 79 N87-17114

Atmospheric correction of TMS data p 79 N87-17115

Enhancement of time images for photointerpretation p 66 N87-17116

Thermal imaging spectroscopy in the Kelso-Baker Region, California p 30 N87-17117

Lithologic mapping of silicate rocks using TMS p 30 N87-17118

Detection and mapping of volcanic rock assemblages and associated hydrothermal alteration with Thermal Infrared Multiband Scanner (TIMS) data Comstock Lode Mining District, Virginia City, Nevada p 31 N87-17119

Simulation modeling and preliminary analysis of TIMS data from the Carlin area and the northern Grapevine Mountains, Nevada p 31 N87-17120

Application of TIMS data in stratigraphic analysis p 31 N87-17121

Monitoring vegetation recovery patterns on Mount St. Helens using thermal infrared multispectral data p 14 N87-17122

Investigation of forest canopy temperatures recorded by the thermal infrared multispectral scanner at H. J. Andrews Experimental Forest p 14 N87-17123

Applications of TIMS data in agricultural areas and related atmospheric considerations p 15 N87-17124

Locating subsurface gravel with thermal imagery p 31 N87-17125

TIMS data applications in Nebraska p 15 N87-17126

The application of remotely sensed data to pedologic and geomorphic mapping on alluvial fan and playa surfaces in Saline Valley, California p 15 N87-17127

The physical basis for spectral variations in thermal infrared emittance of silicates and application to remote sensing p 31 N87-17129

Infrared spectroscopy for geologic interpretation of TIMS data p 31 N87-17130

Calculation of day and night emittance values p 67 N87-17131

Application of Thermal Infrared Multiband Scanner (TIMS) data to mapping of Plutonic and stratified rock and assemblages in accreted terrains of the Northern Sierra, California p 15 N87-17132

A geologic atlas of TIMS data p 32 N87-17133

Airborne Thermal Infrared Multispectral Scanner (TIMS) images over disseminated gold deposits, Osgood Mountains, Humboldt County, Nevada p 32 N87-17134

Concept of a future multispectral Thermal Infrared (TIR) pushbroom mission for Earth observation from space p 80 N87-17169

The use of thermal airborne remote sensing for soil identification: A case study in Limousin (France) p 20 N87-18146

THERMAL RADIATION
Timely thermal infrared data acquisition for soil survey in humid temperature environments p 3 A87-21249

The quantitative use of airborne Thematic Mapper thermal infrared data p 44 A87-30900

THERMAL STABILITY
Group Agromet Monitoring Project (GAMP) methodology integrated mapping of rainfall, evapotranspiration, germination, biomass development and thermal inertia, based on Meteosat and conventional meteorological data p 59 N87-15626

THERMOGRAPHY
Experimental results in soil moisture mapping using IR thermography p 2 A87-21246

Thermography - Principles and application in the Oost-Gelderland remote sensing study project p 3 A87-21247

Aircraft and satellite thermographic systems for wildfire mapping and assessment [AIAA PAPER 87-0187] p 7 A87-24933

Visualization by aerial thermography of hydrodynamic exchanges between the water table, streams and gravel pits in the Rhine plain north of Strasbourg p 58 A87-25746

THICKNESS
Eastern-Western Arctic Sea Ice Analysis, 1985 [AD-A173972] p 55 N87-18298

THUNDERSTORMS
Detecting and forecasting western region flash floods using GOES imagery and conventional data p 58 A87-27883

Forecasting sea breeze thunderstorms at the Kennedy Space Center using the Prognostic Three-Dimensional Mesoscale Model (P 3DM) p 43 A87-27891

TIMBER IDENTIFICATION
The development of procedures for forest interpretation from texture-selective images p 8 A87-26535

Preliminary measurements of leaf spectral reflectance in the 8-14/micron p 10 A87-29018

TIMBER INVENTORY
Estimation of density in young pine plantations using 35mm aerial photography p 5 A87-23819

TIMBER VIGOR
An initial evaluation of two digital airborne imagers for surveying spruce budworm defoliation p 1 A87-20671

Extraction of areas infested by pine bark beetle using Landsat MSS data p 10 A87-30129

TIME SERIES ANALYSIS
A satellite time series of sea surface temperatures in the eastern equatorial Pacific Ocean, 1982-1986 p 39 A87-23718

Bitemporal analysis of Thematic Mapper data for land cover classification p 69 N87-17249

TIROS N SERIES SATELLITES
Atmospheric corrections of NOAA-AVHRR data verification of different methods by ground truth measurements p 70 N87-17274

TOPOGRAPHY
Comparison between satellite image advective velocities, dynamic topography, and surface drifter trajectories p 38 A87-20692

Pre-assessment for large scale civil engineering projects by integrated analysis with the data numerical topography and remote sensing p 57 A87-23815

Use of topographic and climatological models in a geographical data base to improve Landsat MSS classification for Olympic National Park p 25 A87-30128

Application of Thermal Infrared Multiband Scanner (TIMS) data to mapping of Plutonic and stratified rock and assemblages in accreted terrains of the Northern Sierra, California p 15 N87-17132

Spaceborne imaging radar research in the 90's p 79 N87-17141

A scanning radar altimeter for mapping continental topography p 33 N87-17146

SAR imaging of bottom topography in the ocean: Results from an improved model p 48 N87-17298

Analysis of Large Format Camera images from the Black Hills, USA, for topographic and thematic mapping p 71 N87-18189

TOWERS
Tower-based broadband backscattering measurements from the ocean surface in the North Sea p 47 N87-17217

TRACE ELEMENTS
Arctic haze: Natural or pollution? [AD-A174025] p 55 N87-18931

TRACKING NETWORKS
NROSS (Navy Remote Ocean Sensing System) tracking network analysis [AD-A172132] p 45 N87-16384

TRADEOFFS
Some trade-offs in modest-resolution radars for space p 82 N87-17278

TRANSFORMATIONS (MATHEMATICS)
Vegetation and soils information contained in transformed Thematic Mapper data p 22 N87-18185

TREES (PLANTS)
The use of remote sensing in estimating biomass of fish tree areas in the Richard B. Russell Lake p 40 A87-23834

Tree attenuation at 869 MHz derived from remotely piloted aircraft measurements p 9 A87-28414

TROPICAL METEOROLOGY
Annual and interannual variability in large-scale convection over the eastern Pacific and tropical South America p 57 A87-23414

Vertical structure of the temperature field above the North Atlantic p 40 A87-24374

TROPICAL REGIONS
Using Landsat to assess tropical forest habitat for migratory birds in the Yucatan Peninsula p 4 A87-23807

Canopy reflectance modeling in a tropical wooded grassland [NASA-CR-180097] p 11 N87-15518

Evaluation of geophysical parameters measured by the Nimbus-7 microwave radiometer for the TOGA Heat Exchange Project [NASA-CR-180151] p 78 N87-17110

Report of the Fourth Session of the JSC/CCCO Tropical Ocean Global Atmosphere (TOGA) Scientific Steering Group [WCP-120] p 54 N87-18283

TUNGSTEN
Integration of surficial geochemistry and LANDSAT imagery to discover skarn tungsten deposits using image analysis techniques [CONTRIB-19586] p 35 N87-17248

TUNISIA
Spectral brightness and surface soil characteristics in an arid Mediterranean region (southern Tunisia) p 2 A87-21242

Processing thematic mapper data for mapping in Tunisia p 2 A87-21244

An application of thematic mapper data in Tunisia - Estimation of daily amplitude in near-surface soil temperature and discrimination of hypersaline soils p 2 A87-21245

TURBIDITY
Influence of the Yukon River on the Bering Sea [NASA-CR-180356] p 56 N87-19877

TURBULENT FLOW
Effects of a downstream disturbance on the structure of a turbulent plane mixing layer [AIAA PAPER 87-0197] p 74 A87-22476

TURBULENT MIXING

Effects of a downstream disturbance on the structure of a turbulent plane mixing layer [AIAA PAPER 87-0197] p 74 A87-22476

TURKEY

Remote sensing activities in Turkey: Possible contributions to climate studies p 77 N87-15624
The use of remote sensing (including aerial photographs) to devise cost-effective methods for soil conservation in the Kocaeli Peninsula, Turkey p 20 N87-18149

U

U.S.S.R. SPACE PROGRAM

Soviet remote sensing p 86 A87-27452

ULTRAHIGH FREQUENCIES

Proposal of a remote sensing method for measuring soil moisture of bare soils in the frequency range 100 MHz-1 GHz p 8 A87-26974
Tree attenuation at 869 MHz derived from remotely piloted aircraft measurements p 9 A87-28414
L to X-band scatter and emission measurements of vegetation p 19 N87-17347
Bare soil measurements with the Delft University Scatterometer (DUTSCAT) system (L-band) [REPT-64-220-86-T-1LH] p 24 N87-19797

UNITED STATES

Applications of remote sensing in the US Department of Agriculture p 17 N87-17285
The use of space technology in federally funded land processes research in the United States p 88 N87-18152

UNMANNED SPACECRAFT

Aeronautics and space report of the President: 1985 activities p 87 N87-16662

UPWELLING WATER

Mesoscale hydrographic variability in the vicinity of Points Conception and Arguello during April-May 1983 - The OPUS 1983 experiment p 39 A87-23719

URBAN DEVELOPMENT

Detection of new urban build-up in Ardmore and McAlester, Oklahoma using Landsat MSS data p 25 A87-23829

URBAN PLANNING

Environmental modification of metropolitan areas through satellite images: Study of urban design in the tropics p 25 N87-17175

USER REQUIREMENTS

The TIMS investigator's guide p 79 N87-17113
Future user requirements and required technological developments of spaceborne synthetic aperture radars p 82 N87-17320

V

VALLEYS

Assessment of wind and fluvial action by using LANDSAT-MSS color composites in the lower Nile Valley (Egypt) p 13 N87-15612

VEGETABLES

Vegetable crop inventory with Landsat TM data p 5 A87-23833

VEGETATION

Microwave backscattering from a layer of randomly oriented discs with application to scattering from vegetation p 8 A87-28316
Classification of reflectance on colour infrared aerial photographs and sub-tropical salt-marsh vegetation types p 10 A87-29012
Spectral separation of moorland vegetation in airborne Thematic Mapper data p 10 A87-30897
Estimation of vegetation cover at subpixel resolution using LANDSAT data [NASA-CR-177077] p 11 N87-15514
Observations of the seasonal variability of soil moisture and vegetation cover over Africa using satellite microwave radiometry p 12 N87-15593
Vegetation identification and variability in the Tahoua area, Nigeria --- LANDSAT thematic mapper p 13 N87-15610
Vegetation change and desertification in the Caribbean p 14 N87-15619
AVHRR and MSS data based vegetation indices studies over Indian sites --- NOAA radiometer (AVHRR) LANDSAT multispectral scanner (MSS) p 14 N87-15622
The use of remote sensing techniques in the study of vegetation recovery after fire in mediterranean countries (a preliminary study) p 14 N87-15623
Development of EOS-aided procedures for the determination of the water balance of hydrologic budget of a large watershed [NASA-CR-180118] p 60 N87-16383

The effect of measurement error and confusion from vegetation on passive microwave estimates of soil moisture p 18 N87-17304
Proceedings of the 1986 International Geoscience and Remote Sensing Symposium (IGARSS '86) on Remote Sensing: Today's Solutions for Tomorrow's Information Needs, volume 3 [ESA-SP-254-VOL-3] p 84 N87-18142
Off-nadir optical remote sensing from satellites for vegetation identification p 22 N87-18183
Multitemporal analysis of the phenological stage of vegetation using TM-data in the Southern Black Forest (West Germany) p 22 N87-18184
Vegetation and soils information contained in transformed Thematic Mapper data p 22 N87-18185

VEGETATION GROWTH
Satellite remote sensing of primary production p 6 A87-24777
Monitoring East African vegetation using AVHRR data p 6 A87-24781
Rainfall and vegetation monitoring in the Savanna Zone of the Democratic Republic of Sudan using the NOAA Advanced Very High Resolution Radiometer p 6 A87-24783
Monitoring vegetation in the Mali Sahel during summer 1984 p 6 A87-24784
Satellite remote sensing of rangelands in Botswana. I - Landsat MSS and herbaceous vegetation p 7 A87-24785
Growing period and drought early warning in Africa using satellite data p 7 A87-24788
Remote sensing of structurally complex semi-natural vegetation - An example from heathland p 10 A87-30896
Monitoring vegetation recovery patterns on Mount St. Helens using thermal infrared multispectral data p 14 N87-17122
Application of Thermal Infrared Multiband Scanner (TIMS) data to mapping of Plutonic and stratified rock and assemblages in accreted terrains of the Northern Sierra, California p 15 N87-17132

VEGETATIVE INDEX
Evaluation of the mid-infrared (1.45 to 2.0 microns) with a black-and-white infrared video camera p 73 A87-20672
Estimation of canopy parameters for inhomogeneous vegetation canopies from reflectance data. II - Estimation of leaf area index and percentage of ground cover for row canopies p 1 A87-20761
Diurnal-seasonal light interception, leaf area index, and vegetation index interrelations in a wheat canopy - A case study p 5 A87-23822
Maximum normalized difference vegetation index images for sub-Saharan Africa for 1983-1985 p 6 A87-24776
Analysis of the dynamics of African vegetation using the normalized difference vegetation index p 6 A87-24779
Monitoring vegetation in the Mali Sahel during summer 1984 p 6 A87-24784
Satellite remote sensing of rangelands in Botswana. II - NOAA AVHRR and herbaceous vegetation p 7 A87-24786
Monitoring the grasslands of the Sahel 1984-1985 p 7 A87-24787
Growing period and drought early warning in Africa using satellite data p 7 A87-24788
Airborne MSS data to estimate GLAI --- Green Leaf Area Index p 11 A87-30898
The use of aerial remote sensing in a case study of desertification: Quixaba-PE [INPE-3963-PRE/980] p 11 N87-15519
Satellite-derived vegetation index over Europe p 12 N87-15583
Vegetation index models for the assessment of vegetation in marginal areas p 12 N87-15584
Calibration of normalized vegetation index against pasture growth --- NOAA-7 data p 12 N87-15585
SIR-B measurements and modeling of vegetation p 15 N87-17160

VELOCITY MEASUREMENT
An objective method for computing advective surface velocities from sequential infrared satellite images p 39 A87-23717

VERY HIGH FREQUENCIES
Proposal of a remote sensing method for measuring soil moisture of bare soils in the frequency range 100 MHz-1 GHz p 8 A87-26974

VERY LARGE SCALE INTEGRATION
High speed image processing system based on the custom VLSI for Digital Signal Processing (DSP) --- SAR imagery p 71 N87-18179

VERY LONG BASE INTERFEROMETRY
The application of geodetic radio interferometric surveying to the monitoring of sea-level p 39 A87-21367

Mobile very long baseline interferometry and Global Positioning System measurement of vertical crustal motion p 26 A87-21931

VIDEO DATA
Assessment of grassland phytomass with airborne video imagery p 8 A87-25590

VIDEO EQUIPMENT
Evaluation of the mid-infrared (1.45 to 2.0 microns) with a black-and-white infrared video camera p 73 A87-20672

VIEW EFFECTS
Viewing angle corrections of airborne multispectral scanner data acquired over forested surfaces p 17 N87-17273

VISIBLE SPECTRUM
Detection of bottom-related surface patterns on visible spectrum imagery --- ocean bottom p 53 N87-18158

VISUAL OBSERVATION
A cognitive measure of texture in imagery p 64 A87-23800

VOLCANOES
Detection and mapping of volcanic rock assemblages and associated hydrothermal alteration with Thermal Infrared Multiband Scanner (TIMS) data Comstock Lode Mining District, Virginia City, Nevada p 31 N87-17119
Monitoring vegetation recovery patterns on Mount St. Helens using thermal infrared multispectral data p 14 N87-17122
Variability in the Earth radiation budget as determined from the Nimbus ERB experiments p 84 N87-17410
Thematic mapper studies of central Andean volcanoes [NASA-CR-180252] p 36 N87-18910

VOLCANOLOGY
Volcanology from space - Using Landsat thematic mapper data in the central Andes p 27 A87-20689
Preliminary analyses of SIB-B radar data for recent Hawaii lava flows p 29 A87-25588
Discrimination of altered basaltic rocks in the southwestern United States by analysis of Landsat Thematic Mapper data p 30 A87-30126
On the relationship between age of lava flows and radar backscattering p 35 N87-17348

VORTEX RINGS
Shedding of an Agulhas ring observed at sea p 44 A87-30146

VORTEX SHEDDING
Shedding of an Agulhas ring observed at sea p 44 A87-30146

VORTICES
Temperature-plant pigment-optical relations in a recurrent offshore mesoscale eddy near Point Conception, California [AD-A176666] p 39 A87-23720
Biological consequences of a recurrent eddy off Point Conception, California p 40 A87-23721
Island wakes and headland eddies - A comparison between remotely sensed data and laboratory experiments p 44 A87-30925

WADIS
Results of tectonic and spectral investigations along the Wadi Araba fault in Jordan using special processed Thematic Mapping (TM) data p 34 N87-17247

WAKES
Island wakes and headland eddies - A comparison between remotely sensed data and laboratory experiments p 44 A87-30925

WASHINGTON
Monitoring vegetation recovery patterns on Mount St. Helens using thermal infrared multispectral data p 14 N87-17122

WATER BALANCE
Development of EOS-aided procedures for the determination of the water balance of hydrologic budget of a large watershed [NASA-CR-180118] p 60 N87-16383

WATER COLOR
A description of large-scale variability in the ocean using the diffuse attenuation coefficient p 53 N87-18160

WATER DEPTH
An improved method for the determination of water depth from surface wave refraction patterns --- SAR imagery p 49 N87-17299

WATER EROSION
Assessment of wind and fluvial action by using LANDSAT-MSS color composites in the lower Nile Valley (Egypt) p 13 N87-15612

WATER MANAGEMENT
Towards snowmelt runoff forecast using LANDSAT-MSS and NOAA/AVHRR data p 61 N87-17317
A climatological-hydrological study of lake ice in the southwestern mountain area in Norway by use of satellite sensing p 61 N87-17319

W

The use of remote sensing (including aerial photographs) to devise cost-effective methods for soil conservation in the Kocaeli Peninsula, Turkey p 20 N87-18149
 Evaluation of remote sensing results for the benefit of water quality research on the North Sea [NZ-R-86.15] p 62 N87-19799

WATER QUALITY

Mapping of water quality in coastal waters using Airborne Thematic Mapper data p 58 A87-30899
 Evaluation of remote sensing results for the benefit of water quality research on the North Sea [NZ-R-86.15] p 62 N87-19799

WATER RESOURCES

Pre-assessment for large scale civil engineering projects by integrated analysis with the data numerical topography and remote sensing p 57 A87-23815
 An assessment of evapotranspirational water losses in a Sierran Mixed Conifer forest using remotely sensed data p 4 A87-23816
 Application of remote sensing in hydrology and water resources [INPE-3986-PRE/991] p 60 N87-16382

WATER TEMPERATURE

The utility of Thematic Mapper data for temperature mapping in the Great Lakes p 57 A87-23824
 The results of sea-surface temperature determinations from IR and microwave measurements aboard the Cosmos-1151 satellite p 40 A87-24376
 An extension of the split window technique for the retrieval of precipitable water [AD-A173008] p 60 N87-16386

WATER VAPOR

Mobile very long baseline interferometry and Global Positioning System measurement of vertical crustal motion p 26 A87-21931
 Verification of small-scale water vapor features in VAS imagery using high resolution MAMS imagery --- VISSR Atmospheric Sounder - Multispectral Atmospheric Mapping Sensor p 62 A87-23348
 An extension of the split window technique for the retrieval of precipitable water [AD-A173008] p 60 N87-16386
 Atmospheric water vapor corrections for altimetry measurements p 85 N87-18197

WATER WAVES

Optical and radar observations of the nonlinear interaction of gravity waves p 37 A87-20350
 Operational wave forecasting with spaceborne SAR: Prospects and pitfalls p 45 N87-17149
 C and Ku-band scatterometer results from the SCATMOD internal wave experiment p 47 N87-17215
 Estimation of internal wave currents from SAR and infrared scatterometer imagery p 48 N87-17295
 Observations of surface currents at Nantucket Shoals and implications for radar imaging of the bottom p 48 N87-17296
 Characteristics of a very low altitude spacecraft for collecting global directional wave spectra with spaceborne synthetic aperture radar p 49 N87-17333
 The SAR image modulation transfer function derived from SIR-B image spectra and airborne measurements of ocean wave height spectra p 49 N87-17334
 SIR-B observations of ocean waves in the NE Atlantic p 49 N87-17335
 Deriving two-dimensional ocean wave spectra and surface height maps from the Shuttle Imaging Radar (SIR-B) p 49 N87-17336
 Spatial evolution of wave spectra in the vicinity of the Agulhas current from SIR-B p 50 N87-17337
 Characterisation of internal wave surface patterns on airborne SAR imagery p 50 N87-17338
 Proceedings of an ESA Workshop on ERS-1 Wind and Wave Calibration [ESA-SP-262] p 84 N87-17363
 ERS-1 mission constraints related to wind and wave calibration p 84 N87-17364
 Gathering and processing a comparative data set for the calibration and validation of ERS-1 data products; preparatory work at the UK-ERS-DC --- Data Center (DC) p 50 N87-17367
 Requirements and constraints in the calibration and validation of ERS-1 wind and wave parameters p 51 N87-17369
 Comparison concept of satellite derived wind and wave data with ground truth p 51 N87-17373
 A procedure for estimation of two-dimensional ocean height-variance spectra from SAR imagery p 52 N87-17381
 Measurement of the directional spectrum of ocean waves using a conically-scanning radar p 52 N87-17383
 Wave modeling activities of the Wave Modeling (WAM) group relevant to ERS-1 p 52 N87-17389
 Marine climate program p 52 N87-17390
 A scatterometer research program p 53 N87-17391

Detection of bottom-related surface patterns on visible spectrum imagery --- ocean bottom p 53 N87-18158
 SEASAT microwave altimeter measurement of the ocean gravity wave equilibrium-range spectral behavior using full-wave theory p 53 N87-18165

WATERSHEDS

Development of EOS-aided procedures for the determination of the water balance of hydrologic budget of a large watershed [NASA-CR-180118] p 60 N87-16383

WAVELENGTHS

A statistical approach to select the optimal wavelength bands for separating rocks in the wavelength region 0.4 to 2.3 microns p 34 N87-17244

WEATHER

A case study of GWE satellite data impact on GLA assimilation analyses of two ocean cyclones p 41 A87-25787

WEATHER FORECASTING

Satellite contributions to convective scale weather analysis and forecasting p 76 A87-27882
 Rainfall estimation over the Sahel using Meteosat thermal infra-red data p 59 N87-15587
 Utilization of satellite data in mesoscale modeling of severe weather [NASA-CR-179917] p 78 N87-15669

WETLANDS

Remote sensing of wetland plant stress p 21 N87-18171

WHEAT

Diurnal-seasonal light interception, leaf area index, and vegetation index interrelations in a wheat canopy - A case study p 5 A87-23822
 Microcomputer-assisted video image analysis of lodging in winter wheat p 10 A87-30130
 Analysis of the spatial structure of Synthetic Aperture Radar (SAR) imagery for a better separability of cereal crops, wheat and barley p 17 N87-17287

WIND (METEOROLOGY)

A new semi-empirical sea spectrum for estimating the scattering coefficient p 38 A87-20769
 Ocean surface pressure fields from satellite-sensed winds p 41 A87-25797

WIND DIRECTION

Tower-based broadband backscattering measurements from the ocean surface in the North Sea p 47 N87-17217
 Application of the Seasat scatterometer to observations of wind speed and direction and Arctic ice/water boundaries p 48 N87-17259

WIND EFFECTS

Interpretation characteristics of space photographs of sea coasts with wind-induced surges p 43 A87-28509

WIND EROSION

Assessment of wind and fluvial action by using LANDSAT-MSS color composites in the lower Nile Valley (Egypt) p 13 N87-15612

WIND MEASUREMENT

NROSS (Navy Remote Ocean Sensing System) tracking network analysis [AD-A172132] p 45 N87-16384
 Application of the Seasat scatterometer to observations of wind speed and direction and Arctic ice/water boundaries p 48 N87-17259
 Proceedings of an ESA Workshop on ERS-1 Wind and Wave Calibration [ESA-SP-262] p 84 N87-17363
 ERS-1 mission constraints related to wind and wave calibration p 84 N87-17364
 Gathering and processing a comparative data set for the calibration and validation of ERS-1 data products; preparatory work at the UK-ERS-DC --- Data Center (DC) p 50 N87-17367
 Requirements and constraints in the calibration and validation of ERS-1 wind and wave parameters p 51 N87-17369
 Satellite scatterometer comparisons with surface measurements: Techniques and Seasat results p 51 N87-17372
 Comparison concept of satellite derived wind and wave data with ground truth p 51 N87-17373
 Validation of ERS-1 wind data using observations from research and voluntary observing ships p 51 N87-17374
 The accuracy and availability of operational marine surface wind data for ERS-1 sensor calibration and validation from fixed platforms and free drifting buoys p 51 N87-17376
 An overview of the NSCAT/N-ROSS program p 52 N87-17384

WIND VELOCITY
 Wind-wave relationship from Seasat radar altimeter data p 41 A87-24748

Application of the Seasat scatterometer to observations of wind speed and direction and Arctic ice/water boundaries p 48 N87-17259

WIND VELOCITY MEASUREMENT

Further development of an improved altimeter wind speed algorithm p 42 A87-27848
 Retrieval of near-surface wind speed in the Baltic Sea from NIMBUS-7 Scanning Multichannel Microwave Radiometer (SMMR) observations p 50 N87-17342
 Intersensor comparisons for validation of wind speed measurements from ERS-1 altimeter and scatterometer --- Seasat p 52 N87-17386
 Retrieval and global comparison of oceanic winds from SEASAT radiometer, scatterometer and altimeter p 85 N87-18219

WINTER

Possibilities of using satellite data for computations of the ocean/atmosphere heat exchange in the Newfoundland energy-active ocean zone in winter p 41 A87-24379

WORLD DATA CENTERS

The design of an international data centre for remote sensing p 67 N87-17176

WORLD METEOROLOGICAL ORGANIZATION

An overview of the implementation of the World Climate Research program p 26 N87-17388
 Report of the Fourth Session of the JSC/CCCO Tropical Ocean Global Atmosphere (TOGA) Scientific Steering Group [WCP-120] p 54 N87-18283

WYOMING
 Application of TIMS data in stratigraphic analysis p 31 N87-17121

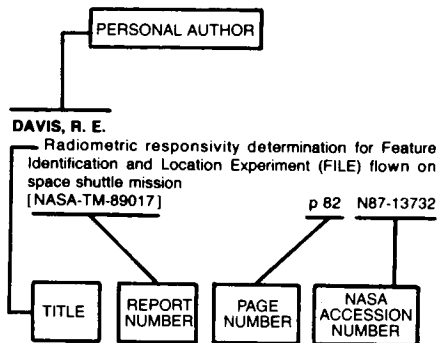
X**X RAY DIFFRACTION**

Nature and origin of mineral coatings on volcanic rocks of the Black Mountain, Stonewall Mountain, and Kane Springs, Wash volcanic centers, Southern Nevada [NASA-CR-180183] p 36 N87-18255

Y**YAGI ANTENNAS**

The FRS-68010: A new concept for the acquisition and analysis of NOAA HRPT data p 68 N87-17206

Typical Personal Author Index Listing



Listings in this index are arranged alphabetically by personal author. The title of the document provides the user with a brief description of the subject matter. The report number helps to indicate the type of document listed (e.g., NASA report, translation, NASA contractor report). The page and accession numbers are located beneath and to the right of the title. Under any one author's name the accession numbers are arranged in sequence with the AIAA accession numbers appearing first.

A

- ABBOTT, ELSA**
The TIMS Data User's Workshop
[NASA-CR-180130] p 78 N87-17111
A geologic atlas of TIMS data p 32 N87-17133
- ABDELLAOUI, A.**
The fundamental problems for the energy balance study by satellite imagery p 66 N87-15590
- ABEDNEGO, B.**
Description of a methodology for biomass change mapping with the use of LANDSAT TM data p 22 N87-18186
- ABEL, N. O. J.**
Estimating and mapping grass cover and biomass from low-level photographic sampling p 9 A87-29005
- ABRAMS, M. J.**
Imaging spectrometry: Aircraft and space program p 81 N87-17202
- ABRAMS, MICHAEL**
Kinematics at the intersection of the Garlock and Death Valley fault zones, California: Integration of TM data and field studies
[NASA-CR-180182] p 36 N87-18256
- ADAMS, L.**
The SEU risk assessment of Z80A, 8086 and 80C86 microprocessors intended for use in a low altitude polar orbit p 74 A87-22025
- ADAMS, S. L.**
Analysis of AIS radiometry at Mono Lake, California p 81 N87-17204
- ADAMS, STEVEN**
Landsat Thematic Mapper digital information content for agricultural environments p 5 A87-23830
- ADEFOLALU, D. O.**
Regional studies with satellite data in Africa on the desertification of the Sudan-Sahel belt in Nigeria p 13 N87-15605
- AHERN, F. J.**
An initial evaluation of two digital airborne imagers for surveying spruce budworm defoliation p 1 A87-20671
- ALLEY, R. E.**
Analysis of AIS radiometry at Mono Lake, California p 81 N87-17204
- ALMAZOV, I. V.**
Investigation of spectral correlations of vegetation growing on different types of geological structures p 29 A87-28508
- ALMEIDA, R.**
Digital satellite imagery acquisition and processing p 68 N87-17207
- ALPERS, W.**
On the discrimination between crude oil spills and monomolecular sea slicks by airborne remote sensors: Today's possibilities and limitations p 53 N87-18167
- AMBROSIA, V. G.**
Aircraft and satellite thermographic systems for wildfire mapping and assessment
[AIAA PAPER 87-0187] p 7 A87-24933
- ANDERSON, DONALD L.**
Thermal imaging spectroscopy in the Kelso-Baker Region, California p 30 N87-17117
- ANDERSON, J. M.**
The quantitative use of airborne Thematic Mapper thermal infrared data p 44 A87-30900
- ANDERSON, JAMES E.**
Estimation of absolute water surface temperature based on atmospherically corrected thermal infrared multispectral scanner digital data p 79 N87-17114
- ANDREEV, G. G.**
Automation of thematic processing of space images in evaluating crop condition p 8 A87-26539
- ANTHONY, D. A.**
Forest cover analysis using SIR-B data p 23 N87-18220
- ANUTA, P.**
Parameter space techniques for image registration p 70 N87-17327
- APEL, J. R.**
Hydrodynamics of internal solitons and a comparison of SIR-A and SIR-B data with ocean measurements p 45 N87-17147
- ARAI, KOHEI**
Development, status, prospects of marine observation satellite p 45 N87-15989
- ARANOFF, S.**
Integration of surficial geochemistry and LANDSAT imagery to discover skarn tungsten deposits using image analysis techniques
[CONTRIB-19586] p 35 N87-17248
- ARCHER, PAUL**
Spot data distribution p 62 A87-20683
- ARDANUY, PHILIP EDWARD**
Variability in the Earth radiation budget as determined from the Nimbus ERB experiments p 84 N87-17410
- ARKIN, PHILLIP A.**
Annual and interannual variability in large-scale convection over the eastern Pacific and tropical South America p 57 A87-23414
- ARTAMONOV, M. A.**
Analysis of correlations between structural elements detected on space images and metallogenic zones p 28 A87-24380
- ARVESEN, J. C.**
Aircraft and satellite thermographic systems for wildfire mapping and assessment
[AIAA PAPER 87-0187] p 7 A87-24933
- ARWYN, R. JONES**
Monitoring sediment transfer processes on the desert margin
[NASA-CR-180181] p 23 N87-18222
- ASEM, A.**
Design of a data base system for inferring land surface parameters and fluxes from satellite radiances p 66 N87-15625
- ASFAR, L.**
Design of a data base system for inferring land surface parameters and fluxes from satellite radiances p 66 N87-15625
- ASKNE, J.**
Atmospheric water vapor corrections for altimetry measurements p 85 N87-18197
- ASRAR, G.**
Assessing grass canopy condition and growth from combined optical-microwave measurements p 17 N87-17286

- ASTLE, W. L.**
Rainfall and vegetation monitoring in the Savanna Zone of the Democratic Republic of Sudan using the NOAA Advanced Very High Resolution Radiometer p 6 A87-24783
Satellite remote sensing of rangelands in Botswana. I - Landsat MSS and herbaceous vegetation p 7 A87-24785
- ATAMAN, E.**
LANDSAT-5 Thematic Mapping (TM) data applications to land use classification on around the Bosphorus area, Turkey p 19 N87-17351
- ATKINSON, LARRY P.**
Mesoscale hydrographic variability in the vicinity of Points Conception and Arguello during April-May 1983 - The OPUS 1983 experiment p 39 A87-23719
- ATLAS, DAVID**
Simultaneous ocean cross section and rainfall measurements from space with a nadir-looking radar p 38 A87-20956
- AXELSSON, SUNE**
Experimental results in soil moisture mapping using IR thermography p 2 A87-21246
- AZUMA, Y.**
Some results of Marine Observation Satellite (MOS-1) airborne verification experiment Multispectral Electronic Self Scanning Radiometer (MESSR) p 46 N87-17166
Outline of SAR-850 data processing method in Japan p 71 N87-18176

B

- BACCI, L.**
An integrated data bank for agricultural productivity by remote sensing p 21 N87-18153
- BAHAR, E.**
SEASAT microwave altimeter measurement of the ocean gravity wave equilibrium-range spectral behavior using full-wave theory p 53 N87-18165
- BAKLIWAL, P. C.**
Comparative study of LANDSAT MSS, Salyut-7 (TERRA) and radar (SIR-A) images for geological and geomorphological applications: A case study from Rajasthan and Gujarat, India p 34 N87-17236
- BANGERT, JOHN A.**
Preliminary evaluation of Doppler-determined pole positions computed using world geodetic system 1984 [AD-A173467] p 27 N87-18225
- BANKS, BARBARA A.**
The effect of Hurricane Gloria on sea surface temperature patterns p 39 A87-23362
- BANNINGER, C.**
Influence of canopy shadow on stress detection in coniferous forests using LANDSAT data p 21 N87-18173
Relationship between tree density, leaf area index, soil metal content, and LANDSAT MSS canopy radiance values p 21 N87-18174
- BARALE, VITTORIO**
Space and time variability of the surface color field in the northern Adriatic Sea p 40 A87-23722
- BARRICK, D. E.**
SEASAT microwave altimeter measurement of the ocean gravity wave equilibrium-range spectral behavior using full-wave theory p 53 N87-18165
- BARTHOLOMEW, MARY JANE**
Infrared spectroscopy for geologic interpretation of TIMS data p 31 N87-17130
- BARTON, G.**
Satellite remote sensing of the marine environment: Literature and data sources
[PB86-245446] p 56 N87-18971
- BARTON, IAN J.**
Australian validation plans for ERS-1 p 84 N87-17387
- BARTSCH, N.**
Contributions to oil spill detection and analysis with radar and microwave radiometry, results of the Archimedes 2 campaign p 54 N87-18170

- BASHMAKOV, V. A.**
Quantitative processing procedures and the information content of space imagery in predictions of structural inhomogeneities of the sedimentary cover p 29 A87-26534
- BAUMGARTNER, M. F.**
Towards snowmelt runoff forecast using LANDSAT-MSS and NOAA/AVHRR data p 61 N87-17317
- BEAL, R. C.**
Operational wave forecasting with spaceborne SAR: Prospects and pitfalls p 45 N87-17149
Characteristics of a very low altitude spacecraft for collecting global directional wave spectra with spaceborne synthetic aperture radar p 49 N87-17333
- BECK, L.**
Remote sensing of wetland plant stress p 21 N87-18171
- BECKER, F.**
Design of a data base system for inferring land surface parameters and fluxes from satellite radiances p 66 N87-15625
Future European plans in the framework of the International Satellite Land Surface Climatology Project (ISLSCP) p 78 N87-15628
- BELOBORODOV, M. A.**
The principles and procedures of modeling ore-related objects in predictive metallogenic investigations (using satellite-borne data) p 29 A87-26533
- BELWARD, A. S.**
The influence of resampling method and multitemporal LANDSAT imagery on crop classification accuracy in the United Kingdom p 16 N87-17250
- BENELLI, G.**
Multispectral classification of microwave remote sensing images p 16 N87-17238
- BENNETT, J. R.**
An improved method for the determination of water depth from surface wave refraction patterns p 49 N87-17299
- BENNETT, JACK**
The Red River Valley archeological project p 31 N87-17128
- BENNETT, W. J.**
An initial evaluation of two digital airborne imagers for surveying spruce budworm defoliation p 1 A87-20671
- BERGEN, WILLIAM R.**
Performance of selected spatial domain edge detection algorithms for earth resources application p 64 A87-23798
- BERLIN, GRAYDON L.**
Discrimination of altered basaltic rocks in the southwestern United States by analysis of Landsat Thematic Mapper data p 30 A87-30126
- BERNARD, R.**
The Along Track Scanning Radiometer (ATSR) for ERS1 p 73 A87-19660
Toward a satellite system to monitor the spatial and temporal behavior of soil water content p 18 N87-17288
- BERNSTEIN, RALPH**
Remote sensing from space - An overview p 87 A87-30881
- BERNSTEIN, ROBERT L.**
Ocean remote sensing p 44 A87-30883
Equatorial long-wave characteristics determined from satellite sea surface temperature and in situ data p 44 A87-30923
- BHAVSAR, P. D.**
Indian remote sensing program p 77 N87-15242
- BICHSEL, M.**
Sri Lanka's solution to land use mapping and monitoring for Third World countries development p 67 N87-17174
- BIEGEL, JOSEPH D.**
Radiometric analysis of the longwave infrared channel of the Thematic Mapper on LANDSAT 4 and 5 [NASA-CR-180180] p 86 N87-18221
- BINNENKADE, P.**
The processing of and information extraction from airborne SLAR data [NLR-MP-86004-U] p 23 N87-18919
- BIRKS, ANDREW ROBERT**
Measurement of the directional spectrum of ocean waves using a conically-scanning radar p 52 N87-17383
- BIRNIE, R. W.**
Discrimination of lithologic units using geobotanical and LANDSAT TM spectral data p 34 N87-17246
- BISHOP, M. P.**
IRSAP: An improved approach in processing remotely sensed data p 70 N87-17332
- BISHOP, WILLIAM P.**
Partnerships in remote sensing - A theme with some examples p 86 A87-25531
- BLAETTLER, D. K.**
Merging spaceborne image data of optical and microwave sensors p 69 N87-17267
- BLAIR, ROBERT W., JR.**
Geomorphology from space: A global overview of regional landforms [NASA-SP-486] p 36 N87-18139
- BLAKE, P.**
The quantitative use of airborne Thematic Mapper thermal infrared data p 44 A87-30900
- BLAKLEY, EARL**
Detection of new urban build-up in Ardmore and McAlester, Oklahoma using Landsat MSS data p 25 A87-23829
- BLANCHARD, A. J.**
The effect of measurement error and confusion from vegetation on passive microwave estimates of soil moisture p 18 N87-17304
- BLAZQUEZ, C. H.**
Evaluation of the mid-infrared (1.45 to 2.0 microns) with a black-and-white infrared video camera p 73 A87-20672
- BLEIER, MARY**
The data dilemma - How to properly construct and utilize aerial photo volume tables p 63 A87-23790
- BLOM, R. G.**
On the relationship between age of lava flows and radar backscattering p 35 N87-17348
- BLOOM, ARTHUR L.**
Tectonic geomorphology of the Andes with SIR-A and SIR-B p 32 N87-17136
- BLUEMEL, KLAUS**
Satellite-derived vegetation index over Europe p 12 N87-15583
- BOBERG, GORAN**
Distribution and biomass of *Fucus vesiculosus* L. near a cooling-water effluent from a nuclear power plant in the Baltic Sea estimated by aerial photography p 43 A87-29014
- BOCHAROV, V. P.**
Automation of thematic processing of space images in evaluating crop condition p 8 A87-26539
- BOGATYREV, V. E.**
Use of space imagery and geophysical data in metallogenic prediction studies in central Kyzylkum p 28 A87-24383
- BOLLE, H.-J.**
Vegetation identification and variability in the Tahoua area, Nigeria p 13 N87-15610
- BONHAM-CARTER, G. F.**
Integration of surficial geochemistry and LANDSAT imagery to discover skarn tungsten deposits using image analysis techniques [CONTRIB-19586] p 35 N87-17248
- BORAN, DEBORAH A.**
Ozone in the boundary layer of the equatorial Pacific Ocean p 41 A87-25534
- BORENGASSER, MARCUS**
Detection and mapping of volcanic rock assemblages and associated hydrothermal alteration with Thermal Infrared Multiband Scanner (TIMS) data Comstock Lode Mining District, Virginia City, Nevada p 31 N87-17119
Application of Thermal Infrared Multiband Scanner (TIMS) data to mapping of Plutonic and stratified rock and assemblages in accreted terrains of the Northern Sierra, California p 15 N87-17132
- BORN, G. H.**
Accurate measurement of mean sea level changes by altimetric satellites p 38 A87-20524
- BRACEWELL, R. N.**
Automated remote sensing of sea ice using synthetic aperture radar p 46 N87-17186
- BRACHET, GERARD**
SPOT IMAGE and commercialisation of remote sensing data p 65 A87-29430
- BRADY, ROLAND**
Kinematics at the intersection of the Garlock and Death Valley fault zones, California: Integration of TM data and field studies [NASA-CR-180182] p 36 N87-18256
- BRAILE, LAWRENCE W.**
Improving the geological interpretation of magnetic and gravity satellite anomalies [NASA-CR-180149] p 35 N87-17418
- BRANDANI, ALDO**
Multiple incidence angle SIR-B experiment over Argentina p 80 N87-17157
- BRASS, J. A.**
Aircraft and satellite thermographic systems for wildfire mapping and assessment [AIAA PAPER 87-0187] p 7 A87-24933
- BRAUN, H. M.**
Future user requirements and required technological developments of spaceborne synthetic aperture radars p 82 N87-17320
- BREED, CAROL S.**
The megageomorphology of the radar rivers of the eastern Sahara p 32 N87-17139
- BREZHNIANSKII, K.**
Lineaments of eastern Cuba - Geological interpretation of aerial and space imagery p 28 A87-24384
- BRINK, KENNETH H.**
Mesoscale hydrographic variability in the vicinity of Points Conception and Arguello during April-May 1983 - The OPUS 1983 experiment p 39 A87-23719
- BROWN, R.**
Canadian plans for operational demonstrations of satellite imaging radar applications p 68 N87-17229
- BROWN, R. J.**
An overview of remote sensing agricultural applications in North America: Past, present and future p 17 N87-17284
- BROWN, ROBERT A.**
Ocean surface pressure fields from satellite-sensed winds p 41 A87-25797
- BRYANT, NEVIN**
Landsat Thematic Mapper digital information content for agricultural environments p 5 A87-23830
- BULATOV, IU. V.**
Exact determination of wave parameters from the results of Fourier analysis of sea-surface radar imagery p 41 A87-24377
- BURLESHIN, M. I.**
Methods of geological interpretation of lineaments of platform areas (with reference to Ustiurt) p 29 A87-26532
- BURNS, B. A.**
Active/passive microwave sensor comparison of MIZ-ice concentration estimates p 46 N87-17185
Geophysics of the marginal ice zone from SAR p 47 N87-17219
SAR ice floe kinematics and correlation with mesoscale oceanic structure within the marginal ice zone p 48 N87-17222
Analysis of multichannel SAR data of Spitsbergen p 60 N87-17223
- BUSACCA, ALAN**
Spectral characteristics and the extent of paleosols of the Palouse formation [NASA-CR-180357] p 24 N87-19826
- BUTLER, DAVID R.**
Impact of environmental variables on spectral signatures acquired by the Landsat Thematic Mapper p 9 A87-29003

C

- CAHALAN, ROBERT F.**
Large-scale short-period sea ice atmosphere interaction p 42 A87-27546
- CALHES, G.**
Exploitation of the SPOT system p 62 A87-21095
- CALLAHAN, PHILLIP S.**
An overview of the NSCAT/N-ROSS program p 52 N87-17384
- CALLISON, R. D.**
The quantitative use of airborne Thematic Mapper thermal infrared data p 44 A87-30900
- CALOZ, R.**
Description of a methodology for biomass change mapping with the use of LANDSAT TM data p 22 N87-18186
- CAMPBELL, JAMES B.**
The effect of training data variability on classification accuracy p 64 A87-23796
- CAPPELLINI, V.**
An integrated system to assess agricultural productivity p 14 N87-15621
- CAPPELLINI, V.**
Multispectral classification of microwave remote sensing images p 16 N87-17238
An integrated data bank for agricultural productivity by remote sensing p 21 N87-18153
- CARLA, R.**
An integrated system to assess agricultural productivity p 14 N87-15621
An integrated data bank for agricultural productivity by remote sensing p 21 N87-18153
- CARLOTTO, M. J.**
Extracting surface features in multispectral imagery p 68 N87-17211
- CARLSON, TOBY N.**
Soil moisture estimates from satellite infrared temperatures and their relation to surface measurements p 3 A87-23389
- CAROPPO, C.**
UMUS: A project for usage of LANDSAT MSS and ancillary data in land cover mapping of large areas in southern Italy p 72 N87-18191

- CARPENTER, D. J.**
The Coastal Zone Color Scanner views the Bismarck Sea p 42 A87-26970
- CARR, FREDERICK H.**
Observations and analysis of a polar low over the Great Lakes region p 76 A87-27872
- CARROLL, DOUGLAS M.**
Radar images for soil survey in England and Wales p 3 A87-21251
- CARTER, W. E.**
The application of geodetic radio interferometric surveying to the monitoring of sea-level p 39 A87-21367
- CARUTHERS, C. G.**
Geophysics of the marginal ice zone from SAR p 47 N87-17219
- CASEY, DAREN**
Multiple incidence angle SIR-B experiment over Argentina p 80 N87-17157
- CATTS, G. P.**
Modelling of estuarine chlorophyll-A from an airborne scanner p 61 N87-18172
- CAVALIERI, D. J.**
Active/passive microwave sensor comparison of MIZ-ice concentration estimates p 46 N87-17185
- CAVANIE, ALAIN**
Evaluation of the different parameters in Long's C-band model p 51 N87-17370
- CEBULA, R. P.**
Instrument characterization for the detection of long-term changes in stratospheric ozone - An analysis of the SBUV/2 radiometer p 74 A87-20961
- CHABAN, L. N.**
Automation of thematic processing of space images in evaluating crop condition p 8 A87-26539
- CHADWICK, O. A.**
An iterative Landsat-MSS classification methodology for soil survey p 3 A87-23797
- CHAHINE, M. T.**
Remote sensing of land-surface temperature from HIRS/MSU data p 77 N87-15573
- CHAMPION, RICHARD**
The production of orthophotographs by digital image processing techniques p 63 A87-23787
- CHANDICA, A. L.**
Classification of reflectance on colour infrared aerial photographs and sub-tropical salt-marsh vegetation types p 10 A87-29012
- CHANDRASEKHARAM, D.**
Significance of space image, air photo and drainage linears in relation to west coast tectonics, India p 33 N87-17232
- CHARI, S. T.**
AVHRR and MSS data based vegetation indices studies over Indian sites p 14 N87-15622
- CHASE, JUANITA R.**
The impact of satellite infrared sea surface temperatures on FNOOC (Fleet Numerical Oceanography Center) ocean thermal analyses [AD-A173333] p 54 N87-18295
- CHAUDRY, A. H.**
Tower-based broadband backscattering measurements from the ocean surface in the North Sea p 47 N87-17217
- CHAVEZ, PAT S., JR.**
Discrimination of altered basaltic rocks in the southwestern United States by analysis of Landsat Thematic Mapper data p 30 A87-30126
- CHELTON, DUDLEY B.**
Further development of an improved altimeter wind speed algorithm p 42 A87-27848
- CHEN, SHUPENG**
Atlas of geo-science analyses of Landsat imagery in China p 65 A87-24542
- CHENG, YAAN**
Spectral characteristics and the extent of paleosols of the Palouse formation [NASA-CR-180357] p 24 N87-19826
- CHHONKAR, R. P. S.**
AVHRR and MSS data based vegetation indices studies over Indian sites p 14 N87-15622
- CHIARANTINI, L.**
Contribution of passive microwave remote sensing in soil moisture and evapotranspiration measurements p 12 N87-15589
- CHIU, LONG S.**
Satellite rainfall retrieval by logistic regression p 56 A87-23370
Large-scale short-period sea ice atmosphere interaction p 42 A87-27546
- CHOI, B. H.**
Study of ocean bottom coupling process using satellite altimeter data p 54 N87-18199
- CHOY, L. W.**
Comparison of ocean tide models with satellite altimeter data [AD-A174698] p 56 N87-19879
- CHRISTENSEN, PHILIP R.**
Thermal imaging spectroscopy in the Kelso-Baker Region, California p 30 N87-17117
- CIBULA, WILLIAM G.**
Use of topographic and climatological models in a geographical data base to improve Landsat MSS classification for Olympic National Park p 25 A87-30128
- CICONE, R. C.**
Vegetation and soils information contained in transformed Thematic Mapper data p 22 N87-18185
- CIMINO, J.**
Space Shuttle radargrammetry results p 65 A87-23827
- CIMINO, JOBEA**
Multiple incidence angle SIR-B experiment over Argentina p 80 N87-17157
- CIVCO, D. L.**
Identification of forest and agricultural edges using Landsat Thematic Mapper data - Preliminary results p 5 A87-23832
- CLANCY, R. M.**
The impact of satellite infrared sea surface temperatures on FNOOC (Fleet Numerical Oceanography Center) ocean thermal analyses [AD-A173333] p 54 N87-18295
- CLERKE, WILLIAM H.**
Locating subsurface gravel with thermal imagery p 31 N87-17125
- CLOERN, J. E.**
Modelling of estuarine chlorophyll-A from an airborne scanner p 61 N87-18172
- COFFIN, MILLARD F.**
Structure of the Kerguelen Plateau province from Seasat altimetry and seismic reflection data p 28 A87-24866
- COLLET, C.**
Description of a methodology for biomass change mapping with the use of LANDSAT TM data p 22 N87-18186
- COLLINS, M. B.**
Mapping of water quality in coastal waters using Airborne Thematic Mapper data p 58 A87-30899
- COLLINS, M. J.**
Comparison between satellite image advective velocities, dynamic topography, and surface drifter trajectories p 38 A87-20692
An objective method for computing advective surface velocities from sequential infrared satellite images p 39 A87-23717
Automated extraction of pack ice motion from advanced very high resolution radiometer imagery p 42 A87-27547
- COLLINS, MICHAEL**
Island wakes and headland eddies - A comparison between remotely sensed data and laboratory experiments p 44 A87-30925
- COLLINS, W. G.**
Discrimination of land features using LANDSAT false colour composite in N Iran p 19 N87-17352
- COLWELL, ROBERT N.**
Land applications for remote sensing from space p 25 A87-30882
- CONDE, JUAN JOSE**
Marine climate program p 52 N87-17390
- CONEL, J. E.**
Analysis of AIS radiometry at Mono Lake, California p 81 N87-17204
- CONESE, C.**
An integrated system to assess agricultural productivity p 14 N87-15621
An integrated data bank for agricultural productivity by remote sensing p 21 N87-18153
- CONGALTON, RUSSELL G.**
An assessment of evapotranspirational water losses in a Sierran Mixed Conifer forest using remotely sensed data p 4 A87-23816
Development of EOS-aided procedures for the determination of the water balance of hydrologic budget of a large watershed [NASA-CR-180118] p 60 N87-16383
- COOK, ELIZABETH A.**
Interpreting forest and grassland biome productivity utilizing nested scales of image resolution and biogeographical analysis [NASA-CR-180213] p 23 N87-18912
- COOLEY, P.**
On the relationship between age of lava flows and radar backscattering p 35 N87-17348
- CORDEY, R. A.**
SIR-B observations of ocean waves in the NE Atlantic p 49 N87-17335
- COURTOIS, M.**
The SPOT satellites - From SPOT 1 to SPOT 4 p 74 A87-21094
- COVRE, MARCOS**
CANASATE: Sugar cane mapping by satellite, area 3 [INPE-4068-RPE/526] p 24 N87-19790
- CRAWFORD, D. R.**
SAR imaging of bottom topography in the ocean: Results from an improved model p 48 N87-17298
- CRAWFORD, W. R.**
Comparison between satellite image advective velocities, dynamic topography, and surface drifter trajectories p 38 A87-20692
An objective method for computing advective surface velocities from sequential infrared satellite images p 39 A87-23717
- CRIST, E. P.**
Vegetation and soils information contained in transformed Thematic Mapper data p 22 N87-18185
- CROMBIE, MICHAEL A.**
Sparse area stereo matching experiment [AD-A173601] p 66 N87-16388
- CSILLAG, FERENC**
Comparison of some classification methods on a test site (Kiskore, Hungary) - Separability as a measure of accuracy p 9 A87-29006
- CUMMING, I. G.**
Resolving the Doppler ambiguity for spaceborne synthetic aperture radar p 72 N87-18212
- CUNNINGHAM, JAMES P.**
Preliminary evaluation of Doppler-determined pole positions computed using world geodetic system 1984 [AD-A173467] p 27 N87-18225
- CURRAN, P. J.**
Airborne MSS data to estimate GLAI p 11 A87-30898
- CUSHNIE, JANIS L.**
The interactive effect of spatial resolution and degree of internal variability within land-cover types on classification accuracies p 77 A87-30895

D

- DACOSTAFREITASYANASSE, CORINA**
Agricultural crop estimates using information gathered by remote sensing satellites, as well as ground data, through samples of geographic layers [INPE-4102-RPE/534] p 24 N87-19786
- DAELS, L.**
Assessment of wind and fluvial action by using LANDSAT-MSS color composites in the lower Nile Valley (Egypt) p 13 N87-15612
Assessment of soil degradation in an arid region using remote sensing p 20 N87-18148
- DAIDA, J. M.**
Automated remote sensing of sea ice using synthetic aperture radar p 46 N87-17186
- DALE, P. E. R.**
Classification of reflectance on colour infrared aerial photographs and sub-tropical salt-marsh vegetation types p 10 A87-29012
- DALY, E. J.**
The SEU risk assessment of Z80A, 8086 and 80C86 microprocessors intended for use in a low altitude polar orbit p 74 A87-22025
- DAMS, R. V.**
SAR imagery for forest management p 18 N87-17313
- DANCY, K. J.**
Estimating and mapping grass cover and biomass from low-level photographic sampling p 9 A87-29005
- DASARATHY, BELUR V.**
An information processing system for integration of data from remote sensors, aerial photographs and existing maps p 63 A87-23791
- DASILVAFAGUNDESFILHO, EDGAR**
Remote sensing applied to basic geological surveys: A methodological approach for the northeast region [INPE-4041-TDL/246] p 37 N87-19788
- DAVIDSON, JOHN M.**
Mobile very long baseline interferometry and Global Positioning System measurement of vertical crustal motion p 26 A87-21931
- DAVIES, A. F.**
Application of the Seasat scatterometer to observations of wind speed and direction and Arctic ice/water boundaries p 48 N87-17259
- DAVIES, HUGH L.**
Structure of the Kerguelen Plateau province from Seasat altimetry and seismic reflection data p 28 A87-24866
- DAVIS, A. W.**
Calibration of Landsat data for sparsely vegetated semi-arid rangelands p 9 A87-29008

- DAVIS, BRUCE A.**
Remote sensing of aquatic macrophyte distribution in upper Lake Marion p 57 A87-23826
- DAVIS, DAVID**
Application of Thermal Infrared Multiband Scanner (TIMS) data to mapping of Plutonic and stratified rock and assemblages in accreted terrains of the Northern Sierra, California p 15 N87-17132
- DAVIS, PHILIP A.**
Discrimination of altered basaltic rocks in the southwestern United States by analysis of Landsat Thematic Mapper data p 30 A87-30126
- DAVIS, RUSS E.**
Mesoscale hydrographic variability in the vicinity of Points Conception and Arguello during April-May 1983 - The OPUS 1983 experiment p 39 A87-23719
- DE JAVEL, Y.**
The Along Track Scanning Radiometer (ATSR) for ERS1 p 73 A87-19660
- DEAN, K.**
Influence of the Yukon River on the Bering Sea [NASA-CR-180065] p 54 N87-18293
Influence of the Yukon River on the Bering Sea [NASA-CR-180356] p 56 N87-19877
- DEANDRADE, LUIS ANTONIO**
Methodology for the elaboration of thematic maps utilizing LANDSAT-TM data [INPE-3893-TDL/225] p 72 N87-19792
- DEBLONDE, G.**
Remote sensing of hydrological variables from the DMSP microwave mission sensors p 57 A87-23374
- DECARVALHO, VITOR CELSO**
The use of aerial remote sensing in a case study of desertification: Quixaba-PE [INPE-3963-PRE/980] p 11 N87-15519
- DEFARIA, KLEBER**
CANASATE: Sugar cane mapping by satellite, area 3 [INPE-4068-RPE/526] p 24 N87-19790
- DEFEQO, N. J.**
Discrimination of lithologic units using geobotanical and LANDSAT TM spectral data p 34 N87-17246
- DEFRAIPONT, P.**
Design of a data base system for inferring land surface parameters and fluxes from satellite radiances p 66 N87-15625
- DEGNER, JANET D.**
Landsat Thematic Mapper data analysis within the Suwannee River Basin p 57 A87-23825
- DELDERFIELD, J.**
The Along Track Scanning Radiometer (ATSR) for ERS1 p 73 A87-19660
- DELRE, E.**
Multispectral classification of microwave remote sensing images p 16 N87-17238
- DEMURGER, JOELLE**
Evaluation of the different parameters in Long's C-band model p 51 N87-17370
- DENYER, N.**
Canadian plans for operational demonstrations of satellite imaging radar applications p 68 N87-17229
- DERENYI, EUGENE**
Control extension utilizing Large Format Camera imagery p 75 A87-23804
- DERRYBERRY, B. A.**
Preliminary analyses of SIR-B radar data for recent Hawaii lava flows p 29 A87-25588
Hawaiian lava flows and SIR-B results p 69 N87-17245
- DESAI, PRANAV S.**
Equatorial Indian Ocean evaporation estimates from operational meteorological satellites and some inferences in the context of monsoon onset and activity p 39 A87-22041
- DESCHAMPS, P. Y.**
Design of a data base system for inferring land surface parameters and fluxes from satellite radiances p 66 N87-15625
- DESHAYES, JEAN-PIERRE**
In flight calibration of push broom remote sensing instruments p 73 A87-19652
- DEV, S.**
Remote sensing applications in the study of land use and soils of aeolian cover of the western part of Haryana State, India p 22 N87-18187
- DIAMANTE, J.**
The application of geodetic radio interferometric surveying to the monitoring of sea-level p 39 A87-21367
- DIAMANTOPOULOS, J.**
The use of remote sensing techniques in the study of vegetation recovery after fire in mediterranean countries (a preliminary study) p 14 N87-15623
- DIETZ, K. R.**
Analysis of Large Format Camera images from the Black Hills, USA, for topographic and thematic mapping p 71 N87-18189
- DIGENNARO, V.**
UMUS: A project for usage of LANDSAT MSS and ancillary data in land cover mapping of large areas in southern Italy p 72 N87-18191
- DIMOTAKIS, P. E.**
Effects of a downstream disturbance on the structure of a turbulent plane mixing layer [AIAA PAPER 87-0197] p 74 A87-22476
- DINI, P. W.**
Calibration of normalized vegetation index against pasture growth p 12 N87-15585
- DIXON, T. H.**
A scanning radar altimeter for mapping continental topography p 33 N87-17146
- DOBSON, M. CRAIG**
SIR-B measurements and modeling of vegetation p 15 N87-17160
- DOMIK, G.**
Space Shuttle radargrammetry results p 65 A87-23827
Using secondary image products to aid in understanding and interpretation of radar imagery p 68 N87-17239
Digital terrain mapping with STAR-1 SAR data p 69 N87-17269
- DOMIK, GITTA**
Multiple incidence angle SIR-B experiment over Argentina p 80 N87-17157
- DONELAN, M. A.**
Verification results for a two-scale model of microwave backscatter from the sea surface p 47 N87-17213
- DOOGE, JAMES C. I.**
Hydrologic models of land surface processes p 58 N87-15547
- DOSSANTOS, RENATO**
CANASATE: Sugar cane mapping by satellite, area 3 [INPE-4068-RPE/526] p 24 N87-19790
- DOSSO, M.**
First step in the use of remote sensing for regional mapping of soil organization data: Application in Brittany (France) and French Guiana p 23 N87-18193
- DOWDESWELL, J.**
Analysis of multichannel SAR data of Spitsbergen p 60 N87-17223
- DREYER, GUENTHER**
Multilens cameras for high velocity/low altitude photoreconnaissance p 75 A87-23650
- DUBE, C.**
Analysis of the spatial structure of Synthetic Aperture Radar (SAR) imagery for a better separability of cereal crops, wheat and barley p 17 N87-17287
- DUCHOSSOIS, G.**
Overview and status of the ERS-1 program p 47 N87-17190
- DUESMANN, B. J.**
Homogeneous plate deformations on a sphere as monitored by Satellite Laser Ranging (SLR) networks analyzed with the multi-epoch method [ETN-87-99221] p 27 N87-18908
- DUGDALE, G.**
Rainfall estimation over the Sahel using Meteorast thermal infra-red data p 59 N87-15587
Hydrological studies in Niger p 59 N87-15609
- DURBEC, ANDRE**
Visualization by aerial thermography of hydrodynamic exchanges between the water table, streams and gravel pits in the Rhine plain north of Strasbourg p 58 A87-25746
- DURKIN, J. W.**
Growing period and drought early warning in Africa using satellite data p 7 A87-24788

E

- EAGLESON, PETER S.**
Estimation of vegetation cover at subpixel resolution using LANDSAT data [NASA-CR-177077] p 11 N87-15514
- ECHOLS, PATRICK F.**
Landsat Thematic Mapper data analysis within the Suwannee River Basin p 57 A87-23825
- EGAN, WALTER G.**
Proposed design of an imaging spectropolarimeter/photometer for remote sensing of earth resources p 73 A87-20795
- ELACHI, CHARLES**
Spaceborne imaging radar research in the 90's p 79 N87-17141
- ELGERED, G.**
Atmospheric water vapor corrections for altimetry measurements p 85 N87-18197
- ELIASON, J. R.**
Surface reflectance correction and stereo enhancement of LANDSAT thematic mapper imagery for structural geologic exploration [DE87-003095] p 37 N87-19796
- ELLWOOD, D. J.**
Integration of surficial geochemistry and LANDSAT imagery to discover skarn tungsten deposits using image analysis techniques [CONTRIB-19586] p 35 N87-17248
- EMERY, W. J.**
Comparison between satellite image advective velocities, dynamic topography, and surface drifter trajectories p 38 A87-20692
An objective method for computing advective surface velocities from sequential infrared satellite images p 39 A87-23717
Automated extraction of pack ice motion from advanced very high resolution radiometer imagery p 42 A87-27547
- ENGBERG, A.**
Marrying geocoded image data with other types of geographic information in a PC environment p 21 N87-18154
- ENGMANN, E. T.**
Evaluating roughness models of radar backscatter p 19 N87-17344
- EPEMA, GERRIT F.**
The thematic mapper - A new tool for soil mapping in arid areas p 2 A87-21243
Processing thematic mapper data for mapping in Tunisia p 2 A87-21244
- EPPLER, DUANE T.**
Classification of sea ice types with single-band (33.6 GHz) airborne passive microwave imagery p 42 A87-27545
- ERDIN, K.**
LANDSAT-5 Thematic Mapping (TM) data applications to land use classification on around the Bosphorus area, Turkey p 19 N87-17351
- ESAIAS, WAYNE**
Ideas for a future earth observing system from geosynchronous orbit p 74 A87-23419
- ESCADAFAL, RICHARD**
Spectral brightness and surface soil characteristics in an arid Mediterranean region (southern Tunisia) p 2 A87-21242
- ESCOBAR, D. E.**
Evaluation of the mid-infrared (1.45 to 2.0 microns) with a black-and-white infrared video camera p 73 A87-20672
Assessment of grassland phytomass with airborne video imagery p 8 A87-25590
- ESSER, G.**
Evaluation of climate relevant land surface characteristics from remote sensing p 12 N87-15572
- ESTES, JOHN E.**
Remote Sensing Information Sciences Research Group, year four [NASA-CR-180198] p 88 N87-18907
- ETKIN, V. S.**
Optical and radar observations of the nonlinear interaction of gravity waves p 37 A87-20350
- EVANS, DIANE L.**
Geological applications of multipolarization SAR data p 33 N87-17140
- EVANS, ROBERT**
Radar images for soil survey in England and Wales p 3 A87-21251
- EVERITT, J. H.**
Evaluation of the mid-infrared (1.45 to 2.0 microns) with a black-and-white infrared video camera p 73 A87-20672
Assessment of grassland phytomass with airborne video imagery p 8 A87-25590
- EWING, J. A.**
Effect of surface properties on the narrow to broadband spectral relationship in clear sky satellite observations p 65 A87-25587
- EYRE, L. ALAN**
Vegetation change and desertification in the Caribbean p 14 N87-15619
- EZRATY, ROBERT**
Using buoys and ships to calibrate ERS-1 altimeter and scatterometer p 51 N87-17377

F

- FABRICIUS, JENS S.**
The ice conditions in the Greenland waters, 1980 [REPT-551.467.3.068(988)] p 53 N87-17428
- FAEST, O.**
On the discrimination between crude oil spills and monomolecular sea slicks by airborne remote sensors: Today's possibilities and limitations p 53 N87-18167
- FAGBAMI, A.**
Machine processing of Landsat data for soil survey - The Benue Valley savanna case study p 1 A87-20759

- FAGBAMI, AYODELE**
Remote sensing options for soil survey in developing countries p 2 A87-21239
- FARMER, L. DENNIS**
Classification of sea ice types with single-band (33.6 GHz) airborne passive microwave imagery p 42 A87-27545
- FEDCHENKO, P. P.**
Remote sensing of the state of crops and soils p 1 A87-20758
- FELDMAN, GENE CARL**
Variability of the productive habitat in the eastern equatorial Pacific p 38 A87-20687
- FERGUSON, H. M.**
Antarctica - Measuring glacier velocity from satellite images p 57 A87-23699
- FIELDING, ERIC J.**
Tectonic geomorphology of the Andes with SIR-A and SIR-B p 32 N87-17136
- FIMIN, R. I.**
Investigation of spectral correlations of vegetation growing on different types of geological structures p 29 A87-28508
- FINNERTY, TONY**
Kinematics at the intersection of the Garlock and Death Valley fault zones, California: Integration of TM data and field studies [NASA-CR-180182] p 36 N87-18256
- FISCHER, CHARLES J.**
Ozone in the boundary layer of the equatorial Pacific Ocean p 41 A87-25534
- FLANNIGAN, M. D.**
Forest fire monitoring using the NOAA satellite series p 3 A87-23360
- FLITCROFT, I. D.**
Hydrological studies in Niger p 59 N87-15609
- FLOUZAT, G.**
Computer-aided interpretation of complex geological patterns in remote sensing p 35 N87-17294
- FOERSTNER, WOLFGANG**
Digital image matching techniques for standard photogrammetric applications p 63 A87-23785
- FOOTE, H. P.**
Surface reflectance correction and stereo enhancement of LANDSAT thematic mapper imagery for structural geologic exploration [DE87-003095] p 37 N87-19796
- FORD, JOHN P.**
Space shuttle radar images of Indonesia p 32 N87-17137
- FORD, P. G.**
Delineation of fault zones using imaging radar p 32 N87-17138
- FORMEL, F.**
Lineaments of eastern Cuba - Geological interpretation of aerial and space imagery p 28 A87-24384
- FRANCIS, C. R.**
ERS-1 radar altimeter: Performance, calibration and data validation p 80 N87-17194
- FRANCIS, P. W.**
Volcanology from space - Using Landsat thematic mapper data in the central Andes p 27 A87-20689
- FRANCIS, PETER E.**
The use of numerical wind and wave models to provide areal and temporal extension to instrument calibration and validation of remotely sensed data p 51 N87-17371
- FRANCIS, PETER W.**
Thematic mapper studies of central Andean volcanoes [NASA-CR-180252] p 36 N87-18910
- FRANK, THOMAS**
Interpreting forest and grassland biome productivity utilizing nested scales of image resolution and biogeographical analysis [NASA-CR-180213] p 23 N87-18912
- FRANKLIN, J.**
Thematic mapper analysis of coniferous forest structure and composition p 1 A87-20762
- FRANKLIN, JANET**
Canopy reflectance modeling in a tropical wooded grassland [NASA-CR-180097] p 11 N87-15518
- FRANKLIN, STEVEN E.**
Terrain analysis from digital patterns in geomorphometry and Landsat MSS spectral response p 66 A87-30127
- FRAZIER, B. E.**
Spectral characteristics and the extent of paleosols of the Palouse formation [NASA-CR-180357] p 24 N87-19826
- FREDERICK, J. E.**
Instrument characterization for the detection of long-term changes in stratospheric ozone - An analysis of the SBUV/2 radiometer p 74 A87-20961
- FREEMAN, N.**
Canadian plans for operational demonstrations of satellite imaging radar applications p 68 N87-17229
- FREEMAN, NELSON G.**
Canada Center for Remote Sensing (CCRS) Convair 580 results relevant to ERS-1 wind and wave calibration p 84 N87-17379
- FREILICH, MICHAEL H.**
Satellite scatterometer comparisons with surface measurements: Techniques and Seasat results p 51 N87-17372
An overview of the NSCAT/N-ROSS program p 52 N87-17384
- FREISE, CLARK B.**
Analysis of surface patterns over Cobb Seamount using synthetic-aperture radar imagery [AD-A171670] p 45 N87-16493
- FUJIMURA, S.**
Models for temperature estimation from remotely sensed thermal IR data p 83 N87-17325
- FUJITA, MASAHARU**
Development and experiment of airborne microwave rain-scatterometer/radiometer system. III - Rain measurement and its data analysis p 58 A87-28436
- FUKAI, M.**
A satellite-borne SAR transmitter and receiver p 83 N87-17358

G

- GAD, A.**
Assessment of wind and fluvial action by using LANDSAT-MSS color composites in the lower Nile Valley (Egypt) p 13 N87-15612
Assessment of soil degradation in an arid region using remote sensing p 20 N87-18148
- GADDIS, L. R.**
Preliminary analyses of SIB-B radar data for recent Hawaii lava flows p 29 A87-25588
Hawaiian lava flows and SIR-B results p 69 N87-17245
- GAIROLA, R. M.**
Wind-wave relationship from Seasat radar altimeter data p 41 A87-24748
- GALLIMORE, R. G.**
A case study of GWE satellite data impact on GLA assimilation analyses of two ocean cyclones p 41 A87-25787
- GALLO, K. P.**
Land surface climatic variables monitored by NOAA-AVHRR satellites p 4 A87-23811
- GALLOTTIFLORENZANO, TERESA**
Evaluation of LANDSAT 4 MSS data for geomorphological mapping in the semiarid environment for regional planning purposes: An integrated approach (study site, the Juazeiro region) [INPE-3984-TDL/236] p 72 N87-19787
- GALPEROV, G. V.**
Use of space imagery and geophysical data in metallogenic prediction studies in central Kyzylkum p 28 A87-24383
- GANNING, BJORN**
Distribution and biomass of *Fucus vesiculosus* L. near a cooling-water effluent from a nuclear power plant in the Baltic Sea estimated by aerial photography p 43 A87-29014
- GARCIA, OSWALDO**
Atmospheric characteristics of the equatorial Pacific during the 1982-1983 El Nino, deduced from satellite and aircraft observations p 41 A87-25543
- GARDNER, ELAINE C.**
Mobile very long baseline interferometry and Global Positioning System measurement of vertical crustal motion p 26 A87-21931
- GASPAROVIC, R. F.**
Hydrodynamics of internal solitons and a comparison of SIR-A and SIR-B data with ocean measurements p 45 N87-17147
- GAUTHIER, F.**
The use of thermal airborne remote sensing for soil identification: A case study in Limousin (France) p 20 N87-18146
- GAYDOS, LEONARD**
The production of orthophotographs by digital image processing techniques p 63 A87-23787
- GEORGE, P.**
A very fast synthetic-aperture radar signal processor for ERS-1 and Radarsat p 85 N87-18180
- GERSTL, S. A. W.**
Canopy hot-spot as crop identifier [DE86-011258] p 19 N87-17395
Off-nadir optical remote sensing from satellites for vegetation identification p 22 N87-18183
Off-nadir optical remote sensing from satellites for vegetation identification [DE86-012387] p 23 N87-18916
- GERTEN, D. M.**
Microcomputer-assisted video image analysis of lodging in winter wheat p 10 A87-30130
- GIANNINI, J. A.**
A description of large-scale variability in the ocean using the diffuse attenuation coefficient p 53 N87-18160
- GILL, STEVE**
Spectral characteristics and the extent of paleosols of the Palouse formation [NASA-CR-180357] p 24 N87-19826
- GILLANI, N. V.**
Ozone formation in pollutant plumes: A reactive plume model with arbitrary crosswind resolution [PB86-236973] p 26 N87-18246
- GILLESPIE, A. R.**
Enhancement of time images for photointerpretation p 66 N87-17116
Lithologic mapping of silicate rocks using TIMS p 30 N87-17118
- GILLESPIE, D. A.**
Identification of forest and agricultural edges using Landsat Thematic Mapper data - Preliminary results p 5 A87-23832
- GILLESPIE, D. D.**
Analysis of multiple incidence angle SIR-B data for determining forest stand characteristics p 15 N87-17156
- GIRARD, MICHEL C.**
Soil science interpretation of photographs taken by Spacelab 1 p 2 A87-21241
- GOEL, N. S.**
Estimation of canopy parameters for inhomogeneous vegetation canopies from reflectance data. II - Estimation of leaf area index and percentage of ground cover for row canopies p 1 A87-20761
- GOETTING, H. R.**
Spatial analysis of the dynamics of an ecosystem by multistage remote sensing in Kenya p 16 N87-17173
A knowledge-based software environment for the analysis of spectroradiometer data p 68 N87-17203
- GOGINENI, S. P.**
Tower-based broadband backscattering measurements from the ocean surface in the North Sea p 47 N87-17217
- GOHIL, B. S.**
Wind-wave relationship from Seasat radar altimeter data p 41 A87-24748
- GOLDHIRSH, JULIUS**
Tree attenuation at 869 MHz derived from remotely piloted aircraft measurements p 9 A87-28414
- GOMES, I.**
Digital satellite imagery acquisition and processing p 68 N87-17207
- GOODENOUGH, D. G.**
Viewing angle corrections of airborne multispectral scanner data acquired over forested surfaces p 17 N87-17273
- GOODFELLOW, W.**
Integration of surficial geochemistry and LANDSAT imagery to discover skarn tungsten deposits using image analysis techniques [CONTRIB-19586] p 35 N87-17248
- GORDON, A. L.**
Shedding of an Agulhas ring observed at sea p 44 A87-30146
- GORDON, DANIEL K.**
Fruit tree inventory with Landsat Thematic Mapper data p 8 A87-28387
- GORODETSKII, A. K.**
The results of sea-surface temperature determinations from IR and microwave measurements aboard the Cosmos-1151 satellite p 40 A87-24376
- GOYAL, V. P.**
Application of remote sensing in the study of the soil hazards of Haryana State, India p 20 N87-18150
Remote sensing applications in the study of land use and soils of aeolian cover of the western part of Haryana State, India p 22 N87-18187
- GRAETZ, R. D.**
Calibration of Landsat data for sparsely vegetated semi-arid rangelands p 9 A87-29008
- GRAF, JAMES E.**
Earth Observing System - The earth research system of the 1990's [AIAA PAPER 87-0320] p 74 A87-22556
- GRAF, K. CH.**
Merging spaceborne image data of optical and microwave sensors p 69 N87-17267
- GRAHAM, ROBIN L.**
Interpreting forest and grassland biome productivity utilizing nested scales of image resolution and biogeographical analysis [NASA-CR-180213] p 23 N87-18912
- GRANKOV, A. G.**
Use of decimeter waves in studies of water bodies by methods of microwave radiometry p 58 A87-26537

GRAPE, G.

Marrying geocoded image data with other types of geographic information in a PC environment p 21 N87-18154

GRASSL, HARTMUT

Multiangle or multiwavelength technique for remote sensing of sea surface temperature p 45 N87-15652

GRAY, A. L.

C and Ku-band scatterometer results from the SCATTMOD internal wave experiment p 47 N87-17215
Canada Center for Remote Sensing (CCRS) Convair 580 results relevant to ERS-1 wind and wave calibration p 84 N87-17379

GREEN, K. M.

Using Landsat to assess tropical forest habitat for migratory birds in the Yucatan Peninsula p 4 A87-23807

GRIER, T.

Estimation of canopy parameters for inhomogeneous vegetation canopies from reflectance data. II - Estimation of leaf area index and percentage of ground cover for row canopies p 1 A87-20761

GRIFFITHS, H.

New techniques in satellite altimeter tracking systems p 85 N87-18164

GRUEN, A.

Point positioning and mapping with Large Format Camera data p 71 N87-18188

GRUENER, K.

Contributions to oil spill detection and analysis with radar and microwave radiometry, results of the Archimedes 2 campaign p 54 N87-18170

GRUNES, M.

Comparison of ocean tide models with satellite altimeter data [AD-A174698] p 56 N87-19879

GRUSHIN, V. A.

Optical and radar observations of the nonlinear interaction of gravity waves p 37 A87-20350

GUBIN, V. N.

Identification of reclaimed landscapes of Belorussia from space images p 28 A87-24382

GUENTHER, K. P.

Laser-induced chlorophyll-A fluorescence of terrestrial plants p 23 N87-18207

GUIGNARD, J. P.

ERS-1 fast delivery processing and products p 81 N87-17224

GUILLAUME, A. M.

A two-step algorithm for the separate retrieval of ocean surface and atmospheric parameters from microwave radiometers p 50 N87-17341

GUILLON, L.

Soil degradation evaluation by digital image processing p 20 N87-18147

GUISARD, A.

A two-step algorithm for the separate retrieval of ocean surface and atmospheric parameters from microwave radiometers p 50 N87-17341

GULEN, L.

Delineation of fault zones using imaging radar p 32 N87-17138

GUPTA, R. K.

AVHRR and MSS data based vegetation indices studies over Indian sites p 14 N87-15622

GUTINEZDELACAMARAARA, JESUS

Remote Sensing Laboratory [ETN-87-98850] p 88 N87-18227

GUYENNE, T. D.

Proceedings of the 1986 International Geoscience and Remote Sensing Symposium (IGARSS '86) on Remote Sensing: Today's Solutions for Tomorrow's Information Needs, volume 1 [ESA-SP-254-VOL-1] p 80 N87-17163

Proceedings of the 1986 International Geoscience and Remote Sensing Symposium (IGARSS '86) on Remote Sensing: Today's Solutions for Tomorrow's Information Needs, volume 2 [ESA-SP-254-VOL-2] p 82 N87-17283

Proceedings of the 1986 International Geoscience and Remote Sensing Symposium (IGARSS '86) on Remote Sensing: Today's Solutions for Tomorrow's Information Needs, volume 3 [ESA-SP-254-VOL-3] p 84 N87-18142

GUYMER, TREVOR H.

Requirements and constraints in the calibration and validation of ERS-1 wind and wave parameters p 51 N87-17369

GUYOT, L.

Monitoring of large phenomena in developing countries through satellite imagery p 67 N87-17172

GUZKOWSKA, M. A. J.

The prospects for hydrological measurements using ERS-1 p 59 N87-15588

Satellite altimeter measurements over land and inland water p 61 N87-18200

GWYNN, M. D.

Monitoring East African vegetation using AVHRR data p 6 A87-24781

H

HAACK, BARRY

Landsat Thematic Mapper digital information content for agricultural environments p 5 A87-23830

HAEFNER, H.

Monitoring of land-surface change in Sri Lanka p 13 N87-15618

HAJA, S. R.

Spatial remote sensing to land management p 70 N87-18157

HALL, FORREST

Ideas for a future earth observing system from geosynchronous orbit p 74 A87-23419

HALLIKAINEN, M.

Developpement of algorithms to retrieve the water equivalent of snow cover from satellite microwave radiometer data p 60 N87-17264

Classification of forest and surface types by satellite microwave radiometry p 18 N87-17305

Retrieval of near-surface wind speed in the Baltic Sea from NIMBUS-7 Scanning Multichannel Microwave Radiometer (SMRM) observations p 50 N87-17342

Sea ice studies in the Baltic Sea using satellite microwave radiometer data p 50 N87-17343

HALPERN, DAVID

Equatorial long-wave characteristics determined from satellite sea surface temperature and in situ data p 44 A87-30923

HARBOE-SORENSEN, R.

The SEU risk assessment of Z80A, 8086 and 80C86 microprocessors intended for use in a low altitude polar orbit p 74 A87-22025

HARDING, JOHN M.

The impact of satellite infrared sea surface temperatures on FNOC (Fleet Numerical Oceanography Center) ocean thermal analyses [AD-A173333] p 54 N87-18295

HARRIS, R.

Vegetation index models for the assessment of vegetation in marginal areas p 12 N87-15584

HART, JUDY

Spectral characteristics and the extent of paleosols of the Palouse formation [NASA-CR-180357] p 24 N87-19826

HARTL, PH.

Future user requirements and required technological developments of spaceborne synthetic aperture radars p 82 N87-17320

HASKINS, R.

Remote sensing of land-surface temperature from HIRS/MSU data p 77 N87-15573

HASSELMANN, KLAUS

Wave modeling activities of the Wave Modeling (WAM) group relevant to ERS-1 p 52 N87-17389

HAUCK, M.

Southern Pantanal Matogrossense (South America) of Modular Optoelectronic Multispectral Scanner (MOMS) data, preliminary results p 71 N87-18182

HAURY, LOREN R.

Temperature-plant pigment-optical relations in a recurrent offshore mesoscale eddy near Point Conception, California [AD-A176666] p 39 A87-23720

Biological consequences of a recurrent eddy off Point Conception, California p 40 A87-23721

HAWKINS, JEFFREY D.

The impact of satellite infrared sea surface temperatures on FNOC (Fleet Numerical Oceanography Center) ocean thermal analyses [AD-A173333] p 54 N87-18295

HAWKINS, R. K.

Canada Center for Remote Sensing (CCRS) Convair 580 results relevant to ERS-1 wind and wave calibration p 84 N87-17379

HAXBY, WILLIAM F.

Structure of the Kerguelen Plateau province from Seasat altimetry and seismic reflection data p 28 A87-24866

HE, DONG-CHEN

Drainage channel network of the Arcachon Basin using Thematic Mapper data obtained at high tide p 58 A87-29013

HEATH, D. F.

Instrument characterization for the detection of long-term changes in stratospheric ozone - An analysis of the SBUV/2 radiometer p 74 A87-20961

HEER, RICHARD C.

Estimation of density in young pine plantations using 35mm aerial photography p 5 A87-23819

HELD, D. N.

Imaging radar polarimetry from wave synthesis p 82 N87-17279

HELD, DANIEL N.

Imaging radar polarimetry from wave synthesis p 76 A87-29849

HELLDEN, ULF

Desertification monitoring: Remotely sensed data for drought impact studies in the Sudan p 12 N87-15604

HENDERSON-SELLERS, A.

Illustration of the influence of shadowing on high latitude information derived from satellite imagery p 62 A87-20768

HENRICKSEN, B. L.

Reflections on drought - Ethiopia 1983-1984 p 6 A87-24780
Growing period and drought early warning in Africa using satellite data p 7 A87-24788

HERMAN, GERALD F.

Data sensitivities of sea ice drift and ocean stress in North Atlantic high latitudes p 38 A87-20520

HEUMBEL, R.

Sri Lanka's solution to land use mapping and monitoring for Third World countries development p 67 N87-17174

HIELKEMA, J. U.

Rainfall and vegetation monitoring in the Savanna Zone of the Democratic Republic of Sudan using the NOAA Advanced Very High Resolution Radiometer p 6 A87-24783

Assessment of ecological conditions associated with the 1980/81 desert locust plague upsurge in West Africa using environmental satellite data p 7 A87-24789

HIERNAUX, P. H. Y.

Monitoring the grasslands of the Sahel using NOAA AVHRR data Niger 1983 p 6 A87-24782
Monitoring vegetation in the Mali Sahel during summer 1984 p 6 A87-24784

HILL, C. T.

Remote sensing of structurally complex semi-natural vegetation - An example from heathland p 10 A87-30896

HILL, J.

Rural land use inventory and mapping in the Ardeche area (France) using multitemporal Thematic Mapping (TM) data p 19 N87-17350

HILLER, K.

Southern Pantanal Matogrossense (South America) of Modular Optoelectronic Multispectral Scanner (MOMS) data, preliminary results p 71 N87-18182

HINZE, WILLIAM J.

Improving the geological interpretation of magnetic and gravity satellite anomalies [NASA-CR-180149] p 35 N87-17418

HIROSHIMA, K.

High speed image processing system based on the custom VLSI for Digital Signal Processing (DSP) p 71 N87-18179

HISADA, Y.

A satellite-borne SAR transmitter and receiver p 83 N87-17358
Pulse compression test results of the SAR transmitter and receiver p 83 N87-17360

HIZAL, A.

LANDSAT-5 Thematic Mapping (TM) data applications to land use classification on around the Bosphorus area, Turkey p 19 N87-17351
The use of remote sensing (including aerial photographs) to devise cost-effective methods for soil conservation in the Kocaeli Peninsula, Turkey p 20 N87-18149

HO, D.

Design of a data base system for inferring land surface parameters and fluxes from satellite radiances p 66 N87-15625
Thermal inertia and soil fluxes by remote sensing p 20 N87-18143

HODGSON, MICHAEL E.

A cognitive measure of texture in imagery p 64 A87-23800

HOETZL, H.

Hydrogeological research in Peloponnesus (Greece) Karst area by support and completion of LANDSAT-thematic data p 33 N87-17234

HOFFER, R. M.

Analysis of multiple incidence angle SIR-B data for determining forest stand characteristics p 15 N87-17156

HOFFMAN, R. N.

Satellite remote sensing of meteorological parameters for global numerical weather prediction p 76 A87-26098

HOFMANN, O.

The stereo-pushbroom scanner system Digital Photogrammetry System (DPS) and its accuracy p 80 N87-17167

- HOGUE, F.**
Oceanographic measurement capabilities of the NASA P-3 aircraft p 52 N87-17380
- HOGUE, FRANK E.**
Chlorophyll pigment concentration using spectral curvature algorithms - An evaluation of present and proposed satellite ocean color sensor bands p 37 A87-20204
- HOLBEN, B. N.**
Monitoring East African vegetation using AVHRR data p 6 A87-24781
- HOLBEN, BRENT N.**
Characteristics of maximum-value composite images from temporal AVHRR data p 75 A87-24778
- HOLECZ, F. M.**
Merging spaceborne image data of optical and microwave sensors p 69 N87-17267
- HOLLIDAY, DENNIS**
A radar ocean imaging model for small to moderate incidence angles p 43 A87-29015
- HOOPER, DAVID**
The production of orthophotographs by digital image processing techniques p 63 A87-23787
- HOOPER, G. L.**
Analysis of AIS radiometry at Mono Lake, California p 81 N87-17204
- HOOPER, MERVYN**
Classification of sea ice types with single-band (33.6 GHz) airborne passive microwave imagery p 42 A87-27545
- HORIGUCHI, K.**
High speed image processing system based on the custom VLSI for Digital Signal Processing (DSP) p 71 N87-18179
- HORII, S.**
High speed image processing system based on the custom VLSI for Digital Signal Processing (DSP) p 71 N87-18179
- HOSHIZAKI, T.**
Remote detection of forest damage p 8 A87-26197
- HSU, LIANG C.**
Nature and origin of mineral coatings on volcanic rocks of the Black Mountain, Stonewall Mountain, and Kane Springs, Wash volcanic centers, Southern Nevada [NASA-CR-180183] p 36 N87-18255
- HSU, SHIN-Y**
Rock type discrimination with AI-based texture analysis algorithms p 28 A87-23782
- HUEHNERFUSS, H.**
On the discrimination between crude oil spills and monomolecular sea slicks by airborne remote sensors: Today's possibilities and limitations p 53 N87-18167
- HUEPPI, R.**
Dielectric and surface parameters related to microwave scatter and emission properties p 16 N87-17262
L to X-band scatter and emission measurements of vegetation p 19 N87-17347
- HUGHES, B. A.**
C and Ku-band scatterometer results from the SCATMOD internal wave experiment p 47 N87-17215
Estimation of internal wave currents from SAR and infrared scatterometer imagery p 48 N87-17295
- HUGHES, S. J.**
C and Ku-band scatterometer results from the SCATMOD internal wave experiment p 47 N87-17215
Estimation of internal wave currents from SAR and infrared scatterometer imagery p 48 N87-17295
- HULSMAN, K.**
Classification of reflectance on colour infrared aerial photographs and sub-tropical salt-marsh vegetation types p 10 A87-29012
- HUMMER-MILLER, SUSANNE**
Simulation modeling and preliminary analysis of TIMS data from the Carlin area and the northern Grapevine Mountains, Nevada p 31 N87-17120
- HUNT, J. J.**
Proceedings of the 1986 International Geoscience and Remote Sensing Symposium (IGARSS '86) on Remote Sensing: Today's Solutions for Tomorrow's Information Needs, volume 1 [ESA-SP-254-VOL-1] p 80 N87-17163
Proceedings of the 1986 International Geoscience and Remote Sensing Symposium (IGARSS '86) on Remote Sensing: Today's Solutions for Tomorrow's Information Needs, volume 2 [ESA-SP-254-VOL-2] p 82 N87-17283
Proceedings of an ESA Workshop on ERS-1 Wind and Wave Calibration [ESA-SP-262] p 84 N87-17363
Proceedings of the 1986 International Geoscience and Remote Sensing Symposium (IGARSS '86) on Remote Sensing: Today's Solutions for Tomorrow's Information Needs, volume 3 [ESA-SP-254-VOL-3] p 84 N87-18142
- HUSSEY, M. A.**
Evaluation of the mid-infrared (1.45 to 2.0 microns) with a black-and-white infrared video camera p 73 A87-20672
Assessment of grassland phytomass with airborne video imagery p 8 A87-25590
- HUTSINPILLER, AMY**
Detection and mapping of volcanic rock assemblages and associated hydrothermal alteration with Thermal Infrared Multiband Scanner (TIMS) data Comstock Lode Mining District, Virginia City, Nevada p 31 N87-17119
- I**
- INCE, F.**
Remote sensing activities in Turkey: Possible contributions to climate studies p 77 N87-15624
- INOMATA, HIDEYUKI**
Development and experiment of airborne microwave rain-scatterometer/radiometer system. IV - Microwave back-scattering experiment of ocean surface p 43 A87-28437
- IOKA, M.**
Evaluation of LANDSAT 5 Thematic Mapping (TM) data for image clustering and classification p 69 N87-17251
- IOKA, MIKIHIRO**
Performance of Landsat-5 TM data in land-cover classification p 25 A87-29007
- IRVINE, D. E.**
Spatial evolution of wave spectra in the vicinity of the Agulhas current from SIR-B p 50 N87-17337
- ISAACS, R. G.**
Remote sensing of hydrological variables from the DMSP microwave mission sensors p 57 A87-23374
Satellite remote sensing of meteorological parameters for global numerical weather prediction p 76 A87-26098
- ISHIWADA, YASUFUMI**
Present status of Japanese ERS-1 Project p 79 N87-17145
- ITO, M. R.**
Resolving the Doppler ambiguity for spaceborne synthetic aperture radar p 72 N87-18212
- ITOH, Y.**
A satellite-borne SAR transmitter and receiver p 83 N87-17358
Pulse compression test results of the SAR transmitter and receiver p 83 N87-17360
- ITEN, K. I.**
Sri Lanka's solution to land use mapping and monitoring for Third World countries development p 67 N87-17174
Viewing angle corrections of airborne multispectral scanner data acquired over forested surfaces p 17 N87-17273
- IVERSON, LOUIS R.**
Interpreting forest and grassland biome productivity utilizing nested scales of image resolution and biogeographical analysis [NASA-CR-180213] p 23 N87-18912
- IZUMI, I.**
A satellite-borne SAR transmitter and receiver p 83 N87-17358
- J**
- JACKSON, F. C.**
Oceanographic measurement capabilities of the NASA P-3 aircraft p 52 N87-17380
- JAMES, ALEC**
Island wakes and headland eddies - A comparison between remotely sensed data and laboratory experiments p 44 A87-30925
- JANTUNEN, H.**
Remote sensing of shallow water areas with reference to environmental and multitemporal monitoring of the Hailuoto area, Finland p 61 N87-18159
- JARAMILLO, LINDA L.**
Thermal imaging spectroscopy in the Kelso-Baker Region, California p 30 N87-17117
- JASINSKI, MICHAEL F.**
Estimation of vegetation cover at subpixel resolution using LANDSAT data [NASA-CR-177077] p 11 N87-15514
- JASSEMM, KHALEEL IBRAHEM**
Photometric functions, reflectance map - Two techniques for determining surface shape and orientation from image intensity p 64 A87-23802
- JAYATILAKA, H. S.**
Sri Lanka's solution to land use mapping and monitoring for Third World countries development p 67 N87-17174
- JEDLOVEC, GARY**
Verification of small-scale water vapor features in VAS imagery using high resolution MAMS imagery p 62 A87-23348
- JENSEN, JOHN R.**
Agricultural remote sensing in South Carolina - A study of crop identification capabilities utilizing Landsat data p 4 A87-23806
Remote sensing of aquatic macrophyte distribution in upper Lake Marion p 57 A87-23826
- JEPSKY, JOSEPH**
Airborne laser profiling and mapping systems come of age p 75 A87-23786
- JIN, Y.-Q.**
Remote sensing of hydrological variables from the DMSP microwave mission sensors p 57 A87-23374
- JOHANNESSEN, J. A.**
Geophysics of the marginal ice zone from SAR p 47 N87-17219
- JOHANNESSEN, O. M.**
Geophysics of the marginal ice zone from SAR p 47 N87-17219
- JOHNSON, D. R.**
A case study of GWE satellite data impact on GLA assimilation analyses of two ocean cyclones p 41 A87-25787
- JOHNSON, L. K.**
Surface reflectance correction and stereo enhancement of LANDSAT thematic mapper imagery for structural geologic exploration [DE87-003095] p 37 N87-19796
- JOLMA, P.**
Development of algorithms to retrieve the water equivalent of snow cover from satellite microwave radiometer data p 60 N87-17264
Classification of forest and surface types by satellite microwave radiometry p 18 N87-17305
- JONES, BURTON H.**
Mesoscale hydrographic variability in the vicinity of Points Conception and Arguello during April-May 1983 - The OPUS 1983 experiment p 39 A87-23719
- JORDAN, DOUGLAS M.**
Landsat Thematic Mapper data analysis within the Suwannee River Basin p 57 A87-23825
- JUSTICE, C. O.**
Analysis of the dynamics of African vegetation using the normalized difference vegetation index p 6 A87-24779
Monitoring East African vegetation using AVHRR data p 6 A87-24781
Monitoring the grasslands of the Sahel using NOAA AVHRR data Niger 1983 p 6 A87-24782
Monitoring vegetation in the Mali Sahel during summer 1984 p 6 A87-24784
Monitoring the grasslands of the Sahel 1984-1985 p 7 A87-24787
- K**
- KAHLE, A. B.**
The application of remotely sensed data to pedologic and geomorphic mapping on alluvial fan and playa surfaces in Saline Valley, California p 15 N87-17127
- KAHLE, ANNE B.**
The TIMS Data User's Workshop [NASA-CR-180130] p 78 N87-17111
Calculation of day and night emittance values p 67 N87-17131
- KANEMASU, E. T.**
Assessing grass canopy condition and growth from combined optical-microwave measurements p 17 N87-17286
- KANESHIGE, THOMAS**
An overview of the implementation of the World Climate Research program p 26 N87-17388
- KAPLAN, L. D.**
Remote sensing of hydrological variables from the DMSP microwave mission sensors p 57 A87-23374
Satellite remote sensing of meteorological parameters for global numerical weather prediction p 76 A87-26098
- KAPLAN, M. S.**
Application of Spaceborne Distributed Aperture/Coherent Array Processing (SDA/CAP) technology to active and passive microwave remote sensing p 82 N87-17277
- KARASKA, MARK A.**
Impact of environmental variables on spectral signatures acquired by the Landsat Thematic Mapper p 9 A87-29003
- KASHIHARA, H.**
A satellite-borne SAR transmitter and receiver p 83 N87-17358
Pulse compression test results of the SAR transmitter and receiver p 83 N87-17360

KASISCHKE, E. S.

Characterisation of internal wave surface patterns on airborne SAR imagery p 50 N87-17338
 Detection of bottom-related surface patterns on visible spectrum imagery p 53 N87-18158

KATO, YUICHI

Pre-assessment for large scale civil engineering projects by integrated analysis with the data numerical topography and remote sensing p 57 A87-23815

KAUFMAN, H.

Results of tectonic and spectral investigations along the Wadi Araba fault in Jordan using special processed Thematic Mapping (TM) data p 34 N87-17247

KAUFMANN, H.

Hydrogeological research in Peloponnesus (Greece) Karst area by support and completion of LANDSAT-thematic data p 33 N87-17234

KAUPP, V. H.

Preliminary analyses of SIB-B radar data for recent Hawaii lava flows p 29 A87-25588
 Hawaiian lava flows and SIR-B results p 69 N87-17245

KAVANAGH, P. F.

Resolving the Doppler ambiguity for spaceborne synthetic aperture radar p 72 N87-18212

KAWATA, Y.

Bitemporal analysis of Thematic Mapper data for land cover classification p 69 N87-17249
 Radiometric correction method which removes both atmospheric and topographic effects from the LANDSAT-MSS data p 83 N87-17329
 Automatic update procedure of the digitized land use map using LANDSAT TM data p 72 N87-18192

KE, YING

Interpreting forest and grassland biome productivity utilizing nested scales of image resolution and biogeographical analysis [NASA-CR-180213] p 23 N87-18912

KEARNEY, JOHN A.

Capabilities for source assessment p 63 A87-23793

KEDEM, BENJAMIN

Satellite rainfall retrieval by logistic regression p 56 A87-23370

KELLER, M.

Snow cover recession in an Alpine ecological system p 18 N87-17316

KELLER, M. R.

Active/passive microwave sensor comparison of MIZ-ice concentration estimates p 46 N87-17185

KENNARD, W. C.

Identification of forest and agricultural edges using Landsat Thematic Mapper data - Preliminary results p 5 A87-23832

KERBER, A. G.

Utility of AVHRR channels 3 and 4 in land-cover mapping p 9 A87-28388

KESSLER, R.

Microwave remote sensing: Its applications and limitations in operational tasks of land use inventory and forest management p 17 N87-17266

KETTEL, E. G.

An initial evaluation of two digital airborne imagers for surveying spruce budworm defoliation p 1 A87-20671

KEYDEL, W.

X-SAR extends the frequency range of Shuttle Imaging Radar p 70 N87-17362
 Contributions to oil spill detection and analysis with radar and microwave radiometry, results of the Archimedes 2 campaign p 54 N87-18170

KEYTE, G. E.

SIR-B observations of ocean waves in the NE Atlantic p 49 N87-17335

KHALSA, SIRI JODHA SINGH

Atmospheric characteristics of the equatorial Pacific during the 1982-1983 El Nino, deduced from satellite and aircraft observations p 41 A87-25543

KHORRAM, S.

Modelling of estuarine chlorophyll-A from an airborne scanner p 61 N87-18172

KIDSON, J. W.

Calibration of normalized vegetation index against pasture growth p 12 N87-15585

KIENKO, IU. P.

Soviet remote sensing p 86 A87-27452

KILGUS, C. C.

Development in radar altimetry: The Navy Geosat mission p 85 N87-18161

KING, W. D.

A thermal device for aircraft measurement of the solid water content of clouds p 56 A87-20951

KIRCHHOF, W.

Comparison of Thematic Mapper (TM) and SPOT simulation data for agricultural applications in south west Germany p 16 N87-17165

KLEESPIES, THOMAS J.

An extension of the split window technique for the retrieval of precipitable water p 60 N87-16386
 [AD-A173008]

KLEMAN, JOHAN

The spectral reflectance of stands of Norway spruce and Scotch pine, measured from a helicopter p 7 A87-25586

KNIGHT, A. W.

Modelling of estuarine chlorophyll-A from an airborne scanner p 61 N87-18172

KOBLINSKY, CHESTER J.

Temperature-plant pigment-optical relations in a recurrent offshore mesoscale eddy near Point Conception, California [AD-A176666] p 39 A87-23720
 Biological consequences of a recurrent eddy off Point Conception, California p 40 A87-23721

KOBRICK, M.

Space Shuttle radargrammetry results p 65 A87-23827

KOCH, WOLFGANG

Comparison concept of satellite derived wind and wave data with ground truth p 51 N87-17373

KODA, M.

Evaluation of LANDSAT 5 Thematic Mapping (TM) data for image clustering and classification p 69 N87-17251

KODA, MASATO

Performance of Landsat-5 TM data in land-cover classification p 25 A87-29007

KOGEN, V. S.

The principles and procedures of modeling ore-related objects in predictive metallogenic investigations (using satellite-borne data) p 29 A87-26533

KOJIMA, M.

Some results of Marine Observation Satellite (MOS-1) airborne verification experiment Multispectral Electronic Self Scanning Radiometer (MESSR) p 46 N87-17166

KOMAR, C. A.

Proceedings of the Second Workshop on Remote Sensing/Lineament Applications for Energy Extraction [DE86-006613] p 36 N87-18915

KONDO, H.

A satellite-borne SAR transmitter and receiver p 83 N87-17358

KONDRATEV, K. IA.

Remote sensing of the state of crops and soils p 1 A87-20758
 Soviet remote sensing p 86 A87-27452

KOCHESFAHANI, M. M.

Effects of a downstream disturbance on the structure of a turbulent plane mixing layer [AIAA PAPER 87-0197] p 74 A87-22476

KOOPMANS, B. N.

A comparative study of lineament analysis from different remote sensing imagery over areas in the Benue Valley and Jos Plateau Nigeria p 30 A87-29010

KOVALEVSKY, JEAN

The shape of the earth in the space age p 26 A87-28442

KOZODEROV, V. V.

Remote sensing of the state of crops and soils p 1 A87-20758

KRASNOZHON, G. F.

Interpretation characteristics of space photographs of sea coasts with wind-induced surges p 43 A87-28509

KRAVTSOVA, V. I.

The development of procedures for forest interpretation from texture-selective images p 8 A87-26535

KROGER, PETER M.

Mobile very long baseline interferometry and Global Positioning System measurement of vertical crustal motion p 26 A87-21931

KROHN, M. DENNIS

Airborne Thermal Infrared Multispectral Scanner (TIMS) images over disseminated gold deposits, Osgood Mountains, Humboldt County, Nevada p 32 N87-17134

KRUG, THELMA

Agricultural crop estimates using information gathered by remote sensing satellites, as well as ground data, through samples of geographic layers [INPE-4102-RPE/534] p 24 N87-19786

KRUL, LEO

Theoretical approach to radar backscattering of soils p 3 A87-21250

KRUSE, FRED A.

Simulation modeling and preliminary analysis of TIMS data from the Carlin area and the northern Grapevine Mountains, Nevada p 31 N87-17120

KUBO, M.

High speed image processing system based on the custom VLSI for Digital Signal Processing (DSP) p 71 N87-18179

KUCHERIAVENKOV, A. I.

An analysis of the potential of satellite-borne bistatic radar sensing of the earth p 75 A87-24385

KUIPERS, H.

Ground water-fed lakes in the Libyan desert: Their varying area as observed by means of LANDSAT-MSS data p 59 N87-15611

KUMAR, R.

A new semi-empirical sea spectrum for estimating the scattering coefficient p 38 A87-20769

KUMMEROW, C.

Microwave radiances from horizontally finite precipitating clouds containing ice and liquid hydrometeors p 61 N87-17340

KUNIYASU, Y.

High speed image processing system based on the custom VLSI for Digital Signal Processing (DSP) p 71 N87-18179

KURBATOVA, I. E.

Interpretation characteristics of space photographs of sea coasts with wind-induced surges p 43 A87-28509

KUSAKA, T.

Bitemporal analysis of Thematic Mapper data for land cover classification p 69 N87-17249
 Radiometric correction method which removes both atmospheric and topographic effects from the LANDSAT-MSS data p 83 N87-17329
 Automatic update procedure of the digitized land use map using LANDSAT TM data p 72 N87-18192

KUTUZA, B. G.

The results of sea-surface temperature determinations from IR and microwave measurements aboard the Cosmos-1151 satellite p 40 A87-24376

KUUSK, A. E.

A photographic technique for studying reflection indicatixes of vegetation cover p 5 A87-24388

KUX, H.

Southern Pantanal Matogrossense (South America) of Modular Optoelectronic Multispectral Scanner (MOMS) data, preliminary results p 71 N87-18182

KUZNETSOV, A. A.

Geological nature of early Precambrian formations (considering the example of the Anabar shield) p 28 A87-24274

L**LADNER, LYMAN**

The production of orthophotographs by digital image processing techniques p 63 A87-23787

LAMACRAFT, R. R.

Calibration of Landsat data for sparsely vegetated semi-arid rangelands p 9 A87-29008

LAN, F. KH.

The use of Doppler observations to obtain initial geodetic data and to derive plumbline deviations and quasi-geoid heights p 27 A87-28504

LANG, H. R.

Application of TIMS data in stratigraphic analysis p 31 N87-17121

LANGE, P. A.

On the discrimination between crude oil spills and monomolecular sea slicks by airborne remote sensors: Today's possibilities and limitations p 53 N87-18167

LANGHAM, E.

Canadian plans for operational demonstrations of satellite imaging radar applications p 68 N87-17229

LANGRAN, KENNETH J.

Monitoring vegetation recovery patterns on Mount St. Helens using thermal infrared multispectral data p 14 N87-17122

LANNELONGUE, N.

VARAN-S radar image interpretation [CNES-CT/DRT/TIT/RL-54-T] p 66 N87-16963

LATHROP, RICHARD G., JR.

The utility of Thematic Mapper data for temperature mapping in the Great Lakes p 57 A87-23824

LAURIN, R.

Vegetation and soils information contained in transformed Thematic Mapper data p 22 N87-18185

LAUSTRUP, MARK

The Red River Valley archeological project p 31 N87-17128

LAVROVA, N. P.

Investigation of spectral correlations of vegetation growing on different types of geological structures p 29 A87-28508

LAWRENCE, G. R.

Thermal infrared remote sensing: One of today's solutions p 83 N87-17324

- LEAR, JOHN W.**
Instrumentation for optical remote sensing from space; Proceedings of the Meeting, Cannes, France, November 27-29, 1985 [SPIE-589] p 73 A87-19647
- LEBERL, F.**
Space Shuttle radargrammetry results p 65 A87-23827
Using secondary image products to aid in understanding and interpretation of radar imagery p 68 A87-17239
Digital terrain mapping with STAR-1 SAR data p 69 A87-17269
- LEBERL, FRANZ**
Multiple incidence angle SIR-B experiment over Argentina p 80 A87-17157
- LECLERC, A.**
Spatial remote sensing to land management p 70 A87-18157
- LECOMTE, PASCAL**
Evaluation of the different parameters in Long's C-band model p 51 A87-17370
- LEGECKIS, RICHARD**
A satellite time series of sea surface temperatures in the eastern equatorial Pacific Ocean, 1982-1986 p 39 A87-23718
- LEVINE, D.**
The Electronically Steered Thinned Array Radiometer (ESTAR) p 82 A87-17260
- LEVY, GAD**
Ocean surface pressure fields from satellite-sensed winds p 41 A87-25797
- LEWIS, JAMES K.**
Modeling energy flow and nutrient cycling in natural semiarid grassland ecosystems with the aid of thematic mapper data [NASA-CR-179903] p 11 A87-15517
- LI, F. K.**
An overview of the NSCAT/N-ROSS program p 52 A87-17384
- LIETH, H.**
Evaluation of climate relevant land surface characteristics from remote sensing p 12 A87-15572
- LILLESAND, THOMAS M.**
The utility of Thematic Mapper data for temperature mapping in the Great Lakes p 57 A87-23824
- LINDGREN, RALF**
A comparative test of photogrammetrically sampled digital elevation models p 66 A87-29499
- LIST, F. K.**
LANDSAT-MSS remote sensing and satellite cartography: An integrated approach to the preparation of a new geological map of Egypt at a scale of 1:500 000 p 36 A87-18190
- LIU, W. TIMOTHY**
Month-to-month variability of ocean-atmosphere latent heat flux as observed from the Nimbus microwave radiometer p 39 A87-23391
Evaluation of geophysical parameters measured by the Nimbus-7 microwave radiometer for the TOGA Heat Exchange Project [NASA-CR-180151] p 78 A87-17110
- LIU, Z. K.**
Snow survey from meteorological satellite images in the Qilian Mountain Basin in northwest China p 56 A87-20765
- LIVINGSTONE, C. E.**
Canada Center for Remote Sensing (CCRS) Convair 580 results relevant to ERS-1 wind and wave calibration p 84 A87-17379
- LLEWELLYN-JONES, D. T.**
The Along Track Scanning Radiometer (ATSR) for ERS1 p 73 A87-19660
- LLOYD, ROBERT E.**
A cognitive measure of texture in imagery p 64 A87-23800
- LO, C. P.**
Accuracy of population estimation from medium-scale aerial photography p 24 A87-23777
- LOFFET, A.**
On the discrimination between crude oil spills and monomolecular sea slicks by airborne remote sensors: Today's possibilities and limitations p 53 A87-18167
- LOHANICK, ALAN W.**
Classification of sea ice types with single-band (33.6 GHz) airborne passive microwave imagery p 42 A87-27545
- LOMBARDO, M. A.**
Environmental modification of metropolitan areas through satellite images: Study of urban design in the tropics p 25 A87-17175
- LOPES, A.**
Extraction of the backscatter coefficient of agricultural fields from an airborne SAR image p 16 A87-17265
- LORENZINI, M.**
Integrated analysis of geological and remote sensing data aimed at mineral deposits detection in the Monapo area (northern Mozambique) p 34 A87-17243
- LORKEERS, ALOISIUS**
An application of thematic mapper data in Tunisia - Estimation of daily amplitude in near-surface soil temperature and discrimination of hypersaline soils p 2 A87-21245
- LOUET, J.**
The ESA approach for ERS-1 sensor calibration and performance verification p 80 A87-17192
- LOUET, JACQUES**
ERS-1 mission constraints related to wind and wave calibration p 84 A87-17364
- LOWENTHAL, DOUGLAS H.**
Arctic haze: Natural or pollution? [AD-A174025] p 55 A87-18931
- LOWRY, R. T.**
Digital terrain mapping with STAR-1 SAR data p 69 A87-17269
SAR imagery for forest management p 18 A87-17313
STAR-VUE: A tactical ice navigation workstation p 54 A87-18181
- LOZANO-GARCIA, D. F.**
Analysis of multiple incidence angle SIR-B data for determining forest stand characteristics p 15 A87-17156
- LUCCHITTA, B. K.**
Antarctica - Measuring glacier velocity from satellite images p 57 A87-23699
- LUEPKE, DOUGLAS E.**
Locating subsurface gravel with thermal imagery p 31 A87-17125
- LUIS, JOSIE ENRIQUE**
Marine climate program p 52 A87-17390
- LULLA, K.**
IRSAP: An improved approach in processing remotely sensed data p 70 A87-17332
- LUNDEN, B.**
A statistical approach to select the optimal wavelength bands for separating rocks in the wavelength region 0.4 to 2.3 microns p 34 A87-17244
- LUNDEN, BENGT**
Experimental results in soil moisture mapping using IR thermography p 2 A87-21246
- LUTJEHARMS, J. R. E.**
Shedding of an Agulhas ring observed at sea p 44 A87-30146
- LYDEN, J. D.**
Geophysics of the marginal ice zone from SAR p 47 A87-17219
- LYNCH, J. F.**
Using Landsat to assess tropical forest habitat for migratory birds in the Yucatan Peninsula p 4 A87-23807
- LYNN, DAVID W.**
Timely thermal infrared data acquisition for soil survey in humid temperature environments p 3 A87-21249
- LYON, R. J. P.**
A knowledge-based software environment for the analysis of spectroradiometer data p 68 A87-17203
Interrelationship between field spectra and airborne MSS systems in the Singatse range, (Yerington) Nevada p 34 A87-17242
- LYONS, WALTER A.**
Forecasting sea breeze thunderstorms at the Kennedy Space Center using the Prognostic Three-Dimensional Mesoscale Model (P 3DM) p 43 A87-27891

M

- MACARTHUR, J. L.**
Development in radar altimetry: The Navy Geosat mission p 85 A87-18161
- MACDONALD, H. C.**
Preliminary analyses of SIB-B radar data for recent Hawaii lava flows p 29 A87-25588
Hawaiian lava flows and SIR-B results p 69 A87-17245
- MACK, MARILYN J. P.**
POLYSITE - An interactive package for the selection and refinement of Landsat image training sites p 65 A87-23805
- MACKAS, D. L.**
Comparison between satellite image advective velocities, dynamic topography, and surface drifter trajectories p 38 A87-20692
An objective method for computing advective surface velocities from sequential infrared satellite images p 39 A87-23717
- MACKLIN, J. T.**
SIR-B observations of ocean waves in the NE Atlantic p 49 A87-17335
- MAECKEL, R.**
Spatial analysis of the dynamics of an ecosystem by multistage remote sensing in Kenya p 16 A87-17173
- MAEDA, K.**
Some results of Marine Observation Satellite (MOS-1) airborne verification experiment Multispectral Electronic Self Scanning Radiometer (MESSR) p 46 A87-17166
Outline of SAR-850 data processing method in Japan p 71 A87-18176
- MAETZER, C.**
Dielectric and surface parameters related to microwave scatter and emission properties p 16 A87-17262
- MAKAREVICH, A. A.**
Identification of reclaimed landscapes of Belorussia from space images p 28 A87-24382
- MAKAROV, V. I.**
Lineaments of eastern Cuba - Geological interpretation of aerial and space imagery p 28 A87-24384
- MALANOTTE-RIZZOLI, PAOLA**
Space and time variability of the surface color field in the northern Adriatic Sea p 40 A87-23722
- MALILA, A.**
Components and comparisons of potential information from several imaging satellites p 67 A87-17164
- MALIN, MICHAEL C.**
Thermal imaging spectroscopy in the Kelso-Baker Region, California p 30 A87-17117
- MALKEVICH, M. S.**
The results of sea-surface temperature determinations from IR and microwave measurements aboard the Cosmos-1151 satellite p 40 A87-24376
- MALMSTROEM, H.**
Marrying geocoded image data with other types of geographic information in a PC environment p 21 A87-18154
- MANDL, P.**
Land surface models as collateral data in satellite image interpretation p 70 A87-18155
- MANLEY, T. O.**
SAR ice floe kinematics and correlation with mesoscale oceanic structure within the marginal ice zone p 48 A87-17222
- MAPPER, D.**
The SEU risk assessment of Z80A, 8086 and 80C86 microprocessors intended for use in a low altitude polar orbit p 74 A87-22025
- MARACCHI, G.**
An integrated system to assess agricultural productivity p 14 A87-15621
An integrated data bank for agricultural productivity by remote sensing p 21 A87-18153
- MARCKWARDT, W.**
Optical visual evaluation and interpretation of remote sensing data p 83 A87-17353
- MARON, ADOLFO**
Marine climate program p 52 A87-17390
- MARTIN, B. D.**
An overview of the NSCAT/N-ROSS program p 52 A87-17384
- MARTIN, R. D.**
Assessing grass canopy condition and growth from combined optical-microwave measurements p 17 A87-17286
- MARTINEC, J.**
Towards snowmelt runoff forecast using LANDSAT-MSS and NOAA/AVHRR data p 61 A87-17317
- MASON, I. M.**
The prospects for hydrological measurements using ERS-1 p 59 A87-15588
Satellite altimeter measurements over land and inland water p 61 A87-18200
- MASUKO, HARUNOBU**
Measurement of microwave backscattering signatures of the ocean surface using X band and K(a) band airborne scatterometers p 40 A87-23725
Development and experiment of airborne microwave rain-scatterometer/radiometer system. III - Rain measurement and its data analysis p 58 A87-28436
Development and experiment of airborne microwave rain-scatterometer/radiometer system. IV - Microwave back-scattering experiment of ocean surface p 43 A87-28437
- MATARESE, J.**
Delineation of fault zones using imaging radar p 32 A87-17138
- MATZLER, C.**
Analysis of multichannel SAR data of Spitsbergen p 60 A87-17223
- MAUSEL, P.**
IRSAP: An improved approach in processing remotely sensed data p 70 A87-17332
- MAUSER, W.**
Comparison of Thematic Mapper (TM) and SPOT simulation data for agricultural applications in south west Germany p 16 A87-17165

- Multitemporal analysis of the phenological stage of vegetation using TM-data in the Southern Black Forest (West Germany) p 22 N87-18184
- MAXWELL, M. S.**
The Sequential Filter Imaging Radiometer (SFIR), a new instrument configuration for Earth observations p 81 N87-17205
- MAXWELL, MARVIN**
Ideas for a future earth observing system from geosynchronous orbit p 74 A87-23419
- MAZIKOV, V. M.**
Determination of the properties of a plowed soil layer from multispectral space imagery p 8 A87-26536
- MCALLISTER, R.**
Volcanology from space - Using Landsat thematic mapper data in the central Andes p 27 A87-20689
- MCARDLE, R.**
The use of space technology in federally funded land processes research in the United States p 88 N87-18152
- MCAVOY, G.**
STAR-VUE: A tactical ice navigation workstation p 54 N87-18181
- MCCAULEY, JOHN F.**
The megageomorphology of the radar rivers of the eastern Sahara p 32 N87-17139
- MCCLAIN, CHARLES R.**
Space and time variability of the surface color field in the northern Adriatic Sea p 40 A87-23722
- MCCORMICK, M. P.**
SAM II measurements of Antarctic PSC's and aerosols p 75 A87-23546
- MCCELROY, JOHN**
Space remote sensing p 86 A87-20682
- MCCELROY, JOHN H.**
Space science and applications: Progress and potential p 87 A87-30876
- MCFARLAND, MARSHALL J.**
Nimbus-7 SMMR multispectral passive microwave correlations with an antecedent precipitation index p 74 A87-23390
- MGILLEM, C.**
Parameter space techniques for image registration p 70 N87-17327
- MCGINNIS, D. F., JR.**
Land surface climatic variables monitored by NOAA-AVHRR satellites p 4 A87-23811
- MCGUFFIE, K.**
Illustration of the influence of shadowing on high latitude information derived from satellite imagery p 62 A87-20768
- MCMILLIN, LARRY M.**
An extension of the split window technique for the retrieval of precipitable water [AD-A173008] p 60 N87-16386
- MCDONNELL, L.**
An overview of operational SAR data collection and dissemination plans for ERS-1 ice data in Canada p 47 N87-17189
Canadian plans for operational demonstrations of satellite imaging radar applications p 68 N87-17229
- MCPHERRON, ROBERT L.**
Geophysical remote sensing p 30 A87-30884
- MCROY, C. P.**
Influence of the Yukon River on the Bering Sea [NASA-CR-180065] p 54 N87-18293
Influence of the Yukon River on the Bering Sea [NASA-CR-180356] p 56 N87-19877
- MEGIER, J.**
Rural land use inventory and mapping in the Ardeche area (France) using multitemporal Thematic Mapping (TM) data p 19 N87-17350
- MEIER, E. H.**
Merging spaceborne image data of optical and microwave sensors p 69 N87-17267
- MEISSNER, B.**
LANDSAT-MSS remote sensing and satellite cartography: An integrated approach to the preparation of a new geological map of Egypt at a scale of 1:500 000 p 36 N87-18190
- MELICE, J. L.**
Estimation of surface albedo using satellite data. A simple formulation for atmospheric effects p 25 N87-15579
- MENDONCA, FRANCISCO JOSE**
CANASATE: Sugar cane mapping by satellite, area 3 [INPE-4068-RPE/526] p 24 N87-19790
- MENEGHINI, ROBERT**
Simultaneous ocean cross section and rainfall measurements from space with a nadir-looking radar p 38 A87-20956
- MENENTI, M.**
Future European plans in the framework of the International Satellite Land Surface Climatology Project (ISLSCP) p 78 N87-15628
- MENENTI, MASSIMO**
An application of thematic mapper data in Tunisia - Estimation of daily amplitude in near-surface soil temperature and discrimination of hypersaline soils p 2 A87-21245
- MENETI, M.**
Ground water-fed lakes in the Libyan desert: Their varying area as observed by means of LANDSAT-MSS data p 59 N87-15611
- MENZ, G.**
Deduction of a synthetic bioclimatological map by means of remote sensing data and a digital terrain model using a correlation approach p 72 N87-18194
- MENZEL, PAUL W.**
Verification of small-scale water vapor features in VAS imagery using high resolution MAMS imagery p 62 A87-23348
- MERCER, J. B.**
Digital terrain mapping with STAR-1 SAR data p 69 N87-17269
- MERCIER, J. L.**
Design of a data base system for inferring land surface parameters and fluxes from satellite radiances p 66 N87-15625
- MEYER, DAVID S.**
Earth sensing - New tools enable scientists to gain insight into the structure of our planet's surface p 29 A87-25890
- MEYER, P.**
Viewing angle corrections of airborne multispectral scanner data acquired over forested surfaces p 17 N87-17273
- MEYER, WALTER**
Multiangle or multiwavelength technique for remote sensing of sea surface temperature p 45 N87-15652
- MEYLAN, P.**
Description of a methodology for biomass change mapping with the use of LANDSAT TM data p 22 N87-18186
- MIGLIETTA, F.**
An integrated system to assess agricultural productivity p 14 N87-15621
- MIKHAILOV, V. I.**
Identification of reclaimed landscapes of Belorussia from space images p 28 A87-24382
- MIKKOLA, P.-V.**
Sea ice studies in the Baltic Sea using satellite microwave radiometer data p 50 N87-17343
- MILEKHIN, O. E.**
An analysis of the potential of satellite-borne bistatic radar sensing of the earth p 75 A87-24385
- MILFORD, J. R.**
Rainfall estimation over the Sahel using Meteosat thermal infra-red data p 59 N87-15587
Hydrological studies in Niger p 59 N87-15609
- MILLER, D. A.**
The application of remotely sensed data to pedologic and geomorphic mapping on alluvial fan and playa surfaces in Saline Valley, California p 15 N87-17127
- MILLINGTON, ANDREW C.**
Monitoring sediment transfer processes on the desert margin [NASA-CR-180181] p 23 N87-18222
- MILTON, E. J.**
Ground radiometry and airborne multispectral survey of bare soils p 10 A87-30894
Remote sensing of structurally complex semi-natural vegetation - An example from heathland p 10 A87-30896
- MINNETT, P. J.**
On the use of synthetic 12-micron data in a split-window retrieval of sea surface temperature from AVHRR measurements p 43 A87-29019
- MOCK, DONALD R.**
Evaluation of geophysical parameters measured by the Nimbus-7 microwave radiometer for the TOGA Heat Exchange Project [NASA-CR-180151] p 78 N87-17110
- MOGNARD, N. M.**
Intersensor comparisons for validation of wind speed measurements from ERS-1 altimeter and scatterometer p 52 N87-17386
- MOLLO-CHRISTENSEN, ERIK**
Oceanographic measurement capabilities of the NASA P-3 aircraft p 52 N87-17380
- MONALDO, F.**
The SAR image modulation transfer function derived from SIR-B image spectra and airborne measurements of ocean wave height spectra p 49 N87-17334
- MONALDO, FRANK**
A procedure for estimation of two-dimensional ocean height-variance spectra from SAR imagery p 52 N87-17381
- MONFILS, ANDRE**
Instrumentation for optical remote sensing from space; Proceedings of the Meeting, Cannes, France, November 27-29, 1985 [SPIE-589] p 73 A87-19647
- MONTEJANO, RITA BARCALA**
Remote Sensing Laboratory [ETN-87-98850] p 88 N87-18227
- MOON, W.**
Application of 2-D Hilbert transform in the interpretation of remotely sensed potential field data p 35 N87-17293
Study of ocean bottom coupling process using satellite altimeter data p 54 N87-18199
- MOORE, R. K.**
Tower-based broadband backscattering measurements from the ocean surface in the North Sea p 47 N87-17217
Some trade-offs in modest-resolution radars for space p 82 N87-17278
- MORALEV, V. M.**
Analysis of correlations between structural elements detected on space images and metallogenic zones p 28 A87-24380
- MORD, A. J.**
Improved multispectral earth imaging from space using electronic image alignment p 73 A87-19655
- MORLEY, BRUCE M.**
Development and demonstration of ALARM (Airborne Lidar Agent Remote Monitor) [AD-A172886] p 78 N87-16387
- MORTON, A. J.**
Moorland plant community recognition using Landsat MSS data p 7 A87-25589
- MOUEDDENE, K.**
Computer-aided interpretation of complex geological patterns in remote sensing p 35 N87-17294
- MOUGINIS-MARK, P.**
Hawaiian lava flows and SIR-B results p 69 N87-17245
- MOUGINIS-MARK, P. J.**
Preliminary analyses of SIB-B radar data for recent Hawaii lava flows p 29 A87-25588
- MUELLER, P. W.**
Analysis of multiple incidence angle SIR-B data for determining forest stand characteristics p 15 N87-17156
- MUKAI, YUKIO**
Extraction of areas infested by pine bark beetle using Landsat MSS data p 10 A87-30129
- MULDERS, MICHEL A.**
The thematic mapper - A new tool for soil mapping in arid areas p 2 A87-21243
- MULLANE, T.**
An overview of operational SAR data collection and dissemination plans for ERS-1 ice data in Canada p 47 N87-17189
Canadian plans for operational demonstrations of satellite imaging radar applications p 68 N87-17229
- MULLER, JAMES R.**
Capabilities for source assessment p 63 A87-23793
- MUNTZER, PAUL**
Visualization by aerial thermography of hydrodynamic exchanges between the water table, streams and gravel pits in the Rhine plain north of Strasbourg p 58 A87-25746
- MURRAY, GENE**
TIMS data applications in Nebraska p 15 N87-17126
- MUTTIT, G.**
Application of the Seasat scatterometer to observations of wind speed and direction and Arctic ice/water boundaries p 48 N87-17259
- MWENDWA, H.**
Estimating pre-harvest production of maize in Kenya using large-scale aerial photography and radiometry p 9 A87-29004
- MYERS, J. S.**
Aircraft and satellite thermographic systems for wildfire mapping and assessment [AIAA PAPER 87-0187] p 7 A87-24933
- MYERS, RICHARD K.**
The use of remote sensing in estimating biomass of fish tree areas in the Richard B. Russell Lake p 40 A87-23834

N

- NAKAMURA, KENJI**
Development and experiment of airborne microwave rain-scatterometer/radiometer system. III - Rain measurement and its data analysis p 58 A87-28436

NAKAMURA, MASAHARU

Pre-assessment for large scale civil engineering projects by integrated analysis with the data numerical topography and remote sensing p 57 A87-23815

NAKAYAMA, N.

High speed image processing system based on the custom VLSI for Digital Signal Processing (DSP) p 71 N87-18179

NAWAYAKKARA, S. D. F. C.

Monitoring of land-surface change in Sri Lanka p 13 N87-15618
Sri Lanka's solution to land use mapping and monitoring for Third World countries development p 67 N87-17174

NATH, J.

Remote sensing applications in the study of land use and soils of aeolian cover of the western part of Haryana State, India p 22 N87-18187

NAVARRO, A. A.

Cartographic analysis of remote sensing data through Landsat mosaic scaling p 65 A87-23809

NAVONE, S.

Soil degradation evaluation by digital image processing p 20 N87-18147

NEJEDLY, G.

Atmospheric corrections of NOAA-AVHRR data verification of different methods by ground truth measurements p 70 N87-17274

NELSON, CRAIG S.

The effect of Hurricane Gloria on sea surface temperature patterns p 39 A87-23362

NEMOTO, YOSHIKI

Present statue of Japanese ERS-1 Project p 79 N87-17145

NEWTON, LAURENCE

Control extension utilizing Large Format Camera imagery p 75 A87-23804

NIELSEN, NORM B.

Development and demonstration of ALARM (Airborne Lidar Agent Remote Monitor) [AD-A172886] p 78 N87-16387

NIEUWENHUIS, GERARD J. A.

Thermography - Principles and application in the Coast-Gelderland remote sensing study project p 3 A87-21247

NIGRO, L.

Multispectral classification of microwave remote sensing images p 16 N87-17238

NINNIS, R. M.

Automated extraction of pack ice motion from advanced very high resolution radiometer imagery p 42 A87-27547

NISHIKAWA, K.

A satellite-borne SAR transmitter and receiver p 83 N87-17358

Pulse compression test results of the SAR transmitter and receiver p 83 N87-17360

NISHINO, H.

A satellite-borne SAR transmitter and receiver p 83 N87-17358

Pulse compression test results of the SAR transmitter and receiver p 83 N87-17360

NIWA, SHUNTARO

Measurement of microwave backscattering signatures of the ocean surface using X band and K(a) band airborne scatterometers p 40 A87-23725

NIXON, P. R.

Evaluation of the mid-infrared (1.45 to 2.0 microns) with a black-and-white infrared video camera p 73 A87-20672

Assessment of grassland phytomass with airborne video imagery p 8 A87-25590

NJOKU, ENI G.

Observations of the seasonal variability of soil moisture and vegetation cover over Africa using satellite microwave radiometry p 12 N87-15593

NOACK, W.

Results of an airborne synthetic-aperture radar (SAR) experiment over a SIR-B (Shuttle Imaging Radar) test site in Germany p 76 A87-27999

Intelligent SAR Processor (ISAR), a new concept for high throughput and high precision digital SAR processing p 85 N87-18178

NOBLE, DONALD C.

Nature and origin of mineral coatings on volcanic rocks of the Black Mountain, Stonewall Mountain, and Kane Springs, Wash volcanic centers, Southern Nevada [NASA-CR-180183] p 36 N87-18255

NORDIUS, H.

Atmospheric water vapor corrections for altimetry measurements p 85 N87-18197

NOVO, EVELYN MARCIA LEO DEMORAES

Application of remote sensing in hydrology and water resources [INPE-3986-PRE/991] p 60 N87-16382

NUESCH, D. R.

Merging spaceborne image data of optical and microwave sensors p 69 N87-17267

NYQUIST, MAURICE O.

Use of topographic and climatological models in a geographical data base to improve Landsat MSS classification for Olympic National Park p 25 A87-30128

O**OCHIAI, H.**

Estimation of maximum snow volume distribution using NOAA-AVHRR data p 60 N87-17314

OCHOA, M. C.

Applications of TIMS data in agricultural areas and related atmospheric considerations p 15 N87-17124

ODERWALD, RICHARD

The data dilemma - How to properly construct and utilize aerial photo volume tables p 63 A87-23790

OFFILER, DAVID

The use of aircraft for wind scatterometer calibration p 84 N87-17382

OKAMOTO, KENICHI

Measurement of microwave backscattering signatures of the ocean surface using X band and K(a) band airborne scatterometers p 40 A87-23725

Development and experiment of airborne microwave rain-scatterometer/radiometer system. III - Rain measurement and its data analysis p 58 A87-28436

Development and experiment of airborne microwave rain-scatterometer/radiometer system. IV - Microwave back-scattering experiment of ocean surface p 43 A87-28437

OLAUSSEN, T.

Geophysics of the marginal ice zone from SAR p 47 N87-17219

OLORY-HECHINGER, E.

Design of a data base system for inferring land surface parameters and fluxes from satellite radiances p 66 N87-15625

OLORY, P.

Design of a data base system for inferring land surface parameters and fluxes from satellite radiances p 66 N87-15625

OLSON, JERRY S.

Interpreting forest and grassland biome productivity utilizing nested scales of image resolution and biogeographical analysis [NASA-CR-180213] p 23 N87-18912

ONORATI, G.

Integrated analysis of geological and remote sensing data aimed at mineral deposits detection in the Monapo area (northern Mozambique) p 34 N87-17243

ONSTOTT, R. G.

An inter-sensor comparison of the microwave signatures of Arctic sea ice p 46 N87-17184

OOST, WIEBE A.

The accuracy and availability of operational marine surface wind data for ERS-1 sensor calibration and validation from fixed platforms and free drifting buoys p 51 N87-17376

OSAKI, E.

High speed image processing system based on the custom VLSI for Digital Signal Processing (DSP) p 71 N87-18179

OSHIMA, TAICHI

Pre-assessment for large scale civil engineering projects by integrated analysis with the data numerical topography and remote sensing p 57 A87-23815

OSHIMA, Y.

High speed image processing system based on the custom VLSI for Digital Signal Processing (DSP) p 71 N87-18179

OSTMAN, ANDERS

A comparative test of photogrammetrically sampled digital elevation models p 66 A87-29499

OTENGI, SILVERY B. B.

Use of remote sensing application for agricultural expansion into semi-arid areas of Kenya p 13 N87-15607

OTTICHILO, W. K.

Estimating pre-harvest production of maize in Kenya using large-scale aerial photography and radiometry p 9 A87-29004

OVECHKIN, V. N.

Investigation of spectral correlations of vegetation growing on different types of geological structures p 29 A87-28508

P**PAETZOLD, RON F.**

NMR instrument for soil moisture ground-truth data collection p 2 A87-21240

PALLUCONI, FRANK D.

The TIMS investigator's guide p 79 N87-17113

PALOSCIA, S.

Contribution of passive microwave remote sensing in soil moisture and evapotranspiration measurements p 12 N87-15589

PALUSZKIEWICZ, THERESA

Mesoscale hydrographic variability in the vicinity of Points Conception and Arguello during April-May 1983 - The OPUS 1983 experiment p 39 A87-23719

PAMPALONI, P.

Contribution of passive microwave remote sensing in soil moisture and evapotranspiration measurements p 12 N87-15589

PANDEY, P. C.

Wind-wave relationship from Seasat radar altimeter data p 41 A87-24748
Retrieval and global comparison of oceanic winds from SEASAT radiometer, scatterometer and altimeter p 85 N87-18219

PANENKO, V. V.

Exact determination of wave parameters from the results of Fourier analysis of sea-surface radar imagery p 41 A87-24377

PANFILOVICH, ANATOLY I.

Mapping of agricultural lands in the USSR p 11 N87-15507

PARASHAR, S.

Canadian plans for operational demonstrations of satellite imaging radar applications p 68 N87-17229

PARASKEVOPOULOS, S.

The use of remote sensing techniques in the study of vegetation recovery after fire in mediterranean countries (a preliminary study) p 14 N87-15623

PARSONS, A. J.

An analysis of geologic lineaments seen on Landsat MSS imagery p 30 A87-29011

PARTON, M. C.

An iterative Landsat-MSS classification methodology for soil survey p 3 A87-23797

PASQUARIELLO, G.

UMUS: A project for usage of LANDSAT MSS and ancillary data in land cover mapping of large areas in southern Italy p 72 N87-18191

PATEL, INDU R.

Observations of the seasonal variability of soil moisture and vegetation cover over Africa using satellite microwave radiometry p 12 N87-15593

PATTIARATCHI, C. B.

Mapping of water quality in coastal waters using Airborne Thematic Mapper data p 58 A87-30899

PATTIARATCHI, CHARITHA

Island wakes and headland eddies - A comparison between remotely sensed data and laboratory experiments p 44 A87-30925

PAVELEV, A. G.

An analysis of the potential of satellite-borne bistatic radar sensing of the earth p 75 A87-24385

PECH, R. P.

Calibration of Landsat data for sparsely vegetated semi-arid rangelands p 9 A87-29008

PEDEN, D. G.

Estimating pre-harvest production of maize in Kenya using large-scale aerial photography and radiometry p 9 A87-29004

PEDERSEN, L. T.

Sea ice in the Greenland sea observed by the Nimbus-7 Scanning Multichannel Microwave Radiometer (SMMR) p 48 N87-17221

PEDROFERNANDES, A. T.

Computer-aided analysis of LANDSAT data for mapping geologic and geomorphic features, North Bombay, India p 33 N87-17235

PELAEZ, JOSE

Temperature-plant pigment-optical relations in a recurrent offshore mesoscale eddy near Point Conception, California [AD-A176666] p 39 A87-23720

Biological consequences of a recurrent eddy off Point Conception, California p 40 A87-23721

PELLETIER, R. E.

Applications of TIMS data in agricultural areas and related atmospheric considerations p 15 N87-17124

PERTSOV, A. V.

Use of space imagery and geophysical data in metallogenic prediction studies in central Kyzykum p 28 A87-24383

PESSANHA, L.

Digital satellite imagery acquisition and processing p 68 N87-17207

PETERHERYCH, S.

PETERHERYCH, S.

Application of the Seasat scatterometer to observations of wind speed and direction and Arctic ice/water boundaries p 48 N87-17259

PETERS, ALPHEN

Evaluation of remote sensing results for the benefit of water quality research on the North Sea [NZ-R-86.15] p 62 N87-19799

PETERSEN, G. W.

The application of remotely sensed data to pedologic and geomorphic mapping on alluvial fan and playa surfaces in Saline Valley, California p 15 N87-17127

PETRENKO, B. Z.

The results of sea-surface temperature determinations from IR and microwave measurements aboard the Cosmos-1151 satellite p 40 A87-24376

PETTINGILL, G. H.

Delineation of fault zones using imaging radar p 32 N87-17138

PHILIPSON, W. R.

Landsat Thematic Mapper images for hydrologic land use and cover p 58 A87-23831
Vegetable crop inventory with Landsat TM data p 5 A87-23833

PHILIPSON, WARREN R.

Fruit tree inventory with Landsat Thematic Mapper data p 8 A87-28387

PHILPOT, W. D.

Landsat Thematic Mapper images for hydrologic land use and cover p 58 A87-23831
Vegetable crop inventory with Landsat TM data p 5 A87-23833

PHILPOT, WILLIAM D.

Fruit tree inventory with Landsat Thematic Mapper data p 8 A87-28387

PICH, M.

Intelligent SAR Processor (ISAR), a new concept for high throughput and high precision digital SAR processing p 85 N87-18178

PICHEL, WILLIAM G.

The effect of Hurricane Gloria on sea surface temperature patterns p 39 A87-23362

PICKARD, G. L.

The Coastal Zone Color Scanner views the Bismarck Sea p 42 A87-26970

PIELKE, ROGER A.

Forecasting sea breeze thunderstorms at the Kennedy Space Center using the Prognostic Three-Dimensional Mesoscale Model (P 3DM) p 43 A87-27891

PIERCE, LARS L.

An assessment of evapotranspirational water losses in a Sierran Mixed Conifer forest using remotely sensed data p 4 A87-23816

PIERSON, W. J., JR.

Verification results for a two-scale model of microwave backscatter from the sea surface p 47 N87-17213

PINKER, R. T.

Effect of surface properties on the narrow to broadband spectral relationship in clear sky satellite observations p 65 A87-25587

PINKERTON, B.

Assessment of grassland phytomass with airborne video imagery p 8 A87-25590

PIOTROWICZ, STEPHEN R.

Ozone in the boundary layer of the equatorial Pacific Ocean p 41 A87-25534

PLUMMER, DAVID W.

Data sensitivities of sea ice drift and ocean stress in North Atlantic high latitudes p 38 A87-20520

POEHLMANN, G.

LANDSAT-MSS remote sensing and satellite cartography: An integrated approach to the preparation of a new geological map of Egypt at a scale of 1:500 000 p 36 N87-18190

POKROVSKAIA, I. V.

Spatial-statistical characteristics of sea surface foam fields (from optical sounding data) p 42 A87-26531

POLLARD, R. T.

SeaSoar CTD surveys during FASINEX [IOS-230] p 55 N87-18970

POPELLA, A.

Intelligent SAR Processor (ISAR), a new concept for high throughput and high precision digital SAR processing p 85 N87-18178

POSCOLIERI, M.

Integrated analysis of geological and remote sensing data aimed at mineral deposits detection in the Monapo area (northern Mozambique) p 34 N87-17243

POUGET, MARCEL

Spectral brightness and surface soil characteristics in an arid Mediterranean region (southern Tunisia) p 2 A87-21242

POWELL, REDVERS JOHN

Gathering and processing a comparative data set for the calibration and validation of ERS-1 data products; preparatory work at the UK-ERS-DC p 50 N87-17367

POWERS, B. J.

Canopy hot-spot as crop identifier [DE86-011258] p 19 N87-17395

PRANGE, M.

Delineation of fault zones using imaging radar p 32 N87-17138

PRICE, J. C.

Applications of remote sensing in the US Department of Agriculture p 17 N87-17285

PRINCE, S. D.

Rainfall and vegetation monitoring in the Savanna Zone of the Democratic Republic of Sudan using the NOAA Advanced Very High Resolution Radiometer p 6 A87-24783

Satellite remote sensing of rangelands in Botswana. I - Landsat MSS and herbaceous vegetation p 7 A87-24785

Satellite remote sensing of rangelands in Botswana. II - NOAA AVHRR and herbaceous vegetation p 7 A87-24786

Monitoring the grasslands of the Sahel 1984-1985 p 7 A87-24787

PROULX, H.

Analysis of the spatial structure of Synthetic Aperture Radar (SAR) imagery for a better separability of cereal crops, wheat and barley p 17 N87-17287

PULLEN, PATRICIA E.

Equatorial long-wave characteristics determined from satellite sea surface temperature and in situ data p 44 A87-30923

PUNJABI, A.

Correlation between time- and depth-resolved simulated lidar signals p 38 A87-20770

PURDOM, JAMES F. W.

Satellite contributions to convective scale weather analysis and forecasting p 76 A87-27882

PYLE, T. E.

The application of geodetic radio interferometric surveying to the monitoring of sea-level p 39 A87-21367

Q

QUARMBY, N. A.

Preliminary analysis of SPOT HRV multispectral products of an arid environment p 10 A87-29017

QUARMBY, NEIL

Monitoring sediment transfer processes on the desert margin [NASA-CR-180181] p 23 N87-18222

QUEEN, LLOYD

TIMS data applications in Nebraska p 15 N87-17126

R

RAFFY, M.

Design of a data base system for inferring land surface parameters and fluxes from satellite radiances p 66 N87-15625

RAGGAM, J.

Space Shuttle radargrammetry results p 65 A87-23827

RAGHAVAN, V.

Significance of space image, air photo and drainage linears in relation to west coast tectonics, India p 33 N87-17232

Computer-aided analysis of LANDSAT data for mapping geologic and geomorphic features, North Bombay, India p 33 N87-17235

RAHN, KENNETH A.

Arctic haze: Natural or pollution? [AD-A174025] p 55 N87-18931

RAI, R. K.

Structural and geomorphic evolution of Meghalaya plateau, India on LANDSAT imagery p 33 N87-17233

RAITALA, J.

Remote sensing of shallow water areas with reference to environmental and multitemporal monitoring of the Hailuoto area, Finland p 61 N87-18159

RAIZER, V. I.

Optical and radar observations of the nonlinear interaction of gravity waves p 37 A87-20350

RAJASENAN, C.

NROSS (Navy Remote Ocean Sensing System) tracking network analysis [AD-A172132] p 45 N87-16384

RAMSEIER, R.

Comparison concept of satellite derived wind and wave data with ground truth p 51 N87-17373

RANGANATH, B. K.

AVHRR and MSS data based vegetation indices studies over Indian sites p 14 N87-15622

RAPLEY, C. G.

The prospects for hydrological measurements using ERS-1 p 59 N87-15588

New techniques in satellite altimeter tracking systems p 85 N87-18164

Satellite altimeter measurements over land and inland water p 61 N87-18200

RASOOL, S. ICHTIAQUE

Weather and atmosphere remote sensing p 77 A87-30885

RAST, M.

Concept of a future multispectral Thermal Infrared (TIR) pushbroom mission for Earth observation from space p 80 N87-17169

RATTI, BRUNO

Business approach to earth observation applications p 87 A87-29433

RAYMOND, WILLIAM H.

Data sensitivities of sea ice drift and ocean stress in North Atlantic high latitudes p 38 A87-20520

READ, J. F.

SeaSoar CTD surveys during FASINEX [IOS-230] p 55 N87-18970

REICHART, B.

Hydrogeological research in Peloponnesus (Greece) Karst area by support and completion of LANDSAT-thematic data p 33 N87-17234

REUTER, D.

Remote sensing of land-surface temperature from HIRS/MSU data p 77 N87-15573

REYNOLDS, M. L.

Concept of a future multispectral Thermal Infrared (TIR) pushbroom mission for Earth observation from space p 80 N87-17169

RICCIO, E.

Satellite remote sensing of the marine environment: Literature and data sources [PB86-245446] p 56 N87-18971

RICHARDS, J. A.

Radar signature determination: Trends and limitations p 67 N87-17159

RICHARDSON, ARTHUR J.

Diurnal-seasonal light interception, leaf area index, and vegetation index interrelations in a wheat canopy - A case study p 5 A87-23822

Detection of new urban build-up in Ardmore and McAlester, Oklahoma using Landsat MSS data p 25 A87-23829

RICHTER, K.

On the discrimination between crude oil spills and monomolecular sea slicks by airborne remote sensors: Today's possibilities and limitations p 53 N87-18167

RICKMAN, DOUG

Atmospheric correction of TIMS data p 79 N87-17115

RIES, J. C.

Accurate measurement of mean sea level changes by altimetric satellites p 38 A87-20524

NROSS (Navy Remote Ocean Sensing System) tracking network analysis [AD-A172132] p 45 N87-16384

RIGGAN, P. J.

Aircraft and satellite thermographic systems for wildfire mapping and assessment [AIAA PAPER 87-0187] p 7 A87-24933

RIKHTER, D. G.

Analysis of correlations between structural elements detected on space images and metallogenic zones p 28 A87-24380

RIKIMARU, ATSUSHI

Pre-assessment for large scale civil engineering projects by integrated analysis with the data numerical topography and remote sensing p 57 A87-23815

RIMMER, J. C.

Mapping of water quality in coastal waters using Airborne Thematic Mapper data p 58 A87-30899

RIPPLE, WILLIAM J.

Phenological effects on grass canopy/spectral relationships p 4 A87-23818

RISSEY, PAUL G.

Interpreting forest and grassland biome productivity utilizing nested scales of image resolution and biogeographical analysis [NASA-CR-180213] p 23 N87-18912

ROBERTS, B.

Satellite remote sensing of the marine environment: Literature and data sources [PB86-245446] p 56 N87-18971

ROBERTSON, D. S.

The application of geodetic radio interferometric surveying to the monitoring of sea-level p 39 A87-21367

ROBINSON, DAVID A.

Remotely sensed albedo of snow-covered lands p 56 A87-23361

- ROCHON, G.**
Spatial remote sensing to land management
p 70 N87-18157
- ROCK, B. N.**
Assessing forest decline in coniferous forests of Vermont using NS-001 Thematic Mapper Simulator data
p 1 A87-20763
Remote detection of forest damage p 8 A87-26197
Use of TMS/TM data for mapping of forest decline damage in the northeastern United States
p 22 N87-18175
- ROFFEY, J.**
Assessment of ecological conditions associated with the 1980/81 desert locust plague upsurge in West Africa using environmental satellite data
p 7 A87-24789
- ROSEMA, A.**
Group Agromet Monitoring Project (GAMP) methodology integrated mapping of rainfall, evapotranspiration, germination, biomass development and thermal inertia, based on Meteosat and conventional meteorological data
p 59 N87-15626
- ROSENTHAL, DANIEL ALFREDO**
CANASATE: Sugar cane mapping by satellite, area 3 [INPE-4068-RPE/526]
p 24 N87-19790
- ROSS, BECKY**
Data sensitivities of sea ice drift and ocean stress in North Atlantic high latitudes
p 38 A87-20520
- ROSS, M. N.**
Tidal heating in an internal ocean model of Europa
p 43 A87-30143
- ROTHROCK, DREW**
Observing the polar oceans with spaceborne radar
p 46 N87-17151
- ROWNTREE, P. R.**
Remote sensing identified in climate model experiments with hydrological and albedo changes in the Sahel
p 59 N87-15569
- RUF, C.**
The Electronically Steered Thinned Array Radiometer (ESTAR)
p 82 N87-17260
- RUNCO, SUSAN K.**
The relationship between marine aerosol optical depth and satellite-sensed sea surface temperature [AD-A174337]
p 55 N87-18963
- RUSSAK, SIDNEY L.**
Instrumentation for optical remote sensing from space: Proceedings of the Meeting, Cannes, France, November 27-29, 1985 [SPIE-589]
p 73 A87-19647
- RUTH, BYRON E.**
Landsat Thematic Mapper data analysis within the Suwannee River Basin
p 57 A87-23825
- RUZEK, M. J.**
Analysis of multiple incidence angle SIR-B data for determining forest stand characteristics
p 15 N87-17156
- RZHEPLINSKII, D. G.**
Possibilities of using satellite data for computations of the ocean/atmosphere heat exchange in the Newfoundland energy-active ocean zone in winter
p 41 A87-24379
- S**
- SABINS, FLOYD F.**
Space shuttle radar images of Indonesia
p 32 N87-17137
- SACCO, V.**
An integrated system to assess agricultural productivity
p 14 N87-15621
- SADER, STEVEN A.**
Investigation of forest canopy temperatures recorded by the thermal infrared multispectral scanner at H. J. Andrews Experimental Forest
p 14 N87-17123
- SAFFMAN, P. G.**
SAR imaging of bottom topography in the ocean: Results from an improved model
p 48 N87-17298
- SALISBURY, JOHN W.**
Preliminary measurements of leaf spectral reflectance in the 8-14/micron
p 10 A87-29018
- SALVI, S.**
Integrated analysis of geological and remote sensing data aimed at mineral deposits detection in the Monapo area (northern Mozambique)
p 34 N87-17243
- SAMADANI, R.**
Automated remote sensing of sea ice using synthetic aperture radar
p 46 N87-17186
- SAMUELS, BONITA L.**
The impact of satellite infrared sea surface temperatures on FNOC (Fleet Numerical Oceanography Center) ocean thermal analyses [AD-A173333]
p 54 N87-18295
- SANDWELL, D. T.**
Undersea volcano production versus lithospheric strength from satellite altimetry [NASA-CR-179984]
p 78 N87-15660
- SANGSTER, A. B.**
Remote sensing identified in climate model experiments with hydrological and albedo changes in the Sahel
p 59 N87-15569
- SANSOE, C.**
The SEU risk assessment of Z80A, 8086 and 80C86 microprocessors intended for use in a low altitude polar orbit
p 74 A87-22025
- SARKAR, A.**
A new semi-empirical sea spectrum for estimating the scattering coefficient
p 38 A87-20769
- SASSI, K.**
Proposal of a remote sensing method for measuring soil moisture of bare soils in the frequency range 100 MHz-1 GHz
p 8 A87-26974
- SAULSKII, V. K.**
Method for computing the periodicity of a remote-sensing survey
p 65 A87-26540
- SAVITSKY, BASIL G.**
Agricultural remote sensing in South Carolina - A study of crop identification capabilities utilizing Landsat data
p 4 A87-23806
- SAZONOV, N. V.**
Automation of thematic processing of space images in evaluating crop condition
p 8 A87-26539
- SCARPACE, FRANK L.**
Performance of selected spatial domain edge detection algorithms for earth resources application
p 64 A87-23798
- SCHABER, GERALD G.**
The megageomorphology of the radar rivers of the eastern Sahara
p 32 N87-17139
- SCHANDA, E.**
L to X-band scatter and emission measurements of vegetation
p 19 N87-17347
- SCHENCK, L. R.**
On the relationship between age of lava flows and radar backscattering
p 35 N87-17348
- SCHERZ, JAMES P.**
Photometric functions, reflectance map - Two techniques for determining surface shape and orientation from image intensity
p 64 A87-23802
- SCHMID, P.**
Monitoring land use changes in Sri Lanka for land use planning using a geographic information system and satellite imagery
p 26 N87-18151
- SCHMUGGE, T. J.**
The first International Satellite Land Surface Climatology Project (ISLSCP) Field Experiment - FIFE
p 14 N87-15629
- SCHNEIDER, G.**
Sri Lanka's solution to land use mapping and monitoring for Third World countries development
p 67 N87-17174
- SCHOLEN, DOUGLAS E.**
Locating subsurface gravel with thermal imagery
p 31 N87-17125
- SCHOTT, JOHN R.**
Radiometric analysis of the longwave infrared channel of the Thematic Mapper on LANDSAT 4 and 5 [NASA-CR-180180]
p 86 N87-18221
- SCHOTTER, R.**
Digital realtime SAR processor for C- and X-band applications
p 71 N87-18177
- SCHREIBER, H.**
Contributions to oil spill detection and analysis with radar and microwave radiometry, results of the Archimedes 2 campaign
p 54 N87-18170
- SCHRIEL, R. C.**
On the discrimination between crude oil spills and monomolecular sea slicks by airborne remote sensors: Today's possibilities and limitations
p 53 N87-18167
- SCHROEDER, LYLE C.**
Archival of Seasat-A satellite scatterometer data merged with in situ data at selected, illuminated sites over the ocean [NASA-TM-87736]
p 45 N87-16492
- SCHUBERT, G.**
Tidal heating in an internal ocean model of Europa
p 43 A87-30143
- SCHUCHMAN, R. A.**
Geophysics of the marginal ice zone from SAR
p 47 N87-17219
- SCHUH, JEROME A.**
Forecasting sea breeze thunderstorms at the Kennedy Space Center using the Prognostic Three-Dimensional Mesoscale Model (P 3DM)
p 43 A87-27891
- SCHULTZ, S.**
Analysis of AIS radiometry at Mono Lake, California
p 81 N87-17204
- SCHUTT, J. B.**
Utility of AVHRR channels 3 and 4 in land-cover mapping
p 9 A87-28388
- SEELEY, JOHN S.**
Instrumentation for optical remote sensing from space: Proceedings of the Meeting, Cannes, France, November 27-29, 1985 [SPIE-589]
p 73 A87-19647
- SEGAL, MOTI M.**
Forecasting sea breeze thunderstorms at the Kennedy Space Center using the Prognostic Three-Dimensional Mesoscale Model (P 3DM)
p 43 A87-27891
- SEGER, M.**
Land surface models as collateral data in satellite image interpretation
p 70 N87-18155
- SEIDEL, K.**
Snow cover recession in an Alpine ecological system
p 18 N87-17316
Towards snowmelt runoff forecast using LANDSAT-MSS and NOAA/AVHRR data
p 61 N87-17317
- SEKER, S. S.**
Microwave backscattering from a layer of randomly oriented discs with application to scattering from vegetation
p 8 A87-28316
- SEKI, T.**
Estimation of maximum snow volume distribution using NOAA-AVHRR data
p 60 N87-17314
- SELLERS, P. J.**
Satellite remote sensing of primary production
p 6 A87-24777
The first International Satellite Land Surface Climatology Project (ISLSCP) Field Experiment - FIFE
p 14 N87-15629
- SEYLER, F.**
First step in the use of remote sensing for regional mapping of soil organization data: Application in Brittany (France) and French Guiana
p 23 N87-18193
- SHAIN, WILLIAM A.**
The use of remote sensing in estimating biomass of fish tree areas in the Richard B. Russell Lake
p 40 A87-23834
- SHARKOV, E. A.**
Spatial-statistical characteristics of sea surface foam fields (from optical sounding data)
p 42 A87-26531
- SHEMDIN, OMAR H.**
Investigation of physics of synthetic aperture radar in ocean remote sensing toward 84/86 field experiment. Volume 1: Data summary and early results [AD-A174197]
p 55 N87-18913
Investigation of physics of synthetic aperture radar in ocean remote sensing TOWARD 84/86 field experiment. Volume 2: Contributions of individual investigators [AD-A174527]
p 55 N87-18966
- SHENK, WILLIAM E.**
Ideas for a future earth observing system from geosynchronous orbit
p 74 A87-23419
- SHEREMET, O. G.**
Analysis of correlations between structural elements detected on space images and metallogenic zones
p 28 A87-24380
- SHIMADA, MASANOBU**
Measurement of microwave backscattering signatures of the ocean surface using X band and K(a) band airborne scatterometers
p 40 A87-23725
Development and experiment of airborne microwave rain-scatterometer/radiometer system. IV - Microwave back-scattering experiment of ocean surface
p 43 A87-28437
- SHINOHARA, H.**
Pulse compression test results of the SAR transmitter and receiver
p 83 N87-17360
- SHORT, NICHOLAS M.**
Geomorphology from space: A global overview of regional landforms [NASA-SP-486]
p 36 N87-18139
- SHUCHMAN, R.**
Analysis of multichannel SAR data of Spitsbergen
p 60 N87-17223
- SHUCHMAN, R. A.**
SAR ice floe kinematics and correlation with mesoscale oceanic structure within the marginal ice zone
p 48 N87-17222
- SHUCHMAN, ROBERT A.**
Imaging radar contributions to a major air-sea-ice interaction study in the Greenland Sea
p 46 N87-17150
- SHUTKO, A. M.**
Use of decimeter waves in studies of water bodies by methods of microwave radiometry
p 58 A87-26537
- SHVYRKOV, N. N.**
Possibilities of using satellite data for computations of the ocean/atmosphere heat exchange in the Newfoundland energy-active ocean zone in winter
p 41 A87-24379

T

SIEBER, A.

Results of an airborne synthetic-aperture radar (SAR) experiment over a SIR-B (Shuttle Imaging Radar) test site in Germany p 76 A87-27999

SIMMER, C.

Canopy hot-spot as crop identifier [DE86-011258] p 19 N87-17395

SIMON, BABY

Equatorial Indian Ocean evaporation estimates from operational meteorological satellites and some inferences in the context of monsoon onset and activity p 39 A87-22041

SIMONETT, DAVID

Canopy reflectance modeling in a tropical wooded grassland [NASA-CR-180097] p 11 N87-15518

SIMPSON, JAMES J.

Temperature-plant pigment-optical relations in a recurrent offshore mesoscale eddy near Point Conception, California [AD-A176666] p 39 A87-23720
Biological consequences of a recurrent eddy off Point Conception, California p 40 A87-23721

SINGH, M.

Application of remote sensing in the study of the soil hazards of Haryana State, India p 20 N87-18150
Remote sensing applications in the study of land use and soils of aeolian cover of the western part of Haryana State, India p 22 N87-18187

SIVERTSON, W. E., JR.

Space Shuttle cloud detection and earth feature classification experiment p 77 A87-31139

SKORVE, J. E.

A climatological-hydrological study of lake ice in the southwestern mountain area in Norway by use of satellite sensing p 61 N87-17319

SKOU, N.

On the discrimination between crude oil spills and monomolecular sea slicks by airborne remote sensors: Today's possibilities and limitations p 53 N87-18167

SLANEY, V. R.

Canadian plans for operational demonstrations of satellite imaging radar applications p 68 N87-17229

SLATER, PHILIP N.

Variations in in-flight absolute radiometric calibration p 77 N87-15594

SLOGGETT, D. R.

The design of an international data centre for remote sensing p 67 N87-17176

SLOTH, P.

Sea ice in the Greenland sea observed by the Nimbus-7 Scanning Multichannel Microwave Radiometer (SMMR) p 48 N87-17221

SMART, JOHN R.

Observations and analysis of a polar low over the Great Lakes region p 76 A87-27872

SMIRNOV, A. V.

Optical and radar observations of the nonlinear interaction of gravity waves p 37 A87-20350

SMITH, GARY S.

Techniques for deriving land use information from Landsat data through the use of a geographic information system p 24 A87-23828

SMITH, JAMES

The data dilemma - How to properly construct and utilize aerial photo volume tables p 63 A87-23790

SMITH, JAMES L.

Estimation of density in young pine plantations using 35mm aerial photography p 5 A87-23819

SMITH, LAWSON

The Red River Valley archeological project p 31 N87-17128

SMITH, M. P.

Automated remote sensing of sea ice using synthetic aperture radar p 46 N87-17186

SMITH, P.

Observations of surface currents at Nantucket Shoals and implications for radar imaging of the bottom p 48 N87-17296

SMITH, TERENCE

Remote Sensing Information Sciences Research Group, year four [NASA-CR-180198] p 88 N87-18907

SMITHERS, J.

SeaSoar CTD surveys during FASINEX [IOS-230] p 55 N87-18970

SNYDER, MICHAEL W.

Classification of multivariate Thematic Mapper data p 64 A87-23795

SOBIESKI, P.

A two-step algorithm for the separate retrieval of ocean surface and atmospheric parameters from microwave radiometers p 50 N87-17341

SPATZ, DAVID M.

Nature and origin of mineral coatings on volcanic rocks of the Black Mountain, Stonewall Mountain, and Kane Springs, Wash volcanic centers, Southern Nevada [NASA-CR-180183] p 36 N87-18255

SPAYD, LEROY E., JR.

Detecting and forecasting western region flash floods using GOES imagery and conventional data p 58 A87-27883

SPECTER, C.

The transfer of remote sensing technology to developing countries: A survey of experts in the field p 87 N87-17170

SPENCE, THOMAS

Physical oceanography program science abstracts [AD-A174019] p 55 N87-18961

SPIESS, E.

Point positioning and mapping with Large Format Camera data p 71 N87-18188

ST-CYR, GAETAN

A radar ocean imaging model for small to moderate incidence angles p 43 A87-29015

STAENZ, K.

Viewing angle corrections of airborne multispectral scanner data acquired over forested surfaces p 17 N87-17273

STANICH, CHUCK

The TIMS instrument p 79 N87-17112

STAR, JEFFREY L.

Remote Sensing Information Sciences Research Group, year four [NASA-CR-180198] p 88 N87-18907

STEINER, ELLEN J.

Atmospheric characteristics of the equatorial Pacific during the 1982-1983 El Nino, deduced from satellite and aircraft observations p 41 A87-25543

STEVENS, PAYSON R.

Ocean remote sensing p 44 A87-30883

STEWART, R. H.

Accurate measurement of mean sea level changes by altimetric satellites p 38 A87-20524

STIBIG, H.-J.

Comparison of Thematic Mapper (TM) and SPOT simulation data for agricultural applications in south west Germany p 16 N87-17165

STORY, MICHAEL H.

Classification of multivariate Thematic Mapper data p 64 A87-23795

STORY, MICHAEL H.

The effect of training data variability on classification accuracy p 64 A87-23796

STOTZER, E.

Dielectric and surface parameters related to microwave scatter and emission properties p 16 N87-17262

STREET-PERROTT, F. A.

The prospects for hydrological measurements using ERS-1 p 59 N87-15588

SUGIMURA, TOSHIRO

Extraction of areas infested by pine bark beetle using Landsat MSS data p 10 A87-30129

SUOMI, VERNER E.

Ideas for a future earth observing system from geosynchronous orbit p 74 A87-23419

SUSSKIND, J.

Remote sensing of land-surface temperature from HIRS/MSU data p 77 N87-15573

SUZUKI, K.

High speed image processing system based on the custom VLSI for Digital Signal Processing (DSP) p 71 N87-18179

SVENDSEN, E.

Geophysics of the marginal ice zone from SAR p 47 N87-17219

SWEET, JON L.

Archival of Seasat-A satellite scatterometer data merged with in situ data at selected, illuminated sites over the ocean [NASA-TM-87736] p 45 N87-16492

SWIFT, C. T.

The Electronically Steered Thinned Array Radiometer (ESTAR) p 82 N87-17260

SWIFT, CALVIN

Intersensor comparisons for validation of wind speed measurements from ERS-1 altimeter and scatterometer p 52 N87-17386

SWIFT, ROBERT N.

Chlorophyll pigment concentration using spectral curvature algorithms - An evaluation of present and proposed satellite ocean color sensor bands p 37 A87-20204

TABBAGH, A.

Proposal of a remote sensing method for measuring soil moisture of bare soils in the frequency range 100 MHz-1 GHz p 8 A87-26974

The use of thermal airborne remote sensing for soil identification: A case study in Limousin (France) p 20 N87-18146

TACONET, O.

Modelisation of evapotranspiration and soil available water over an agricultural region applicable for remote sensing p 12 N87-15554

Toward a satellite system to monitor the spatial and temporal behavior of soil water content p 18 N87-17288

TAKEDA, K.

Estimation of maximum snow volume distribution using NOAA-AVHRR data p 60 N87-17314

TAKERKIA, H.

Discrimination of land features using LANDSAT false colour composite in Iran p 19 N87-17352

TAKEUCHI, S.

Estimation of maximum snow volume distribution using NOAA-AVHRR data p 60 N87-17314

TALMOLA, P.

Retrieval of near-surface wind speed in the Baltic Sea from NIMBUS-7 Scanning Multichannel Microwave Radiometer (SMMR) observations p 50 N87-17342

TANAKA, K.

A satellite-borne SAR transmitter and receiver p 83 N87-17358

Pulse compression test results of the SAR transmitter and receiver p 83 N87-17360

TANG, R.

Study of ocean bottom coupling process using satellite altimeter data p 54 N87-18199

TANIS, F. J.

Detection of bottom-related surface patterns on visible spectrum imagery p 53 N87-18158

TANNER, A.

The Electronically Steered Thinned Array Radiometer (ESTAR) p 82 N87-17260

TAPLEY, B. D.

Accurate measurement of mean sea level changes by altimetric satellites p 38 A87-20524

Undersea volcano production versus lithospheric strength from satellite altimetry [NASA-CR-179984] p 78 N87-15660

NROSS (Navy Remote Ocean Sensing System) tracking network analysis [AD-A172132] p 45 N87-16384

TARANIK, JAMES V.

Detection and mapping of volcanic rock assemblages and associated hydrothermal alteration with Thermal Infrared Multiband Scanner (TIMS) data Comstock Lode Mining District, Virginia City, Nevada p 31 N87-17119

Application of Thermal Infrared Multiband Scanner (TIMS) data to mapping of Plutonic and stratified rock and assemblages in accreted terrains of the Northern Sierra, California p 15 N87-17132

Nature and origin of mineral coatings on volcanic rocks of the Black Mountain, Stonewall Mountain, and Kane Springs, Wash volcanic centers, Southern Nevada [NASA-CR-180183] p 36 N87-18255

TARIQUE, S. M.

Computer-aided analysis of LANDSAT data for mapping geologic and geomorphic features, North Bombay, India p 33 N87-17235

TARPLEY, J. D.

Land surface climatic variables monitored by NOAA-AVHRR satellites p 4 A87-23811

TAVARES, C.

Digital satellite imagery acquisition and processing p 68 N87-17207

TAYLOR, B. F.

Calibration of normalized vegetation index against pasture growth p 12 N87-15585

TAYLOR, J. C.

The influence of resampling method and multitemporal LANDSAT imagery on crop classification accuracy in the United Kingdom p 16 N87-17250

TAYLOR, PETER K.

Validation of ERS-1 wind data using observations from research and voluntary observing ships p 51 N87-17374

TEILLET, P. M.

Viewing angle corrections of airborne multispectral scanner data acquired over forested surfaces p 17 N87-17273

TEMPFLI, K.

Composite/progressive sampling - A program package for computer supported collection of DTM data p 62 A87-23784

- THEIS, S. W.**
The effect of measurement error and confusion from vegetation on passive microwave estimates of soil moisture p 18 N87-17304
- THIES, PAUL R.**
Performance of selected spatial domain edge detection algorithms for earth resources application p 64 A87-23798
- THIESSEN, R. L.**
Surface reflectance correction and stereo enhancement of LANDSAT thematic mapper imagery for structural geologic exploration [DE87-003095] p 37 N87-19796
- THOMAS, A. C.**
Comparison between satellite image advective velocities, dynamic topography, and surface drifter trajectories p 38 A87-20692
An objective method for computing advective surface velocities from sequential infrared satellite images p 39 A87-23717
- THOMAS, R. W.**
Utility of remote sensing data in renewable resource sample survey p 18 N87-17289
- THOMAS, RANDALL W.**
Development of EOS-aided procedures for the determination of the water balance of hydrologic budget of a large watershed [NASA-CR-180118] p 60 N87-16383
- THOMPSON, D. R.**
Hydrodynamics of internal solitons and a comparison of SIR-A and SIR-B data with ocean measurements p 45 N87-17147
- THOMPSON, K. P. B.**
Analysis of the spatial structure of Synthetic Aperture Radar (SAR) imagery for a better separability of cereal crops, wheat and barley p 17 N87-17287
- THORLEY, G. A.**
The use of space technology in federally funded land processes research in the United States p 88 N87-18152
- THORNTON, S. D.**
STAR-VUE: A tactical ice navigation workstation p 54 N87-18181
- TILLEY, D. G.**
Deriving two-dimensional ocean wave spectra and surface height maps from the Shuttle Imaging Radar (SIR-B) p 49 N87-17336
- TOKSOZ, M. N.**
Delineation of fault zones using imaging radar p 32 N87-17138
- TOLMUNEN, T.**
Retrieval of near-surface wind speed in the Baltic Sea from NIMBUS-7 Scanning Multichannel Microwave Radiometer (SMMR) observations p 50 N87-17342
- TOM, V. T.**
A synergistic approach for multispectral image restoration using reference imagery p 69 N87-17255
- TONN, W.**
Satellite-derived vegetation index over Europe p 12 N87-15583
- TORLEGARD, KENNETH**
A comparative test of photogrammetrically sampled digital elevation models p 66 A87-29499
- TOUTIN, T.**
Spatial remote sensing to land management p 70 N87-18157
- TOUZI, R.**
Extraction of the backscatter coefficient of agricultural fields from an airborne SAR image p 16 N87-17265
- TOWNSHEND, J. R. G.**
Analysis of the dynamics of African vegetation using the normalized difference vegetation index p 6 A87-24779
Preliminary analysis of SPOT HRV multispectral products of an arid environment p 10 A87-29017
- TOWNSHEND, JOHN R. G.**
Monitoring sediment transfer processes on the desert margin [NASA-CR-180181] p 23 N87-18222
- TRACEY, J. P.**
Thermal infrared remote sensing: One of today's solutions p 83 N87-17324
- TRAZET, M.**
The SPOT satellites - From SPOT 1 to SPOT 4 p 74 A87-21094
- TREMPAT, Y.**
Exploitation of the SPOT system p 62 A87-21095
- TREPTE, C. R.**
SAM II measurements of Antarctic PSC's and aerosols p 75 A87-23546
- TREWORGY, COLIN**
Interpreting forest and grassland biome productivity utilizing nested scales of image resolution and biogeographical analysis [NASA-CR-180213] p 23 N87-18912
- TRIFONOV, V. G.**
Lineaments of eastern Cuba - Geological interpretation of aerial and space imagery p 28 A87-24384
- TROLIER, L. J.**
Landsat Thematic Mapper images for hydrologic land use and cover p 58 A87-23831
- TRUBINA, M. A.**
Vertical structure of the temperature field above the North Atlantic p 40 A87-24374
- TSUJI, T.**
A satellite-borne SAR transmitter and receiver p 83 N87-17358
- TUCKER, C. J.**
Maximum normalized difference vegetation index images for sub-Saharan Africa for 1983-1985 p 6 A87-24776
Satellite remote sensing of primary production p 6 A87-24777
Satellite remote sensing of rangelands in Botswana. II - NOAA AVHRR and herbaceous vegetation p 7 A87-24786
Monitoring the grasslands of the Sahel 1984-1985 p 7 A87-24787
Assessment of ecological conditions associated with the 1980/81 desert locust plague upsurge in West Africa using environmental satellite data p 7 A87-24789
- TURVEY, D. E.**
A thermal device for aircraft measurement of the solid water content of clouds p 56 A87-20951
- TUZET, ANDREE**
Hydrological Atmospheric Pilot Experiment (HAPEX) hydrology budget modeling (MOBILHY): Outline of the program p 59 N87-15632
- U**
- UENO, S.**
Bitemporal analysis of Thematic Mapper data for land cover classification p 69 N87-17249
Radiometric correction method which removes both atmospheric and topographic effects from the LANDSAT-MSS data p 83 N87-17329
Automatic update procedure of the digitized land use map using LANDSAT TM data p 72 N87-18192
- ULABY, FAWWAZ T.**
SIR-B measurements and modeling of vegetation p 15 N87-17160
- USHAH, A.**
Application of 2-D Hilbert transform in the interpretation of remotely sensed potential field data p 35 N87-17293
- UTHE, EDWARD E.**
Development and demonstration of ALARM (Airborne Lidar Agent Remote Monitor) [AD-A172886] p 78 N87-16387
- V**
- VAN ZYL, JAKOB J.**
Imaging radar polarimetry from wave synthesis p 76 A87-29849
- VANECK, P.**
SAR imagery for forest management p 18 N87-17313
- VANHALSEMA, D.**
C and Ku-band scatterometer results from the SCATMOD internal wave experiment p 47 N87-17215
- VANLEEUWEN, H. J. C.**
Bare soil measurements with the Delft University Scatterometer (DUTSCAT) system (L-band) [REPT-64-220-86-T-1LH] p 24 N87-19797
- VANRENSBURG, P. A. J.**
Integrating vector and satellite data to evaluate the adequacy of a grain silo network p 21 N87-18156
- VANT, M. R.**
A very fast synthetic-aperture radar signal processor for ERS-1 and Radarsat p 85 N87-18180
- VANVUUREN, E. J.**
Integrating vector and satellite data to evaluate the adequacy of a grain silo network p 21 N87-18156
- VANZYL, J. J.**
Imaging radar polarimetry from wave synthesis p 82 N87-17279
- VASILEV, L. N.**
Determination of the properties of a plowed soil layer from multispectral space imagery p 8 A87-26536
- VASILEV, V. A.**
Vertical structure of the temperature field above the North Atlantic p 40 A87-24374
- VERDIN, JAMES P.**
Satellite observations of snow covered area in the High Atlas Mountains of Morocco p 57 A87-23808
- VERESHCHAKA, T. V.**
Interpretation characteristics of space photographs of sea coasts with wind-induced surges p 43 A87-28509
- VEROSUB, KEN**
Kinematics at the intersection of the Garlock and Death Valley fault zones, California: Integration of TM data and field studies [NASA-CR-180182] p 36 N87-18256
- VESECKY, J. F.**
Automated remote sensing of sea ice using synthetic aperture radar p 46 N87-17186
- VIANNARODRIGUES, RICARDO L.**
CANASATE: Sugar cane mapping by satellite, area 3 [INPE-4068-RPE/526] p 24 N87-19790
- VIDAL-MADJAR, D.**
Toward a satellite system to monitor the spatial and temporal behavior of soil water content p 18 N87-17288
- VISSERS, MARTIN**
An application of thematic mapper data in Tunisia - Estimation of daily amplitude in near-surface soil temperature and discrimination of hypersaline soils p 2 A87-21245
- VOGEL, WOLFHARD J.**
Tree attenuation at 869 MHz derived from remotely piloted aircraft measurements p 9 A87-28414
- VOGELMANN, A. F.**
Remote detection of forest damage p 8 A87-26197
- VOGELMANN, J. E.**
Assessing forest decline in coniferous forests of Vermont using NS-001 Thematic Mapper Simulator data p 1 A87-20763
Remote detection of forest damage p 8 A87-26197
Use of TMS/TM data for mapping of forest decline damage in the northeastern United States p 22 N87-18175
- VOLCHKOVA, G. I.**
Lineaments of eastern Cuba - Geological interpretation of aerial and space imagery p 28 A87-24384
- VOLCHOK, WILLIAM J.**
Radiometric analysis of the longwave infrared channel of the Thematic Mapper on LANDSAT 4 and 5 [NASA-CR-180180] p 86 N87-18221
- VOLIAK, K. I.**
Exact determination of wave parameters from the results of Fourier analysis of sea-surface radar imagery p 41 A87-24377
- VON BUN, FRITZ**
Ideas for a future earth observing system from geosynchronous orbit p 74 A87-23419
- VONDER HAAR, T. H.**
Forest fire monitoring using the NOAA satellite series p 3 A87-23360
- VONFRESE, RALPH R. B.**
Improving the geological interpretation of magnetic and gravity satellite anomalies [NASA-CR-180149] p 35 N87-17418
- VONSOLMS, S. H.**
Integrating vector and satellite data to evaluate the adequacy of a grain silo network p 21 N87-18156
- VOROBEV, V. IA.**
Integration of space-geological and geophysical methods in regional and local predictions of tectonic structures in the Caspian depression p 28 A87-24381
Quantitative processing procedures and the information content of space imagery in predictions of structural inhomogeneities of the sedimentary cover p 29 A87-26534
- W**
- WACHARAKITTI, S.**
The application of LANDSAT imagery for land cover assessment p 13 N87-15614
- WAHR, JOHN M.**
The earth's C21 and S21 gravity coefficients and the rotation of the core p 27 A87-29977
- WAITE, W. P.**
Hawaiian lava flows and SIR-B results p 69 N87-17245
- WAKAMORI, KUNIYASU**
Extraction of areas infested by pine bark beetle using Landsat MSS data p 10 A87-30129
- WALL, STEPHEN**
Multiple incidence angle SIR-B experiment over Argentina p 80 N87-17157
- WALSH, E. J.**
Oceanographic measurement capabilities of the NASA P-3 aircraft p 52 N87-17380
- WALSH, JOHN E.**
Data sensitivities of sea ice drift and ocean stress in North Atlantic high latitudes p 38 A87-20520

- WALSH, STEPHEN J.**
Impact of environmental variables on spectral signatures acquired by the Landsat Thematic Mapper p 9 A87-29003
- WALTER, LOUIS S.**
The physical basis for spectral variations in thermal infrared emittance of silicates and application to remote sensing p 31 N87-17129
- WANG, J. R.**
Evaluating roughness models of radar backscatter p 19 N87-17344
- WANG, LI**
Drainage channel network of the Arcachon Basin using Thematic Mapper data obtained at high tide p 58 A87-29013
- WARD, IAN A.**
A scatterometer research program p 53 N87-17391
- WARDLEY, N. W.**
Remote sensing of structurally complex semi-natural vegetation - An example from heathland p 10 A87-30896
- WARNER, ROBERT A.**
The effect of Hurricane Gloria on sea surface temperature patterns p 39 A87-23362
- WARNER, THOMAS T.**
Utilization of satellite data in mesoscale modeling of severe weather [NASA-CR-179917] p 78 N87-15669
- WATANABE, HIROSHI**
Extraction of areas infested by pine bark beetle using Landsat MSS data p 10 A87-30129
- WATSON, KEN**
Simulation modeling and preliminary analysis of TIMS data from the Carlin area and the northern Grapevine Mountains, Nevada p 31 N87-17120
- WEAVER, R. E.**
Spectral separation of moorland vegetation in airborne Thematic Mapper data p 10 A87-30897
- WEBB, J. P.**
Ground radiometry and airborne multispectral survey of bare soils p 10 A87-30894
- WEBSTER, R.**
Estimating and mapping grass cover and biomass from low-level photographic sampling p 9 A87-29005
- WEGENER, M.**
The FRS-68010: A new concept for the acquisition and analysis of NOAA HRPT data p 68 N87-17206
- WEGMUELLER, U.**
Dielectric and surface parameters related to microwave scatter and emission properties p 16 N87-17262
- WEINMAN, J. A.**
Microwave radiances from horizontally finite precipitating clouds containing ice and liquid hydrometeors p 61 N87-17340
- WENTZ, FRANK J.**
Further development of an improved altimeter wind speed algorithm p 42 A87-27848
- WESTER, K.**
A statistical approach to select the optimal wavelength bands for separating rocks in the wavelength region 0.4 to 2.3 microns p 34 N87-17244
- WETZEL, PETER J.**
The effect of local advection on the inference of soil moisture from thermal infrared radiances p 3 A87-23388
- WHERRY, DAVID**
Spectral characteristics and the extent of paleosols of the Palouse formation [NASA-CR-180357] p 24 N87-19826
- WIEGAND, CRAIG L.**
Diurnal-seasonal light interception, leaf area index, and vegetation index interrelations in a wheat canopy - A case study p 5 A87-23822
- WIESE, M. V.**
Microcomputer-assisted video image analysis of lodging in winter wheat p 10 A87-30130
- WIESENHAHN, DAVID**
Temperature-plant pigment-optical relations in a recurrent offshore mesoscale eddy near Point Conception, California [AD-A176666] p 39 A87-23720
- WILKE, GREGORY D.**
Nimbus-7 SMMR multispectral passive microwave correlations with an antecedent precipitation index p 74 A87-23390
- WILLIAMS, C. P.**
Commercial opportunities in Earth observation from space p 87 N87-17177
- WILLIAMS, D. L.**
Remote detection of forest damage p 8 A87-26197
- WILLIAMS, ROSS N.**
Current achievements and future projects/useful applications of weather satellites and future remote sensing p 76 A87-29431
- WILLIAMS, V. L.**
Vegetable crop inventory with Landsat TM data p 5 A87-23833
- WILLIAMSON, E. J.**
The Along Track Scanning Radiometer (ATSR) for ERS1 p 73 A87-19660
- WILLIAMSON, H. D.**
Airborne MSS data to estimate GLAI p 11 A87-30898
- WILSON, GREGORY**
Verification of small-scale water vapor features in VAS imagery using high resolution MAMS imagery p 62 A87-23348
- WINGHAM, D. J.**
An automatic tracking mode switching algorithm for the ERS-1 altimeter p 81 N87-17195
New techniques in satellite altimeter tracking systems p 85 N87-18164
- WISENHAHN, DAVID**
Biological consequences of a recurrent eddy off Point Conception, California p 40 A87-23721
- WITTE, F.**
On the discrimination between crude oil spills and monomolecular sea slicks by airborne remote sensors: Today's possibilities and limitations p 53 N87-18167
Oil slick detection with a sidelooking airborne radar p 53 N87-18169
Contributions to oil spill detection and analysis with radar and microwave radiometry, results of the Archimedes 2 campaign p 54 N87-18170
- WOLANSKI, E.**
The Coastal Zone Color Scanner views the Bismarck Sea p 42 A87-26970
- WOOD, B.**
Remote sensing of wetland plant stress p 21 N87-18171
- WOODS, NANCY E.**
A radar ocean imaging model for small to moderate incidence angles p 43 A87-29015
- WOODWARD, ROBERT H.**
The effect of local advection on the inference of soil moisture from thermal infrared radiances p 3 A87-23388
- WORSHAM, R. D.**
Remote sensing of hydrological variables from the DMSP microwave mission sensors p 57 A87-23374

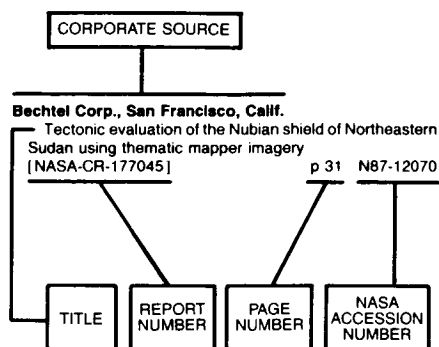
Y

- YAMADA, HIROYOSHI**
Development and experiment of airborne microwave rain-scatterometer/radiometer system. IV - Microwave back-scattering experiment of ocean surface p 43 A87-28437
- YEARLEY, R. J.**
An analysis of geologic lineaments seen on Landsat MSS imagery p 30 A87-29011
- YOKOTA, T.**
Models for temperature estimation from remotely sensed thermal IR data p 83 N87-17325
- YOSHIKADO, SHIN**
Development and experiment of airborne microwave rain-scatterometer/radiometer system. III - Rain measurement and its data analysis p 58 A87-28436
- YTTERBORN, KARL, H.**
Distribution and biomass of *Fucus vesiculosus* L. near a cooling-water effluent from a nuclear power plant in the Baltic Sea estimated by aerial photography p 43 A87-29014
- YUEN, H. C.**
SAR imaging of bottom topography in the ocean: Results from an improved model p 48 N87-17298

Z

- ZATONSKII, L. K.**
The use of space photography to create and renew small-scale maps p 65 A87-25249
- ZEBKER, H. A.**
Imaging radar polarimetry from wave synthesis p 82 N87-17279
- ZEBKER, HOWARD A.**
Imaging radar polarimetry from wave synthesis p 76 A87-29849
- ZELL, L.-O.**
Surface albedo change in arid regions in the Sudan p 13 N87-15615
- ZENG, Q. Z.**
Snow survey from meteorological satellite images in the Qilian Mountain Basin in northwest China p 56 A87-20765

- ZENKER, S.**
Marrying geocoded image data with other types of geographic information in a PC environment p 21 N87-18154
- ZHENG, S. Y.**
Snow survey from meteorological satellite images in the Qilian Mountain Basin in northwest China p 56 A87-20765
- ZHOU, GUOPING**
Accurate determination of ellipse centers in digital imagery p 63 A87-23788
- ZILLOX, LOTHAIRE**
Visualization by aerial thermography of hydrodynamic exchanges between the water table, streams and gravel pits in the Rhine plain north of Strasbourg p 58 A87-25746
- ZIMMERMANN, R.**
Laser-induced chlorophyll-A fluorescence of terrestrial plants p 23 N87-18207
- ZINKE, PAUL J.**
Development of EOS-aided procedures for the determination of the water balance of hydrologic budget of a large watershed [NASA-CR-180118] p 60 N87-16383

Typical Corporate Source
Index Listing

Listings in this index are arranged alphabetically by corporate source. The title of the document is used to provide a brief description of the subject matter. The page number and the accession number are included in each entry to assist the user in locating the abstract in the abstract section. If applicable, a report number is also included as an aid in identifying the document.

A

- Agricultural Research Service, Beltsville, Md.**
Applications of remote sensing in the US Department of Agriculture p 17 N87-17285
- Air Force Geophysics Lab., Hanscom AFB, Mass.**
An extension of the split window technique for the retrieval of precipitable water [AD-A173008] p 60 N87-16386
- Alaska Univ., Anchorage.**
Influence of the Yukon River on the Bering Sea [NASA-CR-180065] p 54 N87-18293
Influence of the Yukon River on the Bering Sea [NASA-CR-180356] p 56 N87-19877
- Analytic Sciences Corp., Reading, Mass.**
Extracting surface features in multispectral imagery p 68 N87-17211
A synergistic approach for multispectral image restoration using reference imagery p 69 N87-17255
- Applied Research Corp., Landover, Md.**
Large-scale short-period sea ice atmosphere interaction p 42 A87-27546
- Arizona State Univ., Tempe.**
Thermal imaging spectroscopy in the Kelso-Baker Region, California p 30 N87-17117
- Arizona Univ., Tucson.**
Variations in in-flight absolute radiometric calibration p 77 N87-15594
- Arkansas Univ., Fayetteville.**
Preliminary analyses of SIB-B radar data for recent Hawaii lava flows p 29 A87-25588
Hawaiian lava flows and SIR-B results p 69 N87-17245
- Army Engineer Topographic Labs., Fort Belvoir, Va.**
Sparse area stereo matching experiment [AD-A173601] p 66 N87-16388
- Army Engineer Waterways Experiment Station, Vicksburg, Miss.**
The Red River Valley archeological project p 31 N87-17128

Aster, Inc., Fort Collins, Colo.

Forecasting sea breeze thunderstorms at the Kennedy Space Center using the Prognostic Three-Dimensional Mesoscale Model (P 3DM) p 43 A87-27891

Aston Univ., Birmingham (England).

Discrimination of land features using LANDSAT false colour composite in N Iran p 19 N87-17352

Atmospheric Environment Service, Downsview (Ontario).

Application of the Seasat scatterometer to observations of wind speed and direction and Arctic ice/water boundaries p 48 N87-17259

Auburn Univ., Ala.

Applications of TIMS data in agricultural areas and related atmospheric considerations p 15 N87-17124

B

Bern Univ. (Switzerland).

Dielectric and surface parameters related to microwave scatter and emission properties p 16 N87-17262
Atmospheric corrections of NOAA-AVHRR data verification of different methods by ground truth measurements p 70 N87-17274
L to X-band scatter and emission measurements of vegetation p 19 N87-17347

C

Calabar Univ. (Nigeria).

Regional studies with satellite data in Africa on the desertification of the Sudan-Sahel belt in Nigeria p 13 N87-15605

California Univ., Berkeley.

Development of EOS-aided procedures for the determination of the water balance of hydrologic budget of a large watershed [NASA-CR-180118] p 60 N87-16383
Utility of remote sensing data in renewable resource sample survey p 18 N87-17289

California Univ., La Jolla.

Temperature-plant pigment-optical relations in a recurrent offshore mesoscale eddy near Point Conception, California [AD-A176666] p 39 A87-23720

Biological consequences of a recurrent eddy off Point Conception, California p 40 A87-23721
Space and time variability of the surface color field in the northern Adriatic Sea p 40 A87-23722

California Univ., Los Angeles.

Tidal heating in an internal ocean model of Europa p 43 A87-30143
Geophysical remote sensing p 30 A87-30884

California Univ., Santa Barbara.

Canopy reflectance modeling in a tropical wooded grassland [NASA-CR-180097] p 11 N87-15518

Remote Sensing Information Sciences Research Group, year four [NASA-CR-180198] p 88 N87-18907

Canada Centre for Remote Sensing, Ottawa (Ontario).

An overview of operational SAR data collection and dissemination plans for ERS-1 ice data in Canada p 47 N87-17189

Canadian plans for operational demonstrations of satellite imaging radar applications p 68 N87-17229

An overview of remote sensing agricultural applications in North America: Past, present and future p 17 N87-17284

Canada Center for Remote Sensing (CCRS) Convair 580 results relevant to ERS-1 wind and wave calibration p 84 N87-17379

A very fast synthetic-aperture radar signal processor for ERS-1 and Radarsat p 85 N87-18180

Centre d'Etude Spatiale des Rayonnements, Toulouse (France).

Extraction of the backscatter coefficient of agricultural fields from an airborne SAR image p 16 N87-17265

Computer-aided interpretation of complex geological patterns in remote sensing p 35 N87-17294

Centre de Developpement des Techniques Avancees, Alger-Gare (Algeria).

The fundamental problems for the energy balance study by satellite imagery p 66 N87-15590

Centre de Recherches en Physique de l'Environnement, Issy-les-Moulineaux (France).

Modelisation of evapotranspiration and soil available water over an agricultural region applicable for remote sensing p 12 N87-15554

Centre for Earth Science Studies, Trivandrum (India).

Significance of space image, air photo and drainage linears in relation to west coast tectonics, India p 33 N87-17232

Computer-aided analysis of LANDSAT data for mapping geologic and geomorphic features, North Bombay, India p 33 N87-17235

Centre National d'Etudes des Telecommunications, Issy-les-Moulineaux (France).

Toward a satellite system to monitor the spatial and temporal behavior of soil water content p 18 N87-17288

Centre National d'Etudes Spatiales, Toulouse (France).

VARAN-S radar image interpretation [CNES-CT/DRT/TIT/RL-54-T] p 66 N87-16963

Centre National de la Recherche Scientifique, Garchy (France).

The use of thermal airborne remote sensing for soil identification: A case study in Limousin (France) p 20 N87-18146

Centre National de la Recherche Scientifique, Strasbourg (France).

Design of a data base system for inferring land surface parameters and fluxes from satellite radiances p 66 N87-15625

Centre Oceanologique de Bretagne, Brest (France).

Evaluation of the different parameters in Long's C-band model p 51 N87-17370

Using buoys and ships to calibrate ERS-1 altimeter and scatterometer p 51 N87-17377

Centro Studi ed Applicazioni in Tecnologia Avanzate, Bari (Italy).

UMUS: A project for usage of LANDSAT MSS and ancillary data in land cover mapping of large areas in southern Italy p 72 N87-18191

Chalmers Univ. of Technology, Goeteborg (Sweden).

Atmospheric water vapor corrections for altimetry measurements p 85 N87-18197

Chevron Oil Field Research Co., La Habra, Calif.

Space shuttle radar images of Indonesia p 32 N87-17137

City Coll. of the City Univ. of New York.

Verification results for a two-scale model of microwave backscatter from the sea surface p 47 N87-17213

Colorado State Univ., Fort Collins.

Satellite contributions to convective scale weather analysis and forecasting p 76 A87-27882

Colorado Univ., Boulder.

The earth's C21 and S21 gravity coefficients and the rotation of the core p 27 A87-29977

Columbia Univ., Palisades, N.Y.

SAR ice floe kinematics and correlation with mesoscale oceanic structure within the marginal ice zone p 48 N87-17222

Comision Nacional de Investigaciones Espaciales, Buenos Aires (Argentina).

Soil degradation evaluation by digital image processing p 20 N87-18147

Commonwealth Scientific and Industrial Research Organization, Aspendale (Australia).

Australian validation plans for ERS-1 p 84 N87-17387

Consiglio Nazionale delle Ricerche, Florence (Italy).

Contribution of passive microwave remote sensing in soil moisture and evapotranspiration measurements p 12 N87-15589

An integrated system to assess agricultural productivity p 14 N87-15621

An integrated data bank for agricultural productivity by remote sensing p 21 N87-18153

Consiglio Nazionale delle Ricerche, Frascati (Italy).

Integrated analysis of geological and remote sensing data aimed at mineral deposits detection in the Monapo area (northern Mozambique) p 34 N87-17243

Cornell Univ., Ithaca, N.Y.

Tectonic geomorphology of the Andes with SIR-A and SIR-B p 32 N87-17136

Crnfield Inst. of Tech., Bedford (England).

The influence of resampling method and multitemporal LANDSAT imagery on crop classification accuracy in the United Kingdom p 16 N87-17250

D**Daedalus Enterprises, Inc., Ann Arbor, Mich.**

The TIMS instrument p 79 N87-17112

Danish Meteorological Inst., Copenhagen.

The ice conditions in the Greenland waters, 1980 [REPT-551.467.3.068(988)] p 53 N87-17428

Dartmouth Coll., Hanover, N.H.

Discrimination of lithologic units using geobotanical and LANDSAT TM spectral data p 34 N87-17246

Defence Research Establishment Pacific, Victoria (British Columbia).

Estimation of internal wave currents from SAR and infrared scatterometer imagery p 48 N87-17295

Defense Mapping Agency, Washington, D.C.

Preliminary evaluation of Doppler-determined pole positions computed using world geodetic system 1984 [AD-A173467] p 27 N87-18225

Department of Energy, Morgantown, W. Va.

Proceedings of the Second Workshop on Remote Sensing/Lineament Applications for Energy Extraction [DE86-006613] p 36 N87-18915

Deutsche Forschungs- und Versuchsanstalt fuer Luft- und Raumfahrt, Oberpfaffenhofen (West Germany).

X-SAR extends the frequency range of Shuttle Imaging Radar p 70 N87-17362

Contributions to oil spill detection and analysis with radar and microwave radiometry, results of the Archimedes 2 campaign p 54 N87-18170

Intelligent SAR Processor (ISAR), a new concept for high throughput and high precision digital SAR processing p 85 N87-18178

Southern Pantanal Matogrossense (South America) of Modular Optoelectronic Multispectral Scanner (MOMS) data, preliminary results p 71 N87-18182

Deutsche Forschungs- und Versuchsanstalt fuer Luft- und Raumfahrt, Wessling (West Germany).

Oil slick detection with a sidelooking airborne radar p 53 N87-18169

Digim (1983), Inc. Montreal (Quebec).

Spatial remote sensing to land management p 70 N87-18157

Dornier-Werke G.m.b.H., Friedrichshafen (West Germany).

Digital realtime SAR processor for C- and X-band applications p 71 N87-18177

Durham Univ. (England).

Vegetation index models for the assessment of vegetation in marginal areas p 12 N87-15584

E**Earth Observation Satellite Co., Va.**

Commercial opportunities in Earth observation from space p 87 N87-17177

Ecole Polytechnique Federale de Lausanne (Switzerland).

Description of a methodology for biomass change mapping with the use of LANDSAT TM data p 22 N87-18186

EG and G Washington Analytical Services Center, Inc., Pocomoke City, Md.

Chlorophyll pigment concentration using spectral curvature algorithms - An evaluation of present and proposed satellite ocean color sensor bands p 37 A87-20204

Eidgenoessische Technische Hochschule, Zurich (Switzerland).

Point positioning and mapping with Large Format Camera data p 71 N87-18188

Environmental Analysis and Remote Sensing, Delft (Netherlands).

Group Agromet Monitoring Project (GAMP) methodology integrated mapping of rainfall, evapotranspiration, germination, biomass development and thermal inertia, based on Meteosat and conventional meteorological data p 59 N87-15626

Environmental Research Inst. of Michigan, Ann Arbor.

Imaging radar contributions to a major air-sea-ice interaction study in the Greenland Sea p 46 N87-17150

An inter-sensor comparison of the microwave signatures of Arctic sea ice p 46 N87-17184

Geophysics of the marginal ice zone from SAR p 47 N87-17219

Analysis of multichannel SAR data of Spitsbergen p 60 N87-17223

An improved method for the determination of water depth from surface wave refraction patterns p 49 N87-17299

Characterisation of internal wave surface patterns on airborne SAR imagery p 50 N87-17338

Detection of bottom-related surface patterns on visible spectrum imagery p 53 N87-18158

Vegetation and soils information contained in transformed Thematic Mapper data p 22 N87-18185

European Space Agency, Paris (France).

Proceedings of the 1986 International Geoscience and Remote Sensing Symposium (IGARSS '86) on Remote Sensing: Today's Solutions for Tomorrow's Information Needs, volume 1 [ESA-SP-254-VOL-1] p 80 N87-17163

Overview and status of the ERS-1 program p 47 N87-17190

Proceedings of the 1986 International Geoscience and Remote Sensing Symposium (IGARSS '86) on Remote Sensing: Today's Solutions for Tomorrow's Information Needs, volume 2 [ESA-SP-254-VOL-2] p 82 N87-17283

Proceedings of an ESA Workshop on ERS-1 Wind and Wave Calibration [ESA-SP-262] p 84 N87-17363

Proceedings of the 1986 International Geoscience and Remote Sensing Symposium (IGARSS '86) on Remote Sensing: Today's Solutions for Tomorrow's Information Needs, volume 3 [ESA-SP-254-VOL-3] p 84 N87-18142

European Space Agency, European Space Research and Technology Center, ESTEC, Noordwijk (Netherlands).

Concept of a future multispectral Thermal Infrared (TIR) pushbroom mission for Earth observation from space p 80 N87-17169

The ESA approach for ERS-1 sensor calibration and performance verification p 80 N87-17192

ERS-1 radar altimeter: Performance, calibration and data validation p 80 N87-17194

ERS-1 fast delivery processing and products p 81 N87-17224

ERS-1 mission constraints related to wind and wave calibration p 84 N87-17364

Executive Office of the President, Washington, D. C.

Aeronautics and space report of the President: 1985 activities p 87 N87-16662

F**Flinders Univ., Bedford Park (Australia).**

The FRS-68010: A new concept for the acquisition and analysis of NOAA HRPT data p 68 N87-17206

Florence Univ. (Italy).

Multispectral classification of microwave remote sensing images p 16 N87-17238

Florida International Univ., Miami.

The transfer of remote sensing technology to developing countries: A survey of experts in the field p 87 N87-17170

Florida State Univ., Tallahassee.

Variability in the Earth radiation budget as determined from the Nimbus ERB experiments p 84 N87-17410

Food and Agriculture Organization of the United Nations, Rome (Italy).

Assessment of ecological conditions associated with the 1980/81 desert locust plague upsurge in West Africa using environmental satellite data p 7 A87-24789

Forest Service, Atlanta, Ga.

Locating subsurface gravel with thermal imagery p 31 N87-17125

Freiburg Univ. (West Germany).

Comparison of Thematic Mapper (TM) and SPOT simulation data for agricultural applications in south west Germany p 16 N87-17165

Microwave remote sensing: Its applications and limitations in operational tasks of land use inventory and forest management p 17 N87-17266

Multitemporal analysis of the phenological stage of vegetation using TM-data in the Southern Black Forest (West Germany) p 22 N87-18184

Deduction of a synthetic bioclimatological map by means of remote sensing data and a digital terrain model using a correlation approach p 72 N87-18194

Forest cover analysis using SIR-B data p 23 N87-18220

Freie Univ., Berlin (West Germany).

Satellite-derived vegetation index over Europe p 12 N87-15583

LANDSAT-MSS remote sensing and satellite cartography: An integrated approach to the preparation of a new geological map of Egypt at a scale of 1:500 000 p 36 N87-18190

G**General Software Corp., Landover, Md.**

The effect of local advection on the inference of soil moisture from thermal infrared radiances p 3 A87-23388

Geological Survey, Denver, Colo.

Simulation modeling and preliminary analysis of TIMS data from the Carlin area and the northern Grapevine Mountains, Nevada p 31 N87-17120

Geological Survey, Flagstaff, Ariz.

The megageomorphology of the radar rivers of the eastern Sahara p 32 N87-17139

Geological Survey, Reston, Va.

Airborne Thermal Infrared Multispectral Scanner (TIMS) images over disseminated gold deposits, Osgood Mountains, Humboldt County, Nevada p 32 N87-17134

The use of space technology in federally funded land processes research in the United States p 88 N87-18152

Geological Survey of Canada, Ottawa (Ontario).

Integration of surficial geochemistry and LANDSAT imagery to discover skarn tungsten deposits using image analysis techniques [CONTRIB-19586] p 35 N87-17248

Geological Survey of India, Jaipur.

Comparative study of LANDSAT MSS, Salyut-7 (TERRA) and radar (SIR-A) images for geological and geomorphological applications: A case study from Rajasthan and Gujarat, India p 34 N87-17236

George Mason Univ., Fairfax, Va.

Landsat Thematic Mapper digital information content for agricultural environments p 5 A87-23830

Ghent Univ. (Belgium).

Assessment of wind and fluvial action by using LANDSAT-MSS color composites in the lower Nile Valley (Egypt) p 13 N87-15612

Assessment of soil degradation in an arid region using remote sensing p 20 N87-18148

GKSS-Forschungszentrum Geesthacht (West Germany).

Multiangle or multiwavelength technique for remote sensing of sea surface temperature p 45 N87-15652

Comparison concept of satellite derived wind and wave data with ground truth p 51 N87-17373

Graz Univ. (Austria).

Space Shuttle radargrammetry results p 65 A87-23827

H**Hamburg Univ. (West Germany).**

On the discrimination between crude oil spills and monomolecular sea slicks by airborne remote sensors: Today's possibilities and limitations p 53 N87-18167

Haryana Agricultural Univ., Hissar (India).

Application of remote sensing in the study of the soil hazards of Haryana State, India p 20 N87-18150

Remote sensing applications in the study of land use and soils of aeolian cover of the western part of Haryana State, India p 22 N87-18187

Hawaii Inst. of Geophysics, Honolulu.

Preliminary analyses of SIB-B radar data for recent Hawaii lava flows p 29 A87-25588

Helsinki Univ. of Technology, Espoo (Finland).

Development of algorithms to retrieve the water equivalent of snow cover from satellite microwave radiometer data p 60 N87-17264

Classification of forest and surface types by satellite microwave radiometry p 18 N87-17305

Retrieval of near-surface wind speed in the Baltic Sea from NIMBUS-7 Scanning Multichannel Microwave Radiometer (SMRM) observations p 50 N87-17342

Sea ice studies in the Baltic Sea using satellite microwave radiometer data p 50 N87-17343

I**IBM France S. A., Paris.**

Thermal inertia and soil fluxes by remote sensing p 20 N87-18143

First step in the use of remote sensing for regional mapping of soil organization data: Application in Brittany (France) and French Guiana p 23 N87-18193

IBM Japan.

Evaluation of LANDSAT 5 Thematic Mapping (TM) data for image clustering and classification p 69 N87-17251

- Illinois Natural History Survey, Champaign.**
Interpreting forest and grassland biome productivity utilizing nested scales of image resolution and biogeographical analysis
[NASA-CR-180213] p 23 N87-18912
- INAP, Paris (France).**
Hydrological Atmospheric Pilot Experiment (HAPEX) hydrology budget modeling (MOBILHY): Outline of the program p 59 N87-15632
- Indian Space Research Organization, Ahmedabad.**
Indian remote sensing program p 77 N87-15242
AVHRR and MSS data based vegetation indices studies over Indian sites p 14 N87-15622
Retrieval and global comparison of oceanic winds from SEASAT radiometer, scatterometer and altimeter p 85 N87-18219
- Indiana State Univ., Terre Haute.**
IRSAF: An improved approach in processing remotely sensed data p 70 N87-17332
- Innsbruck Univ. (Austria).**
Vegetation identification and variability in the Tahoua area, Nigeria p 13 N87-15610
- Institut fuer Angewandte Geodäsie, Frankfurt am Main (West Germany).**
Mapping of agricultural lands in the USSR p 11 N87-15507
- Institut Geographique National, Paris (France).**
Monitoring of large phenomena in developing countries through satellite imagery p 67 N87-17172
- Institute of Oceanographic Sciences, Wormley (England).**
Requirements and constraints in the calibration and validation of ERS-1 wind and wave parameters p 51 N87-17369
Validation of ERS-1 wind data using observations from research and voluntary observing ships p 51 N87-17374
SeaSoar CTD surveys during FASINEX [IOS-230] p 55 N87-18970
- Instituto de Pesquisas Espaciais, Sao Jose dos Campos (Brazil).**
The use of aerial remote sensing in a case study of desertification: Quixaba-PE [INPE-3963-PRE/980] p 11 N87-15519
Application of remote sensing in hydrology and water resources [INPE-3986-PRE/991] p 60 N87-16382
Agricultural crop estimates using information gathered by remote sensing satellites, as well as ground data, through samples of geographic layers [INPE-4102-RPE/534] p 24 N87-19786
Evaluation of LANDSAT 4 MSS data for geomorphological mapping in the semiarid environment for regional planning purposes: An integrated approach (study site, the Juazeiro region) [INPE-3984-TDL/236] p 72 N87-19787
Remote sensing applied to basic geological surveys: A methodological approach for the northeast region [INPE-4041-TDL/246] p 37 N87-19788
CANASATE: Sugar cane mapping by satellite, area 3 [INPE-4068-RPE/526] p 24 N87-19790
Methodology for the elaboration of thematic maps utilizing LANDSAT-TM data [INPE-3893-TDL/225] p 72 N87-19792
- Instituto de Pesquisas Espaciais, Sao Paulo (Brazil).**
Environmental modification of metropolitan areas through satellite images: Study of urban design in the tropics p 25 N87-17175
- Instituto Nacional de Meteorologia e Geofisica, Lisbon (Portugal).**
Digital satellite imagery acquisition and processing p 68 N87-17207
- Instituto Nacional de Tecnica Aeroespacial, Madrid (Spain).**
Remote Sensing Laboratory [ETN-87-98850] p 88 N87-18227
- Instituut voor Cultuurtechniek en Waterhuishouding, Wageningen (Netherlands).**
Ground water-fed lakes in the Libyan desert: Their varying area as observed by means of LANDSAT-MSS data p 59 N87-15611
Future European plans in the framework of the International Satellite Land Surface Climatology Project (ISLSCP) p 78 N87-15628
- INTERA Environmental Consultants Ltd., Calgary (Alberta).**
Digital terrain mapping with STAR-1 SAR data p 69 N87-17269
STAR-VUE: A tactical ice navigation workstation p 54 N87-18181
- INTERA Environmental Consultants Ltd., Ottawa (Ontario).**
SAR imagery for forest management p 18 N87-17313
Thermal infrared remote sensing: One of today's solutions p 83 N87-17324
- Istanbul Univ. (Turkey).**
LANDSAT-5 Thematic Mapping (TM) data applications to land use classification on around the Bosphorus area, Turkey p 19 N87-17351
The use of remote sensing (including aerial photographs) to devise cost-effective methods for soil conservation in the Kocaeli Peninsula, Turkey p 20 N87-18149
- J**
- Jet Propulsion Lab., California Inst. of Tech., Pasadena.**
Assessing forest decline in coniferous forests of Vermont using NS-001 Thematic Mapper Simulator data p 1 A87-20763
Mobile very long baseline interferometry and Global Positioning System measurement of vertical crustal motion p 26 A87-21931
Earth Observing System - The earth research system of the 1990's [AIAA PAPER 87-0320] p 74 A87-22556
Month-to-month variability of ocean-atmosphere latent heat flux as observed from the Nimbus microwave radiometer p 39 A87-23391
Space Shuttle radargrammetry results p 65 A87-23827
Landsat Thematic Mapper digital information content for agricultural environments p 5 A87-23830
Remote detection of forest damage p 8 A87-26197
Imaging radar polarimetry from wave synthesis p 76 A87-29849
Equatorial long-wave characteristics determined from satellite sea surface temperature and in situ data p 44 A87-30923
Observations of the seasonal variability of soil moisture and vegetation cover over Africa using satellite microwave radiometry p 12 N87-15593
Evaluation of geophysical parameters measured by the Nimbus-7 microwave radiometer for the TOGA Heat Exchange Project [NASA-CR-180151] p 78 N87-17110
The TIMS Data User's Workshop [NASA-CR-180130] p 78 N87-17111
The TIMS investigator's guide p 79 N87-17113
Enhancement of time images for photointerpretation p 66 N87-17116
Lithologic mapping of silicate rocks using TIMS p 30 N87-17118
Application of TIMS data in stratigraphic analysis p 31 N87-17121
Infrared spectroscopy for geologic interpretation of TIMS data p 31 N87-17130
Calculation of day and night emittance values p 67 N87-17131
A geologic atlas of TIMS data p 32 N87-17133
The Second Spaceborne Imaging Radar Symposium [NASA-CR-180131] p 67 N87-17135
Geological applications of multipolarization SAR data p 33 N87-17140
Spaceborne imaging radar research in the 90's p 79 N87-17141
Present status of Japanese ERS-1 Project p 79 N87-17145
A scanning radar altimeter for mapping continental topography p 33 N87-17146
Multiple incidence angle SIR-B experiment over Argentina p 80 N87-17157
Imaging spectrometry: Aircraft and space program p 81 N87-17202
Analysis of AIS radiometry at Mono Lake, California p 81 N87-17204
Imaging radar polarimetry from wave synthesis p 82 N87-17279
On the relationship between age of lava flows and radar backscattering p 35 N87-17348
Satellite scatterometer comparisons with surface measurements: Techniques and Seasat results p 51 N87-17372
An overview of the NSCAT/N-ROSS program p 52 N87-17384
Use of TMS/TM data for mapping of forest decline damage in the northeastern United States p 22 N87-18175
Kinematics at the intersection of the Garlock and Death Valley fault zones, California: Integration of TM data and field studies [NASA-CR-180182] p 36 N87-18256
Shuttle imaging radar-C science plan [NASA-CR-180241] p 86 N87-18697
Investigation of physics of synthetic aperture radar in ocean remote sensing toward 84/86 field experiment. Volume 1: Data summary and early results [AD-A174197] p 55 N87-18913
- Johns Hopkins Univ., Laurel, Md.**
Tree attenuation at 869 MHz derived from remotely piloted aircraft measurements p 9 A87-28414
Hydrodynamics of internal solitons and a comparison of SIR-A and SIR-B data with ocean measurements p 45 N87-17147
Operational wave forecasting with spaceborne SAR: Prospects and pitfalls p 45 N87-17149
Characteristics of a very low altitude spacecraft for collecting global directional wave spectra with spaceborne synthetic aperture radar p 49 N87-17333
The SAR image modulation transfer function derived from SIR-B image spectra and airborne measurements of ocean wave height spectra p 49 N87-17334
Deriving two-dimensional ocean wave spectra and surface height maps from the Shuttle Imaging Radar (SIR-B) p 49 N87-17336
Spatial evolution of wave spectra in the vicinity of the Agulhas current from SIR-B p 50 N87-17337
A procedure for estimation of two-dimensional ocean height-variance spectra from SAR imagery p 52 N87-17381
A description of large-scale variability in the ocean using the diffuse attenuation coefficient p 53 N87-18160
Development in radar altimetry: The Navy Geosat mission p 85 N87-18161
- Joint Publications Research Service, Arlington, Va.**
Development, status, prospects of marine observation satellite p 45 N87-15989
- Joint Research Centre of the European Communities, Ispra (Italy).**
Rural land use inventory and mapping in the Ardeche area (France) using multitemporal Thematic Mapping (TM) data p 19 N87-17350
- K**
- Kalamazoo Coll., Mich.**
Mobile very long baseline interferometry and Global Positioning System measurement of vertical crustal motion p 26 A87-21931
- Kanazawa Inst. of Tech. (Japan).**
Bitemporal analysis of Thematic Mapper data for land cover classification p 69 N87-17249
Automatic update procedure of the digitized land use map using LANDSAT TM data p 72 N87-18192
- Kanazawa Univ. (Japan).**
Radiometric correction method which removes both atmospheric and topographic effects from the LANDSAT-MSS data p 83 N87-17329
- Kansas State Univ., Manhattan.**
Assessing grass canopy condition and growth from combined optical-microwave measurements p 17 N87-17286
- Kansas Univ. Center for Research, Inc., Lawrence.**
Tower-based broadband backscattering measurements from the ocean surface in the North Sea p 47 N87-17217
Some trade-offs in modest-resolution radars for space p 82 N87-17278
- Karlsruhe Univ. (West Germany).**
Hydrogeological research in Peloponnesus (Greece) Karst area by support and completion of LANDSAT-thematic data p 33 N87-17234
Results of tectonic and spectral investigations along the Wadi Araba fault in Jordan using special processed Thematic Mapping (TM) data p 34 N87-17247
- Kasetsart Univ., Bangkok (Thailand).**
The application of LANDSAT imagery for land cover assessment p 13 N87-15614
- Kenya Meteorological Dept., Nairobi.**
Use of remote sensing application for agricultural expansion into semi-arid areas of Kenya p 13 N87-15607
- Klagenfurt Univ. (Austria).**
Land surface models as collateral data in satellite image interpretation p 70 N87-18155
- Kombinet VEB Carl Zeiss, Jena (East Germany).**
Optical visual evaluation and interpretation of remote sensing data p 83 N87-17353
- L**
- Laval Univ. (Quebec).**
Analysis of the spatial structure of Synthetic Aperture Radar (SAR) imagery for a better separability of cereal crops, wheat and barley p 17 N87-17287
- Liege Univ. (Belgium).**
Instrumentation for optical remote sensing from space; Proceedings of the Meeting, Cannes, France, November 27-29, 1985 [SPIE-589] p 73 A87-19647

London Univ. (England).

- Satellite remote sensing of rangelands in Botswana. II
- NOAA AVHRR and herbaceous vegetation p 7 A87-24786
Monitoring the grasslands of the Sahel 1984-1985 p 7 A87-24787

Los Alamos National Lab., N. Mex.

- Canopy hot-spot as crop identifier [DE86-011258] p 19 N87-17395
Off-nadir optical remote sensing from satellites for vegetation identification [DE86-012387] p 23 N87-18916

Los Alamos Scientific Lab., N. Mex.

- Off-nadir optical remote sensing from satellites for vegetation identification p 22 N87-18183

Ludwig-Maximilians-Universitaet, Munich (West Germany).

- Analysis of Large Format Camera images from the Black Hills, USA, for topographic and thematic mapping p 71 N87-18189

Lunar and Planetary Inst., Houston, Tex.

- Thematic mapper studies of central Andean volcanoes [NASA-CR-180252] p 36 N87-18910

Lund Univ. (Sweden).

- Desertification monitoring: Remotely sensed data for drought impact studies in the Sudan p 12 N87-15604
Surface albedo change in arid regions in the Sudan p 13 N87-15615

M**MacDonald, Dettwiler and Associates Ltd., Richmond (British Columbia).**

- Resolving the Doppler ambiguity for spaceborne synthetic aperture radar p 72 N87-18212

Manitoba Univ., Winnipeg.

- Application of 2-D Hilbert transform in the interpretation of remotely sensed potential field data p 35 N87-17293

- Study of ocean bottom coupling process using satellite altimeter data p 54 N87-18199

Marconi Co. Ltd., Chelmsford (England).

- SIR-B observations of ocean waves in the NE Atlantic p 49 N87-17335
A scatterometer research program p 53 N87-17391

Marmara Research Inst., Gebze (Turkey).

- Remote sensing activities in Turkey: Possible contributions to climate studies p 77 N87-15624

Martin Marietta Aerospace, Denver, Colo.

- Instrumentation for optical remote sensing from space; Proceedings of the Meeting, Cannes, France, November 27-29, 1985 [SPIE-589] p 73 A87-19647

Maryland Univ., College Park.

- Simultaneous ocean cross section and rainfall measurements from space with a nadir-looking radar p 38 A87-20956
Analysis of the dynamics of African vegetation using the normalized difference vegetation index p 6 A87-24779

- Monitoring East African vegetation using AVHRR data p 6 A87-24781

- Monitoring the grasslands of the Sahel using NOAA AVHRR data Niger 1983 p 6 A87-24782
Monitoring the grasslands of the Sahel 1984-1985 p 7 A87-24787

Massachusetts Inst. of Tech., Cambridge.

- Space and time variability of the surface color field in the northern Adriatic Sea p 40 A87-23722

- Estimation of vegetation cover at subpixel resolution using LANDSAT data [NASA-CR-177077] p 11 N87-15514
Delineation of fault zones using imaging radar p 32 N87-17138

Massachusetts Univ., Amherst.

- Intersensor comparisons for validation of wind speed measurements from ERS-1 altimeter and scatterometer p 52 N87-17386

Max-Planck-Inst. fuer Meteorologie, Hamburg (West Germany).

- Wave modeling activities of the Wave Modeling (WAM) group relevant to ERS-1 p 52 N87-17389

Messerschmitt-Boelkow-Blohm G.m.b.H., Munich (West Germany).

- The stereo-pushbroom scanner system Digital Photogrammetry System (DPS) and its accuracy p 80 N87-17167

Meteorological Office, Bracknell (England).

- Remote sensing identified in climate model experiments with hydrological and albedo changes in the Sahel p 59 N87-15569

- The use of numerical wind and wave models to provide areal and temporal extension to instrument calibration and validation of remotely sensed data p 51 N87-17371

- The use of aircraft for wind scatterometer calibration p 84 N87-17382

Michigan Univ., Ann Arbor.

- SIR-B measurements and modeling of vegetation p 15 N87-17160

- Components and comparisons of potential information from several imaging satellites p 67 N87-17164

Ministerio de Obras Publicas, Madrid (Spain).

- Marine climate program p 52 N87-17390

Minnesota Univ., Minneapolis.

- Microwave radiances from horizontally finite precipitating clouds containing ice and liquid hydrometeors p 61 N87-17340

Mullard Space Science Lab., Dorking (England).

- The prospects for hydrological measurements using ERS-1 p 59 N87-15588

- An automatic tracking mode switching algorithm for the ERS-1 altimeter p 81 N87-17195

- New techniques in satellite altimeter tracking systems p 85 N87-18164

- Satellite altimeter measurements over land and inland water p 61 N87-18200

N**National Aeronautics and Space Administration, Washington, D.C.**

- Ideas for a future earth observing system from geosynchronous orbit p 74 A87-23419

National Aeronautics and Space Administration. Ames Research Center, Moffett Field, Calif.

- Aircraft and satellite thermographic systems for wildfire mapping and assessment [AIAA PAPER 87-0187] p 7 A87-24933

- Remote sensing of wetland plant stress p 21 N87-18171

National Aeronautics and Space Administration. Earth Resources Lab., Bay St. Louis, Miss.

- Estimation of absolute water surface temperature based on atmospherically corrected thermal infrared multispectral scanner digital data p 79 N87-17114

- Atmospheric correction of TIMS data p 79 N87-17115

- Monitoring vegetation recovery patterns on Mount St. Helens using thermal infrared multispectral data p 14 N87-17122

- Investigation of forest canopy temperatures recorded by the thermal infrared multispectral scanner at H. J. Andrews Experimental Forest p 14 N87-17123

- Applications of TIMS data in agricultural areas and related atmospheric considerations p 15 N87-17124

National Aeronautics and Space Administration. Goddard Space Flight Center, Greenbelt, Md.

- Chlorophyll pigment concentration using spectral curvature algorithms - An evaluation of present and proposed satellite ocean color sensor bands p 37 A87-20204

- Variability of the productive habitat in the eastern equatorial Pacific p 38 A87-20687

- Simultaneous ocean cross section and rainfall measurements from space with a nadir-looking radar p 38 A87-20956

- Instrument characterization for the detection of long-term changes in stratospheric ozone - An analysis of the SBUV/2 radiometer p 74 A87-20961

- The effect of local advection on the inference of soil moisture from thermal infrared radiances p 3 A87-23388

- Ideas for a future earth observing system from geosynchronous orbit p 74 A87-23419

- Temperature-plant pigment-optical relations in a recurrent offshore mesoscale eddy near Point Conception, California [AD-A176666] p 39 A87-23720

- Biological consequences of a recurrent eddy off Point Conception, California p 40 A87-23721

- Space and time variability of the surface color field in the northern Adriatic Sea p 40 A87-23722

- POLYSITE - An interactive package for the selection and refinement of Landsat image training sites p 65 A87-23805

- Maximum normalized difference vegetation index images for sub-Saharan Africa for 1983-1985 p 6 A87-24776

- Satellite remote sensing of primary production p 6 A87-24777

- Characteristics of maximum-value composite images from temporal AVHRR data p 75 A87-24778

- Monitoring East African vegetation using AVHRR data p 6 A87-24781

- Satellite remote sensing of rangelands in Botswana. II - NOAA AVHRR and herbaceous vegetation p 7 A87-24786

- Monitoring the grasslands of the Sahel 1984-1985 p 7 A87-24787

- Assessment of ecological conditions associated with the 1980/81 desert locust plague upsurge in West Africa using environmental satellite data p 7 A87-24789

- Remote detection of forest damage p 8 A87-26197

- Large-scale short-period sea ice atmosphere interaction p 42 A87-27546

- Utility of AVHRR channels 3 and 4 in land-cover mapping p 9 A87-28388

- Remote sensing of land-surface temperature from HIRS/MSU data p 77 N87-15573

- The first International Satellite Land Surface Climatology Project (ISLSCP) Field Experiment - FIFE p 14 N87-15629

- The physical basis for spectral variations in thermal infrared emittance of silicates and application to remote sensing p 31 N87-17129

- Active/passive microwave sensor comparison of MLZ-ice concentration estimates p 46 N87-17185

- The Electronically Steered Thinned Array Radiometer (ESTAR) p 82 N87-17260

- Evaluating roughness models of radar backscatter p 19 N87-17344

- Oceanographic measurement capabilities of the NASA P-3 aircraft p 52 N87-17380

- Geomorphology from space: A global overview of regional landforms [NASA-SP-486] p 36 N87-18139

National Aeronautics and Space Administration. Langley Research Center, Hampton, Va.

- SAM II measurements of Antarctic PSC's and aerosols p 75 A87-23546

- Space Shuttle cloud detection and earth feature classification experiment p 77 A87-31139

- Archival of Seasat-A satellite scatterometer data merged with in situ data at selected, illuminated sites over the ocean [NASA-TM-87736] p 45 N87-16492

National Aeronautics and Space Administration. Marshall Space Flight Center, Huntsville, Ala.

- Verification of small-scale water vapor features in VAS imagery using high resolution MAMS imagery p 62 A87-23348

National Aeronautics and Space Administration. National Space Technology Labs., Bay Saint Louis, Miss.

- Use of topographic and climatological models in a geographical data base to improve Landsat MSS classification for Olympic National Park p 25 A87-30128

- National Aerospace Lab., Amsterdam (Netherlands).**
The processing of and information extraction from airborne SLAR data [NLR-MP-86004-U] p 23 N87-18919

National Environmental Satellite Service, Madison, Wis.

- Verification of small-scale water vapor features in VAS imagery using high resolution MAMS imagery p 62 A87-23348

National Oceanic and Atmospheric Administration, Fort Collins, Colo.

- Satellite contributions to convective scale weather analysis and forecasting p 76 A87-27882

National Oceanic and Atmospheric Administration, Seattle, Wash.

- Equatorial long-wave characteristics determined from satellite sea surface temperature and in situ data p 44 A87-30923

National Oceanic and Atmospheric Administration, Washington, D. C.

- Satellite remote sensing of the marine environment: Literature and data sources [PB86-245446] p 56 N87-18971

National Park Service, Gunnison, Colo.

- Use of topographic and climatological models in a geographical data base to improve Landsat MSS classification for Olympic National Park p 25 A87-30128

National Space Development Agency, Ibaraki (Japan).

- A satellite-borne SAR transmitter and receiver p 83 N87-17358

- Pulse compression test results of the SAR transmitter and receiver p 83 N87-17360

- Outline of SAR-850 data processing method in Japan p 71 N87-18176

National Space Development Agency, Tokyo (Japan).

- Some results of Marine Observation Satellite (MOS-1) airborne verification experiment Multispectral Electronic Self Scanning Radiometer (MESSR) p 46 N87-17166

Naval Academy, Annapolis, Md.

- Analysis of surface patterns over Cobb Seamount using synthetic-aperture radar imagery [AD-A171670] p 45 N87-16493

Naval Ocean Research and Development Activity, Bay St. Louis, Miss.

- Observations of surface currents at Nantucket Shoals and implications for radar imaging of the bottom p 48 N87-17296

- The impact of satellite infrared sea surface temperatures on FNOG (Fleet Numerical Oceanography Center) ocean thermal analyses
[AD-A173333] p 54 N87-18295
- Naval Polar Oceanography Center, Washington, D.C.**
Eastern-Western Arctic Sea Ice Analysis, 1985
[AD-A173972] p 55 N87-18298
- Naval Postgraduate School, Monterey, Calif.**
The relationship between marine aerosol optical depth and satellite-sensed sea surface temperature
[AD-A174337] p 55 N87-18963
- Naval Research Lab., Washington, D. C.**
Application of Spaceborne Distributed Aperture/Coherent Array Processing (SDA/CAP) technology to active and passive microwave remote sensing p 82 N87-17277
Comparison of ocean tide models with satellite altimeter data
[AD-A174698] p 56 N87-19879
- Nebraska Univ., Lincoln.**
TIMS data applications in Nebraska p 15 N87-17126
- Nevada Univ., Reno.**
Detection and mapping of volcanic rock assemblages and associated hydrothermal alteration with Thermal Infrared Multiband Scanner (TIMS) data Cornstock Lode Mining District, Virginia City, Nevada p 31 N87-17119
Application of Thermal Infrared Multiband Scanner (TIMS) data to mapping of Plutonic and stratified rock and assemblages in accreted terrains of the Northern Sierra, California p 15 N87-17132
Nature and origin of mineral coatings on volcanic rocks of the Black Mountain, Stonewall Mountain, and Kane Springs, Wash volcanic centers, Southern Nevada
[NASA-CR-180183] p 36 N87-18255
- New South Wales Univ., Kensington (Australia).**
Radar signature determination: Trends and limitations p 67 N87-17159
- New York State Univ., Binghamton.**
Estimation of canopy parameters for inhomogeneous vegetation canopies from reflectance data. II - Estimation of leaf area index and percentage of ground cover for row canopies p 1 A87-20761
- New Zealand Meteorological Service, Wellington.**
Calibration of normalized vegetation index against pasture growth p 12 N87-15585
- North Carolina State Coll., Raleigh.**
Modelling of estuarine chlorophyll-A from an airborne scanner p 61 N87-18172
- O**
- Oak Ridge National Lab., Tenn.**
Interpreting forest and grassland biome productivity utilizing nested scales of image resolution and biogeographical analysis
[NASA-CR-180213] p 23 N87-18912
- Ocean Surface Research, Boulder, Colo.**
SEASAT microwave altimeter measurement of the ocean gravity wave equilibrium-range spectral behavior using full-wave theory p 53 N87-18165
- Office of Naval Research, Arlington, Va.**
Physical oceanography program science abstracts
[AD-A174019] p 55 N87-18961
Investigation of physics of synthetic aperture radar in ocean remote sensing TOWARD 84/86 field experiment. Volume 2: Contributions of individual investigators
[AD-A174527] p 55 N87-18966
- Ohio State Univ., Columbus.**
Basic research for the geodynamics program
[NASA-CR-180137] p 27 N87-17415
Improvement of the Earth's gravity field from terrestrial and satellite data
[NASA-CR-180139] p 27 N87-17416
- Oldenburg Univ. (West Germany).**
Laser-induced chlorophyll-A fluorescence of terrestrial plants p 23 N87-18207
- Operations Research, Inc., Rockville, Md.**
The Sequential Filter Imaging Radiometer (SFIR), a new instrument configuration for Earth observations p 81 N87-17205
- Oregon State Univ., Corvallis.**
Further development of an improved altimeter wind speed algorithm p 42 A87-27848
- Oslo Univ. (Norway).**
A climatological-hydrological study of lake ice in the southwestern mountain area in Norway by use of satellite sensing p 61 N87-17319
- Osnabrueck Univ. (West Germany).**
Evaluation of climate relevant land surface characteristics from remote sensing p 12 N87-15572
- Oulu Univ. (Finland).**
Remote sensing of shallow water areas with reference to environmental and multitemporal monitoring of the Hailuoto area, Finland p 61 N87-18159

P

- Pacific Northwest Labs., Richland, Wash.**
Surface reflectance correction and stereo enhancement of LANDSAT thematic mapper imagery for structural geologic exploration
[DE87-003095] p 37 N87-19796
- Pennsylvania State Univ., University Park.**
Utilization of satellite data in mesoscale modeling of severe weather
[NASA-CR-179917] p 78 N87-15669
The application of remotely sensed data to pedologic and geomorphic mapping on alluvial fan and playa surfaces in Saline Valley, California p 15 N87-17127
- Physics and Electronics Lab. TNO, The Hague (Netherlands).**
C and Ku-band scatterometer results from the SCATMOD internal wave experiment p 47 N87-17215
- Purdue Univ., West Lafayette, Ind.**
Analysis of multiple incidence angle SIR-B data for determining forest stand characteristics p 15 N87-17156
Parameter space techniques for image registration p 70 N87-17327
Improving the geological interpretation of magnetic and gravity satellite anomalies
[NASA-CR-180149] p 35 N87-17418

R

- R Scan Corp., Minneapolis, Minn.**
Forecasting sea breeze thunderstorms at the Kennedy Space Center using the Prognostic Three-Dimensional Mesoscale Model (P 3DM) p 43 A87-27891
- Rand Afrikaans Univ., Johannesburg (South Africa).**
Integrating vector and satellite data to evaluate the adequacy of a grain silo network p 21 N87-18156
- Reading Univ. (England).**
Instrumentation for optical remote sensing from space; Proceedings of the Meeting, Cannes, France, November 27-29, 1985
[SPIE-589] p 73 A87-19647
Analysis of the dynamics of African vegetation using the normalized difference vegetation index p 6 A87-24779
Rainfall estimation over the Sahel using Meteosat thermal infra-red data p 59 N87-15587
Hydrological studies in Niger p 59 N87-15609
Monitoring sediment transfer processes on the desert margin
[NASA-CR-180181] p 23 N87-18222
- Remote Sensing Systems, Sausalito, Calif.**
Further development of an improved altimeter wind speed algorithm p 42 A87-27848
- Rhode Island Univ., Kingston.**
Arctic haze: Natural or pollution?
[AD-A174025] p 55 N87-18931
- Rijkswaterstaat, The Hague (Netherlands).**
Evaluation of remote sensing results for the benefit of water quality research on the North Sea
[NZ-R-86.15] p 62 N87-19799
- Rochester Inst. of Tech., N. Y.**
Radiometric analysis of the longwave infrared channel of the Thematic Mapper on LANDSAT 4 and 5
[NASA-CR-180180] p 86 N87-18221
- Royal Netherlands Meteorological Inst., De Bilt.**
The accuracy and availability of operational marine surface wind data for ERS-1 sensor calibration and validation from fixed platforms and free drifting buoys p 51 N87-17376

S

- SASC Technologies, Inc., Hampton, Va.**
SAM II measurements of Antarctic PSC's and aerosols p 75 A87-23546
- SASC Technologies, Inc., Hyattsville, Md.**
Instrument characterization for the detection of long-term changes in stratospheric ozone - An analysis of the SBUV/2 radiometer p 74 A87-20961
- Science Research Council, Chilton (England).**
Gathering and processing a comparative data set for the calibration and validation of ERS-1 data products; preparatory work at the UK-ERS-DC p 50 N87-17367
Measurement of the directional spectrum of ocean waves using a conically-scanning radar p 52 N87-17383
- SeaSpace, San Diego, Calif.**
Equatorial long-wave characteristics determined from satellite sea surface temperature and in situ data p 44 A87-30923

Software Sciences Ltd., Farnborough (England).

- The design of an international data centre for remote sensing p 67 N87-17176
- South Dakota State Univ., Brookings.**
Modeling energy flow and nutrient cycling in natural semiarid grassland ecosystems with the aid of thematic mapper data
[NASA-CR-179903] p 11 N87-15517
- SRI International Corp., Menlo Park, Calif.**
Development and demonstration of ALARM (Airborne Lidar Agent Remote Monitor)
[AD-A172886] p 78 N87-16387
- Stanford Univ., Calif.**
Spatial analysis of the dynamics of an ecosystem by multistage remote sensing in Kenya p 16 N87-17173
Automated remote sensing of sea ice using synthetic aperture radar p 46 N87-17186
A knowledge-based software environment for the analysis of spectroradiometer data p 68 N87-17203
Interrelationship between field spectra and airborne MSS systems in the Singatse range, (Yerington) Nevada p 34 N87-17242
- Stockholm Univ. (Sweden).**
A statistical approach to select the optimal wavelength bands for separating rocks in the wavelength region 0.4 to 2.3 microns p 34 N87-17244
- Stuttgart Univ. (West Germany).**
Future user requirements and required technological developments of spaceborne synthetic aperture radars p 82 N87-17320
- Swedish Space Corp., Soina.**
Marrying geocoded image data with other types of geographic information in a PC environment p 21 N87-18154
- T**
- Technical Univ. of Denmark, Lyngby.**
Sea ice in the Greenland sea observed by the Nimbus-7 Scanning Multichannel Microwave Radiometer (SMMR) p 48 N87-17221
- Technicolor Government Services, Inc., Moffett Field, Calif.**
Aircraft and satellite thermographic systems for wildfire mapping and assessment
[AIAA PAPER 87-0187] p 7 A87-24933
- Technische Hogeschool, Delft (Netherlands).**
Homogeneous plate deformations on a sphere as monitored by Satellite Laser Ranging (SLR) networks analyzed with the multi-epoch method
[ETN-87-99221] p 27 N87-18908
Bare soil measurements with the Delft University Scatterometer (DUTSCAT) system (L-band)
[REPT-64-220-86-T-1LH] p 24 N87-19797
- Technische Univ., Graz (Austria).**
Influence of canopy shadow on stress detection in coniferous forests using LANDSAT data p 21 N87-18173
Relationship between tree density, leaf area index, soil metal content, and LANDSAT MSS canopy radiance values p 21 N87-18174
- Texas Instruments, Inc., Dallas.**
The effect of measurement error and confusion from vegetation on passive microwave estimates of soil moisture p 18 N87-17304
- Texas Univ., Austin.**
Accurate measurement of mean sea level changes by altimetric satellites p 38 A87-20524
Tree attenuation at 869 MHz derived from remotely piloted aircraft measurements p 9 A87-28414
Undersea volcano production versus lithospheric strength from satellite altimetry
[NASA-CR-179984] p 78 N87-15660
NROSS (Navy Remote Ocean Sensing System) tracking network analysis
[AD-A172132] p 45 N87-16384
- Thessaloniki Univ. (Greece).**
The use of remote sensing techniques in the study of vegetation recovery after fire in mediterranean countries (a preliminary study) p 14 N87-15623
- Toba Merchant Marine Coll. (Japan).**
Estimation of maximum snow volume distribution using NOAA-AVHRR data p 60 N87-17314
- Tokyo Univ. (Japan).**
Models for temperature estimation from remotely sensed thermal IR data p 83 N87-17325
- Toshiba Research and Development Center, Kawasaki (Japan).**
High speed image processing system based on the custom VLSI for Digital Signal Processing (DSP) p 71 N87-18179
- TRW Space Technology Labs., Redondo Beach, Calif.**
SAR imaging of bottom topography in the ocean: Results from an improved model p 48 N87-17298

United Nations. General Assembly.

U

United Nations. General Assembly. Committee on the Peaceful Uses of Outer Space.

Monitoring East African vegetation using AVHRR data
p 6 A87-24781

Universite Catholique de Louvain (Belgium).

Estimation of surface albedo using satellite data. A simple formulation for atmospheric effects
p 25 N87-15579

A two-step algorithm for the separate retrieval of ocean surface and atmospheric parameters from microwave radiometers
p 50 N87-17341

University Coll., Dublin (Ireland).

Hydrologic models of land surface processes
p 58 N87-15547

University of North-Eastern Hill, Shillong (India).

Structural and geomorphic evolution of Meghalaya plateau, India on LANDSAT imagery
p 33 N87-17233

University of the West Indies, Kingston (Jamaica).

Vegetation change and desertification in the Caribbean
p 14 N87-15619

V

Vexcell Corp., Boulder, Colo.

Space Shuttle radargrammetry results
p 65 A87-23827

Using secondary image products to aid in understanding and interpretation of radar imagery
p 68 N87-17239

W

Washington State Univ., Pullman.

Spectral characteristics and the extent of paleosols of the Palouse formation
[NASA-CR-180357]
p 24 N87-19826

Washington Univ., Seattle.

Ocean surface pressure fields from satellite-sensed winds
p 41 A87-25797

Observing the polar oceans with spaceborne radar
p 46 N87-17151

Washington Univ., St. Louis, Mo.

Ozone formation in pollutant plumes: A reactive plume model with arbitrary crosswind resolution
[PB86-236973]
p 26 N87-18246

Wisconsin Univ., Madison.

Verification of small-scale water vapor features in VAS imagery using high resolution MAMS imagery
p 62 A87-23348

Ideas for a future earth observing system from geosynchronous orbit
p 74 A87-23419

A case study of GWE satellite data impact on GLA assimilation analyses of two ocean cyclones
p 41 A87-25787

World Climate Programme, Geneva (Switzerland).

Report of the Fourth Session of the JSC/CCCO Tropical Ocean Global Atmosphere (TOGA) Scientific Steering Group
[WCP-120]
p 54 N87-18283

World Meteorological Organization, Geneva

(Switzerland).
An overview of the implementation of the World Climate Research program
p 26 N87-17388

Z

Zurich Univ. (Switzerland).

Monitoring of land-surface change in Sri Lanka
p 13 N87-15618

Sri Lanka's solution to land use mapping and monitoring for Third World countries development
p 67 N87-17174

Merging spaceborne image data of optical and microwave sensors
p 69 N87-17267

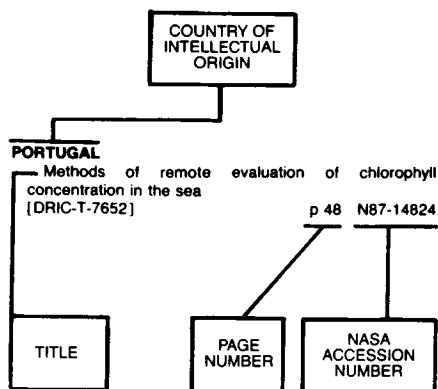
Viewing angle corrections of airborne multispectral scanner data acquired over forested surfaces
p 17 N87-17273

Snow cover recession in an Alpine ecological system
p 18 N87-17316

Towards snowmelt runoff forecast using LANDSAT-MSS and NOAA/AVHRR data
p 61 N87-17317

Monitoring land use changes in Sri Lanka for land use planning using a geographic information system and satellite imagery
p 26 N87-18151

Typical Foreign Technology Index Listing



Listings in this index are arranged alphabetically by country of intellectual origin. The title of the document is used to provide a brief description of the subject matter. The page number and the accession number are included in each entry to assist the user in locating the citation in the abstract section.

A

ALGERIA
The fundamental problems for the energy balance study by satellite imagery p 66 N87-15590

AUSTRALIA
A thermal device for aircraft measurement of the solid water content of clouds p 56 A87-20951
Structure of the Kerguelen Plateau province from Seasat altimetry and seismic reflection data p 28 A87-24866
The Coastal Zone Color Scanner views the Bismarck Sea p 42 A87-26970
Calibration of Landsat data for sparsely vegetated semi-arid rangelands p 9 A87-29008
Classification of reflectance on colour infrared aerial photographs and sub-tropical salt-marsh vegetation types p 10 A87-29012
Radar signature determination: Trends and limitations p 67 N87-17159
The FRS-68010: A new concept for the acquisition and analysis of NOAA HRPT data p 68 N87-17206
Australian validation plans for ERS-1 p 84 N87-17387

AUSTRIA
Vegetation identification and variability in the Tahoua area, Nigeria p 13 N87-15610
Land surface models as collateral data in satellite image interpretation p 70 N87-18155
Influence of canopy shadow on stress detection in coniferous forests using LANDSAT data p 21 N87-18173
Relationship between tree density, leaf area index, soil metal content, and LANDSAT MSS canopy radiance values p 21 N87-18174

B

BELGIUM
Estimation of surface albedo using satellite data. A simple formulation for atmospheric effects p 25 N87-15579
Assessment of wind and fluvial action by using LANDSAT-MSS color composites in the lower Nile Valley (Egypt) p 13 N87-15612
A two-step algorithm for the separate retrieval of ocean surface and atmospheric parameters from microwave radiometers p 50 N87-17341
Assessment of soil degradation in an arid region using remote sensing p 20 N87-18148

BRAZIL
The use of aerial remote sensing in a case study of desertification: Quixaba-PE [INPE-3963-PRE/980] p 11 N87-15519
Application of remote sensing in hydrology and water resources [INPE-3986-PRE/991] p 60 N87-16382
Environmental modification of metropolitan areas through satellite images: Study of urban design in the tropics p 25 N87-17175
Soil degradation evaluation by digital image processing p 20 N87-18147
Agricultural crop estimates using information gathered by remote sensing satellites, as well as ground data, through samples of geographic layers [INPE-4102-RPE/534] p 24 N87-19786
Evaluation of LANDSAT 4 MSS data for geomorphological mapping in the semiarid environment for regional planning purposes: An integrated approach (study site, the Juazeiro region) [INPE-3984-TDL/236] p 72 N87-19787
Remote sensing applied to basic geological surveys: A methodological approach for the northeast region [INPE-4041-TDL/246] p 37 N87-19788
CANASATE: Sugar cane mapping by satellite, area 3 [INPE-4068-RPE/526] p 24 N87-19790
Methodology for the elaboration of thematic maps utilizing LANDSAT-TM data [INPE-3893-TDL/225] p 72 N87-19792

C

CANADA
An initial evaluation of two digital airborne imagers for surveying spruce budworm defoliation p 1 A87-20671
Comparison between satellite image advective velocities, dynamic topography, and surface drifter trajectories p 38 A87-20692
Forest fire monitoring using the NOAA satellite series p 3 A87-23360
An objective method for computing advective surface velocities from sequential infrared satellite images p 39 A87-23717
Control extension utilizing Large Format Camera imagery p 75 A87-23804
Automated extraction of pack ice motion from advanced very high resolution radiometer imagery p 42 A87-27547
Terrain analysis from digital patterns in geomorphometry and Landsat MSS spectral response p 66 A87-30127
An overview of operational SAR data collection and dissemination plans for ERS-1 ice data in Canada p 47 N87-17189
Canadian plans for operational demonstrations of satellite imaging radar applications p 68 N87-17229
Integration of surficial geochemistry and LANDSAT imagery to discover skarn tungsten deposits using image analysis techniques [CONTRIB-19586] p 35 N87-17248
Application of the Seasat scatterometer to observations of wind speed and direction and Arctic ice/water boundaries p 48 N87-17259
Digital terrain mapping with STAR-1 SAR data p 69 N87-17269
An overview of remote sensing agricultural applications in North America: Past, present and future p 17 N87-17284

Analysis of the spatial structure of Synthetic Aperture Radar (SAR) imagery for a better separability of cereal crops, wheat and barley p 17 N87-17287
Application of 2-D Hilbert transform in the interpretation of remotely sensed potential field data p 35 N87-17293
Estimation of internal wave currents from SAR and infrared scatterometer imagery p 48 N87-17295
SAR imagery for forest management p 18 N87-17313
Thermal infrared remote sensing: One of today's solutions p 83 N87-17324
Canada Center for Remote Sensing (CCRS) Convoir 580 results relevant to ERS-1 wind and wave calibration p 84 N87-17379
Spatial remote sensing to land management p 70 N87-18157
A very fast synthetic-aperture radar signal processor for ERS-1 and Radarsat p 85 N87-18180
STAR-VUE: A tactical ice navigation workstation p 54 N87-18181
Study of ocean bottom coupling process using satellite altimeter data p 54 N87-18199
Resolving the Doppler ambiguity for spaceborne synthetic aperture radar p 72 N87-18212

CHINA, PEOPLE'S REPUBLIC OF
Snow survey from meteorological satellite images in the Qilian Mountain Basin in northwest China p 56 A87-20765
Atlas of geo-science analyses of Landsat imagery in China p 65 A87-24542

D

DENMARK
Sea ice in the Greenland sea observed by the Nimbus-7 Scanning Multichannel Microwave Radiometer (SMMR) p 48 N87-17221
The ice conditions in the Greenland waters, 1980 [REPT-551.467.3.068(988)] p 53 N87-17428

E

ESTONIA
A photographic technique for studying reflection indicatrices of vegetation cover p 5 A87-24388

ETHIOPIA
Reflections on drought - Ethiopia 1983-1984 p 6 A87-24780
Growing period and drought early warning in Africa using satellite data p 7 A87-24788

F

FINLAND
Developpement of algorithms to retrieve the water equivalent of snow cover from satellite microwave radiometer data p 60 N87-17264
Classification of forest and surface types by satellite microwave radiometry p 18 N87-17305
Retrieval of near-surface wind speed in the Baltic Sea from NIMBUS-7 Scanning Multichannel Microwave Radiometer (SMMR) observations p 50 N87-17342
Sea ice studies in the Baltic Sea using satellite microwave radiometer data p 50 N87-17343
Remote sensing of shallow water areas with reference to environmental and multitemporal monitoring of the Hailuoto area, Finland p 61 N87-18159

FRANCE
In flight calibration of push broom remote sensing instruments p 73 A87-19652
The SPOT satellites - From SPOT 1 to SPOT 4 p 74 A87-21094
Exploitation of the SPOT system p 62 A87-21095
Soil science interpretation of photographs taken by Spacelab 1 p 2 A87-21241
Visualization by aerial thermography of hydrodynamic exchanges between the water table, streams and gravel pits in the Rhine plain north of Strasbourg p 58 A87-25746

- Proposal of a remote sensing method for measuring soil moisture of bare soils in the frequency range 100 MHz-1 GHz p 8 A87-26974
- The shape of the earth in the space age p 26 A87-28442
- Drainage channel network of the Aracchon Basin using Thematic Mapper data obtained at high tide p 58 A87-29013
- SPOT IMAGE and commercialisation of remote sensing data p 65 A87-29430
- Weather and atmosphere remote sensing p 77 A87-30885
- Modelisation of evapotranspiration and soil available water over an agricultural region applicable for remote sensing p 12 N87-15554
- Design of a data base system for inferring land surface parameters and fluxes from satellite radiances p 66 N87-15625
- Hydrological Atmospheric Pilot Experiment (HAPEX) hydrology budget modeling (MOBILHY): Outline of the program p 59 N87-15632
- VARAN-S radar image interpretation [CNES-CT/DRT/TIT/RL-54-T] p 66 N87-16963
- Proceedings of the 1986 International Geoscience and Remote Sensing Symposium (IGARSS '86) on Remote Sensing: Today's Solutions for Tomorrow's Information Needs, volume 1 p 80 N87-17163
- Monitoring of large phenomena in developing countries through satellite imagery p 67 N87-17172
- Automated remote sensing of sea ice using synthetic aperture radar p 46 N87-17186
- Overview and status of the ERS-1 program p 47 N87-17190
- The ESA approach for ERS-1 sensor calibration and performance verification p 80 N87-17192
- Extraction of the backscatter coefficient of agricultural fields from an airborne SAR image p 16 N87-17265
- Proceedings of the 1986 International Geoscience and Remote Sensing Symposium (IGARSS '86) on Remote Sensing: Today's Solutions for Tomorrow's Information Needs, volume 2 p 82 N87-17283
- [ESA-SP-254-VOL-2] p 82 N87-17283
- Toward a satellite system to monitor the spatial and temporal behavior of soil water content p 18 N87-17288
- Computer-aided interpretation of complex geological patterns in remote sensing p 35 N87-17294
- Proceedings of an ESA Workshop on ERS-1 Wind and Wave Calibration [ESA-SP-262] p 84 N87-17363
- Evaluation of the different parameters in Long's C-band model p 51 N87-17370
- Using buoys and ships to calibrate ERS-1 altimeter and scatterometer p 51 N87-17377
- Proceedings of the 1986 International Geoscience and Remote Sensing Symposium (IGARSS '86) on Remote Sensing: Today's Solutions for Tomorrow's Information Needs, volume 3 p 84 N87-18142
- [ESA-SP-254-VOL-3] p 84 N87-18142
- Thermal inertia and soil fluxes by remote sensing p 20 N87-18143
- The use of thermal airborne remote sensing for soil identification: A case study in Limousin (France) p 20 N87-18146
- First step in the use of remote sensing for regional mapping of soil organization data: Application in Brittany (France) and French Guiana p 23 N87-18193

G

GERMANY, FEDERAL REPUBLIC OF

- Multilens cameras for high velocity/low altitude photoreconnaissance p 75 A87-23650
- Measurement of microwave backscattering signatures of the ocean surface using X band and K(a) band airborne scatterometers p 40 A87-23725
- Digital image matching techniques for standard photogrammetric applications p 63 A87-23785
- Results of an airborne synthetic-aperture radar (SAR) experiment over a SIR-B (Shuttle Imaging Radar) test site in Germany p 76 A87-27999
- Evaluation of climate relevant land surface characteristics from remote sensing p 12 N87-15572
- Satellite-derived vegetation index over Europe p 12 N87-15583
- Multiangle or multiwavelength technique for remote sensing of sea surface temperature p 45 N87-15652
- Comparison of Thematic Mapper (TM) and SPOT simulation data for agricultural applications in south west Germany p 16 N87-17165
- The stereo-pushbroom scanner system Digital Photogrammetry System (DPS) and its accuracy p 80 N87-17167

- Hydrogeological research in Peloponnesus (Greece) Karst area by support and completion of LANDSAT-thematic data p 33 N87-17234
- Results of tectonic and spectral investigations along the Wadi Araba fault in Jordan using special processed Thematic Mapping (TM) data p 34 N87-17247
- Microwave remote sensing: Its applications and limitations in operational tasks of land use inventory and forest management p 17 N87-17266
- Future user requirements and required technological developments of spaceborne synthetic aperture radars p 82 N87-17320
- Optical visual evaluation and interpretation of remote sensing data p 83 N87-17353
- X-SAR extends the frequency range of Shuttle Imaging Radar p 70 N87-17362
- Comparison concept of satellite derived wind and wave data with ground truth p 51 N87-17373
- Wave modeling activities of the Wave Modeling (WAM) group relevant to ERS-1 p 52 N87-17389
- On the discrimination between crude oil spills and monomolecular sea slicks by airborne remote sensors: Today's possibilities and limitations p 53 N87-18167
- Oil slick detection with a sidelooking airborne radar p 53 N87-18169
- Contributions to oil spill detection and analysis with radar and microwave radiometry, results of the Archimedes 2 campaign p 54 N87-18170
- Digital realtime SAR processor for C- and X-band applications p 71 N87-18177
- Intelligent SAR Processor (ISAR), a new concept for high throughput and high precision digital SAR processing p 85 N87-18178
- Southern Pantanal Matogrossense (South America) of Modular Optoelectronic Multispectral Scanner (MOMS) data, preliminary results p 71 N87-18182
- Multitemporal analysis of the phenological stage of vegetation using TM-data in the Southern Black Forest (West Germany) p 22 N87-18184
- Analysis of Large Format Camera images from the Black Hills, USA, for topographic and thematic mapping p 71 N87-18189
- LANDSAT-MSS remote sensing and satellite cartography: An integrated approach to the preparation of a new geological map of Egypt at a scale of 1:500 000 p 36 N87-18190
- Deduction of a synthetic bioclimatological map by means of remote sensing data and a digital terrain model using a correlation approach p 72 N87-18194
- Laser-induced chlorophyll-A fluorescence of terrestrial plants p 23 N87-18207
- Forest cover analysis using SIR-B data p 23 N87-18220

GREECE

- The use of remote sensing techniques in the study of vegetation recovery after fire in mediterranean countries (a preliminary study) p 14 N87-15623

H

HUNGARY

- Comparison of some classification methods on a test site (Kiskore, Hungary) - Separability as a measure of accuracy p 9 A87-29006

I

INDIA

- A new semi-empirical sea spectrum for estimating the scattering coefficient p 38 A87-20769
- Equatorial Indian Ocean evaporation estimates from operational meteorological satellites and some inferences in the context of monsoon onset and activity p 39 A87-22041
- Wind-wave relationship from Seasat radar altimeter data p 41 A87-24748
- Indian remote sensing program p 77 N87-15242
- AVHRR and MSS data based vegetation indices studies over Indian sites p 14 N87-15622
- Significance of space image, air photo and drainage linears in relation to west coast tectonics, India p 33 N87-17232
- Structural and geomorphic evolution of Meghalaya plateau, India on LANDSAT imagery p 33 N87-17233
- Computer-aided analysis of LANDSAT data for mapping geologic and geomorphic features, North Bombay, India p 33 N87-17235
- Comparative study of LANDSAT MSS, Salyut-7 (TERRA) and radar (SIR-A) images for geological and geomorphological applications: A case study from Rajasthan and Gujarat, India p 34 N87-17236
- Application of remote sensing in the study of the soil hazards of Haryana State, India p 20 N87-18150

- Remote sensing applications in the study of land use and soils of aeolian cover of the western part of Haryana State, India p 22 N87-18187
- Retrieval and global comparison of oceanic winds from SEASAT radiometer, scatterometer and altimeter p 85 N87-18219

INTERNATIONAL ORGANIZATION

- The SEU risk assessment of Z80A, 8086 and 80C86 microprocessors intended for use in a low altitude polar orbit p 74 A87-22025
- Rainfall and vegetation monitoring in the Savanna Zone of the Democratic Republic of Sudan using the NOAA Advanced Very High Resolution Radiometer p 6 A87-24783
- Assessment of ecological conditions associated with the 1980/81 desert locust plague upsurge in West Africa using environmental satellite data p 7 A87-24789
- On the use of synthetic 12-micron data in a split-window retrieval of sea surface temperature from AVHRR measurements p 43 A87-29019

IRELAND

- Hydrologic models of land surface processes p 58 N87-15547

ITALY

- Business approach to earth observation applications p 87 A87-29433
- Contribution of passive microwave remote sensing in soil moisture and evapotranspiration measurements p 12 N87-15589
- An integrated system to assess agricultural productivity p 14 N87-15621
- Multispectral classification of microwave remote sensing images p 16 N87-17238
- Integrated analysis of geological and remote sensing data aimed at mineral deposits detection in the Monapo area (northern Mozambique) p 34 N87-17243
- Rural land use inventory and mapping in the Ardeche area (France) using multitemporal Thematic Mapping (TM) data p 19 N87-17350
- An integrated data bank for agricultural productivity by remote sensing p 21 N87-18153
- UMUS: A project for usage of LANDSAT MSS and ancillary data in land cover mapping of large areas in southern Italy p 72 N87-18191

J

JAMAICA

- Vegetation change and desertification in the Caribbean p 14 N87-15619

JAPAN

- Pre-assessment for large scale civil engineering projects by integrated analysis with the data numerical topography and remote sensing p 57 A87-23815
- Development and experiment of airborne microwave rain-scatterometer/radiometer system. III - Rain measurement and its data analysis p 58 A87-28436
- Development and experiment of airborne microwave rain-scatterometer/radiometer system. IV - Microwave back-scattering experiment of ocean surface p 43 A87-28437
- Performance of Landsat-5 TM data in land-cover classification p 25 A87-29007
- Extraction of areas infested by pine bark beetle using Landsat MSS data p 10 A87-30129
- Development, status, prospects of marine observation satellite p 45 N87-15989
- Some results of Marine Observation Satellite (MOS-1) airborne verification experiment Multispectral Electronic Self Scanning Radiometer (MESSR) p 46 N87-17166
- Bitemporal analysis of Thematic Mapper data for land cover classification p 69 N87-17249
- Evaluation of LANDSAT 5 Thematic Mapping (TM) data for image clustering and classification p 69 N87-17251
- Estimation of maximum snow volume distribution using NOAA-AVHRR data p 60 N87-17314
- Models for temperature estimation from remotely sensed thermal IR data p 83 N87-17325
- Radiometric correction method which removes both atmospheric and topographic effects from the LANDSAT-MSS data p 83 N87-17329
- A satellite-borne SAR transmitter and receiver p 83 N87-17358
- Pulse compression test results of the SAR transmitter and receiver p 83 N87-17360
- Outline of SAR-850 data processing method in Japan p 71 N87-18176
- High speed image processing system based on the custom VLSI for Digital Signal Processing (DSP) p 71 N87-18179
- Automatic update procedure of the digitized land use map using LANDSAT TM data p 72 N87-18192

K

KENYA

- Estimating pre-harvest production of maize in Kenya using large-scale aerial photography and radiometry p 9 A87-29004
- Use of remote sensing application for agricultural expansion into semi-arid areas of Kenya p 13 N87-15607

M

MALI

- Monitoring vegetation in the Mali Sahel during summer 1984 p 6 A87-24784

N

NETHERLANDS

- The thematic mapper - A new tool for soil mapping in arid areas p 2 A87-21243
- Processing thematic mapper data for mapping in Tunisia p 2 A87-21244
- An application of thematic mapper data in Tunisia - Estimation of daily amplitude in near-surface soil temperature and discrimination of hypersaline soils p 2 A87-21245
- Thermography - Principles and application in the Oost-Gelderland remote sensing study project p 3 A87-21247
- Theoretical approach to radar backscattering of soils p 3 A87-21250
- Composite/progressive sampling - A program package for computer supported collection of DTM data p 62 A87-23784
- A comparative study of lineament analysis from different remote sensing imagery over areas in the Benue Valley and Jos Plateau Nigeria p 30 A87-29010
- Ground water-fed lakes in the Libyan desert: Their varying area as observed by means of LANDSAT-MSS data p 59 N87-15611
- Group Agromet Monitoring Project (GAMP) methodology integrated mapping of rainfall, evapotranspiration, germination, biomass development and thermal inertia, based on Meteosat and conventional meteorological data p 59 N87-15626
- Future European plans in the framework of the International Satellite Land Surface Climatology Project (ISLSCP) p 78 N87-15628
- Concept of a future multispectral Thermal Infrared (TIR) pushbroom mission for Earth observation from space p 80 N87-17169
- ERS-1 radar altimeter: Performance, calibration and data validation p 80 N87-17194
- C and Ku-band scatterometer results from the SCATMOD internal wave experiment p 47 N87-17215
- ERS-1 fast delivery processing and products p 81 N87-17224
- ERS-1 mission constraints related to wind and wave calibration p 84 N87-17364
- The accuracy and availability of operational marine surface wind data for ERS-1 sensor calibration and validation from fixed platforms and free drifting buoys p 51 N87-17376
- Homogeneous plate deformations on a sphere as monitored by Satellite Laser Ranging (SLR) networks analyzed with the multi-epoch method [ETN-87-99221] p 27 N87-18908
- The processing of and information extraction from airborne SLAR data [NLR-MP-86004-U] p 23 N87-18919
- Bare soil measurements with the Delft University Scatterometer (DUTSCAT) system (L-band) [REPT-64-220-86-T-1LH] p 24 N87-19797
- Evaluation of remote sensing results for the benefit of water quality research on the North Sea [NZ-R-86.15] p 62 N87-19799
- NEW ZEALAND**
- Calibration of normalized vegetation index against pasture growth p 12 N87-15585
- NIGERIA**
- Machine processing of Landsat data for soil survey - The Benue Valley savanna case study p 1 A87-20759
- Remote sensing options for soil survey in developing countries p 2 A87-21239
- Regional studies with satellite data in Africa on the desertification of the Sudan-Sahel belt in Nigeria p 13 N87-15605
- NORWAY**
- A climatological-hydrological study of lake ice in the southwestern mountain area in Norway by use of satellite sensing p 61 N87-17319

P

PHILIPPINES

- Cartographic analysis of remote sensing data through Landsat mosaic scaling p 65 A87-23809

PORTUGAL

- Digital satellite imagery acquisition and processing p 68 N87-17207

S

SOUTH AFRICA, REPUBLIC OF

- Shedding of an Agulhas ring observed at sea p 44 A87-30146
- Integrating vector and satellite data to evaluate the adequacy of a grain silo network p 21 N87-18156

SPAIN

- Marine climate program Remote Sensing Laboratory [ETN-87-98850] p 52 N87-17390 p 88 N87-18227

SWEDEN

- Experimental results in soil moisture mapping using IR thermography p 2 A87-21246
- The spectral reflectance of stands of Norway spruce and Scotch pine, measured from a helicopter p 7 A87-25586
- Distribution and biomass of Fucus vesiculosus L. near a cooling-water effluent from a nuclear power plant in the Baltic Sea estimated by aerial photography p 43 A87-29014
- A comparative test of photogrammetrically sampled digital elevation models p 66 A87-29499
- Desertification monitoring: Remotely sensed data for drought impact studies in the Sudan p 12 N87-15604
- Surface albedo change in arid regions in the Sudan p 13 N87-15615
- A statistical approach to select the optimal wavelength bands for separating rocks in the wavelength region 0.4 to 2.3 microns p 34 N87-17244
- Marrying geocoded image data with other types of geographic information in a PC environment p 21 N87-18154
- Atmospheric water vapor corrections for altimetry measurements p 85 N87-18197

SWITZERLAND

- Monitoring of land-surface change in Sri Lanka p 13 N87-15618
- Sri Lanka's solution to land use mapping and monitoring for Third World countries development p 67 N87-17174
- Dielectric and surface parameters related to microwave scatter and emission properties p 16 N87-17262
- Merging spaceborne image data of optical and microwave sensors p 69 N87-17267
- Viewing angle corrections of airborne multispectral scanner data acquired over forested surfaces p 17 N87-17273
- Atmospheric corrections of NOAA-AVHRR data verification of different methods by ground truth measurements p 70 N87-17274
- Snow cover recession in an Alpine ecological system p 18 N87-17316
- Towards snowmelt runoff forecast using LANDSAT-MSS and NOAA-AVHRR data p 61 N87-17317
- L to X-band scatter and emission measurements of vegetation p 19 N87-17347
- An overview of the implementation of the World Climate Research program p 26 N87-17388
- Monitoring land use changes in Sri Lanka for land use planning using a geographic information system and satellite imagery p 26 N87-18151
- Description of a methodology for biomass change mapping with the use of LANDSAT TM data p 22 N87-18186
- Point positioning and mapping with Large Format Camera data p 71 N87-18188
- Report of the Fourth Session of the JSC/CCCC Tropical Ocean Global Atmosphere (TOGA) Scientific Steering Group [WCP-120] p 54 N87-18283

T

THAILAND

- The application of LANDSAT imagery for land cover assessment p 13 N87-15614

TUNISIA

- Spectral brightness and surface soil characteristics in an arid Mediterranean region (southern Tunisia) p 2 A87-21242

TURKEY

- Microwave backscattering from a layer of randomly oriented discs with application to scattering from vegetation p 8 A87-28316

- Remote sensing activities in Turkey: Possible contributions to climate studies p 77 N87-15624
- LANDSAT-5 Thematic Mapping (TM) data applications to land use classification on around the Bosphorus area, Turkey p 19 N87-17351
- The use of remote sensing (including aerial photographs) to devise cost-effective methods for soil conservation in the Kocaeli Peninsula, Turkey p 20 N87-18149

U

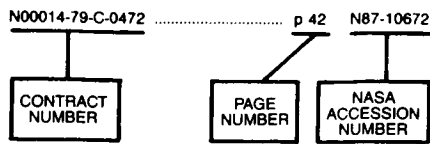
U.S.S.R.

- Optical and radar observations of the nonlinear interaction of gravity waves p 37 A87-20350
- Remote sensing of the state of crops and soils p 1 A87-20758
- Geological nature of early Precambrian formations (considering the example of the Anabar shield) p 28 A87-24274
- Vertical structure of the temperature field above the North Atlantic p 40 A87-24374
- The results of sea-surface temperature determinations from IR and microwave measurements aboard the Cosmos-1151 satellite p 40 A87-24376
- Exact determination of wave parameters from the results of Fourier analysis of sea-surface radar imagery p 41 A87-24377
- Possibilities of using satellite data for computations of the ocean/atmosphere heat exchange in the Newfoundland energy-active ocean zone in winter p 41 A87-24379
- Analysis of correlations between structural elements detected on space images and metallogenic zones p 28 A87-24380
- Integration of space-geological and geophysical methods in regional and local predictions of tectonic structures in the Caspian depression p 28 A87-24381
- Identification of reclaimed landscapes of Belorussia from space images p 28 A87-24382
- Use of space imagery and geophysical data in metallogenic prediction studies in central Kyzylkum p 28 A87-24383
- Lineaments of eastern Cuba - Geological interpretation of aerial and space imagery p 28 A87-24384
- An analysis of the potential of satellite-borne bistatic radar sensing of the earth p 75 A87-24385
- The use of space photography to create and renew small-scale maps p 65 A87-25249
- Spatial-statistical characteristics of sea surface foam fields (from optical sounding data) p 42 A87-26531
- Methods of geological interpretation of lineaments of platform areas (with reference to Usturt) p 29 A87-26532
- The principles and procedures of modeling ore-related objects in predictive metallogenic investigations (using satellite-borne data) p 29 A87-26533
- Quantitative processing procedures and the information content of space imagery in predictions of structural inhomogeneities of the sedimentary cover p 29 A87-26534
- The development of procedures for forest interpretation from texture-selective images p 8 A87-26535
- Determination of the properties of a plowed soil layer from multispectral space imagery p 8 A87-26536
- Use of decimeter waves in studies of water bodies by methods of microwave radiometry p 58 A87-26537
- Automation of thematic processing of space images in evaluating crop condition p 8 A87-26539
- Method for computing the periodicity of a remote-sensing survey p 65 A87-26540
- Soviet remote sensing p 86 A87-27452
- The use of Doppler observations to obtain initial geodetic data and to derive plumbline deviations and quasi-geoid heights p 27 A87-28504
- Investigation of spectral correlations of vegetation growing on different types of geological structures p 29 A87-28508
- Interpretation characteristics of space photographs of sea coasts with wind-induced surges p 43 A87-28509
- Mapping of agricultural lands in the USSR p 11 N87-15507
- UNITED KINGDOM**
- Instrumentation for optical remote sensing from space: Proceedings of the Meeting, Cannes, France, November 27-29, 1985 [SPIE-589] p 73 A87-19647
- The Along Track Scanning Radiometer (ATSR) for ERS1 p 73 A87-19660
- Space remote sensing p 86 A87-20682
- Spot data distribution p 62 A87-20683
- Illustration of the influence of shadowing on high latitude information derived from satellite imagery p 62 A87-20768

- Timely thermal infrared data acquisition for soil survey in humid temperature environments p 3 A87-21249
- Radar images for soil survey in England and Wales p 3 A87-21251
- Analysis of the dynamics of African vegetation using the normalized difference vegetation index p 6 A87-24779
- Satellite remote sensing of rangelands in Botswana. I - Landsat MSS and herbaceous vegetation p 7 A87-24785
- Satellite remote sensing of rangelands in Botswana. II - NOAA AVHRR and herbaceous vegetation p 7 A87-24786
- Moorland plant community recognition using Landsat MSS data p 7 A87-25589
- Estimating and mapping grass cover and biomass from low-level photographic sampling p 9 A87-29005
- An analysis of geologic lineaments seen on Landsat MSS imagery p 30 A87-29011
- Preliminary analysis of SPOT HRV multispectral products of an arid environment p 10 A87-29017
- Ground radiometry and airborne multispectral survey of bare soils p 10 A87-30894
- The interactive effect of spatial resolution and degree of internal variability within land-cover types on classification accuracies p 77 A87-30895
- Remote sensing of structurally complex semi-natural vegetation - An example from heathland p 10 A87-30896
- Spectral separation of moorland vegetation in airborne Thematic Mapper data p 10 A87-30897
- Airborne MSS data to estimate GLAI p 11 A87-30898
- Mapping of water quality in coastal waters using Airborne Thematic Mapper data p 58 A87-30899
- The quantitative use of airborne Thematic Mapper thermal infrared data p 44 A87-30900
- Island wakes and headland eddies - A comparison between remotely sensed data and laboratory experiments p 44 A87-30925
- Remote sensing identified in climate model experiments with hydrological and albedo changes in the Sahel p 59 N87-15569
- Vegetation index models for the assessment of vegetation in marginal areas p 12 N87-15584
- Rainfall estimation over the Sahel using Meteosat thermal infra-red data p 59 N87-15587
- The prospects for hydrological measurements using ERS-1 p 59 N87-15588
- Hydrological studies in Niger p 59 N87-15609
- The design of an international data centre for remote sensing p 67 N87-17176
- An automatic tracking mode switching algorithm for the ERS-1 altimeter p 81 N87-17195
- The influence of resampling method and multitemporal LANDSAT imagery on crop classification accuracy in the United Kingdom p 16 N87-17250
- SIR-B observations of ocean waves in the NE Atlantic p 49 N87-17335
- Discrimination of land features using LANDSAT false colour composite in N Iran p 19 N87-17352
- Gathering and processing a comparative data set for the calibration and validation of ERS-1 data products; preparatory work at the UK-ERS-DC p 50 N87-17367
- Requirements and constraints in the calibration and validation of ERS-1 wind and wave parameters p 51 N87-17369
- The use of numerical wind and wave models to provide areal and temporal extension to instrument calibration and validation of remotely sensed data p 51 N87-17371
- Validation of ERS-1 wind data using observations from research and voluntary observing ships p 51 N87-17374
- The use of aircraft for wind scatterometer calibration p 84 N87-17382
- Measurement of the directional spectrum of ocean waves using a conically-scanning radar p 52 N87-17383
- A scatterometer research program p 53 N87-17391
- New techniques in satellite altimeter tracking systems p 85 N87-18164
- Satellite altimeter measurements over land and inland water p 61 N87-18200
- Monitoring sediment transfer processes on the desert margin [NASA-CR-180181] p 23 N87-18222
- SeaSoar CTD surveys during FASINEX [IOS-230] p 55 N87-18970

CONTRACT NUMBER INDEX

Typical Contract Number Index Listing

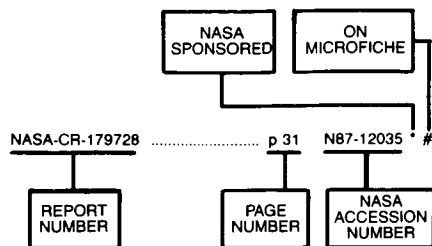


Listings in this index are arranged alpha-numerically by contract number. Under each contract number, the accession numbers denoting documents that have been produced as a result of research done under that contract are arranged in ascending order with the AIAA accession numbers appearing first. The accession number denotes the number by which the citation is identified in the abstract section. Preceding the accession number is the page number on which the citation may be found.

N00014-79-C-0472	p 42	N87-10672
AF-AFOSR-84-0120	p 74	A87-22476
AF-AFOSR-86-0053	p 56	A87-23361
CEC-STI-022-J-C	p 43	A87-29019
DAAG29-82-K-0175	p 78	N87-16387
DE-AC06-76RL-01830	p 37	N87-19796
ESA-6153/WL-MS	p 16	N87-17265
ESTEC-6079/84-NL-PB(SC)	p 85	N87-18164
ESTEC-6375/85-NL-BI	p 81	N87-17195
F19628-83-C-0027	p 57	A87-23374
	p 76	A87-26098
F19628-84-C-0134	p 57	A87-23374
	p 76	A87-26098
F19628-86-C-0141	p 76	A87-26098
F30602-82-C-0148	p 63	A87-23793
JAP-MIN-OF-ED-60129032	p 69	N87-17249
JPL-956520	p 9	A87-28414
JPL-956925	p 29	A87-25588
JPL-956937	p 34	N87-17246
NAGW-334	p 46	N87-17184
NAGW-455	p 88	N87-18907
NAGW-504	p 76	A87-27882
NAGW-679	p 41	A87-25797
NAGW-690	p 47	N87-17213
NAGW-730	p 42	A87-27848
NAGW-736	p 35	N87-17418
NAGW-788	p 11	N87-15518
NAGW-881	p 60	N87-16383
NAG5-399	p 6	A87-24779
	p 6	A87-24781
	p 6	A87-24782
NAG5-485	p 27	A87-29977
NAG5-510	p 11	N87-15514
NAG5-542	p 38	A87-20956
NAG5-580	p 61	N87-17340
NAG5-583	p 40	A87-23722
NAG5-587	p 40	A87-23722
NAG5-787	p 78	N87-15660
NAG5-81	p 41	A87-25787
NASW-4046	p 42	A87-27848
NASW-4049	p 34	N87-17246
NASW-4066	p 27	A87-20689
NAS10-11142	p 43	A87-27891
NAS5-27323	p 86	N87-18221
NAS5-28057	p 81	N87-17205
NAS5-28758	p 24	N87-19826
NAS5-28759	p 27	A87-20689
	p 36	N87-18910
NAS5-28765	p 36	N87-18255
NAS5-28766	p 11	N87-15517
NAS5-28769	p 54	N87-18293
	p 56	N87-19877
NAS5-28781	p 23	N87-18912
NAS7-100	p 65	A87-23827
NAS7-17022	p 75	A87-23546
NAS7-918	p 5	A87-23830
	p 78	N87-17110
	p 78	N87-17111
	p 67	N87-17135
	p 86	N87-18697
NERC-F60/G6/03	p 10	A87-29017
	p 77	A87-30895
NERC-F60/G6/12	p 10	A87-29017
NERC-GR/3/4994	p 10	A87-30894
NERC-GR/3/5096	p 11	A87-30898
NGL-05-007-004	p 30	A87-30884
NGR-36-008-161	p 27	N87-17416
NOAA-NA-800AAD00086	p 57	A87-23824
NOAA-NA-84AAD00017	p 76	A87-27882
NOAA-NA-84AAH00020	p 76	A87-27882
NOAA-NA-84AAH00026	p 65	A87-25587
NOAA-NA-85RAH05045	p 76	A87-27882
NOAA-NA80AA-D-00120	p 61	N87-18172
NSERC-A-7400	p 35	N87-17293
	p 54	N87-18199
NSERC-A-8454	p 66	A87-30127
NSF ATM-83-18676	p 56	A87-23361
NSF DPP-81-18563	p 38	A87-20520
NSF DPP-81-19155	p 38	A87-20520
NSF EAR-84-07110	p 27	A87-29977
NSF ECS-82-15539	p 70	N87-17327
NSF OCE-82-13456	p 39	A87-23719
NSF OCE-82-13872	p 39	A87-23719
NSF OCE-85-06468	p 39	A87-23719
NSF OCE-85-07438	p 39	A87-23719
NSF OCE-85-11526	p 39	A87-23719
NSG-5205	p 78	N87-15669
NSG-5265	p 27	N87-17415
NSG-7315	p 43	A87-30143
N000-14-81-C-0295	p 46	N87-17184
N000-14-83-C-0404	p 47	N87-17219
	p 46	N87-17184
	p 47	N87-17219
N000-14-85-K-0200	p 46	N87-17184
N00014-81-C-0259	p 48	N87-17222
N00014-81-C-0692	p 50	N87-17338
N00014-83-C-0404	p 48	N87-17222
N00014-84-C-0132	p 44	A87-30146
N00014-84-C-2312	p 49	N87-17299
	p 53	N87-18158
N00014-85-C-0132	p 48	N87-17222
N00014-85-K-2034	p 45	N87-16384
N00014-86-K-0752	p 39	A87-23720
	p 40	A87-23721
N00014-86-K-2001	p 61	N87-17340
N00024-85-C-5301	p 9	A87-28414
N00024-86-PR-69506	p 85	N87-18161
OSURF PROJ. 711055	p 27	N87-17415
OSURF PROJ. 783210	p 27	N87-17416
PROJ. R/CZ-68	p 61	N87-18172
W-7405-ENG-36	p 19	N87-17395
	p 23	N87-18916
149-21-00-01	p 45	N87-16492
161-80-15-40-00	p 78	N87-17110
666-31-01-00-64	p 67	N87-17135
677-80-23-01-00	p 78	N87-17111

REPORT NUMBER INDEX

Typical Report Number Index Listing

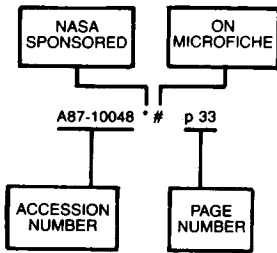


Listings in this index are arranged alphabetically by report number. The page number indicates the page on which the citation is located. The accession number denotes the number by which the citation is identified. An asterisk (*) indicates that the item is a NASA report. A pound sign (#) indicates that the item is available on microfiche.

AD-A171670	p 45	N87-16493	#
AD-A172132	p 45	N87-16384	#
AD-A172886	p 78	N87-16387	#
AD-A173008	p 60	N87-16386	#
AD-A173333	p 54	N87-18295	#
AD-A173467	p 27	N87-18225	#
AD-A173601	p 66	N87-16388	#
AD-A173972	p 55	N87-18298	#
AD-A174019	p 55	N87-18961	#
AD-A174025	p 55	N87-18931	#
AD-A174197	p 55	N87-18913	#
AD-A174337	p 55	N87-18963	#
AD-A174527	p 55	N87-18966	#
AD-A174698	p 56	N87-19879	#
AD-A176666	p 39	A87-23720	* #
AD-B107864L	p 23	N87-18919	#
AFGL-TR-86-0201	p 60	N87-16386	#
AIAA PAPER 87-0187	p 7	A87-24933	* #
AIAA PAPER 87-0197	p 74	A87-22476	#
AIAA PAPER 87-0320	p 74	A87-22556	* #
ARO-18954.2-GS	p 78	N87-16387	#
B8679799	p 23	N87-18919	#
CNES-CT/DRT/TIT/RL-54-T	p 66	N87-16963	#
CONF-860244	p 36	N87-18915	#
CONF-860888-1	p 19	N87-17395	#
CONF-8609200-1	p 37	N87-19796	#
CONF-860997-1	p 23	N87-18916	#
CONTRIB-19586	p 35	N87-17248	#
DE86-006613	p 36	N87-18915	#
DE86-011258	p 19	N87-17395	#
DE86-012387	p 23	N87-18916	#
DE87-003095	p 37	N87-19796	#
DOE/METC-86-6039	p 36	N87-18915	#
EPA-600/3-86-051	p 26	N87-18246	#
ESA-SP-254-VOL-1	p 80	N87-17163	#
ESA-SP-254-VOL-2	p 82	N87-17283	#
ESA-SP-254-VOL-3	p 84	N87-18142	#
ESA-SP-262	p 84	N87-17363	#
ETL-0424	p 66	N87-16388	#
ETN-87-98535	p 80	N87-17163	#
ETN-87-98536	p 82	N87-17283	#
ETN-87-98537	p 84	N87-18142	#
ETN-87-98806	p 66	N87-16963	#
ETN-87-98836	p 84	N87-17363	#
ETN-87-98850	p 88	N87-18227	#
ETN-87-98901	p 54	N87-18283	#
ETN-87-99074	p 24	N87-19797	#
ETN-87-99137	p 55	N87-18970	#
ETN-87-99215	p 62	N87-19799	#
ETN-87-99221	p 27	N87-18908	#
ETN-87-99511	p 23	N87-18919	#
IEEE-86CH2268-VOL-3	p 84	N87-18142	#
IEEE-86CH2268-1-VOL-1	p 80	N87-17163	#
IEEE-86CH2268-1-VOL-2	p 82	N87-17283	#
INPE-3893-TDL/225	p 72	N87-19792	#
INPE-3963-PRE/980	p 11	N87-15519	#
INPE-3984-TDL/236	p 72	N87-19787	#
INPE-3986-PRE/991	p 60	N87-16382	#
INPE-4041-TDL/246	p 37	N87-19788	#
INPE-4068-RPE/526	p 24	N87-19790	#
INPE-4102-RPE/534	p 24	N87-19786	#
IOS-230	p 55	N87-18970	#
ISBN-87-7478-275-4	p 53	N87-17428	#
ISSN-0072-6566	p 84	N87-17363	#
ISSN-0379-6566	p 80	N87-17163	#
ISSN-0379-6566	p 82	N87-17283	#
ISSN-0379-6566	p 84	N87-18142	#
JPL-PUB-86-26	p 67	N87-17135	* #
JPL-PUB-86-29	p 86	N87-18697	* #
JPL-PUB-86-38	p 78	N87-17111	* #
JPL-PUB-86-50	p 78	N87-17110	* #
L-16156	p 45	N87-16492	* #
LA-UR-86-1596	p 19	N87-17395	#
LA-UR-86-1927	p 23	N87-18916	#
LANDSAT-TM-019	p 36	N87-18256	* #
LC-86-17974	p 36	N87-18139	* #
LC-86-80109-VOL-1	p 80	N87-17163	#
LC-86-80109-VOL-2	p 82	N87-17283	#
LC-86-80109	p 84	N87-18142	#
NAS 1.15:87736	p 45	N87-16492	* #
NAS 1.21:486	p 36	N87-18139	* #
NAS 1.26:177077	p 11	N87-15514	* #
NAS 1.26:179903	p 11	N87-15517	* #
NAS 1.26:179917	p 78	N87-15669	* #
NAS 1.26:179984	p 78	N87-15660	* #
NAS 1.26:180065	p 54	N87-18293	* #
NAS 1.26:180097	p 11	N87-15518	* #
NAS 1.26:180118	p 60	N87-16383	* #
NAS 1.26:180130	p 78	N87-17111	* #
NAS 1.26:180131	p 67	N87-17135	* #
NAS 1.26:180137	p 27	N87-17415	* #
NAS 1.26:180139	p 27	N87-17416	* #
NAS 1.26:180149	p 35	N87-17418	* #
NAS 1.26:180151	p 78	N87-17110	* #
NAS 1.26:180180	p 86	N87-18221	* #
NAS 1.26:180181	p 23	N87-18222	* #
NAS 1.26:180182	p 36	N87-18256	* #
NAS 1.26:180183	p 36	N87-18255	* #
NAS 1.26:180198	p 88	N87-18907	* #
NAS 1.26:180213	p 23	N87-18912	* #
NAS 1.26:180241	p 86	N87-18697	* #
NAS 1.26:180252	p 36	N87-18910	* #
NAS 1.26:180356	p 56	N87-19877	* #
NAS 1.26:180357	p 24	N87-19826	* #
NASA-CR-177077	p 11	N87-15514	* #
NASA-CR-179903	p 11	N87-15517	* #
NASA-CR-179917	p 78	N87-15669	* #
NASA-CR-179984	p 78	N87-15660	* #
NASA-CR-180065	p 54	N87-18293	* #
NASA-CR-180097	p 11	N87-15518	* #
NASA-CR-180118	p 60	N87-16383	* #
NASA-CR-180130	p 78	N87-17111	* #
NASA-CR-180131	p 67	N87-17135	* #
NASA-CR-180137	p 27	N87-17415	* #
NASA-CR-180139	p 27	N87-17416	* #
NASA-CR-180149	p 35	N87-17418	* #
NASA-CR-180151	p 78	N87-17110	* #
NASA-CR-180180	p 86	N87-18221	* #
NASA-CR-180181	p 23	N87-18222	* #
NASA-CR-180182	p 36	N87-18256	* #
NASA-CR-180183	p 36	N87-18255	* #
NASA-CR-180198	p 88	N87-18907	* #
NASA-CR-180213	p 23	N87-18912	* #
NASA-CR-180241	p 86	N87-18697	* #
NASA-CR-180252	p 36	N87-18910	* #
NASA-CR-180356	p 56	N87-19877	* #
NASA-CR-180357	p 24	N87-19826	* #
NASA-CR-180131	p 67	N87-17135	* #
NASA-CR-180137	p 27	N87-17415	* #
NASA-CR-180139	p 27	N87-17416	* #
NASA-CR-180149	p 35	N87-17418	* #
NASA-CR-180151	p 78	N87-17110	* #
NASA-CR-180180	p 86	N87-18221	* #
NASA-CR-180181	p 23	N87-18222	* #
NASA-CR-180182	p 36	N87-18256	* #
NASA-CR-180183	p 36	N87-18255	* #
NASA-CR-180198	p 88	N87-18907	* #
NASA-CR-180213	p 23	N87-18912	* #
NASA-CR-180241	p 86	N87-18697	* #
NASA-CR-180252	p 36	N87-18910	* #
NASA-CR-180356	p 56	N87-19877	* #
NASA-CR-180357	p 24	N87-19826	* #
NASA-SP-486	p 36	N87-18139	* #
NASA-TM-87736	p 45	N87-16492	* #
NEDRES-5	p 56	N87-18971	#
NLR-MP-86004-U	p 23	N87-18919	#
NORDA-142	p 54	N87-18295	#
NRL-MR-5866	p 56	N87-19879	#
NZ-R-86.15	p 62	N87-19799	#
PB86-236973	p 26	N87-18246	#
PB86-245446	p 56	N87-18971	#
PNL-SA-13832	p 37	N87-19796	#
REPT-551.467.3.068(988)	p 53	N87-17428	#
REPT-64-220-86-T-1LH	p 24	N87-19797	#
RIT/DIRS-86/87-51-112	p 86	N87-18221	* #
RR-12	p 55	N87-18298	#
SAPR-2	p 11	N87-15517	* #
SAPR-3	p 24	N87-19826	* #
SASR-17	p 27	N87-17415	* #
SPIE-589	p 73	A87-19647	* #
SR-42	p 27	N87-17416	* #
TMWR-PR-3	p 23	N87-18912	* #
TS-BPP-1987-1	p 23	N87-18912	* #
USNA-TSPR-136	p 45	N87-16493	#
WCP-120	p 54	N87-18283	#
WMO/TD-129	p 54	N87-18283	#

ACCESSION NUMBER INDEX

Typical Accession Number Index Listing



Listings in this index are arranged alpha-numerically by accession number. The page number listed to the right indicates the page on which the citation is located. An asterisk (*) indicates the item is a NASA report. A pound sign (#) indicates that the item is available on microfiche.

A87-19647	#	p 73	A87-23389	#	p 3	A87-29011	#	p 30	N87-16382	#	p 60
A87-19652	#	p 73	A87-23390	#	p 74	A87-29012	#	p 10	N87-16383	*	p 60
A87-19655	#	p 73	A87-23391	*	p 39	A87-29013	#	p 58	N87-16384	#	p 45
A87-19660	#	p 73	A87-23414	#	p 57	A87-29014	#	p 43	N87-16386	#	p 60
A87-20204	*	p 37	A87-23419	#	p 74	A87-29015	#	p 43	N87-16387	#	p 78
A87-20350	#	p 37	A87-23546	#	p 75	A87-29017	#	p 10	N87-16388	#	p 66
A87-20520	#	p 38	A87-23650	#	p 75	A87-29018	#	p 10	N87-16492	*	p 45
A87-20524	#	p 38	A87-23699	#	p 57	A87-29019	#	p 43	N87-16493	*	p 45
A87-20671	#	p 1	A87-23717	#	p 39	A87-29430	#	p 65	N87-16662	#	p 87
A87-20672	#	p 73	A87-23718	#	p 39	A87-29431	#	p 76	N87-16963	#	p 66
A87-20682	#	p 86	A87-23719	#	p 39	A87-29433	#	p 87	N87-17110	#	p 78
A87-20683	#	p 62	A87-23720	*	p 39	A87-29499	#	p 66	N87-17111	#	p 78
A87-20687	*	p 38	A87-23721	#	p 40	A87-29849	*	p 76	N87-17112	*	p 79
A87-20689	*	p 27	A87-23722	#	p 40	A87-29977	*	p 27	N87-17113	*	p 79
A87-20692	#	p 38	A87-23723	#	p 40	A87-30126	#	p 30	N87-17114	*	p 79
A87-20758	#	p 1	A87-23725	#	p 40	A87-30127	#	p 66	N87-17115	*	p 79
A87-20759	#	p 1	A87-23777	#	p 24	A87-30128	*	p 25	N87-17116	*	p 66
A87-20761	*	p 1	A87-23782	#	p 28	A87-30129	#	p 10	N87-17117	*	p 30
A87-20762	#	p 1	A87-23785	#	p 62	A87-30130	#	p 10	N87-17118	*	p 30
A87-20763	#	p 1	A87-23786	#	p 63	A87-30143	*	p 43	N87-17119	*	p 31
A87-20765	#	p 56	A87-23787	#	p 63	A87-30146	#	p 44	N87-17120	*	p 31
A87-20768	#	p 62	A87-23788	#	p 63	A87-30876	#	p 87	N87-17121	*	p 31
A87-20769	#	p 38	A87-23789	#	p 63	A87-30881	#	p 87	N87-17122	*	p 14
A87-20770	#	p 38	A87-23791	#	p 63	A87-30882	#	p 25	N87-17123	*	p 14
A87-20795	#	p 73	A87-23793	#	p 63	A87-30883	#	p 44	N87-17124	*	p 15
A87-20951	#	p 56	A87-23795	#	p 64	A87-30884	*	p 30	N87-17125	*	p 31
A87-20956	*	p 38	A87-23796	#	p 64	A87-30885	#	p 77	N87-17126	*	p 15
A87-20961	#	p 74	A87-23797	#	p 3	A87-30889	#	p 10	N87-17127	*	p 15
A87-21094	#	p 74	A87-23798	#	p 64	A87-30895	#	p 77	N87-17128	*	p 31
A87-21095	#	p 62	A87-23800	#	p 64	A87-30896	#	p 10	N87-17129	*	p 31
A87-21239	#	p 2	A87-23802	#	p 64	A87-30897	#	p 10	N87-17130	*	p 31
A87-21240	#	p 2	A87-23804	#	p 75	A87-30898	#	p 11	N87-17131	*	p 67
A87-21241	#	p 2	A87-23805	*	p 65	A87-30899	#	p 58	N87-17132	*	p 15
A87-21242	#	p 2	A87-23806	#	p 4	A87-30900	#	p 44	N87-17133	*	p 32
A87-21243	#	p 2	A87-23807	#	p 4	A87-30923	*	p 44	N87-17134	*	p 32
A87-21244	#	p 2	A87-23808	#	p 4	A87-30925	#	p 44	N87-17135	*	p 67
A87-21245	#	p 2	A87-23809	#	p 57	A87-31139	#	p 77	N87-17136	*	p 32
A87-21246	#	p 2	A87-23810	#	p 4	N87-15242	#	p 77	N87-17137	*	p 32
A87-21249	#	p 3	A87-23811	#	p 4	N87-15507	#	p 11	N87-17138	#	p 32
A87-21250	#	p 3	A87-23815	#	p 57	N87-15514	*	p 11	N87-17139	#	p 32
A87-21251	#	p 3	A87-23816	#	p 4	N87-15517	#	p 11	N87-17140	#	p 33
A87-21367	#	p 39	A87-23818	#	p 4	N87-15518	#	p 11	N87-17141	*	p 79
A87-21931	#	p 26	A87-23819	#	p 5	N87-15519	#	p 11	N87-17145	*	p 79
A87-22025	#	p 74	A87-23822	#	p 5	N87-15547	#	p 58	N87-17146	*	p 33
A87-22041	#	p 39	A87-23824	#	p 57	N87-15547	#	p 58	N87-17147	#	p 45
A87-22476	#	p 74	A87-23825	#	p 57	N87-15554	#	p 12	N87-17149	#	p 45
A87-22556	*	p 74	A87-23826	#	p 57	N87-15554	#	p 12	N87-17150	*	p 46
A87-23348	#	p 62	A87-23827	*	p 65	N87-15556	#	p 59	N87-17151	*	p 46
A87-23360	#	p 3	A87-23828	#	p 24	N87-15572	#	p 12	N87-17156	*	p 15
A87-23361	#	p 56	A87-23829	#	p 25	N87-15573	*	p 77	N87-17159	*	p 67
A87-23362	#	p 39	A87-23830	*	p 5	N87-15579	#	p 25	N87-17160	*	p 15
A87-23370	#	p 56	A87-23831	#	p 58	N87-15583	#	p 12	N87-17163	#	p 80
A87-23374	#	p 57	A87-23832	#	p 5	N87-15584	#	p 12	N87-17164	#	p 67
A87-23388	*	p 3	A87-23833	#	p 5	N87-15585	#	p 12	N87-17165	#	p 16
			A87-23834	#	p 40	N87-15587	#	p 59	N87-17166	#	p 46
						N87-15588	#	p 59	N87-17167	#	p 80
						N87-15589	#	p 12	N87-17169	#	p 80
						N87-15593	*	p 12	N87-17170	#	p 87
						N87-15594	*	p 77	N87-17172	#	p 67
						N87-15604	#	p 12	N87-17173	#	p 16
						N87-15605	#	p 13	N87-17174	#	p 67
						N87-15607	#	p 13	N87-17175	#	p 25
						N87-15609	#	p 59	N87-17176	#	p 67
						N87-15610	#	p 13	N87-17177	#	p 87
						N87-15611	#	p 59	N87-17184	*	p 46
						N87-15612	#	p 13	N87-17185	*	p 46
						N87-15614	#	p 13	N87-17186	*	p 46
						N87-15615	#	p 13	N87-17189	#	p 47
						N87-15618	#	p 13	N87-17190	#	p 47
						N87-15619	#	p 14	N87-17192	#	p 80
						N87-15621	#	p 14	N87-17194	#	p 80
						N87-15622	#	p 14	N87-17195	#	p 81
						N87-15623	#	p 14	N87-17202	*	p 81
						N87-15624	#	p 77	N87-17203	#	p 68
						N87-15625	#	p 66	N87-17204	*	p 81
						N87-15626	#	p 59	N87-17205	*	p 81
						N87-15628	#	p 78	N87-17206	#	p 68
						N87-15629	#	p 14	N87-17207	#	p 68
						N87-15632	#	p 59	N87-17211	#	p 68
						N87-15652	#	p 45	N87-17213	*	p 47
						N87-15660	#	p 78	N87-17215	#	p 47
						N87-15669	*	p 78	N87-17217	#	p 47
						N87-15989	#	p 45			

N87-17219 #	p 47	N87-17381 #	p 52	N87-18971 #	p 56
N87-17221 #	p 48	N87-17382 #	p 84	N87-19786 #	p 24
N87-17222 #	p 48	N87-17383 #	p 52	N87-19787 #	p 72
N87-17223 #	p 60	N87-17384 * #	p 52	N87-19788 #	p 37
N87-17224 #	p 81	N87-17386 #	p 52	N87-19790 #	p 24
N87-17229 #	p 68	N87-17387 #	p 84	N87-19792 #	p 72
N87-17232 #	p 33	N87-17388 #	p 26	N87-19796 #	p 37
N87-17233 #	p 33	N87-17389 #	p 52	N87-19797 #	p 24
N87-17234 #	p 33	N87-17390 #	p 52	N87-19799 #	p 62
N87-17235 #	p 33	N87-17391 #	p 53	N87-19826 * #	p 24
N87-17236 #	p 34	N87-17395 #	p 19	N87-19877 * #	p 56
N87-17238 #	p 16	N87-17410 #	p 84	N87-19879 #	p 56
N87-17239 #	p 68	N87-17415 * #	p 27		
N87-17242 #	p 34	N87-17416 * #	p 27		
N87-17243 #	p 34	N87-17418 * #	p 35		
N87-17244 #	p 34	N87-17428 #	p 53		
N87-17245 #	p 69	N87-18139 * #	p 36		
N87-17246 * #	p 34	N87-18142 #	p 84		
N87-17247 #	p 34	N87-18143 #	p 20		
N87-17248 #	p 35	N87-18146 #	p 20		
N87-17249 #	p 69	N87-18147 #	p 20		
N87-17250 #	p 16	N87-18148 #	p 20		
N87-17251 #	p 69	N87-18149 #	p 20		
N87-17255 #	p 69	N87-18150 #	p 20		
N87-17259 #	p 48	N87-18151 #	p 26		
N87-17260 * #	p 82	N87-18152 #	p 88		
N87-17262 #	p 16	N87-18153 #	p 21		
N87-17264 #	p 60	N87-18154 #	p 21		
N87-17265 #	p 16	N87-18155 #	p 70		
N87-17266 #	p 17	N87-18156 #	p 21		
N87-17267 #	p 69	N87-18157 #	p 70		
N87-17269 #	p 69	N87-18158 #	p 53		
N87-17273 #	p 17	N87-18159 #	p 61		
N87-17274 #	p 70	N87-18160 #	p 53		
N87-17277 #	p 82	N87-18161 #	p 85		
N87-17278 #	p 82	N87-18164 #	p 85		
N87-17279 #	p 82	N87-18165 #	p 53		
N87-17283 #	p 82	N87-18167 #	p 53		
N87-17284 #	p 17	N87-18169 #	p 53		
N87-17285 #	p 17	N87-18170 #	p 54		
N87-17286 #	p 17	N87-18171 * #	p 21		
N87-17287 #	p 17	N87-18172 #	p 61		
N87-17288 #	p 18	N87-18173 #	p 21		
N87-17289 #	p 18	N87-18174 #	p 21		
N87-17293 #	p 35	N87-18175 * #	p 22		
N87-17294 #	p 35	N87-18176 #	p 71		
N87-17295 #	p 48	N87-18177 #	p 71		
N87-17296 #	p 48	N87-18178 #	p 85		
N87-17298 #	p 48	N87-18179 #	p 71		
N87-17299 #	p 49	N87-18180 #	p 85		
N87-17304 #	p 18	N87-18181 #	p 54		
N87-17305 #	p 18	N87-18182 #	p 71		
N87-17313 #	p 18	N87-18183 #	p 22		
N87-17314 #	p 60	N87-18184 #	p 22		
N87-17316 #	p 18	N87-18185 #	p 22		
N87-17317 #	p 61	N87-18186 #	p 22		
N87-17319 #	p 61	N87-18187 #	p 22		
N87-17320 #	p 82	N87-18188 #	p 71		
N87-17324 #	p 83	N87-18189 #	p 71		
N87-17325 #	p 83	N87-18190 #	p 36		
N87-17327 #	p 70	N87-18191 #	p 72		
N87-17329 #	p 83	N87-18192 #	p 72		
N87-17332 #	p 70	N87-18193 #	p 23		
N87-17333 #	p 49	N87-18194 #	p 72		
N87-17334 #	p 49	N87-18197 #	p 85		
N87-17335 #	p 49	N87-18199 #	p 54		
N87-17336 * #	p 49	N87-18200 #	p 61		
N87-17337 #	p 50	N87-18207 #	p 23		
N87-17338 #	p 50	N87-18212 #	p 72		
N87-17340 * #	p 61	N87-18219 #	p 85		
N87-17341 #	p 50	N87-18220 #	p 23		
N87-17342 #	p 50	N87-18221 * #	p 86		
N87-17343 #	p 50	N87-18222 * #	p 23		
N87-17344 * #	p 19	N87-18225 #	p 27		
N87-17347 #	p 19	N87-18227 #	p 88		
N87-17348 * #	p 35	N87-18246 #	p 26		
N87-17350 #	p 19	N87-18255 * #	p 36		
N87-17351 #	p 19	N87-18256 * #	p 36		
N87-17352 #	p 19	N87-18283 #	p 54		
N87-17353 #	p 83	N87-18293 * #	p 54		
N87-17358 #	p 83	N87-18295 #	p 54		
N87-17360 #	p 83	N87-18298 #	p 55		
N87-17362 #	p 70	N87-18697 * #	p 86		
N87-17363 #	p 84	N87-18907 * #	p 88		
N87-17364 #	p 84	N87-18908 #	p 27		
N87-17367 #	p 50	N87-18910 * #	p 36		
N87-17369 #	p 51	N87-18912 * #	p 23		
N87-17370 #	p 51	N87-18913 #	p 55		
N87-17371 #	p 51	N87-18915 #	p 36		
N87-17372 * #	p 51	N87-18916 #	p 23		
N87-17373 #	p 51	N87-18919 #	p 23		
N87-17374 #	p 51	N87-18931 #	p 55		
N87-17376 #	p 51	N87-18961 #	p 55		
N87-17377 #	p 51	N87-18963 #	p 55		
N87-17379 #	p 84	N87-18966 #	p 55		
N87-17380 * #	p 52	N87-18970 #	p 55		

AVAILABILITY OF CITED PUBLICATIONS

IAA ENTRIES (A87-10000 Series)

Publications announced in *IAA* are available from the AIAA Technical Information Service as follows: Paper copies of accessions are available at \$10.00 per document (up to 50 pages), additional pages \$0.25 each. Microfiche⁽¹⁾ of documents announced in *IAA* are available at the rate of \$4.00 per microfiche on demand. Standing order microfiche are available at the rate of \$1.45 per microfiche for *IAA* source documents and \$1.75 per microfiche for AIAA meeting papers.

Minimum air-mail postage to foreign countries is \$2.50. All foreign orders are shipped on payment of pro-forma invoices.

All inquiries and requests should be addressed to: Technical Information Service, American Institute of Aeronautics and Astronautics, 555 West 57th Street, New York, NY 10019. Please refer to the accession number when requesting publications.

STAR ENTRIES (N87-10000 Series)

One or more sources from which a document announced in *STAR* is available to the public is ordinarily given on the last line of the citation. The most commonly indicated sources and their acronyms or abbreviations are listed below. If the publication is available from a source other than those listed, the publisher and his address will be displayed on the availability line or in combination with the corporate source line.

Avail: NTIS. Sold by the National Technical Information Service. Prices for hard copy (HC) and microfiche (MF) are indicated by a price code preceded by the letters HC or MF in the *STAR* citation. Current values for the price codes are given in the tables on NTIS PRICE SCHEDULES.

Documents on microfiche are designated by a pound sign (#) following the accession number. The pound sign is used without regard to the source or quality of the microfiche.

Initially distributed microfiche under the NTIS SRIM (Selected Research in Microfiche) is available at greatly reduced unit prices. For this service and for information concerning subscription to NASA printed reports, consult the NTIS Subscription Section, Springfield, Va. 22161.

NOTE ON ORDERING DOCUMENTS: When ordering NASA publications (those followed by the * symbol), use the N accession number. NASA patent applications (only the specifications are offered) should be ordered by the US-Patent-Appl-SN number. Non-NASA publications (no asterisk) should be ordered by the AD, PB, or other *report* number shown on the last line of the citation, not by the N accession number. It is also advisable to cite the title and other bibliographic identification.

Avail: SOD (or GPO). Sold by the Superintendent of Documents, U.S. Government Printing Office, in hard copy. The current price and order number are given following the availability line. (NTIS will fill microfiche requests, as indicated above, for those documents identified by a # symbol.)

(1) A microfiche is a transparent sheet of film, 105 by 148 mm in size containing as many as 60 to 98 pages of information reduced to micro images (not to exceed 26.1 reduction).

- Avail: BLL (formerly NLL): British Library Lending Division, Boston Spa, Wetherby, Yorkshire, England. Photocopies available from this organization at the price shown. (If none is given, inquiry should be addressed to the BLL.)
- Avail: DOE Depository Libraries. Organizations in U.S. cities and abroad that maintain collections of Department of Energy reports, usually in microfiche form, are listed in *Energy Research Abstracts*. Services available from the DOE and its depositories are described in a booklet, *DOE Technical Information Center - Its Functions and Services* (TID-4660), which may be obtained without charge from the DOE Technical Information Center.
- Avail: ESDU. Pricing information on specific data, computer programs, and details on ESDU topic categories can be obtained from ESDU International Ltd. Requesters in North America should use the Virginia address while all other requesters should use the London address, both of which are on page vi.
- Avail: Fachinformationszentrum, Karlsruhe. Sold by the Fachinformationszentrum Energie, Physik, Mathematik GMBH, Eggenstein Leopoldshafen, Federal Republic of Germany, at the price shown in deutschmarks (DM).
- Avail: HMSO. Publications of Her Majesty's Stationery Office are sold in the U.S. by Pendragon House, Inc. (PHI), Redwood City, California. The U.S. price (including a service and mailing charge) is given, or a conversion table may be obtained from PHI.
- Avail: NASA Public Document Rooms. Documents so indicated may be examined at or purchased from the National Aeronautics and Space Administration, Public Documents Room (Room 126), 600 Independence Ave., S.W., Washington, D.C. 20546, or public document rooms located at each of the NASA research centers, the NASA Space Technology Laboratories, and the NASA Pasadena Office at the Jet Propulsion Laboratory.
- Avail: Univ. Microfilms. Documents so indicated are dissertations selected from *Dissertation Abstracts* and are sold by University Microfilms as xerographic copy (HC) and microfilm. All requests should cite the author and the Order Number as they appear in the citation.
- Avail: US Patent and Trademark Office. Sold by Commissioner of Patents and Trademarks, U.S. Patent and Trademark Office, at the standard price of \$1.50 each, postage free. (See discussion of NASA patents and patent applications below.)
- Avail: (US Sales Only). These foreign documents are available to users within the United States from the National Technical Information Service (NTIS). They are available to users outside the United States through the International Nuclear Information Service (INIS) representative in their country, or by applying directly to the issuing organization.
- Avail: USGS. Originals of many reports from the U.S. Geological Survey, which may contain color illustrations, or otherwise may not have the quality of illustrations preserved in the microfiche or facsimile reproduction, may be examined by the public at the libraries of the USGS field offices whose addresses are listed in this Introduction. The libraries may be queried concerning the availability of specific documents and the possible utilization of local copying services, such as color reproduction.
- Avail: Issuing Activity, or Corporate Author, or no indication of availability. Inquiries as to the availability of these documents should be addressed to the organization shown in the citation as the corporate author of the document.

PUBLIC COLLECTIONS OF NASA DOCUMENTS

DOMESTIC: NASA and NASA-sponsored documents and a large number of aerospace publications are available to the public for reference purposes at the library maintained by the American Institute of Aeronautics and Astronautics, Technical Information Service, 555 West 57th Street, 12th Floor, New York, New York 10019.

EUROPEAN: An extensive collection of NASA and NASA-sponsored publications is maintained by the British Library Lending Division, Boston Spa, Wetherby, Yorkshire, England for public access. The British Library Lending Division also has available many of the non-NASA publications cited in *STAR*. European requesters may purchase facsimile copy or microfiche of NASA and NASA-sponsored documents, those identified by both the symbols # and * from ESA - Information Retrieval Service European Space Agency, 8-10 rue Mario-Nikis, 75738 CEDEX 15, France.

FEDERAL DEPOSITORY LIBRARY PROGRAM

In order to provide the general public with greater access to U.S. Government publications, Congress established the Federal Depository Library Program under the Government Printing Office (GPO), with 50 regional depositories responsible for permanent retention of material, inter-library loan, and reference services. At least one copy of nearly every NASA and NASA-sponsored publication, either in printed or microfiche format, is received and retained by the 50 regional depositories. A list of the regional GPO libraries, arranged alphabetically by state, appears on the inside back cover. These libraries are *not* sales outlets. A local library can contact a Regional Depository to help locate specific reports, or direct contact may be made by an individual.

STANDING ORDER SUBSCRIPTIONS

NASA SP-7041 and its supplements are available from the National Technical Information Service (NTIS) on standing order subscription as PB 86-903800 at the price of \$14.50 domestic and \$29.00 foreign. Standing order subscriptions do not terminate at the end of a year, as do regular subscriptions, but continue indefinitely unless specifically terminated by the subscriber.

ADDRESSES OF ORGANIZATIONS

American Institute of Aeronautics and
Astronautics
Technical Information Service
555 West 57th Street, 12th Floor
New York, New York 10019

British Library Lending Division,
Boston Spa, Wetherby, Yorkshire,
England

Commissioner of Patents and
Trademarks
U.S. Patent and Trademark Office
Washington, D.C. 20231

Department of Energy
Technical Information Center
P.O. Box 62
Oak Ridge, Tennessee 37830

ESA-Information Retrieval Service
ESRIN
Via Galileo Galilei
00044 Frascati (Rome) Italy

ESDU International, Ltd.
1495 Chain Bridge Road
McLean, Virginia 22101

ESDU International, Ltd.
251-259 Regent Street
London, W1R 7AD, England

Fachinformationszentrum Energie, Physik,
Mathematik GMBH
7514 Eggenstein Leopoldshafen
Federal Republic of Germany

Her Majesty's Stationery Office
P.O. Box 569, S.E. 1
London, England

NASA Scientific and Technical Information
Facility
P.O. Box 8757
B.W.I. Airport, Maryland 21240

National Aeronautics and Space
Administration
Scientific and Technical Information
Office (NTT-1)
Washington, D.C. 20546

National Technical Information Service
5285 Port Royal Road
Springfield, Virginia 22161

Pendragon House, Inc.
899 Broadway Avenue
Redwood City, California 94063

Superintendent of Documents
U.S. Government Printing Office
Washington, D.C. 20402

University Microfilms
A Xerox Company
300 North Zeeb Road
Ann Arbor, Michigan 48106

University Microfilms, Ltd.
Tylers Green
London, England

U.S. Geological Survey Library
National Center - MS 950
12201 Sunrise Valley Drive
Reston, Virginia 22092

U.S. Geological Survey Library
2255 North Gemini Drive
Flagstaff, Arizona 86001

U.S. Geological Survey
345 Middlefield Road
Menlo Park, California 94025

U.S. Geological Survey Library
Box 25046
Denver Federal Center, MS914
Denver, Colorado 80225

NTIS PRICE SCHEDULES

(Effective January 1, 1987)

Schedule A STANDARD PRICE DOCUMENTS AND MICROFICHE

PRICE CODE	PAGE RANGE	NORTH AMERICAN PRICE	FOREIGN PRICE
A01	Microfiche	\$ 6.50	\$13.00
A02	001-025	9.95	19.90
A03	026-050	11.95	23.90
A04-A05	051-100	13.95	27.90
A06-A09	101-200	18.95	37.90
A10-A13	201-300	24.95	49.90
A14-A17	301-400	30.95	61.90
A18-A21	401-500	36.95	73.90
A22-A25	501-600	42.95	85.90
A99	601-up	*	*
NO1		45.00	80.00
NO2		48.00	80.00

Schedule E EXCEPTION PRICE DOCUMENTS AND MICROFICHE

PRICE CODE	NORTH AMERICAN PRICE	FOREIGN PRICE
E01	\$ 7.50	15.00
E02	10.00	20.00
E03	11.00	22.00
E04	13.50	27.00
E05	15.50	31.00
E06	18.00	36.00
E07	20.50	41.00
E08	23.00	46.00
E09	25.50	51.00
E10	28.00	56.00
E11	30.50	61.00
E12	33.00	66.00
E13	35.50	71.00
E14	38.50	77.00
E15	42.00	84.00
E16	46.00	92.00
E17	50.00	100.00
E18	54.00	108.00
E19	60.00	120.00
E20	70.00	140.00
E99	*	*

*Contact NTIS for price quote.

IMPORTANT NOTICE

NTIS Shipping and Handling Charges

U.S., Canada, Mexico — ADD \$3.00 per TOTAL ORDER

All Other Countries — ADD \$4.00 per TOTAL ORDER

Exceptions — Does NOT apply to:

ORDERS REQUESTING NTIS RUSH HANDLING
ORDERS FOR SUBSCRIPTION OR STANDING ORDER PRODUCTS ONLY

NOTE: Each additional delivery address on an order
requires a separate shipping and handling charge.

1. Report No. NASA SP-7041 (54)	2. Government Accession No.	3. Recipient's Catalog No.	
4. Title and Subtitle EARTH RESOURCES A Continuing Bibliography (Issue 54)		5. Report Date August, 1987	
		6. Performing Organization Code	
7. Author(s)		8. Performing Organization Report No.	
		10. Work Unit No.	
9. Performing Organization Name and Address National Aeronautics and Space Administration Washington, DC 20546		11. Contract or Grant No.	
		13. Type of Report and Period Covered	
12. Sponsoring Agency Name and Address		14. Sponsoring Agency Code	
15. Supplementary Notes			
16. Abstract This bibliography lists 562 reports, articles and other documents introduced into the NASA scientific and technical information system between April 1 and June 30, 1987. Emphasis is placed on the use of remote sensing and geophysical instrumentation in spacecraft and aircraft to survey and inventory natural resources and urban areas. Subject matter is grouped according to agriculture and forestry, environmental changes and cultural resources, geodesy and cartography, geology and mineral resources, hydrology and water management, data processing and distribution systems, instrumentation and sensors, and economic analysis.			
17. Key Words (Suggested by Authors(s)) Bibliographies Earth Resources Remote Sensors		18. Distribution Statement Unclassified - Unlimited	
19. Security Classif. (of this report) Unclassified	20. Security Classif. (of this page) Unclassified	21. No. of Pages 162	22. Price * A08/HC

*For sale by the National Technical Information Service, Springfield, Virginia 22161